Advanced Analysis in Nanospace: Research with the XFEL

H. Dosch, MPI, Stuttgart

Abstract

Little happens in industrialised countries without the use of high-tech materials which are the building blocks of all modern technologies ranging from information, communication, health, energy and environment to transport. In the last decades the development of novel materials has progressed at a breathtaking rate. This has become possible through our microscopic insight into the atomistic structure of condensed matter which finally enabled us to assemble new material systems atom-by-atom. These days, we are facing a revolution in the investigation of nanospace: Through new concepts in accelerator physics, electrons can be forced to emit short-pulsed x-ray laser radiation. Such a futuristic European x-ray free electron laser (XFEL) laboratory is currently being constructed and will allow mankind to finally get holographic snapshots of the motion of atoms and electrons in materials. Ultimate insights into matter, as the realtime-observation of the formation and the breaking of molecular bonds, sound like science fiction, but could become reality in less than a decade, if Europe embarks today into this bold adventure which will lead us into unexplored dimensions of nanospace.

NO SUBMISSION RECEIVED

ACCELERATOR LAYOUT OF THE XFEL

R. Brinkmann, Deutsches Elektronen-Synchrotron, Hamburg, Germany
for the XFEL Group

Abstract

The X-ray Free Electron Laser XFEL is a 4th generation synchrotron radiation facility based on the SASE FEL concept and the superconducting TESLA technology for the linear accelerator. In February 2003 the German government decided that the XFEL should be realised as a European project and located at DESY/Hamburg. The Ministry for Education and Research also announced that Germany is prepared to cover half of the investment and personnel costs of the project. This paper gives an overview of the overall layout and parameters of the facility, with emphasis on the accelerator design, technology and physics.

INTRODUCTION

X-rays have played for many decades a crucial role in the study of structural and electronic properties of matter on an atomic scale. With the ultra-high brilliant and sub-100 fs pulse length coherent radiation achievable with free electron laser X-ray sources the research in this field will enter a new era [1]. It will become possible to take holographic snapshots with atomic resolution in space and time resolution on the scale of chemical bond formation and breaking. Linear accelerator driven FELs using the principle of self-amplified spontaneous emission (SASE) [2] appear to be the most promising approach to produce this radiation with unprecedented quality in the Å-wavelength regime. The first facility of this type, using part of the existing SLAC linac, was proposed at Stanford and is now under construction [3,4]. The XFEL was originally proposed as integral part of the TESLA project together with a 500 – 800 GeV e+e- Linear Collider based on superconducting RF (SRF) technology [5]. In a later update [6], the proposal was modified such as to build the XFEL with its own, separate linac for the benefit of flexibility regarding construction, commissioning and operation of the facility, maintaining the SRF technology identical to the collider linac and a common experimental site 16km northwest from the DESY site in Hamburg. The German government decision in 2003 to go ahead with the XFEL as a European project and to postpone the decision on the collider led to a revision of the site, with synergy arguments for a common site no longer in effect. The new site layout, sketched in Fig. 1, has the XFEL linac starting on the DESY site, permitting to make optimum use of existing infrastructure, and the user facility in a rural area about 3km west-northwest from DESY. The legal procedure to obtain permission for construction is in preparation and expected to be completed by end of 2005.

The project organisation at the European level is ongoing. A steering committee and two working groups, on scientific-technical and administrative-financial issues, have been established early in 2004, with members from all European countries which are interested in participating in the project. The main task of these groups is to prepare the documents required for the technical definition and organisational structure of the project by 2005. The final decision to move into the construction phase is expected for 2006. The construction time until beam operation will be 6 years. The total project cost is estimated at 684 M€ (year 2000 price level), of which Germany will cover 50%.

Figure 1: Sketch of the XFEL site near DESY.

The electron beam quality and stability required by the SASE process presents considerable challenges to the linear accelerator community. SASE test facilities in the visible and ultra-violet wavelength range were built and operated during the last years [7]. The results have demonstrated the viability of the challenging accelerator subsystems and the good understanding of the SASE process. In particular the successful operation of the TESLA Test Facility (TTF) linac and FEL at DESY provides a firm basis for the XFEL, regarding the SRF technology, beam dynamics and the FEL process [8] and the conduction of user experiments [9]. In its 2nd phase, just about to start, operation of the VUVFEL, designed for FEL radiation down to 6nm wavelength, will continue to deliver a vast amount of experience as a pilot facility for the future project [10].

OVERALL LAYOUT AND PARAMETERS

The XFEL is laid out as a multi-user facility. In its 1st stage, it will have 5 undulator beamlines, 3 of which are SASE-FELs (two for the Å wavelength regime, one for softer X-rays), the other two for hard X-ray spontaneous radiation. Initially, 10 experimental stations are foreseen. The underground experimental hall has a floor space of $50\times90m^2$ and more stations can be added later. The site allows to extend the user facility for more beam lines in a later stage (see Figure 2).

Linac Coherent Light Source (LCLS) Accelerator System Overview

P. Krejcik, Z. Huang, J. Wu, SLAC, Menlo Park, California;
P. Emma, SLAC/ARDA, Menlo Park, California

Abstract

The Linac Coherent Light Source (LCLS) will be the world's first x-ray free-electron laser (FEL). Pulses of LCLS x-ray FEL will be several orders of magnitude brighter and shorter than most existing sources. These characteristics will enable frontier new science in several areas. To ensure the vitality of FEL lasing, it is critical to preserve the high quality of the electron beam during the acceleration and compression. We will give an overview of the LCLS accelerator system. We will address design essentials and technique challenges to satisfy the FEL requirements. We will report studies on the microbunching instability suppression via a Laser-Heater. The studies clearly prove the necessary of adding the Laser-Heater and show how effectively this Laser-Heater suppresses the instability by enhancing the Landau damping. We will report how to minimize the sensitivity of the final energy spread and the peak current to various system jitters. To minimize this sensitivity, a feedback system is required together with other diagnostics. With all these considerations, full start-to-end simulations show saturation at 1.5 , though the LCLS is expected to be a very challenging machine.

NO SUBMISSION RECEIVED

HIGH-INTENSITY, HIGH CHARGE-STATE HEAVY ION SOURCES*

J. G. Alessi
Brookhaven National Laboratory, Upton, NY 11973, USA

Abstract

There are many accelerator applications for high intensity heavy ion sources, with recent needs including dc beams for RIA, and pulsed beams for injection into synchrotrons such as RHIC and LHC. The present status of sources producing high currents of high charge state heavy ions is reviewed. These sources include ECR, EBIS, and Laser ion sources. Benefits and limitations for these type sources are described. Possible future improvements in these sources are also mentioned.

INTRODUCTION

In heavy ion preinjectors, the choice of charge state, (or minimum charge-to-mass ratio), to be designed for, is an important consideration. Higher Q/M from an ion source makes the downstream accelerators more compact and less costly, but generally there is a tradeoff between intensity and charge state from a source, which may or may not be acceptable. If one can select a charge state high enough to eliminate one or more subsequent stripping stages, however, this lower initial intensity may result in equal or higher final intensities.

Examples of future applications which are pushing requirements for high intensity, high charge state heavy ion sources include the following:

- At Brookhaven, a new heavy ion preinjector is planned as a simpler, more modern replacement for the two Tandem Van de Graaff accelerators which are presently used for the heavy ion program at RHIC. As an example, ion source requirements for Au ions include the following a.) charge state 32+, to eliminate the need for stripping before injection into the Booster synchrotron; b.) pulse width ~ 10 µs, to allow simple single turn injection into the Booster; c.) Au^{32+} current from the source of 1.7 emA, in order to deliver the required intensity of 3 x 10^9 ions/pulse to the Booster; d.) 5 Hz repetition rate. In addition, in order to support simultaneously the beam requirements for the NASA Space Radiation Laboratory (NSRL), the ion source must be able to deliver to Booster a second beam species, with pulses interleaved with the RHIC beam pulses, *switching species at the 5 Hz repetition rate*. Examples of the beams required for NSRL include He^{2+}, C^{6+}, O^{8+}, Si^{14+}, Ti^{18+}, Fe^{21+}, and Cu^{22+}, all at currents of 2-3 emA, and pulse widths of ~ 10 µs. As will be discussed below, an Electron Beam Ion Source (EBIS), similar to that which has been developed at Brookhaven [1], can meet these requirements.
- Driver accelerators for rare ion production, such as the Rare Ion Accelerator (RIA), require dc beams of essentially any ion species. Examples of required beams and intensities for RIA are 230 eµA of $U^{28+, 29+}$, 280 eµA of $Pb^{25+,26+}$, 220 eµA of Xe^{18+}, 350 eµA of Ni^{12+}, 230 eµA of Ar^{8+} [2]. In applications such as this, which require high current dc beams, the ECR ion source is essentially the only option. Present state-of-the-art ECRs can exceed RIA requirements for gaseous beams, and are close to meeting the requirements for the more difficult beams produced from solids.
- At CERN, LHC requirements for heavy ions depend on the acceleration scheme used. While initial operation is with Pb ions, ions such as He, O, Ar, Kr, and In have also been requested [3]. The baseline plan for Pb ions requires an upgraded ECR producing > 200 eµA of Pb^{27+}, in 200 µs pulses, at 5 Hz. This scheme also requires the use of LEIR for ion storage and cooling. In an alternative scheme, one could avoid the use of LEIR if one would produce directly from the source ~ 5 emA of Pb^{25+}, in 5.5 µs pulses, at 1 Hz. A laser ion source (LIS) was being developed for this option [4], and an EBIS with a reasonable scaling from Brookhaven parameters could also be considered. A third option, also not needing LEIR, would be to produce ions in a charge state which would also eliminate a stripping stage. In this case, one would need 2-3 emA of Pb^{54+} ions, in 5.5 µs pulses at 1 Hz. Parameters for an EBIS meeting these requirements were presented in [5].

ION SOURCE CONSIDERATIONS

As seen from the above examples, source requirements can depend strongly on the application. Some important considerations are common to almost all accelerator applications, such as source lifetime, reliability, stability (both pulse-to-pulse and long term), magnitude of current fluctuations (noise), and beam emittance. Other aspects have varying importance depending on the application. For instance, the ease and speed of changing species is important for RHIC, but nearly irrelevant for the other applications. Some applications have less flexibility than others regarding the choice of beam species, so sources favoring ions coming either from gases (ECR) or solids (LIS), may be at a disadvantage. Finally, for these high current applications, the charge state distribution of ions coming from the source can be an important

*Work performed under Contract Number DE-AC02-98CH10886 with the auspices of the US Department of Energy.

NON-INTERFERING BEAM DIAGNOSTIC DEVELOPMENTS

A. Peters, P. Forck, GSI, Darmstadt, Germany

Abstract

New high power proton and heavy ion LINAC projects are a big challenge for beam diagnostic developments. Due to the high inherent beam power mostly all destructive measurement techniques are not applicable. Thus a lot of beam diagnostic developments are under way from enhancements of well-known systems like current transformers to new designs for profile or bunch length measurements using e.g. the interaction of the high power beams with the residual gas in the LINACs. The latest progress in this field will be reviewed with descriptions of some remarkable solutions.

INTRODUCTION

The development of new high power proton/ion LINACs is still going on. The aims of such new accelerators are highest beam pulse or D.C. currents and highest brilliances. The demands for new beam diagnostic devices are as follows:

- As much as possible the devices shall work non-interfering to measure even beams of highest power which destroy every material put into the beam line.
- The length of diagnostics mechanics in beam direction shall be as small as possible to have nearly 100 % space for accelerating and focusing elements, which is necessary because of the high space charge forces.

All these parameters together are very challenging, but those developing beam diagnostic equipment can profit from the following trends in the industry:

- A huge market of remote controllable devices has grown, which can be used as parts of diagnostic systems without modifications.
- Digital data treatment methods and devices like FPGAs and DSPs have become cheap and their capabilities are growing fast.
- A special industry segment, the vision systems, shows these trends exemplarily. Digital cameras with fast speeds and/or high resolution are capable to send their image data without any loss directly digital to the user [1].

This overview will report about some examples following the above mentioned tendencies – the focus is glanced at the latest developments in the field of transformers, optical profile measurement devices and a nonintersecting bunch length measuring techniques.

NEW TRANSFORMER APPLICATIONS

BNL Developments for SNS

An interesting example for the use of digital data treatment in connection with a well-known transformer technique was developed by M. Kesselman et al. for the SNS facility [2]. The time structures of the beams range from sub-µs bunches to 1 ms long macro-pulses.

Figure 1: SNS transformer for the DTL section.

To realize only one current measurement device which is capable to observe these different beams with a rise time of about 1 ns and a droop of 0.1 %/ms is normally not possible: an extremely large and expensive core of a (passive) transformer would meet the low droop but not the necessary rise time. In addition, the required space for such a device is not given in a linac. An active-passive transformer would have the same problems, only the size would shrink. To meet both requirements a digital compensation scheme was developed to use a commercial available Fast Current Transformer [3], see Fig. 1 and 2.

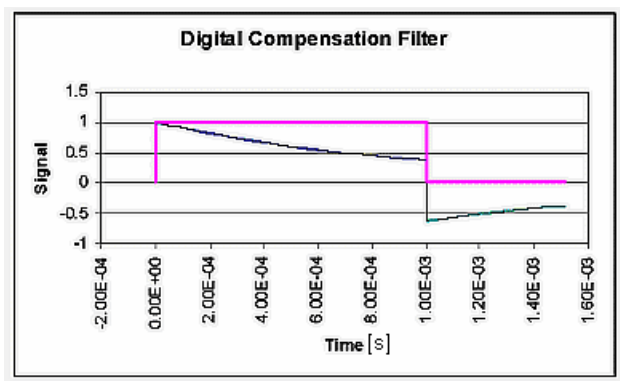

Figure 2: Compensation of an ideal exponentially decaying transformer output signal (blue drooping trace) with a 1ms time constant compensated by an IIR filter that introduces a 1s time constant instead of the 1ms time constant (squared-up magenta trace).

The reconstruction of the original current pulse is based on using an IIR (infinite impulse response) filter. The realization shows that the transformer time constant has to be known with high accuracy that could only be achieved by implementing an online calibration procedure [4]. The IIR filter can easily be realized in a field programmable

STATUS OF REX-ISOLDE*

O. Kester#, D. Habs, S. Emhofer, K. Rudolph, LMU München, 85748 Garching, Germany
T. Sieber, F. Wenander, F. Ames, P. Delahaye, M. Lindroos, P. Butler, CERN, Geneva, Switzerland
R. von Hahn, H. Scheit, R. Repnow, D. Schwalm, MPI-K, Heidelberg, Germany
and the REX-ISOLDE collaboration

Abstract

After commissioning of the radioactive beam experiment at ISOLDE (REX-ISOLDE) and the ν-Detector array MINIBALL first series of physics experiments have been performed in 2002 and 2003. The REX-ISOLDE charge state breeder adjusts the charge-to-mass ratio of isotopes from the whole nuclear chart to the LINAC requirements. A variety of isotopes from different mass regions of the nuclear chart have been charge bred with REXEBIS [1] to the required A/q < 4.5. A variety of tests with REXTRAP, REXEBIS and the LINAC structures have been done, in order to study the beam parameters, transmission efficiency and upgrade options. The LINAC now consists of six resonators and one re-buncher cavity. The beam energy, which can be delivered towards the target areas, can be varied between 0.8 and 2.2. An additional boost to 3 MeV/u is now possible because of the upgrade with a 202.56 MHz IH-cavity developed for the MAFF project. In addition beams from the RFQ at 0.3 MeV/u have been used for solid state physics experiments. The present status of the projects and the commissioning measurements will be presented.

INTRODUCTION

Radioactive ion beam (RIB) facilities give rich opportunities for nuclear structure research as well as for nuclear astrophysics and applied physics. RIB facilities drive the increasing understanding of the evolution of nuclear structure and the growing wealth of nuclear structure data. As yet only relatively small part of the nuclear landscape has been explored, especially on the neutron-rich side where the limit of stable nuclei is only known for the lightest elements. The European nuclear physics community, represented by NuPECC, has identified the need for a second generation of Radioactive Ion Beam (RIB) facilities in Europe. The design of such a second generation RIB facility, based on the ISOL technique, has been investigated, under the auspices of the EU Fifth Framework as the RTD proposal EURISOL [2]. Therefore huge effort is spent on extrapolation from running RIB facilities and present techniques towards those new intense ISOL facilities like EURISOL or RIA [3]. Running ISOL facilities in Europe that provide post accelerated RIBs for nuclear physics experiments are ARENAS (Leuven), ISOLDE (CERN) and SPIRAL (GANIL). Preparation work for future facilities is carried out by those facilities, which is important for the EURISOL design study.

*supported by BMBF under contract number 06 ML 185, 06 ML 186 I and 06 ML 188.
#oliver.kester@physik.uni-muenchen.de

The Radioactive Beam Experiment at ISOLDE, REX-ISOLDE, delivers post accelerated beams of exotic isotopes for nuclear physics research and it has been the dominant experiment in the past two ISOLDE running periods [4]. REX-ISOLDE profits from the vast experience of ISOLDE in production of radioactive beams of more than 600 isotopes from 72 elements. In addition the resonant ionisation laser ion source (RILIS) can provide beams with high selectivity, even isomeric beams. Since end of 2001 the LINAC provides radioactive beams from the ISOLDE online separators with energies of 2.2 MeV/u towards two target stations. One target station is used for the efficient ν-ray MINIBALL array [5] and the other target station is dedicated for smaller experimental set-ups. In order to make the full variety of beams from ISOLDE available for nuclear physics experiments the method of charge breeding of the singly charged radioactive ions has been employed [1]. Hence the concept of REX-ISOLDE is based on a large Penning trap which accumulates the radioactive ions from the ISOLDE mass separators and allows phase space cooling of the RIBs. The prepared ions are then injected into an Electron Beam Ion Source (EBIS), which raises the charge state of the radioactive ion to an A/q < 4.5. The extracted highly charged ions are charge state selected with subsequent acceleration in a short LINAC

THE LOW ENERGY SYSTEM

The low energy part of REX-ISOLDE has several tasks. The low energy part transports the 60 keV beam from the ISOLDE main beam line towards the accelerator and prepares the ion beam for injection into the LINAC. The size of the post-accelerator needed to bring the unstable nuclei to the energies required to study nuclear reactions depends linear on the charge state of the radioactive ions. The capability to raise the charge state of the radioactive ions before injection into an accelerator leads to an enormous reduction of construction and running costs of the accelerator and of the infrastructure. In addition it allows in principle to accelerate ions from all regions of the nuclear chart to the same energy per mass unit.

The principal scheme of the charge multiplication (charge breeding) in case of REX-ISOLDE is shown in fig.1. An EBIS delivers high charge states and is employed as breeder for the radioactive isotopes at REX-ISOLDE. The ISOLDE beam can not be injected into the Electron Beam Ion Source (EBIS) with high efficiency without any beam preparation, because of the small

SPIRAL2 AT GANIL

M.-H. Moscatello for the Spiral2 Project Group, GANIL-CEA/CNRS, Caen, FRANCE

ABSTRACT

The SPIRAL2 project has been under detailed design study since beginning of 2003. The aim of this facility is to produce rare ion beams, using a Uranium carbide target fission process, based on a fission rate of 10^{13} to 10^{14} fissions/s.

The driver accelerator accelerates a 5 mA deuteron beam up to 20 MeV/u, impinging on a carbon converter to produce the neutrons necessary to the fission process. It has also to accelerate q/A=1/3 heavy ions, to energies between 0.75 and 14.5 MeV/A for different types of nuclear and non-nuclear physics experiments.

The accelerator is based on a RFQ followed by an independently phased superconducting cavity linac with warm focusing sections.

This paper presents the reference design chosen for the SPIRAL2 driver accelerator, and gives the design status of the different components: Sources, RFQ, Superconducting linac, RF Systems, Cryogenics, Mechanical layout.

INTRODUCTION

The Spiral2 project is originally based on the LINAG1 conceptual design [1], that proposed a facility aiming at delivering high intensity radioactive beams produced by different methods (fission of uranium target via a carbon converter, direct target irradiation), as well as high intensity stable ion beams.

Since the creation of the Spiral2 project group at the beginning of 2003, many detailed studies have been undertaken [2], and have led now to new solutions and technical choices for the accelerator design as well as for the target ion source system and radioactive beam transport lines.

SPIRAL2 GENERAL LAYOUT

The facility consists of a linac driver able to accelerate a 5mA deuteron beam up to 20A.MeV as well as light ion (q/A=1/3), 1mA beams up to 14.5 A.MeV. The deuteron beam impinges on a carbon converter to produce neutrons, used then in the fission process of a uranium carbide for the production of radioactive ion beams (RIB). Theses fission products, extracted from a source, are transported towards a charge breeder, and accelerated by the existing CIME cyclotron to maximum energies between 5 and 10 A.MeV, according to the ion q/A ratio. The stable ion beams can be used also for the production of RIBS on different target types, or sent directly towards an experimental cave, for nuclear physics experiments. Fig.1 shows a schematic layout of the planned facility.

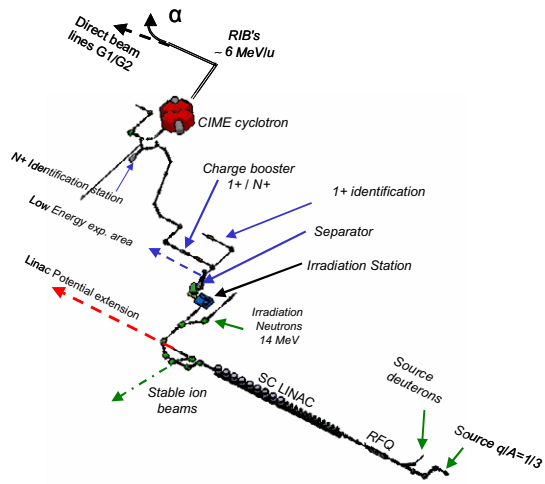

Figure 1: Spiral2 facility schematic layout

THE LINAC ACCELERATOR

Linac Main Specifications and Parameters

The accelerator has been designed with the following main specifications:

- CW accelerator.
- 0.15–5 mA of, 40-MeV deuterons.
- Up to 1 mA (Argon) for q/A=1/3 ions, 14.5 MeV/u.
- Two ion sources, one for the deuterons, the other one for the ions q/A=1/3.
- Normal conducting RFQ injector designed for both D^+ and q/A=1/3 ions.
- Optimisation of the accelerator for 1mA q/A=1/3 ion beams, with the capability of accelerating a 5 mA deuteron beam to the required energy.
- Possibility for the SC linac to accelerate ion beams of q/A=1/6 (up to 1 mA) in the future, and to be extended towards higher energies.
- Maximum energy gain for each kind of ion, which implies independently phased cavities.

A principle layout of the accelerator is presented in fig.2.

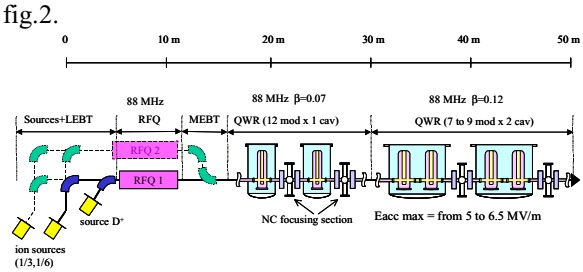

Figure 2: Principle layout of the accelerator

Detailed beam dynamics studies have led to the final frequency choice of 88.05 MHz for the whole

DEVELOPMENT OF ROOM TEMPERATURE AND SUPERCONDUCTING CH-STRUCTURES

H. Podlech
IAP, Universität Frankfurt/Main, Germany

Abstract

In the last decades several types of H-mode cavities have been developed for a wide range of applications. Several drift tube cavities (IH-structure) are in routine operation [1][2]. At the IAP (University of Frankfurt, Germany) a new type of H-mode cavity, the Cross-Bar-H-mode or CH-structure is presently under development. This multicell drift tube cavity is operated in the $H_{21(0)}$-mode. The CH-structure is an excellent candidate for high power proton accelerators in the energy range from 3 to 100 MeV. We present the status of the room temperature (r.t.) CH-cavity development for a dedicated 70 MeV proton injector for the international accelerator facility FAIR at GSI [3]. Due to its mechanical rigidity this cavity can be realized not only for room temperature but also for superconducting (s.c.) operation. To prove the very promising properties of superconducting CH-structures obtained by simulations, a 352 MHz prototype CH-cavity has been designed. Presently, this cavity is in the final stage of production. We present recent results of the s.c. cavity development and different applications which could take advantage of the s.c. CH-structure (XADS, IFMIF, cw-linac for the production of superheavy elements).

INTRODUCTION

A common property of all H-mode cavities is the high shunt impedance and the uniform power loss distribution which simplifies the cooling, especially at higher duty factors or cw operation . Figure 1 shows the effective shunt impedance as function of the particle velocity for different kinds of drift tube cavities. The well known IH-structure ($TE_{11(0)}$-mode) has no competitor in the low β-range from 0.01 to 0.1. The main reason for the high shunt impedance is the low capacitive load by using slim drift tubes without transverse focusing elements inside the tubes. Very high accelerating gradients up to 10.7 MV/m have been achieved in pulsed operation [1], and cw operation has been realized successfully, too [4][5]. Limitation of IH-structures are the lack of mechanical stability for s.c. operation and the upper operation frequency of about 300 MHz. Above this frequency the tank diameter becomes unreasonable small.
The CH-structure which is operated in the $H_{21(0)}$-mode has a larger diameter for a given frequency compared with the IH-structure. Cavities with frequencies from 150 to 800 MHz can be realized. This means that the CH-structure fits well to the popular frequency of proton drivers at around 350 MHz.
Unlike cavities with only two gaps as half wave or spoke resonators which cover typically a broad velocity range, the CH-structure is a multi cell cavity with a fixed velocity profile. Therefore this cavity has a constant high transit time factor larger than 0.8. Additionally, the KONUS beam dynamics (Kombinierte Null Grad Struktur) [1] is used to optimise the individual cavity cells. Due to the reduced transverse rf defocusing, long lens free sections can be realized even at high beam currents. This results in very high real estate gradients

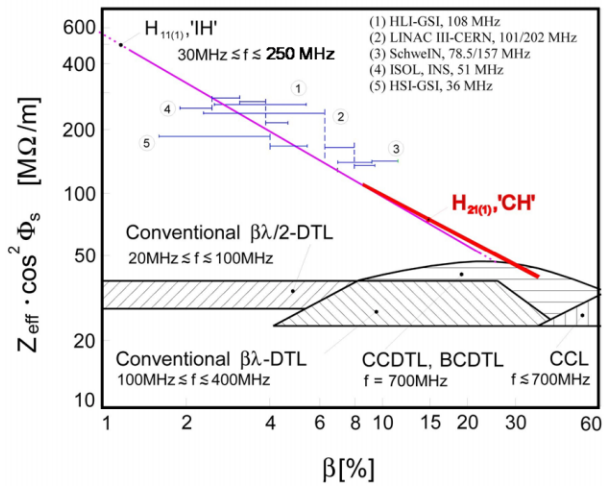

Figure 1: Effective shunt impedance as function of β for different rf structures. The horizontal blue bars represent existing IH-structures and the red line is the expected shunt impedance of the designated CH-proton linac for FAIR/GSI.

R.T. CAVITY DEVELOPMENT FOR THE GSI PROTON-INJECTOR

The existing Unilac at GSI is a fixed velocity heavy ion linac and can fill the synchrotron SIS12 only to about a few percent of the space charge limit for protons [1]. For the physics program, especially for the antiproton producton at FAIR, it is required to increase the proton current by a factor of 70 compared with the present capabilities. This can only be fulfilled by a dedicated proton injector. The key parameters are the final energy of 70 MeV, the neccessary peak current of 70 mA and the rf frequency of 352 MHz.
A combination of a 4-rod-RFQ [6] and of a CH-linac consisting of 11 r.t. CH-cavities is planned [7]. The design goal

BEAM INTENSITY ADJUSTMENT IN THE RIA DRIVER LINAC*

P. N. Ostroumov#, J.A. Nolen, S.I. Sharamentov, ANL, 9700 S. Cass Avenue, Argonne, IL, 60439
A.V. Novikov-Borodin, INR, Moscow 117312, Russia

Abstract

The Rare Isotope Accelerator Facility currently being designed in the U.S. will use both heavy ion and light ion beams to produce radionuclides via the fragmentation and spallation reactions, respectively. Driver beam power of up to 400 kW will be available so that beam sharing between target stations is a viable option to increase the number of simultaneous users. Using a combination of rf-sweepers and DC magnets the driver beams can be delivered to up to four targets simultaneously. With simultaneous beam delivery to more than one target independent adjustment of the relative beam intensities is essential. To enable such intensity adjustment we propose to use a fast chopper in the Medium Energy Beam Transport (MEBT) section. Several design options for the fast chopper are discussed. The MEBT beam optics is being designed to accommodate and match the chopper technical specifications.

BEAM SWITCHYARD

A preliminary design for a driver linac switchyard has been discussed in the recent RIA Facility Workshop [1]. The proposed switchyard will deliver beams to four production targets. The design of the switchyard for the driver beams of RIA is a complex problem due to the following features: 1) Sharing beams of various ion species accelerated over a wide range of energies; 2) Delivery of beams to four target stations simultaneously; 3) Providing high quality beam optics with higher order corrections for multiple charge state beams. The accelerated beam in the RIA driver can be distributed to four targets simultaneously using rf sweepers. A low frequency rf sweeper is appropriate for the deflection of heavy ion beams and the delivery to two or more targets simultaneously. The deflector design is based on an H-type rf cavity. The fundamental frequency of the bunch sequence is determined by the multiharmonic buncher at the front-end of the driver linac. In the two-charge state injector mode all four harmonics are applied and the bunch repetition rate will be 57.5 MHz. In the single charge state injector mode only three harmonics of the multi-harmonic buncher will be used and the bunch repetition rate is still 57.5 MHz. Therefore the rf sweeper can operate at 86.25 MHz to split the beam intensity 50/50 to two directions. The length of the rf sweeper's electrode is chosen to provide a phase slippage of 180° inside the cavity for uranium beams. This condition eliminates any effect of fringing fields on uranium beams but produces negligible momentum spread for lighter ions because of their higher velocity and shorter time-of-flight. A room temperature rf cavity operating at 86.25 MHz can provide a maximum electric field on the surface of ~18 MV/m in cw mode. We have conservatively designed for a maximum electric field of ~7.2 MV/m between the electrodes. The main parameters of the rf sweeper are shown in Table 1. Two such sweepers are used in series. The rf sweeper is followed by two DC septum magnets.

Table 1: Basic parameters of the rf deflector for the RIA switchyard

Maximum electric field between the plates	7.2 MV/m
Effective length	1.2 m
Deflecting angle	± 3 mrad
Aperture	3.0 cm
Tank diameter	68 cm
Required rf power according to the MWS Studio	25 kW

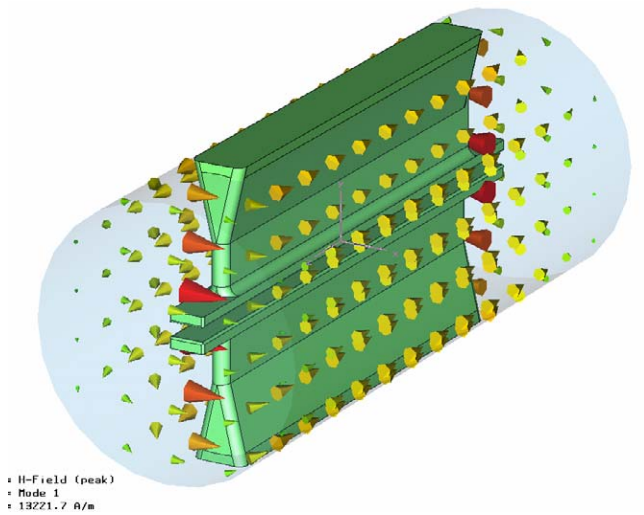

Figure 1: MWS design of the 86 MHz rf sweeper.

BEAM INTENSITY ADJUSTMENT

The switchyard will deliver beams to 4 targets simultaneously. Using rf sweepers beam microbunches will be alternatively sent to different targets. In this mode, all targets will receive equally distributed beam power. For most experiments it is desirable to have adjustable level of beam intensity on the targets. This problem can be solved by using a chopper which could remove any fraction of the beam. The chopper can be made as a device with a deflecting electric field and should be located in the MEBT to minimize the required voltage as well as to reduce the power on the beam dump. The

* This work was supported by the U.S. Department of Energy, Office of Nuclear Physics, under Contract No. W-31-109-ENG-38.
#ostroumov@phy.anl.gov

PROPOSAL FOR REDUCTION OF TRANSVERSE EMITTANCE OF BNL 200 MEV LINAC*

D. Raparia, J. Alessi, J. Beebe Wang, W. T. Weng, Collider-Accelerator Department,
Brookhaven National Laboratory, Upton, New York 11973, USA

Abstract

BNL has a plan to upgrade the AGS proton beam from the current 0.14 MW to higher than 1.0 MW and beyond for a neutrino facility which consists of two major subsystems. First is a 1.45 GeV superconducting linac (SCL) to replace the Booster as injector for the AGS. Second is the performance upgrade for the AGS itself for the higher intensity and repetition rate. For high intensity proton accelerators, such as the upgraded AGS, there are very stringent limitations on uncontrolled beam losses. A direct effect of increased linac beam emittance is the halo/tail generation in the circulating beam. Studies show the estimated halo/tail generation in the beam for the present normalized RMS emittance of the linac beam is unacceptable. To reduce the transverse emittance of the 200 MeV linac, the existing radio frequency quadrupole linac (RFQ) has to be relocated closer to drift tube linac (DTL) tank 1 to meet the emittance requirement for AGS injection with low loss. This paper will present the various options of matching between RFQ and DTL, and chopping options in the low energy beam transport (LEBT).

INTRODUCTION

We have examined possible upgrades to the AGS complex that would meet the requirements of the proton beam for a 1.0 MW neutrino superbeam facility [1]. We are proposing to upgrade the existing 200 MeV linac to 400 MeV using the Fermilab style CCL, followed by a superconducting linac to an energy of 1.45 GeV for direct H^- injection into the AGS [1].

The requirements of the proton beam for the super neutrino beam are summarized in Table 1. Since the present number of protons per fill is already close to the required number, the upgrade focuses on increasing the repetition rate and reducing beam losses (to avoid excessive shielding requirements and to keep activation of the machine components to a workable level). It is also important to preserve all the present capabilities of the AGS, in particular its role as injector to RHIC. Present injection into the AGS requires the accumulation of four Booster loads in the AGS, which takes about 0.6 sec, and is therefore not suited for high average beam power operation.

Table 1: AGS Proton Driver Parameters

Total beam power	1 MW
Beam energy	28 GeV
Average beam current	42 μA
Cycle time	400 msec
Number of protons per fill	0.9×10^{14}
Number of bunches per fill	24
Protons per bunch	0.4×10^{13}
Injection turns	230
Repetition rate	2.5 Hz
Pulse length	0.72 msec
Chopping rate	0.75
Linac average/peak current	20 / 30 mA

To reduce the injection time to about 1 msec, the Booster will be replaced by a 1.45 GeV linac. The injection linac consists of the existing warm linac of 200 MeV upgraded to 400 MeV and a new superconducting linac to 1.45 GeV. The multi-turn injection from a source of 28 mA and 720 μsec pulse width is sufficient to accumulate 0.9×10^{14} particle per pulse in the AGS. The minimum ramp time of the AGS to full energy is presently 0.5 sec. This must be reduced to 0.2 sec to reach the required repetition rate of 2.5 Hz to deliver the required 1 MW beam to the target.

HALO/TAIL GENERATION VS. LINAC EMITTANCE

For high intensity proton accelerators, such as the upgraded AGS, there are very stringent limitations on uncontrolled beam losses. We have examined the emittance growth and uncontrolled beam losses as a function of linac emittance by computer simulations.

All of the physical quantities used in the simulations (Table 1 and 2) are chosen according to the design specifications. Correlated painting is chosen for injection into AGS, considering the available aperture at injection and beam halo/tail control. The average stripping foil thickness is assumed to be 300 $\mu g/cm^2$. In order to separate the effects of linac emittance from the other issues, the effects of space charge and magnet errors are not included in this study.

A direct effect of linac beam emittance is the halo/tail generation in the circulating beam. Figure 2 shows the estimated halo/tail generation in the AGS beam as a function of normalized RMS emittance of linac beam.
Here, the halo/tail generation is defined as the ratio of the number of particles with emittance larger than the designed acceptance of 49π mm-mrad to the total number of particles in the circulating beam.

* Work performed under the auspices of the US Department of Energy
** E-mail raparia@bnl.gov

THE HITRAP-DECELERATOR FOR HEAVY HIGHLY-CHARGED IONS

L. Dahl*, W. Barth, Th. Beier, W. Vinzenz
Gesellschaft für Schwerionenforschung, D-64291 Darmstadt, Germany

C. Kitegi, U. Ratzinger, A. Schempp
J.W. Goethe-University, D-60054 Frankfurt a.M., Germany

Abstract

The GSI accelerator facility provides highly-charged ions up to U^{92+} by stripping the ions at 400 MeV/u in the transfer line from the SIS18 (Heavy Ion Synchrotron) to the ESR (Experimental Storage Ring). The ESR provides high quality beams by means of stochastic cooling and electron cooling. Deceleration down to 4 MeV/u was already successfully demonstrated. After suitable rebunching, further deceleration down to 6 keV/u, necessary for the capture of the ions by a penning trap, is done by IH/RFQ-structures. All cavities are operated at 108 MHz. Recently the HITRAP-project (Heavy Ion Trap), described in a Technical Design Report, was approved. The layout of the decelerator and the beam dynamics in different sections are reported.

INTRODUCTION

Up to now, GSI is the world´s only facility (Fig. 1) which provides heavy highly-charged ions up to U^{92+} for atomic-physics experiments. The high energy, necessary for stripping the ions up to bare nuclei, is obtained by a first acceleration stage of Uranium to 11.4 MeV/u in the UNILAC. Through a transfer line the SIS18 is fed with single macro pulses of 100 µs length which are accelerated up to 400 MeV/u. After extraction and during the transfer to the ESR finally a foil stripper enables a high yield of U^{92+}-ions.

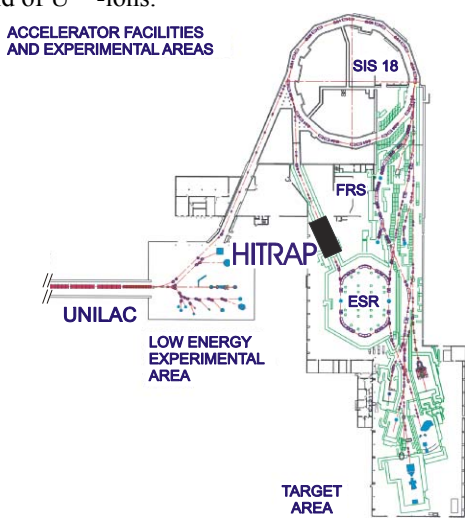

Figure 1: GSI accelerator facility and location of the HITRAP facility.

* L.Dahl@gsi.de

In a multi-stage process the ESR decelerates the U^{92+}-beam down to 4 MeV/u and extracts it to the HITRAP-linear decelerator, described in a Technical Design Report [1]. This decelerator reduces the energy of the heavy highly-charged ions from 4 MeV/u down to 6 keV/u. After ejection from the ESR, the beam will be rebunched by a λ/4-resonator. In a subsequent step an IH-type structure will decelerate the beam from 4 MeV/u to 0.5 MeV/u. Another rebuncher tank of spiral-type will prepare the beam longitudinally for the second deceleration down to 6 keV/u by an RFQ-structure. With this energy the highly-charged ions can be captured in a cylindrical Penning trap and be cooled further by electron and resistive cooling to cryogenic temperatures. The cold ions can be extracted again and transported to the final experiments.

PRODUCTION OF BARE NUCLEI

To provide highly-charged ions up to U^{92+}, which is the design ion for the HITRAP facility, the beam has to pass through three stripping processes. After the U^{4+}-ions are generated either in a high current MEVVA ion source or in a PIG ion source they are accelerated to 1.4 MeV/u by the HSI (High Current Injector) [2] of the UNILAC. Subsequently, a nitrogen gas jet stripper increases the charge state from 4+ to 28+ as the equilibrium charge state, which is needed for acceleration in the Alvarez main accelerator. The fraction of U^{28+} particles amounts to 12 %.

At 11.4 MeV/u a foil stripper, located in the transfer beam line to the SIS18, increases the charge state to 73+ using carbon foils of 600 µg/cm². Again, by the loss of neighbouring charge states only 15 % of the uranium particles remain for injection of 100 µs macro beam pulses into the SIS18 for acceleration to 400 MeV/u. Finally, a copper sheet of 40 mg/cm², located in the beam transfer line between SIS18 extraction and ESR injection strips about 30 % of the uranium ions at the energy of 400 MeV/u to bare nuclei.

The ESR [3] was designed for the deceleration of ions to a minimum energy of 3 MeV/u. Machine experiments have successfully demonstrated the feasibility of U^{92+}-beam deceleration. At 5 MeV/u a U^{92+}-beam intensity of $1 \cdot 10^6$ particles per cycle was achieved and $2 \cdot 10^5$ particles at 3 MeV/u. The corresponding momentum spread was $dp/p = 2.4 \cdot 10^{-4}$ and $dp/p = 1 \cdot 10^{-4}$, detected by Schottky diagnostics. Due to electron cooling the normalized transverse emittances were measured with

A DEDICATED 70 MEV PROTON LINAC FOR THE ANTIPROTON PHYSICS PROGRAM OF THE FUTURE FACILITY FOR ANTIPROTON AND ION RESEARCH (FAIR) AT DARMSTADT

L. Groening, W. Barth, L. Dahl, R. Hollinger, P. Spädtke, W. Vinzenz, S. Yaramishev*, GSI, Darmstadt, Germany
B. Hofmann, Z. Li, U. Ratzinger, A. Schempp, R Tiede, Johann Wolfgang Goethe University, Frankfurt a.M., Germany

Abstract

The antiproton physics program of the proposed International Accelerator Facility at Darmstadt is based on a rate of $7{\cdot}10^{10}$ cooled antiprotons per hour. To provide the primary proton intensities a proton linac is planned, which will be operated independently from the existing UNILAC for heavy ions. The proposed linac comprises a proton source, a RFQ, and a DTL. Its operation frequency of 352 MHz allows for an efficient acceleration to up to 70 MeV using normal conducting Crossed-bar H-cavities. These CH-cavities show high shunt impedances as known from IH-structures, but allow for much higher relative particle velocities of up to 50 %. The beam pulses with a length of at least 25 µs, a current of 70 mA, and total normalized transverse emittances of 2.8 µm will allow to fill the existing synchrotron SIS within one multi-turn-injection up to its space charge limit of $7{\cdot}10^{12}$ protons. The maximum SIS ramping rate limits the applied proton linac repetition rate to 4 Hz. This paper gives an overview of the proposed proton linac. The status of the design including beam dynamic studies will be reported. We acknowledge the support of the European Community-Research Infrastructure Activity under the FP6 "Structuring the European Research Area" programme (CARE, contract number RII3-CT-2003-506395).

INTRODUCTION

A new international Facility for Antiproton and Ion Research (FAIR) is projected at GSI in Darmstadt [1], for which the existing UNILAC and the synchrotron will serve as injectors. Beside radioactive ion research a major part of the experimental program is dedicated to pbar physics (Fig. 1). The need at FAIR sums up to $7{\cdot}10^{10}$ cooled pbar/h. Taking into account the pbar production and cooling rate this is equivalent to $2{\cdot}10^{16}$ primary protons/h to be provided by a chain of accelerators comprising an injector linac and two synchrotrons. The achievable primary proton rate is limited by the repetition rate and by the space charge limit (SCL) of the first synchrotron SIS12 (4 Hz). The scaling of its SCL with $\beta^2\gamma^3$ in connection with the cycle times of the two synchrotrons requires an injector providing protons of at least 18 MeV. The SIS12 is filled during one injection pulse by horizontal multi-turn injection (MTI). To reach the SCL, the beam brilliance B_n provided by the injector linac must be above a minimum value, which depends on the specific parameters of the MTI [2]:

$$B_n \equiv \frac{I}{\beta\gamma\varepsilon_x} \geq 63.6\frac{\text{mA}}{\mu\text{m}}\cdot\frac{(\beta\gamma)^2}{\eta_{MTI}} \equiv B_{n,\min}\ , \quad (1)$$

where I is the proton beam current, ε_x is the total horizontal emittance, and η_{MTI} is the efficiency of the

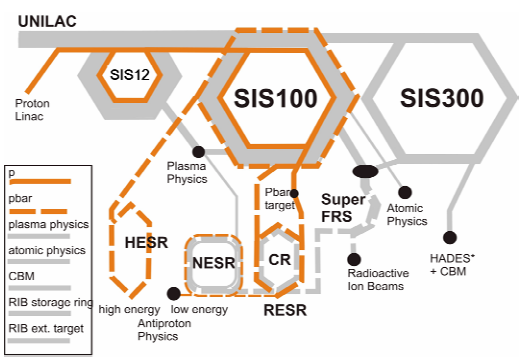

Figure 1: Schematic overview of the accelerator chain to provide cooled antiprotons at FAIR.

*on leave from ITEP, Moscow, Russia

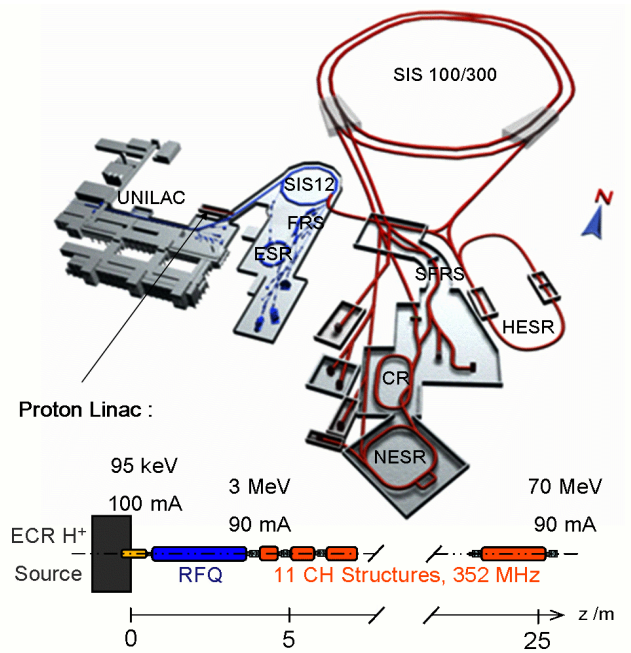

Figure 2: Schematic overview of the new proton injector linac and its implementation into FAIR. The quoted proton currents include safety margins.

HIGH CURRENT BEAM TRANSPORT TO SIS18

S. Richter[#], W. Barth, L. Dahl, J. Glatz, L. Groening, S. Yaramishev[1],
Gesellschaft für Schwerionenforschung, D-64291 Darmstadt, Germany

Abstract

The optimized transversal and longitudinal matching of space charged dominated ion beams to the heavy ion synchrotron SIS18 is essential for minimizing injection losses. This paper focuses on the beam dynamics in the transfer line (TK) from the post-stripper accelerator of the Unilac to the SIS18. Transverse beam emittance measurements at different positions along the TK were done. In particular, the different foil stripping modes were investigated. A longitudinal emittance measurement set-up was commissioned at the entry to the TK. It is used extensively to tune all the rebunchers along the Unilac. In addition, a test bench is in use for measurements of longitudinal bunch profiles, enabling the monitoring of the final debunching to SIS18. Multi particle simulations by means of PARMILA allow a detailed analysis of experimental results for different ion currents.

INTRODUCTION

For the FAIR project the Unilac and SIS18 combination is foreseen to serve as an injector for the SIS100 [1]. To gain the envisaged intensities, up to 10^{12} U^{28+} particles/s must be injected from the Unilac into the synchrotron. To reach this number, different measures must be undertaken to achieve this goal.

Since the successful commissioning of the Unilac High Current Injector (HSI) the particle numbers for the heaviest ions have steadily increased due to constant machine improvement [2].

The high current within the 100 µs pulses offered by the HSI/poststripper accelerators must be transported via the 130 m transfer line (TK) to SIS18. The TK is divided into nine sections (TK1-TK9). A foil stripper in section three allows stripping to higher charge states for SIS18 injection, the charge state analysis is done by using dipole magnets in section 4; the beam is inserted during 20 turns. Typically the ions are stripped at a foil stripper in the TK for SIS18 operation. The ion beam may either be kicked, or in order to reduce the thermal stress, be swept over the foil. For the design ion uranium the charge state equilibrium changes from U^{28+} to U^{73+}. The beam can be manipulated longitudinally after the poststripper by two bunchers.

Table 1: Beam parameters required for SIS18 injection at 11.4 MeV/u.

$\varepsilon_{n,x}$ [mm mrad]	0.8
$\varepsilon_{n,y}$ [mm mrad]	2.5
$\Delta W/W$	$\pm 2 \cdot 10^{-3}$

[#] S.Richter@gsi.de
[1] on leave from ITEP, Moscow, Russia

For an optimum SIS injection both the transversal and longitudinal matching conditions have to be met (see table 1).

Until the end of 2003 the only available longitudinal diagnosis in the Unilac were the phase probe signals, and after a successful injection into SIS18 the Schottky analysis of the circulating beam on the injection plateau.

The TK is currently equipped with two transverse emittance measurement devices and one longitudinal emittance measurement device which was recently commissioned.

PARMILA SIMULATIONS

The multi particle simulations indicate different regions where further experimental investigations should be carried out and additional beam diagnosis elements should be installed. A full description of the beam transport line from the Alvarez accelerator section to the SIS18 injection point at the end of the transfer channel was compiled for PARMILA simulations [3]. After the Alvarez a single gap resonator is used as a rebuncher.

As an outcome of the simulations, the region after the foil stripper is identified as a beam transport line where strong space charge influences are expected. This is due to the approx. 25 m drift of the not yet analyzed multi-charge beam to the charge state separator. Thus, a comparison between the theoretically determined emittances at the exit of the Alvarez section, the stripper section and before SIS injection (see Fig. 1) can be performed. The installed beam diagnostic elements allow a comparison of simulations and measurement.

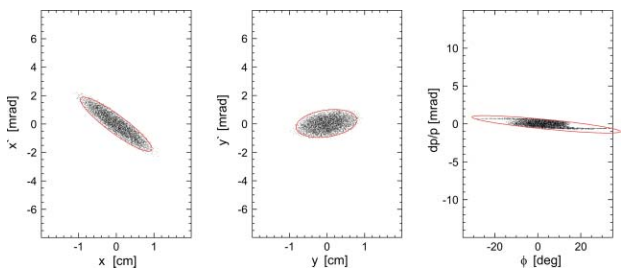

Figure 1: Calculated transversal and longitudinal emittances at the end of the TK.

TRANSVERSE EMITTANCE MEASUREMENTS

Machine development strongly focused on the systematic investigation of emittance growth along the whole Unilac. The results from the last campaigns during 2003 and 2004 are presented here [4]. Two ion species – uranium and argon - delivered by the HSI were investigated. The uranium beam was produced in a MEVVA ion source, whereas argon beam was delivered

INVESTIGATION OF THE BEAM MATCHING TO THE GSI-ALVAREZ DTL UNDER SPACE CHARGE CONDITIONS

S. Yaramishev[1,2], W. Barth, L. Dahl, L. Groening, S. Richter
Gesellschaft für Schwerionenforschung, D-64291 Darmstadt, Germany

Abstract

The main part of the UNILAC consists of the 36 MHz high current RFQ/IH-injector, a gas stripper at an energy of 1.4 MeV/u and a 108 MHz Alvarez poststripper, accelerating ions up to 11.4 MeV/u. The design beam current for U^{28+} is 12.6 emA at full energy. After the stripping process the electrical beam current is increased by a factor of 7 for uranium. This leads to a significant beam emittance growth during the transport through the charge state separator and the matching section to the Alvarez DTL. This paper reports results of numerical studies and beam experiments focused on the matching of the high intensity beams to the Alvarez for different ion species. Possible improvements of the transverse focusing in the Alvarez linac are discussed and the total impact to the beam quality at the synchrotron injection is evaluated.

GSI UNILAC

The UNILAC [1] is designed to accelerate all ion species with mass over charge ratios of up to 8.5 and to fill the heavy ion synchrotron SIS up to its space charge limit. The main part of the UNILAC consists of the 36 MHz high current injector (HSI), a gas stripper section at energy of 1.4 MeV/u and a 108 MHz Alvarez type poststripper, accelerating ions up to 11.4 MeV/u (Fig.1).

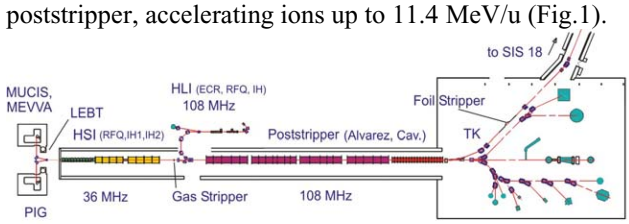

Figure 1: Schematic overview of the GSI UNILAC.

The prestripper section HSI [2] consists of two ion source terminals (PIG and MUCIS/MEVVA), the Low Energy Beam Transport (LEBT), a Radio Frequency Quadrupole accelerator (RFQ), a short matching section (superlens), and two IH (Interdigital H-structure) tanks.

The HSI has been in routine operation since 1999 and has achieved the design intensities for light and medium ions with a significant surplus of the primary beam current coming from the ion source. For heavy ions the achieved beam intensities behind HSI are about factor of two lower than the design values. Several measures were proposed and partially realized for the increase of the beam current and brilliance at the entrance of the synchrotron SIS 18 [3].

[1] S.Yaramishev@gsi.de
[2] On leave from ITEP, Moscow, Russia.

GAS STRIPPER SECTION

In the UNILAC gas stripper section [4] the charge states of incoming ions at energy of 1.4 Mev/u with a charge to mass ratio of $A/q \leq 65$ are increased by stripping in a nitrogen gas jet to allow for further acceleration at $A/q \leq 8.5$. The design U^{4+} beam current of 15 emA rises up to 7 times during stripping. The U^{28+} ions with design beam current of up to 12.6 emA have to be separated entirely from the neighbouring charge states.

Space charge parameter (SCP), calculated from the results of the uranium beam dynamics simulation in the UNILAC, is shown on Fig.2. As can be seen, the SCP is the highest in the stripper area, but it decreases rapidly with particle separation. Another significant peak at the entrance of the 1st Alvarez tank appears due to the small size of the beam in all three dimensions, as required for the beam matching.

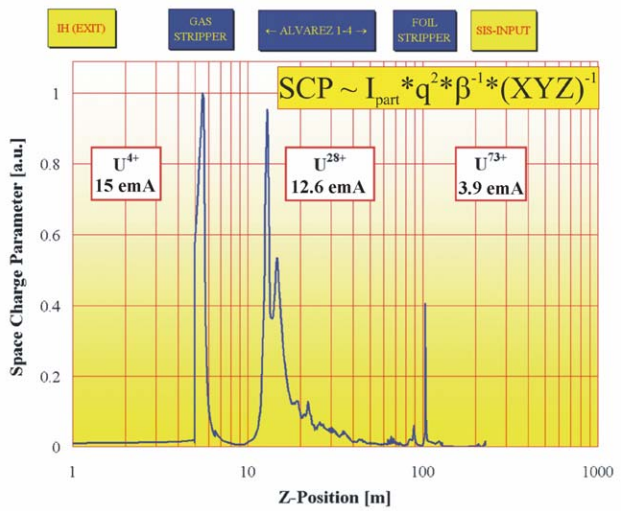

Figure 2: Space charge parameter along UNILAC.

Therefore the separation of the required ion species and the beam matching to the DTL structure are taking place under extremely high space charge influence.

A special optimization procedure, described below in detail, was proposed for the beam matching to the DTL and successfully implemented during machine experiments. It must be pointed out that the recently described procedure does not take into account the defocusing space charge forces. Nevertheless, for the maximum achieved beam current behind the stripper section for the U^{28+} (4 emA), the proposed method was implemented and transmission through the whole Alvarez section up to 100% was reached.

However, the design beam current behind the stripper section is about factor of three higher (12.6 emA for

STATUS OF THE 7 MeV/u, 217 MHz INJECTOR LINAC FOR THE HEIDELBERG CANCER THERAPY FACILITY

B. Schlitt, K. Dermati, G. Hutter, F. Klos, C. Muehle, W. Vinzenz, C. Will, O. Zurkan
GSI, Darmstadt, Germany
A. Bechtold, Y.R. Lu, U. Ratzinger, A. Schempp, IAP, Frankfurt am Main, Germany

Abstract

A clinical synchrotron facility designed by GSI for cancer therapy using energetic proton and ion beams (C, He and O) is under construction and will be installed at the university hospital in Heidelberg, Germany, starting in 2005. The status of the ECR ion source systems, the beam line components, the 400 keV/u RFQ and the 20 MV IH cavity as well as the linac RF system is reported. The production of most of the components is in progress. First devices have been delivered to GSI already. The RF cavities of the injector linac have been designed in close cooperation between GSI and IAP. A beam test stand for the RFQ using proton beams is presently being set up at the IAP. Two prototype magnets of the linac quadrupole magnets have been built at GSI and have been tested successfully. An 1.4 MW, 217 MHz cavity amplifier has been delivered by BERTRONIX recently. A test bench for this system has been installed at GSI including a 120 kW driver amplifier.

INTRODUCTION

A dedicated clinical Heavy Ion CAncer Therapy facility (HICAT) has been designed at GSI and will be built at the university hospital in Heidelberg, Germany [1][2]. The accelerator chain is designed to accelerate low-LET (linear energy transfer) ions (p, He) as well as high-LET ions (C, O) to cover the specific medical requirements. It consists of two ECR ion sources, a 7 MeV/u injector linac and a compact 6.5 Tm synchrotron to accelerate the ions to final energies of 48 – 430 MeV/u. Three treatment stations (two fixed horizontal beam lines and one isocentric ion gantry) as well as a quality assurance place for R&D activities are planned. The facility is designed to treat more than 1000 patients per year using the intensity controlled rasterscan method, which has been developed at GSI and has been successfully applied with carbon ion beams to about 230 patients since more than six years within the GSI therapy project [3]. The requested maximum beam intensities at the treatment places are 1×10^9 $^{12}C^{6+}$ ions/spill and 4×10^{10} protons/spill. Only active and no passive beam manipulating systems are planned.

The layout of the injector linac is presented in Fig. 1 [4][5], major linac parameters are listed in Table 1. The low energy beam transport lines (LEBT) consist of two independent spectrometer lines and allow for a fast selection between two different ion species by a switching magnet. DC operation is planned for the ion sources. A short beam pulse with a length of up to about 300 µs will be formed by a macropulse chopper. The RF linac consists of an 1.4 m long four-rod type RFQ for acceleration of the ions to 400 keV/u [6][7], a very compact intertank matching section [4] and a 3.8 m long 20 MV IH-type drift tube cavity [4][5][8][9]. The remaining electrons of the ions will be stripped off for all ion species in a thin stripper foil behind of the linac.

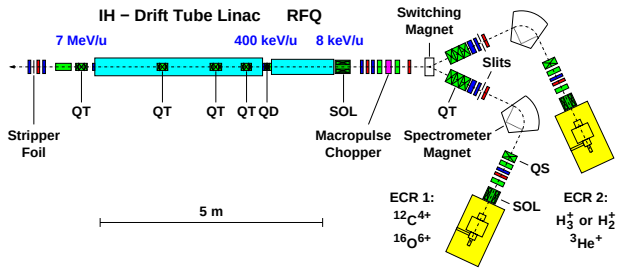

Figure 1: Schematic drawing of the injector linac. SOL ≡ solenoid magnet; QS, QD, QT ≡ magnetic quadrupole singlet, doublet, triplet.

Table 1: Selection of major linac parameters.

Ion species (from ion sources) and required ion source currents	$^{12}C^{4+}$: 130 µA H_3^+: 440 µA $^{16}O^{6+}$: 100 µA $^3He^+$: 320 µA
Ion mass-to-charge ratio	$A/q \leq 3$
Final beam energy	7 MeV/u
Operating frequency	216.816 MHz
RF pulse length	≤ 500 µs @ PRR ≤ 10 Hz

GENERAL STATUS

The components for the complete HICAT facility like vacuum chambers, magnets, power supplies, the RF systems and the accelerator control system have been ordered from industry in 2003. Most of the manufacturing drawings are completed and the production of the components is in progress. The first solenoid magnet for the LEBT has been delivered by SIGMAPHI to GSI last week.

Two complete 14.5 GHz SUPERNANOGAN ECR ion source systems have been ordered from PANTECHNIK [10]. Major components of the ion sources are fabricated and assembled already. Factory acceptance tests are planned for the fourth quarter of this year.

An overview of the beam diagnostics devices for the complete HICAT facility is given in Ref. [11]. The mechanical parts such as detector housings, stepping motor and pneumatic drives are produced or integrated by GSI whereas for the software and the electronic devices industrial solutions are preferred. The production of first

THE IH CAVITY FOR HITRAP

C. Kitegi, U. Ratzinger, IAP, University Frankfurt/Main, Germany
S. Minaev, ITEP, Moscow, Russia

Abstract

RFQs are already successfully used to decelerate ions and to match them to ion traps. Within the Heavy Ions TRAP project HITRAP at GSI a combination of an IH drift tube cavity operating at the $H_{11(0)}$ mode and a 4-rod RFQ is proposed to decelerate the 1 µs long heavy ion bunches (up to U^{92+}) from 4 A·MeV to 6 A keV after storage ring extraction. The transition energy from the IH into the RFQ is 0.5AmeV. The operating frequency is 108.408 MHz. The A/q range of the linac is up to 3.

A 4-gap quarter wave resonator working at 108.408MHz provides the micro bunch structure for the IH. The transmission mainly defined by the buncher is about 30%. An alternative 2nd harmonic bunching section, which allows higher transmission and/or smaller longitudinal emittance, will be discussed.

By applying the KONUS dynamics, the 2.7 meter long IH cavity will perform a high efficient deceleration by up 10.5 MV with 200kW rf power. The beam dynamics performed with the LORASR simulation code will be shown. It is aimed to reach an effective shunt impedance around 220MΩ/m for the IH cavity.

IH CAVITY

General Parameters

The HITRAP decelerator will enlarge the variety of decelerated ion beams to Highly Charged Ions up to U^{92+}. The decelerator linac will be installed in the re-injection beam line between ESR and synchrotron SIS. The decelerator is designed for a A/q range up to 3. The HCI are extracted from the ESR at 4 AMeV in a 1 µs long cooled bunch [1]. As for such an A/q range the input energy is too high for an efficient RFQ solution, an IH cavity is proposed to decelerate to an intermediate energy of 0.5 AMeV. A 4-rod RFQ performs the deceleration down to 6AkeV. The chosen intermediate energy allows for a design of an IH tank with one internal lens. Only the IH cavity will be discussed in this paper. The succeeding RFQ will be of the 4-rod type and is designed at IAP as well. The needed repetition time is approximately 10 seconds at a low duty cycle of 0.15%. Intermediate rf pulses may be needed to keep the linac in resonance.

Table1: General IH parameters

	IH LINAC	
	input	output
W [A.MeV]	4	0.5
β	0.0924	0.0328
frequency in MHz	108.408	
duty factor	0.15%	

Beam Dynamics

IH drift tube linacs using the KONUS beam dynamics concept [2] (KOmbinierte NUll grad struktur) are used as injectors for the Alvarez section of UNILAC. The same beam dynamics concept can be applied for beam deceleration.

Within the KONUS scheme particle bunches are decelerated in successive gaps with 180° synchronous phase in order to reduce the transverse defocusing effect. This allows the use of slim drift tubes without any optical element. Consequently the decelerating H mode cavity using the Konus dynamics is composed by:

-One main decelerating section with 180° synchronous phase.

-One quadrupole triplet to focus the beam.

-One short section with positive synchronous phase, typically 215° to focus longitudinally and match the beam.

Due to the rf buncher ahead of the cavity, the micro-bunch is convergent in the first gaps of the IH. To avoid over focusing, which could lead to beam instability, the 145° synchronous phase is used in the first gaps to "defocus" the bunch.

Deceleration of 10.5MV is then achieved within the 2.7m long IH cavity; Figure 2 shows the 98% transverse envelopes in the cavity calculated with LORASR, which is an adequate code to study the KONUS dynamics. As the beam is cooled in the ESR, transverse emittances are very small. The beam radius in the IH tank is less than 4mm.

Figure 3 shows the longitudinal output emittance obtained for an arbitrary reference input emittance. For such emittance the beam dynamics is rather safe as the acceptance of the IH is twice.

The simulations of the matching section were performed in order to match micro bunches into this emittance.

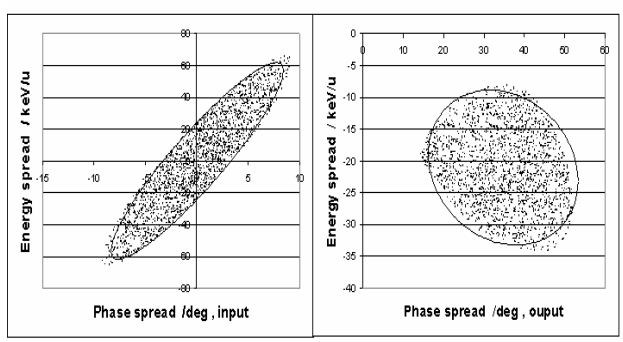

Figure 1: 98% input (left) and output (right) longitudinal emittance.

THE COMPACT 20 MV IH-DTL FOR THE HEIDELBERG THERAPY FACILITY

Y.R. Lu[*,#,§], S. Minaev[*,$], U. Ratzinger[*], B. Schlitt[#], R. Tiede[*]
[*]IAP, Universität Frankfurt/Main, Germany
[#]Gesellschaft für Schwerionenforschung mbH, Darmstadt, Germany
[§]Institute of Heavy Ion Physics, Peking University, P.R.China
[$]Institute of Theoretical and Experimental Physics, Moscow, Russia

Abstract

A clinical facility for cancer therapy using energetic proton and ion beams (C, He and O) is under construction and will be installed at the Radiologische Universitaetsklinik in Heidelberg, Germany, starting in 2005. It consists of two ECR ion sources, a 7 AMeV linac injector and a 6.5 Tm synchrotron to accelerate the ions to final energies of 50-430 AMeV[1-3]. The linac is the combination of a 400 AkeV RFQ and a 20MV IH-DTL operating at 216.8MHz. The accelerator project is coordinated by GSI; IAP is responsible for the Linac cavities in cooperation with GSI. The different RF tuning concepts and tuning results for a 1:2 scaled IH-DTL model cavity are presented. Microwave Studio simulations have been carried out for the model and for the real power cavity. Results from the model measurements and the field simulations agree very well also for the higher order modes. The beam matching from the RFQ to the IH-DTL was optimised. The IH drift tube array was matched with the gap voltage distribution resulting from RF model measurements. Simulated RFQ output particle distributions were used in the final beam dynamics investigations along the IH cavity.

INTRODUCTION

By comparing cancer therapy with proton and carbon beams, one important aspect next to the medical efficiency is the treatment costs per patient. Since 1997 a very compact and efficient 7 AMeV C^{4+} linac has been developed. The status of the whole injector including ECR ion sources, linac, RF power system, and quadruple magnets will be discussed in another paper in this conference [4]. The beam matching from the RFQ to the IH-DTL ,the improved beam dynamics simulations with the software LORASR along the IH cavity as well as the RF tuning of the 1:2 scaled RF model cavity and accompanying simulations with Microwave Studio will be discussed in these proceedings.

KONUS BEAM DYNAMICS

The IH-DTL consists of four KONUS sections with a total of 56 gaps, and with three magnetic quadruple triplets, which are housed in one cavity with 3.77m in length and 0.32m equivalent cavity diameter. The beam dynamics simulations have been optimised with the code LORASR [5] for the beam matching from the RFQ exit to the IH-DTL with new geometry [6] and real particle distributions at the RFQ exit as calculated with the PARMTEQ code. The effective gap voltage distributions and real drift tube parameters are adapted from the results of the cold RF model cavity tuning measurements. RFQ internal buncher[7] effective voltage has been optimised to get normalized emittance growth factors as low as 1.18 in x-x', 1.05 in y-y' and 1.23 in w-z plane, respectively (Figure1). Figure 2 shows IH-DTL output particle distributions at the synchrotron injection point. The exit ellipses contain 95% of the particles. The transversal 98% envelopses up to the stripper foil are shown in Figure 3.

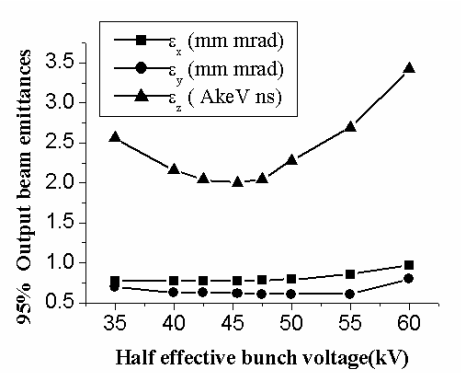

Figure 1: Output emittance at the stripper foil vs. the effective voltage of the RFQ internal 2 gap buncher.

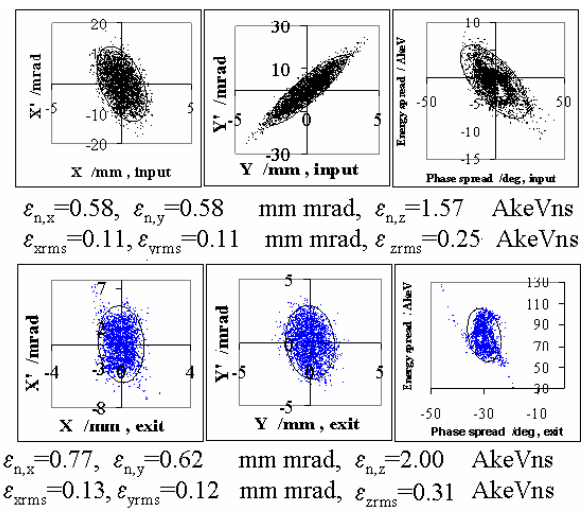

Figure 2: Particle distributions at the RFQ exit and at the stripper foil behind of the IH-DTL ,normalized as well as rms emittance values.

KONUS BEAM DYNAMICS DESIGN OF A 70 mA, 70 MeV PROTON CH-DTL FOR GSI-SIS12*

R. Tiede, G. Clemente, H. Podlech, U. Ratzinger, IAP, University of Frankfurt/Main, Germany,
W. Barth, L. Groening, GSI, Darmstadt, Germany,
Z. Li, IMP, Lanzhou, China, S. Minaev, ITEP, Moscow, Russia

Abstract

The future scientific program at GSI needs a dedicated proton injector into the synchrotron SIS, in order to increase the proton intensity of the existing UNILAC/SIS12 combination by a factor of 70, resulting in $7x10^{12}$ protons in the synchrotron. A compact and efficient 352 MHz RFQ - CH-DTL combination based on novel structure developments for RFQ and DTL was worked out. For DTL's operated in an H-mode like CH-cavities (H210-mode), the shunt impedance is optimized by use of the KONUS beam dynamics. Beam dynamics simulation results of the CH-DTL section, covering the energy range from 3 to 70 MeV, with emphasis on the low energy front end are presented. Optimization aims are the reduction of emittance growth, of beam losses and of capital costs, by making use of the high acceleration gradients and shunt impedance values provided by the Crossbar H-Type (CH) structure. In addition, the beam dynamics design of the overall DTL layout has to be matched to the power limits of the available 352 MHz power klystrons. The aim is to power each cavity by one klystron with a peak rf power of around 1 MW.

DESIGN CRITERIA AND PARAMETERS

KONUS Beam Dynamics and H-Mode Cavities

First investigations on proton beam acceleration with a CH-DTL were presented in ref. [1].

For the proposed GSI Proton Injector the KONUS beam dynamics ("Kombinierte Null Grad Struktur" – Combined 0° Structure [2]), together with the use of H-mode structures ("Crossbar H-Type" - CH) are foreseen for the energy range from 3 to 70 MeV. The advantages of this concept are:

- High accel. gradients (up to 6 MV/m) due to the high shunt impedance of the CH-DTL and the KONUS beam dynamics concept ("slim" drift tubes without integrated quadrupole lenses housed in each multi-cell cavity).
- Simplified construction, maintenance and reduced number of components.
- Reduction of project costs and overall linac size.

Design Parameters

Compared with the initial layout presented in ref. [3] the following modifications were necessary, leading to an updated overall linac design:

- The optimum RFQ-DTL transition energy was investigated and finally fixed at 3 MeV. This opens the option to realize the RFQ as 352 MHz 4 rod-RFQ in one cavity [4].
- The linac output energy has been increased and fixed at 70 MeV.
- The design current has been increased from 50 to 90 mA (safety factor included): for operation a maximum linac output current of 70 mA is specified.
- The operating rf frequency of 352 MHz along the whole linac has been fixed now.

The latter decision was motivated by the manifold offer of rf hardware (power klystrons) at that frequency. The exit energy and beam current were chosen with regard to a 10 – 15 turn injection scheme into the horizontal acceptance (150 π mm mrad) of SIS.

Table 1 summarizes the CH-DTL relevant Proton Linac beam parameters:

Table 1: Basic beam parameters specified for the Proton CH-DTL section

General	
rf frequency	352 MHz
macro pulse length	0.1 ms
rep. rate	5 Hz
macro pulse current at linac exit	90 mA (design current; 70 mA spec. for operation)
RFQ exit	
beam energy	3 MeV
transverse beam emittance (norm.)	1.5 mm mrad
CH-DTL exit	
beam energy	70 MeV
transverse beam emittance (norm.)	2.8 mm mrad
beam momentum spread	$\pm 5x10^{-4}$

Design Criteria and Restrictions

For the design of the 3-70 MeV CH-DTL section some constraints had to be taken into account:

- The choice of the RFQ-DTL transition energy is a trade-off between an adequate maximum output energy of the RFQ and the minimum input energy acceptable for the DTL. Covering a larger energy range by the RFQ reduces the acceleration efficiency and can lead to problems with respect to tank length, flatness and coupling between structure cells. In the DTL short period lengths

*Work supported by the EU (CARE, cont. no. RII3-CT-2003-506395), BMBF, contr. no. 06F134I

DEVELOPMENT OF INTENSE BEAM PROTON LINAC IN CHINA

S.N.Fu[1], X.L.Guan[2], H.F.Ouyang[1], S.C.Zhao[1], B.Q.Cui[2], Z.Y.Guo[3], J.X.Fang[3], S.X.Fang[1]
[1]IHEP, Institute of High Energy Physics, P.O.Box 918, Beijing 100039, China
[2]CIAE, China Institute of Atomic Energy, Beijing 102413, China
[3]IHIP, Institute of Heavy Ion Physics, Peking University, Beijing 100871, China

Abstract

Study on intense beam proton linac was started about four years ago in a national program for the basic research on ADS in China. This ADS program is meant for the future development of the clean nuclear power generation. Another important application of HPPA for Chinese Spallation Neutron Source was also proposed recently in China, and it is now financially supported by Chinese Academy of Sciences. In this paper, the research progress on intense beam proton linac in these two application fields will be outlined including the test result of a high-current ECR proton source, construction status of a 3.5MeV RFQ accelerator, medium-β superconducting cavity test and the design of a DTL linac.

INTRODUCTION

Shortage of electricity supply is becoming a bottleneck for the rapid economy growth in China. However, fossil energy resources in the newly-increased power supply must be reduced for the environment protection (at present, coal contributes about 70% electricity). Nuclear power must play a more important role, especially, in the eastern part of China. So, there is a rapid development of nuclear power plant in China: 25 new nuclear power stations are going to be built within next 15 years. It means the electricity from nuclear power will increase from 3.8% to 9% of the total electricity supply in China.

Accelerator Driven Subcritical system (ADS) is recognized as one of the best options of fission nuclear power source. A basic research program of ADS[1] was lunched in 2000 under the support of the Ministry of Science and Technology, China. In this program, we have studied some key technologies of an intense beam proton linac, including construction of an ECR proton source and a pulsed beam RFQ accelerator. Chinese Academy of Sciences also gave a support to the linac research in the field of medium-β superconducting cavity. Institute of High Energy Physics, China Institute of Atomic Energy and Institute of Heavy Ion Physics of Peking University jointly conduct the researches.Chinese Spallation Neutron Source (CSNS) is a multidiscipline platform, as a complementary to synchrotron radiation (SR) facility. China will soon have 3 SR facilities in the mainland, but no spallation neutron source at all. There is a common sense among Chinese scientists that China should build a spallation neutron source as soon as possible, and it should rank in the world-class but within the limitation of financial capability of China, as a developing country. A preliminary research program for CSNS with a small budget was lunched in 2002 under the support of CAS. Institute of Physics and Institute of High Energy Physics undertook this task. A physics design and R&D prototyping program has been proposed and is now waiting for the ratification of our government. In comparison with ADS, CSNS is a near-term program with relatively mature technology.

In this paper, we will present our research progress in intense beam proton linac, including the test result of a high-current ECR proton source, construction status of a 3.5MeV RFQ accelerator, medium-β superconducting cavity test and the design of a DTL linac.

THE ECR PROTON SOURCE[2]

An ECR proton source and LEBT have been built at CIAE as the injector of the RFQ. Fig.1 shows the source and its major performance parameters. Our great efforts were made on the reliability and stability of the source operation. We have overcome the problems associated with the breakdown of the RF input ceramic window resulted from the electron back strike. The electrodes have been optimized for minimum spark rate. At present a high reliability of 99.9% is achieved during an 120 hours continuous operation.

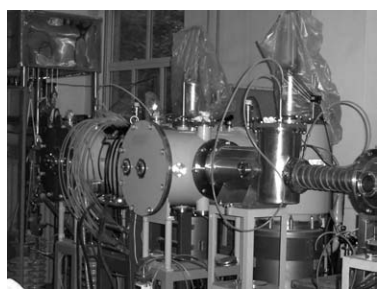

E(KeV)	75
I(mA)	70
f_{RF}(GHz)	2.45
P_{RF}(kw)	1
$E_{n,rms}$ (π mm-mrad)	0.13
H^+ Ratio	80%
Raliability	99%

Figure 1: The ECR source and its major parameters.

DEVELOPMENT OF THE RFQ[3-4]

The major parameters of the RFQ are listed in Table 1. It is separated into two segments and each segment consists of two technological modules. On each module there are 16 tuners distributed on the 4 quadrants for frequency and field tuning. Dipole stabilizer rods on both

TRASCO-RFQ AS INJECTOR FOR THE SPES-1 PROJECT

P. A. Posocco, M. Comunian, E. Fagotti†, A. Pisent,
INFN - Laboratori Nazionali di Legnaro (LNL), Legnaro, Italy
†Università degli Studi di Milano, Milano, Italy

Abstract

The funded first phase of SPES foresees the realization at LNL of a facility able, on one hand, to accelerate a 10 mA protons beam up to 20 MeV for nuclear studies and, on the other hand, to accelerate a 30 mA protons beam up to 5 MeV for BNCT and preliminary ADS studies. In this two-way facility, the TRASCO RFQ will operate in two different current regimes. Moreover a specific MEBT has to be designed able to match the beam to the following superconducting linac and to deliver a beam with the correct characteristics to the neutron production target for the BNCT studies.

INTRODUCTION

The first phase of SPES facility (see Fig. 1) will produce a CW proton beam at 20 MeV 10 mA for nuclear studies and at 5 MeV 30 mA for BNCT (Boron Neutron Capture Therapy) studies [1]. The accelerator chain comprises the proton source TRIPS developed at LNS, a low energy beam transport (LEBT) [2] and the 352 MHz TRASCO RFQ [3], which can handle a beam up to 50 mA of current and 5 MeV of energy. After the RFQ a MEBT is necessary to inject the beam to the following superconducting linac [4] and to switch the line when the BNCT facility is operated.

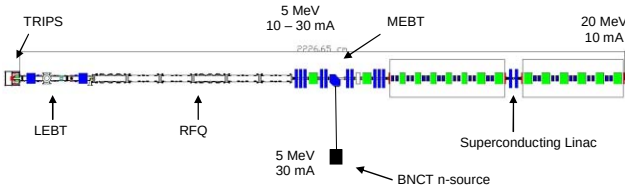

Figure 1: The SPES-1 project.

MEBT DESIGN

The MEBT lattice matches the 10 mA beam from the RFQ through 5 normal-conducting magnetic doublets and 2 longitudinal focusing 3-gap buncher into the first period of the superconducting linac and, at the same time, it should bend the 30 mA beam out of the linac direction for the BNCT studies. As shown in Fig. 2, the line to the BNCT target starts almost from the centre of the MEBT with a 90° degree bend (200 mm radius), for which a free length of 600 mm has been left: this choice is made in order to have a very short MEBT ensuring a high beam quality to the linac and, at the same time, to restrict the interferences between the BNCT facility and the RFQ-linac building.

The lattice of the BNCT line doesn't include any longitudinal focusing system because the BNCT target [5] requires a well defined transverse distribution and prefers a non bunched beam. Differently from the linac case, for which the requirements are on the 6 Twiss parameters, the focusing condition for the BNCT target is described by the transverse spot dimensions and by the condition of a very small dispersion to reduce error on beam position. These requirements are obtained with a simple combination of 4 normal-conducting doublets before the 4.5 m long drift to the collimator of the target (the drift is necessary for the radiation shielding walls and for the remote handling of the neutron converter).

Table 1: MEBT characteristics (line to BNCT from the dipole to the last doublet).

Line to		**Linac** (10 mA)		**BNCT** (30 mA)	
Total length (m)		3.15		5.9	
No. Doublets		5		4	
Length (mm)		100-70-100		150-100-150	
Bore radius (mm)		20		50	
Max env. (mm)		7.5		20	
Max gradient (T/m)		25		10	
		In	*Out*	*In*	*Out*
$\varepsilon_{n,RMS}$	x (mm.mrad)	0.204	0.208	0.217	0.709
	y (mm.mrad)	0.201	0.204	0.212	0.215
*ΔE/E	z (deg.MeV)	0.253	0.240	*0.83%	*1.9%

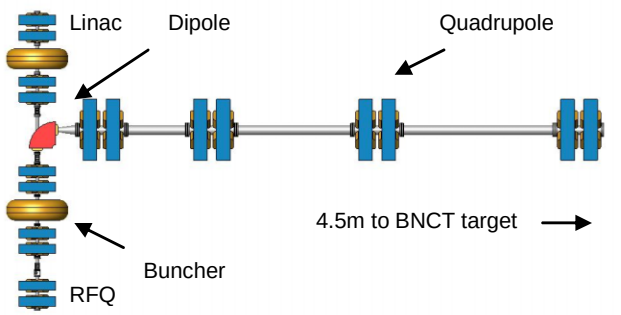

Figure 2: MEBT and BNCT line overview.

THE LINE TO THE LINAC

The choice of having 2 current regimes and the need for a dedicated line to the BNCT facility forces the shared part of the lattice to be flexible: this requirement is obtained with the use of normal conducting doublets (see Tab. 1) with independent power supply for each magnet.

The MEBT can be ideally divided in 2 parts, before and after the dipole, where the second one is specific designed to match the beam into the linac. More in details:

- the first doublet, also required in order to place the RFQ vacuum valve and some diagnostics in the following drift, should reduce the RMS differences

THE TRASCO-SPES RFQ

A. Pisent, M.Comunian, A. Palmieri INFN/LNL, Legnaro, Padova, Italy
E. Fagotti, Università degli Studi di Milano, Milano, Italy - INFN/LNL, Legnaro, Padova, Italy
G.V. Lamanna, CINEL Strumenti Scientifici, Vigonza (PD), Italy
S. Mathot, CERN, Geneva Switzerland

Abstract

A high intensity RFQ is under construction at LNL. Developed within TRASCO research program, the Italian feasibility study an ADS (Accelerator Driven System), it will be employed as the first accelerating element of SPES facility, the ISOL project of LNL. The RFQ operates at the frequency of 352 MHz in CW mode. It delivers a proton current up to 30 mA and consists of six brazed segments whose length is 1.2 m. In this article the results obtained from the construction of a 20 cm "technological model", aimed at testing the construction procedure of the final structure, will be discussed. Finally we will report about the machining and the outcomes obtained after RF testing of the first two segments built up to now.

INTRODUCTION

The high intensity RFQ under construction at LNL, developed within TRASCO project [1] for ADS application, will be used as the front-end of a new generation ISOL facility for the production of exotic beams (SPES project [2]). The 5 MeV beam of the RFQ will also be used for the production of the neutrons necessary for the BNCT (Boron Neutron Capture Therapy); the first studies will be devoted to the application of this therapy for the treatment of skin melanoma. The construction of both this facility and a 20MeV, 10 mA superconducting proton linac (SPES-1) has been funded and is starting. In Table 1 the main RFQ parameters are listed.

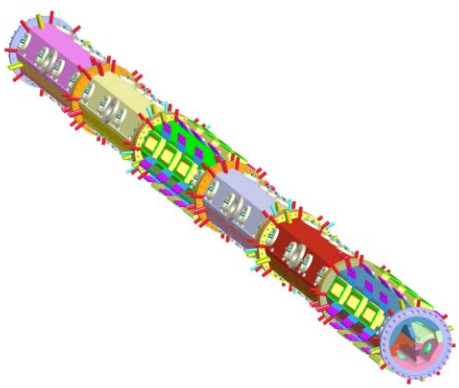

Figure 1: Layout of the TRASCO-SPES RFQ

CONSTRUCTION PROCEDURE

The RFQ consists of three modules 2.4 meters long resonantly coupled via two coupling cells in order to reduce sensitivity to machining errors. Each module consists of two 1.2 meters long segments, which are the basic construction units (Figure 1). Each segment, built in OFE copper, is made of four main parts (A, B, C, and D in Figure 2). The head flanges between segments and the rectangular vacuum flanges are made of SS (LN316). To reduce the number of brazing joints, the longitudinal cooling passages are deep-hole drilled from one side and closed with brazed plugs on the flat surfaces of the RFQ segment (opposite to the coupling or end cells). Moreover, the vacuum grids with their cooling channels are directly machined on the copper bulk.

Table 1: Main RFQ parameters

Energy Range	0.08-5	MeV
Frequency	352.2	MHz
Proton current	30	mA
Duty cycle	100	%
Emittance T RMS in/out	0.20/0.21	mm mrad norm.
Emittance L RMS	0.19	MeV deg
RFQ length	7.13	m (8.4 λ)
Intervane voltage	68	kV (1.8 Kilp.)
Transmission	95	%
Q (80% of Superfish result)	8000	
Beam Loading	0.148	MW
RF Power	0.726	MW

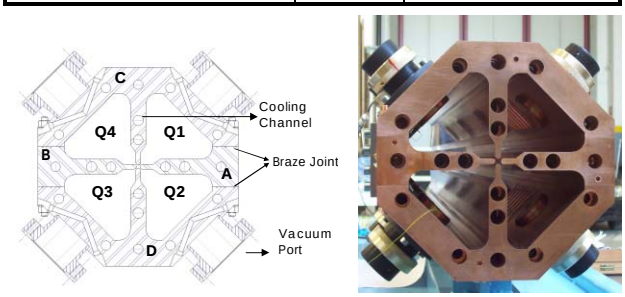

Figure 2: Transverse section of the RFQ with the indication of quadrants and pieces to be brazed.

Two brazing steps occur. In the first the four main parts are brazed in horizontal position in a horizontal vacuum furnace, as well as the OFE plugs for the cooling channels. The brazing alloy is B-Ag68CuPd-807/810 (according to ISO 3677) and the brazing temperature is 820^{O}C. After first brazing, the seat for the head flanges and the flat end surfaces (where the cooling channel plugs are located) are machined. In the second brazing cycle the head SS flanges, the inlet and outlet cooling water SS tubes and the SS flanges for vacuum ports or couplers are brazed in vertical position in a vertical vacuum furnace. The brazing alloy is B-Ag72Cu-780 (according to ISO 3677) and the brazing temperature is 790^{O}C.

DESIGN OF THE SPES-1 LEBT

E. Fagotti*, Universita' degli studi di Milano, Milano, Italy - INFN/LNL, Legnaro, Padova, Italy
M. Comunian, A. Pisent, INFN/LNL, Legnaro, Padova, Italy

Abstract

The low-energy-beam transport (LEBT) system for the SPES-1 accelerator transports the beam at 80 keV and 30 mA from the ion-source TRIPS [1] to the TRASCO RFQ entrance. A second mode of operation corresponding to 10 mA current is also foreseen. The code PARMELA [2] performed these simulations of the beam transport through the LEBT. This code is used to transport H+ and H2+ in the electrostatic fields of the ion-source extraction, in the magnetic fields of both the source and the solenoid lenses and under space charge and neutralization influence.

INTRODUCTION

AXCEL code [3] is used to derive a first estimation of the radius of curvature r_p of the plasma boundary in the ion-source-extraction aperture. Beam is then generated on a spherical cathode with radius r_p and accelerated through the electrostatic fields of the ion source's accelerating column. Then beam goes through the LEBT (see Fig. 1), which has two magnetic solenoids and arrives at RFQ input after passing some collimators and an electrons trap. PARMELA code has been chosen for simulation because it allows transporting three different ion types in the electrostatic and magneto-static fields generated with SUPERFISH code [4]. This is a very interesting feature that allows simulating neutralization of H^+ and H_2^+ beams extracted from TRIPS source.

EXTRACTION AND NEUTRALIZATION

Being a t-code, PARMELA is able to simulate transient effects. A consequence is that simulation starts with no beam at all [5]. This means that a long enough stream of H^+ and H_2^+ ions must be injected to avoid head and tail effects due to the finite longitudinal dimension of the beam as shown in Fig. 2. Moreover time moves faster for H_2^+ ions in order to compensate the lower velocity and minimize simulation time.

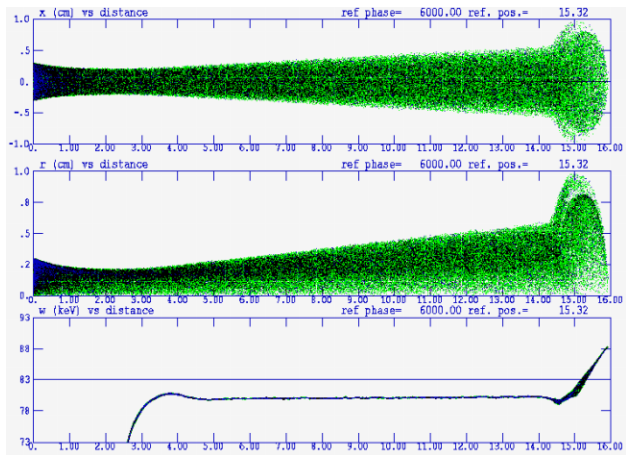

Figure 2: Head effect in beam generation. Cause to this effect, only central part of the beam enters the calculation.

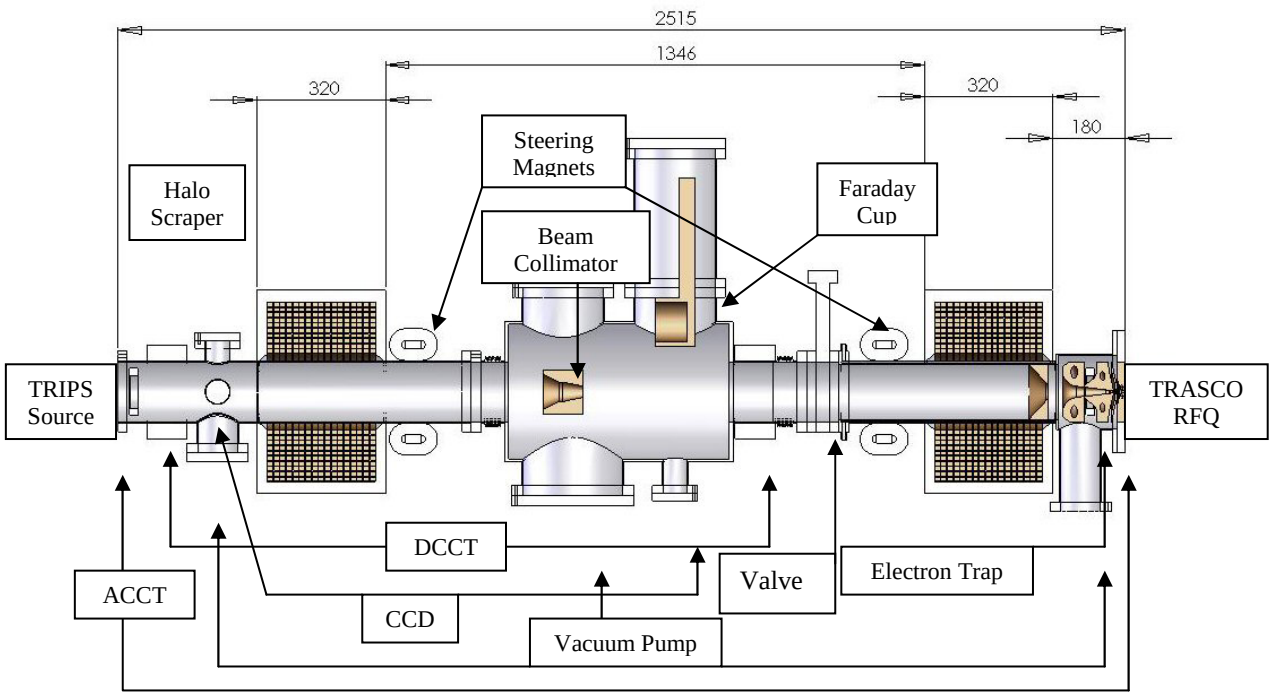

Figure 1: LEBT design. The location of five Bergoz dc and ac current transformers and two video camera diagnostics are indicated.

*Enrico.Fagotti@lnl.infn.it

COLD-MODEL TESTS AND FABRICATION STATUS FOR J-PARC ACS

H. Ao#, H. Akikawa, A. Ueno, K. Hasegawa, Y. Yamazaki, JAERI, Tokai, Ibaraki, 319-1195, Japan

M. Ikegami, S. Noguchi KEK, Tsukuba, Ibaraki, 305-0801, Japan

N. Hayashizaki, TIT, Meguro, Tokyo, 152-8550, Japan

V. Paramonov, INR RAS, Russia

Abstract

The J-PARC (Japan Proton Accelerator Research Complex) LINAC will be commissioned with energy of 181-MeV using 50-keV ion source, 3-MeV RFQ, 50-MeV DTL and 181-MeV SDTL (Separated DTL) on September 2006. It is planed to be upgraded by using a 400-MeV ACS (Annular Coupled Structure), which is a high-beta structure most suitable for the J-PARC, in a few years from the commissioning. The first ACS type cavity, which will be used as the first buncher between the SDTL and the ACS, is under fabrication. Detailed design and tuning procedure of ACS cavities has been studied with RF simulation analysis and cold-model measurements. The results of cold-model measurements, fabrication status, and related development items are described in this paper.

INTRODUCTION

An Annular Coupled Structure (ACS) has been developed for upgrade of a J-PARC linac from 180 MeV to 400 MeV. An operation frequency is 972 MHz.[1]

An ACS-type buncher cavity has been fabricated from Apr.2002. This cavity consists of two 5-cell ACS accelerating cavities and a bridge cavity, which will be installed to a matching section from the SDTL to the ACS as the first cavity of two buncher cavities. It is the first fabrication of an ACS-type cavity for the J-PARC linac. It will be finished at the end of FY2004.

For the study of tuning procedure and RF measurement, we machined some aluminium and OFC intermediate cells that were designed for a periodical symmetry part. RF measurement procedure, tools, and frequency tuning process have been improved with these test cells.

10-cell half-scale aluminum models (beta=0.7114) were also fabricated in FY2003. Intermediate cells and end-cells were tuned for an operating frequency, and then total properties and end-cell effects were measured with this model.

This paper reports a fabrication status and measurement results.

BUNCHER CAVITY

Intermediate Cell

Trial machining and RF measurement for the buncher cavity has been developed. [2,3,4,5]. The frequency has to be adjusted to an operating one by final machining with RF measurement. Because a cavity design based on a 2D and 3D electromagnetic analysis has some errors, and machining process also has certain errors.

In FY2004, we tried final frequency tuning process and measured a frequency correction factor (amount of cutting versus a frequency shift) for frequency tuning regions.

An accelerating mode and a coupling mode have to be considered for the ACS cavity. In the accelerating cell, outer diameter of the cell has a tuning margin, and in the coupling cell, a ledge part has a tuning margin. Figure 1 shows the tuning parts for each cell and the frequency correction factor.

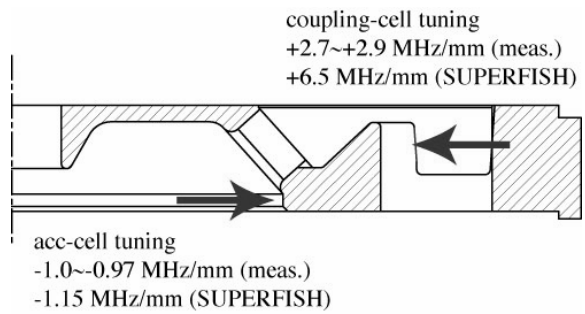

Figure 1: Tuning part and frequency shift.

About the accelerating cell, we consider that expanded volume of an electromagnetic field through a coupling slot makes the frequency shift of the accelerating cell smaller than the SUPERFISH analysis. About the coupling cell, eight vacuum ports cut the tuning ledge part, so that the frequency shift is smaller than the analysis. These results suggest the initial amount of cutting in frequency tuning procedure.

We also added a 5 mm vertical straight at bottom of the ledge part to make it easy for 3D profile measurement after machining.

The test brazing with these cells is planned to confirm a frequency shift before and after brazing.

The cell dimensions of the buncher cavity are almost fixed except for minor corrections required the mechanical restriction. Test cavities for an end-cell and bridge cavity were not fabricated, so that we design and correct dimensions based on a 2D and 3D electromagnetic analysis and the measurement of an half-scale aluminum model.

#aohi@linac.tokai.jaeri.go.jp

PARTICLE DISTRIBUTIONS AT THE EXIT OF THE J-PARC RFQ

Yasuhiro Kondo*, Akira Ueno, JAERI, Tokai, Ibaraki 319-1195, Japan
Masanori Ikegami, Kiyoshi Ikegami, KEK, Tsukuba, Ibaraki 305-0801, Japan

Abstract

A 3.115m long, 324MHz, 3MeV radio-frequency quadrupole (RFQ) linac is used as the first RF accelerator of the J-PARC linac. We have performed RFQ simulations to provide a particle distribution for an end-to-end (from the RFQ entrance to the injection point of the rapid cycling synchrotron (RCS)) simulation of the J-PARC linac. Two simulation codes, PARMTEQM and TOUTATIS are used for the RFQ simulations. The simulated emittances show good agreements with the ones measured at the exit of the medium energy beam transport (MEBT).

INTRODUCTION

Beam characteristics of the J-PARC linac are being discussed in detail by performing the end-to-end simulation, as described in separate papers [1][2][3]. The results of the simulation strongly depend on the initial particle distribution, therefore, "realistic" distribution should be adopted. The commissioning of the front-end part (from an ion source(IS) to the MEBT) of the J-PARC linac was done at KEK by February 2003 [4][5]. In this paper, we perform the RFQ simulations using a distribution based on measurement at the low energy beam transport (LEBT). Obtained distributions at the RFQ exit are transported to the MEBT exit. Simulation results are compared with the measurement at the MEBT exit to confirm the validity as an initial distribution for the J-PARC-linac end-to-end simulation.

PARTICLE DISTRIBUTION AT THE RFQ ENTRANCE

We assume following particle distribution at the RFQ entrance; A Gaussian distribution in the x-x' and y-y' planes (truncated at 4σ), the energy is 50keV with no spread and the phase is uniform. The width of the Gaussian is decided based on the measured distribution obtained with emittance monitors at the LEBT. Figure1 shows the measured distribution at the LEBT and the distribution used for the RFQ simulations. Since the LEBT emittance monitors are located between two solenoid magnets of the LEBT, neutral particles, such as H^0, are included in the measurement. Therefore, we regard the tails of the measured emittances as a background. The injection beam parameters used for the RFQ simulations are summarized in Table 1. The beam current is a measured value at the LEBT.

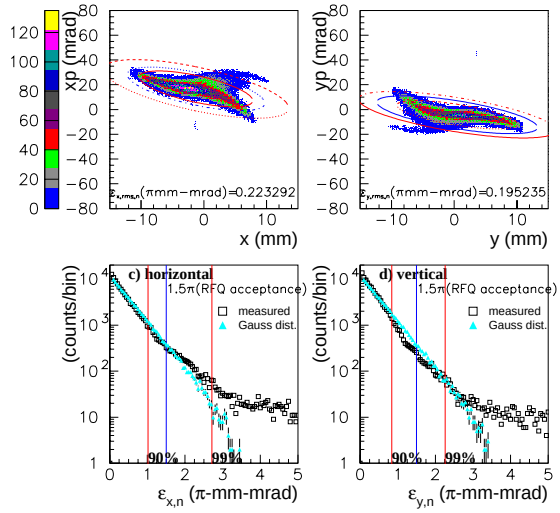

Figure 1: Measured emittances of the LEBT. The left-top and right-top show the phase space plots in the x-x' and y-y' planes, respectively. The ellipses are 90%, 1.5π mm·mrad (design acceptance of the RFQ) and 99% emittances. The bottom figures represent the beam current in the slices of the ellipses. The beam current is normalized to 100000. Open squares show the experimental result and closed triangles represent the distribution used for the simulation.

Table 1: Injection beam parameters used for the RFQ simulations

Parameters	values
Beam current	32 mA
Number of particles	100000
α_t	2.23
β_t	0.112 mm/mrad
ϵ_t(rms, normalized)	0.217π mm·mrad
Distribution(x-x', y-y')	Gaussian (truncated at 4 σ)
(phase)	Uniform
(energy)	50keV, no spread

SIMULATION RESULTS AT THE RFQ EXIT

We use two simulation codes, PARMTEQM[6] and TOUTATIS[7] for the RFQ simulations. Table 2 shows emittances and Twiss parameters at the RFQ exit obtained with use of the distribution described in the previous section. The rms emittances are not significantly different be-

* yasuhiro.kondo@j-parc.jp

DESIGN OF THE R.T. CH-CAVITY AND PERSPECTIVES FOR A NEW GSI PROTON LINAC*

Zhihui Li, IMP, Lanzhou, China
R. Tiede, U. Ratzinger, H. Podlech, G.Clemente, IAP, Universitaet Frankfurt/Main, Germany
K.Dermati, Winfried Barth, Lars Groening, GSI, Darmstadt, Germany

Abstract

The CH-Structure has been studied at the IAP Frankfurt and at GSI for several years. Compared with the IH structure (110-mode), the CH structure (210-mode) can operate at higher frequencies (150 - 700 MHz) and can accelerate ions to higher energies (up to 150 AMeV). Detailed Microwave Studio (MWS) simulations were performed for this structure. Since a multi-gap cavity can be approximated as a quasi-periodic structure, it is possible to analyse one βλ/2-cell at an energy corresponding to the cavity centre. A reduced copper conductivity of 85% was adopted in effective shunt impedance calculations. Geometry variations with respect to RF frequency and shunt impedance can be performed rapidly by that method in the first stage of optimization. Using the transit time factor calculated by the beam dynamics simulation code LORASR, effective shunt impedances from 100 MΩ/m down to 45 MΩ/m were obtained for the energy range from 6MeV to 66 MeV by this method. The RF frequency was 352 MHz. A systematic analysis of the influence of the cell number in long CH-cavities on the effective shunt impedance is presented. Actually, a 70 MeV, 70 mA, 352 MHz proton linac design for GSI Darmstadt is developed. About 12 CH-cavities will cover the energy range from 3 MeV up to the final energy, the DTL total length will be around 22m.

INTRODUCTION

The Interdigital H-type (IH) structure is well known for its high shunt impedance at low beta values. It is successfully used as front part for ion linacs like the Unilac at GSI [1] or the CERN Linac3 [2] and for rare isotope acceleration. Since a couple of years, a new type of H-structure was proposed and studied at IAP, Frankfurt and GSI, Darmstadt, that is the Cross Bar H-type (CH) structure. Compared with the IH-structure, the CH-structure is providing new features. Working in the H_{21} mode, the transverse cavity dimensions are significantly larger than that of the IH-cavity at a given frequency and velocity profile, thus it can work at higher frequencies up to around 700 MHz. This allows to close the velocity gap with respect to attractive structures at the low energy end of Coupled Cavity Linacs CCL. It can be designed for operation at about 350 MHz in the first section and at 700 MHz in the high-energy section up to about 150 AMeV. Furthermore, the CH cavity exceeds by far the mechanical rigidity of the IH cavity. This opens the possibility to develop superconducting multi-cell cavities as well [3].
A set of formulas based on a simple field model was derived for H-type structures to describe the main RF parameters as a function of the geometrical dimensions. A normal conducting 70 MeV, 70 mA proton injector based on a 3 Mev RFQ followed by a CH-DTL is designed for the future FAIR facility at GSI. The beam dynamics [4] and the cavity design are studied in parallel. The construction of a model cavity will start this year.

In the following sections we present the results got from cavity simulations for room temperature CH structures, the emphasis is put on the effective shunt impedance.

*Work supported by the GSI, BMBF, contr. no. 06F134I and EU contr. nr. RII3-CT-2003-506395

SIMULATION METHOD

In general a high level of accuracy is needed in the simulation of multi-cell cavities to achieve relevant results and in particular with respect to the cell voltage distribution. However, many important aspects can be investigated already with single cell calculations, which are very fast and reliable. In case of a quasi-periodic H-structure the following strategy was applied:

- For every cavity a single cell optimisation with respect to shunt impedance was performed for the relevant beam velocity at the tank mid plane.
- The capabilities of these geometries with respect to mechanical stability, cooling etc. were checked.
- Simulation of multi-cell cavities with steadily increasing cell numbers. Investigation the dependence of the main parameters on the cell number.

GEOMETRY OPTIMIZATION

The geometry optimization has been done for a sequence of discrete energies from 3 MeV up to 70 MeV. Figure 1(a) schematically shows the 50 MeV cavity cell used in MWS simulations. Figure 1(b) shows a design alternative with a drift tube geometry relevant for tank 1. The main difference is the central ring around the drift tube similar to the superconducting version [3].

For the real multi-cell cavity, the transverse geometries are kept unchanged, but in longitudinal direction, the period length will change with the velocity profile of the beam. In the investigation of the dependence of the RF parameters on the cell number, however, a constant periodic length along the cavity is used. The zero-mode can be achieved by a simple end cell geometry like shown in fig. 2.

In order to test the validity of the cell-cavity approximation, we calculate the CERN Linac3, tank3 that

THE PRE-INJECTOR LINAC FOR THE DIAMOND LIGHT SOURCE

C. Christou*, V. Kempson, Diamond Light Source, Rutherford Appleton Laboratory, Chilton, Didcot, Oxfordshire OX11 0QX, UK
K. Dunkel, C. Piel, Accel Instruments GmbH, Bergisch-Gladbach, Germany.

Abstract

The Diamond Light Source (DLS) is a new medium-energy high brightness synchrotron light facility which is under construction on the Rutherford Appleton Laboratory site in the U.K [1]. The accelerator facility can be divided into three major components; a 3 GeV 561 m circumference storage ring, a 158.4 m circumference full-energy booster synchrotron and a 100 MeV pre-injector linac. This paper describes the linac design and plans for operation.

LINAC PARAMETERS

The DLS linac generates an electron beam suitable for injection through the linac-to-booster transfer line (LTB) into the booster synchrotron. The Diamond master oscillator frequency is 499.654 MHz† and linac operation is synchronised to this at 2.997924 GHz‡. Two modes of operation are planned; short-pulse mode, in which a single electron bunch is injected into one booster RF bucket, and long-pulse mode in which a train of single bunches is injected into the booster at an operational frequency of 500 MHz.

Table 1: Linac parameters

Parameter	Short-pulse mode	Long-pulse mode
Energy	100 MeV	100 MeV
Pulse-to-pulse energy variation	0.25% rms	0.25% rms
Relative energy spread	0.25% rms, ±1.5% full spread	0.25% rms, ±1.5% full spread
Repetition rate	Single shot to 5 Hz	Single shot to 5 Hz
Normalised emittance (1σ)	50 π mm mrad in each transverse plane	50 π mm mrad in each transverse plane
Pulse duration	1 ns	300 ns to 1000 ns
Output charge	50 pC to 1.5 nC	50 pC to 3 nC
Pulse purity	1% of total charge	-

The linac will be capable of performing continuous top-up injection in both short-pulse and long-pulse modes. During top-up, 1-5 Hz repetitive operation in both modes will be maintained for 1-10 seconds, and repeated every 1-5 minutes, or single pulses (or pulse trains in long-pulse mode) will be repeated every 10-300 seconds.

LINAC COMPONENTS

The linac is supplied by ACCEL Instruments GmbH under a turn-key contract, with Diamond Light Source Ltd. providing linac beam diagnostics, control system hardware and standard vacuum components. The design chosen for the DLS linac is very similar to that operating at the Swiss Light Source (SLS) [2, 3], also supplied by ACCEL Instruments.

Electron gun

The electron gun assembly contains an EIMAC YU 171 thermionic dispenser cathode with integrated heater and grid. Cathode lifetime is estimated to be several thousand hours. The gun pulser contains two independent driving circuits, a 1 ns fwhm pulser driving the cathode for short-pulse operation, and a 500 MHz sine-wave driver modulating the cathode. Separation of the two driving circuits avoids the excitation of the cathode-grid resonance by the 500 MHz Fourier component of the short-pulse waveform. The electron gun is maintained at -90 kV relative to earth.

Bunching system

The linac buncher will consist of the following components:

- Subharmonic pre-buncher (SHPB): one copper single-cell 500 MHz standing-wave cavity
- Primary bunching unit (PBU): one copper four-cell constant-impedance travelling-wave structure operating in 2π/3 mode at 3 GHz
- Final bunching unit (FBU): one copper sixteen-cell constant-impedance travelling wave structure operating in 8π/9 mode at 3 GHz

The SHPB acts to velocity modulate the non-relativistic electron beam emerging from the gun, compressing the pulse before it passes into the PBU. In the PBU, the beam is given a 3 GHz S-band structure, and then this S-band beam is accelerated to a relativistic level in the FBU, and the S-band bunches are further compressed. Phase velocities in the bunching units are 0.6 c in the PBU and 0.95 c in the FBU.

A laminar flow tent will be used for SHPB installation to minimise the possibility of multipactoring during linac operation. Use of a driving amplifier with a higher duty

*chris.christou@diamond.ac.uk
†Rounded to 500 MHz for the remainder of this document
‡Rounded to 3 GHz for the remainder of this document

USING A SOLID STATE SWITCH FOR A 60KV BOUNCER TO CONTROL ENERGY SPREAD DURING THE BEAM PULSE *

L. Donley, J.C. Dooling, G.E. McMichael and V. F. Stipp, ANL, Argonne, Illinois, 60439

Abstract

The beam injected into the IPNS Linac is from a column utilizing a Cockcroft-Walton voltage source. The accelerating column consists of a single high gradient gap. To lessen the likelihood of gap voltage breakdown we pulse ("bounce") the column voltage up during the beam pulse allowing the column DC voltage to be lower. The accelerating voltage is supplied through a 5 MΩ resistor and has only small capacitance to hold the voltage constant during the beam pulse. A capacitor is connected between the high voltage end of the column and the bouncer pulse generator. The bouncer pulse increases the column voltage to the proper level just microseconds before the beam pulse. A slope on the top of the bouncer pulse allows for correction to be added, compensating for the voltage droop that results from beam loading. The bouncer that has served this purpose in the past utilized a tube amplifier. In searching for a suitable replacement system it was decided that the system should be able to deliver a 60 kV pulse and the slope on the top of the pulse could be controlled by an RC rise. A solid state switch was purchased for this application. Switch protection and other design decisions will be discussed

INTRODUCTION

The Intense pulsed Neutron Source (IPNS) injector linac[1] delivers 70 to 80 microsecond long pulses of 50 MeV H- particles to the 450 MeV synchrotron. The H- ion source is capable of delivering about 1.6×10^{13} particles per pulse at a 30 Hz rate. The linac is designed for a 750 keV input beam, but can operate at a reduced efficiency with input beams as low as 700 keV[2].

Column arc rate is acceptable if the DC voltage is below 700 kV. Our present operating energy is 730 keV out of the column. The DC voltage is operated at 690 kV, the extractor is 20 kV and the bouncer makes up the remaining 20 kV. The bouncer coupling network couples 50% of the supplied pulse so this requires that the bouncer supply a 40 kV pulse to the coupling network. The old bouncer meets these requirements but the tubes are no longer manufactured. Recent plans to upgrade the synchrotron by adding a third rf cavity may require more charge per pulse out of the linac, leading to a need to improve linac transmission efficiency. Furthermore, calculations indicate that much better control of linac output longitudinal emittance is possible if injection is at the design 750 keV. This could improve capture and lower losses in the synchrotron independent of the new rf cavity. Column redesign was a possibility but had no guarantee of success and would have required a long downtime for the modifications and commissioning. However improving the capability of the bouncer added little additional risk and could be incrementally tested during our regular machine research periods. To replace our present bouncer, the new bouncer would need to run at 40 kV; to meet future plans a 60kV bouncer and 700kV DC will provide a 750keV beam from the column.

Ideally, the bouncer should rapidly increase and decrease the column voltage in time for the beam pulse, and should compensate for the beam loading voltage droop of the Cockcroft-Walton during the pulse. This led to the following specifications:

1 Operate at 30Hz
2 Output up to 60 kV
3 Rise time ≈100 μs
4 Top slope of 5 0 V/μs
5 Top width of 90 μs
6 Fall time ≈ 1 ms
7 Survive in an environment where 700 kV pulses at several amperes are frequently generated.

DESIGN

Recent advances in semiconductor technology have made available fast high-voltage solid-state switches that can be cascaded to provide current and voltage capabilities unreachable only a few years ago. We now use these devices for our 20 kV extractor as well as for the bouncer. Figure 1 shows the 60 kV switch that we purchased from Diversified Technologies, Inc.

Figure 1: 60Kv 20A-50A switch as installed at the base of the IPNS ion source.

This switch has 6 plates assembled on a fiberglass channel and a control box with leads ready for connection

*This work is supported by the US DOE under contract no. W-31-109-ENG-38.

THE LEBRA 125 MEV ELECTRON LINAC FOR FEL AND PXR GENERATION

K.Hayakawa#, T.Tanaka, Y.Hayakawa, K.Yokoyama*, I.Sato,
LEBRA, Nihon University, Funabashi, Japan
K.Kanno, K.Nakao, K.Ishiwata and T.Sakai,
Graduate School of Science and Technology Nihon University, Funabashi, Japan

Abstract

A 125MeV electron linac has been constructed at Laboratory for Electron Beam Research and Application (LEBRA) in Nihon University for Free Electron Laser (FEL) and Parametric X-ray (PXR)[1] generation. Electron bunches of 3 - 4 psec width formed at the injector are compressed to within 1 psec during passing through the magnetic bunching system. Peak current of the electron beam injected to the FEL system is expected to be about 50 A. FEL lasing has been achieved at the wavelength range from 0.9 to 6 μm. Estimated peak power of the extracted FEL light pulse is about 4 MW. Applied researches using the FEL started last autumn. Preliminary experiment for the PXR generation has been proceeded. First light of the PXR is observed at April in this year.

INTRODUCTION

The specifications of the electron linac are listed in Table 1. The beam injection system and the regular accelerator sections of the linac were moved from KEK Photon Factory positron injector linac as a part of collaboration on development of a high quality electron linac. Schematic layout of the accelerating structures and RF system are shown in Fig.1.

FEL beam line has been installed to feed near infrared laser for application users [2]. To improve FEL gain, magnetic bunch compressor has been adopted.

To generate monochromatic X-ray, PXR beam line has been installed next to FEL beam line. Several interesting results are obtained.

LINAC

The electron linac has a conventional configuration. It consists of a DC electron gun with a dispenser cathode, a prebuncher which is a 7-cell travelling wave structure, a buncher which is a 21-cell travelling wave structure and three 4-m long normal accelerator sections.

Table 1:Specifications for LEBRA 125MeV linac.

Accelerating rf frequency	2856	MHz
Klystron peak output rf Power	30	MW
Number of klystrons	2	
Electron energy	30~125	MeV
Energy spread (FWHM)	0.5~1	%
Macropulse beam current	200	mA
Macropulse duration	20	μsec
Repletion rate	12.5	Hz

RF System

Two klystrons feed rf power of approximately 20MW peak and 20μsec pulse duration each to accelerating structures. Phase of the rf fed to each component is controlled independently.

Output RF phase of the solid state RF amplifier and the klystron drifts with a room temperature variation. Since RF amplifier is operated in pulse mode, RF phase change

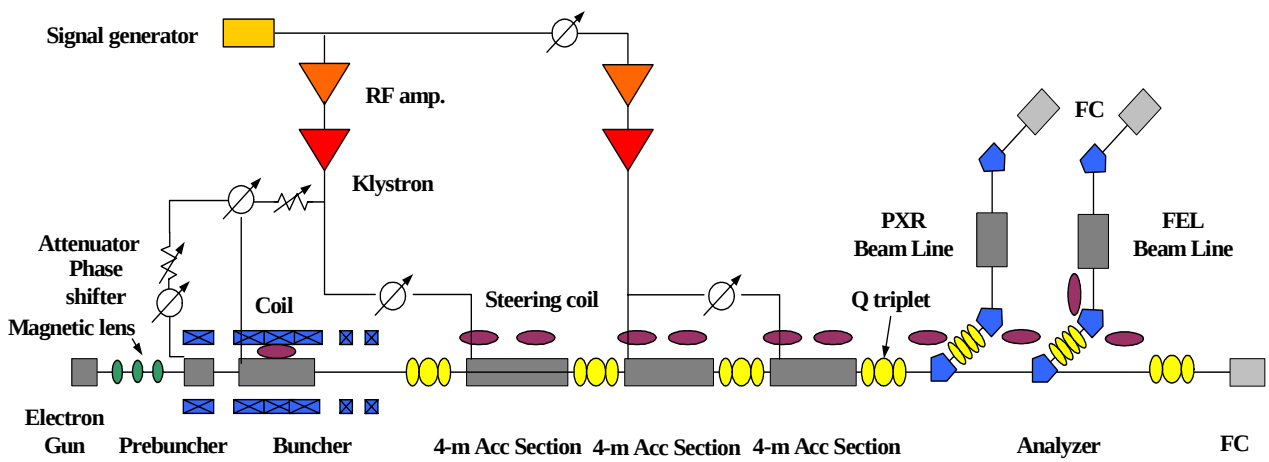

Figure1: Schematic layout of the LEBRA linac and the FEL and the PXR beam line.

#hayakawa@lebra.nihon-u.ac.jp
*Present affiliation: KEK, Tsukuba, Japan

ERLP GUN COMMISSIONING BEAMLINE DESIGN

D.J. Holder, C. Gerth, F.E. Hannon and R.J. Smith,

ASTeC, Daresbury Laboratory, Warrington, WA4 4AD, UK

Abstract

The 4GLS project is a novel next-generation solution for a UK national light source. It is based on an energy recovery linac (ERL) operating at high average beam currents up to 100mA and with compression schemes producing pulses in the 10-100 fs range. This challenging accelerator technology, new to Europe, necessitates a significant R&D programme and a major part of this is a low-energy prototype, the ERLP, which is currently under construction at Daresbury Laboratory, in the north-west of England. The first components of ERLP to be built will be the DC photocathode gun and low-energy beam transport and diagnostics. The gun will initially be operated with a diagnostic beamline in order to measure the properties of the high-brightness beams generated as fully as possible. This will allow comparison of its performance with the results of multi-particle tracking codes, prior to its integration into the ERLP machine. The diagnostic beamline will include diagnostics for measuring the transverse and longitudinal properties of the electron beam.

This paper will describe the design of this diagnostic beamline and demonstrate through simulation, the expected characteristics and performance achievable from this system.

INTRODUCTION

The ERLP uses a replica of the DC photocathode gun used in the IR Demo and Upgrade FELs at Thomas Jefferson National Accelerator Facility (J-Lab), which has already been producing high-brightness, high average-current electron beams [1]. The gun is currently being built at Daresbury Laboratory, and will be operated with a negative affinity GaAs photocathode which will be illuminated with a mode-locked Nd:YVO_4 laser with an oscillator frequency of 81.25MHz. The 350keV electron beam from the gun is transported via a normal conducting buncher cavity and accelerated by a superconducting booster to 8.35 MeV before entering the recirculating section. The fundamental frequency of both the buncher and the booster is 1.3GHz, and are based on ELBE designs [2]. A second superconducting linac module accelerates the beam to 35 MeV before it is then redirected back to the linac (for energy recovery) by the return transport line. The return path incorporates a FEL based on a permanent magnet wiggler (previously used in the Jefferson Laboratory IR-Demo machine) and two dipole chicanes. The layout of ERLP is illustrated in Fig. 1.

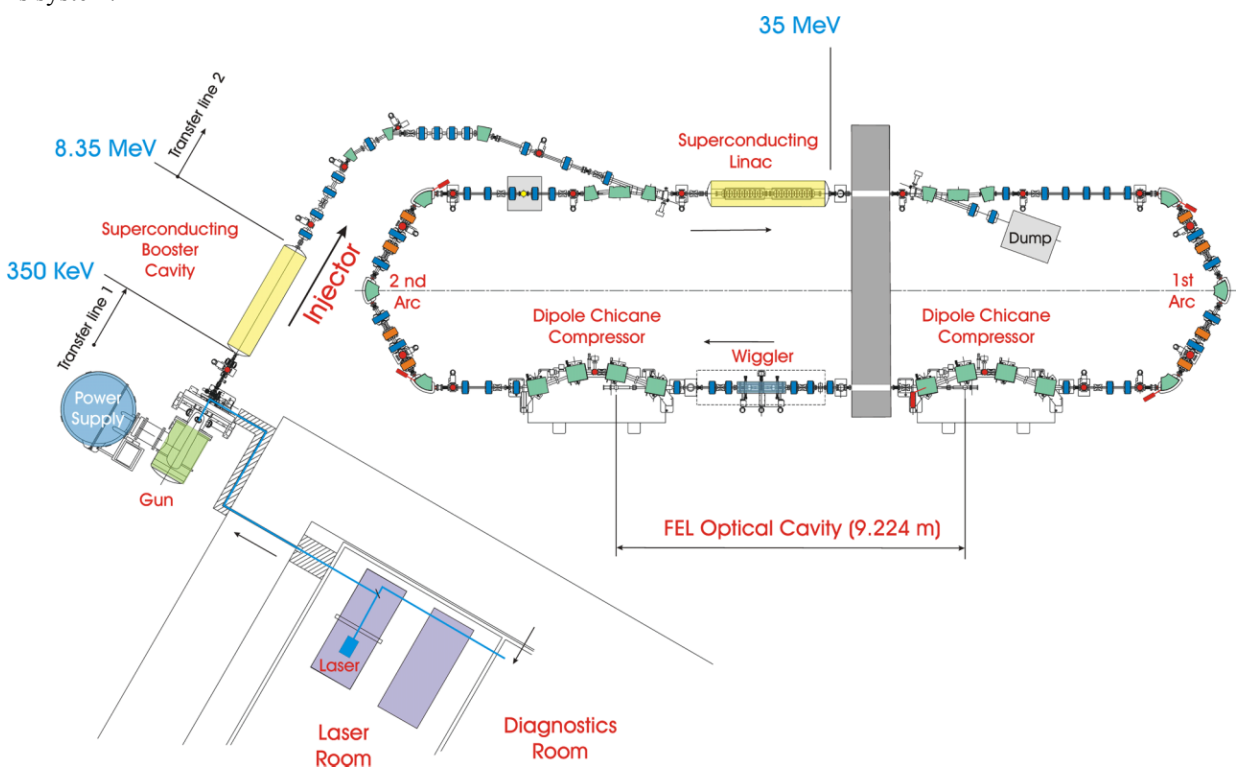

Figure 1: ERLP Layout.

COMMISSIONING OF A 6 MEV X-BAND SW ACCELERATING GUIDE

Qingxiu Jin, Dechun Tong, Yuzheng Lin, Xiang Sun, Xaokui Tao, Jingqing Sun, Xiuming Duan
Department of Engineering Physics, Tsinghua University Beijing 100084, P.R.China
Bingyi Chen, Baoyu Sun, Yang Zou, Yaozeng Li,
Beijing Institute of Electronics & Vacuum Technology, Beijing 100016, P.R.China

Abstract

A 6 MeV, X-band on axis-coupled SW electron linear accelerating guide was developed in Accelerator Laboratory of Tsinghua University. It can be suitable for portable radiotherapy and radiography. The design, manufacture and high power test of the guide are given in this paper.

The length of the guide is 47cm long. It includes a 38cm long accelerating structure, a Pierce electron gun and a target. A 1.5MW pulsed magnetron at 9300MHz is served as its RF power source.

This paper presents the design performance characteristics of the guide and the results of the high-power tests.

INTRODUCTION

New generation portable electron linear accelerator requires small size, less weight and reliable. X-band electron linac can meet these requirements. In order to reduce side and weight of accelerator, in general, magnetron is adopted as microwave power source for X-band linac. The X-band accelerating structure has been studying by Tsinghua University since 1990. For developing X-band linac, we pushed Beijing Institute of Electron & Vacuum Technology to develop a 1MW, X-band magnetron. Using the magnetron, as RF power source a 2.5MeV X-band SW linac was made and successfully was applied to the large container inspection system produced by NUCTECH Company Limited in 1998. For the need of new radiotherapy techniques and radiography, a 6MeV, X-band on axis-coupled SW accelerating guide which operated in the $\pi/2$ mode has been developed by Accelerator Laboratory of Tsinghua University. Using a 1.5MW X-band magnetron was supplied by E2V Technologies Limited, England, the guide of the high-power test has been completed.

GENERAL DESCRIPTION

The geometry of the accelerating structure is a 38cm long, which consists of 49 cavities concluding 9 cavities of buncher. Main parameters of accelerating structure are as following the beam energy being 6MeV, while the pulse beam currents being 50mA.

The microwave power source is an X-band 1.5MW magnetron at 9.3GHz.

The accelerating structure can be used in two modes: electron and X-ray generation. To obtain small size and less weight of the structure, the phase-focusing technique was used without any external magnetic focusing device. As a result, the beam spot size of the accelerating structure is less than 1.5mm in diameters. The accelerating structure characteristics are listed in table 1[1].

Table 1: Accelerating Structure parameter Characteristics

Length	38cm
Beam Energy	6MeV
Beam Current Peak	50mA
Spot Size	<1.5mm
Frequency	9300MHz
RF Peak Power	1.5MW
Input Coupling	1.36
Shunt Impedance	143M Ω /m
Injection Voltage	~ 15KV
Q_0	9000
Q_L	6800
Coupling coefficient K	22%

Figure 1 shows a photograph of the 6MeV SW accelerating guide after brazing. Due to excellence brazing technology, it did not need further tuning after brazing.

Figure 1: The accelerating guide after brazing.

Figure 2: MG6005 magnetron.

A STUDY OF HIGHER-BAND DIPOLE WAKEFIELDS IN X-BAND ACCELERATING STRUCTURES FOR THE G/NLC

R.M. Jones†, SLAC, Stanford, CA 94309, USA

Abstract

The X-band linacs for the G/NLC (Global/Next Linear Collider) [1] have evolved from the DDS (Damped Detuned Structure) [2] series. The present accelerating structures are 60 cm in length and incorporate damping and detuning of the dipole modes which comprise the wakefield. In order to adequately damp the wakefield, frequencies of adjacent structures are interleaved. Limited analysis has been done previously on the higher order dipole bands. Here, we calculate the contribution of higher order bands of interleaved structures to the wakefield. Beam dynamics issues are also studied.

INTRODUCTION

In the operation of the X-band linacs of the G/NLC, wakefields left behind a train of charged bunches can disrupt particles within bunches and can cause severe emittance dilution. For this reason the wakefield is damped by detuning the cell frequencies and by coupling out a portion of the wake to four manifolds that surround the accelerator structure [3].

All previous analyses of the interleaved wakefields for the G/NLC accelerating structures have been exclusively concerned with the 1st dipole band [4]. Herein, this is extended to higher order bands using a mode matching code *Smart2D* [5]. This is applied to the accelerating structure H60VG3 which consists of 55 cells and has an initial fundamental group velocity of 0.03c. Prior to applying the mode matching method we require the geometrical parameters of each cell. The method used to obtain the cell geometry is discussed in [6].

The detailed geometry of the cells is not taken into account with the mode matching method (the curvature of the irises for example is approximated by sharp transitions). However, previous analysis [7] of higher order modes has indicated that making these approximations in the geometry have a small effect on the synchronous frequencies and kick factors [8].

The following section presents the results of calculations on the dipole wakefield for interleaved and non-interleaved accelerating structures. Beam dynamics issues are discussed in the final main section.

TRANSVERSE WAKEFIELDS

Single Structure Wakefield

Smart2D is used to calculate the beam impedance of H60VG3 and the results are presented in Fig. 1. The 1st band is the dominant one. Significant impedances are also located in the 3rd and 6th bands. The kick factor is calculated from the beam impedance by the expanding the impedance into a summation of Lorentzian functions over all modes. A single Lorentzian for the nth mode is:

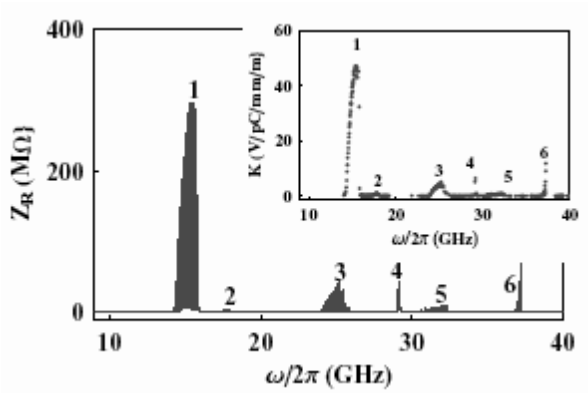

Figure 1: Real part of the beam impedance (Z_R). Kick factors (K) versus synchronous frequencies are shown inset. The approximate band locations are numbered.

$$L_n(\omega) = \frac{2Q_n}{\pi\omega_n}\frac{K_n}{1+4Q_n^2\left(\omega/\omega_n - 1\right)^2}. \qquad (1)$$

Here $\omega_n/2\pi$ is the resonant frequency of a mode with a quality factor Q_n and loss factor $K_n = \int_{-\infty}^{\infty} L(\omega)\,d\omega$. The kick factor is given in terms of the loss factor by $K_n = K_n c/\omega_n r_{off}^2 P$, where P is the period of a cell, and r_{off} the offset of the particle from the axis. Kick factors that result from this fitting procedure are shown inset to Fig. 1. The envelope of the long-range transverse wakefield is calculated from the absolute value of the modal sum:

$$\hat{W}(s) = 2\left|\sum_{n=1}^{N} K_n e^{i\omega_n s/c} e^{-\omega_n s/2Q_n c}\right| \qquad (2)$$

Various components of this wakefield are illustrated in Fig 2. We impose a Q of 700 for the first dipole band and 4000 for all subsequent bands. The optimized first-band wake is also shown in Fig 2 A (for the sake of clarity the wake at the location of the bunch is not shown in this case). This wake has been calculated with the spectral function method [9] which directly incorporates manifold-cell coupling (eliminating the need for an *a posteriori* imposition of a damping Q). Up until the first 20 m or so both wakes are quantitatively similar. However, the 1st band wake calculated with *Smart2D* is significantly larger for the 1st trailing bunch where it is more than 2 V/pC/mm/m. For both calculations in Fig. 2 A the wakefield is larger than 1 V/pC/mm/m in the neighborhood of 10 m and this will readily drive the beam into an unstable BBU mode [10]. In order to prevent this we interleave the frequencies of neighboring accelerator structures.

† Supported by the Department of Energy, grant number DE-AC03-76SF00515

RHIC Electron Cooler *

J. Kewisch, I. Ben-Zvi, X.Y. Chang, V. Litvinenko, C. Montag,
R. Calaga, A. Jain, V. Yakimenko,
Brookhaven National Laboratory, Upton, NY 11973, USA

Abstract

Electron cooling has been applied in many accelerators. All of them operate at low energies where cooling times are short. Electron cooling is now considered for RHIC where gold ions are stored at 100 GeV/u. The corresponding electron energy is 55 MeV. This energy cannot be reached with a DC source like a Fermilab's pelletron. The cooling time is proportional to the square of the energy. In order to have a cooling time of of less than one hour it is necessary to maintain a transverse normalized emittance of 50 mm mrad and an energy spread with a charge of 20 nC per bunch. Such beam quality cannot be achieved with a storage ring. Only a Photocathode Energy Recovery LINAC (PERL) promises success [1].

A special super-conducting cavity was developed for the RHIC electron cooler. It is optimized for high current operation and uses ferrite beam pipes outside the cryostat for higher order mode damping. First simulations with the TBBU computer code [2] show a beam breakup threshold of 3 Amperes.

A strong longitudinal field in the cooling section enhances the cooling process. A solenoid magnet with a field of 1Tesla and a field error of less than is being developed. For a minimum transverse temperature inside the solenoid it is necessary to have a "magnetized beam", i.e. a beam from a cathode immersed in a longitudinal magnetic field. The usual emittance compensation scheme needed to be adapted so that the magnetization does not lead to strong emittance growth.

The RF gun is super-conducting, providing high accelerating fields to minimize the effects of space charge. A cathode insert with a diamond window uses secondary electrons to produce the high charge and avoids a breakdown of superconductivity through surface contamination by the cathode material and the magnetic field required for the magnetization.

Finally, the bunch is lengthened and the energy spread in the cooling section is reduced by bunch rotation in the longitudinal phase space. This also reduces the space charge effect between electrons and ions. The original bunch length must be restored by a second rotation before deceleration and energy recovery.

INTRODUCTION

Electron cooling has been known for many years and is practiced in many machines around the world. The physics of cooling takes place in the reference frame of the ions (and electrons) bunch, which is independent of the energy of the machine. However, there are a number of differences between this electron cooler and any other built so far:

- The RHIC cooler will be by far the highest energy cooler, requiring electron energy of over 50 MeV as compared to the few hundred KeV of any previously built cooler (the only exception is the recycler cooler of FNAL, which is under construction and will have 4.3 MeV electron energy).
- The RHIC cooler is the only machine planned for cooling with bunched electron beams.
- The RHIC II will be the first instance of a directly cooled collider.
- The RHIC cooler will operate with electrons that are much "hotter" than in previous coolers.
- The RHIC cooler will use a very long, high-field, ultra-high precision solenoid.

The electron beam technology of this cooler will be different than any other, requiring high-energy, high-current and low-emittance (temperature) electron beams. In order to reach the goals R&D is taken along the following fronts:

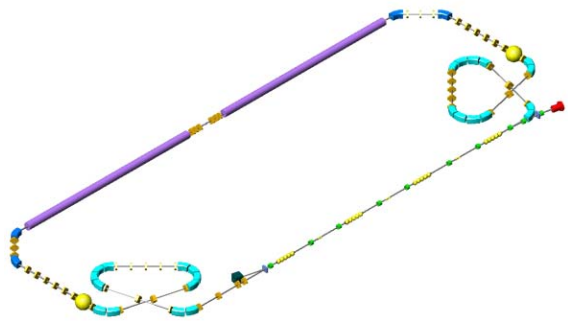

Figure 1: Electron bunches are produced in the gun and accelerated in the super-conducting linac. A beam-transport loop stretches the bunch length and a debunching cavity reduces the energy spread before the electrons are merged with the ion beams. A strong solenoid must be installed in the cooling section to enhance the cooling effect [10]. The electron bunches are then shortened by a combination of a second cavity / transport loop, and then decelerated in the linac before they are dumped. The start of operation is planned for January 2010.

* Work performed under the auspices of the U.S. Department of Energy

LINEAR ACCELERATOR LINAC-800 OF THE DELSY PROJECT

V.V. Kobets, N.I. Balalykin, I.N. Meshkov, I.A. Seleznev, G.D. Shirkov,
JINR, Moscow region, 141980, Dubna, Russia

Abstract

In the report the modernization of electron linear accelerator MEA (Medium Energy Accelerator) is discussed. The goal of the work is to create on the base of MEA a complex of free electron lasers overlaying a range of radiation waves from infrared to ultraviolet. Status of the work is reported.

THE DELSY PROJECT

The DELSY (Dubna Electron Synchrotron) project is being under development at the JINR, Dubna, Russia [1]. It is based on an accelerator facility presented to JINR by the NIKHEF, Amsterdam. The construction of the DELSY facility will proceed in three phases. Phase I will be accomplished with the construction of a complex of FEL covering continuously the spectrum from far infrared down to ultraviolet [2]. Phase II will be accomplished with commissioning of the storage ring DELSY. The optics of the DELSY storage ring is characterized by its 2-fold symmetry, low horizontal emittance (11.4 nm), low-beta section at the wiggler location and section for miniundulator. Synchrotron radiation from the dipole magnets with critical photon energy up to 1.16 keV has rather high intensity in both ultraviolet and infrared regions. This radiation can be used in photoelectron microscopy, time-resolved fluorescent studies of biological objects, in absorption spectroscopy, metrology and photometry. Hard X-ray radiation from wiggler can be used for researches on VUV luminescence of crystal and pumping of VUV-lasers, time-resolved Moessbauer spectroscopy, EXAFS spectroscopy, DANES, DAFS. Phase III of the project is construction of an X-ray FEL. Recent studies have shown that the DELSY complex has a reliable potential for upgrading into a fourth-generation SR light source.

Phase I

Phase I will be accomplished with the construction of a complex of free electron lasers covering continuously the spectrum from far infrared down to ultraviolet (of about 150 nm). The far-infrared coherent source will cover continuously the submillimeter wavelength range. Realization of this phase will not require a significant modification of the JINR infrastructure. In Table 1 we present a summary of the radiation properties from coherent radiation sources being planned to build in Phase I. Notations G1-G4 refer to the FEL oscillators, and FIR stands for the far-infrared coherent source.

ACCELERATOR LINAC-800

The electron beam with necessary parameters for the Free Electron Laser will be generated with the electron linac, which is a modified version of the Medium Energy Accelerator (MEA) transferred to JINR from NIKHEF[3]. The energy of electrons at the linac exit is 800 MeV and peak current of 30-60 A, with subharmonic buncher of the frequency of 476 MHz, a buncher at the frequency of 2856 MHz and 24 acceleration sections, which are combined in 14 acceleration stations (A00 – A13).

Table 1: Summary of radiation properties from coherent radiation sources in Phase I.

	FIR	G1	G2	G3	G4
Radiation wavelength, [μm]	150-1000	20-150	50-30	1-6	0.15-1.2
Peak output power, [MW]	10-100	1-5	1-5	3-15	10-20
Micropulse energy, [μJ]	500	50-200	25-100	25-100	50-100
Micropulse duration (FWHM),[ps]	5-10	10-30	10	10	3-5
Spectrum bandwidth (FWHM),[%]		0.2-0.4	0.6	0.6	0.6
Micropulse repetition rate, [MHz]			19.8/ 39.7/ 59.5		
Macropulse duration, [μs]			5-10		
Repetition rate, [Hz]			1-100		
Average output power (max.), [W]	10-50		0.2-1		

To operate FEL, one needs an injector with a special subharmonic prebuncher. Such an injector has to be developed at JINR.

MEA Injector

To start the linac operation and test its condition, we plan to use the MEA injector consisting of an electron gun, chopper, prebuncher and buncher [4].

The electron gun (Table 2) has a dispenser thermocathode with the diameter of 8 mm. Its heater current is 15 A at the heater filament voltage of 12 V. The cathode lifetime is of the order of 20 thousand hours. The gun optics elements contain Pirce electrode at the cathode potential, control electrode and acceleration tube, which has 15 diaphragms forming homogeneous acceleration field. Linear potential distribution along the tube is provided with the divider, the voltage between two

DEVELOPMENT OF A C-BAND ACCELERATING MODULE FOR SUPERKEKB

S. Ohsawa, T. Kamitani, T. Sugimura, K. Kakihara, M. Ikeda, T. Oogoe,

S. Yamaguchi, and K. Yokoyama

High Energy Accelerator Research Organization, KEK, 1-1, Oho, Tsukuba, Ibaraki, Japan

Abstract

A C-band accelerating module has been constructed in KEKB/PF linac, and beam acceleration tests have been performed during 10-month operation. The purpose is to investigate C-band feasibility and stability of acceleration in the region beyond 40MV/m. The C-band accelerating module is expected to be promising for accelerating positrons up to 8GeV instead of 3.5GeV for both of the present KEK B-factory and SuperKEKB project in order to upgrade the luminosity. Last summer a 1m-long C-band accelerating section installed in the KEKB/PF linac. Accelerating field corresponding to 41 MV/m was successfully achieved in October in a beam test. Present status of C-band accelerator development is reported.

INTRODUCTION

The KEK-B factory is making highest luminosities ($>1.3\times10^{34}$ $cm^{-1}s^{-1}$) in the world, where 3.5-GeV electrons and 8-GeV positrons are colliding. Toward higher luminosities a future project SuperKEKB is under consideration, of which target luminosities arise in the order of 1-5 $\times10^{35}$ $cm^{-1}s^{-1}$ [1]. In order to put into practice such a high goal, requirements to the injector linac should inevitably become severe for all values such as beam intensities, energies and emittances etc., as are listed in table 1. Some schemes of linac upgrade have been considered what should be improved to meet the requirements as well as possibility and feasibility, and consideration is still going on.

Table 1: Upgrade requirements

		KEKB	SuperKEKB
Beam energy	e+	3.5 GeV	8.0 GeV
	e-	8.0 GeV	3.5 GeV
Stored current	e+	2.6 A	4.1 A
	e-	1.1 A	9.4 A
Linac beam	e+	0.6 nC x 2	1.2 nC x 2
	e-	1.0 nC x 1	2.5 nC x 2
Smaller emittance to fit IR&C-band structure aperture			
Faster e+/e- mode switching for continuous injection			

Among the requirements, there has been a subject useful not only SuperKEKB but also for the KEKB. It is a plan to exchange energies of electrons and positrons: positrons become 8GeV instead of 3.5GeV, and electrons become 3.5GeV from 8GeV. The purpose is to avoid positron instability in the ring due to electron cloud, of which influence depends on the positron energy: higher the energy, smaller the effect. Therefore 8GeV positrons would be useful and desirable also for the KEKB instead of the present energy 3.5GeV. The requirement and importance of the beam seem to be growing, especially so under the present status in which beam intensities are still kept rising in both KEKB rings to increase luminosity.

Then exchange of energies would be more urgent issue that should be realized quickly, if possible, before the SuperKEKB project starts. It would have an important role to escape the influence of the electron cloud effect on positrons. Our strategy to get 8GeV positrons is basically simple [2].

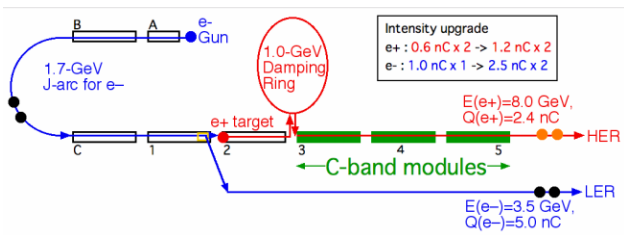

Figure 1: Layout of an upgrade scheme of the KEKB/PF linac

Presently positrons are produced at a production target which is installed halfway of the KEKB/PF linac, as is shown in Fig.1, and then accelerated up to 3.5 GeV in the following half of the linac. The most simple and feasible way to get 8-GeV positrons would be increasing the accelerating fields in the second half of the linac. This scheme is direct method and does not request any new buildings; however, the accelerating field strengths should be increased double from the present value of 21MV/m to 42 MV/m. How can we realise such a high accelerating field, that is the question to be solved. It is obvious that such a high field could not be obtained without increasing

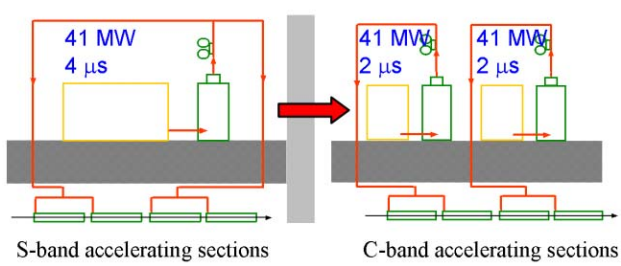

Figure 2: Layouts are showing how to replace accelerating modules from S-band to C-band.

satoshi.ohsawa@kek.jp

INJECTOR LINAC UPGRADE FOR THE BEPCII PROJECT

Shu-Hong Wang† for BEPCII-Linac Group
Institute of High Energy Physics, IHEP, Beijing, P. O. Box 918, 100039, China

Abstract

BEPCII- an upgrade project of Beijing Electron Positron Collider (BEPC) is a factory type of e+e- collider. It requires its injector linac to have a higher beam energy (1.89 GeV) for on-energy injection and a higher beam current (40 mA e+ beam) for a higher injection rate (≥50 mA/min.). The low beam emittance (1.6πmm-mrad for e+ beam, and 0.2πmm-mrad for 300 mA e- beam) and low beam energy spread (±0.5%) are also required to meet the storage ring acceptance [1]. Hence the original BEPC injector linac must be upgraded to have a new electron gun with its complete tuning system, a new positron source with a flux concentrator, a new RF power system with its phasing loops and a new beam tuning system with orbit correction and optics tuning devices. These new components have been designed, fabricated, tested and now being installed in their final positions, which are described in this paper. The beam commissioning is expected to start from October of 2004.

INTRODUCTION

BEPCII is an upgrade project of Beijing Electron Positron Collider with a high luminosity of $1\times10^{33}\,cm^{-2}s^{-1}$ in the Tau-Charm energy region (2-5 GeV) in the centre of mass. The full energy injection with a high injection rate of > 50 mA/min (ten times of present value) for the e+ beam requires the original BEPC injector linac to be upgraded with its higher performances as listed in the Table 1.

Table 1: Beam Parameters of the BEPCII-Linac

	Unit	e- beam	e+ beam
Beam Energy	GeV	1.89	1.89
Beam Current	mA	~ 40	~ 300
Beam emittance	πmm-mrad	1.60	0.20
Energy spread	%	0.50	0.50
Injection rate	mA / min	> 50	> 300
Pulse repet. rate	Hz	50	50
Beam pulse length	ns	1.0	1.0

To meet these specifications, we need a new electron gun with its complete tuning system, a new positron source with a flux concentrator, a new RF power system with its phasing loop and a beam tuning system with the orbit correction and optics tuning. These new components have been designed, fabricated and now being installed in their final positions.

ELECTRON GUN SYSTEM

In order to increase the positron current as well as the injection rate, a new electron gun that can emit higher current is needed. A thermionic triode gun with a cathode-grid assembly of Y796 is employed with the gun beam parameters of 10 A, 1 ns, 10 nC, 150-200 keV and 50 Hz. The computed province is 0.22 μP. At the end port the beam radius is about 6.0 mm, and the emittance is 17.6 mm·mrad. The beam trajectories present that the current density is relatively uniform, which indicate a good beam performance. A Kentech pulser is employed which can be operated at 1ns of either one pulse or two pulses separated by about 56 ns for the two-bunch operation. Between the gun exit and the prebuncher, there are two focusing lens, two steering coils and two BPMs, and a profile monitor for having a well beam alignment and tuning, as shown in the Figure 1.

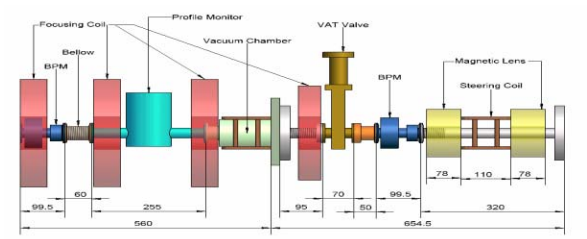

Figure 1: Components downstream the electron gun.

POSITRON SOURCE SYSTEM

A 250 MeV and 6 A primary electron beam at the e+ production target is designed. To have a maximum e+ yield, a tungsten target thickness is optimized at 8 mm and a primary e- beam spot size of 1.0 - 1.5 mm on the target is expected by the beam modeling. A flux concentrator (FC) of 10 cm long is employed to provide a maximum transverse acceptance of 0.31π (MeV/c)-cm, which provides the pulsed longitudinal magnet field of 5.3 T and 0.5 T at the input and output of the FC, respectively, with a 12 kA pulsed power supply. In the downstream FC, there is a 7.5 m long, 0.5 T, DC-solenoid to further focus the e+ beam and matches the beam into the downstream quadrupole focusing system. In addition to the available 15 triplet quads, 24 big aperture quads installed on the downstream accelerating structures will be employed to strongly focus the large emittance e+ beam. In order to bunch the beam longitudinally, the e+ beam is decelerated in the first 1 m of the structure just downstream the FC, and then to be soon accelerated with a high gradient so that the most of the positrons are bunched into a phase spread of $\pm5^0$ at the DC solenoid exit with the positron yield of 4.3%(e+/e-.GeV)[2]. The 8 accelerating structures of 3 meters long each in the e+ production system will be replaced by the new ones in order to have high stability and reliability in high gradient

† wangsh@sun.ihep.ac.cn

THE RESEARCH OF A NOVEL SW ACCELERATING STRUCTURE WITH SMALL BEAM SPOT

Xingfan Yang, Zhou Xu, Xiao Jin, Ming Li, Hao Chen, Yanan Chen, Heping Lu

CAEP,P.R.China

Abstract

A new kind of on-axis coupled biperiodic standing-wave (SW) accelerating structure has been built for a 9MeV accelerator. The research progress was introduced in this paper; it includes the choice of the accelerating structure, the analysis of electron beam dynamics, the tuning of the cavity, the measurement of the accelerating tube and the powered test. The small beam spot is the most interesting feature of this accelerating structure, the diameter of the beam spot is 1.4mm.This accelerator has been used for the x photons generation and the x-ray dose rate is about 3400rad/min/m.

INTRODUCTION

The high energy industrial computed tomography (ICT) which uses accelerator as the driving source has important applications in the fields of aerospace, non-destructive inspection, precise machining etc, the result of the ICT was determined by the performance of the accelerator which used for the generation of x photons, so the accelerating structure with small beam spot is the key of obtaining high space solution and density solution. Usually in order to increasing the transit-time factor and so the effective shunt impedance, nose cone was set in the accelerating cells[1], but the transverse electric field was increased at the same time, so in order to decreasing the beam spot ,we attempt to take out of the nose of the accelerating cell .

DESIGN OF THE ACCELERATING STRUCTURE

This accelerating structure was an on-axis coupled biperiodic SW structure and was made of 11 accelerating cells and 10 coupling cells, illustrated in Figure 1.

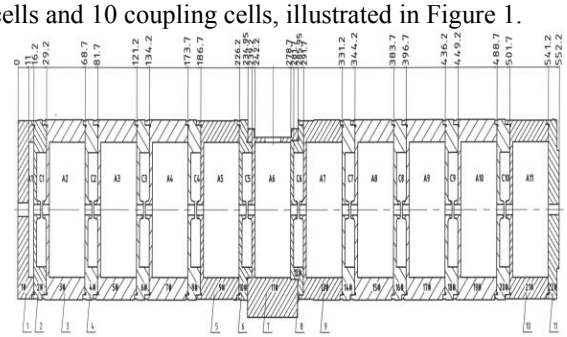

Figure 1: The accelerating tube

There are no nose cones in the accelerating cells and in order to making the electric field cutting off, the nose cones were set in the coupling cell. Adjacent cells are coupled magnetically, through slots cut in the outer walls and so the accelerating structure is a resonant system. In order to decreasing the secondary coupling. The SUPERFISH code was used in the design and optimised of the cavity; the distribution, the stored energy and the power dissipation of the wall were calculated. The electric field in the cells were illustrated in Figure 2 and electric field on the axis was illustrated in Figure 3.

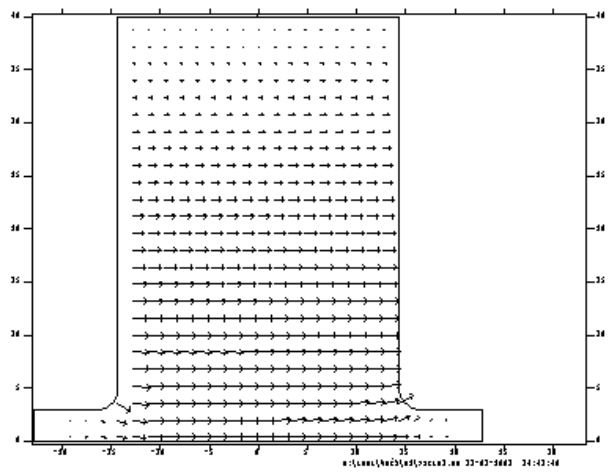

Figure 2: The electric field in the cell

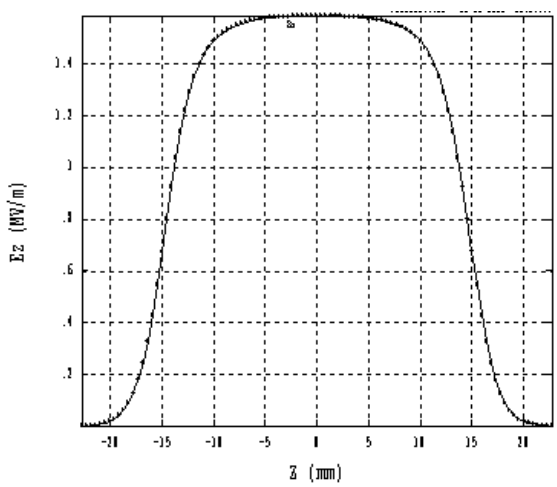

Figure 3: The on-axis electric field

There are no nose cone in the accelerating cells, this makes the longitudinal electric field much smooth, and

PRELIMINARY STUDY ON HOM-BASED BEAM ALIGNMENT IN THE TESLA TEST FACILITY

N. Baboi, G. Kreps, M. Wendt, DESY, Hamburg
G. Devanz, O. Napoly, R.G. Paparella, CEA/Saclay, DSM/DAPNIA, Gif-sur-Yvette

Abstract

The interaction of the beam with the higher order modes (HOM) in the TESLA cavities has been studied in the past at the TESLA Test Facility (TTF) in order to determine whether the modes with the highest loss factor are sufficiently damped. The same modes can be used actively for beam alignment. At TTF2 a first study on the beam alignment based on the HOM signals has been made in the first cryo-module, containing 8 accelerating cavities. Four modes with highest R/Q in the first two cavities have been monitored. One bunch has been usually used. The cavity center could be found for each of the modes. The results are presented in this paper.

INTRODUCTION

The TESLA Test Facility – phase 2 (TTF2) [1] at DESY is equipped with various monitors: beam position monitors, beam loss monitors, screens, wire scanner etc. However difficulties have been encountered to align the beam over long sections of the linac constituted by the cryo-modules. These contain eight 9-cell superconducting accelerating cavities, which are cooled together to about 2K. Each cavity is about 1 m long. Beam alignment in the cavities is important in order to avoid transverse kicks on the beam from higher-order modes (HOM), which may lead both to a single-bunch deformation and to beam break-up along the bunch train.

These monitor-free long sections can be filled by the signals from the HOM couplers. Such couplers are placed at either side of each cavity in order to extract energy from the fields excited by charged particles and hence damp the higher-order modes. In the past, signals from the HOM couplers have been used to study the modes, and to find out if the damping is sufficient for the dipole modes with high R/Q, i.e. good coupling to an off-axis beam [2]. The same HOM signals can be used to monitor the offset of the beam with respect to the cavity axis [3], since their amplitude is proportional to it. To improve the alignment tolerances for both the collider and the FEL applications of TTF superconducting modules, this beam-based method should achieve a positioning resolution significantly better than 500 µm obtained by the cavity mechanical alignments.

First studies on the possibility to align the beam in the cavities have been made. The amplitude of the fields excited by the beam at several resonances in the first two cavities of the first TTF module has been measured as a function of the beam position. In this paper the measurements are described and the results are discussed.

THE METHOD

Setup

Fig. 1 shows schematically the first part of the TTF2 injector in the first phase of commissioning. A gun accelerates the electrons emitted by a photo-cathode to 4.5 MeV. A horizontal and a vertical steerer can deflect the beam, correcting for possible errors in the transverse and angular alignment of the gun. Eight cavities in module ACC1 accelerate the beam with a gradient of 12 MV/m.

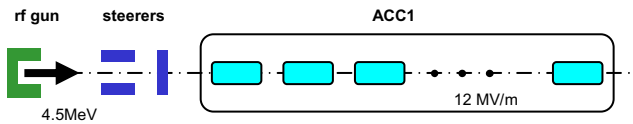

Figure 1: Schematic view of the alignment setup

The frequency spectrum of the wake fields excited by the beam is monitored with a spectrum analyzer. The spectrum of each cavity consists of resonant modes grouped in passbands by the type of the mode. There are 9 modes in each passband, and for the case of dipole modes there are 2 polarizations for each mode.

Fig. 2 shows such a spectrum for one mode of the first dipole passband of the first cavity. The two polarizations can be distinguished and their quality factors Q, of about $9.3 \cdot 10^3$ and $2.4 \cdot 10^4$, have been measured a priori with a network analyzer. This mode is one with highest R/Q. Four modes with highest R/Q have been used. Their frequencies and R/Q as predicted from simulations for an ideal TESLA cavity are shown in Table 1.

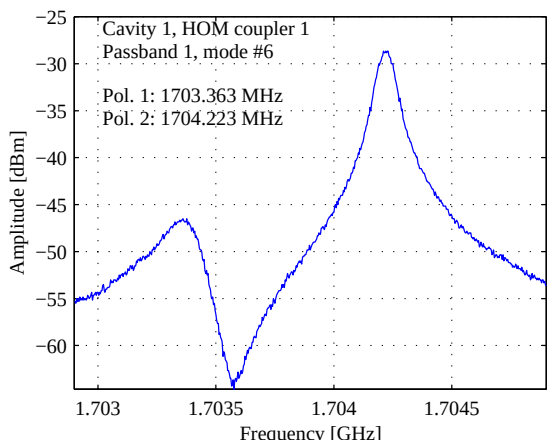

Figure 2: Mode #6 of the first dipole passband in cavity 1 of ACC1

Table 1: Dipole modes with highest R/Q used for beam monitoring as predicted by simulations

OPTIMIZATION OF POSITRON CAPTURE IN NLC*

Yuri K. Batygin, SLAC, Stanford, CA 94309, USA

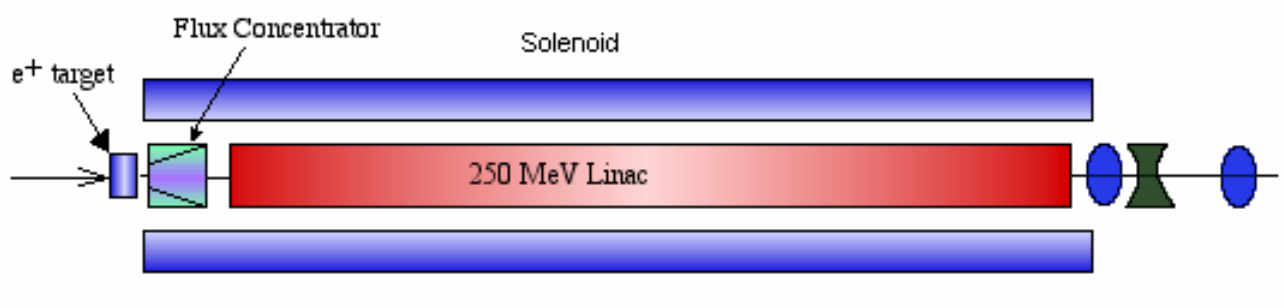

Figure 1: Layout of the NLC positron injector.

Abstract

In the Next Linear Collider design [1], the positron capture system includes a positron production target, followed by a short solenoid with a strong magnetic field (flux concentrator), a 250 MeV linac with solenoidal focusing, a 1.73 GeV linac with quadrupole focusing and an energy compressor system before injection into the positron pre-damping ring (see Fig. 1 for initial part of collector). Two schemes for positron production have been studied: (i) a conventional approach with a 6.2 GeV electron beam interacting with a high-Z target and (ii) polarized positron production using polarized photons generated in a helical undulator by a 150 GeV electron beam which then interact with a positron production target. The capture system has been optimized to insure high positron yield into the 6-dimensional acceptance of the pre-damping ring. As a result of these optimization studies, the positron yield in the conventional scheme has been increased from 1.0 to at least 1.5 and captuire for the polarized positron scheme from 0.25 to 0.30 while maintaining 60% positron polarization.

POSITRON YIELD, CAPTURE AND POLARIZATION

Generated positron beam is characterized by large value of beam emittance and wide energy spread (see Fig. 2). At the time of injection into the pre-damping ring, positron capture is restricted by the acceptance of the pre-damping ring. It is convenient to select an energy-invariant 6-dimensional phase space volume and compare positron capture within this volume at different stages of the injector. To provide positrons injection into the pre-damping ring, the normalized positron beam emittance is selected to be $\varepsilon_x, \varepsilon_y \le 0.03$ π m rad and the energy spread $\Delta E/E = \pm 1\%$ at the injection energy of 1.98 GeV (see Fig. 3).

For analysis, we use several criteria, which characterize efficiency of positron collection. Positron capture is a ratio of the number of positrons within invariant 6-dimensional volume, N_{e+}, to the number of positrons generated after the positron production target, $N_{e+,target}$. Positron yield is defined as a ratio of accepted positrons into the pre-damping ring at the energy of 1.98 GeV to the number of incident electrons, N_{e-}, or to the number of incident photons, N_γ, interacting with the target. Longitudinal polarization of a positron beam, $\langle P_z \rangle = \langle S_z P \rangle$, is an average of the product of the longitudinal component of positron spin vector, S_z, and the value of positron polarization, P, over all positrons.

Table 1 illustrates dependence of positron yield in the conventional production scheme with respect to different values of 6-dimensional acceptance of the pre-damping ring.

Table 1: Positron yield at 1.98 GeV as a function of 6D acceptance.

6-D phase space	$\varepsilon_x, \varepsilon_y$ <0.03 π m rad, $\Delta E/E$ =2%	$\varepsilon_x, \varepsilon_y$ <0.045 π m rad, $\Delta E/E$ =2%	$\varepsilon_x, \varepsilon_y$ <0.06 π m rad, $\Delta E/E$ =2%	$\varepsilon_x, \varepsilon_y$ <0.03 π m rad, $\Delta E/E$ =4%	$\varepsilon_x, \varepsilon_y$ <0.045 π m rad, $\Delta E/E$ =4%	$\varepsilon_x, \varepsilon_y$ <0.06 π m rad, $\Delta E/E$ =4%
Positron yield	1.01	1.26	1.36	1.25	1.55	1.69

*Work supported by the Department of Energy Contract No. DE-AC03-76SF00515

BACKGROUND FROM UNDULATOR IN THE PROPOSED EXPERIMENT WITH POLARIZED POSITRONS*

Yuri K. Batygin, SLAC, Stanford, CA 94309, USA

Abstract

In the proposed E-166 experiment [1], 50 GeV electrons pass through helical undulator, and produce circularly polarized photons, which interact with a tungsten target and generate longitudinally polarized positrons. The background is an issue for a considered experiment. GEANT3 simulations were performed to model production of secondary particles from high-energy electrons hitting an undulator. The energy density of generated photons at the target was analysed. Results of the simulations are presented and discussed.

INTRODUCTION

E-166 is the proposed experiment for the verification of polarized positron production for the Next Linear Collider [1]. According to the original suggestion of Ref. [2], high-energy electrons pass through a helical undulator and produce circularly polarized photons, which after interaction with tungsten target, generate longitudinally polarized positrons. In the E-166 experiment (see Fig. 1), the 50 GeV electron beam propagates inside 1 m long undulator followed by a drift space of 35 m. Polarized positrons generated in an undulator are analyzed by Si-W calorimeter which is placed along the axis. Polarized positrons are analyzed by a Cs-I calorimeter after reconversion of positrons to photons at the second target shifted by 45 cm from the axis. In this paper we discuss the effect of background particles generated by primary high-energy electrons hitting undulator tube.

SIMULATION SET-UP

Fig. 2 illustrates the simulation set-up of the Final Focus Test Beam (FFTB) line of SLAC linac. Beamline includes undulator (1), quadrupole magnet (2), bending magnets (3) and lead shields (4), (5). The undulator was substituted by a thin iron tube with length of 1 m and internal diameter of 0.88 mm. To prevent background, in front of the undulator a tungsten collimator with the length of 30 RL (10.5 cm) is used. Simulations were performed for two cases: illumination of the internal part of the undulator and illumination of collimator by halo electrons.

To define divergence of halo electrons, let us take into account that normalized rms beam emittance in FFTB line is $\gamma\varepsilon = 3\text{x}10^{-5}\ \pi$ m rad, and rms beam size is $\sigma = 40\cdot10^{-6}$ m. Therefore, rms beam divergence for beam energy of $\gamma = 10^5$ is

$$\left(\frac{dx}{dz}\right)_{rms} = \frac{\varepsilon}{\sigma} = 7.5\cdot10^{-6}. \quad (1)$$

The internal undulator radius is approximately 10 times larger than the rms beam size. As soon as halo electrons are distributed in a phase space within a 10 times larger ellipse than the beam core, the divergence of the halo electrons was selected to be

$$\left(\frac{dx}{dz}\right)_{halo} = 10\cdot\left(\frac{dx}{dz}\right)_{rms} = 7.5\cdot10^{-5}. \quad (2)$$

The generated secondary particles were collected and analyzed at the distance of 35 m from undulator.

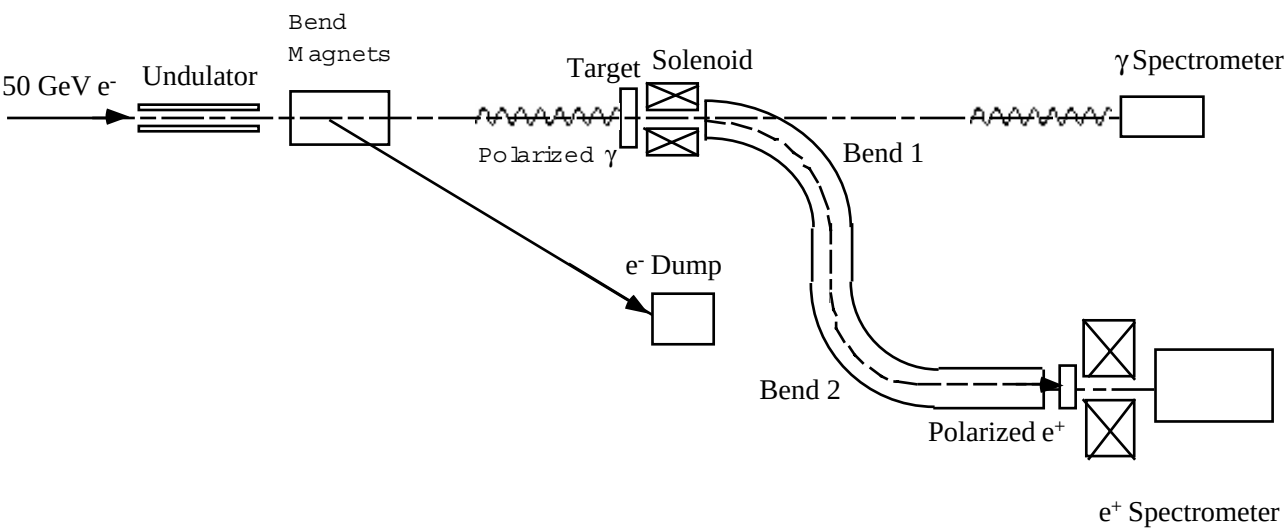

Figure 1: Layout of experiment.

*Work is supported by Department of Energy under Contract No. DE-AC03-76SF00515

POSITRON TRANSMISSION AND POLARIZATION IN E-166 EXPERIMENT*

Yuri K. Batygin, SLAC, Stanford, CA 94309, USA

Abstract

The proposed experiment E-166 at SLAC is designed to demonstrate the possibility of producing longitudinally polarized positrons from circularly polarized photons. The experimental set-up utilizes a low emittance 50 GeV electron beam passing through a helical undulator in the Final Focus Test Beam line of the SLAC accelerator. Circularly polarized photons generated by the electron beam in the undulator hit a target and produce electron-positron pairs. The purpose of the post-target spectrometer is to select the positron beam and to deliver it to a polarimeter, keeping the positron beam polarization as high as possible. The paper analyzes the positron transmission and polarization in the E-166 spectrometer both numerically and analytically. The value of positron transmission has a maximum of 5% for positron energy of 7 MeV, while positron polarization is around 80%.

INTRODUCTION

The polarized positron production experiment E-166 uses a strongly collimated 50 GeV electron beam to generate circularly polarized photons in a helical undulator. Photons, after interaction with a target, create polarized positrons. The layout and general description of experiment are given in Ref. [1]. The purpose of a spectrometer is to select the positron beam after the target from electron and photon beams and to deliver positrons to a reconversion target, keeping beam polarization as high as possible.

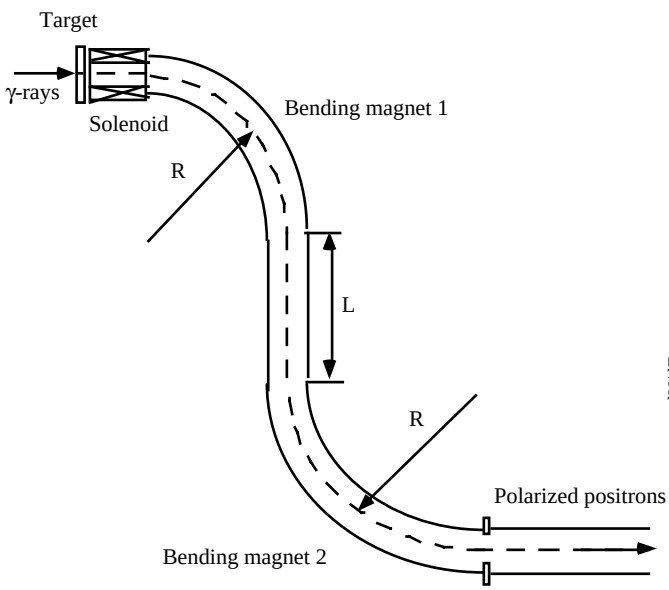

Figure 1: Layout of spectrometer.

Table 1: Parameters of spectrometer

Positron beam energy	0..10 MeV
Bending radius, R	12.5 cm
Bending angle, θ	90°
Drift space, L	20 cm
Positron transmission	5%
Positron polarization	80 %

POLARIZED POSITRON DISTRIBUTION AFTER TARGET

The initial distribution of positrons produced by circularly polarized photons was calculated by J.C.Sheppard using the program EGS4, modified for polarized positrons [2, 3]. Positron distribution after the target is presented in Fig. 2. The distribution is characterized by a large emittance of the positron beam and a large energy spread. The correlation between energy, polarization, and transverse momentum spread is illustrated by partial distributions presented in Figs. 3 – 5. Low energy positrons are less polarized and more transversely divergent, while high-energy positrons are strongly polarized and less divergent. The energy spectrum peaks near the low-energy end of the distribution.

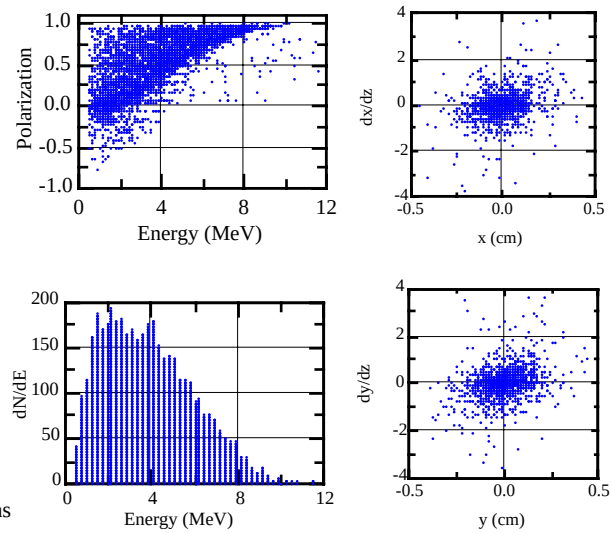

Figure 2: Initial distribution of positrons.

*Work is supported by Department of Energy under Contract No. DE-AC03-76SF00515

A STUDY OF COUPLER-TRAPPED MODES IN X-BAND LINACS FOR THE GLC/NLC†

R.M. Jones, V.A. Dolgashev, Z. Li, J.W. Wang, SLAC

Abstract

Each of the X-band accelerating structures for the GLC/NLC (Global Linear Collider/Next Linear Collider) consists of 55 cells which accelerate a train of charged bunches. The cells are carefully designed to ensure that the transverse wakefield left behind each bunch does not disrupt the trailing bunches, but some modes are trapped in the region of the coupler cells. These modes can give rise to severe emittance dilution if care is not taken to avoid a region of resonant growth in the emittance. Here, we present results on simulations, cold test experimental measurements and beam dynamics simulations arising as a consequence of modes trapped in the coupler. The region in which trapped modes have little influence on the beam is delineated.

INTRODUCTION

In the design of a next generation linear collider operating at room temperature there are two main issues that must be faced: firstly, operating at high gradients with minimal electrical breakdowns and secondly, damping the wakefield that the charged bunches leave behind such that disruptive Beam Break Up (BBU) instabilities do not develop. Means of controlling electrical breakdown is under intensive investigation at SLAC [1] and is not the subject of this paper.

Here we study the second major issue, namely, wakefield effects. The short range, or intra-bunch, wakefield affects particles within a given bunch and it is proportional to $a^{-3.8}$ (where a is the average iris radius of the accelerator structure). An $a/\lambda \sim 0.17$ (where λ is the free-space wave number at the accelerating frequency) gives rise to manageable short-range wakefields and this is the number used in several designs for the GLC/NLC. The long-range wakefield affects trailing bunches and it falls by almost two orders of magnitude by the time of the first trailing bunch (separated from its neighbor by 1.4 ns). This decay is achieved by varying the geometry of the accelerator cells in a careful controlled manner [2]. We have investigated Gaussian and Sech functional behavior in the fall-off of the long-range wakefield. Eventually the modes would re-cohere and, in order to damp these modes [3] down to acceptable levels we couple out a significant fraction of the remaining wakefield to 4 attached manifolds.

These detuned and moderately damped accelerating structures have been verified to behave as expected from simulations in several ASSET (Accelerator Structure Setup) experiments [4] conducted in the SLC. However, modes can readily become trapped in the regions of the fundamental mode RF couplers. We refer to these modes being trapped in the sense that they are localized in the waveguide coupler [5] and the next cell. They are weakly coupled to the regular cells and output waveguides. We make the distinction between these modes and the structure modes with some fields in the coupler region [3]. The trapped modes can cause transverse instabilities which may significantly dilute the beam emittance. It is the purpose of this paper to carefully analyze these modes and ascertain their influence on the beam dynamics.

The following section provides an analysis of these modes based on experimental measurements of the scattering matrix properties of the coupler and on *HFSS* [6] modeling of the eigenmodes of the structure. The impact of the trapped modes on the beam dynamics is presented in the final main section.

MEASUREMENT AND SIMULATION OF TRAPPED EIGENMODES

Reflection and transmission were measured using one port of the fundamental coupler and an antenna inserted into the beam pipe. To measure the frequency and Q of the trapped mode it was necessary to insert the probe in the field of the trapped mode. The inserted probe, obviously perturbs the frequency and Q of the mode. The perturbation is minimized by withdrawing the probe to the extent that the resonance in S_{11} is just discernable. We observed two highest Q modes in this accelerator structure: each are located in the regions of the input and output coupler. The Qs of these modes are determined entirely by the copper losses.

The eigenmodes together with their Q values were calculated with its eigenmode module of *HFSS*. The complete set of modes simulated for a waveguide coupler, a matching iris and the first iris of the structure, are shown in Fig. 1. Further modes were observed during the experimental measurements but only those we believe to be modes trapped in the region of the coupler are shown in Fig. 1. The highest Q modes are illustrated in Fig. 1A and Fig. 1B. All of the modes displayed are dipole-like in character, except the mode in Fig. 1F. This mode is monopole-like with a finite quadrupole field. This mode has some focusing in one plane and defocusing in the other. Properties are of such modes are discussed in [7]. A summary of the experimentally determined frequencies and those computed with *HFSS* is given in Table 1. Additionally we have made limited *Omega3P* [8] simulations of the high Q input and output modes. These *Omega3P* calculations indicate that the input fundamental coupler has a mode frequency of 10.658 GHz and the output fundamental mode coupler is 11.534 GHz. These values are in better agreement with the experimentally determined frequencies. This may be due to the *Omega3P*

† Supported by the DOE, grant number DE-AC03-76SF00515

EMITTANCE-IMPOSED ALIGNMENT AND FREQUENCY TOLERANCES FOR THE TESLA LINEAR COLLIDER

N. Baboi, DESY, Hamburg, Germany and R.M. Jones†, SLAC, Stanford, CA 94309, USA

Abstract

One option in building a future 500 GeV c.m. linear collider is to use superconducting 1.3 GHz 9-cell cavities. However, wakefields excited by the bunch train in the TESLA (TeV-Energy Super Conducting Linear Accelerator) collider can resonantly drive the beam into unstable operation such that a BBU (Beam Break Up) mode results or at the very least significant emittance dilution occurs. The largest kick factors (proportional to the transverse fields which kick the beam off axis) are found in the first three dipole bands and hence multi-bunch emittance growth is mainly determined from these bands. These higher order dipole modes are damped by carefully orientating special couplers placed at both ends of the cavities. We investigate the dilution in the emittance of a beam with a random misalignment of cavities down the complete main linac. The beneficial effects of frequency errors on ameliorating the beam dilution are discussed.

INTRODUCTION

The fundamental consideration in a linear collider is the luminosity of the colliding beams at the interaction point. The luminosity of flat beams is proportional to $L \propto P_b / \sqrt{\varepsilon_{y,n}}$, where $P_b \propto f_{rep} n_b q$ is the beam power and $\varepsilon_{y,n}$ the normalized vertical emittance at the interaction point. For TESLA a high P_b is achieved by compensating the low pulse repetition frequency, f_{rep}, with a high bunch charge q, and a large number of bunches n_b. In order to maximize the luminosity it is however also important to minimize the vertical emittance.

As the highly charged bunches traverse the linac any misalignment in the structure, focusing magnets, or initial offset in the leading bunch, gives rise to wakes [1] which dilute the emittance and the beam may break up down the linac. This BBU [2] can result from short range wakes over the bunch itself, in which the head drives the tail, or from a long range wake, in which trailing bunches are driven by leading ones and BBU occurs due to the coupled motion of the bunches.

Table 1: Fundamental L-band TESLA RF parameters

Quantity	Symbol	L
Accelerating freq. (GHz.)	f_{acc}	1.300
Loaded gradient (MV/m)	G_{acc}	23.4
Bunch train length (T_{fill})	T_b	2.3
Bunch spacing (T_{RF})	T_{bb}	438
Charge per bunch (10^{10})	N_e	2
Structure Iris radius (λ_{RF})	A	0.15
Bunch length (μm)	σ_z	300
Pulse rate	f_{rep}	5

We investigate the emittance dilution due to the long-range wakefield left behind accelerated bunches in the main linacs of the TESLA collider [3,4]. RF parameters for the linacs of this L-band collider are given in Table 1. For the TESLA design, as the cavities are superconducting, the losses are minimal and the fill time and the length of the train of particle bunches can be very long. For this reason 2820 bunches are in the charged particle train, which is 950 μs long. Each cavity consists of 9 cells, operating in the standing wave mode and with a π phase advance per cell. A typical 9-cell cavity structure is illustrated in Fig. 1. There will be close to 21,000 of these cavities in the collider.

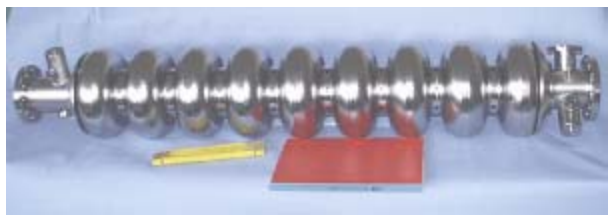

Figure 1: Fabricated nine-cell niobium TESLA cavity.

In this paper, due to space considerations, we concern ourselves entirely with how the emittance of the beam is diluted due to misaligned accelerator cavities. However, we refer the interested reader to [5] for an analysis of the impact on emittance dilution of a beam injected offset from the axis of the accelerator.

This paper is organized in two main sections. The following section describes the transverse wakefields calculated from numerically evaluated kick factors, and measured Qs and synchronous frequencies. The second section investigates the alignment tolerances that are allowable for a specified emittance dilution.

TRANSVERSE WAKEFIELDS

For the TESLA cavities, there are no more than a few modes that interact strongly with the beam in the first three pass-bands. Using HOM couplers attached to the beam pipe at either side of each cavity, the Q of these modes is reduced from the order of 10^9 to below 10^5. Measurements made in the majority of cavities built to date indicate this damping level is achieved. Fig. 2 shows the Qs and kick factors [6] of the dipole modes. It is clear that only a few modes have appreciable kick factors. The frequencies and quality factors given here are results from

† Supported by the U.S. Department of Energy grant number DE-AC03-76SF00515

LINAC ALIGNMENT AND FREQUENCY TOLERANCES FROM THE PERSPECTIVE OF CONTAINED EMITTANCES FOR THE G/NLC

R.M. Jones†, SLAC, Stanford, CA 94309, USA

Abstract

The next generation of linear colliders will consist of several tens of thousands of accelerating structures and this will entail inevitable errors in the dimensions and alignments of cells and groups thereof. These errors result in a dilution of the beam emittance and consequently a loss in overall luminosity of the collider. For this reason it is important to understand the alignment tolerances and frequency tolerances that are imposed for a specified emittance budget. Here we specify an emittance dilution of no more than 10% of the injected nominal value of 20 nm.rads and we track the progress of the beam down the linac whilst accelerating structures (and sub-sections thereof) are misaligned in a random manner. Random frequencies are also incorporated in the misalignment analyses. Tolerances are specified for both frequency errors and misalignment errors.

INTRODUCTION

The main X-band linacs of the G/NLC (Global/Next Linear Collider) [1] are required to sustain an unloaded gradient of 65 MV/m (with a loaded gradient of 55 MV/m) and be able to accelerate 192 bunches of charged particles for almost 14 km. In order to prevent breakdown occurring in the accelerating structures, surface cleanliness, surface electromagnetic fields and several other parameters have been carefully studied and the breakdown events have been reduced to manageable rates [2].

It is also important to minimize the wakefield left behind each accelerated bunch in the train as cumulative BBU [3] or severe emittance dilution [4] will occur. The wakefield is reduced by almost 2 order of magnitude at the first trailing bunch by detuning the cell frequencies such that the characteristic modal frequencies add destructively [5]. However, soon thereafter the wakefield re-coheres and further down the train succeeding bunches would experience a wake large enough to drive a BBU instability. This is prevented by coupling out the wake from each cell to four waveguide-like manifolds [6] that lie co-linear with the axis of the accelerating structure. This method of wakefield damping has been successful in reducing the wakefield for earlier structures [7].

However, the latest structures, motivated by electrical breakdown considerations [2], are a factor of 3 shorter than the original DDS series [5]. Reducing the accelerating structure's length increases the dipole wakefield mode spacing and hence reduces the effectiveness of the overlapping of neighbouring modes. For this reason we interleave the modes of neighbouring structures and effectively fill-in the space between modes in a single structure. The focus herein is on the G/NLC baseline design structure H60VG3S17. This accelerating structure is 60 cm in length and consists of 55 cells with an initial fundamental group velocity of 0.03c. The average iris to free space wavelength is 0.17.

The final emittance of the beam can be diluted by a beam injected off axis (injection offset) and by misalignment of cells. Space considerations prevent the former being presented. However, we refer the interested reader to [8] for some details on the remarkably loose frequency tolerances for a beam subjected to an injection offset.

Here we investigate the emittance growth due to long-range transverse wakefields for misaligned cells in the accelerator structure. We study the case of a beam injected on-axis but with misaligned cells (and groups thereof). In particular, we include frequency errors and calculate their impact on misalignment tolerances.

The paper is organized such that the next section discusses the wakefield of the G/NLC baseline design and the second main section analyzes misalignment tolerances.

TRANSVERSE WAKEFIELDS

The G/NLC baseline design uses four-fold interleaving of the dipole frequencies of accelerator structures [9]. The dominant first dipole band wake [10] that results from this process is illustrated in Fig. 1. For the sake of comparison, the decay in the envelope of the wakefield that occurs due to purely Ohmic damping together with that which occurs due to detuning the cell frequencies is also shown. Detuning the cell frequencies gives rise to destructive interference of the modes and results in the

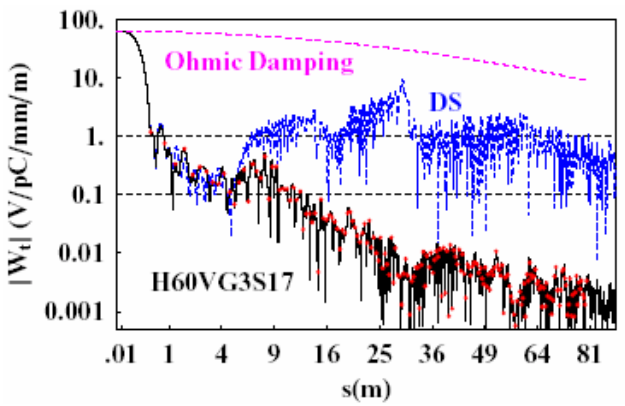

Figure 1: Envelope of the four-fold interleaved long-range transverse wakefield $|W_t|$ for H60VG3S17. The red dots indicate the location of each bunch. Also shown, in blue, is the wake that results from detuning only (DS), and in magenta, the decay of the wake that results from copper losses in the cells (Ohmic damping).

† Supported by the Department of Energy, grant number DE-AC03-76SF00515

THE IMPACT OF LONGITUDINAL DRIVE BEAM JITTER ON THE CLIC LUMINOSITY

D. Schulte, E. J. N. Wilson, F. Zimmermann, CERN

Abstract

In the Compact Linear Collider (CLIC) now under study at CERN, the RF power which accelerates the main beam is provided by decelerating a high current drive beam. Errors in the timing and intensity of the drive beam can turn into RF phase and amplitude errors that are coherent along the whole main linac and the resulting error of the final beam energy, in combination with the limited bandwidth of the beam delivery system, can lead to a significant loss of luminosity. We discuss the stability tolerances that must be met by the drive beam to avoid this loss. We also examine one of the most important sources of this jitter, which stems from the combination of RF jitter in the drive beam accelerator and subsequent bunch compression. Finally we give details of a potential feedback system that can reduce the drive beam jitter.

MAIN LINAC RF JITTER TOLERANCE

The RF can jitter in phase and amplitude; both result in a change of the effective gradient. The RF jitter tolerance is given by two main constraints. First, the luminosity loss should be limited to less than 2%. Second, the energy jitter should not lead to a significant widening of the luminosity spectrum at collision. Since the mean RF phase in the linac is about 15°, a coherent error of the RF phase all along the main linac of 0.225° corresponds to an effective gradient error of about $\Delta G/G \approx 10^{-3}$. The final energy error and the luminosity loss will be quite similar in the two cases.

In CLIC the single bunch RMS energy spread is about $\sigma_E/E \approx 3.5 \times 10^{-3}$. Consequently a beam energy jitter of $\sigma_{jitt}/E \approx 1 \times 10^{-3}$ leads to a negligible broadening of this spread, while $\sigma_{jitt}/E = 2 \times 10^{-3}$ results in probably acceptable but noticeable change of the total spread to $\sigma_E/E \approx 4 \times 10^{-3}$. We prefer to aim for $\sigma_{jitt}/E \leq 10^{-3}$.

To estimate the luminosity loss resulting from the RF jitter integrated simulations of the main linac, beam delivery system and beam-beam interaction have been performed, using PLACET [1] and GUINEA-PIG [2]. It has been found that the jitter tolerance arising from the luminosity loss due to multi-pulse emittance growth in the main linac is more relaxed than that from the above energy stability [3]. However, the limited bandwidth of the current beam delivery system results in a tighter energy error tolerance of $\sigma_{jitt}/E = 0.7 \times 10^{-3}$ for 2% luminosity reduction [5], see Fig. 1. This limitation is to a large extent due to the collimation system. Removing it from the simulation yields a tolerance of $\sigma_{jitt}/E = 1.2 \times 10^{-3}$.

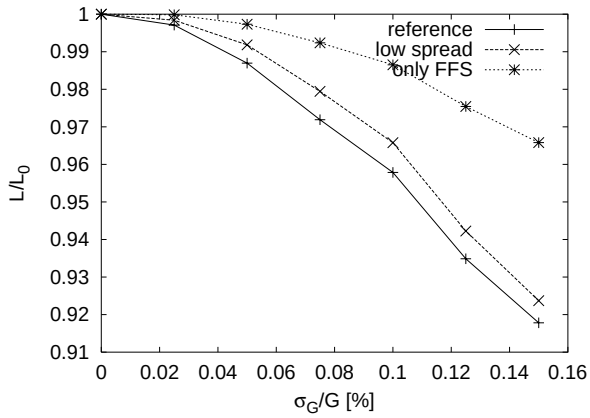

Figure 1: The relative luminosity as a function of a coherent gradient error in the main linac.

Table 1: Some important drive beam parameters.

parameter	symbol	unit	value
particles per bunch	N	$[10^{10}]$	6
energy before DBA	E_0	[MeV]	50
energy after BDA	E_f	[MeV]	2000
bunch length before DBA	$\sigma_{z,0}$	[mm]	4
bunch length after DBA	$\sigma_{z,f}$	[mm]	0.4

DRIVE BEAM TOLERANCES

The RF phase and amplitude in the main linac depends directly on the drive beam; the drive beam intensity and phase tolerances are hence $\delta I/I \leq 10^{-3}$ and $\delta\Phi \leq 0.225^\circ$ (equivalent to $\delta z \leq 6\mu\mathrm{m}$), respectively. After a short overview of the drive beam generation system one of the main jitter generation mechanisms will be discussed, focusing on coherent errors of the whole drive beam.

The drive beam is generated in a complex that is located centrally between the two linacs, for parameters see table 1. Each $92\mu\mathrm{s}$ long drive beam pulse is produced in the drive beam injector complex and then accelerated in the drive beam accelerator (DBA), with an RF frequency of $30.0/32\mathrm{GHz} = 937\mathrm{MHz}$. In a delay loop the pulse is then split into $130\mathrm{ns}$ long sub-pulses. At the end of the delay loop these pulses are pairwise merged forming new pulses of $130\mathrm{ns}$ length but with twice the previous bunch frequency. In two following combiner rings 16 of these new pulses are again merged, increasing the beam intensity as well as the bunch frequency by another factor of 16. Each of the generated 22 pulses is then sent through a transport line to the start of one drive beam decelerator, where it will arrive in time to produce the RF power needed for the main beam.

ELECTRON-CLOUD EFFECTS IN THE POSITRON LINACS OF FUTURE LINEAR COLLIDERS

A. Grudiev, D. Schulte, F. Zimmermann, CERN; K. Oide, KEK

Abstract

Inside the rf structures of positron (or electron) linacs for future linear colliders, electron multipacting may occur under the combined influence of the beam field and the electro-magnetic rf wave. The multipacting can lead to an electron-cloud build up along the bunch train. Electrons are also created by collisional and field ionization of the residual gas. We present simulation results of the electron build up for various proposed designs, and discuss possible consequences.

INTRODUCTION

Table 1 lists beam and rf parameters for the linacs of 3 different linear-collider projects. In the following, we discuss the primary-electron generation, electron accumulation and multipacting under the influence of beam and rf fields, as well as mechanisms of emittance degradation.

Table 1: Beam and RF cell parameters

design	TESLA	N(G)LC	CLIC
particles/bunch N_b [10^9]	20	7.5	4
bunch spacing $L_{\rm sep}$ [ns]	337	1.4	0.67
rms bunch length σ_z [μm]	300	110	35
initial energy E_b [GeV]	5	8	9
rms hor. size σ_x [μm]	260	57	14
rms vert. size σ_y [μm]	11	6	2
norm. h. emit. $\epsilon_{N;x}$ [μm]	8	3.6	0.55
norm. v. emit. $\epsilon_{N;y}$ [nm]	20	40	5
beta function $\beta_{x,y}$ [m]	80	14	5
pressure [ntorr]	10	10	10
frequency $f_{\rm rf}$ [GHz]	1.3	11.42	30
radius R [mm]	107	10.4	4
cell length L [mm]	115	7.5	3.3
rf wave length $\lambda_{\rm rf}$ [mm]	230	26	10
field E_0 [MV/m]	23.4	45.1	150

IONIZATION RATES

Primary electrons are created by ionization of the residual gas. The collisional ionization cross section $\sigma_{\rm ion}$ is abut 2 Mbarn for nitrogen or carbon monoxide molecules at utrarelativistic beam energies, yielding 6×10^{-8} electrons per meter and per positron for a pressure of 10 ntorr. Another ionization process that can become important in linear colliders is field ionization [1]. In the quasistatic limit, its ionization rate is [2, 3]

$$w = 4\omega_0 \left(\frac{E_i}{E_h}\right)^{5/2} \frac{E_a}{E} \exp\left[-\frac{2}{3}\left(\frac{E_i}{E_h}\right)^{3/2}\frac{E_a}{E}\right] , \quad (1)$$

where $\omega_0 = \alpha^2 m_e c^2/\hbar$ is the atomic frequency unit, E_h and E_i are the ionization potentials of hydrogen (13.6 eV) and the gas atom or molecule in question (11.26 eV for carbon monoxide, 14.5 eV for nitrogen), and $E_a = m_e c^2\alpha^4/(r_e e)$ is the atomic unit of the electric field. A different formula whose numerical evaluation yields similar results was given in [1]. The ionization probability is further enhanced at high frequencies [4], i.e., for short bunch lengths σ_z and large ionization energies E_i [3], namely at $E_i > e^2E_0^2\sigma_z^2/(4m_ec^2)$; the right-hand side is 24.1 eV for TESLA, 12.0 eV for NLC/GLC and 13.5 eV for CLIC. Field ionization may also occur for electron beams and could there enhance fast beam-ion instabilities. The probability of field ionization rises steeply from 0 to 1 at a field of about 20 GV/m. Such beam fields are expected at higher beam energies in CLIC and possibly in NLC/GLC. Assuming that, at 500 GeV/c, the beam is ionized within a few rms beam sizes, the ionization rate amounts to the production of several 10^7 electrons per meter and per passing bunch, which is some orders of magnitude more than from collisional ionization. The progress of field ionization over successive bunches depends on the thermal motion of molecules. At room temperature, the rms vertical distance travelled by a gas molecule between two successive bunches is about 0.3–1 σ_y for CLIC, and larger for the other designs.

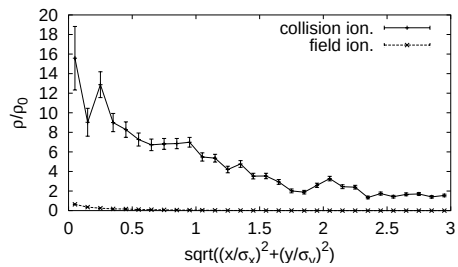

Figure 1: Electron density in units of local gas density as a function of the radial position in units of 0.1σ during a bunch passage at the end of the CLIC linac for collisional and field ionization.

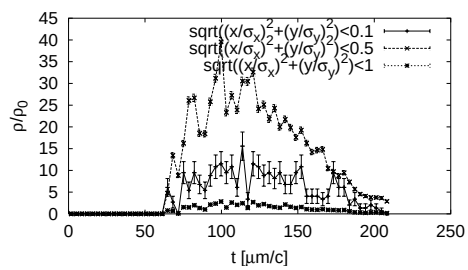

Figure 2: Average electron density, inside the 3 ellipses defined by $((x/\sigma_x)^2+(y/\sigma_y)^2)^{1/2}$ equal to 0.1, 0.5 and 1, in units of the local gas density as a function of time during the passage of a CLIC bunch with field ionization.

Figure 1 shows the radial distribution of electrons during a bunch passage at the end of the CLIC linac. The com-

A POTENTIAL SIGNAL FOR LUMINOSITY OPTIMISATION IN CLIC

D. Schulte, CERN, Geneva, Switzerland

Abstract

Luminosity optimisation will be challenging in the compact linear collider (CLIC) studied at CERN. In particular, the signals which can be used for luminosity optimisation need to be identified. The strong beam-beam interaction in CLIC will give rise to the emission of a few megawatts of beamstrahlung; this is a potential candidate for such a signal. In this paper luminosity optimisation using the beamstrahlung is attempted for realistically shaped bunches.

INTRODUCTION

In the Compact Linear Collider (CLIC) [1], very small emittance beams are focused to a vertical spot size of about $0.7\mathrm{nm}$ in the interaction point, see table 1. The collision parameters, such as collision offset and angle, need to be carefully tuned in order to maximise luminosity. In order to optimise these parameters a fast luminosity signal is needed. Three candidate processes that could provide such a signal have been investigated in [3], beamstrahlung, bremsstrahlung and incoherent pair creation. In CLIC also a fourth process, the coherent pair creation is significant enough to be used as a signal.

Beam-Beam Interaction and Beamstrahlung

Due to the high beam density at collision each beam produces strong electro-magnetic fields, which focus the oncoming beam. The resulting acceleration of the particles towards the beam axis leads to a reduction of the effective beam size during collision, which results in increased luminosity. However, this acceleration also leads to the emission of beamstrahlung, a process comparable to the emission of synchrotron radiation in a magnetic field. Due to this effect, each particle emits on average about 1.5 photons, which carry away about 20% of the particle energy. The total energy of the photons depends on the dimensions and charges of the beams but also on other parameters, e.g. their relative offsets.

Bremsstrahlung

The bremsstrahlung or radiative Bhabha scattering has frequently been used for luminosity measurements. If two charged particles collide the exchange of a virtual photon can induce the emission of a real photon by one of the beam particles and hence a significant energy loss. The emitting particles receive little transverse kick and needs to be seperated from the beam by use of dispersion. In CLIC, these particles cannot be distinguished from beam particles which lost most of their energy by emission of beamstrahlung.

Incoherent Pair Creation

Two colliding beamstrahlung photons can produce a secondary electron-positron pair. Equivalently a pair can be produced by the collision of a photon and an electron or positron, in which case the original electron or positron is preserved. Finally a colliding electron-positron pair can create an additional pair. The total number of these particles is of the order of 10^5 per bunch crossing and most of them have small transverse momenta at production but are deflected by the beam fields. The electron of the pair can either fly into the direction of the electron or the positron beam. If it follows the electron beam it will be focused by the positron beam. If it flies in the other direction it will be deflected away from the axis by the electron beam. The pair particles can therefore reach quite large angles. This makes it possible to detect them at some distance from the beam. While the total number of pairs depends on many variables it is strongly dependent on the luminosity. By measuring the integrated energy of the pairs above a certain angle with respect to the beam axis it is thus possible to obtain a signal for luminosity optimisation [2][3]. The procedure consists of modifying one beam parameter at the time (e.g. the longitudinal position of the waist) and aiming to maximise the pair signal. In the case of CLIC the low energy tail of the particles from coherent pair creation may mask the incoherent pairs.

Coherent Pair Creation

In a very intense field the beamstrahlung photons can directly turn into an electron-positron pair. This is called coherent pair production because the photon interacts with the coherent field of the oncoming particles. The number of these pairs depends strongly on the field strength; in the case of CLIC it is only one order of magnitude smaller than the number of original beam particles.

The coherent pairs are deflected by the beam fields in the same way as the incoherent ones. The coherent pairs add a significant positron component to the spent electron beam and vice versa, which can easiliy be seperated from the rest of the spent beam using a dipole field. The power of the coherent pairs will in many cases depend in a similar fashion on the beam properties as the beamstrahlung, so it can also be used as a tuning signal. The relative changes

EXPERIMENTAL INVESTIGATION OF THE LONGITUDINAL BEAM DYNAMICS IN A PHOTOINJECTOR USING A TWO-MACROPARTICLE BUNCH

R. Tikhoplav, A.C. Melissinos, University of Rochester, Rochester, NY 14627, USA
P. Piot, Fermi National Accelerator Laboratory, Batavia IL 60510, USA
N. Barov, D. Mihalcea, Northern Illinois University, DeKalb, IL 60115, USA

Abstract

We have developed a two-macroparticle bunch to explore the longitudinal beam dynamics through various component of the Fermilab/NICADD photoinjector laboratory. Such a two-macroparticle bunch is generated by splitting the photocathode drive laser impinging the photocathode. The presented method allows the exploration of rf-induced compression in the 1+1/2 cell rf-gun and in the 9-cell TESLA cavity. It also allows a direct measurement of the magnetic chicane bunch compressor parameters such as its momentum compaction.

INTRODUCTION

Linear accelerators designed to drive FEL-based light sources or advanced accelerator physics R&D experiments (e.g. plasma wakefield accelerators) need to provide small emittance high peak current electron bunches. In order to achieve such high-brightness beams, the bunch, after generation, is generally manipulated both in the transverse (e.g. emittance compensation in photo-injector) and longitudinal (e.g. bunch compression) phase spaces. The beam dynamics associated with such beams is intricate since both external and space charge forces play an important role in the dynamics. It is, therefore, difficult to set-up or optimize the beam manipulation process by simply measuring the bunch properties. Instead, it is first necessary to make sure the lattice is set in a proper way, e.g. as devised by numerical simulations. Directly measuring the lattice properties is generally an easy task in the transverse phase space. However, it is not such an easy matter as far as the longitudinal phase space is concerned. In the present paper we propose a simple method based on generating a bunch that consists of two macroparticles. There are two main advantages of the two-macroparticle method. Firstly, measuring the change of the separation between two macroparticles is much easier than measuring the change of the bunch size. On the other hand the space charge force is negligible for the two-macroparticle case and the evolution of their relative separation is truly a measurement of the longitudinal focussing properties.

EXPERIMENTAL SET-UP

The experimental tests of the two-macroparticle method were performed at the Fermilab/NICADD photoinjector laboratory (FNPL). The bunch length measurement can be performed by a streak camera that streaks optical transition radiation (OTR) pulses emitted as the bunch strikes an Al-coated mirror. An alternative frequency-domain bunch length diagnostics based on Martin-Puplett interferometry of coherent transition radiation is also available. For measurements reported hereafter, only the total power of the CTR emission was detected using a pyroelectric detector. The CTR signal only provide a way to monitor and minimize the bunch length (by maximizing the CTR emission). Downstream of the beamline, the electron beam can be horizontally bent in a dispersive section, to measure the beam energy distribution using a fluorescent screen located downstream at a (horizontal) dispersion of $|\eta_x| = 317\,\mathrm{mm}$.

The double-beam optical set-up used to create a two-macroparticle bunch was initially developed for the witness probe/plasma wake-field experiment. The photoinjector laser beam is split into two and then recombined in such a way that a time-delay is introduced between the two pulses. The delay can be remotely varied from $\sim$7 to $\sim$35 ps. A calibrated potentiometer provide a read-out for the delay between the two pulses. When such double-pulse impinges the photocathode it creates two electron bunches with a time separation much smaller than the rf period (769 ps). Hence both macroparticles fall into the same rf bucket and can be treated as a single bunch. This bunch is henceforth

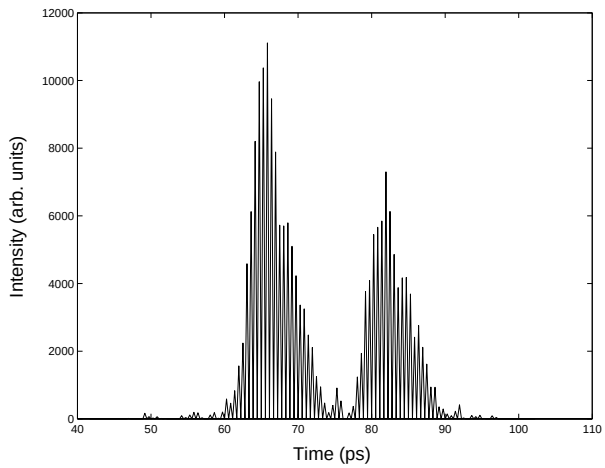

Figure 1: Example of two optical pulse streak camera measurement. The two pulses do not have exactly the same intensity in this measurement.

LIMITING EFFECTS IN THE ROUND-TO-FLAT BEAM TRANSFORMATION

Y.-E Sun*, K.-J. Kim†, University of Chicago, Chicago, IL 60637, USA
P. Piot, FNAL, Batavia, IL 60510, USA

Abstract

In the present paper we study the chromatic effects on transverse beam emittances in the transformation of an angular-momentum-dominated round beam into a flat beam. Analytical results are compared with numerical simulations and found in good agreement. We also attempt to study the effects caused by the asymmetries in the four dimensional transverse phase space distribution.

INTRODUCTION

The theory of generating a beam with high transverse emittance ratio, i.e., a flat beam, from an incoming angular-momentum-dominated beam is treated in several papers [1, 2, 3]. In this paper, we follow the theoretical treatment based on four dimensional beam matrix presented in [4], in which the round-to-flat beam (RTFB) transformation analysis was performed assuming that the beam and the transport channel upstream of the flat beam transformer are cylindrically symmetric and that the particle dynamics is symplectic. The experimental demonstration of such a round-to-flat transformation at Fermilab/NICADD Photoinjector Lab (FNPL) by using a RTFB transformer consists of three skew quadrupole channel is reported in [5].

CHROMATIC EFFECTS

The strength of a quadrupole is related to the particle's momentum. Consider an electron with a small fractional momentum deviation $\delta = \frac{p-p_0}{p_0}$ around the average beam momentum p_0. In practical units, the quadrupole strength q for an electron with momentum p is given by:

$$q[1/\mathrm{m}] = \frac{300g[\mathrm{T/m}]l_{eff}[\mathrm{m}]}{pc[\mathrm{MeV}]} = q_0(1-\delta+\delta^2+\mathcal{O}(\delta^3)),$$

where g the transverse magnetostatic field gradient, l_{eff} is the effective length of the quadrupole and c the speed of light, $q_0[1/\mathrm{m}] \doteq \frac{300g[\mathrm{T/m}]l_{eff}[\mathrm{m}]}{p_0c[\mathrm{MeV}]}$. Correspondingly, in thin lens approximation, the 2×2 transfer matrix M_Q of a normal quadrupole may be written as:

$$M_Q(q,\delta) \approx \begin{bmatrix} 1 & 0 \\ q_0 & 1 \end{bmatrix} + \delta \begin{bmatrix} 0 & 0 \\ -q_0 & 0 \end{bmatrix} + \delta^2 \begin{bmatrix} 0 & 0 \\ q_0 & 0 \end{bmatrix}.$$

Consider a RTFB transformer composed of three skew quadrupoles of strengths q_1, q_2, q_3 and separated dy drift space of lengths d_2 and d_3. The 4×4 transfer matrix of such a transformer takes the form of:

$$M(q_1,q_2,q_3,d_2,d_3) \approx M_0 + \delta\Delta_1 + \delta^2\Delta_2, \qquad (1)$$

where M_0 is the transfer matrix for reference particle with momentum p_0, Δ_1 and Δ_2 are the corrections to the transfer matrix to the first and second order of δ.

The general form of a cylindrically symmetric beam matrix [4] at the entrance of the RTFB transformer is:

$$\Sigma_0 = \begin{bmatrix} \sigma^2 & 0 & 0 & \kappa\sigma^2 \\ 0 & \kappa^2\sigma^2+\sigma'^2 & -\kappa\sigma^2 & 0 \\ 0 & -\kappa\sigma^2 & \sigma^2 & 0 \\ \kappa\sigma^2 & 0 & 0 & \kappa^2\sigma^2+\sigma'^2 \end{bmatrix}, \qquad (2)$$

where $\sigma^2 = \langle x^2\rangle = \langle y^2\rangle, \sigma'^2 = \langle x'^2\rangle = \langle y'^2\rangle, \kappa = \frac{eB_z}{2p}$, B_z is the longitudinal magnetic field on the photocathode and e the electron charge. The beam matrix at the exit of the RTFB transformer is:

$$\Sigma = M\Sigma_0\widetilde{M}, \qquad (3)$$

where $\widetilde{M}$ stands for the transpose of M. Since $\langle\delta\rangle$ vanishes, keeping only the first order modification to the beam matrix, from Eq. 1 and Eq. 3, we have:

$$\Sigma \approx M_0\Sigma_0\widetilde{M_0} + \langle\delta^2\rangle(M_0\Sigma_0\widetilde{\Delta_2} + \Delta_1\Sigma_0\widetilde{\Delta_1} + \Delta_2\Sigma_0\widetilde{M_0}). \qquad (4)$$

Given proper transfer matrix M, the first term of Eq. 4 can be block diagonalized and the two transverse emittances are given by (see, for example, Ref. [4]):

$$\varepsilon^0_{x,y} = \varepsilon_{eff} \mp \mathcal{L}, \qquad (5)$$

where $\varepsilon_{eff} = \sigma\sqrt{\sigma'^2+\kappa^2\sigma^2}$, $\mathcal{L} = \kappa\sigma^2$.

When there is a relative momentum spread in the beam, the beam matrix varies as a function of it. The two transverse emittances can be calculated as the square roots of the determinants of the top left and bottom right 2×2 sub-matrices of the beam matrix expressed in Eq. 4. Let's rewrite the second term of Eq.4 as:

$$\langle\delta^2\rangle \begin{bmatrix} \Delta_{11} & \Delta_{12} \\ \Delta_{21} & \Delta_{22} \end{bmatrix} \doteq \langle\delta^2\rangle(M_0\Sigma_0\widetilde{\Delta_2} + \Delta_1\Sigma_0\widetilde{\Delta_1} + \Delta_2\Sigma_0\widetilde{M_0}). \qquad (6)$$

By using the convenient relation for the determinant of the sum of two 2×2 matrices P and Q,

$$|P+Q| = |P| + |Q| + Tr(P^\dagger Q), \qquad (7)$$

* yinesun@uchicago.edu
† Also APS, ANL, Argonne, IL 60439, USA

GAMMA - RAYS AND X-RAYS PRODUCTION FOR EXPERIMENTS AT ELSA FACILITY

J.-L. Lemaire

CEA/DAM, Bruyères-le-Châtel, France

Abstract

The ELSA facility is a high brightness 18 MeV electron source dedicated to electron irradiation, γ-rays and picosecond hard and soft X-rays. It consists of a 144 MHz RF photo-injector producing short bunches which are further accelerated to an energy varying from 2 to the maximum energy of 18 MeV thanks to three 433 MHz cavities. Former beam compression design used a half turn magnet compressor system. It was recently replaced by a double alpha magnet compressor. Electron beams are now delivered to a new experimental room. We present the new panel of interests offered by this facility in terms of short pulses X-ray production.

INTRODUCTION

The ELSA facility was designed in the late 80's, as a test bench for physics and technology of high efficiency FELs [1]. It consists of a RF photo-injector followed by a linear accelerating structure, a compressor magnet and adapted undulators. After the demonstration of free electron laser operation in the IR range was completed, improvements of the accelerator were needed. Main concerns were on the cavity of the photo-injector and on the stability of the laser system. A renewed cavity was built to fit with ultra high vacuum for photo-cathode life time requirements (10^{-10} mbar is the typical vacuum pressure at present time). The pulse-to-pulse fluctuations of the drive laser which can operate at either 532 nm or 236 nm, depending upon the choice of cathode type, were also solved. In response to new needs, the facility is now mainly used as a high-brightness electron source or as a picosecond hard X-ray source via bremsstrahlung on high Z materials. Due to lack of room to set the experimental devices in the former facility, a contiguous experimental area has been added. In order to achieve short pulses a magnetic compressor was re-design. It is now made of two alpha-magnets type (with field index of 1) [2]. The beam is also tightly radialally focused on production targets. In this ELSA2 facility, new dedicated beam lines built in this experimental area, are now commissioned. This allows to users a panel of versatile experimental conditions with short pulses of electrons, X-rays or γ-rays.

ELSA FACILITY

The ELSA overview facility is presented on figure 1. It is made of a 144 MHz photo-injector delivering for nominal operating conditions, trains of electron bunches at 2.5 MeV. The temporal structure consists of macropulses of 20 to 150μs duration. Maximum repetition rate is 10 Hz. A macropulse is made of 20 ps long micropulses (individual bunch) at a repetition rate of 14.4 MHz (see figure 2). The acceleration is completed by three 433 MHz accelerating cavities. These cavities operate at room temperature. The photo-injector cavity is powered by a tetrode tube supplying 1.5 MW of peak power. This gives an accelerating gradient of 30 MV/m.

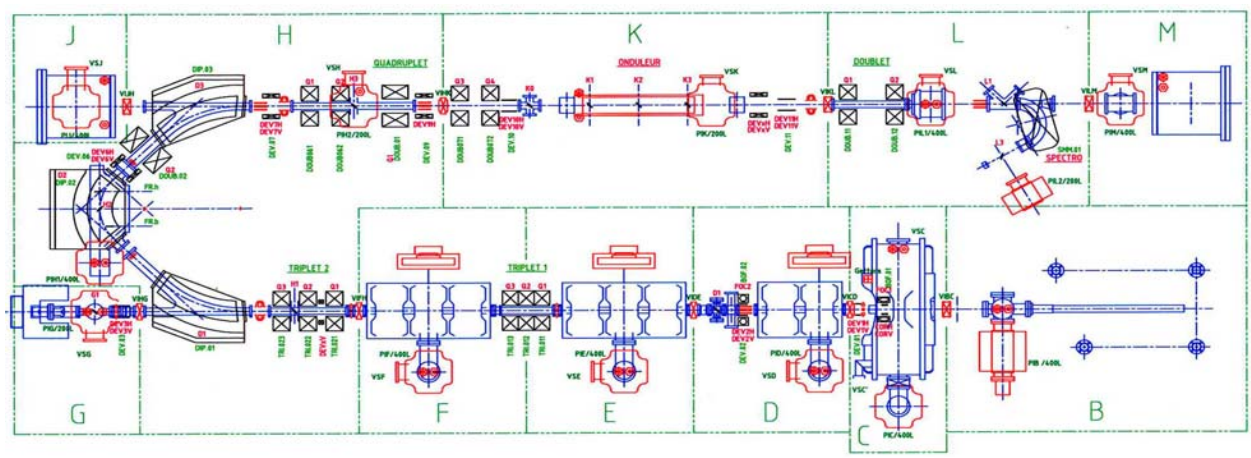

Figure 1: Former overview of the ELSA facility: room size is 12 m x 5 m and beam is bent to 180 ° through a half turn compressor magnet system made of three dipole magnets.

STATUS AND OPERATING EXPERIENCE OF THE TTF COUPLER

D. Kostin, W.–D. Möller, for the TESLA Collaboration, DESY, D-22607 Hamburg, Notkestr. 85

Abstract

Five accelerating modules are installed in the VUV-FEL [1] linac so far. This includes 40 high power couplers connected to the superconducting cavities, eight in a module. All of them are processed and operated up to the cavity performance limits. The coupler processing procedure is described. The performance in relation to the test results on the coupler test stands and the operating experience are discussed.

INTRODUCTION

In the frame of the TESLA Collaboration [2] RF power couplers for superconducting cavities are developed. Three different types [3], [4] of the couplers are fabricated, tested and installed at the 5 modules in the Tesla Test Facility (TTF). The basic design parameters for the TTF couplers are:

- Frequency: 1.3 GHz
- Pulse length: 500 µs rise time, 800 µs flat top with beam
- Repetition rate: 10 Hz
- Coupling: adjustable, Q_{ext}= 10^6-10^7
- Safety: two ceramic windows, protection of the cavity during assembly and against window failures

During the last year the TTF is converted to a Vacuum-Ultra-Violet Free-Electron-Laser (VUV FEL) user facility. The cavities in the 5 modules are processed and operated successfully as described in [5].

Two high gradient tests with electro polished (EP) cavities and TTF3 couplers in the horizontal cryostat (CHECHIA) have been carried out. In these tests the cavity is fully equipped and corresponds to a 1/8th of a module [6].

One of the high gradient EP cavities is installed in the module ACC1 and was tested with beam.

RF COUPLER PROCESSING ON THE TEST STAND AND IN THE HORIZONTAL CRYOSTAT

Prior to the assembly on a cavity all couplers are tested and preconditioned on a test stand at room temperature. On the test stand the couplers are backed at 150 – 200 C and 24 hours. The processing is done with travelling waves. The power is cycled from low to high values, starting with short pulses (20 µs, 2 Hz). After reaching 1 MW the pulse length is doubled and the power rise starts again at low power. This procedure is repeated up to the operating pulse length of 1.3 µs. The rate of the power increase is limited by the different thresholds, set for the coupler vacuum, light and charged particles (e-) in the coupler vacuum. A hardware interlock can switch off the power at high readings of vacuum, light, electrons or ceramic temperature.

The average processing time for such a pair of couplers is 70 to 125 hours (see Fig. 1).

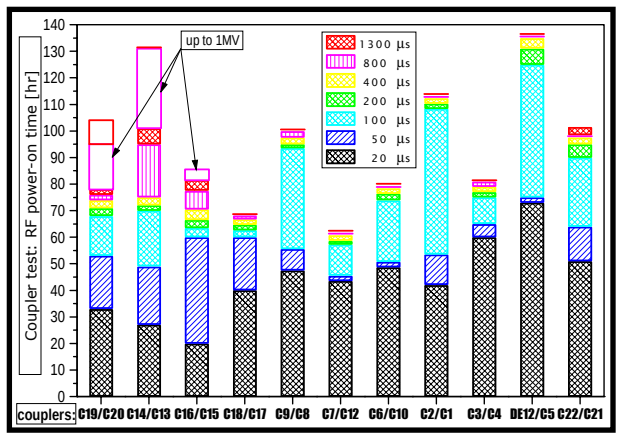

Figure 1: RF Processing times for pairs of couplers on the coupler test stand. The colours distinguish between the different pulse lengths.

After disassembly from the test stand the coupler parts are stored under dry Nitrogen atmosphere.

Due to the limited time schedule, only some of the couplers are tested together with the fully equipped cavities in the horizontal cryostat CHECHIA. Baking of the coupler is done in situ at 150 C and 24 h. The RF processing procedure before cooldown of the cavity is nearly the same that at the test stand.

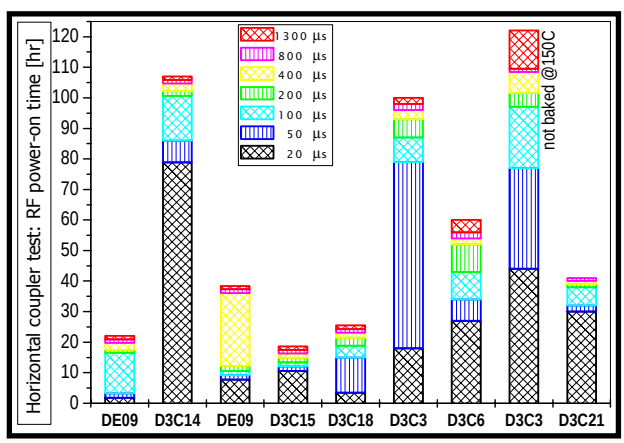

Figure 2: RF processing times for some couplers assembled to the cavities in the horizontal cryostat. The colours distinguish between the different pulse lengths. Without backing the coupler in situ the longest time is needed. Notice the big difference of needed time.

ENERGY SPREAD IN BTW ACCELERATING STRUCTURES AT ELETTRA

P. Craievich, R. J. Bakker, G. D'Auria, S. Di Mitri, Sincrotrone Trieste, Trieste, Italy

Abstract

The FEL project FERMI@ELETTRA will use the existing 1.0 GeV Linac, based on Backward Travelling Wave (BTW) structures, to produce VUV radiation between 100-10 nm. The project will be articulated in two different phases (100-40nm/40-10nm) and will require high quality beam with short bunches (500/160 fsec). Hence, wakefield effects have to be considered with respect to the electron beam quality. The single bunch energy spread induced by the short-range longitudinal wakefield is analyzed and results of start-to-end simulations are reported.

INTRODUCTION

The Fermi@Elettra project aims to construct a single-pass FEL user-facility in the spectral range 100-10 nm using the existing normal conducting 1.0 GeV linac. Fig.1 shows the proposed machine layout for the two phases of the project: FEL-I (100-40 nm) and FEL-II (40-10 nm) [1]. At present the linac is operated less than two hours a day as injector of the storage ring Elettra and, at least for the next two years, until the new injection system will be fully commissioned, this function has to be preserved. This implies that all the activities related to FERMI have to be scheduled without interfering with the normal operation of the machine.

More details on the machine upgrading and layout modifications can be found in [2].

The new scheme for the machine foresees an RF photo-cathode gun [3], providing a high quality electron beam, whose parameters are directly related to the ones required at the entrance of the undulator lines (table 1). Then, a 100 MeV pre-injector, composed by two 3 m accelerating sections with focusing solenoids, get the beam out of the space-charge energy domain and creates an energy-position correlation for bunch compression.

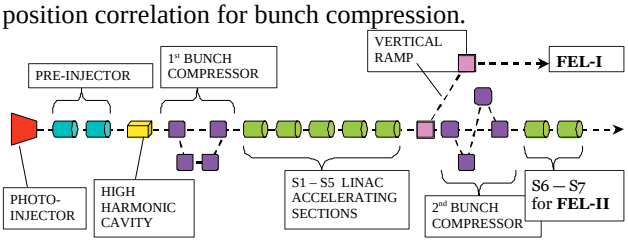

Figure 1: Schematic layout of the configuration for the FEL-I and FEL-II stages.

After the first magnetic chicane, five accelerating structures of the existing linac, equipped with an RF pulse compression system (SLED), allow the beam to reach the target energy required by FEL-I, 700 MeV. In total the present linac includes seven 6 m accelerating sections, 3/4π backward travelling wave (BTW), composed by 164 nose-cone cavities magnetically coupled. The remaining two accelerating sections will be located after the second bunch compression and will be used for the second phase of the project FEL-II up to 1.0 GeV. Quadrupole triplets between the sections provide the necessary transverse focusing. As reported in table 1, FEL operations require a high quality beam with ultra short bunches, hence the wakefield effects have to be considered carefully. That is, the short-range longitudinal wakefields increase the single bunch energy spread, while short-range transverse wakefields may increase the emittance of the bunch.

In this paper the single bunch energy spread induced by short-range longitudinal wakefields and accelerating voltage is analyzed for the FEL-I. The minimum single bunch energy spread at the exit of the linac has been calculated by varying the energy gain and RF phase of the BTW sections. Finally the results have been compared with those obtained from start-to-end simulations with ELEGANT [4] in presence of longitudinal wakefields.

Table 1: Electron beam parameters at the end of the linac for FEL-I and FEL-II

	FEL-I	FEL-II	
Wavelength target	100 40	40 10	nm
Beam energy	0.70	0.55 1.00	GeV
Bunch charge	1.0	1.0	nC
Peak current	0.8	2.5	kA
Bunch duration (σ_t)	500	160	fs
Energy spread (σ_δ)	0.7	1.0	MeV
Emittance	1.5	1.5	μm
Repetition rate	50	50	Hz

LONGITUDINAL DYNAMICS IN FEL-1

The FEL-I wavelengths foresees the acceleration to 700 MeV of a bunch with σ_z=120μm and total charge Q= 1nC at in five BTW sections. Note that with a negligible beam loading each section of the present linac can provide an energy gain up to 170 MeV. The beam energy spread is determined by the accelerating field produced by the external generator and the wakefields excited by the beam in the accelerating structures. For our BTW structures the wake potentials have been numerically evaluated and the wake function obtained by a fitting based on analytical estimations [5]. Figure 2 shows the numerical results obtained for the longitudinal wake potentials of Gaussian bunches with lengths ranging from 1000 μm up to 50 μm (solid lines); the black dashed line represents an analytic approximation of the longitudinal wake function.

As already shown in [6], for a Gaussian bunch the RMS energy spread can be easily evaluated by knowing four integral parameters of the wake fields: the loss factor $K_{\|}$, the average wake energy spread ΔW and the Fourier

NUMERICAL CALCULATION OF COUPLING IMPEDANCES IN KICKER MODULES FOR NON-RELATIVISTIC PARTICLE BEAMS

B. Doliwa, T. Weiland, TEMF, Technische Universität Darmstadt, Germany

Abstract

In the context of heavy-ion synchrotrons, coupling impedances in ferrite-loaded structures (e.g. fast kicker modules) are known to have a significant influence on beam stability. While bench measurements are feasible today, it is desirable to have the coupling impedances in hands already during the design process of the respective components. To achieve this goal, as a first step, we have carried out numerical analyses of simple ferrite-containing test systems within the framework of the Finite Integration Technique. This amounts to solving the full set of Maxwell's equations in frequency domain, the particle beam being represented by an appropriate excitation current. With the resulting electromagnetic fields, one may then readily compute the corresponding coupling impedances. Despite the complicated material properties of ferrites, our results show that their numerical treatment is possible, thus opening up a way to determine a crucial parameter of kicker devices before construction.

INTRODUCTION

Within the design work of the planned heavy-ion synchrotron at the GSI accelerator facility, detailed impedance studies are required. Due to the target vacuum quality of 10^{-12} mbar and particle currents of up to 1 A, beam instabilities would have tremendous effects on the operability of the synchrotron. One unknown is the beam response to the ferrite-loaded kickers. Vice versa, heating of the kicker components may be a problem.

Caspers has addressed the measurement of coupling impedances via the so-called coaxial-wire technique [1], which is most accurate for ultra-relativistic particle beams. The obvious drawback of this approach is that a prototype component has to be at hand. During the design process of new components, therefore, simulations may be helpful.

In this paper we consider the numerical determination of the longitudinal coupling impedance [2]

$$Z_{||}(\omega) = \frac{1}{q^2} \int \mathrm{d}x\mathrm{d}y \rho(x,y) \int \mathrm{d}z E_z(x,y,z;\omega) e^{i\omega z/\beta c} \tag{1}$$

where $\rho(x,y)$ is the transverse charge distribution of the particle beam and $q = \int \mathrm{d}x\mathrm{d}y\rho(x,y)$. The electric field in the above expression is generated by the current density

$$\boldsymbol{J}_{\text{ext}}(x,y,z;t) = \beta c \hat{z} \rho(x,y) \delta(z - \beta c t), \tag{2}$$

which corresponds to an infinitesimally short bunch of particles travelling with velocity βc along the positive z direction. The equivalent expression in frequency domain is

$$\boldsymbol{J}_{\text{ext}}(x,y,z;\omega) = \hat{z} \rho(x,y) e^{-\mathrm{i}\omega z/\beta c}. \tag{3}$$

In the case of kicker impedances, we will restrict ourselves to frequencies below 100 MHz, which are of primary interest for the planned heavy-ion synchrotron.

COMPUTATIONAL APPROACH

In order to determine $Z_{||}$ for a given geometry and excitation current we need to calculate the electric field. Our starting point is

$$\boldsymbol{\partial} \times \nu \boldsymbol{\partial} \times \boldsymbol{E} - \omega^2 \epsilon \boldsymbol{E} = -\mathrm{i}\omega \boldsymbol{J}_{\text{ext}},$$

a descendant of Maxwell's equations in frequency domain. Here $\nu \equiv 1/\mu$, with possibly complex permeability μ and ϵ denoting permittivity.

Within the Finite Integration Technique[3], we carry out an appropriate discretization, which leads to a matrix counterpart of the former equation,

$$\left(\tilde{\boldsymbol{C}} M_\nu \boldsymbol{C} - \omega^2 M_\epsilon \right) \boldsymbol{e} = -\mathrm{i}\omega \boldsymbol{j}_{\text{ext}}. \tag{4}$$

In the presence of ferrites, this system of linear equations may become highly ill-conditioned due to the large jumps in permeability. We therefore do not attempt to solve the matrix equation as a whole but proceed as follows: Firstly, an electrostatic problem is solved yielding a divergence-free source term $\boldsymbol{j}'_{\text{ext}}$ and the 'static' part of the electric field solution. We then note that, at low enough frequencies, the term $\omega^2 M_\epsilon \equiv b$ is small compared with $\tilde{\boldsymbol{C}} M_\nu \boldsymbol{C} \equiv B$ (in the sense of some matrix norm). One may then expand the solution in terms of bB^{-1} (symbolically). It has turned out in our simulations that keeping up to six terms of this series expansion is sufficient (below 100 MHz). The inversion of the matrix B in each expansion term formally corresponds to solving a standard magnetostatic problem, which will therefore not be discussed here.

We finally remark that simulations are carried out using the software tools CST MICROWAVE STUDIO®[4] and MATLAB [5].

BOUNDARY CONDITIONS

One problem in modelling an elementary particle beam traversing an accelerator component is the question of appropriately chosen boundary conditions. This is crucial since the fourier transform of a short bunch, Eq. 3, extends from $z = -\infty$ to $+\infty$. Since our computational domain is finite we have to take one of the following options:

- open boundary conditions, e.g. by using perfectly-matched layers[6]
- periodic boundary conditions

WIRE MEASUREMENT OF IMPEDANCE OF AN X-BAND ACCELERATING STRUCTURE†

N. Baboi, DESY, Hamburg; R.M. Jones, J.R. Lewandowski, G.B. Bowden,
S.G. Tantawi, V.A. Dolgashev, J.W. Wang, SLAC, Stanford, USA

Abstract

Several tens of thousands of accelerator structures will be needed for the next generation of normal conducting linear colliders known as the GLC/NLC (Global Linear Collider/Next Linear Collider). To prevent the beam being driven into a disruptive BBU (Beam Break-Up) mode or at the very least, the emittance being significantly diluted, it is important to damp down the wakefield left by driving bunches to a manageable level. Manufacturing errors and errors in design need to be measured and compared with prediction. In this paper a bench-top method of measuring transverse impedances in X-band accelerating structures is described. Utilizing an off-axis wire the S parameters are measured and converted to impedance. Measurements in a damped and detuned structure built for GLC/NLC are presented and the results are discussed.

INTRODUCTION

One option in building a next generation of linear collider is to use normal conducting X-band accelerating structures. These structures have been carefully designed and studied for over a decade for the GLC/NLC [1]. One main concern in their design is the minimization of wakefield effects. Wakefields are excited by charged particles in the accelerating structures and influence the motion of subsequent particles or bunches. In particular, transverse fields are of concern, as they cause large increase in the emittance or, in the worst case, BBU [2].

To prevent this, the frequencies of the modes which comprise the wakefield are forced to add de-constructively by detuning the frequencies of the cells. Initially the wake decays with a Gaussian functional form. However, as there are a finite number of cells, eventually the modes must add coherently. This causes the wakefield to rise to unacceptably large values. To prevent this from occurring, a fraction of the wake is coupled out to four manifolds, which run collinear with the axis of the accelerator. Several such damped and detuned structures have been built and studied. The most advanced in this series is the RDDS1 (rounded damped detuned structure) [3]. It has a length of 1.8 m with a $2\pi/3$ phase advance per cell. A 60 cm accelerator structure with a $5\pi/6$ phase advance per cell is currently being fabricated [4].

Even though electromagnetic field simulation codes as well as circuit models have proven to give accurate results, the increasing complexity of the structures requires wakefield measurements to be performed in order to be sure that the fabricated structures behave as expected. Previously, the main setup for such measurements in GLC/NLC structures has been the ASSET facility [5], where transverse fields are excited and sampled by a beam. Although this method is quite precise, it has the drawback of requiring expensive beam time at an accelerator facility.

An alternative and somewhat complementary method is the wire method [6,7]. Here a metallic wire takes the place of the beam and a high frequency measurement is conducted in the laboratory. The fundamental idea behind the wire method is to simulate the beam-structure interaction by propagating a short current down a wire inserted in an accelerating structure.

Alternatively, one can measure the transmission curve in the frequency domain in order to study the transverse impedance, which is related to the wakefield $W_\perp$ by:

$$Z_\perp(\omega) = \frac{-i}{c}\int_{-\infty}^{\infty} W_\perp(\zeta)\exp\left(-i\omega\frac{\zeta}{c}\right)d\zeta\,, \qquad (1)$$

where ω is the angular frequency and c the light velocity. In the frequency domain one can distinguish the individual resonances of the structure, the higher order modes (HOM), constituting the wakefield:

$$W_\perp(\zeta) = \sum_n 2k_{\perp,n}\sin\left(\omega_n\frac{\zeta}{c}\right)\exp\left(-\frac{\omega_n}{2Q_n}\frac{\zeta}{c}\right). \qquad (2)$$

Here ω_n, Q_n and $k_{\perp,n}$ are the angular frequency, quality factor and kick factor of mode n.

In our measurements we chose to measure in the frequency domain. For transverse wakefields, two wires placed symmetrically around the axis have been used previously. This kind of measurement has the advantage of decoupling the odd and even modes. On the other hand, aligning the two wires may be rather difficult, particularly for X-band structures. For this reason we chose to use a single off-axis wire for our measurements.

In the next section we present the setup, built at SLAC, to measure transverse wakefields. The measurements made in RDDS1 are described in the final main section.

METHOD

Setup

Fig. 1 shows the setup of the wire measurement. A wire of diameter 300 μm is placed at an offset in the device

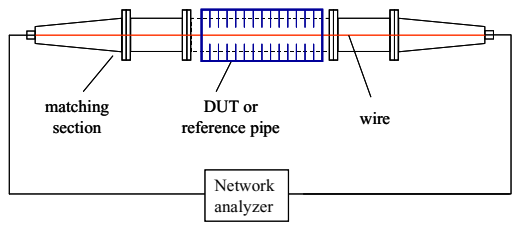

Figure 1: Sketch of the wire measurement setup.

† Supported by the U.S. DOE grant number DE-AC03-76SF00515

SIMPLE THEORY OF THERMAL FATIGUE CAUSED BY RF PULSE HEATING

S.V. Kuzikov, Institute of Applied Physics, Russian Academy of Sciences, Nizhny Novgorod, Russia

Abstract

The electron-positron linear colliders projects imply that accelerating structures and other RF components will undergo action of extremely high RF fields. Except for electrical the breakdown threat there is an effect of the copper surface damage due to multi-pulse mechanical stress caused by Ohmic losses in the skin layer [1].

A new theory of the thermal fatigue is presented. The theory is based on the consideration of the quasi-elastic interaction between neighborhood grains in the metal due to the thermal expansion of the skin-layer. With a proposed method one can estimate a total number of the RF pulses needed for surface to fracture depending on temperature rise, pulse duration, and average temperature. The parameters necessary for the final equation were found, using experimental data points obtained at 11.4 GHz for the copper [2]. Experimental studies of the pulsed heating fatigue of the copper surface at 30 GHz are also under way [3].

FATIGUE MODEL

The copper crystal has a cubic structure. Ideally, each atom has 6 links with neighbors (Fig. 1). Probability to break any link is given by next equation:

$$p_j = \exp\left(-\frac{U_c}{k_B T_c}\right), \qquad (1)$$

which shows that the higher the temperature the higher the probability. Here U_c – energy of the coupling of the atoms, T_c is a stationary temperature, and k_B is a Boltzman's constant. If T_c>0, the probability is not zero and there are some broken links. Should mention that because of (2), the value of p_j is rather small for the temperatures less than metal melting point.

$$\frac{U_c}{k_B T_c} >> 1, \qquad (2)$$

.

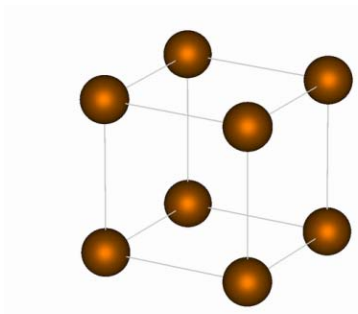

Figure 1: Structure of copper's crystal.

However, real copper has many defects. In particular, any bulk copper consists of grains (Fig. 2). Energy of coupling between grains is weak compared to the ideal crystal, and there is certain expansion of the grains if surface is hot.

During RF pulse, the Ohmic skin layer δ_{ohm} represents a thermal source. A thin layer of copper δ_T, which is exposed to the temperature increase, is a thermal skin layer. Next we suggest that the thermal skin layer is significantly smaller than the typical size of the individual copper grain. In this case the expansion in the thermal skin layer brings to situation when grains start to push each other (Fig. 3). As a result, additional elastic forces come to scene, thus increasing the probability to break links between atoms.

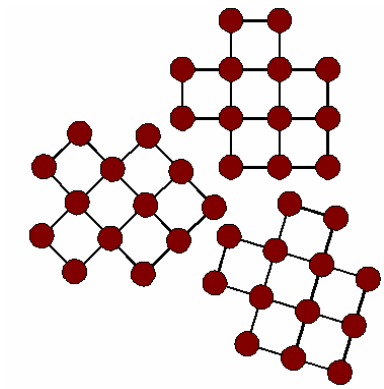

Figure 2: Schematic view of copper's grain structure.

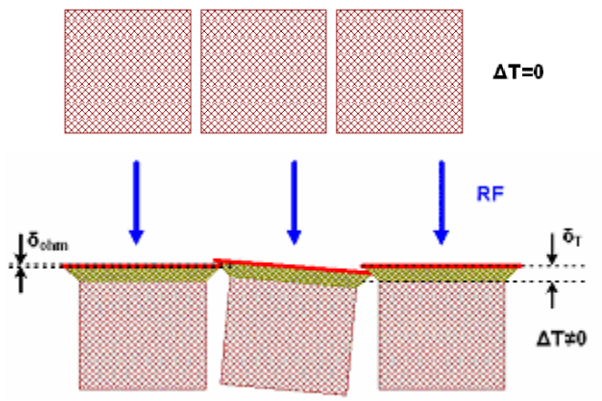

Figure 3: Interaction of grains under pulse RF heating.

High Temperature Region Approach

In the presence of the elastic forces the equation (1) has to be modified:

$$p_j = \exp\left(-\frac{U_c - \overline{U}}{k_B T_c}\right), \qquad (3)$$

where $\overline{U}$ is an energy of the external forces breaking the given link. In assumption that individual grain has n_s links with the other grains, the probability to break all these links can be expressed as:

CALCULATION OF RF PROPERTIES OF THE THIRD HARMONIC CAVITY

K. Rothemund†, D. Hecht, U. van Rienen, Universität Rostock, Institut für Allgemeine Elektrotechnik, D – 18051 Rostock, Germany

Abstract

Recently a third harmonic structure has been proposed for the injector of the TTF-FEL to avoid nonlinear distortions in the longitudinal phase space. This structure consists of four nine cell TESLA-like cavities. For the use of this structure in combination with the TTF-FEL it might be interesting to investigate higher order modes (HOM) in the structure and their effect on the beam dynamics. In the 5th dipole passband one mode with a frequency around 9.05 Ghz was found to be almost trapped in the cavity with very small fields in the end cells and the beam pipes. CST MicrowaveStudio® (MWS) and Coupled S-Parameter Calculation (CSC) have been applied to investigate this frequency range. The CSC method [1] is based on the scattering parameter description of the rf components found with field solving codes or analytically for components of special symmetry. This paper presents the results of the calculation of frequencies and field distributions of dipole modes in the frequency range around 9.05 GHz.

INTRODUCTION

A 3.9 GHz 3rd harmonic superconducting section for the photoinjector of the TTF 2 has been proposed [2] and designed [3] recently. This section consists of four nine cell cavities. Its purpose is to correct for nonlinearities of the longitudinal phase space to produce highly charged bunches. The basic rf parameters for many monopole, dipole and quadrupole modes for one nine cell cavity of the 3rd harmonic section have been calculated [4] using MAFIA eigenmode solver [5]. As a result of these calculations a dipole mode in the frequency range around 9.05 GHz was found which has almost no electric field in the beam pipes and even in the cavity end cells. Therefor this mode might be difficult to be damped by the HOM-couplers.

This paper presents the first results of CSC calculations of frequencies and field distributions for dipole modes in this frequency range and compares the results with the results of calculations done with CST Microwave-Studio® [5] for the same frequency range.

CSC THEORY

The reflection and transmission of waves between the ports of any rf system can be described by scattering-parameters (S-parameters). In general, each S-parameter is a complex function of the frequency containing information about amplitude and phase. S-parameters can be represented by the scattering matrix **S**:

$$\mathbf{b}_k = \mathbf{S}_k\,\mathbf{a}_k \qquad (1)$$

with the vectors $\mathbf{a}_k$ and $\mathbf{b}_k$ describing all input- and output-signals of the k-th object, respectively.

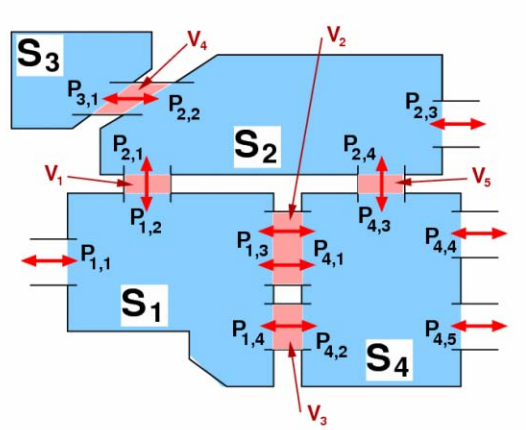

Figure 1: Complex rf-structure consisting of four substructures S_1, S_2, S_3, S_4, connected to each other by the connections V_1, V_2, V_3, V_4, with external ports $P_{1,1}$, $P_{2,3}$, $P_{4,4}$, $P_{4,5}$ and internal ports $P_{1,2}$, $P_{1,3}$, $P_{1,4}$, $P_{2,1}$, $P_{2,2}$, $P_{2,4}$, $P_{3,1}$, $P_{4,1}$, $P_{4,2}$, $P_{4,3}$.

For a complex structure consisting of several subsections the S-parameters of all subsections are arranged in a block diagonal matrix **S**:

$$\mathbf{b} = \mathbf{S}\,\mathbf{a} = \begin{pmatrix} \mathbf{S}_1 & \cdots & \mathbf{0} \\ \vdots & \ddots & \vdots \\ \mathbf{0} & \cdots & \mathbf{S}_N \end{pmatrix} \begin{pmatrix} \mathbf{a}_1 \\ \vdots \\ \mathbf{a}_N \end{pmatrix} = \begin{pmatrix} \mathbf{b}_1 \\ \vdots \\ \mathbf{b}_N \end{pmatrix} \qquad (2)$$

Next all incident signals are collected in a vector $\mathbf{a}_{inc}$ and all signals travelling from one subsection into a neighbouring subsection are grouped together in a coupling vector $\mathbf{a}_{cop}$. These rearrangements are performed by two permutation matrices **P** and **F**:

$$\mathbf{a} = \mathbf{P}\begin{pmatrix} \mathbf{a}_{cop} \\ \mathbf{a}_{inc} \end{pmatrix} \quad ; \quad \begin{pmatrix} \mathbf{a}_{cop} \\ \mathbf{a}_{sct} \end{pmatrix} = \mathbf{P}^{-1}\,\mathbf{F}\,\mathbf{b} \qquad (3)$$

$\mathbf{a}_{sct}$ is the vector of all signals leaving the structure at the external ports. These signals are kept untouched. The combination of the above equations yields:

$$\begin{pmatrix} \mathbf{a}_{cop} \\ \mathbf{a}_{sct} \end{pmatrix} = \underbrace{\mathbf{P}^{-1}\,\mathbf{F}\,\mathbf{S}\,\mathbf{P}}_{\mathbf{G}} \begin{pmatrix} \mathbf{a}_{cop} \\ \mathbf{a}_{inc} \end{pmatrix} \qquad (4)$$

where the matrix $\mathbf{G} = \mathbf{P}^{-1}\mathbf{F}\mathbf{S}\mathbf{P}$ describes the structure of the whole system. According to the dimensions of vectors $\mathbf{a}_{cop}$, $\mathbf{a}_{sct}$ and $\mathbf{a}_{inc}$ this system matrix **G** can be split into submatrices:

† karsten.rothemund@etechnik.uni-rostock.de

TESLA RF POWER COUPLER THERMAL CALCULATIONS

Dohlus M., Kostin D., Möller W.-D., DESY, D-22607 Hamburg, Germany

Abstract

The main RF power coupler is one of the key elements of the accelerating module for the superconducting linac. It provides RF power to the cavity and interconnects different temperature layers in the module. Therefore statistical and dynamical thermal losses have to be optimised. Different operating modes as well as geometries were investigated. Coupler design optimisation studies are carried out for TESLA and for the XFEL case. Especially long pulse operation for the XFEL is being investigated.

THEORETICAL BACKGROUND

Heat Conduction Equations

The general heat conduction equation (see Eq. 1) for the steady state in one dimension becomes the Eq. 2, *P* is internal heating power source, λ - thermal conductivity, ν - material index.

$$\rho C_p \frac{\partial T}{\partial T} = \nabla(\lambda \nabla T) + \frac{dP}{dV} \tag{1}$$

$$\frac{dT}{dz} = R'(z,T(z)) \cdot p(z),\ R'(z,T) = \left(\sum_{\nu} A_{\nu}(z) \lambda_{\nu}(T) \right)^{-1} \tag{2}$$

The thermal resistance *R(z,T)* describes the thermal properties of the material, it can be calculated as:

$$R_i(T_a,T_b) = (T_b - T_a) \frac{l}{A} \Big/ \int_{T_a}^{T_b} \lambda(T) dT \text{ , } l \text{ - length} \tag{3}$$

The radiational thermal resistance is (k_{em} is the emissivity and σ - Boltzmann constant 5.67×10^{-8}):

$$R_{rad}(T_1,T_2,A_{rad}) = \frac{T_1 - T_2}{A_{rad}(T_1^4 - T_2^4) k_{em} \sigma} \tag{4}$$

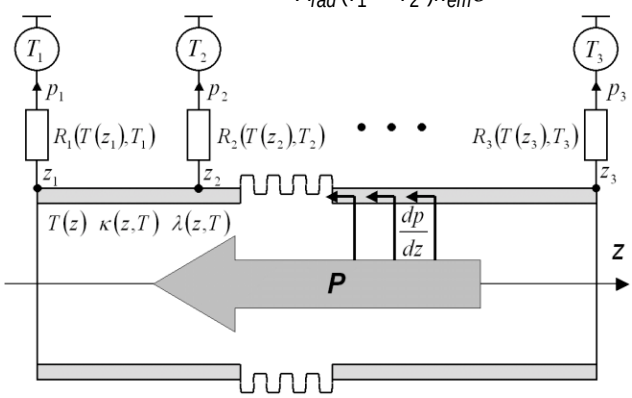

Figure 1: The Boundary Problem.

The problem to solve is a boundary problem with internal power sources introduced by RF power losses and fixed temperature points as boundary conditions (see Fig. 1). RF power losses was calculated using MAFIA and recalculated using Eq. 5, where κ is the electrical conductivity. The coupler bellows are simulated by geometry coefficient *gb(z)>1* (ratio of the material length along the bellow surface to the bellow length, see Eq. 6).

$$\frac{dp}{dz} = \underbrace{\left(\frac{dp}{dz}\right)}_{\substack{\kappa=\kappa_0,\\ P=P_0\\ \text{MAFIA}}} \cdot \frac{P}{P_0} \cdot \sqrt{\frac{\kappa_0}{\kappa(z,T)}} \tag{5}$$

$$\frac{dT}{dz} = R'(z,T(z)) \cdot p(z) \cdot gb(z),\quad gb(z) = \frac{d\tilde{z}}{dz} \tag{6}$$

Numerical Solution

The coupler was simulated by set of discrete elements (see Fig. 2) similar to the electrical circuits, in this case the resistive elements are the thermal resistances, currents are power flows and voltages are the temperature differences (see Eq. 7), for element ***n*** one can write Eq. 8. and for the whole system the matrix equation with tridiagonal matrix **G**(**t**) (see Eq. 9), solved using method of iterations in MathCAD (See Eq. 10).

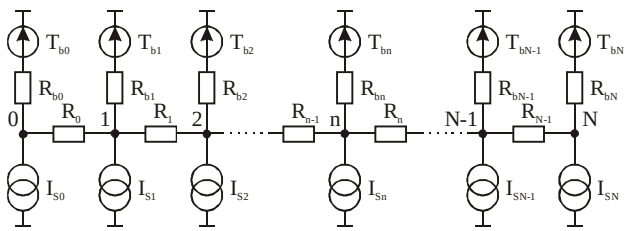

Figure 2: Equivalent Circuit Diagram.

$$G = 1/R, \mathbf{t} = (T_n), \mathbf{i} = (I_n) = \mathbf{i}(\mathbf{t}), I_n = \frac{dp}{dz} \delta z \tag{7}$$

$$(-1/R_{n-1}) T_{n-1} + (1/R_{n-1} + 1/R_n + 1/R_{bn}) T_n + + (-1/R_n) T_{n+1} = (I_{sn} + T_{bn}/R_{bn}) \tag{8}$$

$$\mathbf{i}(\mathbf{t}) = \mathbf{G}(\mathbf{t}) \mathbf{t} + \mathbf{G}_b(\mathbf{t}, \mathbf{T}_b) \mathbf{T}_b \tag{9}$$

$$\mathbf{i}(\mathbf{t}_n) = \mathbf{G}(\mathbf{t}_n) \mathbf{t}_{n+1} + \mathbf{G}_b(\mathbf{t}_n, \mathbf{T}_b) \mathbf{T}_b$$
$$\mathbf{t}_0 \rightarrow \text{linear between } T_1 \text{ and } T_N \tag{10}$$

TESLA RF POWER COUPLER

The RF power input coupler specifications are presented in the Table 1. The coupler is shown in Figure 3, it has 4 fixed temperature points: outside connection to 300 K, 70 K shield connection, 4 K shield connection and the cavity flange at 2K. Coupler inner and outer conductors are made from stainless steel coated by copper, coupler antenna is a whole copper made. Coupler has 2 ceramic windows (warm and cold) and 3 bellows.

RIBBON ION BEAM DYNAMICS IN UNDULATOR LINEAR ACCELERATOR*

E.S. Masunov, S.M. Polozov,
MEPhI, Moscow, 115409, Russia

Abstract

The possibility of non-synchronous radio frequency field harmonics using for ribbon ion beam focusing and acceleration in linac is discussed. In periodical resonant structure the accelerating force is produced by the combination of two spatial harmonics of RF field (two RF undulators). The examples illustrating the efficiency of the proposed method of acceleration are given for longitudinal and transverse undulators.

INTRODUCTION

The space-charge influence is the main factor limiting the beam intensity in low energy RF linac. The ion ribbon beam can be used in order to increase current in linac. The stable motion of ribbon ion beam can be provided by using an external focusing devices or a special configuration of RF fields (RF focusing). The latter approach seems to be more promising for low energy ions. In a conventional RF linac ion beams are accelerated by a synchronous wave. Non-synchronous wave will be used for focusing a charged particles only.

The values of synchronous and nonsynchronous harmonic amplitudes must be chosen to provide both longitudinal and transverse stability. For two wave approach (synchronous and one nonsynchronous harmonics) RF focusing conditions were founded for axisymmetric (ARF) and ribbon (RRF) beams in Ref. [1-2].

Another method to accelerate ions in the RF periodical structure without synchronous wave was suggested in Ref. [3-4]. In this case the acceleration force is to be driven by a combination of two non-synchronous waves (two undulators) and transverse focusing is realized by means of each RF undulator. The peculiarity of a ribbon ion beam focusing and acceleration in RF undulator linear accelerator (UNDULAC-RF) is discussed in this paper.

RF FIELD IN PERIODICAL RESONATOR

The UNDULAC-RF can be realized using an interdigital H-type resonator. The especial form of electrodes must be used in order to provide the transverse focusing along the ribbon width (see Fig.1, [4]). The field excited in a periodical resonator can be found as a periodic solution of the Maxwell equations. Under the assumption that the cross-section size of the accelerator channel is much smaller than the wavelength of the RF field, the Fourier series coefficients for field can be calculated with quasi-electrostatic approximation. The potential of RF field in periodic resonator can be represented as the sum of the spatial harmonics:

$$U = \sum_{n=0}^{\infty} U_n(x,y)\cdot\sin\left(\int h_n dz + \alpha\right)\cos(\omega t) \quad (1)$$

where $h_n = \mu / D + 2\pi n / D$ is a longitudinal wave number of field harmonic, μ is a phase advance of the field per period of RF structure, n is the harmonic number. The n-th harmonic amplitude U_n can be found from the equation

$$\Delta_\perp U_n = h_n^2 U_n \quad (2)$$

Two solutions of this equation are existent: $U_n(x,y) \sim \cosh(h_{n,x}x)\cosh(h_{n,y}y)$ and $\alpha = 0$ for longitudinal radio frequency undulator and $U_n(x,y) \sim \cosh(h_{n,x}x)\sinh(h_{n,y}y)$, $\alpha = \pi/2$ for transverse one. Here $h_{n,x}$ and $h_{n,y}$ are transverse wave number, $h_{n,x}^2 + h_{n,y}^2 = h_n^2$. The ratio $h_{n,x}/h_{n,y}$ is defined by the electrodes form and it's value is small for ribbon beams with large aspect ratio.

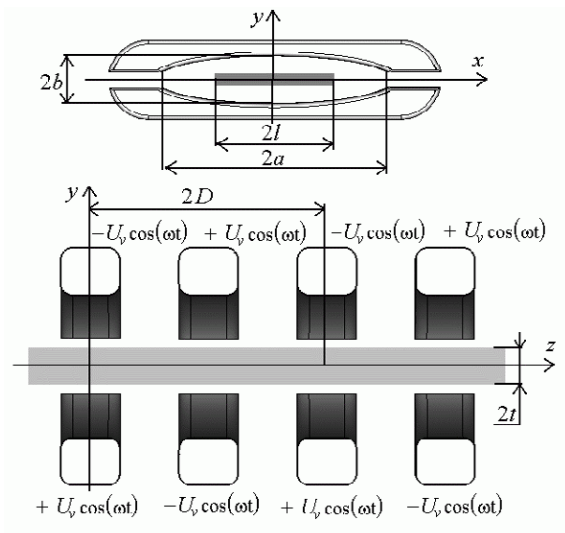

Figure 1: The structure of transverse UNDULAC-RF.

EQUATION OF MOTION

Let us consider the equation of motion for a non-relativistic ion beam in RF field (1) assuming that the particle velocity v differs from the phase velocity of all harmonics: $v_{ph,n} = \omega / h_n$, n=0,1,2… . In general, the interaction of the particles with the non-synchronous harmonic of the RF field does not change the average

*The work was supported by RFBR. Grant 04-02-16667

RF CONTROL MODELLING ISSUES FOR FUTURE SUPERCONDUCTING ACCELERATORS

A.S. Hofler, J.R. Delayen, TJNAF, Newport News, Virginia, USA
V. Ayvazyan, A. Brandt, S.N. Simrock, DESY, Hamburg, Germany
T. Czarski, WUT, Warsaw, Poland; T. Matsumoto, KEK, Ibaraki, Japan

Abstract

The development of superconducting accelerators has reached a high level of maturity following the successes of ATLAS at Argonne, CEBAF at Jefferson Lab, the TESLA Test Facility at DESY and many other operational accelerators. As a result many new accelerators under development (e.g. SNS) or proposed (e.g. RIA) will utilize this technology. Covering all aspects from cw to pulsed rf and/or beam, non-relativistic to relativistic particles, medium and high gradients, light to heavy beam loading, linacs, rings, and ERLs, the demands on the rf control system can be quite different for the various accelerators. For the rf control designer it is therefore essential to understand these issues and be able to predict rf system performance based on realistic rf control models. This paper will describe the features that should be included in such models and present an approach which will drive the development of a generic rf system model.

INTRODUCTION

Nowadays the designer of an rf control system for superconducting accelerators can make use of powerful digital processing hardware including digital signal processors (DSPs) and field programmable gate arrays (FPGAs) allowing processing times reaching from a few hundred nanoseconds for basic field control algorithms to several microseconds or more for complex algorithms. In cases where lowest possible latency is critical (to achieve higher feedback gain and immediate feedback response) the designer may want to choose an analog feedback solution, possibly a hybrid system with fast analog feedback and digital control of operating parameters, built-in diagnostics, and exception handling. In all cases it is desirable to develop a model for the rf control system to be able to predict the expected performance while assuming realistic noise source and performance limitation of the llrf subsystems. The model will allow for comparisons between different controls concept and aid the designer in the synthesis of the optimal controller design [1,2].

RF CONTROL REQUIREMENTS

The rf control requirements for amplitude and phase stability are usually derived from the desired beam parameters. The beam parameters include emittance, energy spread, bunch length and arrival time of the bunch which is critical for seeded XFEL applications. Since the bunch-to-bunch energy spread ranges from around 1% to better than 0.01%, the typical categories for field control are of the order:

Table 1: Typical requirements for field stability rf control

Category	1[a]	2[b]	3[c]
σ_A/A	1e-2	1e-3	1e-4
σ_φ [deg.]	1	0.1	0.01

a. SNS, RIA main linac
b. CEBAF, TESLA, XFEL main linac
c. XFEL critical sections (bunch compressor)

The requirements in Table 1 are considered uncorrelated errors for category 1 and 2 (the correlated error budget is certainly tighter) and correlated errors for class 3 (only few cavities before bunch compressor). The requirements for the phase stability become also more severe for off-crest operation. In the case of the control of the vector-sum of several cavities driven by one klystron, the requirement for the phase calibration of the vector-sum components may become critical depending on the magnitude of microphonics.

Besides field stabilization the RF control system must provide diagnostics for the calibration of gradient and beam phase, measurement of the loop phase, cavity detuning, and control of the cavity frequency tuners. Exception handling capability must be implemented to avoid unnecessary beam loss. Features such as automated fault recovery will help to maximize accelerator up-time. A thorough understanding of the RF system will allow for operation close to the performance envelope while maximizing accelerator availability. Often the RF control must be fully functional over a wide range of operating parameters such as gradients and beam current. For efficiency reasons the RF system should provide sufficient control close to klystron saturation. The cavities are limited in their maximum operable gradients by quench, field emission or coupler sparks. Maximum operable gradient can be achieved with proper exception handling.

SOURCES OF PERTUBATIONS

An essential feature of the rf model will be the appropriate accounting for noise. Evaluating control schemes requires a clear understanding of sources of pertubations and its implementation.

A first classification distinguishes between a modulation of parameters of the model and noise that is added at certain points of the model. The resonance frequency of superconducting cavities is a parameter that undergoes modulations due to mechanical and electromagnetic

A PASS BAND PERFORMANCE SIMULATION CODE OF COUPLED CAVITIES

Tao Xiaokui, Tong Dechun
Tsinghua University, Beijing 100084, P. R. China

Abstract

A simulation code of coupled cavities named PPSC is developed by the solutions of the microwave equivalent circuit equation. It can give the pass band performance of periodic or non-periodic coupled cavity chain, such as the dispersion frequencies and the reflection factor of the cavity, the field distribution of each mode and so on. The natural parameters of the cavity chain, such as the number of the cavities, the resonant frequencies and Q-factors of each cavity, the coupling factor between two cavities and the locations of the couplers, can be changed easily to see the different results of the simulation. The code is written based on MS Visual Basic under MS windows and a user-friendly interface is made. Some simple examples were simulated and gave reliable results.

INTRODUCTION

The tuning of the pass band performance of the coupled cavities is an essential part of the development of a RF linear accelerator. Usually, we need know the pass band performance even on the physical design stage. In general, there are two way to study the coupled cavities. One is to solve the Maxwell equations under certain boundary conditions. The other is based on equivalent circuit model of coupled cavity chain.

For the first way, many codes are developed in recent years, such as URMLT, Superfish, MAFIA, HFSS, ANSYS, etc. These codes can simulate the pass band performance of a RF structure accurately. But for long multi-cell, non-uniform or very complex cavities, the calculating procedure becomes very complicated and time consuming. Sometimes it is almost impossible on a normal PC.

On the contrary, the equivalent circuit method is very simple relatively. It can give the pass band performance of periodic or non-periodic coupled cavity chain, such as the dispersion frequencies and the reflection factor of the cavity, the field flatness, and so on. The natural parameters of the cavity chain that the calculation need are all obtainable by experiments.

During our development of low energy medical linacs and non-destructive inspection linacs, a simulation code (PPSC) based on the equivalent circuit method is written. While designing and tuning a real coupled structure, the information provided by PPSC can be used as a predictive tool to adjust the normal modes and field flatness.

PPSC is a standard Microsoft Windows code. It is written by Microsoft Visual Basic, which allow programmers write large programs easily with user-friendly interfaces by the Object-oriented technology. The idea of this technology is similar to a person's thinking process, so the program is much easier to read.

FUNDAMENTAL PRINCIPLE

The fundamental principle of PPSC is based on the equivalent circuit model of a coupled cavity chain [1] (shown in Figure1).

f_i and Q_i are the resonant frequency and quality factor of the *i*-th cell *(i=1,2,...,N);* k_{0i}*(i=1,2,...,N-1)* and k_{1i} *(i=1,2,...,N-2)* are the nearest and next nearest neighbour couplings between cells. β_1/β_2 is the coupling factor between the waveguide with the input/output coupler respectively.

The equivalent circuit model gives the following matrix:

$$\begin{bmatrix} a_1 & \frac{k_{01}}{2} & \frac{k_{11}}{2} & & & & 0 \\ \frac{k_{01}}{2} & a_2 & \frac{k_{02}}{2} & & & & \\ \frac{k_{01}}{2} & \frac{k_{02}}{2} & a_3 & & & & \vdots \\ \vdots & & & \ddots & & & 0 \\ & & & & & & \frac{k_{1N-2}}{2} \\ & & & & \cdots & a_{N-1} & \frac{k_{0N-1}}{2} \\ 0 & & & 0 & \frac{k_{1N-2}}{2} & \frac{k_{0N-1}}{2} & a_N \end{bmatrix} \bullet \begin{bmatrix} X_1 \\ X_2 \\ X_3 \\ \vdots \\ \vdots \\ \vdots \\ X_N \end{bmatrix} = \begin{bmatrix} I_1 \\ I_2 \\ I_3 \\ \vdots \\ \vdots \\ \vdots \\ I_N \end{bmatrix} \quad (1)$$

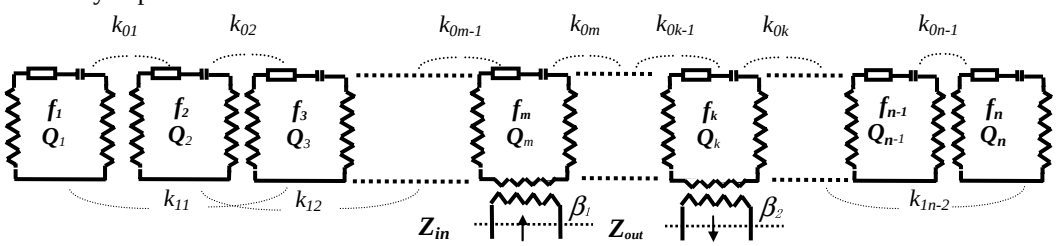

Figure 1: Equivalent circuit model of a coupled cavity chain.

ADVANCED BEAM-DYNAMICS SIMULATION TOOLS FOR RIA*

T. P. Wangler, R. W. Garnett, LANL, Los Alamos, NM, USA
K. R. Crandall, Tech Source, Santa Fe, NM, USA
J. Qiang, R. Ryne, LBNL, Berkeley, CA, USA
N. Aseev, P. Ostroumov, ANL, Argonne, IL, USA
D. Gorelov, R. York, Michigan State University, East Lansing, MI, USA

Abstract

Understanding beam losses is important for the high-intensity RIA driver linac. Small fractional beam losses can produce radioactivation of the beamline components that can prevent or hinder hands-on maintenance, reducing facility availability. Operational and alignment errors in the RIA driver linac can lead to beam losses caused by irreversible beam-emittance growth and halo formation. We are developing multiparticle beam-dynamics simulation codes for RIA driver-linac simulations extending from the low-energy beam transport (LEBT) line to the end of the linac. These codes run on the NERSC parallel supercomputing platforms at LBNL, which allow us to run simulations with large numbers of macroparticles for the beam-loss calculations. The codes have the physics capabilities needed for RIA, including transport and acceleration of multiple-charge-state beams, and beam-line elements such as high-voltage platforms within the linac, interdigital accelerating structures, charge-stripper foils, and capabilities for handling the effects of machine errors and other off-normal conditions. In this paper we present the status of the work, including examples showing some initial beam-dynamics simulations..*

INTRODUCTION

The present concept for the Rare Isotope Accelerator (RIA) project [1] includes a 1.4-GV CW superconducting driver linac. The driver linac is designed for multicharge-state acceleration [2] of all stable species, including protons to 900 MeV and uranium to 400 MeV/u. In conventional heavy-ion linacs, a single charge-state beam of suitably high intensity is extracted from an electron-cyclotron resonance (ECR) ion source and injected into the linac. The linac typically contains one or more strippers at higher energies to further increase the beam charge state and improve acceleration efficiency. However, the limitation to a single charge state from the ion source and from each stripper significantly reduces the beam intensity. This disadvantage is addressed in the RIA driver-linac design concept by the innovative approach of simultaneous acceleration of multiple charge states of a given ion species, which results in high-power beams of several hundred kilowatts for all beams ranging from protons to uranium. Initial beam-dynamics studies [2], supported by experimental confirmation at the Argonne ATLAS facility [3], have demonstrated the feasibility of this new approach.

However, the high-power beam associated with the multiple charge-state acceleration introduces a new design constraint to control beam losses that cause radioactivation of the driver linac [4]. Radioactivation of the linac-beamline components will hinder routine maintenance and result in reduced availability of the facility. Therefore, it will be important for the RIA project to produce a robust beam-dynamics design of the driver linac that minimizes the threat of beam losses. As an important consequence of this design requirement, it will be necessary to develop a computer-simulation code with the capability of accurately modeling the beam dynamics throughout the linac and computing the beam losses, especially at high energies where beam loss translates into greater activation.

The driver linac is made up of three sections. The first is the pre-stripper accelerator section consisting of an ECR ion source, and a low-energy beam transport (LEBT) line, which includes a mass and charge-state-selection system, and a buncher/radiofrequency quadrupole (RFQ) injection system. This is followed by the initial linac stage consisting of a room-temperature RFQ linac, a medium-energy beam transport (MEBT) line, and the low-velocity (low-β) superconducting accelerating structures. The pre-stripper section, accelerates the beam, consisting of two charge states for uranium, to an energy of about 10 MeV/u, where the beam passes through the first stripper and new charge states are produced.

The second section of the linac uses medium-β superconducting structures to accelerate the multicharge-state beam from the first to the second stripper at an energy of about 85 MeV/u. This medium-β section accelerates about five charge states for uranium. This is followed by the third and final section of the linac, which uses high-β superconducting structures to accelerate typically four charge-states for uranium to a final energy of 400 MeV/u.

The overall performance of the driver linac is crucially dependent on the performance of the LEBT and RFQ. The LEBT is designed to focus, bunch, and inject two charge states for uranium into alternate longitudinal buckets of the RFQ. The LEBT RF buncher system consists of two main components. The first RF buncher cavity system (multiharmonic buncher) uses four harmonics and is designed to capture 80% of each charge state within the longitudinal acceptance of the RFQ. A

* This work is supported by the U. S. Department of Energy Contract W-7405-ENG-36

RF BREAKDOWN IN ACCELERATOR STRUCTURES: FROM PLASMA SPOTS TO SURFACE MELTING*

Perry B. Wilson, SLAC, Stanford CA 94309, USA

Abstract

Plasma spots are known to form at field emission sites in regions of high dc or rf electric field. Several mechanisms for the formation of plasma spots in an rf field have been proposed, and one such mechanism which fits experimental data is presented in this paper. However, a plasma spot by itself does not produce breakdown. A single plasma spot, with a lifetime on the order of 30 ns, extracts only a negligible amount of energy from the rf field. The evidence for its existence is a small crater, on the order of 10 μm in diameter, left behind on the surface. In this paper we present a model in which plasma spots act as a trigger to produce surface melting on a macroscopic scale (~ 0.1 mm^2). Once surface melting occurs, a plasma that is capable of emitting several kiloamperes of electrons can form over the molten region. A key observation that must be explained by any theory of breakdown is that the probability of breakdown is independent of time within the rf pulse—breakdown is just as likely to occur at the beginning of the pulse as toward the end. In the model presented here, the conditions for breakdown develop over many pulses until a critical threshold for breakdown is reached.

INTRODUCTION

The theory presented here assumes that, for a gradient-limiting breakdown event to develop in an accelerator structure, a fairly large area near an iris tip (0.01mm^2 or more) must be brought to the melting point in a fairly short time at the beginning of each of many rf pulses. Such an event will produce serious surface damage, and a few hundred of them will produce a measurable change in the iris geometry. The sequence of events leading to such a breakdown starts with the formation of a plasma spot at a field emission site (for a description of the physics of plasma spots see [1]). A proposed mechanism for the formation of plasma spots is given in the next section. Following that, we construct a field emission based model for the breakdown rate after a structure has undergone initial processing, but at gradient levels below the surface damage threshold. Next, we examine the conditions necessary to produce rapid, large-scale surface melting, including the dependence on the physical properties of the surface metal. The predictions of the theory are then compared with experiment. Finally, we give a theory for the development of geometric surface forms over many rf pulses that lead to a gradient-limiting breakdown event.

*Work supported by Department of Energy Contract DE-AC03-76SF00515

LIQUID DROPLET MODEL FOR THE FORMATION OF PLASMA SPOTS

Once initial field emission sites have been processed off, only emitters depending on the topography of the base material remain. A plasma spot formation mechanism must kick in which depends only on the geometry of these emitters. We propose a model that is closely related to the "mechanical breakup" model of Norem *et al.* [2]. In this model the force due to the intense surface field at the emitter tip exceeds the tensile strength of copper, causing a fragment of the tip to break loose. Once this micro-particle has separated from the emitter tip, it is subjected to bombardment and vaporization by the field emission beam from the remaining tip. The rate of vaporization, and the resulting vapor density, is proportional to the field emission current for a given surface field. The rate of ionization in the metallic vapor cloud is proportional to both the vapor density and the current. *Thus the ionization rate should vary roughly as the square of the field emission current.*

A variation in this scenario assumes that tip of the emitter begins to melt due to resistive heating rather than to mechanically break off. The radius of curvature of the molten tip is set by a balance between the force per unit area, F_A, due to the E^2 force pulling on the surface and the surface tension α of the liquid metal (1.3 Nt/m for copper). It is given by [3]

$$r_0 = 2\alpha/F_A = 8\alpha/\varepsilon_0 E_S^2. \quad (1)$$

As the E-field increases the radius of curvature of the molten tip decreases until an unstable point is reached. The tip begins to neck down (possibly due to a pinch effect from the increasing magnetic field associated with the FE current??) and a droplet or a train of droplets are pinched off and pulled away. Many experimental measurements on field emitters have shown that the maximum surface field at the tip of the emitter cannot exceed about 7–10 GV/m before the emitter is destroyed. Also, it is observed that emitters in superconducting cavities cannot be processed (implying creation of a plasma) unless the emitter area is greater than about 10^{-15} m^2 [4]. Using α = 1.9 Nt/m for niobium and E_S = 7 GV/m, Eq. (1) gives an effective emitter area ($\approx 2r^2$) of 2.4×10^{-15} m^2.

A FIELD EMISSION MODEL FOR TRIGGERING BREAKDOWN EVENTS

In the initial stages of processing, we expect that the field emission features with the highest beta values will be burned off first, leaving single isolated craters. When a

DEVELOPMENT OF A PERMANENT MAGNET ECR SOURCE TO PRODUCE A 5 mA DEUTERON BEAM AT CEA/SACLAY

R. Gobin*, P-Y Beauvais, G. Charruau, O. Delferrière, D. De Menezes, R. Ferdinand, Y. Gauthier, F. Harrault, Commissariat à l'Energie Atomique, CEA-Saclay, DSM/DAPNIA, 91191 Gif sur Yvette Cedex, France
N. Comte, Commissariat à l'Energie Atomique, CEA-Saclay, DEN/SAC/DSP/SPR, 91191 Gif sur Yvette Cedex, France
P. Leherissier, J-Y. Paquet, GANIL, Bd Henri Becquerel, 14076 Caen Cedex 5. France

Abstract

The high intensity light ion source (SILHI) is an ECR ion source operating at 2.45 GHz which produces high intensity (over 100 mA) proton or deuteron beams at 95 keV. This encouraged us to propose a permanent magnet source based on the SILHI design to fit in with the injector of the Spiral 2 project, requesting 5 mA of D^+ beam with an energy of 40 keV and a normalized rms emittance lower than 0.2 π mm.mrad. The new source has been recently assembled and the first beam (proton) extracted. The source design improvements and the preliminary results are reported.

INTRODUCTION

In France, CEA and CNRS have been working on high beam power accelerators for several years. In a first step, the SILHI source has been built to produce high intensity proton beams. Experiments were also devoted to the production of deuterons for irradiation tools. Deuterons are now also needed by the future SPIRAL 2 facility [1] and a "low" intensity (5 mA) deuteron source is presently under study at CEA Saclay.

The goal of SPIRAL 2 at GANIL, consists in extending the possible radioactive beam types. SPIRAL 2 is based on the fission of a Uranium carbide target induced by neutrons. The neutron flow will be produced by interaction of deuteron beam with a Carbon target. SPIRAL 2 requires a maximum of 5 mA - 40 keV CW D^+ beam (at the RFQ entrance) with rms normalized emittances lower than 0.2 π mm.mrad. To answer these requirements, an ECR source has been proposed, extending the SILHI design with permanent magnets.

SOURCE DESIGN

Magnetic Structure

The SILHI ECR ion source, operating at 2.45 GHz, is producing more than 100 mA proton beams [2] with a high reliability. Taking into account the deuteron experiments already successfully performed with SILHI (130 mA at 100 keV in pulsed mode) [3], the design of such a source fulfilling the SPIRAL 2 requirements has been undertaken. The reproducible performance led us to propose a permanent magnet 2.45 GHz ECR source: the magnetic field is provided by 3 ring shaped permanent magnets instead of 2 solenoidal coils on SILHI. Electromagnetic simulations have been carried out to reproduce at best the SILHI magnetic field profile on the axis [4]. The plasma chamber and the RF power chaine keep the SILHI design. In order to increase the plasma density, 2 Boron Nitride discs are also located at both ends of the plasma chamber.

No problem occurred when assembling the source but a 6 % deviation has been observed between the magnetic measurements and the simulations. Even if the ECR resonances have been easily placed, we discovered experimentally a major problem. It came from the particular permanent magnet configuration built with no shielding. Consequently, in the extraction region, the magnetic field was 40 times higher than in the SILHI case with coils and magnetic shielding, reaching a value of about 0.2 T. This high magnetic field contributed to initiate a discharge between the electrodes when the high voltage increases. The extraction system is designed for electric fields as high as 60 kV/cm and only few kV/cm between electrodes led to important currents in glow discharge and to a vacuum increase.

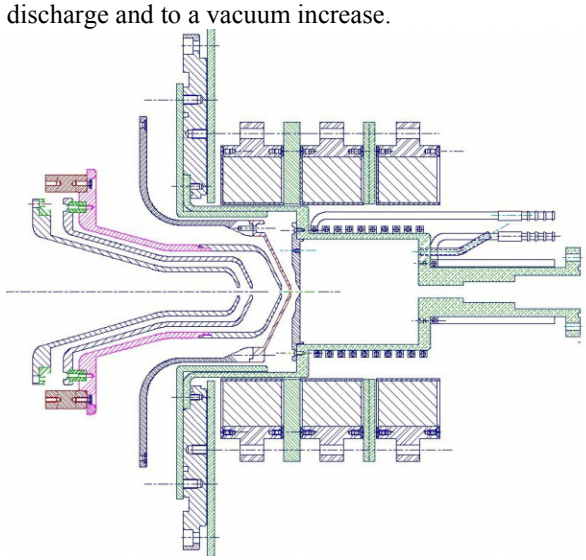

Figure 1: Permanent magnet ECR source with magnetic shielding and discs.

So, new magnetic configurations have been tested to lower the magnetic field between electrodes. But magnetic shielding leads to a decrease of the magnetic field in the plasma chamber. A compromise has finally

RECENT RESULTS OF THE 2.45 GHz ECR SOURCE PRODUCING H⁻ IONS AT CEA/SACLAY

R. Gobin*, K. Benmeziane, O. Delferrière, R. Ferdinand, F. Harrault, Commissariat à l'Energie Atomique, DSM/DAPNIA/SACM, 91 Gif/Yvette, France
A. Girard, Commissariat à l'Energie Atomique, DSM/DRFMC/SBT, 38 Grenoble, France

Abstract

Low frequency ECR plasma sources have demonstrated their efficiency, reproducibility and long life time for the production of positive light ions. In 2003, the new 2.45 GHz ECR test stand based on a pure volume H^- ion production, developed at CEA/Saclay, showed a spectucar increase of the extracted H^- ion beam intensity. In fact, a stainless steel grid now divides the plasma chamber in two different parts: the plasma generator zone and the negative ion production zone. By optimizing the grid position and its potential with respect to the plasma chamber, the negative ion current reached nearly 1 mA. Ceramic plates covering the plasma chamber walls help electron density and lead to an optimisation of the ion production. A 1.32 mA H^- extracted current has been measured. New Langmuir probe measurements have also been done on both sides of the grid. The last results are reported and discussed. This work is supported by the European Union under contract HPRI-CT-2001-50021.

INTRODUCTION

Future high intensity proton accelerators like SNS, ESS or neutrino factories ask for reliable and efficient H^- ion production to inject in compressor rings. These facilities have been planned to work in pulsed mode (roughly 1 to 2.5 ms pulse length at a frequency ranging from 15 to 50 Hz). Many existing machines such as HERA, ISIS, LANCSE and others are also interested in source developments. Taking into account these demands, CEA has undertaken an important R&D program on high intensity light ion sources.

Since the SILHI source [1] showed a good efficiency for high intensity proton beam production with a very long source life time, parallel programs are in progress. A permanent magnet deuteron source is now delivering its first deuteron beams [2] for the SPIRAL 2 project. In parallel, the development of the 2.45 GHz ECR negative ion source is still in progress and the H^- ion production slightly increases.

One year ago, measurements performed with a plasma chamber separated into 2 zones showed an important improvement [3]. These results are shortly reported in the next section. The third section will insist on the last results obtained by testing different materials. Then recent Langmuir probe measurements are presented.

* e-mail : rjgobin@cea.fr

ELECTRIC FILTER

To produce negative hydrogen ions, the sources are generally based on the same principle. In the plasma creation zone, energetic electrons of about 20 to 40 eV interact with the gas to excite the molecules and then in a second zone, slow electrons (about 1 eV) react with these excited molecules to give an H atom and an H^- ion. This process is called the dissociative attachment. Generally, both zones are separated by a magnetic filter to limit the high energy electron flux entering into the negative ion production zone.

At Saclay, the preliminary design of the source based on plasma generated by electron cyclotron resonance, followed this principle. And only few µA of H^- ions have been observed [4].

So the small H^- ion production may be attributed to negative ion destruction close to the plasma electrode. It is possible that microwave power not completely absorbed by the plasma contributes to H^- loss. Simulations show that a simple metallic grid with a large transparency can stop the microwave penetration. As a result, an important improvement has been observed when the plasma chamber has been effectively separated in 2 zones by a stainless steel grid. This grid is polarised at the same potential than the plasma electrode.

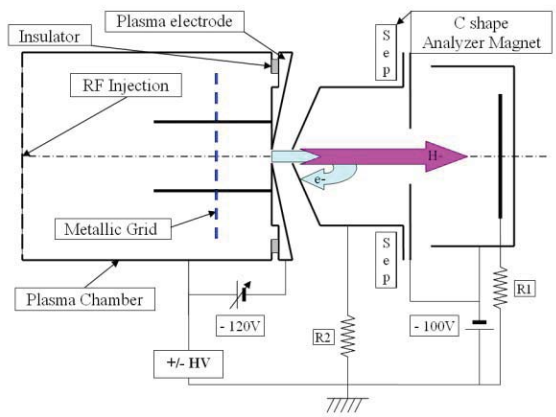

Figure 1: Scheme of the H^- ECR source.

After optimisation of the grid position, the maximum H^- current occurred while the grid was located at 30 mm from the plasma electrode. By tuning the potential of the grid and plasma electrode from 0 to – 120 V compared to

H⁻ DISTRIBUTION IN THE HERA RF-VOLUME SOURCE

J. Peters DESY, Hamburg, Germany

Abstract

The HERA RF-Volume Source is the only source that delivers routinely a H⁻ current of 40 mA without Cs. The production mechanism for H⁻ ions in this type of source is still under discussion. Laser photodetachment measurements have been started at DESY in order to measure the H⁻ distribution in the source. The measurements were done also under extraction conditions at high voltage. Measurements with and without extraction are contributions for the H⁻ sheath theory. Knowing how the H⁻ are distributed and where they are produced makes further source improvements possible.

INTRODUCTION

Photodetachment measurements in order to measure the density of negative ions have been done as early as 1969 [1]. First density measurements of H^- are reported in 1979 [2]. In the HERA source a modification of a technique with a cylindrical metal probe (langmuir probe) aligned parallel to a laser axis [3] was used. The HERA volume H^- source is a RF source with an antenna outside of the plasma chamber. The antenna is shielded by a ceramic. For HERA a current pulse of 40 mA, 120 µsec long is extracted at 35 kV. The details of the source are given in several papers [4],[5],[6].

MEASUREMENT SET UP

The power applied at the RF coil of the HERA H⁻ source is pulsed. With a positive bias (U_{LP}) of 5V close to saturation one draws an electron current to the tip of the probe. This current (I_{LP}) is measured with a toroid (see Fig.1). The current signal is shown in Fig.2a. The affinity of the electron attached to the hydrogen atom is with 0.75eV very low [1]. By photodetachment $H^- + h\nu = H + e^-$ an increase in electron density is produced.

To clearly interpret the signals it has to be made sure that no other photon processes like photoionisation take place. Fig. 2b shows the increase in electrons detected when a 9 nsec, 1064 nm puls of a Nd: YAG laser travels on the axis of the source. The maximum pulse energy of our laser was 650 mJ per pulse. The 8 mm ∅ laser beam was compressed to 3mm ∅ with an optical system.

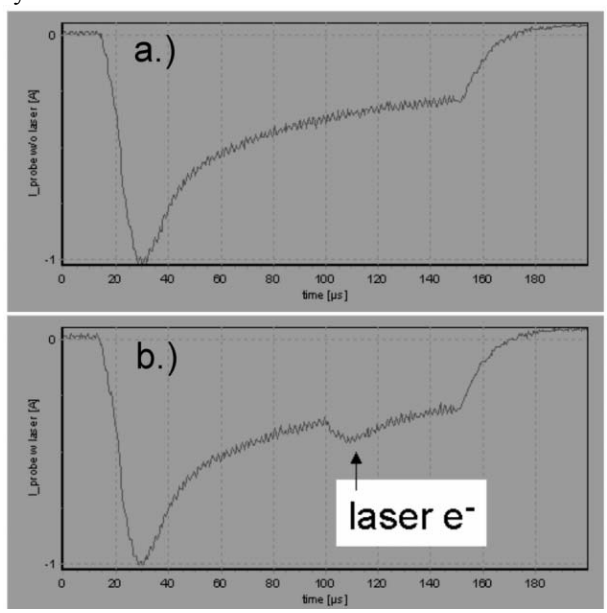

Figure 2: Current pulse of the Langmuir probe (I_{LP}) without laser beam (a) and with photo detached electrons (b).

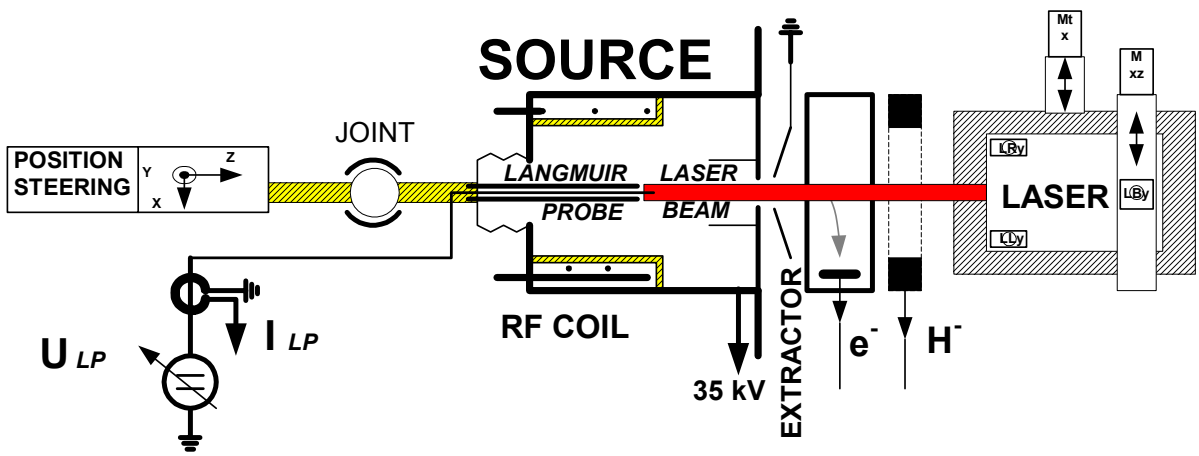

Figure 1: HERA RF source with mounted langmuir probe on the back side and a laser beam shooting through the extractor hole.

ULTRA-HIGH-VACUUM PROBLEM FOR 200 KEV POLARIZED ELECTRON GUN WITH NEA-GaAs PHOTOCATHODE

T. Nakanishi[a], M. Yamamoto[a], N. Yamamoto[a], S. Okumi[a], F. Furuta[a], M. Kuwahara[a],
K. Naniwa[a], K. Yasui[a], H. Kobayakawa[b], Y. Takashima[b],
H. Matsumoto[c], M. Kuriki[c], and M.Yoshioka[c]
[a]Dept. of Physics, Nagoya University, Nagoya 464-8602, Japan
[b]Faculty of Engineering, Nagoya University, Nagoya 464-8602, Japan
[c]KEK High Energy Accelerator Research Organization, 1-1 Oho, Tsukuba 305-0801,Japan

Abstract

A high gradient electron gun with an NEA-GaAs-type photocathode is indispensable to produce the high intensity (polarized) electron beam for a future e^+-e^- linear collider (LC) and the low emittance CW beam for energy recovery linac (ERL) projects. Motivated by these needs, a 200keV (polarized) electron gun has been constructed at Nagoya Univ. The source emittance measurement system is also constructed and preliminary results are obtained. However, the lifetime of the NEA surface is not yet sufficiently long, and this problem is discussed with the efforts for improvement.

INTRODUCTION

A proto-type of 200keV polarized electron gun has been constructed for applications to the LC and ERL projects. As well known, the warm-technology-based LC requires high-intensity (>5A peak current), multi-bunch structure (~500ps bunch width, 1.4ns separation) beam with low emittance (<10π·mm·mrad) at gun exit[1]. The ERL requires large average current (~100mA) beam with the lowest emittance (<0.5π·mm·mrad)[2].

In such applications, the NEA (Negative Electron Affinity) surface makes an indispensable role to extract electrons in conduction band minimum into vacuum. It assures high polarization (P≅90%), high quantum efficiency (QE≥0.5%) [3] and lowest initial emittance (ε≅0.1 π·mm·mrad) [4] of the extracted beam.

On the contrary, there is a serious NEA lifetime problem. The NEA surface is realized by a mono-layer of electric-dipole-moment of Ga(-)–Cs(+) formed by the Cs deposition to the GaAs surface. Thus this surface state is extremely delicate against environment. In fact, the NEA surface is easily degraded by (a) desorption of residual gas molecules, (b) desorption of additional gas molecules created by the dark currents from high voltage electrode, and (c) NEA surface back-bombardment of the positive ions produced by the beam itself. In order to reduce these effects, high quality ultra-high-vacuum (UHV) is required in the vicinity of NEA surface.

The dark current induced by field emission from the cathode electrode surface is enhanced by secondary electron and ion productions. It must be also suppressed below 10nA level to maintain the UHV condition.

For keeping the lowest initial source emittance, on the other side, the higher gradient field at the NEA surface is required to prevent the beam divergence due to the space charge effect. It means that the NEA lifetime problem becomes more and more serious, if we require the higher field gradient to realize the lower source emittance.

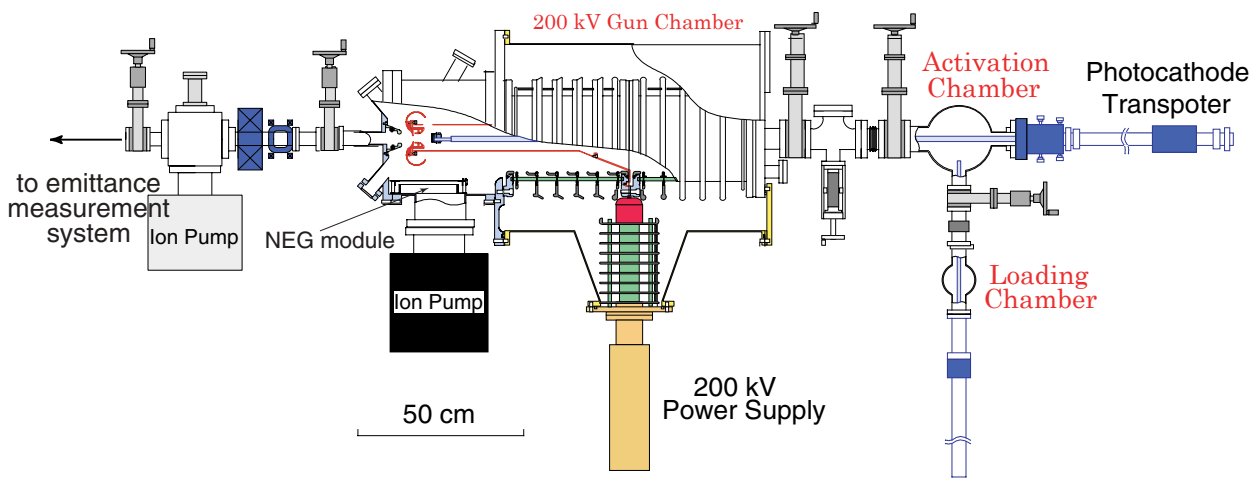

Figure 1: A schematic view of the 200keV polarized electron source.

DESGIGN PARAMETERS OF THE NORMAL CONDUCTING BOOSTER CAVITY FOR THE PITZ-2 TEST STAND

V.V. Paramonov, N.I. Brusova, A.I. Kvasha, A.A. Menshov, O.D. Pronin,
A.K. Skasyrskaya, A.A. Stepanov, INR, 117312 Moscow, Russia
A. Donat, M. Krasilnikov, A. Oppelt, F. Stephan, DESY, Zeuthen, Germany
K. Floettmann, DESY, Hamburg, Germany

Abstract

The normal conducting booster cavity is intended to increase the electron bunch energy in the Photo Injector Test (DESY, Zeuthen) stage 2 experiments [1]. The normal conducting cavity is selected due to infrastructure particularities in DESy Zeuthen. The L-band cavity is designed to provide the accelerating gradient up to 14 MV/m with the total input rf power up to 8.6 MW, rf pulse length up to 900 mks and repetition rate 5 Hz. The multi-cell cavity is based on the CDS compensated accelerating structure with the improved coupling coefficient value. The main design ideas and decisions are described briefly together with cavity parameters - rf properties, cooling and pumping circuits.

GENERAL PARAMETERS

Table 1: Cavity parameters

Parameter	Unit	Value
Operating frequency	MHz	1300
Particle velocity	relative	1.0
Nominal gradient E_0T	$\frac{MV}{m}$	12.5
Maximal gradient E_0T	$\frac{MV}{m}$	14.0
Nominal energy gain	MeV	20.18
Maximal surface field	$\frac{MV}{m}$	40.0
Maximal rf pulse power	MW	8.6
Maximal rf pulse length	μks	900
Nominal repetition rate	Hz	5
Aperture diameter	mm	30.0
Number of periods		14
Coupling coefficient	%	7.2
Calculated Q-factor		23700
Required Q-factor	at $20C^o$	20100
Cavity length	m	≈ 1.8
Operating temperature	C^o	≈ 44
Cooling water consumpt.	$\frac{m^3}{h}$	4.5
Residual gas pressure	$Torr$	$\leq 10^{-7}$

The booster cavity is the component of the test stand for investigations of high brightness electron beam formation. The cavity should combine different, some time contradictory, properties as operating parameters flexibility, reliability, minimal own emittance perturbations. Additionally the cavity realize (in maximal parameters) the full scale high power prototype of the high gradient cavities in the TESLA Positron Pre-Accelerator [2].
The cavity general parameters are summarized in Table 1.

Accelerating structure and beam dynamics

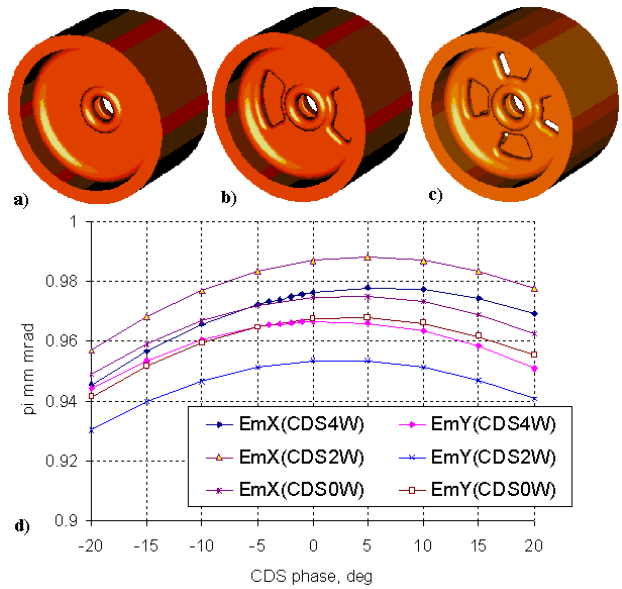

Figure 1: Top - the structure options for BD investigations, a) - axial symmetrical (CDS0W), b) - with two (CDS2W) and c) with four coupling windows. Bottom - d) the transverse rms beam emittance for different CDS options.

The cavity should provide the maximal energy gain for the maximal gradient $E_0T = 14\frac{MV}{m}$ with input rf power $P_i = 8.6MW$ and the structure effective shunt impedance Z_e should be reasonably optimized. The CDS structure [3], which combines improved coupling coefficient k_c, high Z_e value and small dimensions, is chosen. The options with two (CDS2W), Fig. 1b, and four (CDS4W), Fig. 1c, were considered. The axially symmetric option (CDS0W), Fig. 1a, is used as a reference. The moderate, not maximal possible, k_c values, $k_c^{2W} = 9.55\%$ and $k_c^{4W} = 7.2\%$, are chosen to obtain higher Z_e values, which are $Z_e^{2W} = 0.995Z_e^{0W}$ and $Z_e^{4W} = 1.03Z_e^{0W}$ (calculated values). To have higher Z_e value, the coupling windows edges - the place of maximal rf current density - are rounded. It leads to higher sensitivity of k_c value on win-

DEVELOPMENT OF ADAPTIVE FEEDBACK CONTROL SYSTEM OF BOTH SPATIAL AND TEMPORAL BEAM SHAPING FOR UV-LASER LIGHT SOURCE FOR RF GUN

H. Tomizawa[1], H. Dewa[1], T. Taniuchi[1], A. Mizuno[1], T. Asaka[1], K. Yanagida[1], S. Suzuki[1], T. Kobayashi[1], H. Hanaki[1], and F. Matsui[2],
Accelerator Division, Japan Synchrotron Radiation Research Institute (SPring-8),
1-1-1 Kouto, Mikazuki-cho, Sayo-gun, Hyogo 679-5198, Japan[1]
Creative & Advanced Research Department, Industrial Technology Centre of Fukui Prefecture,
61 Kawaiwashiduka-cho, Fukui City 910-0102, Japan[2]

Abstract

We have been developing a stable and highly qualified UV-laser pulse as a light source for the rf gun, which is a potential injector for future light sources. Our gun cavity is a single-cell pillbox, and the copper inner wall is used as a photo cathode. At present, the short pulse energy stability of laser has been improved, with a reduction to 1.3~1.5% (rms) for third harmonic generation.

In this improvement we only passively stabilized the system. We considered environmental controls in the clean room to reduce optical damage accidents and constructed a new humidity-controlled clean room in 2003. We then re-installed the entire laser system in this room in 2004. The relative humidity of this new clean room at room temperature is in the region of 50~60%, with a stability less than 2% (peak-to-peak). On the other hand, the ideal spatial and temporal profiles of a shot-by-shot single-laser pulse are essential in order to suppress the emittance growth of the electron beam from an rf gun.

This laser-shaping project has proceeded in two steps since its inception in 2002. In the first successful test run in 2002, with a microlens array as a simple spatial shaper, we obtained a minimum emittance value of 2π mm•mrad with a beam energy of 3.1 MeV, holding its charge to 0.1 nC/bunch. In the next test run in 2004, we prepared a deformable mirror for spatial shaping and a spatial light modulator based on fused-silica plates for temporal shaping. We are applying both types of adaptive optics to automatically shape both the spatial and temporal UV-laser profiles simultaneously with a feedback routine. We report here the principle and developing process of our laser beam quality control system.

INTRODUCTION

We have been developing a photo-cathode rf gun [1] as a highly qualified electron beam source to achieve future X-ray light sources (FEL (free electron laser), Compton back scattering, etc.) since 1996 in a test facility at the SPring-8 site. Future X-ray light sources will require an electron beam source with a low emittance of ~1 π mm•mrad. Our development of this type of gun is oriented toward a long-lived stable system for user experiments. It is necessary for the copper cathode of the rf gun to have a UV-laser pulse with a pulse width of ~10 ps and a photon energy of ~4 eV.

Since we started to develop the test facility, two issues regarding the laser light source have appeared. One is the energy stability of the UV-laser light source. The other concerns the spatial and temporal laser profiles. The quality of the laser beam is essential to stabilization and generation of a low-emittance electron beam.

We passively stabilized the system. Environmental controls were considered in the clean room to reduce optical damage accidents, and a new humidity-controlled clean room was constructed (relative humidity at room temperature: 50~60%). The pumping source of the laser system was stabilized with a temperature-controlled base plate. As a result of the passive stabilization, the pulse energy stability of the laser has been improved with a reduction to 1.3~1.5% (rms; 10 pps; 10000 shots) for third harmonic generation (THG).

On the other hand, optimal spatial and temporal profiles of a shot-by-shot single laser pulse are essential in order to suppress the emittance growth of the electron beam from a photo-cathode rf gun. This laser-shaping project has proceeded in two steps since its start in 2002. Specifically, higher stability of the pulse energy is required and homogeneous Silk-hat (cylindrical flattop) spatial and rectangular temporal profiles of the UV-laser light source must be generated.

In the first spatial shaping test run, we shaped the laser spatial profiles with a microlens array. Consequently, the horizontal emittance was significantly improved from 6 to 2 π mm•mrad at a beam charge of 0.1 nC/bunch. This experimental data represents a new record for the minimum emittance of an electron beam from a single-cell-cavity rf gun [2].

In the next test run, we applied both types of adaptive optics to automatically shape both the spatial and temporal UV-laser profiles with a feedback routine simultaneously. We prepared a deformable mirror for spatial shaping and a spatial light modulator based on fused-silica plates for temporal shaping. Both adaptive optics were installed in the UV-laser optical transport. The development process of our beam quality control systems are reviewed in the remainder of this paper.

ANALYSIS OF THE QUALIFICATION-TESTS PERFORMANCE OF THE SUPERCONDUCTING CAVITIES FOR THE SNS LINAC*

J. R. Delayen#, J. Mammosser, J. Ozelis, Thomas Jefferson National Accelerator Facility,
12000 Jefferson Avenue, Newport News, VA 23606, USA

Abstract

Thomas Jefferson National Accelerating Facility (Jefferson Lab) is producing superconducting radio frequency (SRF) cryomodules for the Spallation Neutron Source (SNS) cold linac. This consists of 11 medium-beta (0.61) cryomodules of 3 cavities each, and 12 high-beta (0.81) cryomodules of 4 cavities each. Before assembly into cavity strings the cavities undergo individual qualification tests in a vertical cryostat (VTA). In this paper we analyze the performance of the cavities during these qualification tests, and attempt to correlate this performance with cleaning, assembly, and testing procedures. We also compare VTA performance with performance in completed cryomodules.

CAVITY AND CRYOMODULE PERFORMANCE ANALYSIS TOOLS

Jefferson Lab has developed a web-based system that integrates commercial database, data analysis, document archiving and retrieval, and user interface software into a coherent knowledge management product called *Pansophy*. *Pansophy* provides key tools for the successful pursuit of major projects such as accelerator system development and construction by offering elements of process and procedure control, data capture and review, and data mining and analysis. *Pansophy* is being used in Jefferson Lab's SNS superconducting linac construction effort as a means for structuring and implementing the QA program, for process control and tracking, and for cavity and cryomodule test data capture and analysis.

Using *Pansophy*, critical process and performance parameters for individual cavities and cryomodules can be entered in the underlying database, in a systematic fashion, by using a set of "travelers" that provide process control and data input. Typical examples of these data include cavity dimensional data, cavity rinse time, rinse water particulate count, BCP etch rate, cavity performance (gradient, Q_o, radiation onset), and cryomodule performance (gradient, Q_o, radiation onset, tuner performance, thermal behavior, probe couplings, etc.).

* Work supported by the U.S. Department of Energy under contracts DE-AC05-84-ER40150 and DE-AC05-00-OR22725.
#delayen@jlab.org

These data can be analyzed and mined using various standard and user-defined queries. These query tools allow for straightforward investigation of correlations and dependencies between cavity performance parameters and cavity processing variables. For example, the onset of field emission during vertical cavity tests can be investigated with respect to High Pressure Rinse (HPR) water particulate level, with the hope that any observed correlations can be utilized as predictors of cavity performance or water system integrity. Likewise, comparisons between cavity performance in vertical tests and in completed cryomodules can be compared and assessed. The results of such queries can be downloaded to a spreadsheet, or saved as a text file to be used with other analysis programs.

Cavity and Cryomodule *Performance Overview* pages have been added to *Pansophy*. They provide "Single-click" performance summary of cavities tested in the VTA (along with downloadable data and plots), and cryomodules tested in CMTF. An example for such a page for a cavity is shown in Fig.1.

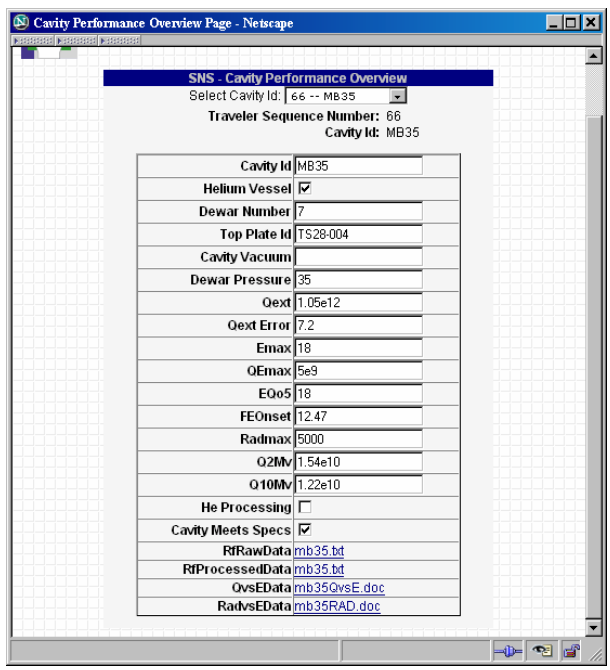

Figure 1: *Performance Overview* page provided by *Pansophy* summarizing processing, testing, and performance data on a cavity.

SRF CAVITY AND MATERIALS R&D AT FERMILAB *

P. Bauer, L. Bellantoni#, T. Berenc, C. Boffo, R. Carcagno, C. Chapman, H. Edwards, L. Elementi, M. Foley, E. Hahn, D. Hicks, T. Khabiboulline, D. Mitchell, A. Rowe, N. Solyak, Y. Terechkine, FNAL, Batavia, IL 60510, USA
M. Jewell, D. Larbalestier, P. Lee, A. Gurevich, A. Polyanskii, A. Squitieri, Applied Superconductivity Center, University of Wisconsin-Madison, WI 53706, USA

Abstract

Fermilab has been steadily developing its SRF cavity expertise, infrastructure and technology base. We particularly emphasize here recent developments in understanding basic material properties and developing a new chemistry treatment facility.

INTRODUCTION

Two types of 3.9 GHz superconducting RF cavities are under development at FNAL for use in the upgraded A0 photo-injector facility. A TM_{110} mode cavity will provide streak capability for bunch slice diagnostics, and a TM_{010} mode cavity will provide linearization of the accelerating gradient before compression for better emittance. Fig. 1 shows the upgraded A0 facility beam line layout including the 3.9 GHz transverse deflecting and 3rd harmonic modules. The performance of recent prototype cavities is given in [1]. The use of a TM_{010} cavity for TESLA bunch compression is discussed in [2].

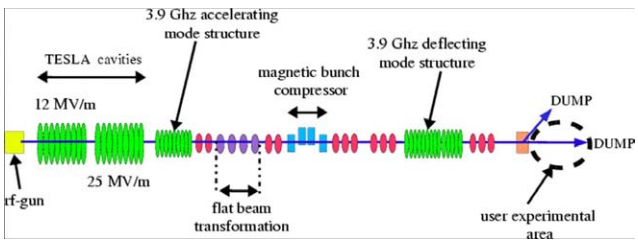

Figure 1: Upgraded A0 facility beam line layout.

CAVITY FABRICATION

We purchase RRR 300 Nb sheet from industry, cut disks via wire EDM, and stamp, coin, and machine them into cells. Prior to forming, the disks are inspected for imperfections and inclusions with an eddy current scanner. The eddy current scanning, which was formerly performed at DESY, is now done at FNAL with a scanner on loan from SNS. RRR measurements on select samples are performed to check if the material meets the specifications. The latest batch of material received from Wah Chang achieves a high RRR~450. Electron beam welding is performed near FNAL at Sciaky Inc. Our vacuum bake facility (1200°C) is used for annealing and hydrogen removal. 1:1:2 BCP acid etching can be done in-house for cavity parts. The fully assembled cavities, however, have been kindly etched for us by Jlab. We are in the process of commissioning a small manual acid etch facility operated jointly with K. Shephard, M. Kelly and M. Kedzie at Argonne National Lab. Additionally, a new, larger, remotely controlled, semi-automatic chemistry facility for FNAL cavities is under development. After commissioning at FNAL, the facility will be transferred to ANL to become a part of the ANL-FNAL Surface Treatment Facility, located at ANL. Recent developments regarding this new chemistry facility are going to be discussed in further detail below. A high pressure rinse with 18 MΩ H_20 in a class 10 clean room can be done on-site. RF field flatness tunings are all performed on-site, as is mechanical 3-dimensional high resolution profilometry. We have contracted with Advanced Energy Systems in Medford, NY to fabricate two cavities, the first of which is currently in the welding stage.

*Supported by the U.S. Department of Energy.
#bellanto@fnal.gov

CHEMISTRY FACILITY

Chemical treatment with BCP is a well-established procedure that allows the removal of a mechanically damaged and chemically contaminated layer of Nb from the cavity surface. It is used several times during the cavity fabrication with varying thicknesses of Nb removed at each step.

Fig. 2 shows the full-scale mockup of the BCP facility at FNAL, where it is being tested with water. The facility will be installed in a ventilated leak-proof process compartment in order to provide acid containment in case of a spill. This facility is designed not only for 3.9 GHz cavities but also for treatment of the larger 9-cell, 1.3 GHz TESLA-type cavities, which require up to 250 liters of acid. Up to one TESLA-sized cavity a day can be processed. To maintain a precise control over the processing time, the cavity fill-time is required to be 1 minute or less. This requirement is met by elevating the gravity feed tank for acid and by using a large (50 mm) diameter filling pipe. The system operates in the pump-through mode with a minimum acid flow speed through the cavity of 1.1 liters/min. When a TESLA-type cavity is processed at a typical etching rate of 1 μm/min, the power required to keep the solution temperature constant (including heat loss) is about 1 kW. A 2 kW heat exchanger keeps the temperature of the acid at 15°C. For a 1 m^2 Nb surface area, about 15 liters of NO_2 are released each minute. Besides NO_2, there is also emission of NO, HNO_3 and HF – fumes that are considered dangerous pollutants. The facility is designed for air exchange and subsequent scrubbing at a rate of 700 m^3/h (200 l/sec).

The acid will be brought into the chemical isolation room in double-walled barrels (HDPE outside, Teflon

FIRST CRYOGENIC TESTS WITH JLAB'S NEW UPGRADE CAVITIES*

P. Kneisel, G. Ciovati, G.R. Myneni, G. Wu, Jefferson Lab, Newport News, VA 23606, USA
J. Sekutowicz, DESY, Notkestrasse 85, 22607 Hamburg, Germany
J. Halbritter, Forschungszentrum Karlsruhe, Karlsruhe, Germany

Abstract

Two types of 7-cell cavities have been developed for the upgrade of CEBAF to 12 GeV. The High Gradient type (HG) has been optimized with respect to the ratio of E_{peak}/E_{acc}. The Low Loss (LL) type has optimized shunt impedance and improved geometric factor. Each cavity type features four DESY–type coaxial Higher Order Mode (HOM) couplers and a waveguide input coupler. Design goals for these cavities have been set to E_{acc} = 20 MV/m with an intrinsic Q_o of $8\cdot10^9$ at 2.05 K. A niobium prototype of each cavity has been fabricated at JLab and both cavities have been evaluated at cryogenic temperatures after appropriate surface treatment. In addition, pressure sensitivity as well as Lorentz force detuning were evaluated. The damping of approximately 20 HOMs has been measured to verify the room temperature data. Several single cell cavities were tested in addition to multi cell cavities. We present in this contribution a summary of tests performed on the prototypes of the proposed cavities.

INTRODUCTION

The rationale for developing two different types of cavities for the upgrade of CEBAF to 12 GeV has been discussed in a previous paper [1] and will be repeated only briefly here. Typically, superconducting niobium cavities are limited in their high field performance by field emission. By optimizing the geometry, the ratio of the surface electric field E_{peak} to the accelerating field E_{acc} can be reduced for a given onset of field emission. The HG cavity has this ratio of E_{peak}/E_{acc}=1.89 making it less sensitive to the field emission phenomenon. A reduction in the cryogenic losses of a cavity can be achieved by maximizing the shunt impedance R/Q and the geometry factor G. These optimised parameters result in lower stored energy and wall losses at a given accelerating gradient compared to non-optimized cavity shapes. Given a fixed cryogenic capacity of the LHe plant higher end energies can be achieved in the CEBAF accelerator with such cavities (LL).

In Figure 1 the shapes of inner cells of both "upgrade" cavities developed at JLab are compared with the original cavities used at present in the accelerator. Table 1 lists their rf parameters.

CAVITY FABRICATION AND SURFACE TREATMENT

Several single cell cavities and one 7-cell cavity of each type were fabricated from high purity niobium with a RRR value of ~250 by the standard method of deep drawing of subcomponents and electron beam welding.

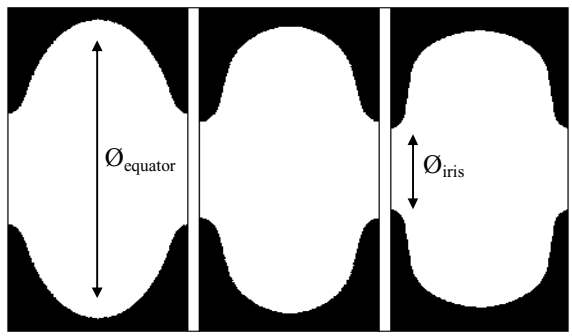

Figure 1: Geometry of the inner cells of the "original CEBAF" (OC) shape and the HG and LL shapes.

Table 1: Parameters of inner cells

Parameter		OC	HG	LL
$Ø_{equator}$	[mm]	187.0	180.5	174.0
$Ø_{iris}$	[mm]	70.0	61.4	53.0
k_{cc}*	[%]	3.29	1.72	1.49
E_{peak}/E_{acc}	[-]	2.56	1.89	2.17
B_{peak}/E_{acc}	[mT/(MV/m)	4.56	4.26	3.74
R/Q	[Ω]	96.5	111.9	128.8
G	[Ω]	273.8	265.5	280.3
R/Q·G	[Ω·Ω]	26422	29709	36103

*cell-to-cell coupling

The single cell cavities were used to develop surface treatment procedures and to verify the absence of multipacting as predicted by simulation [2]. The 7-cell cavities (Fig. 2) feature stiffening rings to resist the Lorentz force. At each end of a multi-cell cavity is a Nb55Ti helium vessel end-dish for an integrated helium vessel and two HOM couplers of the DESY type [3]. The coupling of the rf to the cavity is accomplished by a waveguide coupler situated at one beam pipe 80 mm away from the end cell iris. It provides a Q_{ext}~ $2\cdot10^7$.

All flanges are made from Nb55Ti and Al_3Mg gaskets are used [4] for sealing.

Figure 2: LL seven cell cavity.

* Supported in part by DOE contract DE-AC05-84ER40150
!kneisel@jlab.org

INFLUENCE OF TA CONTENT IN HIGH PURITY NIOBIUM ON CAVITY* PERFORMANCE: PRELIMINARY RESULTS

P. Kneisel *!, G.R. Myneni *, D. Proch +, W. Singer+, X. Singer+, T. Carneiro++, C. Klinkenberg#, M. Imagumbai##,
* Jefferson Lab, Newport News, VA; USA; + DESY, Hamburg, Germany; ++ Reference Metals Co., Inc., Bridgeville, PA, USA; # Niobium Products Co., GmbH, DÜsseldorf, Germany; ## CBMM Asia , Tokyo, Japan

Abstract

In a previous paper [1] a program for reducing the costs of high purity niobium was outlined. This program was based on the fact that niobium prices could be reduced, if a higher content of Ta, which does not significantly affect the RRR–value, could be tolerated for high performance cavities. This contribution reports on the execution of this program and its present status.

Four ingots with different Ta contents have been melted and transformed into sheets. In each manufacturing step material quality has been monitored, using chemical analysis, thermal conductivity measurements and evaluation of mechanical properties. The niobium sheets have been scanned for defects by an eddy current device.

Two single cell cavities (CEBAF geometry) have been fabricated from each of three ingots, with Ta concentrations of 150, 600 and 1300 wtppm. A series of tests have been performed on each cavity with increasing amount of material removal.

This contribution reports on the test results and gives an analysis of the data.

INTRODUCTION

High purity niobium with RRR–values > 250 is exclusively used for the fabrication of high performance cavities for SRF accelerator projects such as SNS, TESLA, RIA or CEBAF Upgrade. Material cost is a significant fraction of total cavity cost, and one reason for the high costs is related to the specifications for tantalum content, which is in some cases required to be < 500 wtppm. Naturally occurring niobium–containing deposits such as columbite/tantalite or pyrochlore typically have high Ta content. Low Ta content in high purity niobium can only be obtained from niobium oxide, which appears as a byproduct of Ta production. Limited supply may be a big barrier to price stability and reliability for large projects such as TESLA.

The RRR–value (and therefore the thermal conductivity) of high purity niobium is mainly determined by interstitial impurities such as nitrogen, oxygen, hydrogen and carbon [2]. The contribution of Ta to the residual resistivity is significantly lower. It seems therefore quite reasonable to investigate the influence of Ta content in high purity niobium. However, one has also to make sure that the Ta is uniformly dispersed throughout the material, avoiding Ta clusters, which have in some cases been identified as causes of premature quenches in cavities. This is done by careful eddy current scanning of the sheets used for cavity fabrication [3].

In 2001 a project was launched to pursue this study with the following major objectives:

- Manufacturing of four niobium ingots with different Ta contents (< 150 wtppm,~ 600 wtppm, ~ 1200 wtppm and ~ 1300 wtppm)
- In these ingots only the Ta content was to be varied, content of other interstitial impurities was kept the same and verified by chemical analysis
- QA steps such as thermal conductivity measurements of ingots and rolled sheets and evaluation of mechanical properties of the rolled sheets accompanied production
- From the niobium sheets two single cell cavities each of the CEBAF variety were fabricated for Ta contents of < 150 ppm, ~ 600 ppm and 1300 ppm
- The rf performance of these cavities was measured at several stages during material removal from the surfaces

In the following the execution of this plan and the results from a total of 21 cavity tests are reported.

NIOBIUM SHEET MANUFACTURE

Ingot Production

The starting material for ingot production was pyrochlore as found at CBMM's deposit in Araxa, Brazil. Standard processing procedures [4] converted the ore to niobium ingots after triple electron beam melting of aluminothermically reduced niobium oxide. Addition of different amounts of Ta produced the four different ingots as mentioned above.

Material samples were taken from each ingot and the RRR-values were measured; the results are listed in Table 1.

Sheet Production

The ingots were converted into 2.8 mm thick sheets at the Tokyo Denkai facility in Japan in accordance with their standard processing procedures [5]. The RRR-values

* Supported in part by DOE contract DE-AC05-84ER40150
!kneisel@jlab.org

COLD TEST RESULTS OF THE ISAC-II MEDIUM BETA HIGH GRADIENT CRYOMODULE

R.E. Laxdal, I. Bylinskii, G.S. Clark, K. Fong, A.K. Mitra, R.L. Poirier, B. Rawnsley,
T.R. Ries, I. Sekachev, G. Stanford, V. Zvyagintsev,
TRIUMF, 4004 Wesbrook Mall, Vancouver, BC, Canada, V6T2A3

Abstract

Many proposals (RIA, Eurisol, ISAC-II) are emerging for a new generation of high gradient heavy ion accelerators. The ISAC-II medium beta cryomodule represents the first realized application that encorporates many new techniques to improve the performance over machines presently being used for beam delivery. Developments include upgraded tuner and coupling loop designs, electronic alignment monitoring systems and a high density lattice using superconducting solenoids. The new developments are described and the results of the first cold tests are presented.

INTRODUCTION

TRIUMF is now preparing a new heavy ion superconducting linac as an extension to the ISAC facility [1], to permit acceleration of radioactive ion beams up to energies of at least 6.5 MeV/u. The superconducting linac is composed of two-gap, bulk niobium, quarter wave rf cavities, for acceleration, and superconducting solenoids, for periodic transverse focussing, housed in several cryomodules. The linac is grouped into low, medium and high beta sections. An initial installation of 18 MV of medium beta cavities ($\beta = 5.8\%$, 7.1%) is due for commissioning in 2005. The first major milestone, reported here and achieved in June 2004, is the first rf cold test of the completed cryomodule.

The ISAC-II medium beta cavity design goal is to operate up to 6 MV/m across an 18 cm effective length with $P_{cav} \leq 7$ W. The gradient corresponds to an acceleration voltage of 1.1 MV, a challenging peak surface field of $E_p = 30$ MV/m and a a stored energy of $U_o = 3.2$ J and is a significant increase over other operating heavy ion facilities. This goal not only demands clean rf surfaces but an rf system capable of achieving stable performance. To achieve stable phase and amplitude control the cavity natural bandwidth of $\pm$0.1 Hz is broadened by overcoupling to accomodate detuning by microphonic noise and helium pressure fluctuation. The chosen tuning bandwidth of $\pm$20 Hz demands a cw forward power of $\sim$200 W and peak power capability of $\sim$400 W to be delivered to the coupling loop.

The large accelerating gradients produce a large rf defocussing. A linac lattice consisting of modules of four cavities with a single high field (9 T) superconducting solenoid in the center is adopted. Beam diagnostics are positioned between modules at a waist in the beam envelope. The lattice is compatible with acceleration of multi-charge beams of $\Delta Q/Q \leq 7\%$.

MEDIUM BETA CRYOMODULE

The engineering description and cryogenic tests are reported in a separate article.[6] The vacuum tank consists of a stainless steel rectangular box and lid. All services and feedthroughs are located on the lid. A serial LN2 piping circuit cools both the copper panels formed into a thermal shielding box and the rf coupling loops. Magnetic shielding in the form of high μ sheet is suspended between the warm wall and the cold shield. Cavities and solenoids are suspended from a common support frame itself suspended from the tank lid (Fig. 1). Each cryomodule has a single vacuum system for thermo-isolation and beam acceleration. This demands extreme cleanliness of internal components and precludes the use of volatile lubricants and flux, as well as particulate generators, to avoid superconducting surface contamination. Assembly is done in the new ISAC-II clean room.

Figure 1: Cryomodule top assembly in the assembly frame prior to the cold test.

Alignment

The cavities must be aligned to within 0.4 mm and the solenoid to 0.2 mm. A wire position monitor (WPM)[7] system has been developed to monitor the position of the cold mass during thermal cycling. The monitors each consisting of four striplines are attached to the cavities and solenoid by off-center 'L' brackets. A wire running parallel to the beam axis and through the monitors carries an rf signal that is measured by the striplines and is converted to an x-y position. In addition optical targets are placed in

CONCEPTUAL LAYOUT OF THE EUROPEAN X-FEL LINEAR ACCELERATOR CRYOGENIC SUPPLY

H.Lierl, B.Petersen, A.Zolotov, DESY, Hamburg, Germany

Abstract

As a source for the European X-ray Free Electron Laser (European X-FEL project) at DESY a superconducting linear accelerator will deliver a pulsed electron beam of about 20-GeV. A conceptual layout for the cryogenic supply of the linac is presented. The linac will consist of about 1000 superconducting niobium 1.3-GHz 9-cell cavities, which will be cooled in a liquid-helium bath at a temperature of 2-K. In addition to the main linac of about 1.6-km length, two injector sections have to be supplied separately by means of helium refrigerators and the related helium distribution system.

THE EUROPEAN X-FEL PROJECT

In order to reach the X-ray region (0.1 nm) by means of a Free Electron Laser the European X-FEL-Project is presently under development at DESY [1].

A new superconducting linear accelerator will supply a pulsed electron beam of 20-GeV for the operation of the FEL. The TESLA technology will be applied for the linear accelerator:

The X-FEL linear accelerator will consist of about 1000 superconducting niobium 1.3-GHz 9-cell cavities, which will be cooled in a liquid-helium bath at a temperature of 2-K. Eight cavities and one superconducting magnet package will be assembled in cryomodules of 12.2-m length. The 2-K cryostat will be protected against heat radiation by means of two thermal shields cooled to temperatures of 5-K to 8-K and 40-K to 80-K respectively. A cross-section of a cryomodule is shown in Fig. 1.

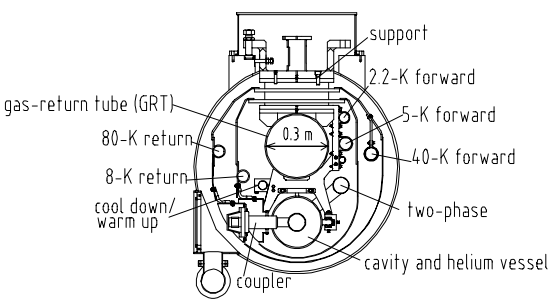

Figure 1: A cross-section of a XFEL-cryomodule.

CRYOGENICS

The XFEL-linac consists of two parallel injector cryomodules, a booster section, a bunch compressor section and the main linac cryomodules. The cryogenic supply of the two parallel injector cyromodules is separated from the supply of the booster and the cryomodules in the main tunnel. From the cryogenic point of view the four booster cryomodules including 3rd harmonic cavities and the main linac cryomodules are treated as one unit of about 1.6-km length. The 2-K cryogenic supplies of the main linac unit will be separated in 10 parallel cryogenic sections each of 12 cryomodules. These sections are called 'strings.' Including the booster cryomodules, 108 cryomodules of the main linac unit will be normally used for beam acceleration. Twelve spare cryomodules are kept in stand-by.

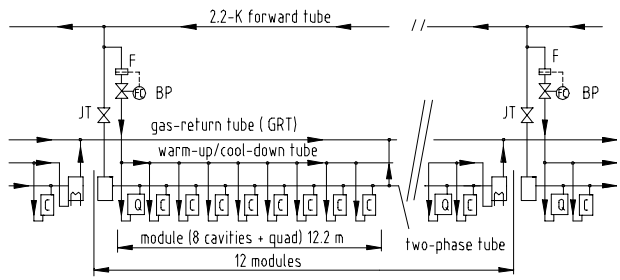

Figure 2 : A simplified scheme of the equipment and instrumentation of a XFEL-linac cryogenic string, which consists of 12 cryomodules, is shown. 'Q' corresponds to a superconducting magnet package.

The strings are separated by string connection boxes. Each box contains a Joule-Thomson valve (JT) for the steady-state operation and a bypass valve (BP) for the cool-down/warm-up. The JT-valves are supplied with helium at a temperature of 2.2-K and a pressure of 0.12 MPa by means of the 2.2-K forward tube (see Fig.1 and Fig.2). Here the helium is expanded to 0.0031-MPa into the two-phase tube and the individual helium vessels of the cavities are filled with liquid helium at 2-K. The helium vapour is directed back to the refrigerator by means of the gas return tube (GRT, see Fig.1). The string connection boxes are equipped with a vacuum barrier, which separates the insulation vacuum of the strings. The GRT as well as the supply and return tubes of the thermal shields will not be separated in string sections. At the end of each cryomodule the two-phase tube is connected to the GRT. The first string of the main linac unit is sub-divided by a bunch compressor section of 120 m length. This warm section separates the first four booster cryomodules from the main linac cyromodules. The bunch compressor section is bridged by a bypass transfer line (BCBTL), which contains all cryogenic process tubes. Inside the BCBTL the process tube diameters can not be reduced to smaller sizes, if unacceptable large

RF COUPLER DESIGN FOR THE TRIUMF ISAC-II SUPERCONDUCTING QUARTER WAVE RESONATOR

R. Poirier, K. Fong, P. Harmer, R. Laxdal, A. Mitra, I. Sekatchev, B. Waraich, V. Zvyagintsev,
TRIUMF*, Vancouver, 4004 Wesbrook Mall, Vancouver, Canada, V6T2A3

Abstract

An rf Coupler for the ISAC-II medium beta (β=0.064 and 0.074) superconducting quarter wave resonators was designed and tested at TRIUMF. The main goal of this development was to achieve stable operation of superconducting cavities at high acceleration gradients and low thermal load to the helium refrigeration system. The cavities will operate at a 6 MV/m acceleration gradient in overcoupled mode at a forward power of 200 watts at 106 MHz. The overcoupling provides ± 20 Hz cavity bandwidth, which improves the stability of the rf control system for fast helium pressure fluctuations, microphonics and environmental noise. Choice of materials, cooling with liquid nitrogen, aluminum nitride rf window and thermal shields insures a small thermal load on the helium refrigeration system by the Coupler. An rf finger contact, which caused micro dust in the coupler housing, was eliminated without any degradation of the coupler performance. Rf and thermal calculations, design and test results on the coupler are presented in this paper.

INTRODUCTION

The ISAC II [1] medium beta cavities have a design gradient of 6 MV/m. This corresponds to a peak surface fields of ~ 30 MV/m and ~60mT, and a stored energy of U=3.2 J. This is a significant increase over other operating heavy ion facilities. To achieve stable phase and amplitude control the natural bandwidth of +/- 0.1 Hz is broadened by overcoupling to accommodate detuning by microphonic noise and helium pressure fluctuations (~1-2 Hz/Torr). The ISAC II medium beta cavities are outfitted with a passive mechanical damper [2] and the microphonics are not expected to be more than a few hertz RMS. The chosen tuning bandwidth of +/- 20 Hz demands a cw forward power of 200 watts and a peak power capability of 400 watts to be delivered to the coupling loop at the cavity.

The various prototypes of the coupler design are reported in [3]. We started with a copy of an INFN-Legnaro design for gradients of 3-4 MV/m and forward power of 50 W, which we identified as Mark I. In the Mark II design we changed the loop assembly materials and added LN2 cooling. We initially tried to cool the outer conductor of the cable with an LN2 cooling loop as well but opted to add a thermal shield inside the cryostat along the rf drive cable which performed a more efficient job in reducing the added thermal load on the helium system. The thermal shield is connected to the LN2 shield of the cryostat and restricts heat radiation flux from the coupler rf cable to the helium system. In the Mark III version we added a 1-inch long split ring piece of Aluminum Nitride (AIN) dielectric to thermally connect the inner and outer conductors of the loop near the heat exchange block to reduce inner conductor heating. In the Mark IV prototype shown in Fig.1, the outer conductor and heat exchange block are formed from a solid piece of copper and a cooling channel running through the block allows direct cooling with LN2. All of these modifications allowed us to reach our design goal of 200 watts forward power at the coupling loop with less than 1 watt of power being added to the helium load. The Mark V (Fig.2 and Fig.6) is the final design for the cryomodule and differs from the Mark IV only by the heat exchange block design, which is adapted for the cryomodule assembly. The thermal shield and heat exchange block are cooled with the same LN2 flux.

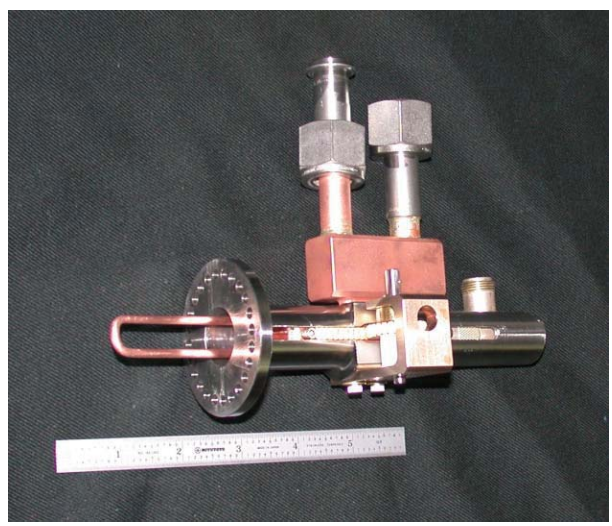

Figure 1: Mark IV Coupling Loop Assembly ready for installation into the cavity.

RF COUPLER

Coupling Loop Assembly

The housing of the coupling loop is made from thin stainless steel for thermal isolation from the cavity. The inner and outer conductors of the coupling loop assembly are made of copper. The outer conductor, which includes an integrated heat exchange block, is driven in and out through a rotating shaft attached to a stepping motor on the cryostat lid via a rack and pinion mechanism on the loop housing. The position of the AIN dielectric and the

* TRIUMF receives funding via a contribution agreement through the National Research Council of Canada

A WIRE POSITION MONITOR SYSTEM FOR THE ISAC-II CRYOMODULE COMPONENTS ALIGNMENT

W. Rawnsley, Y. Bylinski, G. Dutto, K. Fong, R. Laxdal, T. Ries, TRIUMF, Vancouver, Canada
D. Giove, INFN, Milan, Italy

Abstract

TRIUMF is developing ISAC-II, a superconducting (SC) linac. It will comprise 9 cryomodules with a total of 48 niobium cavities and 12 SC solenoids. They must remain aligned at liquid He temperatures: cavities to ±400 µm and solenoids to ±200 µm after a vertical contraction of ~4 mm. A wire position monitor (WPM) system based on a TESLA design has been developed, built, and tested with a prototype cryomodule. The system is based on the measurement of signals induced in pickups by a 215 MHz signal carried by a wire through the WPMs. The wire is stretched between the warm tank walls parallel to the beam axis providing a position reference. The sensors, one per cavity and two per solenoid, are attached to the cold elements to monitor their motion during pre-alignment, pumping and cool down. A WPM consists of four 50 Ω striplines spaced 90° apart. A GaAs multiplexer scans the WPMs and a Bergoz card converts the rf signals to dc X and Y voltages. National Instruments I/O cards read the dc signals. The data acquisition is based on a PC running LabVIEW. System accuracy is ~7 µm. The paper describes system design, WPM calibration and test results.

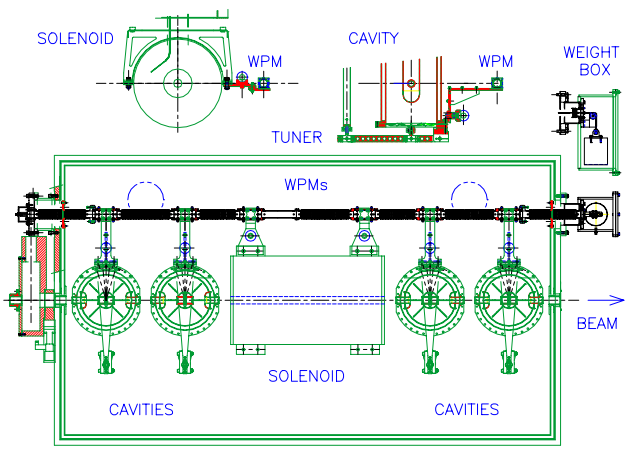

Figure 1: A plan view of a medium beta cryomodule and cross-sections of the wire weight box and WPM mounting brackets.

INTRODUCTION

TRIUMF is now constructing an extension to the ISAC facility, ISAC-II, to permit acceleration of radioactive ion beams up to energies of at least 6.5 MeV/u for masses up to 150. The proposed acceleration scheme will use the existing ISAC RFQ (E = 150 keV/u) with the addition of an ECR charge state booster to achieve the required mass

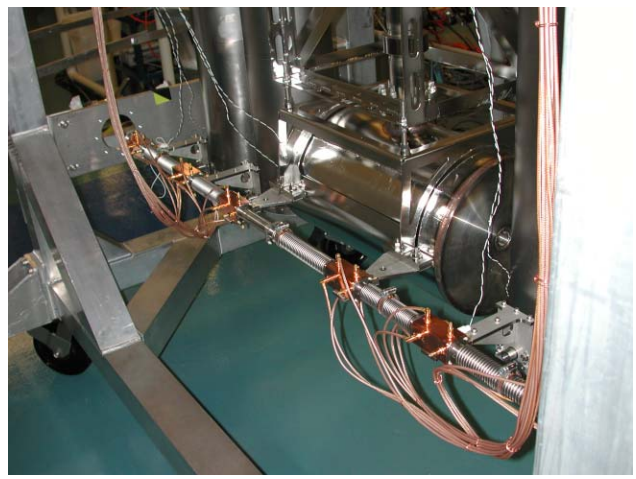

Figure 2: The WPMs and bellows form a coaxial structure. The stripline signals are brought out by 24 rf cables.

to charge ratio ($A/q \leq 30$) for masses up to 150. A new room temperature IH-DTL will accelerate the beam from the RFQ to 400 keV/u followed by a post-stripper heavy ion SC linac designed to accelerate ions of $A/q \leq 7$ to the final energy. The SC linac will be composed of two-gap, bulk niobium quarter wave rf cavities for acceleration and SC solenoids for periodic transverse focussing, housed in several cryomodules. A total of 48 cavities and 12 solenoids will be used. The center line of each cavity must be aligned to within ±400 µm of the true beamline centre while those of the solenoids must be within ±200 µm.

We will discuss the system that has been designed to monitor changes in the alignment of the cavities and solenoids during pump out and cool down. The system has been tested in the first of five medium beta cryomodules, each containing four cavities and a single solenoid, figure 1 [1,2,3].

MEASUREMENT SYSTEM

WPMs

A stretched wire alignment system based on a TESLA Test Facility system has been developed at TRIUMF [4,5]. Six WPMs, one per cavity and two on the solenoid, are positioned along a wire displaced 30.48 mm horizontally from the beam axis to measure lateral displacements. The wire, stretched between the tank walls, provides a position reference and carries a 215 MHz rf signal. The WPMs are supported from the cold masses by stainless steel brackets, figure 2.

SIMULATION OF THE RF COUPLER FOR TRIUMF ISAC-II SUPERCONDUCTING QUARTER WAVE RESONATORS

V. Zvyagintsev, TRIUMF*, 4004 Wesbrook Mall, Vancouver, Canada, V6T2A3

Abstract

The inductive RF coupler for the TRIUMF ISAC-II 106 MHz superconducting accelerating quarter wave resonators [1, 2] was used as a basis for the simulation model of stationary transmission processes of RF power and thermal fluxes. Electromagnetic simulation of the coupler was done with ANSOFT HFSS code. Transmission line theory [3] was used for electromagnetic wave calculations along the drive line to the Coupler. An analogy between electric and thermal processes allows the thermal calculations to be expressed in terms of electrical circuits [4]. The data obtained from the simulation are compared to measured values on the RF coupler.

INTRODUCTION

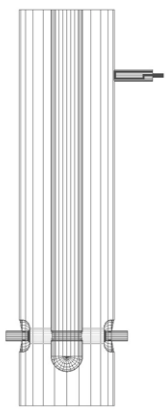

fo	MHz	106
E_a	MV/m	6
P	W	4
Q_o		5.5E+08
U	J	3.3
B_p	mT	60
Δf	Hz	40
β		200
P_f	W	200

$$1/Q_L = 1/Q_o + 1/Q_e \qquad \beta = Q_o/Q_e$$

$$P_f = P\frac{(\beta+1)^2}{4\beta} \qquad \Delta f_L = f_o/Q_L$$

Figure 1: HFSS model of SC TRIUMF ISAC-II medium-β QWR with inductive coupler.

The inductive coupler for the TRIUMF ISAC-II 106 MHz superconducting accelerating quarter wave resonators was designed and successfully tested. The main goal of the design is achieved: the coupler provides more than 200 W forward power which is needed to get an accelerating field E_a=6 MV/m with a bandwidth 40 Hz to maintain a stable cavity operation disturbed by noise and helium pressure fluctuations and thermal load for helium system from the coupler is less than 1 W. Coupler R&D was done with test cryostat and the first TRIUMF ISAC-II cryomodule with 4 medium-β cavities was equipped with new couplers and succesefully tested [1].

* TRIUMF receives funding via a contribution agreement through the National Research Council of Canada

This paper is some attempt to collect the calculation experience from this R&D which can be used for coupler design for next TRIUMF ISAC-II cryomodules which will be equipped with high-β resonators.

HFSS COUPLER SIMULATION

Coupling and Loop Power Dissipation

Due to very high Q of the cavity it is not possible to use the driven mode solution so the eigenmode solution was used instead. For simulation purposes it was assumed that the cavity and coupler were perfect conductors. The coupler port is loaded with an equivalent impedance of 50 Ω. The mesh is refined in the beam and coupler region. The power dissipation on the loop was calculated in the Postprocessor by using normalization for acceleration

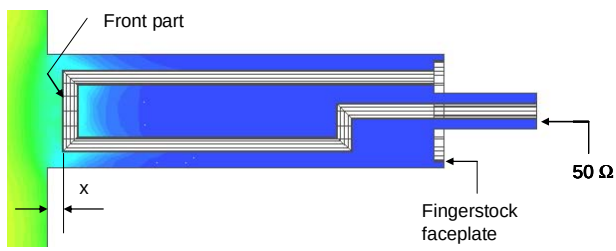

Figure 2: Magnetic field and port bondary condition for HFSS coupling loop model.

field E_a=6 MV/m and conductivity of copper. P_{loop} is the total power dissipated on the loop and P_{front} is the power dissipated on the front part of the loop which is used for analytical check. Data obtained in HFSS calculations at different loop positions are shown in Table 1. Power dissipated on the loop is due to field penetration from the cavity and rf current to the 50 Ω load. In the driven mode which is the real condition for overcoupled operation, the rf current will be very small because a current node appears at the loop as shown in Fig.7. Power dissipation in the load is inversely proportional to the quality factor. By using the external quality factor Q from table 1, and power dissipation P and quality factor Q_o from Fig.1, then power dissipation in the load and power dissipation on the loop due to the rf current through the load P_{loop}* can be calculated (to make a coorection for driven mode). Power dissipation on the loop P_{loop}** for strong overcoupled driven mode is a difference between power dissipation for eigen mode P_{loop} and P_{loop}*. The external quality factor can be defined from the following expression:

$$1/Q_e = 1/Q + 1/Q_{loop} \qquad (1)$$

Loop quality factor defined from loop power dissipation

ENGINEERING AND BUILDING RF STRUCTURES – THE WORKS*

Dale L. Schrage†
Los Alamos National Laboratory, Los Alamos, NM, USA, 87545

Abstract

The translation of the physics designs of linear accelerators into engineering and manufacturing requirements is discussed. The stages of conceptual design, prototyping, final design, construction, and installation are described for both superconducting (LANL $\beta = 0.175$ Spoke Cavity) and normal-conducting (APT/LEDA 6.7 MeV RFQ) accelerators. An overview of codes that have linked accelerator cavity and thermal/structural analysis modules is provided.

INTRODUCTION

Over the past few decades, the field of design of linear accelerators has progressed as the programmatic needs have evolved to requirements for better performance in terms of higher duty factor, higher beam current, and higher accelerating gradient. The requirements for normal-conducting proton accelerators have advanced from such low-power applications as the Beam Experiment Aboard a Rocket (BEAR) of 30 mAmps 1 MeV of H^- at 0.025% duty factor, average beam power of 8 watts [1], to the Low Energy Demonstration Accelerator (LEDA) of 100 mAmps 6.7 MeV of H^+ at CW duty factor, average beam power of 670 Kwatts [2]. These high beam power applications become thermal management challenges. The lower duty factor applications can become similarly difficult if the accelerating gradient becomes sufficiently high that the RF thermal load is high.

For superconducting accelerators, the requirements have advanced from the Continuous Electron Beam Accelerator Facility (CEBAF) at 0.1 mAmps of e^- at CW duty factor with a gradient of 5 Mvolts/meter [3] to pulsed applications of non-relativistic beams such as the Spallation Neutron Source (SNS) [4], 30 mAmps of H^- at $\beta = 0.65$ and pulsed at 60 Hz and to the TESLA accelerator with $\beta = 1$ cavities operated at a gradient of 35 Mvolts/meter [5]. The medium-β ($0.5 \leq \beta < 1.0$) pulsed accelerators, which utilize elliptical cavities, present significant structural challenges in dealing with the Lorentz force detuning and the effects of vibration. Both phenomena cause deformation of the cavity structure and interact with the cavity fields and frequency.

Low velocity applications have advanced from the heavy ion cavities (split-ring resonators @$\beta = 0.06$) for the ATLAS Project [6] to the higher-β spoke cavities for waste transmutation, 30 mAmps of H^+ [7]; both are at CW duty factor. Recent developments on the RIA Project [8] have led to consideration of use of spoke cavities at up to $\beta = 0.6$ [9]. These low-β accelerators utilize much stiffer geometries such as 1/4-λ and spoke resonators. For these, the Lorentz force coefficients are much lower and the structural dynamics considerations are less severe. However, with the low beam current and resulting high loaded Q, there are microphonics concerns that must be addressed. And, there are still static loading issues (e.g., vacuum) and the matter of tuning forces. For spoke cavities with more than two gaps, the development of frequency tuning schemes involves interaction of the RF and structural analyses.

During the past decade, commercial codes have been developed that link the RF cavity, thermal, fluid dynamics, and structural analyses to a single CAD model. The first finite element codes in the US were developed in the 1950's for the structural design of military aircraft. Linked thermal analyses modules were added to these in the 1980's. Three-dimensional RF cavity codes and computational fluid dynamics (CFD) codes were developed independently during the 1980's. In the mid-1990's, the code vendors began linking the CFD module to the thermal module and created RF cavity modules that were then linked.

NORMAL-CONDUCTING CAVITIES

The analysis of normal-conducting cavities falls into two categories: cavities that are basically 2-dimensional and those that have significant 3-dimensional features. Except for the end regions, RFQs are basically two-dimensional structures. The cavity can be analyzed using SUPERFISH [10] for the determination of resonant frequency, quality factor, peak electric and magnetic fields, RF thermal loads, and tuning sensitivity. It is possible to create FORTRAN or C^{++} code to parse the input and output files of SUPERFISH to extract the cavity geometry, RF thermal loads, and tuning sensitivity information and to produce files that can be input to commercial thermal and structural finite element analysis (FEA) codes. The thermal module of the FEA code is run to determine the temperature distribution and that is then input to the structural module to determine the displacements and stresses. The displacement output file of the FEA code is then convolved with the tuning sensitivity data from SUPERFISH to predict the frequency shift. These programs can be run in batch mode and iteratively to solve for the coolant temperature necessary to maintain the cavity on resonance.

This procedure worked very well for the LEDA RFQ [2]. This 8-meter long cavity (Figure 1) had longitudinally variable electric field and vane skirt width. Thus, multiple

* Work Supported by the US Department of Energy
† dls@lanl.gov

SURVEY OF ADVANCED ACCELERATION TECHNIQUES

C. Joshi, UCLA, Los Angeles, CA 90095 USA

Abstract

In this paper I will survey some of the notable progress that has been made on advanced techniques for particle acceleration. Rather than trying to cover every technique superficially I will restrict myself to talking about three schemes that are showing promise: the inverse free electron laser (IFEL), the laser-wakefield acceleration (LWFA), and the beam-driven plasma-wakefield acceleration (PWFA). The progress made in all these schemes was recently presented at the AAC2004 Workshop at Stonybrook in June and in many instances the results presented by the authors are as yet unpublished.

INVERSE FREE ELECTRON LASER RESEARCH (IFEL)

In an IFEL, one uses a periodic magnet array (a.k.a., a wiggler or an undulator) to cause electron trajectory to oscillate as the electron beam traverses the array (Fig. 1). A laser beam is co-propagated with the electron beam. Now net energy exchange is possible from the laser beam to the electron if the resonance condition

$$\gamma^2 = \frac{\lambda_w}{2\lambda_L}\left(1+\frac{K^2}{2}\right) \qquad (1)$$

is satisfied. Here γ is the relativistic Lorentz factor, λ_w and λ_L are the wavelengths of the wiggler and the laser respectively, and $K = eB_o\lambda_w/2\pi mc$ is the wiggler strength parameter. Clearly, as the beam energy (γ) increases one has to either increase λ_w by tapering the wiggler or increase K or both.

The IFEL principle can be used to bunch the electron beam on the laser wavelength scale. Here the idea is to velocity modulate the electron beam by sending it through a short section of an undulator. The velocity modulated beam then bunches as it goes through a magnetic chicane.

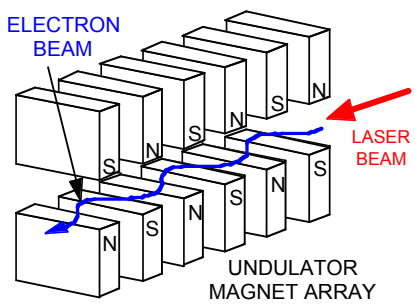

Figure 1: Schematic of the Inverse-Free Electron Laser.

Recent Experiments on the IFEL Scheme

There have been two notable recent experiments on the IFEL scheme. In the first experiment, knows as STELLA[1] for Staged Electron Laser Acceleration, a beam of nominally 45 MeV electrons from the Advanced Test Facility (ATF) at BNL was first sent through an IFEL pre-buncher magnet. This magnet was followed by a chicane compressor and then a second tapered undulator. A CO_2 laser was sent collinearly with the electron beam. The laser was focused at the center of the tapered wiggler to give a peak intensity of $\sim 2 \times 10^{12}$ W/cm^2. This meant that the laser intensity in the pre-buncher section was much lower. Nevertheless, it was sufficient to achieve a ±0.5% momentum modulation. The chicane delivered a bunched beam at the entrance of the tapered undulator. Since the same CO_2 laser beam is used to microbunch the beam and accelerate the pre-bunched beam, phasing between the two is preserved. A spectrometer which analyses the beam exiting the tapered undulator shows acceleration of the pre-bunched beam with an average gradient of 27 MeV/m. The capture efficiency of the pre-bunched beam under optimum condition was over 80% and the accelerated beam has $\lesssim$1% energy spread.[2]

This experiment is extremely significant because it showed many firsts: staged laser acceleration, acceleration of monoenergetic beam and extremely good capture efficiency.

The STELLA collaboration is now planning to do a much higher gradient two-staged laser acceleration experiment. In this method an IFEL prebuncher is used as before to micro-bunch the electron beam on the laser wavelength scale. However, this is followed by a plasma wave excited by the same intense laser in a plasma. Since gradients on the order 1 GeV/m are readily observed in plasmas, it is hoped that mono-energetic acceleration at high gradients can be demonstrated using this two-stage approach that combines IFEL and plasma wakefield technologies.[3]

In a second recent experiment at UCLA's Neptune laboratory, a more powerful, 300 GW, CO_2 laser was used in conjunction with a strongly tapered undulator. Consequently, the nominally 14 MeV electron beam was accelerated out to more than 30 MeV with a peak gradient of > 50 MeV/m.[4] These gradients are beginning to get interesting to be of use in practical devices.

LASER WAKEFIELD ACCELERATOR (LWFA)

Now I will describe recent breakthroughs in the laser-plasma accelerator field. In particular I will confine my remarks to the so-called LWFA scheme (see Fig. 2) where

DEVELOPMENT OF THE UNILAC TOWARDS A MEGAWATT BEAM INJECTOR

W. Barth, L. Dahl, J. Glatz, L. Groening, S. Richter, S. Yaramishev*
Gesellschaft für Schwerionenforschung, D-64291 Darmstadt, Germany

Abstract

For the future Facility for Antiproton and Ion Research (FAIR) at Darmstadt the present GSI-accelerator complex, consisting of the linear accelerator UNILAC and the heavy ion synchrotron SIS 18, is foreseen to serve as U^{28+}-injector for up to 10^{12} particles/s. After a new High Current Injector (HSI) was installed, many different ion species were accelerated in the UNILAC for physics experiments. In 2001 a high energy physics experiment used up to $2\cdot10^9$ uranium ions per SIS18-spill (U^{73+}) while a MEVVA ion source was in routine operation for the first time. In the past two years, different hardware measures and careful fine tuning in all sections of the UNILAC resulted in an increase of the beam intensity to $9.5\cdot10^{10}$ U^{27+}-ions per 100 µs or $1.5\cdot10^{10}$ U^{73+}-ions per 100 µs. The contribution reports results of beam measurements during the high current operation with uranium beams (pulse beam power up to 0.5 MW). One of the major tasks was to optimize the beam matching to the Alvarez-DTL. In addition further upgrades, including improved beam diagnostics, are described, which allow to fill the SIS 18 up to the space charge limit (SCL) of $2.7\cdot10^{11}$ U^{28+}-ions per cycle. We acknowledge the support of the European Community-Research Infrastructure Activity under the FP6 "Structuring the European Research Area" programme (CARE, contract number RII3-CT-2003-506395) and INTAS (project 03-54-3543).

INTRODUCTION

The conceptual design of the international Facility for Antiprotons and Ion Research (FAIR) at GSI in Darmstadt (Fig. 1) has evolved from the science requirements: higher intensities will be achieved, compared to the present GSI accelerator facility, through faster cycling and, for heavy ions, lower charge state which enters quadratically into the SCL. The desired energy of up to 1.5 GeV/u for radioactive beam production is delivered by the synchrotron SIS 100, which also generates intense beams of energetic protons up to 30 GeV for pbar-production. The energy of 30 GeV/u for heavy ions is generated by using higher charge states in combination with the slower cycling synchrotron SIS 300. The SIS 300 can also be used as a stretcher for radioactive beams, which can be injected, cooled and stored in a system of rings with internal targets and in-ring experimentation. The various rings may be shared for the use with different beams.

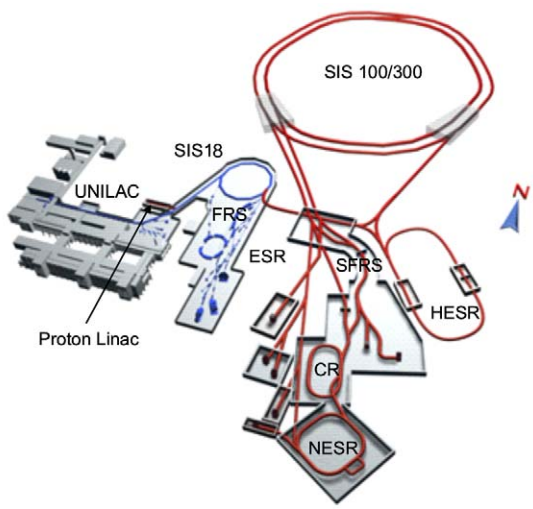

Figure 1: The proposed Accelerator facility FAIR at GSI in Darmstadt [1].

* on leave from ITEP, Moscow, Russia.

Table 1: Design uranium beam parameters at UNILAC and SIS 18 injection [2]

	HSI entrance	HSI exit	Alvarez entrance	SIS 18 injection	**Required for FAIR**
Ion species	$^{238}U^{4+}$	$^{238}U^{4+}$	$^{238}U^{28+}$	$^{238}U^{73+}$	**$^{238}U^{28+}$**
El. Current [mA]	16.5	15	12.5	4.6	**15.0**
Part. per 100µs pulse	$2.6\cdot10^{12}$	$2.3\cdot10^{12}$	$2.8\cdot10^{11}$	$4.2\cdot10^{10}$	**$3.3\cdot10^{11}$**
Energy [MeV/u]	0.0022	1.4	1.4	11.4	**11.4**
ΔW/W	-	$4\cdot10^{-3}$	$\pm1\cdot10^{-2}$	$\pm2\cdot10^{-3}$	**$\pm2\cdot10^{-3}$**
$\varepsilon_{n,x}$ [mm mrad]	0.3	0.5	0.75	0.8	**0.8**
$\varepsilon_{n,y}$ [mm mrad]	0.3	0.5	0.75	2.5	**2.5**

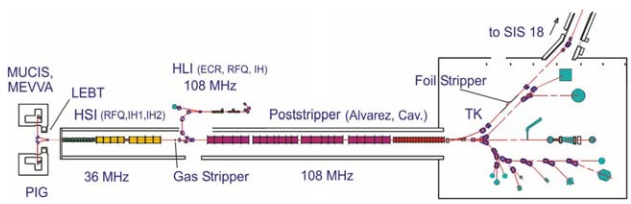

Figure. 2: Schematic overview of the GSI UNILAC [3].

The present GSI accelerator complex will serve as an injector for high intensity heavy ions to fill the SIS 100 to its space charge limit. In the last three years GSI put some effort in increasing the delivered uranium intensities to the SIS 18. An additional upgrade program for the UNILAC is foreseen to reach the required beam brilliance. For uranium (reference ion) the UNILAC has to deliver $3.3\cdot10^{11}$ U^{28+}-particles per 100 µs (see Table 1) to the present synchrotron SIS 18. Currently for a 15 emA $^{238}U^{4+}$ beam from the HSI [4] up to $4\cdot10^{10}$ U^{73+} particles should be delivered to the SIS 18 (during 100 µs), while the SIS 18-SCL is reached by a 20 turn injection into the horizontal phase space. The HSI-front end consists of ion sources of MEVVA-, MUCIS- or Penning-type and a low

DEVELOPMENTS AND FUTURE PLANS AT ISAC/TRIUMF

P. W. Schmor, TRIUMF, Vancouver, Canada

Abstract

The ISAC (Isotope Separator and Accelerator) at TRIUMF uses the ISOL (On Line Isotope Separator) technique with up to 100 microamperes of 500 MeV protons from the TRIUMF cyclotron driver available to create exotic isotopes in a thick target. An ion beam formed from these exotic isotopes is transported at 2 keV/u, mass separated, injected into a room temperature RFQ Linac and then into a five-tank drift tube linac that provides variable-energy accelerated exotic-beams from 0.15 to 1.8 MeV/u for nuclear astrophysics experiments. Super conducting rf cavities are presently being added to the linac chain to permit a further increase in the maximum energy of the exotic beams to 6.5 MeV/u. An ECR-based charge state booster is also being added in front of the RFQ to increase the available mass range of the accelerated isotopes from 30 to about 150. A second proton beam line and new target station for target and ion source development have been proposed for ISAC. In the future this new target station could be used as an independent simultaneous source of exotic beams for the experimental program.

INTRODUCTION

The availability of short-lived exotic beams has become an important goal in the search for solutions to a number of important questions in science. The science includes nuclear astrophysics, nuclear structure, atomic physics & condensed matter physics. There are two main techniques for creating these exotic beams, namely, the fragmentation method and the ISOL method. At TRIUMF the ISOL approach is used.

ISOL type facilities typically use a light-ion driver-accelerator to produce a variety of isotopes in a target. These isotopes are transferred by effusion and diffusion processes to an adjacent ion source where the isotopes are ionized, extracted and formed into an ion beam. A particular isotope is then selected by slits at the focal plane of a mass separator and transported to experimental stations either prior to or following further acceleration. The required beam quality, the beam intensity, the beam energy and the momentum spread of the accelerated exotics depend on the particular experiment. For ISAC the user input led to a continuously variable energy from 0.15 to 1.5 MeV/u for isotopes having an $a/q \leq 30$.

At TRIUMF the driver is an H-, 500 MeV, cyclotron that has been shown to have the capability of accelerating over 400 μA to 500 MeV. The TRIUMF cyclotron can simultaneously extract multiple independent proton beams into different locations. A transport beamline from the cyclotron to the target in ISAC is designed for a maximum of 100 μA of 500 MeV protons. The isotope production target material is located in a tube (2 cm diameter and up to 20 cm long) and the material composition varies depending on the particular isotopes that are being optimized. The target and ion source can be biased up to a voltage of 60 keV. The extracted beam is transported through a beamline with electrostatic focusing and steering elements. This focusing approach allows isotopes with adequate intensities to be used for tuning purposes and then, to adjust only the mass selecting system to the low flux isotopes. These fluxes cannot be, in general, observed on the normal beam diagnostic elements. However, with the electrostatic focusing elements, the beamline tune is not sensitive to the mass, only to the beam energy and that is kept constant. Therefore the low intensity isotope can be transported through the line without needing to readjust the beam optics elements and a minimum of low intensity diagnostics for optimizing the transport efficiency to the experimental target. An off line ion source (OLIS) is used to provide stable beams for commissioning beamlines, accelerators, setting up tunes and experimental calibrations. Figure 1 shows the layout of the TRIUMF facility indicating by color coding the existing and planned modifications.

ISAC I

Although the ISAC I accelerators were initially designed for a maximum energy of 1.5 Mev/u for beams having a $m/q \leq 30$ ratio, isotopes have been accelerated from the injection energy of 2 keV/u up to a maximum energy of 1.8 MeV/u. The accelerating system consists of a multi-harmonic pre-buncher, a cw RFQ, a medium energy beam transport (MEBT) section, an electron stripper, a re-buncher, a cw drift tube linac. The pre-buncher provides a pseudo saw tooth velocity profile at a fundamental frequency of 11.8 MHz, thereby providing approximately 86 nS between beam buckets. Bunched beam from the pre-buncher fills every third bucket of the 35 MHz, cw, 8 m long, split-ring, RFQ. The singly-charged beam out of the RFQ, at energy 0.15 Mev/u, is focused (transversely and longitudinally) and stripped to a higher charge state in the medium energy beam transport line (MEBT). The MEBT has an 106 MHz bunch rotator to provide a time focused beam at the stripper and a double frequency rf chopper to select cleanly separated rf bunches separated by either 85 or 107 ns. The stripped beam is magnetically bent through 90 by two 45 dipoles where silts are used to select only those isotopes having a chosen m/q ($3 \leq m/q \leq 6$) and re-bunched prior to injection into the first tank of the DTL. The DTL provides a beam that can be continuously varied in energy from 0.15 to 1.8 MeV/u. The DTL is a separated-function structure with five DTL tanks, each operating at 0° synchronous phase, with magnetic

THE KEK C-BAND RF SYSTEM FOR A LINEAR COLLIDER

H. Matsumoto#, Shigeru Takeda, S. S. Win, M. Yoshida, KEK, Tsukuba Japan
H. Baba, T. Shintake, SCSS Group, RIKEN, Harima Japan
J. S. Oh, PAL/POSTECH, Pohang, Republic of Korea
Y. Takasu, University of Tokyo, Tokyo Japan
F. Furuta, University of Nagoya, Nagoya Japan

Abstract

C-band (5712-MHz) RF-system hardware R&D for an e^+e^- linear collider started in 1996 at KEK. We have already developed three conventional 50-MW class klystrons, a smart modulator, and a novel HOM-free accelerator structure (Choke-mode type, full-scale high power model) [1], [2], [3], [4]. A very stable ceramic high voltage monitor was successfully tested up to 367-kV with 4.5-µsec pulses. Very good agreement in the expected division ratio and signal waveform fidelity was observed in high power tests. A new C-band SiC type high power rf-load, extending the power handling capability up to 50-MW is now being designed. It should have excellent mass production characteristics as it uses circularly symmetric TM_{011} chained cavities [5]. For the first ever, a high power prototype rf compressor (SLED III) cavity made of a low thermal expansion material (Super Invar) was designed to provide stable operation even with a very high Q of 200-k, it was operated up to a 135-MW peak output power in 0.5-µsec rf pulses compressing input 45-MW 2.5-µsec pulses [6]. The C-band linac rf-system will be used for production work in the SASE-FEL (Spring8 Compact SASE Source, SCSS) project at SPring-8 [7]; SCSS will also serve to not only verify the design concepts and components, but will also provide realistic experience and lessons which can eventually be deployed in the main linac rf system for a future large scale linear collider.

INTRODUCTION

The C-band main linac design and development has been motivated by the increasingly urgent need for a linear collider capable of undertaking the next essential physics programs. Choosing a C-band technology entails a minimum of R&D thus facilitating early deployment and reliable operation. The goal is to enable an early start to the physics program, so as to be as concurrent as possible with the LHC operation. Once a new particle threshold is opened with LHC, all angles of the new physics regime can be thoroughly studied in the more straightforward clean experimental environment of e^+e^- collisions.

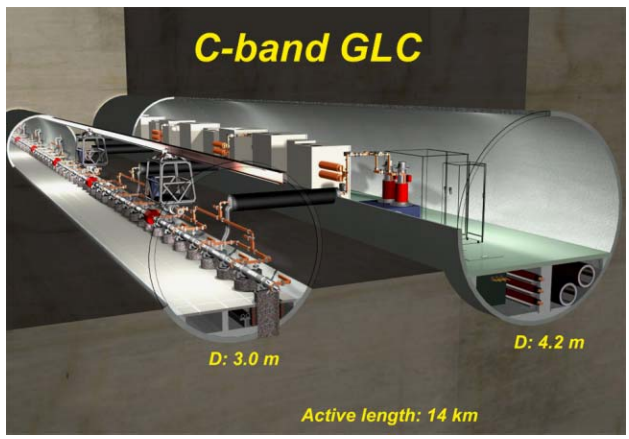

Figure 2: C-band main linac tunnels. The klystron gallery is 4.5-m in diameter and the linac tunnel is 3.0-m in diameter.

The main linac system is the heart of the linear collider. It is a huge system, composed of thousands of repetitions of common RF-units. Therefore, in order to realize a successful physics program, these RF-units have to meet strict requirements for: (1) High reliability, (2) Simplicity, (3) Easy operation, (4) Reasonable power efficiency, and (5) Low cost.

These desiderata provide boundary conditions for our design work. Especially the first three items are crucial for such a large scale system to be operated at all; only after clearing them are the detailed discussions about energy efficiency or upgradeability meaningful. As the C-band frequency is only two times higher than the S-band, the size of the accelerator structure is reduced by half. But more importantly, currently available technology for fabricating the components can easily meet the accuracy required for the C-band, thus removing the risk of a non-manufacturable design. This single choice thus directly results in possibilities for high reliability, simplicity, and hence low cost.

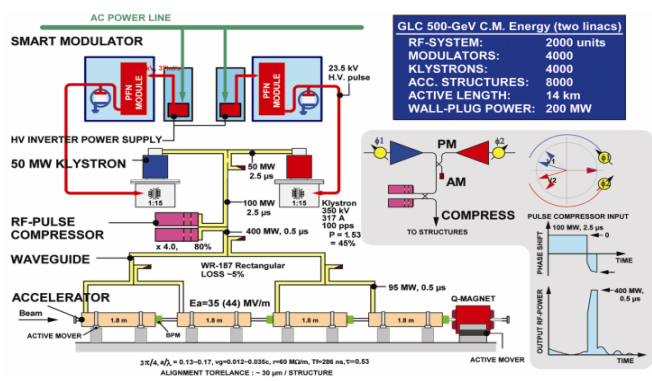

Figure 1: One unit of the C-band main linac.

#hiroshi.matsumoto@kek.jp

LOW EMITTANCE 500 KV THERMIONIC ELECTRON GUN

K. Togawa*, T. Shintake, H. Baba, T. Inagaki, K. Onoe, T. Tanaka, SPring-8 / RIKEN Harima Institute, Hyogo 679-5148, Japan
H. Matsumoto, High Energy Accelerator Research Organization (KEK), Ibaraki 305-5148, Japan

Abstract

A low emittance 500 kV thermionic gun has been developed for the injector system of the X-ray FEL project at SPring-8. A single-crystal CeB_6 cathode is chosen as a thermionic emitter, because of its excellent emission properties, i.e., high resistance against contamination, uniform emission density, and smooth surface. A gun voltage of -500 kV was chosen as a compromise between the need for suppressing emittance growth and reducing the risks of high voltage arcing. We have succeeded in producing a 500 keV beam with 1 A peak current and 3 μsec width. A normalized rms emittance of 1.1π mm.mrad has been measured by means of double-slit method. In this paper, we describe the design of the CeB_6 gun and report on the result of the emittance measurement.

INTRODUCTION

In X-ray FEL theory, it is well known that the fine structure of the beam dominates the FEL gain. To achieve the SASE-FEL in Angstrom wavelength region, the sliced emittance of the beam should be very low and the peak current should be of the order of kA. Moreover from the application point of view, the FEL machine should be stable for long periods of operation.

In the SASE-FEL, the electron beam generated by the gun is accelerated in the main linac, then it is directly injected into the long undulator and generates the X-ray beam there. Therefore, any electron bunch fluctuation in transverse position, timing, size, charge, etc., will directly affect the X-ray lasing. This is markedly different from the storage ring type machine situation. As a result, the stability of the electron gun is essential for producing stable X-ray FEL light.

We decided to use a thermionic cathode followed by a buncher system [1]. Basically, this is a traditional injector system used in many types of electron accelerators. High stability and long lifetimes have been routinely achieved in the present day injectors, however, for these conventional applications, the typical emittance is ~30π mm.mrad or larger. In order to reduce the emittance, we have added the following modifications and upgrades:

1) Small size cathode. The initial emittance of the gun is dominated by its cathode size. We use a single crystal CeB_6 cathode with a 3 mm diameter. The theoretical thermal emittance is 0.4π mm.mrad at ~1400°C. A high beam current of 3 A can be produced from the CeB_6 crystal at this temperature without jeopardising long lifetime.

2) Elimination of the cathode control grid. The emittance of the traditional thermionic cathode gun is degraded by the electric field distortion caused by the grid mesh.

3) Applying 500 kV to the cathode. In order to minimize emittance growth due to space charge effects, a higher gun voltage is desirable. We use a 500 kV pulse just a few μsec in width.

4) Fast beam deflector. To form a nsec single bunch from the long pulse generated by the gun, we use a fast pulsed beam deflector after the gun.

5) Adiabatic bunching and acceleration. In order to minimize emittance growth due to the rf-field, a lower rf frequency is desirable. We use a 238 MHz sub-harmonic buncher, followed by a 1.6 m drift section, and then a 476 MHz booster cavity which raises the beam energy up to 1 MeV. A following S-band pre-linac is used to accelerate the bunch to 20 MeV before injection into the C-band main linac.

THE CEB6 GUN

We have designed and constructed a 500 kV electron gun with a CeB_6 cathode [2]. A side view of the CeB_6 gun with an emittance monitor bench is shown in Fig. 1, and the beam design parameters at the gun exit are summarized in Table 1.

Table1 : The beam design parameters at the gun exit.

Beam energy	500 keV
Peak current	3 A
Pulse width (FWHM)	1.6 μsec
Repetition rate	60 Hz
Normalized emittance (rms)	0.4π mm.mrad

CeB_6 Cathode

The normalized rms thermal emittance of electrons emitted from a hot cathode is described by

$$\varepsilon_{n,rms} = \frac{r_c}{2}\sqrt{\frac{k_B T}{m_e c^2}},$$

where r_c is the cathode radius, k_B is Boltzman's constant, and T is the cathode temperature. From the above relation, in order to obtain the small emittance less than 1π mm.mrad required for the X-ray FEL, the diameter of the cathode must be in the range of a few mm at the temperature of 1000-1500°C. On the other hand, very high emission density (~50 A/cm^2) is required to produce a several ampere peak current from the small surface. Only the rare-earth hexaborides, such as LaB_6 or CeB_6 can emit such an intense current over long lifetimes. A single crystal is preferable for obtaining low emittance because of its extremely flat surface (roughness ≤1 μm)

* togawa@spring8.or.jp

HIGH PRESSURE, HIGH GRADIENT RF CAVITIES FOR MUON BEAM COOLING*

R. P. Johnson#, M. M. Alsharo'a, R. E. Hartline, M. Kuchnir, T. J. Roberts, Muons, Inc., Batavia, IL
C. M. Ankenbrandt, A. Moretti, M. Popovic, Fermi National Accelerator Laboratory, Batavia, IL
D. M. Kaplan, K. Yonehara, Illinois Institute of Technology, Chicago, IL
K. Beard, A. Bogacz, Y. Derbenev, T. Jefferson National Accelerator Facility, Newport News, VA

Abstract

High intensity, low emittance muon beams are needed for new applications such as muon colliders and neutrino factories based on muon storage rings. Ionization cooling, where muon energy is lost in a low-Z absorber and only the longitudinal component is regenerated using RF cavities, is presently the only known cooling technique that is fast enough to be effective in the short muon lifetime. RF cavities filled with high-pressure hydrogen gas bring two advantages to the ionization cooling technique. First, the energy absorption and energy regeneration happen simultaneously rather than sequentially, and second, higher RF gradients and better cavity breakdown behavior are possible due to the Paschen effect. A first step in a program to develop ionization cooling using pressurized cavities is the measurement of RF breakdown of hydrogen at high density. In the study reported here, the linear dependence of breakdown on pressure was verified in an 800 MHz hydrogen-filled test cavity up to 80 MV/m, which was the surface gradient limit of the molybdenum electrodes of the cavity. We note that the conditioning of the electrodes was unusually fast in the gas and needed only a few hundred thousand pulses. Planned research includes experimental measurements of pressurized RF cavity behavior in strong magnetic and ionizing radiation fields. Analytical and simulation calculations are also being made to examine how these cavities might be used in a practical cooling channel, effectively a rather complex Linac.

INTRODUCTION

Accelerators and colliding beam storage rings for High Energy Physics research have used protons and/or electrons and their antiparticles. Muons, despite their short lifetime, have several advantages to make them attractive candidate particles for the next generation of energy frontier colliders. Muons are point like, rather than composite, so that all of their collision energy can be used to create new states of matter. Thus a muon collider can have an energy and footprint one tenth that of the equivalent proton collider. Muons are more massive than electrons so that problems with synchrotron radiation are greatly diminished. Thus a muon collider can be a multi-turn ring of high-field magnets and each beam will not be disrupted by the electromagnetic field of the other at interaction regions. Because of the reduced disruption, a muon collider can be built with center of mass energy much greater than the 1.5 TeV that linear electron-positron colliders are likely to be limited to.

The muon advantage that is the subject of the studies reported here, however, has to do with passage through matter. Unlike protons, muons do not interact through the strong interaction and rarely suffer large scattering angles. Unlike electrons, muons create few electro-magnetic showers since they are more massive. Thus, muons have one other important virtue compared to protons and electrons in that they can pass through material with losses and scattering small enough to still be useful in accelerators, storage rings, and colliders.

This paper describes efforts to use this muon virtue of acceptable scattering through matter to rapidly cool a muon beam and quickly accelerate it to high energy. The new idea that is being exploited is that RF cavities used for muons can be filled with high-pressure gas to suppress high voltage breakdown. The gas, if it is low-Z, can also be the energy absorber for ionization cooling.

Ionization Cooling

Neutrino Factories or Muon Colliders, which require intense beams of muons, are dependent on a scheme to quickly reduce or cool the emittance of a muon beam before it can be injected into a practical accelerator[1]. Ionization cooling of a muon beam involves passing a magnetically focused beam through an energy absorber, where the muon transverse and longitudinal momentum components are reduced, and through RF cavities, where only the longitudinal component is regenerated. After some distance, the transverse components shrink to the point where they come into equilibrium with the heating caused by multiple coulomb scattering.

The equation describing the rate of cooling is a balance between these cooling (first term) and heating (second term) effects[2]:

$$\frac{d\varepsilon_n}{ds} = -\frac{1}{\beta^2}\frac{dE_\mu}{ds}\frac{\varepsilon_n}{E_\mu} + \frac{1}{\beta^3}\frac{\beta_\perp (0.014)^2}{2E_\mu m_\mu X_0}.$$

Here ε_n is the normalized emittance, E_μ is the muon energy in GeV, dE_μ/ds and X_0 are the energy loss and radiation length of the absorber medium, $\beta_\perp$ is the transverse beta-function of the magnetic channel, and β is the particle velocity.

Setting the heating and cooling terms equal defines the equilibrium emittance, the very smallest possible with the given parameters:

* This work is supported in part by US DOE STTR grant DE-AC02-ER86145 and SBIR grant DE-FG02-03ER83722
# Rol@muonsinc.com

EFFECT OF HIGH SOLENOIDAL MAGNETIC FIELDS ON BREAKDOWN VOLTAGES OF HIGH VACUUM 805 MHz CAVITIES

A. Moretti, A. Bross, S. Geer, Z. Qian, (FNAL) , J. Norem, (ANL), D. Li, M. Zisman, (LBNL), Y. Torun, (IIT), R. Rimmer, (TJNAL), D. Errede, (UIUC)

Abstract

There is an on going international collaboration studying the feasibility and cost of building a muon collider or neutrino factory [1,2]. An important aspect of this study is the full understanding of ionization cooling of muons by many orders of magnitude for the collider case. An important muon ionization cooling experiment, MICE [3], has been proposed to demonstrate and validate the technology that could be used for cooling. Ionization cooling is accomplished by passing a high-emittance muon beam alternately through regions of low Z material, such as liquid hydrogen, and very high accelerating RF Cavities within a multi-Tesla solenoidal field. To determine the effect of very large solenoidal magnetic fields on the generation of dark current, x-rays and on the breakdown voltage gradients of vacuum RF cavities, a test facility has been established at Fermilab in Lab G. This facility consists of a 12 MW 805 MHz RF station and a large warm bore 5 T solenoidal superconducting magnet containing a pill box type cavity with thin removable window apertures. This system allowes dark current and breakdown studies of different window configurations and materials. The results of this study will be presented. The study has shown that the peak achievable accelerating gradient is reduced by a factor greater than 2 when solenoidal field of greater than 2 T are applied to the cavity.

INTRODUCTION

The concept of a Muon Collider has been under study internationally for a number of years. High intensity muons are produced from a high-energy high-intensity proton beam hitting a high Z material. Pions are captured and subsequently decay into muons. The capture section consists of a high Z target surrounded by a very high solenoidal capture field of several T. This produces a muon beam of very large 6-D phase space. In order to produce muon beams of high enough quality to be used for a collider, this large phase space must be cooled several orders of magnitude and done quickly, because of the short life time of the muon. Ionization cooling can accomplish the task of cooling the muon beam many orders of magnitude. Ionization cooling consists of passing a high-emittance muon beam alternately through regions of low Z material, such as liquid hydrogen, and very high accelerating RF Cavities within a multi-Tesla solenoidal focusing channel. As the particles pass through the low Z material, they lose momentum in 3-D phase space. The longitudinal component (accelerating frame) is then restored by the RF cavities. This is repeated many times to produce a beam of the quality required for a collider. Although not necessarily required, muon ionization cooling can be used to improve the performance of a neutrino factory.

A key element of the feasibility study is the demonstration of ionization cooling. The Muon Ionization Cooling Experiment, MICE [3], has been proposed and is being planned to demonstrate 10 % cooling which will be enough to validate the technology. This experiment is an international collaborative effort with the US, Europe and Japan as the principle partners. This experiment is planned to take place at Rutherford Appelton Laboratory in England.

Important to any demonstration of muon ionization cooling is the accelerating cavity technology. For the past three years, studies of the limitations of very high electric field gradients in linac type vacuum RF cavities have been taking place in a test facility in Lab G at Fermilab. The purpose of the facility is to determine the effect of very large solenoidal magnetic fields on the generation of dark current and x-rays and its effect on the breakdown voltage gradients of vacuum RF cavities. This facility allows us to test methods and materials to increase the breakdown limit and reduce dark current emissions. Increasing the achievable accelerating gradient would reduce one of the major cost drivers of a future collider or neutrino factory.

THE LAB G TEST FACILITY

The Lab G facility consists of a Fermilab upgrade Linac modulator and controls, a 12 MW pulsed klystron and its waveguide system, a 5 T superconducting magnet with a large warm bore for cavity insertion, cooling water and high vacuum systems for the test cavity and a radiation shielded interlocked test cave. Figure 1 shows a picture of the 5 T superconducting solenoid with the first test cavity (an open cell cavity) being tested in the facility [4]. At its ends are shown thin 125 μm Ti vacuum windows for dark current and x-ray measurements. The facility permits research and development on methods and materials to increase the breakdown limit and reduce dark current emissions. It also allows us to test RF components and qualify RF technology for a future muon collider, neutrino factory or MICE .

The arrangement for the second set of measurements on the LBL Pill box cavity is shown in Figure 2. The single cell LBL cavity is shown in the center of figure 2, [5,6]. It has been designed with removable vacuum end pieces. This arrangement was chosen so that a variety of window configurations and materials could be tested rapidly for

This work supported by the US Department of Energy
Under Contract Number DE-AC02-76H0300.

HIGH POWER CW SUPERCONDUCTING LINACS FOR EURISOL AND XADS

J-L. Biarrotte#, CNRS / IN2P3/ IPNO, Orsay, France

Abstract

A multi-MW superconducting proton linac is proposed as the baseline solution for the EURISOL and the XADS driver accelerators. In the EURISOL project, which studies the design of the next-generation European ISOL facility, it is used to produce both neutron-deficient and neutron-rich exotic nuclei far from the valley of stability. In the PDS-XADS project, which aims to the demonstration of the feasibility of an ADS system for nuclear waste transmutation, it is used to produce the neutron flux required by the associated sub-critical reactor. In this paper, we report the main results and conclusions reached within these preliminary design studies. A special emphasis is given on the on-going and future R&D to be done to accomplish the demonstration of the full technology. Both of these works have been supported and funded by the EC 5th Framework Program, under contracts n° FIKW-CT-2001-00179 (PDS-XADS) and n° HPRI-1999-CT-50001 (EURISOL).

INTRODUCTION

During the period 2000-2004, the European Commission, within its 5th Framework Program, has been supporting in the field of nuclear physics two distinct projects having between them a high level of synergy due to their rather similar driver accelerators.

The EURISOL Project

The first one is the EURISOL project [1], which looks at the feasibility study of a new European isotope-separation-on-line (ISOL) radioactive ion beam facility, aiming at providing exotic beams which are orders of magnitude higher in intensity than presently available. In the light of this general objective and the inherent limits imposed by practical target considerations, a high power proton driver accelerator has been proposed as the base-line solution for producing both neutron-deficient and neutron-rich exotic nuclei far from the valley of stability.

The EURISOL proton beam main specifications are summarized in Table 1. The beam final energy is 1 GeV, with a 2 GeV upgrade capability, and two main intensity regimes are required: at intensities around a few hundred μA, the driver would be operated as a classical ISOL facility, while the full beam power (5 mA mean current) would be used to generate neutrons from a spallation target, which in turn would be used for producing fission products (converter method). Moreover, because of current interest in some cross section properties of heavy-ion induced reactions, the EURISOL proton accelerator should exhibit a strong heavy-ion capability for low-mass species, with ion beam powers of hundreds of kW.

biarrott@ipno.in2p3.fr

The PDS-XADS Project

The second project is the PDS-XADS one, which looks at the feasibility study of an experimental Accelerator Driven System (ADS) for nuclear waste transmutation. Consecutive to the work of the European Technical Working Group on ADS [2], this preliminary design study was launched in 2001 within a large European collaboration [3]. Five work packages (WP) cover the relevant issues, and the WP3 is dedicated to the design of the high power proton accelerator providing the neutron flux to the sub-critical reactor via a spallation target.

The XADS accelerator's main specifications are also quite usual for such a machine (see Table 1): 600 MeV final energy, 6 mA maximum mean beam current on target (10 mA for the demonstration of concept), 2 % beam power stability, 10 % beam size stability on target. On the other hand, less than a few (in the order of 5 per year) beam stops longer than one second are allowed for the successful demonstration of the ADS coupling. Given the state-of-the-art in the field of accelerator reliability, this requirement appears to be highly challenging, and could reveal itself as being a "show-stopper" for ADS technology. From this extremely hard requirement, it is clear that suitable design strategies had to be followed early in the conception stage of the XADS accelerator.

Table 1: EURISOL & XADS beams specifications

	EURISOL	**XADS**
Final proton beam energy	1 GeV	600 MeV
Proton beam mean current	• 5 mA (2-step production mode) • 0.2 to 0.5 mA (direct production mode)	• 6 mA max. on target • 10 mA rated
Main additional specifications	Heavy-ion capability for ions with A/q = 2 & 3	Less than 5 beam trips (>1sec) per year
	The machine must be up-gradable to a 2 GeV machine	The concept must stay valid for a 1 GeV, 20 mA industrial machine

Beam Time Structure

In principle, to avoid thermal stresses on the ADS beam window, target and sub-critical assembly, or in the radioactivity-releasing ISOL target, the maximum smoothing-out of the beam structure is favoured: a continuous wave (CW) beam would thus be the best solution. However, a pulsed operation of the beam could also be feasible, under the condition that the time scales of thermal inertia of the different components of the target and the reactor are much longer than that of the beam

FUTURE DEVELOPMENTS IN ELECTRON LINAC DIAGNOSTICS*

Marc C. Ross, SLAC, Stanford, CA 94025, USA

Abstract

The next generation of electron linacs will fill two different roles:

1. ultra-low emittance, very high power accelerators for linear colliders and

2. ultra-short bunch, high stability accelerators for SASE X-ray production.

In either case, precision control based on non-invasive, reliable, beam instrumentation will be required. For the linear collider, low emittance transport is an important concern for both warm and superconducting linacs. Instrumentation will be used for control and diagnostics will be used to validate emittance preserving strategies, such as beam based alignment and dispersion - free steering. Tests at the KEK ATF and the SLAC FFTB have demonstrated the required performance of beam position and beam size monitors. Linacs intended for FEL's will require precision bunch length diagnostics because of expected non-linear micro-bunching processes. A wide variety of devices are now in development at FEL prototypes, including TTF2 at DESY and SPPS at SLAC. We present a review of the new diagnostic systems.

INTRODUCTION

The last ten years have seen unprecedented growth in electron linac technology development, driven by two main forces: 1) development of ultra-short pulse single pass free electron lasers (FEL) [1] and 2) development of high energy linear colliders (LC) [2]. The underlying physics for these machines has been well understood for 10 – 20 years and the intervening time has been devoted to demonstrations of key subsystems, such as accelerating structures, high-brightness beam generation and related instrumentation. In this paper we review 3 types of beam instruments that play a significant role in this work: 1) sub-micron resolution cavity beam position monitors (BPM's), 2) laser-based profile monitors (laserwires), and 3) bunch length monitors based on deflecting structures.

Demonstration of new beam instrumentation requires substantial accelerator test facilities to provide beams with smaller dimensions, higher brightness and greater stability. Indeed, the development of the instrumentation and the performance of the test facilities are strongly linked. Each is needed to validate and support the operation of the other and this is what has happened at the SLAC Final Focus Test Beam (FFTB) [3], the KEK Accelerator Test Facility (ATF) [4] and the DESY TESLA Test Facility (TTF) [5]. Since starting operation in the mid-1990's, these machines have been used to demonstrate 1) demagnification beyond that needed for the LC (FFTB), 2) generation of ultra-low emittance beams (ATF) and 3) generation of ultra-short pulse saturated ~100nm FEL radiation (TTF). Each of these tests has boosted and allowed aggressive development of related FEL/LC projects.

ULTRA-HIGH RESOLUTION BEAM POSITION MONITORS

The development of high resolution beam pickups for bunched electron beams lags substantially behind proton machine pickups, typically used for un-bunched (or weakly bunched) beams. Those devices, developed roughly 30 years ago for use with broad-band stochastic cooling, typically operate near the thermal, black-body radiation limit and are often cryogenically cooled in order to extend that limit as far as possible. In contrast to the needs of Schottky - signal based devices; most electron machine BPM requirements have been well served by devices that operate well away from the thermal noise limit. This is no longer true.

Third generation light sources require sub-micron resolution and stability, which is achieved using multi-turn digitization schemes that average over many hundreds of thousands of turns [6]. The Stanford Linear Collider (SLC) linac BPM system had 10 micron single reading resolution and an absolute precision of about 5 times larger [7]. This level of performance was well matched to the requirements of the machine. A good, practical way to interpret resolution requirements (r) in an LC or FEL is the view them in units of the beam size. Of course, the size of the vacuum chamber is also critical, so that the two key parameters are: 1) $j=r$/beam size and 2) $p=r$/vacuum chamber diameter. In operational terms, j allows the determination of sources of beam instability (such as poorly performing magnet power supplies or collective effects) with precision that is good compared to the beam's own emittance. In the SLC, with typical beam sizes of 50 μm and a one inch diameter beam tube, 10 μm resolution worked well for the identification most instability sources [8]. At the LC, with expected beam sizes almost 50 times smaller, and a larger beam tube, resolution performance must be substantially improved. Typical beam tube sizes in the FEL will be smaller. Table 1 summarizes these parameters, illustrating the challenge of the next generation linacs.

*Work supported by DOE-AC03-76SF00515.
#mcrec@slac.stanford.edu

RFQ DRIFT-TUBE PROTON LINACS IN IHEP

Yu.A. Budanov#, O.K. Belyaev, S.V. Ivanov, A.P. Maltsev, I.G. Maltsev,
V.B. Stepanov, S.A. Strekalovskyh, V.A. Teplyakov, V.A. Zenin
IHEP, Protvino, Moscow Reg., 142281, Russia

Abstract

The major RFQ Drift-Tube proton Linacs (RFQ-DTL) of IHEP-Protvino are described. The unique feature inherent in these accelerators is use of spatially periodic quadrupole RF focusing. Prospects are outlined for a further progress in R&D of this brand of linacs in IHEP.

PREAMBLE

Stability of a particle motion in a linear accelerator can be attained via choosing a dedicated geometry for accelerating gaps such as to force transverse components of accelerating field to exert the RF quadrupole focusing effect. Primary feasibility studies for this kind of focusing were, mostly, theoretical and foresaw either a weak focusing effect, or an unacceptably low accelerating rate.

A proposal by V.A. Teplyakov [1] to supplement an accelerating gap with a spacer electrode (or, generally, with a few of them), charged under an intermediate potential, has allowed for a noticeable upgrade in performance of the focusing mechanism at issue. Careful tailoring the period geometry allows to attain nearly the same minimal transverse frequency for all phases along bunch which improves beam quality [2].

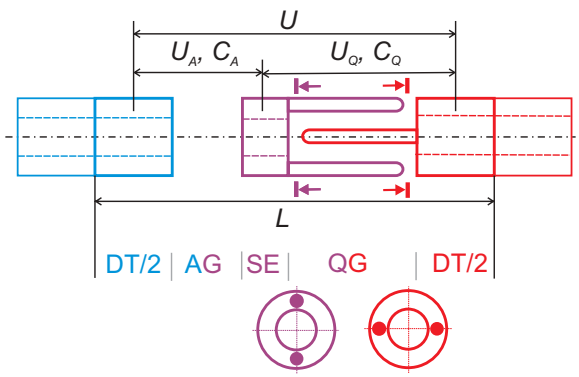

Figure 1: Schematic layout of accelerating cell.

Fig. 1 sketches such an accelerating cell with one spacer electrode SE (AG and QG are accelerating and quadrupole gaps, U_A and U_Q are voltages across them, total $U = U_A + U_Q$, and DT/2 is half of a drift tube, $L = \beta\lambda/2$). It is this structure that is employed in the first sections of URAL-30 and URAL-30M linacs of IHEP (URAL is a Russian acronym for **a**ccelerator **r**esonant **a**uto-focusing and **l**inear — a local code name for the machines).

Since then, a comprehensive R&D program has been pursued in IHEP to manufacture and run RFQ-DT linacs in which accelerating & focusing structure is driven at π-mode by a standing-wave cavity oscillating at a longitudinal-magnetic-field fundamental mode (an *H*-cavity).

In what follows, a 20-year long experience of IHEP-Protvino in R&D of RFQ-DTLs is reviewed.

RFQ-DTL FACILITIES

URAL-30

In 1968, the first experimental model of a linac based on the RFQ principle was assembled [3]. This event has encouraged feasibility studies for implementing RF focusing at lower energies. In 1969, I.M. Kapchinsky (ITEP-Moscow) and V.A. Teplyakov (IHEP-Protvino) put forward the concept of spatially uniform (smooth) quadrupole RF focusing (RFQ). By 1972, initial testing was accomplished, and the first accelerated beam was obtained [3].

The URAL-30 proton linac was commissioned in 1977. It applies a through front-to-end RFQ-focusing up to the top energy of 30 MeV. For a few years to follow diverse and instructive experimental studies of the machine were performed, and a sound practical experience acquired.

Since 1985 till now, this facility routinely operates as an injector to booster proton synchrotron, thus feeding the entire accelerator complex of IHEP (see Fig. 2).

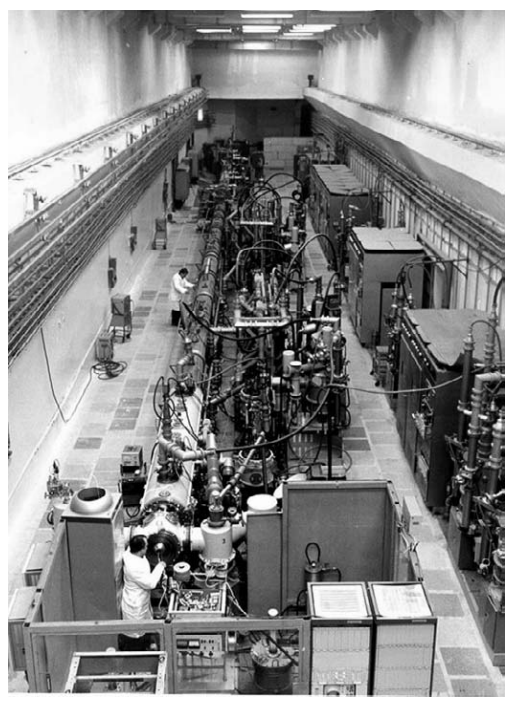

Figure 2: URAL-30 linac in the machine hall. Direction downstream of beam — away from the viewpoint.

#budanov51@mail.ru

DEVELOPMENT OF A 352 MHZ CELL-COUPLED DRIFT TUBE LINAC PROTOTYPE

Y. Cuvet, J. Genest, C. Völlinger, M. Vretenar, CERN, Geneva, Switzerland
F. Gerigk, RAL, Chilton, UK

Abstract

At linac energies above 40 MeV, alternative structures to the conventional Drift Tube Linac can be used to increase efficiency and to simplify construction and alignment. In the frame of the R&D activities for the CERN SPL and Linac4, a prototype of Cell-Coupled Drift Tube Linac (CCDTL) at 352 MHz has been designed and built. This particular CCDTL concept is intended to cover the energy range from 40 to 90 MeV and consists of modules of ~5 m length made of 3-gap DTL tanks linked by coupling cells. The focusing quadrupoles are placed between tanks, and are aligned independently from the RF structure.

The CCDTL prototype consists of two half tanks connected by a coupling cell and requires an RF power of 120 kW to achieve the design gradient. RF tests will be made at low and high power, the latter up to a 20% duty cycle. This paper introduces the main features of this CCDTL design and describes the RF and mechanical design of the prototype.

THE CERN CCDTL

The new Linac4 presently under study at CERN will accelerate an H^- beam to a kinetic energy of 160 MeV, making use of 352 MHz RF equipment (klystrons, waveguides and circulators) recuperated from the LEP machine [1]. This frequency is almost ideal for an H^- linear accelerator, offering a good compromise between size, maximum gradient, efficiency and focalization in the RFQ.

After the RFQ and a 3 MeV chopper line, the present Linac4 layout foresees an Alvarez-type Drift Tube Linac (DTL). The first DTL tank will be equipped with Permanent Magnet Quadrupoles, while the other tanks will have conventional electromagnets. The DTL structure is expensive to build because of its large dimensions and because of the accurate alignment required for the drift tubes. Moreover, the difficult access to the drift tubes is of concern if repairs are needed. However, for a high-intensity linac where beam optics has to be smooth, the choice of the conventional Alvarez DTL is unavoidable at low energy because of its short focusing periods. When the beam energy exceeds a few tens of MeV, the focusing period can become longer, and alternative structures can be considered.

Different alternatives to the DTL have been developed, all relying on the principle of separating the focusing from the RF structure, alternating quadrupoles with short accelerating tanks. Some solutions are based on TE modes, which provide a high shunt impedance, but require relatively long tanks and unconventional beam optics solutions, difficult to apply for high intensity operation due to the longer focusing periods. Other solutions retain the TM010 mode of the DTL, using shorter DTL tanks containing drift tubes of smaller diameter, without quadrupoles which are then placed between tanks. These structures have a lower capacitance between drift tubes than the standard DTL, but have increased losses due to a higher number of end walls, thus arriving at similar shunt impedance values to a conventional DTL. They go under the name of Separated DTL (SDTL) when the accelerating tanks are decoupled one from the other and fed by their own RF coupler, and of Cell-Coupled DTL (CCDTL) when the tanks are coupled together via coupling cells, forming a single resonator. The CCDTL was originally developed at Los Alamos at a frequency of 805 MHz [2].

The solution retained at CERN, shown in Fig. 1, is a CCDTL at the same RF frequency as the DTL, 352 MHz, and composed of 3-gap DTL-like accelerating tanks, connected by standard coupling cells [3]. Single quadrupoles are placed between tanks, giving a focusing period of 7 $\beta\lambda$. A string of 4 tanks forms a module, operating in the $\pi/2$ mode between tanks and coupling cells, which is directly fed by a 1 MW klystron.

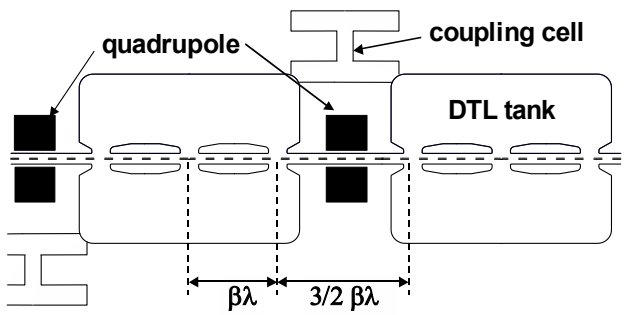

Figure 1: Outline of the CERN Cell-Coupled DTL.

The quadrupoles outside of the tanks can be easily accessed, aligned and cooled. Machining and plating of the relatively small CCDTL tanks requires a smaller and less expensive infrastructure than needed for a DTL. The alignment of the drift tubes is much less critical than in the DTL, the tolerances required for the alignment of an RF gap at this energy being between 5 and 10 times less stringent than for the alignment of the quadrupole. The module is directly fed by a klystron, clearly defining the tank phases and amplitudes. Finally, a CCDTL allows for a continuous focusing lattice, without the DTL intertank spacings, thus reducing the risk of beam mismatch.

Fig. 2 compares the computed shunt impedance of this CCDTL design with a CCDTL design with 2-gap tanks and with two standard DTL designs. In the energy range

DESIGN OF LINAC4, A NEW INJECTOR FOR THE CERN BOOSTER

R. Garoby, K. Hanke, A. Lombardi, C. Rossi, M. Vretenar, CERN, Geneva, Switzerland
F. Gerigk, RAL, Chilton, UK

Abstract

A new H^- linac (Linac4) is presently under study at CERN. This accelerator, based on normal conducting structures at 352 and 704 MHz, will provide a 30 mA 160 MeV H^- beam to the CERN PS Booster (PSB), thus overcoming the present space-charge bottleneck at injection with a 50 MeV proton beam. Linac4 is conceived as the first stage of a future 2.2 GeV superconducting linac (SPL) and it is therefore designed for a higher duty cycle than necessary for the PSB.

This paper discusses the design choices, presents the layout of the facility and illustrates the advantages for the LHC and other CERN users. The R&D and construction strategy, which mainly relies upon international collaborations, is also presented.

INTRODUCTION

A 2.2 GeV, 4 MW Superconducting Proton Linac (SPL) [1] represents a very interesting option for the long-term future of CERN (beyond 2010). This linac would serve as high power driver for neutrino production and/or radioactive ion physics. At the same time, as a high-brightness injector, it would modernise and improve the LHC injection chain, paving the way for an LHC upgrade. The low energy part of the SPL, up to 160 MeV, is normal conducting. It could be built first and used to inject H^- in the PSB, advantageously replacing the present 50 MeV proton Linac2. This new linac injector being the 4th hadron linac to be built at CERN would be named Linac4. Re-using part of the 352.2 MHz RF equipment from the decommissioned LEP accelerator and profiting from the available space and infrastructure in the Proton Synchrotron (PS) South Hall, the construction of Linac4 can be particularly cost-effective.

The main expected benefit of Linac4 is the doubling of the intensity and brightness of the beam from the PSB because of the charge-exchange H^- injection and because of the reduction in the space charge induced tune shift at low energy. That will result in an increased proton flux to the CERN users and an increased bunch population for the LHC. The energy of the new linac is set by the requirement for the PSB to deliver to the PS the LHC beam intensity in a single batch as compared to the present double batch, which corresponds to doubling the intensity per bunch in the PSB. Assuming that the maximum intensity at injection is inversely proportional to the tune shift, which in turn scales like $1/\beta\gamma^2$ (at constant normalized emittances), one can estimate that an energy increase from 50 to 160 MeV, corresponding to a factor 2 in $\beta\gamma^2$, will approximately double the maximum injection intensity. Recent simulations have confirmed this expectation. [2].

A recent study has compared different intensity upgrade scenarios for the CERN accelerators, recommending the construction of Linac4 in the medium term [3]. The estimated performance of the CERN complex with Linac4 together with the decrease of the PSB repetition period from 1.2 to 0.9 s and with upgrades to PS and SPS for higher intensity is shown in Table 1 and compared to present performance. The improvement for neutrino experiments is a factor 1.7, while for radioactive ions a factor of 3.5 is expected. The higher beam brightness would allow the bunch population at PS exit to reach 2×10^{11} protons in a 72 bunch train, corresponding to the LHC ultimate luminosity.

Table 1: Possible improvement to the CERN p beams

	Normal	Improved	
Flux to CNGS (ν beam)	4.5	7.5	$\times10^{19}$ pot/yr
Avg. current to ISOLDE	1.9	6.4	μA
LHC bunch population at PS exit	1.5	2.0	$\times10^{11}$ ppb

PARAMETERS AND LAYOUT

Linac4 will operate in two modes, initially as PSB injector at a maximum repetition frequency of 2 Hz and, at a later stage, at 50 Hz as front-end of the SPL. For injection in the PSB, the beam current is 30 mA, allowing the required number of protons per pulse to be reached in 500 μs, for a duty cycle of 0.1%. For the nominal SPL mode, the available RF power in the SC section limits the beam current to 13 mA, while the pulse length is 2.8 ms, for a duty cycle of 14%. Taking into account the chopping at low energy and the collimation in the front-end, the current required from the source is 50 mA and 30 mA respectively for the two operating modes. The linac structures are designed for the high duty cycle, but they will be operated in a first stage only at low duty cycle. Table 2 summarises the main design parameters.

Table 2: Linac4 parameters

	Phase 1 (PSB)	Phase 2 (SPL)	
Beam Energy	160		MeV
Maximum repetition rate	2	50	Hz
Source current	50	30	mA
RFQ current	40	21	mA
Chopper beam-on factor	75	62	%
Current after chopper	30	13	mA
Pulse length (max.)	0.5	2.8	ms
Average current	15	1820	μA
Max. beam duty cycle	0.1	14	%
Transv. norm. emitt. (rms)	0.33	0.33	π mm mrad
Long. emittance (rms)	0.24	0.24	π deg MeV

THE SPL FRONT END: A 3 MeV H⁻ TEST STAND AT CERN

C. Rossi, L. Bruno, F. Caspers, R. Garoby, J. Genest, K. Hanke, M. Hori, D. Kuchler, A. Lombardi, M. Magistris, A. Millich, M. Paoluzzi, E. Sargsyan, M. Silari, T. Steiner, M. Vretenar, CERN, Geneva, Switzerland
P.-Y. Beauvais, CEA, Saclay, France, P. Ausset, CNRS, Orsay, France

Abstract

In the frame of the SPL (Superconducting Proton Linac) study at CERN, a new 160 MeV proton injector for the CERN PS Booster is presently under development. This linear accelerator (Linac4) would not only be a first step towards a future, multi-MW superconducting linac, but would also improve in the medium term both the beam availability and beam quality for CERN's proton users. Within the framework of the Linac4 study and with the support of the EU funded Joint Research Activity HIPPI (High Intensity Pulsed Proton Injectors), a 3 MeV test stand is under construction at CERN. This test stand will explore some of the most critical issues of the linac, such as the beam dynamics at low energy, with special emphasis on the chopper line that has been designed to generate the required time structure of the beam, to clean the beam halo, and to match it to the subsequent RF structures. In this context, a new Beam Shape and Halo Monitor is under construction. The beam acceleration will be performed by an RFQ that is being developed in France within the IPHI collaboration between CEA and CNRS. Moreover, the test stand will be equipped with an additional 1 MW RF klystron to test different 352 MHz RF structures that are being developed for the Linac4.

INTRODUCTION

During the setting up of the LHC injector chain (Linac2-PSB-PS-SPS) it has been demonstrated that the intensity in the PS ring for the 25 ns LHC beam is limited to 1.5×10^{11} ppb, slightly more than nominal, mainly because of space charge effects at 50 MeV injection into the PS Booster (PSB). This is why the proposal has been made to build the low energy part (160 MeV) of the SPL and use it as an upgraded PSB injector, calling it Linac4 [1], [2]. The charge exchange injection that will be used in the PSB, combined with the higher injection energy, will substantially increase the intensity and brightness of the PSB beam. As a result, the intensity per bunch within the nominal transverse emittances is expected to reach 2.0×10^{11} ppb at the PS exit.

The technology and the beam dynamics issues at low energy, up to 3 MeV, are critical for the performance of Linac4, especially in its potential role as an SPL front-end. The halo formation mechanism has to be accurately studied and the techniques for chopping the beam with the appropriate time structure have to be validated. For these reasons a 3 MeV beam test stand is being built and installed in the position where it will later operate as the Linac4 front-end.

3 MEV TEST STAND LAYOUT

The 3 MeV test stand is designed to become the low energy part of Linac4. As a test stand, its main goal will be to validate the chopper line and to characterize the beam parameters and halo at low energy.

The preliminary layout is shown in Fig.1, integrated in the building where it will be assembled, the PS South Hall Extension.

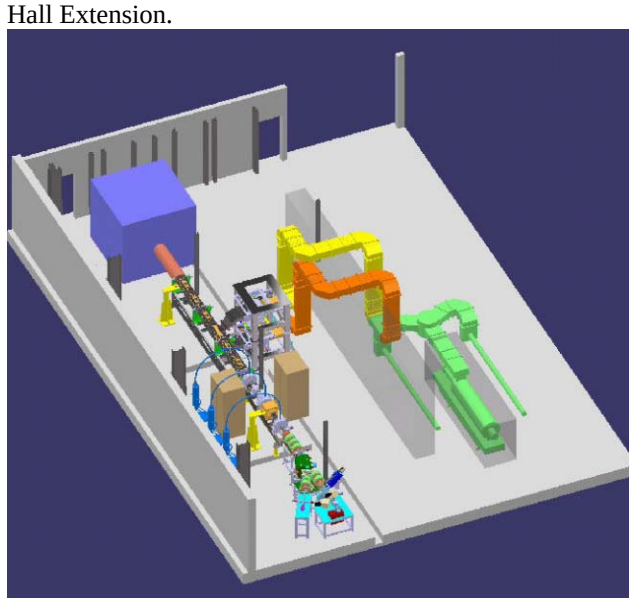

Figure 1: Layout of the 3 MeV test stand.

The test stand is composed of four areas, described below.

Ion Source and LEBT

A high intensity, high performance, micro-wave driven source is presently under development at CERN. It is designed for the requirements of the SPL, that can be considered as a long term development of the less demanding Linac4 H⁻ source.

In Table 1 the parameters for the two cases are listed.

Table 1: Main H⁻ source parameters

Parameter	Linac4	SPL
Instantaneous current	50 mA	>40 mA
Pulse length	0.5 ms	> 2.0 ms
Repetition rate	2 Hz	50 Hz
Extraction voltage	95 kV	95 kV
Duty cycle	1 ‰	15 %

The decision to develop a micro-wave driven source is based on the very satisfying operational experience with

BEAM DYNAMICS FOR A NEW 160 MeV H $^-$ LINAC AT CERN (LINAC4)

F. Gerigk, RAL, Chilton, UK
E. Benedico Mora, A. M. Lombardi, E. Sargsyan, M. Vretenar, CERN, Geneva, Switzerland

Abstract

Linac4 is a normal conducting H^- linac proposed at CERN to provide a higher proton flux to the CERN accelerator chain. It should replace the existing Linac2 as injector for the PS booster (PSB). The same machine can also operate in the future as the front end of the SPL, a 2.2 GeV superconducting linac with 1.8 mA average current. At present Linac4 consists of a Radio Frequency Quadrupole (RFQ), a chopper line, a Drift Tube Linac (DTL), and Cell Coupled DTL (CCDTL) all operating at 352.2 MHz and finally a Side Coupled Linac (SCL) at 704.4 MHz. This paper discusses the overall beam dynamics concept, presents the optics for the different sections of the machine and compares end-to-end simulations realised with two tracking codes (PATH and IMPACT). The influence of phase/energy errors is discussed and the challenging features in the current design are highlighted.

CONCEPT

The guidelines for the design of Linac4 are high beam quality, low losses, low activation and, where possible, reuse of existing equipment. In the initial stage Linac4 will be used as a new injector for the PS Booster, providing 30 mA of H^- at 160 MeV in 0.5 ms long pulses at a 2 Hz repetition rate. At the same time it is conceived and designed as the normal conducting "front-end" of a 2.2 GeV superconducting proton linac with an average power of 4 MW, delivering a 13 mA beam with 2.8 ms pulse length and a repetition rate of 50 Hz [1]. With such high beam power involved, beam quality and halo formation must be carefully controlled in order to avoid activation and to ensure hands-on-maintenance. For this purpose the lattice is designed to provide a smooth evolution of the phase advance per metre across all transitions. This could be achieved for the whole of Linac4 (Fig. 1) with the exception of the LEBT and chopper line where mechanical constraints prevent this approach. Furthermore an effort was made to avoid resonant emittance exchange by adapting the transverse phase advance to the longitudinal one, yielding, in our case, a full current phase advance ratio of $0.5 < k_l/k_t < 0.8$ throughout the machine which successfully prevents any exchange of emittances between the planes (compare Fig. 3).

The fundamental frequency of 352.2 MHz was chosen in order to re-use the LEP klystrons, and the source extraction energy of 95 keV was determined by the availability of the IPHI RFQ [2].

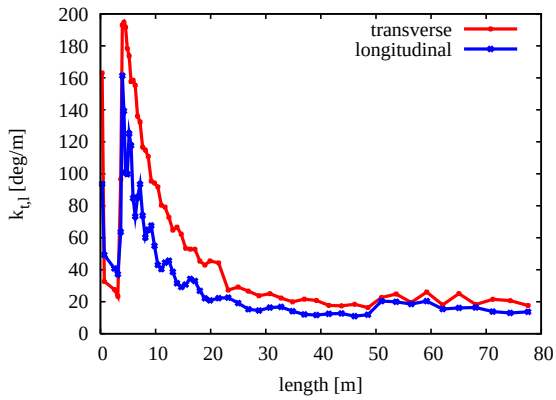

Figure 1: Phase adv. per metre from RFQ (out) to 160 MeV.

BEAM DYNAMICS

LEBT and RFQ

The Linac4 source beam will be matched into the RFQ by means of 2 solenoids and provision is made to house a pre-chopper between the two of them. Space charge effects are not severe as the beam is continuous and they can be compensated for by the solenoids. They account for less than 1% of the simulated emittance increase. The energy spread, expected to be around 4%, has instead a very strong effect, not only generating transverse emittance increase up to 30%, but also significantly spoiling the beam distribution because of the strong chromatic distortion when focused into the RFQ acceptance. The RFQ has been designed and optimised for 100 mA CW operation. It shows excellent transmission and good beam qualities also at 40 mA. The emittance increase, however, which occurs mostly in the first coupling gap, is more pronounced in the presence of the source energy spread.

Chopper Line

The chopper line dynamics is dominated by the chopper structure itself [3], [4]. The requirements for fast rise time (2 ns) and the timing structure of the CERN NuFact accumulator [1]) limit the maximum effective voltage to 800 Volts. In order to separate the beam by more than 1% we are forced to use a 1 m long chopper. The chopper line consists of 5 FODO cells with 2 periods on each side to match from the fast phase advance in the accelerating structures to a slow phase advance in the chopper (see Fig. 2). The chopping takes place in the (20 $\beta\lambda$ long) central FODO cell. The chopper itself is housed inside the first focussing quadrupoles (F5 and F6) and provides a 7 mrad kick to the beam. The separation in phase space is then ampli-

RESULTS OF THE HIGH-POWER CONDITIONING AND THE FIRST BEAM ACCELERATION OF THE DTL-1 FOR J-PARC

F. Naito*, S. Anami, J. Chiba, Y. Fukui, K. Furukawa, Z. Igarashi, K. Ikegami, M. Ikegami
E. Kadokura, N. Kamikubota, T. Kato, M. Kawamura, H. Kobayashi, C. Kubota, E. Takasaki
H.Tanaka, S. Yamaguchi, K. Yoshino, KEK, Tsukuba, JAPAN
K. Hasegawa, T. Itou, T. Kobayashi, Y. Kondo, A. Ueno, Y. Yamazaki, JAERI, Tokai, JAPAN

Abstract

The first tank of the DTL for Japan Proton Accelerator Research Complex (J-PARC) was installed in the test facility at KEK. The DTL tank is 9.9 m in length and consists of 76 cells. The resonant frequency of the tank is 324 MHz. After the installation of the tank, the high-power conditioning was carried out deliberately. Consequently a peak rf power of 1.2 MW (pulse repetition of 50Hz, pulse length of 600 μsec) was put into the tank stably. (The required power is about 1.1 MW for the designed accelerating field of 2.5 MV/m.) Following the conditioning, An H^- ion beam, accelerated by the RFQ linac up to 3 MeV, was injected into the DTL and accelerated up to its design value of 19.7 MeV. The peak current of 30 mA was achieved with almost 100 % transmission in November of 2003.

INTRODUCTION

The construction of a high-intensity proton accelerator facility for J-PARC has been started at Tokai campus of JAERI. The accelerator consists of a 181-MeV linac (which will be extended to 400MeV in near future), a 3-GeV rapid cycle synchrotron and a 50-GeV synchrotron[1]. The 181-MeV injection linac is comprised of the an H^- ion source, an radio frequency quadrupole (RFQ) linac, a drift-tube linac (DTL), a separated DTL (SDTL)[2], and several beam transport lines. The resonant frequency of the RFQ, the DTL and the SDTL is 324 MHz.

The Alvarez-type DTL accelerates the H^- ion beam from 3 to 50 MeV. It consists of the three independent tanks of which the length is about 9 m. Furthermore each tank is comprised of three short unit tanks of which length is approximately 3 m. The inside diameter of the tank is 560 mm. Each drift tube (140 mm in diameter) accommodates the electro-quadrupole magnet. The DTL-1 has 77 magnets. The DTL-2 and -3 have 44 and 28 magnets, respectively.

HIGH-POWER CONDITIONING

The DTL-1 was assembled very precisely and the accelerating field was stabilized by the post-couplers [3]. After the tuning of the field, The DTL-1 was installed in the tunnel of the test facility at KEK for the beam acceleration experiment.

* fujio.naito@kek.jp

Installed DTL-1 into the beam line is shown in figure 1. Left side component in the figure is the MEBT placed precisely in the area between the RFQ and the DTL. The properties of the beam ejected from the DTL are measured by the beam test line which has the current transformer (CT) , the beam position monitors (BPM), the transverse emittance monitor (EM) and the Faraday cup (FC) which works as a beam dump. The emittance monitor and the Faraday cup are installed in the area covered by concrete blocks for radiation shield. The blocks are seen at right side of the figure. The schematic view of the beam test line are shown in figure 2.

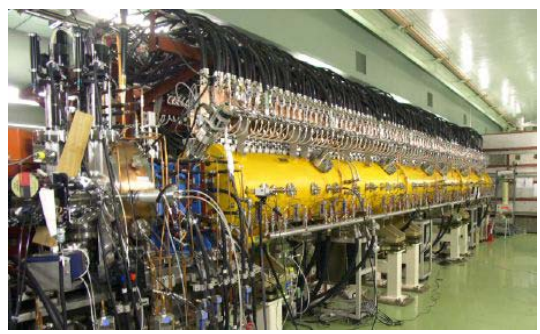

Figure 1: DTL-1 in the beam line.

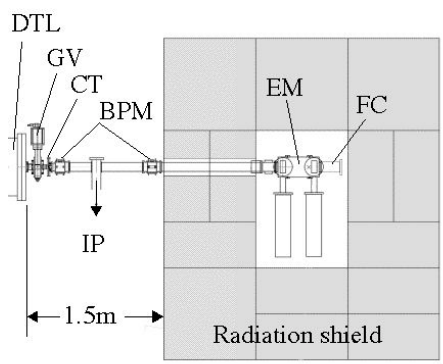

Figure 2: Beam test line.

A lot of black lines on the DTL shown in the figure 1 are the power lines for the quadrupole magnets. Each magnet is supplied the electric power independently. The power sources can supply both DC (600A in maximum) and pulse (1000A in maximum) currents to the magnet.

A LINAC-TO-BOOSTER INJECTION LINE FOR TRANSVERSE MATCHING AND CORRELATED INJECTION PAINTING*

R. W. Garnett, L. J. Rybarcyk, LANL, Los Alamos, USA

Abstract

In this paper we discuss a compact linac-to-booster ring transfer line originally proposed for the Los Alamos Advanced Hydrotest Facility design to vertically inject a 157-MeV H^- beam from the linac into a 4-GeV booster. TRACE 3-D and PARMILA simulations were used to demonstrate the performance of the transfer line to deliver the required transverse beam to the foil while also allowing correlated longitudinal injection painting. Schemes for both transverse and longitudinal matching are important for high-intensity ring applications where low beam loss operation is desirable. The main features of the beam line layout, a proposed longitudinal painting scheme, and the simulation results will be discussed. This work is supported by the U. S. Department of Energy Contract W-7405-ENG-36.

INTRODUCTION

The most recent design of the Advanced Hydrotest Facility (AHF) assumes an injector linac that is a duplication of the SNS linac up to 157 MeV [1]. The linac is followed by an injection line that allows both transverse matching and correlated longitudinal injection painting [2,3] into a 4-GeV booster ring, followed finally by a 50-GeV main ring and associated beam lines for radiography. Here we propose a layout of an injection line that includes the required horizontal and vertical bends necessary to deliver the desired beam to the booster injection foil. Preliminary beam parameters required at the foil, which constrain the proposed transfer line design, and information regarding the booster lattice geometry were provided by the booster designers [4]. TRACE 3-D, PARMILA, and ESME2K simulations were used to demonstrate the performance of the transfer line to deliver the required transverse beam to the foil while also allowing longitudinal injection painting.

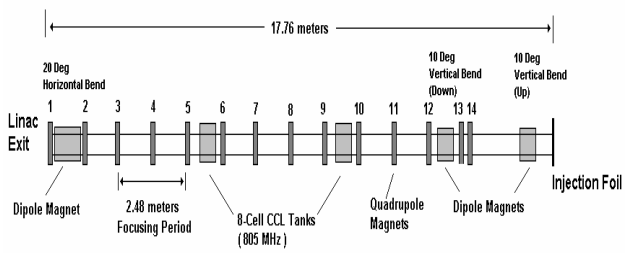

Figure 1: Unfolded layout of the booster transfer line.

TRANSFER LINE LAYOUT

Figure 1 shows the unfolded layout of the transfer line, including its various components. The layout of the transfer line relative to the booster ring is not shown, however, its length constrains the horizontal bend required with respect to the linac beam axis. The horizontal bend angle was chosen to allow sufficient separation between a separate linac tune-up line and the booster transfer line. A 20°-bend angle gives a sufficient separation to allow space for the required shielding so that linac tune-up activities can be in progress while maintenance activities, etc. are performed in the adjacent booster tunnel.

The transfer line focusing lattice is an extension of that used in linac. It was found that doing so maintains the beam size required to clear the relatively small radial apertures (r=1.5cm) of the 805-MHz 8-cell coupled-cavity linac (CCL) tanks of the transfer line that are used to do the correlated painting.

These cavities are identical to those of the last tank of the SNS CCL in order to save construction costs. The first tank will be operated in the bunching mode (ϕ= -90°). The second tank will be varied in phase about -90° and over a range sufficient to give the desired energy variation required to do the painting (typically $-120° \leq \phi \leq -60°$). The amplitude settings of the tanks are not identical, but are well within the expected operating range for SNS.

The quads in the transfer line are all set to identical gradient values with the exception of the final 4 quads (11-14 as shown in Fig. 1) that are used to obtain the transverse beam parameters required at the injection foil. From simulation results it was found that the dispersion at the foil could be reduced significantly by operating the last part of the linac and the transfer line at nearly 90° transverse zero-current phase advance. This results in somewhat higher quadrupole gradients as previously specified for SNS, but well within their operational limits.

Table 1 gives some of the transfer line mechanical and operational parameters. The total unfolded length of the transfer line from the linac exit to the foil is 17.8m. The magnetic field for all three bending dipoles is limited to 0.75 Tesla to avoid magnetic stripping of the H^- beam [5].

BOOSTER INJECTION REQUIREMENTS

Figure 2 shows the vertical injection region into the booster. It has been assumed that all magnets in this region will be operating in DC-mode. The long straight section in the booster is approximately 8.4m long. The injection region is assumed to occupy approximately 7m of the straight section as is shown in the figure. The combination of dipoles in the injection region will bend the beam upward by 10° and then back to horizontal at a new elevation. This displaces the beam approximately 0.53m off the booster axis during injection. This

CARBON ION INJECTOR LINAC FOR A HEAVY ION MEDICAL SYNCHROTRON*

D.A. Swenson, Linac Systems, Albuquerque, NM 87109, USA

Abstract

The design of a Carbon Ion Injector Linac for a heavy ion medical synchrotron will be presented. The linac is designed to accelerate quadruply-ionized carbon ions ($^{12}C^{+4}$) with a charge/mass ratio (q/A) of 0.333, and all other ions with the same or higher charge/mass ratios, such as H^{+1}, H_2^{+1}, D^{+1}, T^{+1}, $^3He^{+1}$, $^4He^{+2}$, $^6Li^{+2}$, $^{10}B^{+4}$, and $^{16}O^{+6}$ to an output energy of 7 MeV/u. The 200-MHz linac consists of a Radio Frequency Quadrupole (RFQ) linac to accelerate the ions from an input energy of 0.008 MeV/u to an intermediate energy of 0.800 MeV/u, and an Rf-Focused Interdigital (RFI) linac to accelerate these ions to the output energy. The combined linac structures have a total length of 7.8 meters and a total peak rf power requirement of about 600 kW. The RFQ linac employs a radial-strut, four-bar design that is about twice as efficient as the conventional four-bar RFQ design. The RFI linac, which is basically an interdigital drift tube structure with rf quadrupole focusing incorporated into each drift tube, is about 5 times more efficient than the conventional Drift Tube Linac (DTL) structure. Details of the linac structures and their calculated performance will be presented.

CARBON LINAC (7 MEV/U)

Linac Systems has designed a 7-MeV/u, Carbon+4 Linac to serve as an injector linac for a heavy-ion synchrotron for medical applications. The linac is designed to operate at 200 MHz and consists of a Radio Frequency Quadrupole (RFQ) linac section, an Rf-Focused Interdigital (RFI) linac[1,2] section, an rf power system, a stripper foil assembly, a debuncher cavity, and associated vacuum, temperature control, and linac control systems. The two linac structures, shown in Fig. 1, have a total length of 7.8 meters and a total peak rf power requirement of about 600 kW.

The low rf power requirement is a tribute to the rf efficiencies of the RFQ and RFI linac structures. The RFQ linac structure employs a radial-strut, four-bar design that is about twice as efficient as conventional four-bar designs. The RFI linac structure[1,2], which is basically an interdigital linac structure with rf quadrupole focusing incorporated into each drift tube, is about 5 times more efficient than the conventional Drift Tube Linac (DTL) structure. Two features of the RFI linac structure contribute to its higher efficiency; namely, the interdigital configuration and the rf electric focusing. The efficiency of the interdigital configuration follows from the fact that the rf electric fields are concentrated in the vicinity of the drift tubes, resulting in very low amounts of electric and magnetic stored energies. The rf electric focusing results in smaller diameter beams, which allows smaller diameter drift tubes, which in turn further reduces the capacitive loading of the structure and associated rf power losses.

The linac system is designed to accelerate quadruply-ionized carbon ions ($^{12}C^{+4}$) with their charge/mass ratio (q/A) of 0.333, and all other ions with higher charge/mass ratios. As all of the accelerating and focusing forces are electric, driven by rf power, the only change required to accommodate the different ion species is a change in the rf drive power. By reducing the rf electric fields by a factor of 3, the accelerating and focusing forces in the linac are appropriate for the acceleration of protons at currents as high as 8 mA.

The rf pulse duty factor requirement for this application is very low. The required beam pulse length is less than 50 μs and the required repetition rate is less that 1 per second. However, for operational and rf conditioning reasons, we have designed for an rf pulse length of 100 μs and a repetition rate of 10 Hz, resulting in a duty factor of 0.1%. The average rf power in the RFQ and RFI linac combination is about 600 W.

The resonant frequency of the resonant units will be maintained by a temperature-controlled, recirculating coolant system mannaged by dedicated temperature control units. The rf frequency of the rf power system will be locked to the resonant frequency of the ensemble of resonant units. The setpoints of the temperature control units will be controlled by the linac control system.

The vacuum system is based on turbomolecular vacuum pumps. Two turbo pumps will be mounted on each of the three resonant units to maintain the vacuum level down to about $5x10^{-7}$ Torr. Several "dry scroll pump" are used to rough down the linac sections and back-up the turbo pumps. The vacuum system will be controlled and monitored by the linac control system.

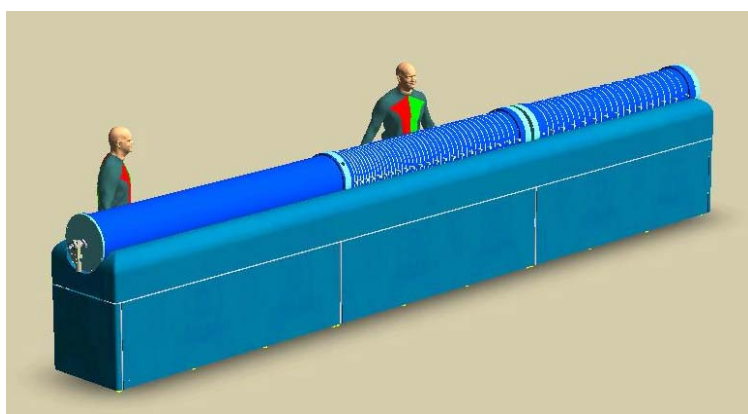

Figure 1: 7-MeV/u, Carbon+4 Injector Linac.

THE HEIDELBERG HIGH CURRENT INJECTOR: A VERSATILE INJECTOR FOR STORAGE RING EXPERIMENTS

R. von Hahn[1], M. Grieser, R. Repnow, D. Schwalm, C.P. Welsch,
MPI-K Heidelberg, Germany

Abstract

The High Current Injector (HCI) was designed and built as a dedicated single turn injector for the Test Storage Ring in Heidelberg to deliver mainly very high intensities of singly charged Li- and Be-ions for laser cooling experiments. After start of routine operation in 1999 the HCI delivered high quality beams for about 25% of the experiments with very high reliability.
Due to the experimental requirements the HCI mutated from a specialized injector to a versatile multipurpose instrument, able to deliver a large variety of atomic and molecular light ions with either positive or negative charge. In addition provisions are far advanced to implement a custom built 18 GHz high power ECR-source for the injection of highly charged heavy ions suitable for further acceleration.
This paper gives an overview of the experience gained so far and presents the status of the upgrade of the HCI.

INTRODUCTION

The High Current Injector (HCI) consists of an ion source, a 6 m long RFQ section [1] and eight drift tube structures with seven accelerating gaps [2]. Most of the components have been designed and built in house. After final construction the first phase of the accelerator was commissioned successfully in 1999 and since then the machine is routinely operated for experiments [3]. The output energy can be flexibly varied from 0.5 MeV/u (RFQ only) to 2 MeV/u (with all 7 gap resonators) and can be boosted up to 5 MeV/u using the room temperature post accelerator of the MP Tandem.
Until now the HCI performed about 10 to 15 one week beam times per year with a large variety of molecules as well as positively or negatively charged ions at the low RFQ-energy or up to the design energy of 1.7 MeV/u with the 7-gap-Linac. Although the second rebuncher is not yet available, the coupling with the post accelerator was successfully used in a few beam times.
The accelerating structures are preferably used at design velocity. After determination of the correct amplitudes and phases in several test runs with $^4He^+$-ions only linear scaling for amplitudes and magnet settings is necessary to achieve beams with good transmission for all ion species in the design range A/q Ò9.
After successful commissioning of the custom built ECR-source at its present test location, various modifications were necessary preparing the second phase of the HCI -project. The platform of the CHORDIS source power supplies was raised up to a height of 3 m to create enough space for the ECR-injection.
The charge-state separator between the HCI and the post accelerator was designed and installed. Moreover, in collaboration with the Moscow University we started to investigate the lifetimes of thin foils for additional stripping behind the HCI [4]. However the time schedule for the installation of the ECR at the HCI or at a new application is presently under discussion as changes in the future orientation of physics research at MPI-K are envisaged.

[1] robert.von.hahn@mpi-hd.mpg.de

THE RFQ

The transmission of the 6 m long RFQ consisting of two directly coupled RFQs was measured as a function of the beam intensity. Up to mass to charge ratio 4:1 the available rf power is sufficient to operate the LINAC in CW mode which is more convenient for rf- and beam diagnostics than pulsed mode operation. With higher masses up to the maximum mass to charge ratio of 9:1 the pulsed mode operation with 20 ms long pulses and a duty cycle of 25% is required. The majority of required beam times were done in CW mode.

The following figures 1 and 2 demonstrate a significant dependence on the beam intensity starting at about 500 µA in CW-mode. At low intensities a bad transmission can be attributed to larger emittances of different ion sources rather than of the RFQ.

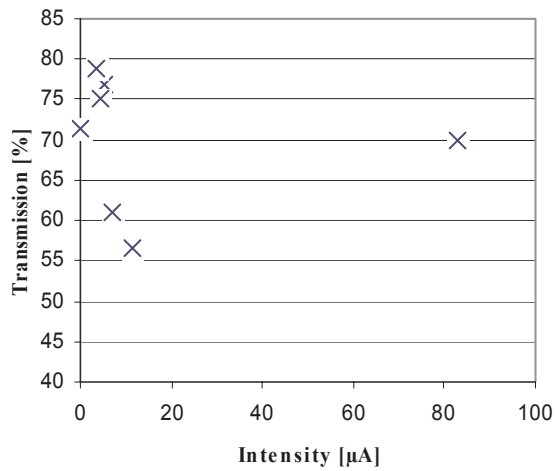

Figure 1: Transmission as a function of the beam intensity in pulsed beam operation.

DESIGN OF A DEUTERON RFQ FOR NEUTRON GENERATION

Z.Y. Guo[1,#], C. Zhang[1,2], A. Schempp[2], J.E. Chen[1], J.X. Fang[1],
Y.R. Lu[1,2], S.X. Peng[1], Z.Z. Song[1], J.X. Yu[1], K. Zhu[1]
[1] Institute of Heavy Ion Physics, Peking University, Beijing 100871, P.R.China
[2] Institute for Applied Physics, Johann Wolfgang Goethe University, Frankfurt am Main, Germany

Abstract

A 201.5 MHz 2.0 MeV deuteron RFQ accelerator for neutron generation has been designed. The general considerations, particle dynamics and RF structure design of the RFQ cavity are discussed. The progress of the studies on ion source, LEBT and RF transmitter are presented.

INTRODUCTION

Neutron has been widely used in various fields. In addition to nuclear reactors, accelerators played an important role in neutron sources. The energy of accelerated proton or deuteron beams ranged from around 100 keV to about 1 GeV depending on the application demand. Low energy accelerators, like DC high voltage accelerator, cyclotron and RFQ, have been used for neutron radiography, boron neutron capture therapy, neutron activation analysis, etc [1].

The neutron sources based on RFQ or RFQ+DTL have been developed in LLNL[2], South Africa[3] and Indiana[4]. In this paper the design of a deuteron RFQ for neutron generation is described.

BASIC DESIGN CONSIDERATIONS

The main design objectives are to get the higher neutron yield with lower RF power. The fast neutron yield depends on the particle species, target element, particle energy and the average beam current. The reaction Be(d, n) was chosen because the Be target is easier to be handled than Li and the beam energy could be lower with deuteron than proton for the same neutron yield (Fig. 1).

The designed parameters of RFQ accelerator largely depend on the available RF output power of transmitter. We decided not to use klystron due to its big dimension and higher cost. The Thales TH781 was chosen as the final RF output tube, which can deliver 400 kW peak power with more than 10% duty factor at around 200 MHz. Considering the available RF power the deuteron energy at exit of RFQ was set to 2.0 MeV, and the peak current of deuteron beam was designed as 50 mA. So the peak beam power is 100 kW and the peak power consumed in RFQ cavity should be limited below 260 – 280 kW. The frequency of RFQ was chosen as 201.5 MHz. From Fig. 1 the expected 4π fast neutron yield is 4×10^{12} n/s.

At the frequency around 200 MHz, both four-vane and four-rod type structure can be used for RFQ cavity. The four-rod structure was chosen due to its smaller diameter and lower machining precision.

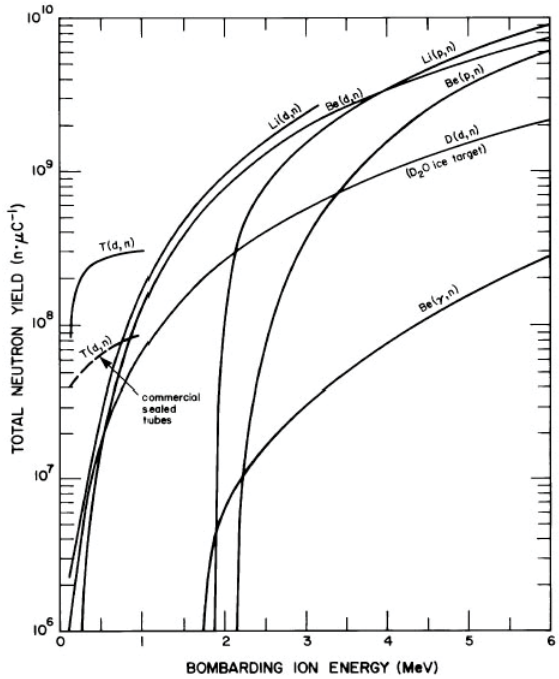

Figure 1: Neutron yields for low energy particle beam reactions[5].

The whole accelerator consists of ion source, LEBT, RFQ cavity and HEBT (Fig. 2), which will be described in the following sections.

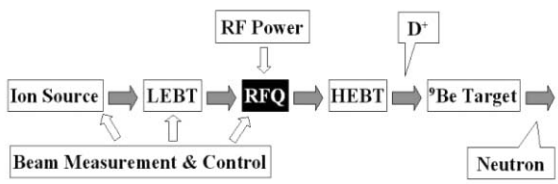

Figure 2: Scheme of the accelerator subsystem.

RFQ CAVITY DESIGN

The RFQ beam dynamics design has been performed with PARMTEQM using the LANL Four Section Procedure[6], but the beam loss is more than the expectation. In order to improve the beam transmission efficiency, two optimization concepts were combined in the new design: (1) the variation of the focusing parameter was adjusted along the RFQ to keep a certain ratio between the focusing force and the space-charge force; (2) main beam dynamics parameters' variation

#zhyguo@pku.edu.cn

HIGH CURRENT RFQ USING LASER ION SOURCE

M. Okamura, R. A. Jameson, J. Takano, K. Yamamoto, RIKEN, Saitama, Japan

H. Kashiwagi, JAERI, Gunma, Japan, T. Hattori, N. Hayashizaki, TIT, Tokyo, Japan

A. Schempp, R. Becker, IAP, Goethe-Universität, Frankfurt, Germany

Y. Iwata, NIRS, Chiba, Japan, T. Fujimoto, S. Shibuya, AEC, Chiba, Japan

Abstract

A new RFQ was built for demonstrating a capability of the "Direct Plasma Injection Scheme". After a few months commissioning period, we could obtain 50 *mA* of Carbon beam from the RFQ. This new heavy ion production scheme could be applied to Cancer therapy facilities and high energy nuclear physics accelerator complexes.

INTRODUCTION

Recently, high current and highly charged state heavy ion sources have been studied intensively in the world. Electron Beam Ion Source (EBIS), Laser Ion Source (LIS) and Metal Vapour Vacuum Arc ion source (MEVVA) are typical sources in this category. Among them, we focused on high brightness of induced plasma in LIS and have studied how to utilize the high density of plasma ablated from solid material.

The plasma is produced by a laser shot on the target and is expanded adiabatically normal to the target surface, with energy of a few hundred *eV*. In the established type of LIS, the plasma drifts with about 100 % momentum spread until obtaining the desired pulse period and then reaches an extraction electrode followed by Low Energy Beam Transport line, LEBT. In order to get about 10 μs of the pulse length, the plasma has to be drifted about 2 *m*. As a result, a solid angle captured by the extraction electrode is very small relative to an emitted angle of the ablation plasma. In addition, we had difficulty overcoming the space charge effect in the LEBT due to highly charged state, voltage limitation in the extractor and relatively higher current compared to standard ion sources, like Electron Cyclotron Resonance (ECR) ion sources.

To prevent the beam loss in the LEBT and take the advantage of the density of the laser plasma, Direct Plasma Injection Scheme (DPIS) has been developed. In general recipe, the beam being injected to an RFQ has to be focused. This scheme is not only for acceptance matching but also having a large beam size in the LEBT to prevent the beam loss caused by the space charge effect. In case of DPIS, we do not need to obey this strategy, because enough injected beam intensity into the RFQ can be achieved even if using diverging injection beam. The diverging beam has a large emittance, but enough beam is accepted by the RFQ. The space charge effect can be neglected during transportation from the source to the RFQ entrance, because the plasma is induced in the box directly attached to the RFQ and the ions fly from the target to the entrance of the RFQ with neutralized plasma state. Moreover the ion source part can be made extremely compact. There are no magnetic or micro wave devices and all the power for ionization is fed by laser light.

Since 2001, we have had experiments to verify the DPIS using an existing RFQ in TITech, Tokyo. Obtained maximum current of Carbon beam was 9.2 *mA* and this value agreed well with our simulation[1]. Upon this experience, we decided to construct a new RFQ to achieve higher current using the DPIS. We believe this new technique will impact the heavy ion accelerator field.

THE NEW RFQ FOR HIGH CURRENT HEAVY ION BEAM

In order to demonstrate the intrinsic performance of the DPIS, the new RFQ was constructed at Institute for Applied Physics, Goethe University, Frankfurt. This RFQ was designed to accelerate Carbon 4+ and 6+. A goal current was set to 100 *mA* with C^{4+}. Operation frequency was chosen as 100 *MHz* by availability of an RF amplifier system. The resonant structure is the 4 rod type, which is well established in IAP and suited for this frequency region and low duty factor operation. It has a reasonably small diameter, and the field distribution is easy to tune. Also it is not difficult to replace vanes in future modification. Total vane length was decided as 2 *m* considering future modification however output beam energy is 100 keV/u limited by a radiation safety regulation. The beam is accelerated up to 100 keV/u within first 1.42 *m* section and then transported through un-modulated vanes to the end of the RFQ. In the un-modulated section, the accelerated beam is completely de-bunched and this will help to reduce space charge effect in an analyzing section, which will be constructed in the near future. The input energy of the beam is a very important value, because in DPIS a high voltage biased slit is located at the entrance of the RFQ and might cause discharge. Part of the very high intensity plasma is guided through the several mm diameter hole in the biased slit and enter the RFQ. To minimize the beam size emitted from the hole, the slit needs to be close to the vanes. At

TEST AND FIRST EXPERIMENTS WITH THE NEW REX-ISOLDE 200 MHZ IH STRUCTURE*

T. Sieber#, CERN, Geneva, Switzerland
D. Habs, O. Kester, LMU, Garching, Ludwig Maximillian Universität, Physics Department

Abstract

For the REX-ISOLDE accelerator, a new accelerating structure is at the moment installed and tested. It will raise the final energy from the present 2.3 MeV/u to 3 MeV/u. The aim is to increase the mass range of the nuclei available for nuclear spectroscopy from mass 40 to mass 80. The new accelerator component is a 0.5 m IH-structure, working at the double REX frequency of 202.56 MHz. It was originally developed as a 7-Gap resonator for the MAFF [1] project and later adapted to the requirements at REX by changing from a 7-Gap to a 9-Gap resonator to match the lower injection energy. We present the design of the resonator and the results of the rf-tests, commissioning and first operation during the 2004 running period.

INTRODUCTION

In order to make a wider range of isotopes from ISOLDE/CERN available for nuclear physics experiments at REX-ISOLDE [2], an energy upgrade of the REX accelerator has been proposed. It was decided to do the upgrade in two separate steps (see fig. 1). The first step – increasing the energy from the previous 2.3 MeV/u to 3 MeV/u – was recently achieved by installing an additional IH 9-gap cavity in the REX beam line. The second step includes major changes in the setup of the machine By replacing two of the existing 7-gap resonators with a 1.5 m IH structure, the energy will be raised from 3 MeV/u to ~4.2 MeV/u. Since this energy is beyond the limits of several currently installed beam optics elements, a redesign of the high energy beam transport is required at the same time.

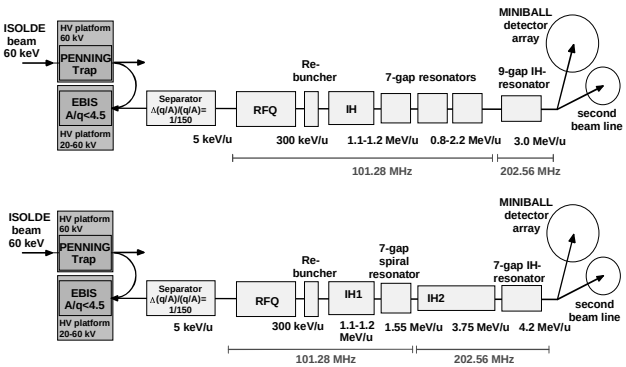

Figure1: Upgrade of the REX-ISOLDE Linac.

For the MAFF project a design has been worked out for two identical short 7-gap IH structures, providing the desired energy variation for the MAFF-Linac. The main advantage of this accelerator type compared to the split-ring resonators of REX-ISOLDE lies in the higher shunt impedance, allowing a variation of the final energy over a comparatively wide range (3.7 – 5.9 MeV/u) with only two short cavities. Since acceleration and deceleration must be possible to cover this energy range, the particle dynamics design at MAFF was very similar to the 7-gap resonators of REX-ISOLDE, which means constant gap lengths and a synchronous phase defined by the phase the particles experience in the middle gap.
In the first design for the REX 3MeV/u upgrade, it was foreseen to change the MAFF resonator from a 7-gap to a 9-gap resonator – keeping a constant cell length, corresponding to 2.5 MeV/u synchronous particle energy. Nine gaps were necessary to match the lower injection energy of 2.2 MeV/u instead of 3.7 MeV/u. However, measurements at the Tandem accelerator of the Maier-Leibnitz Laboratory in Garching showed that this gap geometry leads to a rather low transit time factor [3]. Thus the drift tube geometry was changed to a $\beta\lambda/2$ profile for fixed input and output energies. Table 1 shows the geometry and rf-parameters of the resonator.

Table 1: Resonator parameters of the 9-gap IH-cavity

	IH 9gap
Frequency [MHz]	202.56
outer tank length [mm]	676
inner tank length [mm]	520
half shell radius [mm]	145
cell length [mm]	38.5 – 58.5
gap length [mm]	19 - 27
drift tube length [mm]	32
drift tube diameter in./out. [mm]	16 / 22
maximum rf-power [kW]	100
duty cycle [%]	10
Kilpatrick	1.5
shunt impedance (pert.) [MΩ/m]	218
Q_0	10100

The above 9-gap design includes a smaller diameter of the drift tubes compared to the original 7-gap structure to keep the resonant frequency at 202.56 MHz. The gap voltage distribution used for the LORASR simulations

*work supported by the BMBF and the DFG, # Thomas.Sieber@cern.ch

STATUS OF THE RFI LINAC PROTOTYPE*

D.A. Swenson and W.J. Starling, Linac Systems, Albuquerque, NM 87109, USA

Abstract

A prototype of the Rf Focused Interdigital (RFI) linac structure is currently under construction at Linac Systems. The RFI linac structure is basically an interdigital (or Wideröe) linac structure with rf quadrupole focusing incorporated into each drift tube. The 200-MHz RFI Prototype, consisting of a short RFQ linac followed by a short RFI linac, will accelerate a 20-mA beam of protons from an injection energy of 25 keV to an output energy of 2.50 MeV in a total linac structure length of 1.44 meters. The linac structures are designed for continuous (cw) operation, and will be tested initially at a 33% duty factor. The peak structure power of 66 kW and peak beam power of 50 kW will be supplied by a 144-kW, 33% duty rf power system. A microwave ion source will supply the proton beam and an articulated Einzel lens will steer and focus the beam into the RFQ aperture. The mechanical design of the linac structures will be presented, the calculated performance will be described, the status of the components will be reported. The prototype is scheduled to come into operation in the fall of this year.

THE RFI PROTOTYPE

The Rf Focused Interdigital (RFI) linac structure[1,2] represents an effective combination of the Wideröe (or interdigital) linac structure, used for many low frequency, heavy ion applications, and the rf electric quadrupole focusing used in the Radio Frequency Quadrupole (RFQ) and Rf-Focused Drift tube (RFD) linac structures[3,4]. As in the RFD linac structure, rf focusing is introduced into the RFI linac structure by configuring the drift tubes as two independent pieces operating at different electrical potentials as determined by the rf fields of the linac structure. Each piece (or electrode) of the RFI drift tube supports two fingers pointed inwards towards the opposite end of the drift tube forming a four-finger geometry that produces an rf quadrupole field along the axis of the linac for focusing the beam.

The RFI linac structure is two-to-six times more efficient and three times smaller in diameter than the conventional Drift Tube Linac (DTL) structure in the energy range from 0.75 to 12 MeV. It is ten times more efficient than the RFQ linac structure in the 0.75 to 6 MeV range. This high efficiency reduces the rf power dissipation in the rf structures and the problems associated with cooling them, thereby promoting the prospect for cw operation, which in turn, allows large increases in the average beam currents. This linac structure promises to have significant size, efficiency, performance, and cost advantages over existing linac structures for the acceleration of low energy ion beams of all masses (light to heavy).

An operating prototype of the RFI linac structure, shown in Fig. 1, is under construction at Linac Systems. The RFI Prototype will be designed for an output energy of 2.5 MeV and an output current of 20 mA. It is designed for both pulsed and cw operation. This prototype will serve to verify the performance of the RFI linac structure and demonstrate its capabilities.

The RFI Prototype consists of a microwave ECR ion source, a low energy beam transport (LEBT) system, an RFQ linac section, an RFI linac section, a short beam diagnostics section, an rf power system, a vacuum system, a cooling system, and a computer control system.

ION SOURCE

A 2.45-GHz Microwave Ion Source, similar to the IUCF Ion Source[5], a lower current derivative of the LEDA Ion Source[6], is under construction[7] for the RFI Prototype. The source is designed for a peak proton current of 30 mA at 25 keV, and can be operated in either a continuous (cw) mode or a pulsed mode, with pulse lengths adjustable from 10 to 100 μs and repetition rates adjustable from 10 to 3000 Hz. The magnetic field is supplied by two water-cooled 15,000 A-turn solenoid magnets. The microwave power is adjustable up to 800 W and is capable of cw or pulsed operation.

The performance of the source was analyzed and optimized to the desired parameters with the PBGUNS

Figure 1: The 2.5 MeV, 20 mA RFI Prototype.

* Supported by the U.S. Dept. of Energy.

SPACE CHARGE COMPENSATION IN LOW ENERGY PROTON BEAMS

A. BenIsmaïl[#], R. Duperrier, D. Uriot, CEA Saclay, DSM /DAPNIA, 91191 Gif sur Yvette,
N. Pichoff, CEA Bruyères-le-Châtel, DIF /DPTA, BP12, 91680 Bruyères-le-Châtel, France

Abstract

High-power accelerators are being studied for several projects including accelerator driven neutron or neutrino sources. The low energy part of these facilities has to be carefully optimized to match the beam requirements of the higher energy parts.

In this low energy part, the space charge self force, induced by a high intensity beam, has to be carefully controlled. This nonlinear force can generate a large and irreversible emittance growth of the beam.

To reduce the space charge (SC), neutralization of the beam charge can be done by capturing some particles of the ionised residual gas in the vacuum chamber. This space charge compensation (SCC) regime complicates the beam dynamics study. Modelling the beam behavior in such a regime would be a significant contribution to the development of high intensity accelerators.

INTRODUCTION

In the low energy part of an accelerator, a high intensity beam is space charge dominated. Such a beam can be transported in a neutralization regime using the charge of the ionized residual gas. This regime occurs naturally when the beam propagates through a residual gas. Gas ionization takes place inside the beam and produces electrons and positive ions. For positive beams, electrons are trapped as long as the SC is not fully compensated.

As many experiments show [1], the beam charge is not always fully neutralized. Inside a Low Energy Beam Transport line (LEBT), the time dependent SCC is not necessarily homogeneous in space. These conditions contribute to emittance growth induced by non-linear forces and may lead to particle losses.

The knowledge of such regime is important to predict the optical qualities of the transported beam.

In this paper, we first describe a code CARTAGO for SCC modelization. This PIC code simulates the SCC mechanism during the transient and steady state regimes. We then present a numerical investigation of the SCC behavior for a continuous (DC) and a bunched (AC) proton beam through a drift section.

This work is a part of the theoretical and experimental work for the IPHI project [2].

CARTAGO ALGORITHM

Cartago is a beam dynamics simulation code including the effect of the non linear SCC. The scheme used to simulate the beam and plasma dynamics is composed of four basic parts (Fig.1):

Part1 At each time step, new particles produced by gas ionization are added according to the angular end energy differential cross section [3]. The beam is defined by a particle cloud carrying the main current.

Parts2&3 The charge distribution, is obtained in a 1D mesh (r) with a PIC scheme. The Poisson equation is solved with the grid by integration of the Gauss law. Forces extracted from the resulting potential, are applied to particles via the step by step "leap frog" scheme [4]. This scheme allows to integrate the equation of motion including the SC calculation.

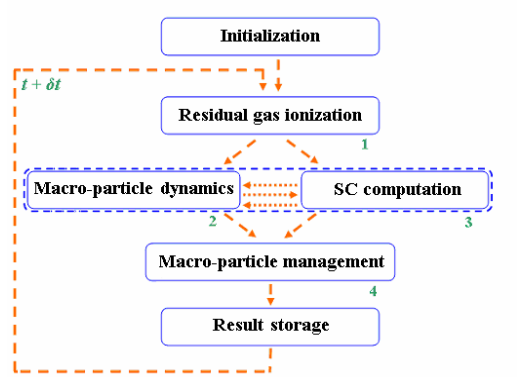

Figure 1: Cartago algorithm.

Part4 The residual gas plasma evolves taking into account the ionization intensity and the extend of the particle losses. This macro-particle system is simulated by using a "chained lists" method [5]. Every particle species is classified on separated lists. The size of each list increases when adding ionized particles, and decreases if some particles are lost on the vacuum chamber walls. Having roughly an idea of the plasma time scale stabilisation [6], and estimating the size for these lists for this moment, we deduce the number of macro-particles generated at every time step. Using this method, we simplify the Read Access Memory management during the computation.

Typical outputs of Cartago are electrostatic field, potential and radial distributions of the studied species. For further information, particle clouds may also be investigated at each time step. The SCC degree at a given azimuth of the beam direction is defined by:

$$\tau(t) = 100 \cdot \left(1 - \frac{\int_0^{r_{beam}} r \cdot \left\| \vec{F}_{SC\_C}(r) \right\| \cdot \rho(r) \cdot dr}{\int_0^{r_{beam}} r \cdot \left\| \vec{F}_{SC}(r) \right\| \cdot \rho(r) \cdot dr} \right), \qquad (1)$$

where $\vec{F}_{SC}$, $\vec{F}_{SC\_C}$ and ρ are respectively SC forces of the initial beam, forces in presence of the SCC and the beam distribution. This SCC degree gives the average reduction of the force acting on the beam. It is 0 if no compensation and 100 if the SC is fully compensated.

[#]bismail@cea.fr

INVESTIGATION ON BEAM DYNAMICS DESIGN OF HIGH-INTENSITY RFQS

C. Zhang*,#,1,2, Z.Y. Guo[1], A. Schempp[2], J.E. Chen[1], J.X. Fang[1]
[1] Key Laboratory of Heavy Ion Physics at Peking University, Ministry of Education, Beijing, China
[2] Institute for Applied Physics, Johann Wolfgang Goethe University, Frankfurt am Main, Germany

Abstract

Recently various potential uses of high-intensity beams bring new opportunities as well as challenges to RFQ accelerator research because of the new problems arising from the strong space-charge effects. Unconventional concepts of beam dynamics design, which surround the choice of basic parameters and the optimization of main dynamics parameters' variation along the machine, are illustrated by the designing Peking University (PKU) Deuteron RFQ. An efficient tool of LANL RFQ Design Codes for beam dynamics simulation and analysis, RFQBAT, is introduced. Some quality criterions are also presented for evaluating design results.

INTRODUCTION

Started by Kapchinsky and Teplyakov in 1970, the Radio Frequency Quadrupole (RFQ) accelerator has been developed as a kind of standard linear accelerator structure for low energy particles. No matter as injectors of large accelerators or independent facilities, a general tendency in the RFQ research field is to work for high-intensity beams.

Because neutrons have widely important applications e.g. clean nuclear power production, non-destructive detection and cancer treatment, the interest of using high-intensity proton or deuteron accelerators to produce neutrons as secondary particles is increasing in the world. As an essential component of such accelerator-based neutron source projects e.g. SNS, China ADS and IFMIF, the RFQ is expected to greatly improve its performance to satisfy some new severe requirements. For example, very low beam loss is a basic demand to limit the possible induced radioactivity to an acceptable level.

A 50 mA, 2.0 MeV RFQ is proposed for neutron radiography at PKU. In the case of high-intensity beams, two obvious negative influences from strong space-charge effects are defocusing and emittance growth. Therefore, some special considerations and optimization methods are required in the design work.

RFQ beam dynamics design is actually a process of choice and optimization for a multi-parameter system. All parameters could be roughly divided into two groups: (a) basic ones giving the boundary conditions of the design, e.g. frequency; (b) three relatively independent functions namely *a(z)*, *m(z)* and $\varphi_s(z)$.

CHOICE OF BASIC PARAMETERS

Basic parameters are mainly decided by four kinds of factors: (a) motivations of projects, (b) available resources like funding, equipments and applicable technologies, (c) analysis from the physical standpoint, (d) practical feasibility. In practice, a basic parameter could not be determined independently. A general case is that basic parameters are chosen as the tradeoffs of several or all kinds of factors.

Usually frequency is the first parameter to be chosen. Singly from the beam dynamics, high-intensity RFQs should use lower frequency for stronger focusing strength, which benefits to capture and accelerate higher current beams (Formula (1)).

$$B = \left(\frac{q \cdot V}{m_0 \cdot f^2 \cdot a^2} \right) \cdot \left(\frac{I_0(ka) + I_0(mka)}{m^2 \cdot I_0(ka) + I_0(mka)} \right) \quad (1)$$

where a=aperture, f= RF frequency, I_0=first order Bessel function, k=wave number, m=electrode modulation, m_0=rest mass, q=charge, V=inter-electrode voltage.

However, lower frequency will significantly increase the cavity dimensions consequently the costs, and higher one could lower the charge per bunch, which is advantageous to avoid undesired resonances and emittance growth in high-intensity RFQs.

For enough neutron production, the ^{9}Be(d, n) reaction using a 50 mA, 2.0 MeV deuteron beam is chosen for the PKU RFQ. Numerical studies show that ~200MHz frequency is suitable for high current deuteron RFQs with adequate focusing strength and aperture size. The available RF power source at ~200 MHz, the THALES tetrode TH781 [1], is adopted for the PKU D^+ RFQ. Consequently, the frequency, the duty factor and the total peak power are fixed at 201.5 MHz, 10% and 400 kW respectively.

Inter-electrode voltage mainly governs the transverse focusing strength (Formula (1)), the current limits and the acceleration efficiency. An integrated consideration of favorable transmission and structure length, ease of machining, low power consumption and the Kilpatrick Law is done for the PKU RFQ. The 80 kV of voltage i.e. $1.8E_k$, which is a reasonable max. surface field proved by the practice of the LEDA RFQ, is finally adopted.

The 50 keV of input energy W_i is a compromising choice of emittance concerns. Lower W_i goes against the

* Supported by Gottlieb Daimler-Karl Benz Stiftung & GSI, Germany
# zhang@iap.uni-frankfurt.de or zhangc@pku.org.cn

BEAM DYNAMICS ISSUES OF SPES-1 LINAC

E. Fagotti, Universita' degli studi di Milano, Milano, Italy - INFN/LNL, Legnaro, Padova, Italy
M. Comunian, A. Palmieri, A. Pisent, INFN/LNL, Legnaro, Padova, Italy

Abstract

An Independent Superconducting Cavity Linac able to accelerate 10 mA CW proton beams up to 20 MeV has been studied for the SPES-1 project. This paper presents the results of beam dynamics studies through SPES linac including mapped fields effects on cavities.

INTRODUCTION

The first time step of SPES [1] realization is the creation of a two-way facility able, on one hand, to accelerate a 10 mA protons beam up to 20 MeV for nuclear studies and, on the other hand, to accelerate a 30 mA protons beam up to 5 MeV for cancer therapy and preliminary ADS studies. TRASCO RFQ [2] is used to accelerate beam up to 5 MeV in both cases. Utilization of an accelerator optimized for high current, for relatively low current requires some care [3]. Even if transversal dynamics may be readjusted through beam re-matching at RFQ input, this is not the case for longitudinal one. Separatrix width results larger than necessary and betatron oscillations are too small in number to let good thermalization of longitudinal distribution.

Linac structure has been optimized for this particular distribution in order to guarantee the lowest possible transversal and longitudinal emittance increase, minimum halo formation and complete transmission.

LINAC DESIGN

Linac is structured in two large cryostats (see Fig. 1) with a warm doublet in between that facilitates transversal matching. The linac lattice is based on a doublets structure. The focusing elements are short quadrupoles mounted inside cryostats; the number of cavities between quadrupoles increases with β. The required quadrupole gradient can be reached both by normal conducting and superconducting magnets. Superferric quadrupoles [4], combining a very compact size with a low power dissipation in the cryostat, have been found to be an excellent solution for this linac. A potential drawback is the residual magnetic field of the iron core, which must be shielded below 1 μT during cavity cooldown to prevent performance degradation of the nearby superconducting cavities. To ensure full transmission, cylindrically symmetric (thus dipole free) reentrant cavities [5] are chosen as accelerating elements. Table 1 summarizes beam characteristics at linac input, while Table 2 presents linac configuration used in matching and tracking calculations.

Table 1: Beam characteristics at Linac input

Current	10 mA	
Energy	5 MeV	
Emit. norm. rms	x	0.208 mm-mrad
	y	0.204 mm-mrad
	z	0.240 deg-MeV

Table 2: Main linac parameters

Period Type	**Type 1**	**Type 2**	**Type 3**
No. Periods	6	3	4
No. Cavity / Period	2	3	4
Energy Range (MeV)	5.0→9.5	9.5→13.2	13.2→20.1
Lattice Type	Doublet		
Lattice Period (m)	0.69	0.87→1.13	1.05
Energy Gain / Period (MeV)	0.6→0.8	1.0→1.4	1.1→2.0
RF Phase	-30°		

BEAM DYNAMICS SIMULATIONS

Trace 3D [6], PARMILA [7] and PARMELA [8] codes are used for beam dynamics simulations, while SUPERFISH [9] is used for cavity real fields generation. Few fundamental rules are followed for beam dynamics calculation:

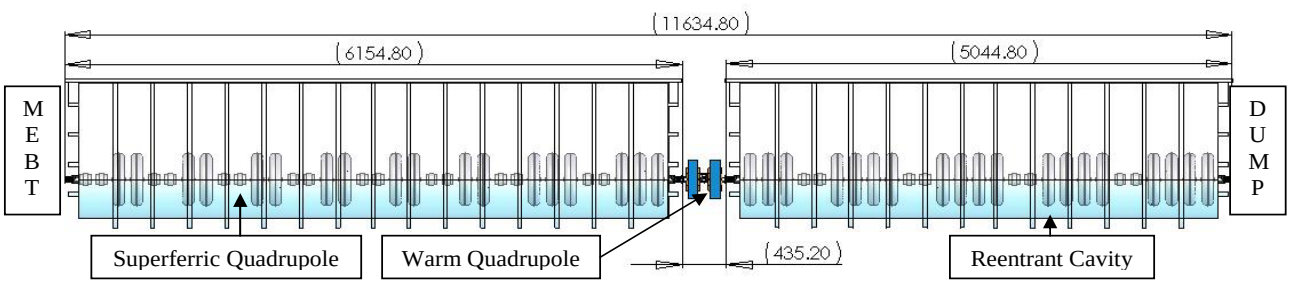

Figure 1: Linac layout. It consists of two large cryostats with a warm section in between.

CHARACTERIZATION OF BEAM PARAMETER AND HALO FOR A HIGH INTENSITY RFQ OUTPUT UNDER DIFFERENT CURRENT REGIMES

E. Fagotti, Universita' degli studi di Milano, Milano, Italy - INFN/LNL, Legnaro, Padova, Italy
M. Comunian, A. Pisent, A. Palmieri, INFN/LNL, Legnaro, Padova, Italy

Abstract

The characterization of the beam distribution at the exit of a high intensity RFQ is a crucial point in view of a correct simulation of beam behaviour in the following linac structure. At this scope we need to know the beam halo quantification as a function of the input beam and RFQ parameters. In this paper, the description of beam halo based upon moments of the particle distribution at the exit of the TRASCO-RFQ [1] is given.

INTRODUCTION

The first time step of SPES [2] realization is the creation of a two-way facility able, on one hand, to accelerate a 10 mA protons beam up to 20 MeV for nuclear studies and, on the other hand, to accelerate a 30 mA protons beam up to 5 MeV for cancer therapy and preliminary ADS studies. This two-way facility, forces the TRASCO RFQ (Fig. 1), which is used to accelerate beam up to 5 MeV in both cases, to work with two very different current regimes. Considering that RFQ design has been optimized for a 50 mA protons beam, it is evident that a very deep RFQ parameters optimization is needed.

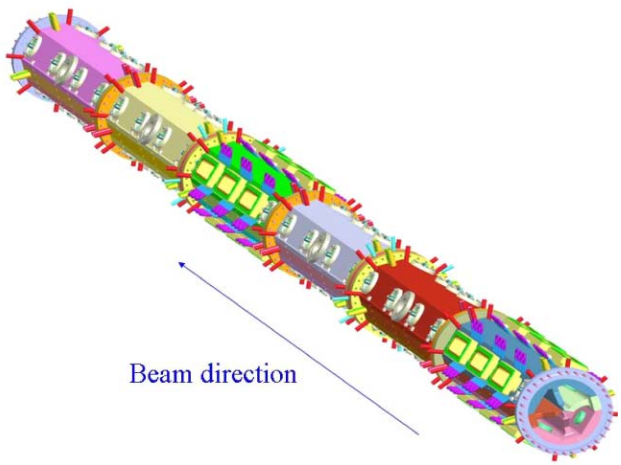

Figure 1: TRASCO-SPES RFQ design.

RFQ BEAM DYNAMICS

Beam dynamics has been simulated with PARMTEQM [3] code. All the simulations are executed starting with a 4-D Waterbag distribution of 100000 macroparticles at RFQ in. All results are obtained analyzing the full distribution output file. Therefore, it has been possible to evaluate parameters that simulation program normally do not calculate. In Tab. 1 and Tab. 2 summarize the main RFQ nominal parameters [4] and Twiss parameters at RFQ in/out for the two current regimes.

Table 1: RFQ characteristics (1)

Particle	Proton
Energy	0.08 – 5 MeV
Frequency	352.2 MHz
Duty Factor	100 %
Length	713 cm
Maximum surface field	<33 MV/m (1.8 Kilpatrick)
RF Power consumption	<800 kW

Table 2: RFQ characteristics (2)

Current (mA)		**10 mA**		**30 mA**	
Transmission		99.6 %		98.0 %	
		in	*out*	*in*	*out*
E.n.rms. *(mm-mrad) (deg-MeV)*	*x*	0.2	0.205	0.2	0.216
	y	0.2	0.2	0.2	0.212
	z	-	0.253	-	0.191
Alpha	*x*	1.37	-1.13	1.57	-1.27
	y	1.37	0.15	1.57	0.29
	z	-	0.288	-	0.05
Beta *(mm/mrad) (deg/MeV)*	*x*	0.049	0.27	0.054	0.32
	y	0.049	0.10	0.054	0.11
	z	-	439.9	-	435.4
H (halo parameter)	*x*	0.25	0.39	0.25	0.68
	y	0.25	0.35	0.25	0.60
	z	0	1.06	0	2.09

Fig. 2 shows simulation results for the two current values. Each plot is divided into four sub-plots showing beam projections in phase space. In particular, x-x', y-y', x-y and $\Delta\varphi$-ΔW plane are plotted from top left to bottom right. As regard the low current case, it can be noticed that phase-energy distribution presents a two picks structure. This has two main reasons: non linear effects due to space charge are too small to remix distribution, separatrix width results larger than necessary allowing beam to expand in longitudinal phase space. Associated with current increase there is a halo formation. In other

SOME RELEVANT ASPECTS IN THE DESIGN AND CONSTRUCTION OF A 30-62 MEV LINAC BOOSTER FOR PROTON THERAPY

D. Davino, University of Sannio, Italy, A. D'Elia, INFN and University of Naples, Italy,
S. Falco, University of Naples, Italy, M.R. Masullo, INFN, Italy,
V. G. Vaccaro*, INFN and University of Naples, Italy

Abstract

Recent results in accelerator physics showed the feasibility of a coupling scheme between a cyclotron and a linac for proton acceleration. Cyclotrons with energies up to 30MeV, mainly devoted to radioisotopes production, are available in a large number of medical centres. This suggested to design a linac booster able to increase the proton energy up to 62MeV as required for treating tumours like the ocular ones. In this paper we will discuss the basic design of a compact 3GHz SCL (Side Coupled Linac). Among the many challenges of such a project one of the most interesting is the tuning of the cavities. Because the tuning can be done only after assembling the system, it is difficult to detect which cavities are responsible for the detuning: indeed the resonant behaviour of single cavity is lost since the resonances merge into the resonant modes of the whole system. It is shown how, from the measured mode frequencies of the system, it is possible to derive the unknown resonances of each cavity and then refine the tuning. The proposed procedure is quite general and is not restricted to the SCL. This procedure is quite attractive because its use may relax the fabrication tolerances and avoids any bead pull procedure. In addition to this one may foresee even an on line computer driven tuning. Examples were given for 13 cavities fed at $\pi/2$ mode.

INTRODUCTION

The effectiveness of proton therapy of deep-seated solid tumours is now well established for the great numbers of the accumulated clinical data since when Bob Wilson proposed this therapy in 1947 in his visionary paper [1].

The potential of proton cancer therapy is now widely accepted. It has already been identified by an EU working group as deserving of priority support [2]. More than 36.000 patients [3] have already been treated world wide with proton beams of energy ranging between 60MeV to 220MeV, according to the tumour depth. The therapeutic activity, which was beforehand mainly concentrated around nuclear physics laboratories, is now moving to ad hoc conceived hospital units. Only in 1991, with the completion of the LOMA LINDA facility, proton therapy became available in a hospital site. Since then several hospital based centres have been developed [3,4,5].

The idea of designing a linac booster able to increase the proton energy up to values adequate for protontherapy was born at the beginning of 90s. A detailed description of the development of this idea and of its outcome can be found in ref. [6,7]. The PALME project concerns the design of a 3GHz linac able to accelerate up to 62MeV proton beams delivered by existing cyclotrons of 30MeV. Many of these cyclotrons are already in use for isotope production in nuclear medicine. The goal is to achieve a mean energy gradient of 11MeV/m, so that the total linac length should not exceed 3m. With 30MeV injection energy booster connected to their cyclotrons these centres could extend their activities to cancer therapy with investments lower than those required for separate installations with the same functions.

THE ACCELERATOR

The SCL is formed by a chain of large number of accelerating cavities (AC) connected via irises to off-set coupling cavities (CC). The principle which governs the frequency behavior of such a device is the resonant coupling [8]: when coupled, the all equal resonances of the cavities split into the resonant modes of the whole system. Each mode is characterized by the phase advance between adjacent cavities. This implies that when excited, all the cavities resonate on this mode with their own phase advances. Therefore, the peculiar aspect of this configuration is the possibility of having only one RF feeder for a very large number of cavities (almost fifty elements AC+CC). For SCL compact accelerators the RF power frequency is matched to the so called $\pi/2$ mode: this means that each second cavity is empty of energy and it has the role of coupling adjacent cavities.

In general the SCL basic bricks are tiles, on the opposite sides of which a half-CC and a half-AC are machined. The fabrication tolerances play a crucial role in the performances of these devices because of the extreme high frequency of the feeder. In fact, the fabrication errors produce deviations from the design nominal values of the most relevant parameters.

Even if we are dealing with devices working in the GigaHertz range, lumped circuit representation very well suits the SCL behaviour [8]. In the next section we resort to the transmission matrix representation of the two-port device for the tiles and we investigate on the overall behaviour of the SCL. In the case of N identical two-port device chain, the whole system exhibits N+1 resonant frequencies, each characterised by its own mode (phase advance). These frequencies are given by simple analytical formulas [9]. The actual situation is quite intricate: after machining the tiles are unequal and the lumped parameter values of the device exhibit slight

*vaccaro@na.infn.it

BEAM DYNAMICS DESIGN OF J-PARC LINAC HIGH ENERGY SECTION

Masanori Ikegami, Takao Kato, Shuichi Noguchi, KEK, Tsukuba, Ibaraki 305-0801, Japan
Hiroyuki Ao, Tomohiro Ohkawa, Akira Ueno, Kazuo Hasegawa,
Yoshishige Yamazaki, JAERI, Tokai, Ibaraki 319-1195, Japan
Noriyosu Hayashizaki, TIT, Meguro, Tokyo 152-8550, Japan
Valentin V. Paramonov, INR RAS, Moscow 117312, Russia

Abstract

Recently, the beam dynamics design of the high-energy part of J-PARC linac has been revised to reduce construction cost. The modifications are described in this paper together with 3D particle simulations results for the revised design.

INTRODUCTION

ACS (Annular-Coupled Structure linac) is the high-energy part of the J-PARC linac, which accelerates 190-MeV negative hydrogen beams up to 400 MeV [1, 2]. Recently, the beam dynamics design of the ACS part has been improved to reduce construction cost. The beam matching section between preceding SDTL (Separate-type Drift Tube Linac) and ACS is also revised correspondingly. The modifications of the design are described in this paper together with 3D particle simulation results for the revised design.

As presented in the reference [1], we start beam commissioning with lower linac energy of 181 MeV, in which the ACS part is replaced with a beam transport line compatible with swift energy upgrade to 400 MeV. Simulation results for the lower energy operation is also presented.

REVISED ACS

Figure 1 shows the layout of a revised ACS module, which consists of two ACS tanks connected with a bridge coupler, and quadrupole doublets placed at inter-tank spacings. Two neighboring ACS tanks are driven by a 2.5-MW klystron. The inter-tank spacing is $4.5\beta\lambda$ with β and λ being the beam velocity scaled by the speed of light and the RF wave length, respectively.

In the original design [3], ACS part consisted of 46 ACS tanks, and each ACS tank had 15 accelerating cells. The total length including inter-tank spacing was 108.3 m.

In the revised design, the number of ACS tanks is reduced from 46 to 42. To maintain the total energy gain, the number of accelerating cells in an ACS tank is increased from 15 to 17. With this design change, the number of klystrons is reduced by two, curtailing the margin for RF power by around 5 %. The averaged field strength E_0 is reduced from 4.26 MV/m to 4.12 MV/m to keep the increase of RF power load in the sustainable range. The total length of the ACS section is slightly reduced to 107.1 m. Cell geometries of an accelerating cell and a coupling cell are not modified. Bridge couplers are placed below the quadruople doublets in the inter-tank spacing, while we originally plan to place them above the beam line. This layout is selected to enable easy handling of beam instrumentation installed in the inter-tank spacing. Table 1 summarizes the main specifications of the revised ACS.

Table 1: Main specifications of the revised ACS

Input beam energy	190.8 MeV
Output beam energy	400.0 MeV
Operation frequency	972 MHz
Beam particle	Negative hydrogen ion
Peak beam current	50 mA
Beam pulse width	0.5 msec
Repetition	50 Hz (25 Hz initially)
Num. of cells per tank	17
Num. of tanks per module	2
Num. of modules	21
Num. of klystrons	21
Inter-tank spacing	$4.5\beta\lambda$
Bore radius	20 mm
Average accelerating field E_0	4.12 MV/m
Synchronous phase	-30 deg
Max. surface field	0.82 Kilpatrick
Peak RF power	42.5 MW
Peak wall loss	32.0 MW
Peak beam loading	10.5 MW
Total length	107.1 m

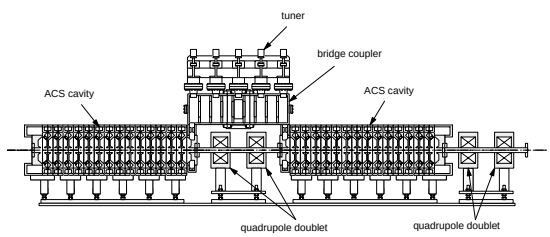

Figure 1: Layout of a revised ACS module. Although the bridge coupler is shown above the beam line in this figure, we plan to place it below.

A SIMULATION STUDY ON CHOPPER TRANSIENT EFFECTS IN J-PARC LINAC

Masanori Ikegami, KEK, Tsukuba, Ibaraki 305-0801, Japan
Tomohiro Ohkawa, Yasuhiro Kondo, Akira Ueno, JAERI, Tokai, Ibaraki 319-1195, Japan

Abstract

J-PARC linac has a chopper system to reduce uncontrolled beam loss in the succeeding ring. The chopper system is located in MEBT (Medium Energy Beam Transport line) between a 3-MeV RFQ and a 50-MeV DTL, and consists of two RFD (Radio-Frequency Deflection) cavities and a beam collector. During the rising- and falling-times of the RFD cavities, the beams are half-kicked and cause excess beam loss downstream. In this paper, the behavior of these half-kicked beams is examined with 3D PARMILA simulations, and resulting beam loss and beam quality deterioration are estimated.

INTRODUCTION

J-PARC linac [1, 2] has a chopper system to reduce uncontrolled beam loss in the succeeding RCS (Rapid Cycling Synchrotron). While we are preparing two-stage chopping system utilizing both LEBT and MEBT choppers [2], we are considering to start beam commissioning only with MEBT chopper, taking account of the following circumstances, namely; we decided to start beam commissioning with lower peak current of 30 mA [1], which eases the heat load problem of the chopper target (collector), and we have experimentally confirmed that surviving ratio in the chopper-on period is less than 10^{-4} only with MEBT chopper [3]. While the experimental data is for the case with 5 mA, it encourages us to seek the possibility of "one-stage chopping" in which the combined transient effects of LEBT and MEBT choppers are avoided. In this paper, we focus on the transient effects in one-stage chopping where only MEBT chopper is used.

The chopper system is located in MEBT between a 3-MeV RFQ and a 50-MeV DTL, and consists of two 324-MHz RFD (Radio-Frequency Deflection) cavities and a beam collector [2, 4]. With this RF chopper system, an intermediate-pulse (or pulse-train) structure is generated as schematically shown in Fig. 1. In the intermediate-pulse structure, the beam-on period continues for $\sim$ 500 nsec followed by the beam-off (chopper-on) period of $\sim$ 500 nsec. The repetition of the intermediate-pulse structure is synchronized with the frequency of the RCS RF system. The intermediate-pulse width will be optimized to have the maximum beam power within the tolerable beam loss limit in RCS. In the beam-off period, beams are horizontally deflected by the RFD cavities and collected by the collector. During the rising- and falling-times of the RFD cavities, the beams are half-kicked and can cause excess beam loss downstream.

Survived half-kicked beams can also cause a beam loss problem in RCS, exceeding the transverse dynamic aperture limit. We have a requirement for the transverse emittance at the injection to RCS to enable effective painting, namely; the normalized transverse emittance should be less than 4πmm·mrad. To achieve the requirement for the transverse emittance, we have transverse halo collimators in the beam transport line between linac and RCS [2]. The collimator edge position is supposed to be set to satisfy the requirement for the transverse emittance, and it is practically important to estimate the collimator load, i.e., the fraction of a beam that must be eliminated with the halo collimators. One of our aims in this simulation study is to estimate the increase of the collimator load during chopper transient.

In this paper, the behavior of these half-kicked beams is examined with 3D PARMILA[5] simulations, and resulting excess beam loss and halo-collimator load are estimated.

SIMULATION CONDITIONS

As discussed in a separate paper [1], we plan to start beam operation with the lower linac energy of 181-MeV. In this paper, simulations are performed with PARMILA from the exit of RFQ to the injection point to RCS for the 181-MeV case. In the simulations, we assume the peak current of 30 mA, which is the design value for 181-MeV operation. The initial distribution at the exit of RFQ is obtained with PARMTEQM [6]. The number of simulation particles is 95,322 and the number of meshes is set to 20x20x40.

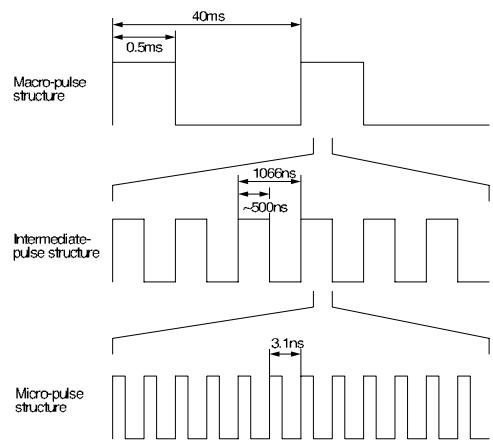

Figure 1: Pulse structure for J-PARC linac (181-MeV injection).

A SIMULATION STUDY ON ERROR EFFECTS IN J-PARC LINAC

Masanori Ikegami, KEK, Tsukuba, Ibaraki 305-0801, Japan
Tomohiro Ohkawa, Yasuhiro Kondo, Akira Ueno, JAERI, Tokai, Ibaraki 319-1195, Japan

Abstract

In this paper, effects of realistic errors on beam loss and beam-quality deterioration in J-PARC linac are examined with systematic simulations with PARMILA. Necessity of transverse collimation is also discussed.

INTRODUCTION

Requirements on the momentum spread and transverse emittance are severe for J-PARC linac [1, 2] to realize effective injection to the succeeding RCS (Rapid Cycling Synchrotron). The requirement for the momentum spread at the RCS injection is less than $\pm 0.1\%$ including beam centroid momentum jitter, and that for the normalized transverse emittance is less than 4πmm·mrad. To achieve the requirement for the transverse emittance, we have transverse halo collimators in the beam transport line between linac and RCS [2]. To meet the requirement for the momentum spread, we have two debuncher cavities in the beam transport line to the RCS, with which the bunch is rotated to minimize momentum spread [2, 3].

As losses and beam-quality deterioration are mainly caused by various errors, such as misalignment, RF setpoint errors, etc, it is essentially important to perform particle simulations for J-PARC linac with as realistic errors as possible to estimate their effects. In this paper, effects of realistic errors on beam loss and beam-quality deterioration in J-PARC linac are examined with systematic 2D and 3D simulations with PARMILA [4].

SIMULATION CONDITIONS

As discussed in a separate paper [1], we plan to start beam operation with the lower linac energy of 181-MeV. In this paper, simulations are performed with PARMILA from the exit of RFQ to the injection point to RCS for the 181-MeV case. In the simulations, we assume the peak current of 30 mA, which is the design value for 181-MeV operation. The initial distribution at the exit of RFQ is obtained with PARMTEQM [5]. The number of simulation particles is 95,322 and the number of meshes is set to 20x20x40 for 3D cases and 20x40 for 2D cases.

The quadrupole magnets in DTL and SDTL sections are set to satisfy the equipartition condition. No halo collimation has been assumed in the simulation.

EFFECTS OF STATIC ERRORS

In error analyses, dynamic errors and static errors should be treated separately. For example, beam orbit distortion is mainly caused by the alignment errors of quadrupole magnets, which are static by nature. Another obvious example is the beam centroid momentum jitter, which is solely determined by the dynamic component of the RF errors. We here refer drift or sway of RF phase and amplitude as "dynamic" regardless of their time-scale, and tuning errors of RF setpoints as "static".

Table 1: Assumed static errors

Errors	Range
Quad alignment error (transverse displacement)	± 0.1 mm
Quad alignment error (roll error)	± 5 mrad
Quad gradient error	$\pm 0.25\%$
RF amplitude error	$\pm 1\%$
RF phase error	± 1 deg

At first, we consider the static errors listed in Table 1. The errors are uniform-randomly distributed in the range. 20 cases with different random seeds have been considered. Simplified beam-orbit correction has been assumed only in the cases where the beam loss is significant, while we have an elaborated beam steering system in the actual linac. At the end of MEBT (in Run #8, 11, 14, and 17), we give a tilt to the beam to minimize the beam loss in DTL1. At the entrance of SDTL (in Run #8), we simply shift the beam center to the origin to avoid the loss in SDTL. Similarly, we shift the beam center to the origin at the exit of SDTL (in Run #5, 9, 11, 16, and 19) to avoid the loss in the beam transport line to RCS.

Figure 1 shows the obtained normalized emittance at the injection to RCS. The result for the case without errors is also shown. As seen in Fig. 1, the emittance exceeds 4πmm·mrad in most cases, and the particles outside 4π ellipse should be eliminated with halo collimators. Then, we estimate the collimator load by counting the number of particles locating outside the 4π boundary. We find that the collimator load ranges from 1 to 3 % and it is typically around 1.5 %, which is tolerable with the current radiation shielding of the halo collimator.

In the 20 cases, we have the beam loss of up to 2 % (typically less than 0.2 %), but they are mostly localized in the first DTL tank as shown in Fig. 2. While small amount of loss (up to 0.2 %) is observed at the DTL-SDTL transition, we have confirmed that it can be reduced to less than 0.01 % (2 W) level with beam steering at MEBT.

Figure 3 shows the energy spread and the longitudinal emittance at RCS injection. While substantial momentum spread increase have be observed, we have confirmed that dynamic RF errors plays a more dominant role in determining the final momentum spread as discussed later. As seen

ALTERNATING PHASE FOCUSING IN LOW-VELOCITY HEAVY-ION SUPERCONDUCTING LINAC*

P.N. Ostroumov#, A.A. Kolomiets†, K.W. Shepard, Physics Division, ANL, 9700 S. Cass Avenue,
E.S. Masunov, MEPhI, Moscow, Russia.

Abstract

The low-charge-state injector linac of the RIA post-accelerator (RIB) is based on ~ 60 independently phased SC resonators providing a total of ~70 MV accelerating potential. The low charge-state beams, however, require stronger transverse focusing, particularly at low velocities, than is used in existing SC ion linacs. For the charge-to-mass ratios considered here (q/A = 1/66) the proper focusing can be reached by using strong SC solenoid lenses with a field of up to 15 T. Both the number of the solenoids and field can be reduced applying Alternating Phase Focusing (APF). A method to set the rf field phases has been developed and studied both analytically [1] and with the help of the three-dimensional ray tracing code TRACK [2]. The paper discusses the results of these studies.

INTRODUCTION

The design goal for the RIB linac is to accelerate heavy ions up to 10 MeV/u and higher in the mass range from 6 to 240, starting with ions at charge state 1+ [3]. The initial section of the RIB linac is a low- charge-to-mass-ratio superconducting rf linac (SRF) which will accelerate any ion with q/A≥1/66 to at least ~1 MeV/u. The low-energy RIB linac will be based on 4-gap quarter wave SC cavities, which can provide typically ~1 MV of accelerating potential per cavity in the velocity range 0.011c<v<0.06c. The initial section of the linac consists of four classes of those cavities designed for different geometrical beta as listed in Table 1. The input beam is formed by upstream RFQs operating at room temperature. The initial normalized transverse emittance is ε_T =0.1 π · mm·mrad and the longitudinal emittance is ε_L =0.3 π · keV/u·nsec. The RIB linac described in this paper is designed using the 4-gap resonators designed for the RIA driver linac. These resonators, modified slightly to match the ATLAS operating frequency [3] are completely applicable for the RIB lianc.

REFERENCE DESIGN

As a reference design of the RIB linac we consider the focusing by high-field SC solenoids alternating with SC resonators. The main parameter which defines specifications to the focusing system is the defocusing factor which is significant due to the high accelerating field in the SC resonators and low velocity of ions.

The phase advance per focusing period of the betatron oscillations μ is defined as

$$\mu^2 = \mu_0^2 + \alpha \sin\varphi , \qquad (1)$$

where $\alpha = \dfrac{\pi eqUL}{2Am_e c^2 \lambda \beta^3 \gamma^3}$, μ_0 is the phase advance without any acceleration, α is the defocusing factor, φ is the particle phase with respect to the accelerating field crest in the resonator, eq and A are the charge and mass number of ion, L is the length of the focusing period, m_e is the atomic unit mass, c is the speed of light, λ is the wavelength of the rf field, β is the ion velocity in units of c. The formula (1) is valid for any particle phase with respect to the crest of the rf electric field in the cavity. There is a large phase slippage of the bunch in a SC resonator therefore it is convenient to introduce an effective phase φ_e which is measured with respect to the maximum energy gain phase angle in the resonator.

The transverse phase advance and average accelerating rate are inversely proportional to the length of the focusing period L. However the lowest possible value of L is limited by practically achievable focusing fields. Figure 1 shows transverse phase advance as a function of the solenoid field. The calculations have been performed for realistic field distributions both in the resonators and solenoids. The effective length of the solenoid is 280 mm,

Table 1: Resonators developed for the RIA driver linac.

Design beta of cavity	Frequency (MHz)	Maximum field (MV/m)	Voltage (MV)
0.017	57.5	20	0.82
0.024	57.5	20	1.07
0.031	57.5	20	1.25
0.061	57.5	20	1.35

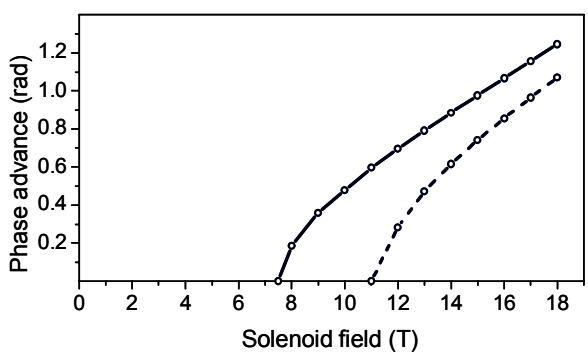

Figure 1: Transverse phase advance as a function of the solenoid field. The solid line corresponds to the bunch center and the dashed line - to the outermost particle phase.

*Work supported by the U.S. Department of Energy, Office of Nuclear Physics, under Contract No. W-31-109-ENG-38.
#ostroumov@phy.anl.gov
† On leave from ITEP, Moscow, Russia

ACCELERATION OF SEVERAL CHARGE STATES OF LEAD ION IN CERN LINAC3

V. Coco, J. Chamings, A. M. Lombardi, E. Sargsyan and R. Scrivens, CERN, Geneva, Switzerland

Abstract

CERN's LINAC3 is designed to accelerate a 100 μAe lead 25+ ion beam from 2.5 keV/u to 4.2 MeV/u. The beam is then stripped using a carbon foil and the resulting 25 μAe 54+ beam is accumulated and cooled in the Low Energy Ion Ring (LEIR) before transfer to the Proton Synchrotron (PS) and ultimately to the Large Hadron Collider (LHC). The lead 25+ ions are selected with a spectrometer from a mixture of ten charge states produced by an Electron Cyclotron Resonance (ECR) source.

In view of the fact that the stripping efficiency to lead 54+ is mostly dependent on energy and not on initial charge state, the feasibility of simultaneously accelerating to 4.2 MeV/u several charge states has been investigated. In this paper we report two possible technical solutions, their advantage in terms of intensity for the downstream machines and the experimental results supporting these conclusions.

MOTIVATION

LINAC3[1], the CERN lead ion injector has been operational since 1993 and providing an intensity of 25 μA of lead 54+ at 4.2 MeV/u to the Proton Synchrotron Booster (PSB). The beam is obtained by selecting a 2.5 keV/u 27+ lead ion beam from an ECR source and further accelerating it to 4.2MeV/u onto a 100 μg/cm^2 carbon foil. The acceleration is done in two stages: a 100MHz RFQ increases the beam energy to 250 keV/u and subsequently a system of three IH tanks (first one at 100MHz, the others at 200MHz) increases the beam energy to 4.2 MeV/u. The theoretical and experimental acceleration efficiency is around 85%, the stripping efficiency around 15% [2]. After stripping one charge state is selected and debunched to prepare for injection into the PSB. From 2006 the LINAC3 beam will be accumulated and cooled in a Low Energy Ion Ring (LEIR) before acceleration to LHC injection energy. The present set-up of LINAC3 is sufficient to meet the LHC needs [3]. Nevertheless, studies for exploring LINAC3 bottlenecks and possible improvements to its output current were pursued in the framework of the Ions for LHC (I-LHC) program. In view of the very good transmission of LINAC3 significant improvements can come either from a new source or from a new approach to producing lead 54+ at 4.2 MeV. In this paper we deal only with the second option. The efficiency of ionisation from lead 27 to lead 54 is quite low, because of the statistical nature of the interaction between charged particles and matter. This means that a good fraction of the intensity is lost due to the fact that more than 80% of the incoming ions are ionised to the "wrong" charge state. For this very same reason, a high charge state can be the result of the ionisation of a slightly different incoming charge state, i.e. lead 54+ can be obtained by stripping 25+ or 26+ or 27+ with the same foil thickness. Therefore, if we had more than one charge state simultaneously on the stripper within the nominal transverse emittance and energy spread, we could increase the overall useful current delivered by LINAC3. In the following we will report some theoretical and experimental observation on how to bring several charge states onto the LINAC3 stripper with minimum modification to the present set-up.

MULTICHARGE OPERATION

The ECR source of LINAC3 delivers, in the afterglow mode, 800 μA of lead shared between about 10 charge states. The source is optimised for delivering a maximum current made of 27+ lead ion and about 400μA of the total current is made of 24+,25+,26+, 27+ and 28+[4].

Low Energy Beam Transport (LEBT)

The LEBT is designed to select a pure single charge state lead ion beam. The 135 degrees spectrometer placed after the source is composed of two 67.5 degrees bending spaced by 700 mm. After the selection, a system of three quadrupoles and a solenoid matches the beam to the RFQ. We have analysed two solutions to bring several charge states at the RFQ entrance. The first one involves eliminating the spectrometer and putting the source in line with the RFQ: the new LEBT line, 2.4 m in length and equipped with three solenoids would allow all the charge states (5 of which also well matched) to the RFQ entrance. This solution, conceptually the easiest, involves major modifications to the present set-up and acquiring a new solenoid. It will be referred to as the "straight injection" solution and its beam dynamics can be seen in Fig. 1.

PROTON BEAM DYNAMICS OF THE SARAF LINAC

A. Shor, D. Berkovits, G. Feinberg and S. Halfon, Soreq NRC Yavne 81800 Israel
K. Dunkel, ACCEL Instruments GmbH, Bergisch-Gladbach, Germany

Abstract

We have performed proton beam dynamics simulations for the SARAF (Soreq Applied Research Accelerator Facility), 40 MeV and 4 mA, linac. The simulations are performed using the GPT code and includes effects of space charge. They demonstrate that for an initial 6D ellipsoid Waterbag distribution beam, a tune can be obtained with a longitudinal rms emittance growth of 5% and a transverse normalized rms emittance growth of 20%. Beam loss is estimated by fitting a radial Gaussian to the particle distribution along the linac. A 1 nA beam envelope is obtained by extrapolating the tail of the radial-Gaussian function. The 1nA beam envelope for an initial Waterbag distribution is well within the beam bore radius. However, benchmark simulations with an initial 6D ellipsoid Gaussian distribution, with the same rms quantities, exhibit a more extended tail that may result in higher beam loss.

INTRODUCTION

Beam dynamics simulations for the SARAF [1] linac (fig. 1) are presently being performed at Soreq. We present results of the simulations performed with the General Particle Tracer (GPT) simulation code [2] and the LANA [3] code. Both codes enable precise calculations of particle tracking, taking into account realistic 3D fields of accelerating and focusing elements and also effects of space charge. GPT contains provisions for generating random particles, and for incorporating user supplied codes.

The SARAF accelerator consists of an ECR ion source (20 keV/u), a low energy beam transport (LEBT), a 176 MHz 4-rod RFQ for bunching and pre-accelerating to 1.5 MeV/u, a medium energy beam transport (MEBT), and a linac. The linac is based on independently phased superconducting (SC) 176 MHz half-wave resonator cavities (HWR) and SC solenoids. The accelerator is based on the ACCEL design [4], consists of two types of HWRs, one optimized for η_0=0.09 and a second for η_0=0.15 [5]. The linac consists of six self-contained SC modules. The first module, referred to as the PSM (Prototype SC Module), consists of three solenoids, each followed by two η_0=0.09 HWRs. The remaining five modules consist of 4 solenoids, each followed by two η_0=0.15 HWRs. Figure 1 shows a schematic of the SARAF linac.

Typically, particles simulations generate the initial particle distribution according to a 6D ellipsoid, with either a Waterbag (WB) or Gaussian (Gauss) distribution. The 6D ellipsoid establishes the particle distribution and correlations in x-x', y-y', and z-z', or π-÷E spaces. The WB option establishes a uniform distribution within the 6D ellipsoid, while the Gauss option establishes a density profile with a Gaussian falloff. ACCEL has performed extensive beam dynamics simulations of the linac assuming an initial 6D ellipsoid with a WB distribution. We use the ACCEL linac lattice and tune and repeat their simulation with the codes GPT and LANA.

INITIAL DISTRIBUTION GENERATOR

GPT version 2.52 has no provisions for a 6D ellipsoid, but it does contain option for linking a user routine to the GPT code. We embarked on developing algorithms for creating a 6D ellipsoid, with a WB or Gauss distribution, and incorporating a reliable code into the GPT particle generator. This code was tested and checked for consistency and reliability.

In the algorithm for generating events within a 6D ellipse we first generate random numbers for x, x', y, y', z and z' uniformly distributed within the given boundaries, according to:

$$4\sqrt{\kappa_x\eta_x}\ \Omega x\ \Omega\sqrt{\kappa_x\eta_x} \text{ and } 4\sqrt{\kappa_x\nu_x}\ \Omega x'\ \Omega\sqrt{\kappa_x\nu_x} \qquad (1)$$

and similarly in the y and z plans, where κ is the emittance and η and ν are the Twiss parameters.

If the event is inside the ellipse, i.e. if the inequality in eq.(2) is satisfied then we accept, otherwise, reject the event. This procedure populates a 6D ellipsoid with a uniform particle distribution (except for statistical fluctuations) - a Waterbag distribution.

We base our algorithm for a 6-D Gauss distribution on the acceptance-rejection method of von Neumann [6]. First, we generate an event according to the prescription described above for the 6D WB. The left side of eq.(2),

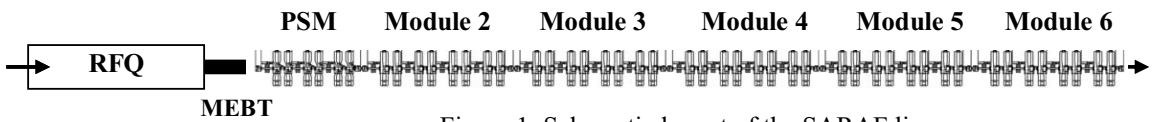

Figure 1: Schematic layout of the SARAF linac.

MULTI-BUNCH BEAM DYNAMICS STUDIES FOR THE EUROPEAN XFEL

N. Baboi*, DESY, Hamburg, Germany

Abstract

In the X-ray free electron laser (XFEL) planned to be built at DESY the acceleration of the electron bunches will be made by 9-cell superconducting cavities. These cavities have been initially developed within the TESLA (TeV Energy Superconducting Linear Accelerator) linear collider study. The impact of the higher order modes (HOM) has been shown to be within the acceptable beam dynamics limits for the collider. For the XFEL the dynamics is relaxed from the point of view of multi-bunch effects (e.g. lower bunch charge, higher bunch emittance). However the lower energy and different time structure of the beam make the study of the HOM effects in the XFEL linac desirable. Multi-bunch beam dynamics simulations have been made. The results of the HOM measurements at the TESLA Test Facility are used. Several options for the beam structure and energy are studied.

INTRODUCTION

In the European XFEL [1, 2, 3] a beam of up to 400 electron bunches with 10 to 20 GeV energy will generate ultrashort, high-intensity, coherent X-rays in long undulators. The design is based on the superconducting technology developed for the TESLA linear collider study [1, 4]. For the SASE FEL process, a good alignment, low emittance and small energy spread of the beam are essential. The main cause of degradation of the multi-bunch beam dynamics is the long-range wakefields generated by each bunch in the accelerating cavities. These may lead to accumulating deflections of the subsequent bunches, so that the multi-bunch emittance increases. The study of the wakefield effects is therefore important.

No dedicated multi-bunch beam dynamics simulations have been made so far for the XFEL. However many estimations could already be made based on the extensive studies made for TESLA [1, 5]. In the linear collider two beams, one of electrons and one of positrons, would be accelerated against each other to an energy of 500 GeV c.m. in an initial stage, and later up to 800 GeV c.m. The emittance preservation in the XFEL is less critical than in the case of TESLA due to the lower bunch charge and length and the higher design emittance (see Table 1). Therefore smaller wakefield effects are expected. However one should take into account some major differences, such as the lower energy, where the wakefield kicks are stronger and the different pulse structure. Therefore a series of simulations have been made of the multi-bunch emittance dilution along the XFEL linac. The results are discussed hereafter.

* nicoleta.baboi@desy.de

Table 1: Comparative parameters for XFEL and TESLA

	XFEL	TESLA
bunch length (fs)	80	1000
bunch spacing (ns)	min. 200	337
bunch train length (μs)	max. 800	950
bunch charge (nC)	1	3.2
beam energy (GeV)	max. 20	250
normalized emittance (m·rad)	$1.4{\cdot}10^{-6}$	$3{\cdot}10^{-8}$

MULTI-BUNCH DYNAMICS SIMULATIONS

Linac layout For the multi-bunch tracking, we have considered the linac design previously used in simulations of single-bunch effects [6]. The layout has been recently slightly changed, to two bunch compression stages in order to increase jitter tolerances [3, 7]. These changes should not affect the multi-bunch effects. A photo-injector produces electrons bunches of 1 nC which are immediately accelerated by four cryo-modules. Each cryo-module contains eight 1 m long 1.3 GHz accelerating cavities (TESLA cavities). Fig. 1 shows the beta function along the linac starting with the last cavity of the first module, where our simulations begin. The linac elements are also schematically shown.

After the first TESLA modules, the bunches pass through a cryo-module with eight cavities working at 3.9 GHz, used to compensate for non-linear distortions of the longitudinal phase space. Two subsequent bunch com-

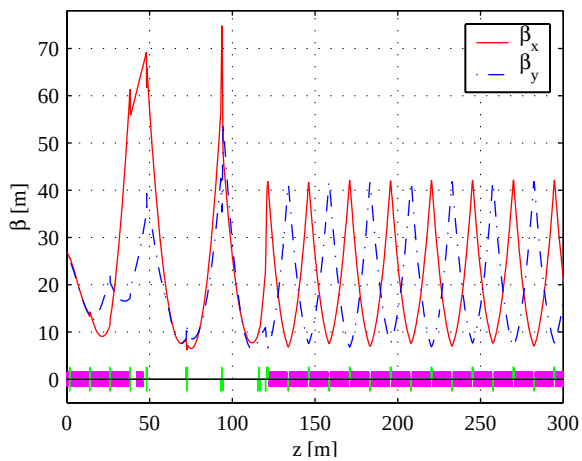

Figure 1: Beta function along the linac. The cryo-modules and quadrupoles are also sketched. The 3.9 GHz module is situated at z ≈ 45 m. Two bunch compressors are placed between about 50 and 120 m.

BEAM OPTICS STUDIES FOR THE TESLA TEST FACILITY LINAC

V. Balandin, P. Castro and N. Golubeva, DESY, Hamburg, Germany

Abstract

The aim of the TESLA Test Facility Phase 2 (TTF2) Linac is to create electron bunches of small transverse emittance and high current with energies up to 1 GeV for the VUV-FEL at DESY. A study of the (linear) beam optics of the linac is presented for the case of beam commissioning for FEL. The requirements of each part of the linac upon the optics are discussed in detail and an appropriate solution for each case is shown, as well as the matching solution to the rest of the accelerator. The chromatic properties of the linac have been studied also.

ACCELERATOR OVERVIEW

Details on components and parts of the TTF2 linac are documented in many technical reports and publications (see, for example, [1, 2, 3, 4] and references therein). The machine layout for the start of operations is shown in Fig. 1.

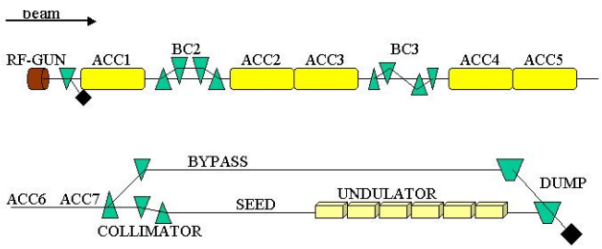

Figure 1: Schematic of TESLA Test Facility Linac.

Electron bunches are produced in an RF gun and accelerated by five cryomodules (ACC1 - ACC5) each containing eight nine-cell superconducting niobium cavities and a doublet of superconducting quadrupoles. To achieve high peak current in the undulator, the bunch is longitudinally compressed in two magnetic chicanes. Downstream the first bunch compressor BC2 (a four bend chicane) there is a diagnostic section arranged in a FODO lattice for the measurement of beam parameters. A second compression stage takes place after the passage through ACC2 and ACC3 and is performed using a S-type chicane (BC3). The last accelerating section, presently containing only two cryomodules (ACC4 and ACC5), accelerates the beam to the chosen final energy. Longitudinal beam profile diagnostics are located in the temporary beam line reserved for two more cryomodules (ACC6 and ACC7). Then, the electron beam is either guided to a bypass beam line (BYPASS) or brought through a collimator section (COLLIMATOR) to the FEL undulator. The collimator section has a dogleg shape and contains transverse and energy collimators for undulator protection purposes. Besides that, the collimator section incorporates a fast orbit feedback system and has to ensure the matching into the downstream beam line. Before the bunch enters the undulator, it passes an FEL seeding section (SEED), which at present is substituted by a temporary beam line with FODO type of focusing. Finally, the electron beams from the undulator and bypass are dumped in the same absorber (DUMP).

OPTICS SEARCH STRATEGY

The transverse optics discussed in this paper starts from the quadrupole doublet of the ACC1 cryomodule and uses as initial values (which eventually have to be corrected after measurement of actual beam parameters) the same Twiss functions which are used in [5]. We consider neither the beam dynamics in the gun area nor the choice of bunch compression schemes. A detailed description of these questions can be found, for example, in [1, 2].

Lattice Constraints

There are several requirements on the local behaviour of the optical functions, which we consider as constraints to the optics design.

- The TTF2 undulator section is a periodic structure consisting of six identical cells. Each cell is built up of an undulator segment (made of permanent magnets) followed by a doublet of electromagnetic quadrupoles to accomplish strong focusing [3, 6]. The quadrupole strength has to be optimized to provide good FEL performance.
- A special choice of Twiss parameters at the entrances of bunch compressors BC2 and BC3 reduces emittance growth due to coherent synchrotron radiation (CSR). That results in an asymmetric behaviour of betatron functions through bunch compression sections with a maximum at the entrance and a minimum between last two dipoles [7, 8, 9].
- The selection of optical functions in the dogleg of the collimator section are completely determined by the need to suppress the linear and second order dispersions and to shape a beam envelop suitable for collimation purposes [10].
- Beam emittance measurements in sections BC2 and SEED are obtained from the beam sizes measured at four separated locations inside a FODO structure. This emittance measurement technique provides its best accuracy for periodic Twiss functions and a 45° phase advance per cell [11].
- Beam spot size at the exit window location should be not smaller than the safety limit defined by the window (and dump) material properties and design. Al-

THE SUPERCONDUCTING CW DRIVER LINAC FOR THE BESSY-FEL USER FACILITY*

J. Knobloch for the BESSY-FEL Design Group
BESSY GmbH, Albert-Einstein-Str. 15, 12489 Berlin, Germany

Abstract

A CW FEL User Facility for the VUV to soft X-ray spectral range using a cascaded HGHG-FEL scheme is planned at the BESSY site. Beam acceleration to 2.3 GeV is provided by a 144-cavity superconducting driver linac based on TESLA technology modified for CW operation. Initially, a high-rep-rate normal-conducting photoinjector will be used but a fully CW superconducting version is being investigated for a future upgrade. The required 2 kA peak current is achieved with two bunch compressors. An overview of the linac layout is provided here. Also discussed are the impact of CW operation, modifications to the TESLA technology that are necessary, as well as the expected linac performance.

INTRODUCTION

Numerous CW FELs are now being proposed to meet the demand of the synchrotron-light community for high-brilliance, fully coherent and short-pulse (fs) light in the VUV to x-ray range. These include the BESSY FEL in Berlin, whose Technical Design Report was published recently[1], and the 4GLS at Daresbury[2].

Such CW machines, which must use superconducting cavities, are very attractive because their intrinsic high average flux and brightness enable multi-beamline operation at a level not possible with pulsed linacs. Furthermore, CW operation provides additional flexibility to tailor the bunch structure to the users' needs. Due to the success of the TESLA Test Facility (TTF) at demonstrating the reliable operation of TESLA technology[3] for FEL applications, these new proposals are also based on this technology.

The BESSY-FEL facility, shown schematically in Fig. 1, comprises a CW linac driving three cascaded High-Gain-Harmonic-Generation (HGHG) FELs. These cover a continuous photon-energy range from 24 eV to 1000 eV.

For efficient lasing, the linac must provide a beam energy of 2.3 GeV at a peak current of 2 kA (2.5 nC per bunch) with a slice emittance of order 1.5 π mm mrad. Bunch compression is achieved in a two-stage system. An arc is included in the layout to reduce the physical length of the machine, leaving space for future upgrades and expansions. Fast kickers[4] at 1020 MeV and 2300 MeV then distribute the electron beam among the three FELs. A collimator section[5] prior to each FEL protects the undulators.

Although much of the pulsed TESLA technology will be transferred directly to the BESSY FEL several issues unique to CW operation have been investigated and necessitate some design and layout changes. These include cryogenic aspects, RF control and the RF distribution which are addressed later.

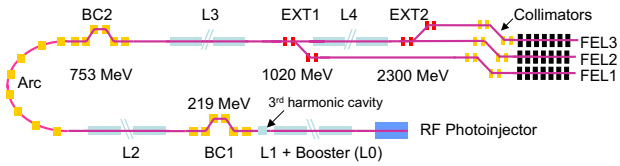

Figure 1: Layout of the driver linac for the BESSY FEL.

INJECTOR

Initially the injector will use a high-rep-rate normal-conducting (NC) RF photogun, but a future upgrade to a fully CW superconducting system is planned.[6] The NC gun is based on the operational PITZ design, which has achieved a *projected* emittance of 1.7 π mm mrad at a peak cavity field of 40 MV/m. Simulations of a layout optimized for 2.5-nC operation have demonstrated that, given a 38 ps flat-top temporal laser profile with short rise and fall times (4 ps), a slice emittance of less than 1.5 π mm mrad can be achieved at the exit of the booster section (L0) (2.1 π mm mrad projected emittance).[6]

Three bunches are accelerated in a 6 μs pulse at a repetition rate of 1 kHz. They are distributed among the three FELs using high-speed kickers[4], so that each FEL is also operated at 1 kHz. But the relatively large duty factor (ca. 2.5% when rise and fall times are included) produces a 75 kW heat load in the RF gun, nearly three times that of PITZ, so that the cooling had to be improved.

The NC, pulsed injector represents a conservative system that will be used to commission the BESSY FEL. However, to fully exploit the CW capability of the main linac, a CW injector will eventually be required. Such systems are currently being investigated[7, 8]. A split superconducting cavity/compensation solenoid layout is also being studied at BESSY. Preliminary simulations of such a layout suggest that the required slice emittance can be achieved at an accelerating field of 34.5 MV/m.

The L0 section, consisting of eight TESLA cavities, follows directly after the RF gun. The average field is 15.7 MV/m, chosen to minimize and preserve the emittance out of the gun. Acceleration is off crest, as in the L1 and L2 linac, to provide an energy chirp which later is used for bunch compression. A third harmonic cavity compensates for the curvature of the RF field as well as the T_{566} of the dispersive sections downstream.

* Work funded by the BMBF and the Land Berlin.

LINAC UPGRADES FOR FERMI@ELETTRA

G. D'Auria, R.J. Bakker, C.J. Bocchetta, P. Craievich, M. Danailov, G. De Ninno, S. Di Mitri, B. Diviacco, M. Ferianis, G. Pangon, L. Rumiz, L. Tosi, V. Verzilov*, D. Zangrando,
Sincrotrone Trieste, SS 14 - km 163,5 in AREA Science Park, 34012 Basovizza, Trieste ITALY

Abstract

To fulfill the stringent requirements expected from the FERMI@ELETTRA project, the existing linac needs some modifications in the layout and an upgrading of the present plants. Moreover, for the next two years, until the new injection system, now under construction, is fully commissioned, the linac has to be kept in operation as injector for the ELETTRA Storage Ring. Therefore most of the planned activities have to be carried out without interfering with the normal operation of the machine. Details on the new linac layout and related activities are discussed.

INTRODUCTION

The FERMI@ELETTRA project [1] is an initiative among Sincrotrone Trieste, INFM and other Italian Institutes, to construct a single-pass FEL user facility located next to the third generation Synchrotron Light Source ELETTRA, utilizing the existing 1.0 GeV linac. The spectral range of the laser will go from 100 nm to 10 nm with two undulator beamlines implemented on the machine in two different phases:

- Phase 1 (FEL-1) will aim to cover 100-40 nm.
- Phase 2 (FEL-2) will extend the FEL wavelength up to 10 nm.

The first proposal of the FERMI project [2] was submitted to Italian Ministry of Education, University and Scientific Research in February 2002, in response to the Italian Government's call for proposals for a multipurpose pulsed laser X-ray source. In July 2004 the project was funded.

Ongoing activities are now evolving from a conceptual design phase to an early stage of a detailed technical design. Table 1 summarizes the main beam parameters for the two phases of the project.

Table 1: Electron beam parameters for phase 1 and 2

	FEL-1		FEL-2		
Wavelength	100	40	40	10	nm
Beam energy	0.7		0.55	1.0	GeV
Bunch charge	1.0		1.0		nC
Peak current	0.8		2.5		kA
Bunch duration	500		160		fs
Energy spread	0.7		1.0		MeV
Emittance	1.5		1.5		10^{-6} m
Repetition rate	50		50		Hz

To produce a beam with the required beam characteristics the existing linac needs some layout modifications, an upgrading of the RF plants, the implementation of a new synchronization system as well as a review of the whole beam optics, including the installation of two bunch compressors.

Figure 1 shows the present layout of the machine (a), the proposed FEL schemes with the two beamlines and the main modifications to be implemented on the existing machine (b) [2], and the new layout to guarantee the injection in the storage ring (c). At present the linac is operated less than 2 hours a day as the ELETTRA injector, the time remaining is completely available for all the activities connected to the FEL development. Therefore, with careful planning, most of the foreseen upgradings could be already activated.

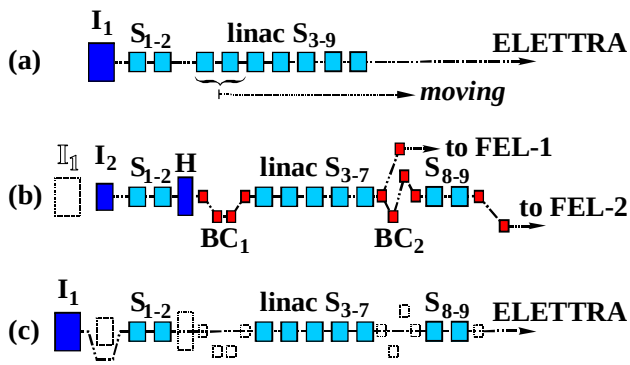

Figure 1: Linac layouts.

Labels meaning:

- I_1: present injector, thermionic gun and bunching sections, beam energy at exit 4.5 MeV.
- I_2: high brightness photoinjector.
- $S_{1\text{-}2}$: 3.2 m long accelerating sections, 2/3π forward TW, iris diameter 16-22 mm, without sled.
- H: 3rd harmonic cavity.
- BC_1 and BC_2: magnetic bunch compressors.
- $S_{3\text{-}9}$: 6.1 m long accelerating sections, 4/5π backward TW, each equipped with its own sled system.

LINAC MODIFICATIONS

Figure 2 gives a schematic overview of the linac building complex with the layout modifications and the expected installations.

Concerning the civil engineering, the present tunnel of the machine is adequate in length to house all the required modifications: roughly 40 m of free space are available at the end of the present accelerator for the relocation of two 6.1 m accelerating sections and the installation of the second bunch compressor as indicated in the FEL layout. The 3rd harmonic cavity, the first bunch compressor and the new diagnostics will be taken up in the space left free from the two moved sections. Additional space, roughly 15 m, is needed for the klystron gallery to relocate two RF plants.

* Now at TRIUMF, Vancouver, B.C., Canada

EXTENDED PARAMETRIC EVALUATION FOR 1Å FEL – EMITTANCE AND CURRENT REQUIREMENTS

M. Pedrozzi, G. Ingold, PSI, Villigen, Switzerland

Abstract

In the synchrotron radiation community there is a strong request for high-brightness, coherent X-ray light pulses, especially in the 1 to 0.1 nm wavelength range. A Free Electron Laser (FEL), driven by a linear single-pass accelerator, is today the most promising mechanism able to produce such radiation. Since the electron beam brightness plays a major role in the laser saturation process and in the final energy of the driving linac, many laboratories are presently working on a new generation of low emittance sources. The present analysis will give an indication about the FEL behaviour versus the undulator parameters and the slice beam quality (emittance, current, energy spread).

INTRODUCTION

At short wavelength the transversal coherence of the FEL radiation and therefore the gain length can strongly be compromized due to the transversal emittance of the electron beam. As shown by L-H Yu and S. Krinsky [1], with an external focusing the normalized emittance will have a negligible effect on the FEL interaction if :

$$\varepsilon_n << \varepsilon_{nc} = \frac{\beta}{L_g}\frac{\gamma\lambda_s}{2\pi} \qquad (1)$$

where β is the betatron function, γ the Lorenz factor, λ_s the radiation wave length and L_g the gain length.

According to equation (1) the beam energy can be reduced and therefore the facility costs only if the emittance is "sufficiently" small.

The present state of the art electron sources intended for the next generation of light source facilities (LCLS [2] and TESLA-FEL [3]) can provide 1 nC beams with normalized slice emittances close to 1 mm mrad [4]. Recently, the importance of developing high brightness beam sources with emittances at least one order of magnitude smaller than the present status has been emphasized [5], and new gun designs proposed [6,7,8]. A systematic parametric analysis of the FEL interaction with an ultra-bright beam is therefore necessary to achieve a consistent set of specifications for the gun, the LINAC and the undulator.

Model

In this analysis we are using the analytical theory developed by L-H Yu et al. [9] which simultaneously includes the effects of the energy spread, emittance, and focusing of the electron beam, as well as the diffraction and the optical guiding of the radiation field. A Gaussian beam energy distribution, a uniform longitudinal density and a uniform water-bag distribution U(R,R') in the 4-dimensional transverse phase space R=(x,y) and R'=(x',y') are assumed:

$$U(\vec{R},\vec{R}') = \frac{\beta^2 n_0}{\pi R_0^2}\,\Theta\left(\frac{R_0^2}{\beta^2} - \frac{R^2}{\beta^2} - R'^2\right) \qquad (2)$$

where Θ(v)=1 for v>0 and Θ(v)=0 for v<0. The transverse electron density profile is then parabolic:

$$g(\vec{R}) = n_0\left(1 - \frac{R^2}{R_0^2}\right) \quad \text{for } R < R_0 \qquad (3)$$

The gain length is calculated by numerically solving the dispersion relation resulting from the linearized Maxwell-Vlasov equations (see [9] for details).

PARAMETRIC ANALYSIS

Reference Case

As a reference we assume a normalized emittance close to the state of the art ε_n=1.2 10^{-6} mrad, and an energy spread σ_E near 10^{-4}, which is comparable to the energy spread induced by the quantum fluctuation along the undulator [10] for energies near 20 GeV. All our evaluations are made for planar undulators.

Table 1: Reference case parameters

ε_n	1.2 10^{-6}
σ_E	10^{-4} and 2 10^{-4}
Peak	5000 [A]
Beta func. β	31 [m]
Radiation λ	1 Å

The gain lengths at optimum detuning versus the undulator period are shown in Fig. 1, and the corresponding beam energies in Fig. 2.

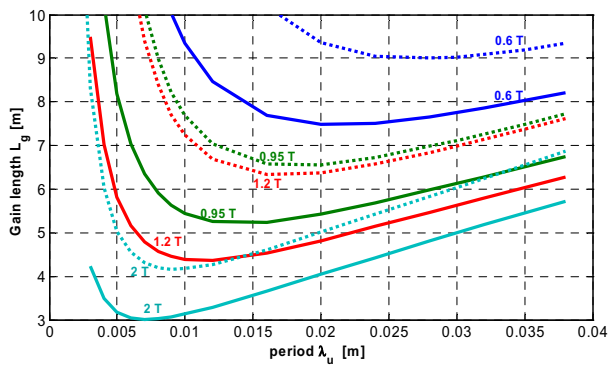

Figure 1: Reference case, gain length vs. undulator period for four peak magnetic fields. Continuous line σ_E =10^{-4}, dotted line σ_E =2 10^{-4}.

A NEW CONTROL SYSTEM FOR THE S-DALINAC[‡]

M. Platz[§], A. Araz, U. Bonnes, M. Brunken, H.-D. Gräf, M. Hertling,
A. Karnaukhov, O. Patalakha, A. Richter, O. Titze, B. Truckses,
Institut für Kernphysik, Technische Universität Darmstadt,
Schlossgartenstrasse 9, 64289 Darmstadt, Germany
W. Ackermann, W. F. O. Müller, B. Steiner, T. Weiland,
Institut Theorie Elektromagnetischer Felder, Technische Universität Darmstadt,
Schlossgartenstrasse 8, 64289 Darmstadt, Germany

Abstract

Recent results with respect to the development of a new control system for the superconducting cw electron accelerator S–DALINAC are presented. The system is based on common industrial standards. Due to the exceptionally large number of devices necessary to control the beam at the S–DALINAC, a simple and inexpensive communication interface is required to replace the current proprietary bus topology. The existing devices will be extended by a microcontroller based CAN-Bus interface as a communication path to one or more control servers. These servers utilize a TCP/IP connection to give application programs (clients) access to the device parameters. The protocol for this communication is composed of a special binary protocol and a text protocol based on XML.

INTRODUCTION

The superconducting recirculating electron accelerator S–DALINAC [1] is designed to deliver a continuous wave (cw) electron beam for nuclear and radiation physics experiments and has commenced operations in 1991. It provides an electron beam with an average current of up to 60 μA at energies of up to 130 MeV. A variety of nuclear physics experiments require the development of a new photoinjector electron gun as well as the increase of energy and intensity of the electron beam. For all experiments a reliable operation of the accelerator based on a modern control system is needed.

The accelerator and its beam transport system shown in fig. 1 consists of about 200 magnets, 80 targets and cameras and several special setups [2], e.g. Faraday cups for beam current measurements, beam position monitors or Compton diodes, to be controlled. The possibility and the demand of controlling additional devices, e.g. new diagnostic elements or parameters of the Helium liquifier, require the development of a new control system which will be realized in three steps.

The human device interface (HDI) used to control the S–DALINAC is a so-called knob board. A knob board is a thumb device emulating an analog tuning of the accelerator. A counter adds up the increments of a rotary encoder and sends the result to a knob server. Button switches are used for digital inputs, e.g. for switching power on/off or toggling between the dial mode for selecting a device from a list, which is defined for a special mode of operation, and the set mode for changing the set value of the selected device. Depending on the mode of operation the server recalculates an internal value, changes the device parameters and displays the result in the LCD elements.

The control system currently used [3] consists of a remote part based on VMS and PSOS including a knob server with an MC68020 processor, giving the possibility of selecting and turning devices, and a VAX 3800 acting as client. As control computers MC68020 microcomputers running under PSOS as operating system (OS) and two AXPvme boards using VxWorks as OS are used. While the MC68020 systems accessing the devices through a local VMEbus, e.g. the HF Control System, the gross of the devices were connected to the AXPvme via a proprietary bus topology. For the communication between the clients and servers, the Linac Control Protocol (LCP) based on Ethernet/DECnet was developed.

Although a reliable operation of the accelerator is possible, this solution has several drawbacks:

- Due to the proprietary bus, an implementation of new types of devices is rather difficult.
- The support for the AXPvme Single Board Computer (SBC) is discontinued.
- The AXPvme board architecture is no longer supported by new versions of VxWorks.
- Therefore, no hardware manufacturer supports the combination of SBC and OS.
- The clients are using VMS as OS.

THE NEW CONTROL SYSTEM

The aim of the new control system is to use a standard transport protocol like TCP/IP instead of the unique LCP used before, which will allow the definition of an application layer protocol independent of operating systems.

[‡] Supported by the Sonderforschungsbereich 634 "Nuclear Structure, Nuclear Astrophysics and Fundamental Experiments at low Momentum Transfer at the Superconducting Darmstadt Electron Accelerator (S–DALINAC)" and by the Graduiertenkolleg 410 "Physics and Technology of Accelerators"

[§] platz@ikp.tu-darmstadt.de

THE PHOTO INJECTOR TEST FACILITY AT DESY ZEUTHEN: RESULTS OF THE FIRST PHASE

A.Oppelt*, K.Abrahamyan, J.Bähr, I.Bohnet, U.Gensch, H.-J.Grabosch,
J.H.Han, M.Krasilnikov, D.Lipka, V.Miltchev, B.Petrosyan, L.Staykov,
F.Stephan, DESY, D-15738 Zeuthen, Germany
M.v.Hartrott, E.Jaeschke, D.Krämer, D.Richter, BESSY, 12487 Berlin, Germany
J.P.Carneiro, K.Flöttmann, S.Schreiber, DESY, D-22603 Hamburg, Germany
P.Michelato, C.Pagani, D.Sertore, INFN Milano, 20090 Segrate, Italy
I.Tsakov, INRNE Sofia, 1784 Sofia, Bulgaria
W.Sandner, I.Will, Max-Born-Institute, D-12489 Berlin, Germany
W.Ackermann, W.F.O.Müller, S.Setzer, T.Weiland, TU Darmstadt, D-64289 Darmstadt, Germany
J.Roßbach, Inst. f. Experimentalphysik, Univ. Hamburg, D-22761 Hamburg, Germany

Abstract

The photo injector test facility at DESY Zeuthen successfully concluded it's first phase of operation in November 2003 (PITZ1). After a complete characterization of the injector, the gun has been transfered to Hamburg and has already been taken into operation on the VUV-FEL.

The measurement program for the year 2003 included RF commissioning, emittance studies, momentum and bunch length measurements, and studies of the influence of the drive laser parameters. We provide an overview on the latest achievements in all of these topics and an outlook on the future plans at PITZ.

INTRODUCTION

The Photo Injector Test Facility at DESY Zeuthen (PITZ) has been built in order to test and optimize electron sources for Free Electron Lasers (FELs) and future linear colliders. The goal of PITZ is to produce intense electron beams with small transverse emittance and short bunch length as required for FEL operation.

The photo injector consists of a 1.5 cell L-band RF gun with a Cs_2Te photo cathode, a solenoid system for space charge compensation, a photo cathode laser system which generates long pulse trains with variable temporal and spatial pulse shape, and an extended diagnostics section. A schematics of the PITZ1 setup is shown in figure 1.

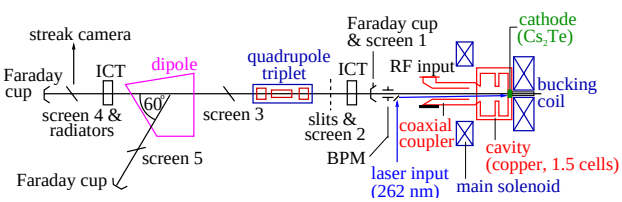

Figure 1: Scheme of the PITZ1 setup.

PITZ has been taken into operation in January 2002. The first stage of the project (PITZ1) has been successfully completed with the transfer of a completely characterized RF gun to the VUV-FEL at DESY Hamburg in November 2003. The results obtained with this gun are briefly summarized in the following section. Meanwhile, a new gun has been installed and conditioned at PITZ. Recent improvements and first measurement results as well as plans for the future of PITZ are reported below.

* corresponding author: anne.oppelt@desy.de

RESULTS OF PITZ1

The measurement program of PITZ1 in the year 2003 included RF commissioning, emittance studies, momentum and bunch length measurements, and studies of the influence of the drive laser parameters.

RF conditioning. The smooth commissioning of the gun allowed an operation with up to 900 μs long RF pulses at 10 Hz repetition rate and about 3.3 MW peak power in the gun. This corresponds to an accelerating gradient at the cathode of about 42 MV/m, and an average power of 27 kW in the gun with 0.9% duty cycle [1]. Such a long RF pulse operation fulfills the TTF2 VUV-FEL requirements.

Photo cathode laser. The optimization of the photo cathode laser parameters included longitudinal and transverse profile. In order to minimize the space charge influence on the transverse beam emittance, a longitudinal flat top profile of 20 ps duration (FWHM) and rise/fall times of 2 ps should be realized. The transverse laser profile is needed to be radially homogeneous, and of adjustable rms size. In reality, these ideal parameters could not yet be reached. Typically, a longitudinal profile of 23 ps FWHM with 6 ps rise/fall time has been used, and a relatively homogeneous transverse profile of size $\sigma_{rms} = 0.5 \ldots 0.6$ mm.

Bunch charge. Detailed studies of the produced electron bunch charge as function of the RF phase and the solenoid settings were performed [1], and comparisons with simulations allowed to improve the understanding of the photo injector. The nominal bunch charge is 1 nC and can be adjusted by tuning the photo cathode laser power.

Momentum and momentum spread. Extensive measurements have been undertaken in order to study longitudinal

PROGRESS REPORT ON THE FLAT BEAM EXPERIMENT AT THE FERMILAB/NICADD PHOTOINJECTOR LABORATORY

Y.-E Sun*, K.-J. Kim, University of Chicago, Chicago, IL 60637, USA
P. Piot†, K. Desler, H. Edwards, M. Hüning,
J. Santucci, J. Wennerberg, FNAL, Batavia, IL 60510, USA
N. Barov, Northern Illinois University, DeKalb, IL 60115, USA
R. Tikhoplav, University of Rochester, Rochester, NY 14627, USA
S. Lidia, LBNL, Berkeley, CA 94720, USA

Abstract

We report on our present progress toward the investigation on the generation of flat beam from an incoming angular momentum-dominated beam. In the present paper we compare our latest experimental results with numerical simulations.

INTRODUCTION

The generation of flat beam from an incoming angular momentum-dominated (magnetized) beam proposed in Reference [1] in the linear collider context has found, since then, other applications, e.g. in the linac-based light source [2]. A proof-of-principle experiment was performed at the Fermilab/NICADD photoinjector laboratory (FNPL) [3] and reported in various papers [4, 5]. In the present paper, we discuss the first results of a second series of experiment dedicated to better understand the production of magnetized beams and the subsequent removal of the longitudinal angular momentum with the round-to-flat beam (RTFB) transformer. The RTFB transformer (see

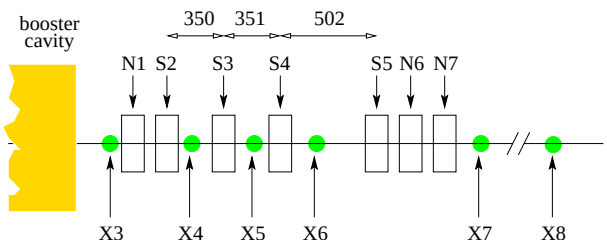

Figure 1: Overview of the RFTB section. The letters N, S and X represents normal and skew quadrupoles, and diagnostic stations. Dimension are in mm.

Fig. 1) consists of four skew quadrupoles located downstream of the booster cavity, at an energy $E \simeq 16$ MeV. Several optical transition radiation (OTR) or scintillating (YaG-based) screens allow the measurement of beam transverse density evolution through the RFTB transformer. The beam transverse emittances can be measured based on the multi-slit, or the quadrupole scan techniques. These emittance diagnostics are available both upstream and downstream of the RFTB section. Compared to the first series

* yinesun@uchicago.edu
† piot@fnal.gov

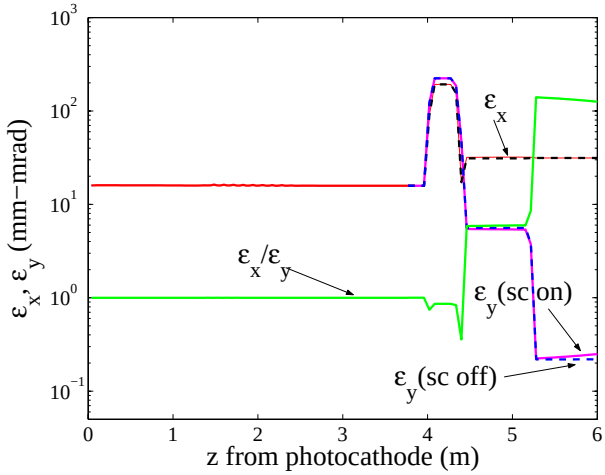

Figure 2: Simulated evolution of transverse emittances along the FNPL beamline for standard nominal settings.

Table 1: Typical settings for the rf-gun, accelerating section, and the photo-cathode drive-laser

parameter	value	units
laser injection phase	25 ± 5	rf-deg
laser radius on cathode	0.6-1.6 ($\pm$ 0.05)	mm
laser pulse duration	4 ($\pm$ 0.5)	ps
bunch charge	0.2-1.6	nC
E_z on cathode	34-35 $\pm$ 0.2	MV/m
B_z on cathode	200-1100	Gauss
booster cavity acc. gradient	~ 12	MV/m

of experiment, our main motivation for reorganizing the RFTB section was to locate all the RFTB section components upstream of the magnetic chicane. Such a relocation was motivated by the potential production of compressed flat beams at a later phase of the flat beam experiment. The typical operating parameters of the photo-injector subsystems during data taking for the flat beam experiment are gathered in Table 1. A series of simulations were performed to study the performance of the RFTB section in term of what transverse emittance ratio could be achieved. An example of evolution of the transverse emittance along the beamline is presented in Fig. 2 for the a magneto-

SIMULATIONS OF THE ION-HOSE INSTABILITY FOR DARHT-II LONG-PULSE EXPERIMENTS

K. C. Dominic Chan, Carl A. Ekdahl Jr., LANL, Los Alamos, NM 87545, USA
Thomas C. Genoni, Thomas P. Hughes, ATK-MRC, NM 87110, USA

Abstract

Computer simulations of the ion-hose effect typically use Particle-In-Cell (PIC) computer codes or codes using the spread-mass model. PIC simulations, though offering more reliable results, require extensive running time on large computers. In order to support commissioning experiments in the DARHT-II induction linac at Los Alamos National Laboratory, we have improved a spread-mass code so that we can survey quickly the parameter space for the experiment. In this paper, we describe the code modifications and the benchmarking against a PIC code, and present results of our simulations for the DARHT-II commissioning experiment.

INTRODUCTION

During Phase-II commissioning of the DARHT (Dual-Axis Radiographic Hydrodynamics Test) Facility [1], beam physics tests (also known as Long-Pulse Experiments, LPE) will focus on the stability of the 2-μs beam pulse against beam-breakup and ion-hose effects. The goal is to demonstrate that beam-breakup and ion-hose instabilities will not cause the DARHT-II beam to become unacceptable for radiographic uses.

The ion-hose instability was studied previously for the DARHT-II induction linac using computer simulations including Particle-In-Cell (PIC) and Spread-Mass (SM) methods [2, 3]. PIC simulations, though offering more reliable results, require extensive running time in large computers. Our goal is to improve a SM simulation code, which has a typical running time of a few minutes, so that it can be used to give fast and reasonably reliable guidance during commissioning.

In this paper, we will describe modifications to the SM code. Numerical results obtained using the improved SM model are compared to PIC simulations to assess the accuracy of the SM simulations. Then we will describe SM simulation results for LPE of Phase-II commissioning.

IMPROVED SPREAD-MASS SIMULATION CODE

Previously, SM simulations for DARHT assumed beam and accelerator parameters that were uniform along the length of the accelerator. These parameters include the solenoidal magnetic field, beam energy, and beam radius. To improve the SM simulations, we modified the SM code to include these parameters as a function of longitudinal distance along the accelerator (z). We also included the effect of the radial magnetic field due to the varying longitudinal magnetic field. This latter effect will introduce a rotation of the beam centroid around the accelerator axis.

Our SM code was based on the SM code written by Genoni with uniform accelerator parameters. Our development and solution of the equations follows closely that by Genoni in Ref. [2], which in turn was a generalization of the original ion-hose SM formulation by Buchanan in Ref [4]. Since details of Genoni's work can be found in Ref. [2], we will highlight here only the new modifications.

Equation (1) in Ref. [2], which considers only the linear ion-hose force, was modified by adding the effect of the radial magnetic field by including a third term on the left-hand side of the equation, i.e.

$$\frac{\partial^2 b}{\partial z^2} = -k_{\beta e}^2 (b-d) + ik_{ce}\frac{\partial b}{\partial z} - ik_{ce}\left(\frac{B_r}{rB_z}\right)b \qquad (1)$$

where b and d, respectively, are the beam and ion-channel centroid-displacements from the axis. In the third term, B_r and B_z are the radial and longitudinal components of the solenoidal magnetic fields and r is the radial position of the beam. Equation (2) in Ref. [2] remains unchanged, i.e.

$$\frac{\partial^2 d}{\partial \tau^2} = -\omega_{\beta i}^2 (d-b) - i\omega_{ci}\frac{\partial d}{\partial \tau} \qquad (2)$$

In equations (1) and (2), $k_{\beta e}^2$ and $\omega_{\beta i}^2$ are given as:

$$k_{\beta e}^2 = \frac{f\nu}{\gamma R^2} \quad and \quad \omega_{\beta i}^2 = \frac{m_e \nu c^2}{m_i R^2}$$

where m_e and m_i are the electron and ion masses, γ is the electron relativistic factor, $\nu = {eI_b}/{m_e c^3}$, $\tau = t - {z}/{c}$, I_b is the beam current and f is the fractional neutralization. k_{ce} and ω_{ci} are defined as:

$$k_{ce} = \frac{eB_z}{\gamma m_e c^2} \quad and \quad \omega_{ci} = \frac{eB_z}{m_i c}$$

Equations (1) and (2) were further transformed by adding the SM formulation and nonlinearity as in Ref. [2], arriving at equations similar to equations (27) and (28) in Ref. [2]. These equations were then solved numerically with the solenoidal magnetic field, beam energy, and beam radius as functions of z.

BENCHMARKING OF SM SIMULATIONS

We benchmarked our SM code against results obtained using LSP, a 3-D PIC code from ATK-MRC [5]. Four

CUMULATIVE BEAM BREAKUP WITH TIME-DEPENDENT PARAMETERS*

J. R. Delayen#, Thomas Jefferson National Accelerator Facility, Newport News, VA 23606, USA

Abstract

A general analytical formalism developed recently for cumulative beam breakup (BBU) in linear accelerators with arbitrary beam current profile and misalignments [1, 2] is extended to include time-dependent parameters, such as energy chirp or rf focusing, in order to reduce BBU-induced instabilities and emittance growth. Analytical results are presented and applied to practical accelerator configurations.

FORMULATION AND SOLUTION

In a continuum approximation, the transverse motion of a relativistic beam under the influence of focusing and BBU can be modeled by [1]

$$\left[\frac{1}{\gamma}\frac{\partial}{\partial\sigma}\left(\gamma\frac{\partial}{\partial\sigma}\right)+\kappa^2\right]x(\sigma,\zeta) = \varepsilon\int_0^{\zeta} d\zeta_1\, w(\zeta-\zeta_1)F(\zeta_1)x(\sigma,\zeta_1) \tag{1}$$

where γ is the usual energy parameter; $\sigma = s/\mathbf{L}$, is the distance from the front of the accelerator normalized to the accelerator length; κ is the normalized focusing wave number; $\zeta = \omega\left(t-\int ds/\beta c\right)$, is the time made dimensionless by the frequency ω and measured after the arrival of the head of the beam at location σ; $F(\zeta) = I(\zeta)/\bar{I}$, the current form factor, is the instantaneous current divided by the average current; $w(\zeta)$ is the wake function, which, in the case of a single dipole mode, is assumed to be $w(\zeta) = u(\zeta)\,\sin\zeta\, e^{-\zeta/2Q}$; ε is the coupling strength between the beam and the dipole mode, and includes properties of the beam and the deflecting mode of the accelerating structure.

While Eq. (1) assumes a perfectly aligned accelerator, misalignment of the cavities and focusing elements can also be included in the following analysis in a straightforward fashion.

Without loss of generality, we will assume a coasting beam. As shown in [1], the analytical results can be extended to an accelerated beam by suitable coordinate and variable transformations. Under these assumptions, the equation of motion becomes

$$\frac{\partial^2}{\partial\sigma^2}x(\sigma,\zeta)+\kappa^2 x(\sigma,\zeta) = \varepsilon\int_0^{\zeta} d\zeta_1\, w(\zeta-\zeta_1)\,F(\zeta_1)\,x(\sigma,\zeta_1). \tag{2}$$

* Work supported by the U.S. Department of Energy under contracts No. DE-AC05-84-ER40150 and DE-AC05-00-OR22725

#delayen@jlab.org

In the following we will make the additional assumption that the injection offsets (lateral displacement and angular divergence) are time-independent. Again, time-dependent injection parameters can be included in the following formalism.

Time-independent Parameters

In [1], Equation (2) was solved under the assumption of constant, time-independent BBU coupling and focusing strengths (ε and κ). Applying to Eq. (2) the Laplace transform with respect to σ: $\mathcal{L}\left[x(\sigma,\zeta)\right] = x^{\dagger}(p,\zeta)$, we obtain

$$x^{\dagger}(p,\zeta) = \sum_{n=0}^{\infty}\frac{\varepsilon^n}{\left(p^2+\kappa^2\right)^{n+1}}\left[\,x_0\,p+x_0'\,\right]f_n(\zeta), \tag{3}$$

with

$$f_{n+1}(\zeta) = \int_0^{\zeta} f_n(\zeta_1)\,w(\zeta-\zeta_1)\,F(\zeta_1)\,d\zeta_1, \qquad f_0(\zeta) = 1. \tag{4}$$

Applying the inverse Laplace transform gives

$$x(\sigma,\zeta) = \sum_{n=0}^{\infty}\varepsilon^n\left[x_0 j_n(\kappa,\sigma)+x_0' i_n(\kappa,\sigma)\right]f_n(\zeta) \quad , \tag{5}$$

where

$$i_n(\kappa,\sigma) = \frac{1}{n!}\left(\frac{\sigma}{2\kappa}\right)^n\frac{1}{\kappa}\sqrt{\frac{\pi\kappa\sigma}{2}}J_{n+\frac{1}{2}}(\kappa\sigma)\ ,$$
$$j_n(\kappa,\sigma) = \frac{1}{n!}\left(\frac{\sigma}{2\kappa}\right)^n\sqrt{\frac{\pi\kappa\sigma}{2}}J_{n-\frac{1}{2}}(\kappa\sigma)\ . \tag{6}$$

Time-dependent Parameters

When the BBU coupling and focusing strengths are time-dependent [$\varepsilon(\zeta)$ and $\kappa(\zeta)$] the beam displacement $x(\sigma,\zeta)$ is not given by Eqs. (3)-(6) anymore and the procedure for solving Eq. (2) needs to be modified. This can be done simply by splitting the focusing strength $\kappa(\zeta)$ in two parts, one constant and the other time-dependent, such that:

$$\kappa^2(\zeta) = \kappa_0^2\left[1+\Delta\kappa(\zeta)\right] \tag{7}$$

The displacement $x(\sigma,\zeta)$ and its Laplace transform $x^{\dagger}(p,\zeta)$ are then given by

$$x^{\dagger}(p,\zeta) = \sum_{n=0}^{\infty}\frac{\left[\,x_0\,p+x_0'\,\right]}{\left(p^2+\kappa_0^2\right)^{n+1}}f_n^*(\zeta) \quad , \tag{8}$$

$$x(\sigma,\zeta) = \sum_{n=0}^{\infty}\left[x_0 j_n(\kappa_0,\sigma)+x_0' i_n(\kappa_0,\sigma)\right]f_n^*(\zeta), \tag{9}$$

METHODS FOR MEASURING AND CONTROLLING BEAM BREAKUP IN HIGH CURRENT ERLS*

C. Tennant#, K. Jordan, E. Pozdeyev, R. Rimmer, H. Wang, TJNAF, Newport News, VA, 23606
S. Simrock, DESY, Hamburg, Germany

Abstract

It is well known that high current Energy Recovery Linacs (ERL) utilizing superconducting cavities are susceptible to a regenerative type of beam breakup (BBU). The BBU instability is caused by the high impedance transverse deflecting higher-order modes (HOMs) of the cavities. This multipass, multibunch instability has been observed at Jefferson Laboratory's FEL Upgrade driver. Some preliminary measurements are presented. To combat the harmful effects of a particularly dangerous mode, two methods of directly damping HOMs through the cavity HOM couplers were demonstrated. In an effort to suppress the BBU in the presence of multiple, dangerous HOMs, a conceptual design for an injector beam-based transverse feedback system has been developed. By implementing beam-based feedback, the threshold for instability can be increased substantially.

INTRODUCTION

The BBU measurement and suppression techniques described in this paper have application to any ERL based machine. However, for simplicity we will restrict ourselves to Jefferson Lab's Free-Electron Laser (FEL) Upgrade. The driver is an energy-recovery based linear accelerator used to condition an electron beam for high power lasing [1]. Electrons are injected at 10 MeV and are accelerated to 145 MeV through three cryomodules (each containing 8 superconducting niobium cavities). The beam is transported to a wiggler where up to 10 kW of laser power is generated. The spent electron beam is recirculated and phased in such a way that the beam is decelerated through the linac region on the second pass. Upon exiting the linac, the 10 MeV beam is extracted to a dump.

MULTIPASS, MULTIBUNCH BBU

At sufficiently high average beam current, ERLs are susceptible to a regenerative type of beam breakup (BBU). The BBU instability is caused by the high impedance transverse deflecting higher-order modes (HOMs) of the cavities. The underlying mechanism is that with insufficient damping of cavity HOMs, a positive feedback loop will be created between the cavity and the recirculated beam. This feedback can create an energy exchange between the cavity fields and beam which can lead to exponential growth of the beam offset. For a single cavity, containing one HOM oriented at an angle α with respect to the horizontal axis and with a single recirculation, the expression for the threshold current of the instability is given by

$$I_{th} = -\frac{2V_b}{k(R/Q)Q\,M_{12}^{*}\sin(\omega T_r)}$$

$$M_{12}^{*} \equiv M_{12}\cos^2\alpha + (M_{14}+M_{32})\sin\alpha\cos\alpha + M_{34}\sin^2\alpha$$

where V_b is the beam voltage at the cavity, k is the wavenumber of the mode, $(R/Q)Q$ is the shunt impedance of the HOM, T_r is the recirculation time and the M_{ij} are the elements of the recirculation transport matrix (which can describe coupled transverse motion) [2]. The purpose of this paper is to present methods of increasing the threshold current by using feedback methods to effectively modify the shunt impedance of the HOM or the M_{12}^{*} term. Other means of suppressing the onset of BBU by a judicious choice of beam optics are given elsewhere [3] [4].

BBU MEASUREMENTS

On May 27, 2004 the multipass, multibunch beam breakup instability was observed at 3 mA of average beam current at the FEL for the first time. Using Schottky diodes on each of the two HOM ports per cavity (8 cavities x 2 ports = 16 diodes total) we were able to monitor the total HOM power levels from each cavity in the second cryomodule – which, for these operating conditions, exhibits insufficient HOM damping. At the onset of the instability we saw the HOM power levels in cavity 4 grow exponentially until the beam losses tripped off the machine (see Figure 1).

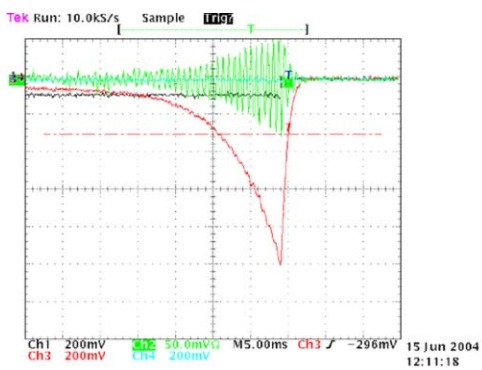

Figure 1: An oscilloscope trace from a BBU induced machine trip. The green trace is the cavity HOM voltage and the red trace is the total HOM power as measured from the Schottky diode. The time scale is 5 msec/div.

Repeated BBU-induced trips continued to be caused by cavity 4, leaving no doubt that the mode causing the instability was located in this cavity. Having successfully located the offending HOM, the next step was to extract

*supported by US DOE Contract No. DE-AC05-84ER40150
#tennant@jlab.org

TEMPORAL PROFILE OF THE LCLS PHOTOCATHODE ULTRAVIOLET DRIVE LASER TOLERATED BY THE MICROBUNCHING INSTABILITY*

Juhao Wu†, P. Emma, Z. Huang, C. Limborg, SLAC, Menlo Park, CA 94025, USA
M. Borland, APS, ANL, Argonne, IL 60439, USA

Abstract

The LCLS electron beam generated in the photoinjector is subject to various instabilities in the downstream acceleration and compression. The instability can be initiated by e-beam density modulation at birth. In this paper, we prescribe the tolerance on the initial e-beam density modulation possibly introduced by the ultraviolet (uv) laser at the cathode. Our study shows that the initial rms density modulation of the e-beam at the photocathode shall be less than 5 % to ensure the FEL lasing and saturation.

Introduction

The success of FEL calls for a high quality e-beam, which is, however, subject to various impedance in the downstream acceleration and compression after being generated from a photocathode. Specifically, the impedance (space charge, wakefield, and CSR) and momentum compaction factor act as an amplifier for initial density and energy modulations. Since the slice emittance and energy spread are extremely small, Landau damping is not effective in suppressing instabilities, which can increase the slice energy spread and emittance, and therefore degrade FEL lasing. FEL operation calls for best achievable beam quality; yet, unnecessarily high quality renders it more susceptible to instabilities described above. To address this quandary, a laser-heater [1] is introduced into the LCLS beamline. The laser-heater is designed to be an adjustable control, which will impose a limited increase on the slice energy spread to the level where FEL lasing is still guaranteed. This 'procured' increase is designed to enhance Landau damping such that downstream instabilities can be suppressed. Density and energy modulations can be initiated by shot noise in the e-beam born at the photocathode. Also, temporal modulation on the ultraviolet (uv) laser pulse itself can be transferred to the e-beam at birth. These initial e-beam density or energy modulations can be amplified to affect the FEL lasing. Hence, we study the tolerance of the e-beam density modulations at birth.

Simulation details and results

In our study, we take the nominal LCLS accelerator system setup including the laser-heater, with parameters in Table 1. The laser-heater is to be installed where the e-beam $E = 135$ MeV. Parameters for the laser-heater are in Table 2. We use a total temporal compression factor of 30. Hence, if we require the rms slice relative energy spread $\sigma_\delta \approx 1 \times 10^{-4}$ at $E = 14.1$ GeV, then the laser-heater should give a maximum rms slice energy spread $\sigma_E \approx 47$ keV, assuming the conservation of the longitudinal phase space area. This slice σ_E then determines the Landau damping strength to suppress instabilities. The laser-heater introduces energy modulation at wavelength of 800 nm; however, the chicane provides an R_{52} large enough, so that the laser-heater induced energy modulation is washed out by the second half of the chicane. Hence, the laser-heater induced energy modulation becomes purely slice energy spread; and will not be converted into density modulation.

In our study, we take two approaches. In the first one, we introduce a density modulation at the injector end ($E = 135$ MeV). In the second one, we introduce a density modulation in the e-beam at birth. Details are the follows.

Approach I: we take a PARMELA output distribution at

Table 1: Main parameters for the LCLS FEL.

Parameter	Symbol	Value
electron energy	γmc^2	14.1 GeV
bunch charge	Q	1 nC
bunch current	I_f	3.4 kA
transverse norm. emittance	$\varepsilon^n_{x,y}$	1 μm
average beta function	$\beta_{x,y}$	25 m
undulator period	λ_u	0.03 m
undulator field	B	1.3 T
undulator parameter	K	3.64
undulator length	L_u	130 m
FEL wavelength	λ_r	1.5 Å
FEL parameter	ρ	4.8×10^{-4}

Table 2: Main parameters for the LCLS laser-heater.

Parameter	Symbol	Value
electron energy	$\gamma_0 mc^2$	135 MeV
average beta function	$\beta_{x,y}$	10 m
transverse rms beam size	$\sigma_{x,y}$	190 μm
undulator period	λ_u	0.05 m
undulator field	B	0.33 T
undulator parameter	K	1.56
undulator length	L_u	0.5 m
laser wavelength	λ_L	800 nm
laser rms spot size	σ_r	175 μm
laser peak power	P_L	1.2 MW
Rayleigh range	Z_R	0.6 m
maximum energy modulation	$\Delta\gamma_L(0)mc^2$	80 keV
rms local energy spread	$\sigma_{\gamma_L}mc^2$	40 keV

* Work supported by the U.S. Department of Energy under Contract No. DE-AC03-76SF00515, and No. W-31-109-ENG-38.

† jhwu@SLAC.Stanford.EDU

RESISTIVE-WALL WAKE EFFECT IN THE BEAM DELIVERY SYSTEM*

J.R. Delayen, Thomas Jefferson National Accelerator Facility, Newport News, VA 23606, USA
Juhao Wu†, T.O. Raubenheimer, SLAC, Menlo Park, CA 94025, USA
Jiunn-Ming Wang, NSLS, BNL, Upton, NY 11973, USA

Abstract

General formulae for resistive-wall induced beam dilution are presented and then applied to the final beam delivery system of linear colliders. Criteria for the design of final beam delivery systems are discussed.

Equation and Solution

Recently, the beam breakup (BBU) problem due to the resistive-wall impedance was studied for uniform single bunch and also point-like bunch train [1, 2]. However for linear collider, the beam at the interaction point normally has some microstructure. This is evidenced by start-to-end simulation. Hence, in this paper, we study the resistive wall BBU problem for the case of arbitrary beam current profile.

We denote the location along the beamline by the variable s. The beam travels in the positive s direction, and the entrance to the beamline is located at $s = 0$. We assume in this paper that the accelerator is uniform and that there is no acceleration. This is not unduly restrictive [3]. In a continuum approximation, the transverse motion $y(\tau, s)$ of a beam in a misaligned beamline under the combined influence of focusing and wake field can be modelled by [4]

$$\frac{\partial^2 y(\sigma,\zeta)}{\partial\sigma^2} + \kappa^2\left[y(\sigma,\zeta) - d_f(\sigma)\right] = \varepsilon\int_0^\zeta w(\zeta-\zeta_1)F(\zeta_1)\left[y(\sigma,\zeta_1) - d_c(\sigma)\right]d\zeta_1\,, \quad (1)$$

where $\sigma = s/\mathcal{L}$, with $\mathcal{L}$ being the length of the element where wakefield is generated; $\zeta = \omega_0\,\tau$, with ω_0 being a reference angular frequency, and $\tau = t - s/v$ describes the relative longitudinal position of the particle inside the bunch, v is the particle velocity; $\kappa = k_y\,\mathcal{L}$, is the betatron phase advance with k_y being the betatron focusing strength; $F(\zeta) = I(\zeta)/\bar{I}$, the current form factor, is the instantaneous current $I(\zeta)$ divided by the average current $\bar{I}$; $d_f(\sigma)$ and $d_c(\sigma)$ are the lateral displacement of the focusing elements and element where the wakefield is generated. The right hand side of Eq. (1) represents the effects due to the wakefield $\mathcal{W}(\tau)$, which is introduced via

$$(\mathcal{L}^2/\omega_0)\,\mathcal{W}(\tau) = \varepsilon\,w(\zeta)\,. \quad (2)$$

The exact meaning of ε and ω_0 will be made clear in the following. The general solution of Eq. (1) is [3]

$$y(\sigma,\zeta) = \sum_{n=0}^{\infty}\varepsilon^n[y_0\,h_n(\zeta)\,j_n(\kappa,\sigma) + y_0'\,g_n(\zeta)\;i_n(\kappa,\sigma)\,] - \sum_{n=0}^{\infty}\varepsilon^{n+1}f_{n+1}(\zeta)\,i_n(\kappa,\sigma) * d_c(\sigma) + \kappa^2\sum_{n=0}^{\infty}\varepsilon^n f_n(\zeta)\,i_n(\kappa,\sigma) * d_f(\sigma) \quad (3)$$

where $i_n(\kappa,\sigma) * d(\sigma) = \int_0^\sigma du\, i_n(\kappa,u)\,d(\sigma-u)$. Via inverse Laplace transform, $i_n(\kappa,\sigma)$ and $j_n(\kappa,\sigma)$ are

$$\begin{aligned} i_n(\kappa,\sigma) &= \mathbf{L}_\sigma^{-1}\left[\frac{1}{(p^2+\kappa^2)^{n+1}}\right] \\ &= \frac{1}{n!}\left(\frac{\sigma}{2\kappa}\right)^n\frac{1}{\kappa}\sqrt{\frac{\pi\kappa\sigma}{2}}J_{n+(1/2)}(\kappa\sigma)\,, \quad (4)\\ j_n(\kappa,\sigma) &= \mathbf{L}_\sigma^{-1}\left[\frac{p}{(p^2+\kappa^2)^{n+1}}\right] \\ &= \frac{d}{d\sigma}i_n(\kappa,\sigma) = \frac{\sigma}{2n}i_{n-1}(\kappa,\sigma) \\ &= \frac{1}{n!}\left(\frac{\sigma}{2\kappa}\right)^n\sqrt{\frac{\pi\kappa\sigma}{2}}J_{n-(1/2)}(\kappa\sigma)\,. \quad (5)\end{aligned}$$

In the absence of focusing $i_n(\kappa,\sigma)$ and $j_n(\kappa,\sigma)$ reduce to $i_n(0,\sigma) = \sigma^{2n+1}/(2n+1)!$, and $j_n(0,\sigma) = \sigma^{2n}/(2n)!$.

The functions $f_n(\zeta)$, $g_n(\zeta)$, and $h_n(\zeta)$ are defined as

$$\begin{Bmatrix} f_{n+1}(\zeta)\\ g_{n+1}(\zeta)\\ h_{n+1}(\zeta)\end{Bmatrix} = \int_{-\infty}^{\zeta}\begin{Bmatrix} f_n(\zeta_1)\\ g_n(\zeta_1)\\ h_n(\zeta_1)\end{Bmatrix} w(\zeta-\zeta_1)\,F(\zeta_1)\,d\zeta_1\,, \quad (6)$$

where

$$f_0(\zeta) = 1\,, \quad (7)$$

$$y_0'\,g_0(\zeta) = y_0'(\zeta) = \frac{\partial}{\partial\sigma}y(\sigma,\zeta)\Big|_{\sigma=0}\,, \quad (8)$$

$$y_0\,h_0(\zeta) = y_0(\zeta) = y(\sigma=0,\zeta)\,. \quad (9)$$

Resistive-Wall Wake

If the wakefield source is the resistive-wall of a circularly cylindrical pipe, then the long-range wakefield is [5]

$$\mathcal{W}(\tau) = \frac{A}{\sqrt{\tau}} \quad \text{for} \quad \tau > 0\,, \quad (10)$$

where

$$A = (4c^2\bar{I})/(v\gamma b^3 I_{\text{Alfvèn}})\sqrt{\epsilon_0/\pi\sigma_c}\,. \quad (11)$$

In the above expression, c is the speed of light in vacuum, γ is the Lorentz factor, b is the radius of the pipe, $I_{\text{Alfvèn}} = 4\pi\epsilon_0 mc^3/e \approx 17,045$ Amp is the Alfvèn current, $\epsilon_0 =$

* Work supported by US Department of Energy under contract No. DE-AC05-84-ER40150 (JRD), No. DE-AC05-00-OR22725 (JRD), No. DE-AC03-76SF00515 (JW&TOR), and No. DE-AC02-98CH10886(JMW).

† jhwu@SLAC.Stanford.EDU

SIMULATION OF RF BREAKDOWN EFFECTS ON NLC BEAM *

V.A. Dolgashev, T. Raubenheimer,
SLAC, Menlo Park, CA, 94025, USA

Abstract

The linacs of the Next Linear Collider (NLC) / Global Linear Collider (GLC) will contain several thousand traveling wave X-band accelerator structures operating at aninput power of about 60 MW. At this input power, prototypes of NLC/GLC structures have breakdown rates lower than one breakdown in ten hours. RF breakdowns disrupt flow of energy inside the structure and create arcs with electron and ion currents. Electromagnetic fields of these currents interact with the NLC beam. We simulated the deflection of the NLC beam caused by breakdown currents using the particle-in-cell code MAGIC. In this paper we present modeling considerations and simulation results.

INTRODUCTION

In the NLC/GLC, electron and positron multibunch beams traverse thousands of traveling wave accelerating structures. Each beam consists of 190 bunches spaced at 1.4 ns. Each 60 cm X-band accelerating structure is driven by about 60 MW of rf power and produces a 65 MV/m unloaded gradient. To fill the structure and accelerate the beam the effective rf pulse length is set to about 400 ns.

RF breakdown in a structure disrupts its operation. Because of that, the NLC has a stringent limit on the breakdown rate: it should be less than one breakdown per few million pulses. With this breakdown rate one breakdown will occur in the linac every few seconds. The structures operate below threshold for breakdown damage, so the rf power does not have to be switched off after the breakdown. Therefore only the beam that is in the linac during the breakdown get distorted. In this report we will discuss the effect of breakdown currents on the NLC beams.

RF Breakdown

RF breakdown is a phenomenon that abruptly and significantly changes transmission and reflection of rf power directed to the structure. Breakdown is accompanied by a burst of x-rays and by a bright flash of visible light. There is copious experimental data on rf breakdowns in the NLC/GLC structures obtained at the Next Linear Collider Test Accelerator (NLCTA) [1, 2]. Listed here are some properties of the rf breakdown phenomenon in the structures [3]:

1. During breakdown the transmitted power drops to unmeasurable levels in 20–200 ns. During the rf pulse the transmission never recovers.
2. Up to 80% of the incident rf power is absorbed by the arc.
3. At the NLCTA the beam current is measured using low-Q cavities located a few centimeters away from the output end of the structure. These current monitors detect a short (order of 10 ns) burst of current concurrent with the first signs of breakdown in rf signals. Typically the sinal from the monitors corresponds to amps of current averaged over an rf pulse.

Breakdown Currents

Knowing that the instantaneous rf power absorbed by the arc reaches 80%, and assuming that this power is absorbed by the electrons, we can estimate the amplitude of the current. The average electron energy for current emitted from a spot on the cell iris tip is about 100 keV (as calculated by a particle tracking code), and the incident rf power is about 100 MW. To absorb this power, the amplitude of the electron current should be about 1 kA. This kA current will interact with the primary electron (or positron) bunches being accelerated in the structure, kick the bunch centroid (assuming that currents are not axially symmetric) and perhaps dilute the beam emittance.

Below, we report results of simulation of the breakdown kick on the centroid of the primary bunch in NLC/GLC structures. We used the commercially available Particle-In-Cell (PIC) code MAGIC3D [4] for the calculations.

PARTICLE-IN-CELL SIMULATIONS

To obtain the beam kick from rf breakdown we have built a 3D PIC model of a 3 cell travelling wave structure. It is a disk loaded waveguide with 120° phase advance per cell, cavity radius of 10.875 mm, period of 8.75 mm, iris radius 4.45 mm, and iris thickness 1.66 mm (the iris tip is rounded). This model was developed for 3D self-consistent simulations of breakdown currents [3]. The geometry is built in cylindrical coordinates with z = constant being the (x, y) plane. The model consists of one cell and two coupler cells that match the impedance of a coaxial waveguide to the impedance of the structure at a frequency of 11.424 GHz (with VSWR better than 1.2). Snapshots of the MAGIC3D screen with the geometry are shown in Fig.1.

To simulate the breakdown, the tip of an iris was divided into upstream and downstream parts. Then one half-tip sector was assigned to emit copper ions using EMISSION BEAM model with current 20 A. The same area is also assigned as a source of space-charge limited electron current. For that we used EMISSION EXPLOSIVE model. EMISSION BEAM and EMISSION EXPLOSIVE are keywords

* This work was supported by the U.S. Department of Energy contract DE-AC02-76SF00515.

ALTERNATIVE LINAC LAYOUT FOR EUROPEAN XFEL PROJECT

Yujong Kim*, K. Flöttmann, and T. Limberg, DESY, D-22603 Hamburg, Germany
Dongchul Son and Y. Kim, The Center for High Energy Physics, Daegu 702-701, Korea

Abstract

To control the microbunching instability at the European XFEL linac, we had optimized one linac layout with a double chicane. However, to relax jitter tolerance further, and to clean ignorable space charge force effects at the second bunch compressor, we have newly designed an alternative linac layout with two bunch compressor stages for the European XFEL project. In this paper, we describe design concepts, Start-to-End (S2E) simulations, and operational flexibility of our alternative linac layout for the European XFEL project.

INTRODUCTION

To supply coherent, ultra-fast, and ultra-bright SASE sources in hard X-ray region, DESY has a plan to construct the largest SASE FEL facility in the world, European XFEL [1]. Its main required parameters are summarized in Table 1. Recently, to control the microbunching instability at bunch compressors for the European XFEL project, we had optimized one linac layout (13JAN04 version) as shown in Fig. 1(top). Here only one bunch compressor (BC) stage with a double chicane is used to obtain a large slice energy spread before the second bunch compressor (BC2) [2], [3]. However it was reported that the jitter tolerance of an FEL driving linac with one BC stage is tighter than that of the other case with two BC stages [4]. Therefore we had investigated the impact of jitters on FEL performances for our current linac layout (13JAN04 version) [3]. According to our recent S2E simulations, rms bunch length, bunch arriving time, and saturation power of SASE source have somewhat large variations under jitters [3]. Since our current linac layout does not have any accelerating module between BCs, space charge force may be increased if bunch length is highly compressed at BC2. Therefore, to avoid any beam quality dilution due to space charge force, we put the double chicane at a somewhat higher beam energy of 510 MeV. According to our CSRtrack simulation considering CSR and space charge force in BCs, the beam quality dilution due to space charge force is ignorable at 510 MeV [3]. By the help of well-damped CSR effects and microbunching instability, all projected and slice beam parameters of our current linac layout are much better than our requirements for the European XFEL project [3]. However, to relax jitter tolerance further, and to clean ignorable space charge force effects at the BC2, we have newly optimized an alternative linac layout (10AUG04 version) with two BC stages for the European XFEL project. In this paper, we describe design concepts, S2E simulations, and operational flexibility of our alternative linac layout for the European XFEL project.

Table 1: Main parameters for XFEL project

Parameter	Unit	Value
beam energy E	GeV	20
single bunch charge Q	nC	1
slice normalized rms emittance ϵ_{ns}	μm	1.4
slice rms relative energy spread $\sigma_{\delta s}$	10^{-4}	1.25
peak current I_{pk}	A	5
maximum bunch train length	μs	650
bunch train repetition rate	Hz	10
minimum bunch spacing in a train	μs	0.2
wavelength of SASE source	nm	0.08-6.4
saturation length of SASE source	m	95-170
total undulator length	m	140.3-250.1

ALTERNATIVE LINAC LAYOUT

Generally, the minimum slice emittance is limited by thermal emittance, which is proportional to beamsize on the cathode [4], [5]. After considering two facts that decelerating electric field at the cathode due to space charge force is inversely proportional to the square of rms beamsize at the cathode, and the available maximum gradient of the L-band RF gun is around 60 MV/m at the cathode, we have reduced the rms beamsize on the cathode from 0.75 mm to 0.70 mm to reduce thermal emittance. Recently, by the help of a flat-top laser profile with about 21 ps (FWHM) length and about 7 ps rising and falling time, TTF2 gun (originally PITZ1 gun) had generated high quality electron beams with a projected normalized rms emittance of about 1.7 μm without any booster linac [6]. Therefore we expect that our XFEL injector can supply much higher quality electron beams by increasing the maximum gradient of gun, by improving uniformity of gun driving laser, by reducing rising and falling time of gun driving laser, and by accelerating beams quickly with a booster linac. According to our new ASTRA optimizations, XFEL injector can supply higher quality electron beams with a projected normalized rms emittance of around 0.88 μm by upgrading TTF2 gun. Detail injector re-optimizations for the European XFEL project are described in reference [7], and its optimized results are summarized in Table 2.

Basic bunch compressor design concepts are well described in reference [8], which is related with the SCSS bunch compressor, and detail bunch compressor design concepts of our current linac layout are described in ref-

* E-Mail : Yujong.Kim@DESY.de, URL : http://TESLA.DESY.de

EXTRACTION OF HIGH CHARGE ELECTRON BUNCH FROM THE ELSA RF INJECTOR – COMPARISON BETWEEN SIMULATION AND EXPERIMENT

N. Pichoff, P. Balleyguier, A. Binet, R. Bailly-Salins, J.-M. Lagniel, V. Le Flanchec, J-L Lemaire, M. Millerioux, C. Quine
CEA/DAM, Bruyères-le-Châtel, France

Abstract

A new scheme based on a photo-injector and an RF linear accelerator operating at 352 MHz has been recently proposed as a versatile radiographic facility. Beam pulses of 60 ns duration containing 20 successive electron bunches that are extracted at 2.5 MeV from a photo-injector are accelerated through the next structure to the final energy of 51 MeV. Bunches carrying 100 nC are required for this purpose. As a first demonstrating step, mora than 50 nC electron bunches have been produced and accelerated to 2.5 MeV with the 144 MHz ELSA photo-injector at Bruyères le Châtel. For this experiment, we compare the results and the numerical simulations made with PARMELA, MAGIC and MAFIA codes.

INTRODUCTION

A proposal for the project named RX2 has been made in view of producing high-flux of short X-ray pulses from a very intense 50 MeV electron beam impinging a high Z material production target. The facility consists of a photo-injector followed by a linear accelerating structure. The beam is finally tightly focused to the target. The 60-ns electron pulse is made of 20 bunches repeated at 352 MHz. Each bunch of 100 ps duration is issued from the photo-injector and carries a 100 nC charge. Several simulation codes have been used to design the photo-injector: PARMELA [1], MAGIC [2], MAFIA [3] and M2V [4].

The space-charge limit is the maximum amount of charge that can be extracted from a gun (at fixed beam size and time duration). This limitation happens when the field induced by the extracted charges (space-charge field) cancels out the gun acceleration field on the cathode. In a stationary 1D model, this is known as the Child-Langmuir current density limit. In the RX2 gun, this limit calculated with the codes [1], [2], [3], [4] is about 600 nC within 20% dispersion from code to code (figure 1). According to these simulations, the RX2 gun 100 nC working point is much lower than the space-charge limit.

To ensure that one can rely on the space-charge limit predicted by the codes, we decided to validate these codes against experimental measurements. In this paper, we present the space charge-limit measured on the ELSA RF photo-injector [5] and we compare it to the code results.

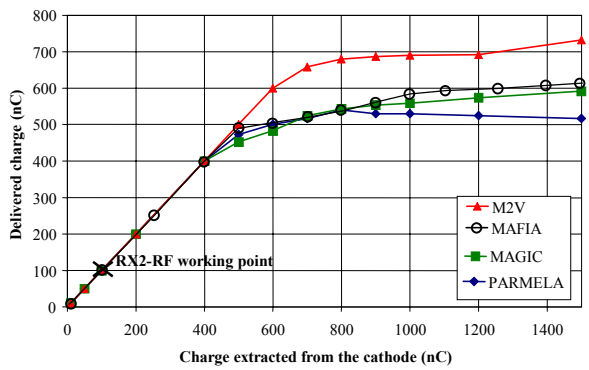

Figure 1: Prediction by four codes for the delivered charge as a function of the expected charge produced from the photo-electric effect. RX2 working point is well below the space charge limit.

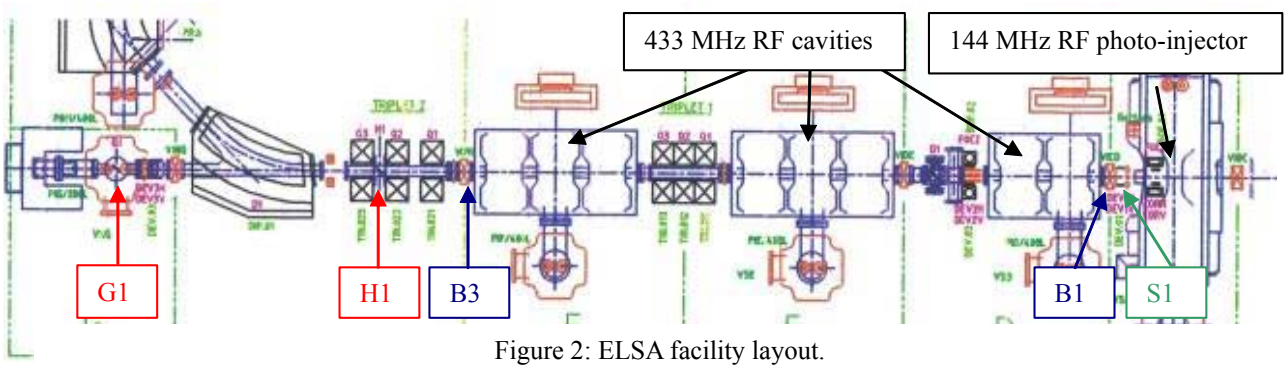

Figure 2: ELSA facility layout.

BEAM ANALYSIS USING THE IPNS LINAC ESEM*

J.C. Dooling, F.R. Brumwell, LI. Donley, G.E. McMichael, and V.F. Stipp
Argonne National Laboratory, Argonne, IL 60439, USA

Abstract

The Energy Spread and Energy Monitor (ESEM) is an on-line, non-intrusive diagnostic used to characterize the output beam from the 200-MHz, 50-MeV linac. The energy spread is determined from a 3-size, longitudinal emittance measurement and energy is derived from TOF analysis. Presently, a single particle distribution is used to yield energy and energy-spread results. Effort is on-going to allow for more realistic distributions to be included. Signals are detected on terminated 50-ohm, stripline BPMs. Each BPM is constructed with four striplines: top, bottom, left and right. Until recently, the ESEM signals were taken solely from bottom striplines in four separate BPM locations in the transport line between the linac and synchrotron. We have begun to use the top stripline data to examine, in more detail, beam position and attempt to measure beam size.

INTRODUCTION

Stripline beam position monitors (BPMs) are an important on-line diagnostic tool[1]. The IPNS BPMs are constructed with four 50-Ω striplines aligned with the horizontal and vertical axes of the accelerator. Each stripline is terminated on the downstream end in its characteristic impedance (50-Ω). A BPM module is shown in Figure 1. There are seven BPM modules in the 50 MeV transport line between the linac and synchrotron; the first four are also used for ESEM measurements.

Figure 1: IPNS 50 MeV line stripline BPMs.

* This work is supported by the US DOE under contract no. W-31-109-ENG-38

The ESEM diagnostic makes use of a three-size technique to determine the beam's longitudinal momentum and energy spread[2]. A drift-length parameter is used to adjust the four three-size permutations until satisfactory agreement is achieved between them. The four BPM permutations are 123, 124, 134, and 234. Figure 2 shows the section of beamline relevant to the ESEM diagnostic.

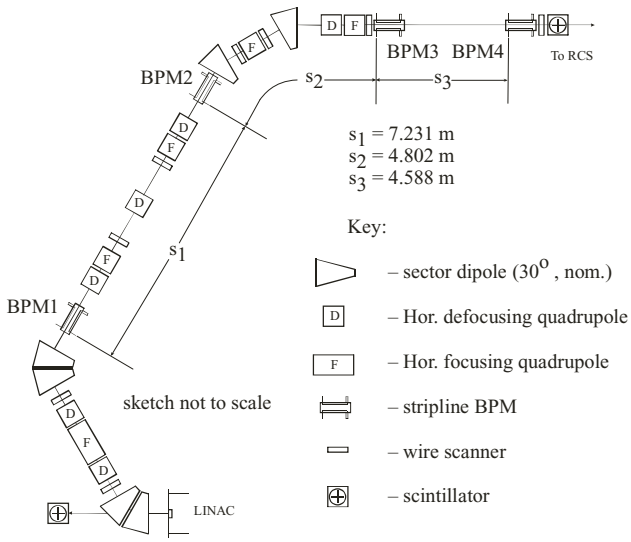

Figure 2: 50-MeV transport line with location of the ESEM stripline BPMs.

BEAM SIZE ANALYSIS

A heuristic approach is used to determine the transverse beam size using stripline BPMs. Two-point models have been used elsewhere[3] to describe beam motion and stability; here, a rigid, two-point model is used to study the beam size.

Two Beamlet Approach

The measurement assumes the beam bunch of charge Q can be represented by two equal point charges of Q/2 separated in one transverse plane by 2a. The center of the two point charges is offset from the axis of the BPM by x_0. The two-beamlet approach is shown schematically in Figure 3. A fraction of the total charge from each beamlet appears on the stripline within a polar angle of $\pi/2\gamma$, centered about $\theta=\pi/2$, where γ is the relativistic ratio of total to rest-mass energy. The charge density on each strip can be expressed as,

$$q_j = \sum_i (Q/2)\cdot(2\pi r_{ij}\, s_{ij})^{-1}\phi_{ij} \qquad (1)$$

THE FIRST RESULTS OF BUNCH SHAPE MEASUREMENTS IN THE SNS LINAC

A. Feschenko*, V. Gaidash, Yu. Kisselev, L. Kravchuk, A. Liyu, A. Menshov, A. Mirzojan,
Institute for Nuclear Research, Moscow 117312, Russia
S. Assadi, W. Blokland, S. Henderson, D.-O. Jeon, E. Tanke, ORNL/SNS, Oak Ridge, Tennessee

Abstract

Three Bunch Shape Monitors with transverse scanning of low-energy secondary electrons have been developed and fabricated for the SNS Linac. A novel feature of the detectors is the use of energy separation of the electrons. The separation allows minimizing the influence of detached electrons originated from dissociation of H-minus ions in the detector wire target. The first detector was used at the exit of the first DTL tank during its commissioning. The results of Bunch Shape measurements are presented and discussed. These results were used to verify beam quality, to set parameters of the accelerating field, to estimate longitudinal beam halo and to estimate the longitudinal beam emittance.

INTRODUCTION

Bunch Shape Monitors (BSMs) are used to measure longitudinal microstructure of the accelerated beam in a number of accelerators. A review report [1] includes details of the principle of operation and description of BSM parameters as well as thorough list of references. Briefly, the principle of operation is based on the coherent transformation of a longitudinal distribution of charge of the analyzed beam into a spatial distribution of low energy secondary electrons through transverse RF modulation. The main parameter of the monitor is its phase resolution. Typically the value of resolution is about 1° at the frequencies of hundreds of MHz.

In the case of an H-minus beam the results of measurements are distorted by the electrons detached from the ions in the wire target of a BSM [2]. The influence of the detached electrons essentially depends on the analyzed beam energy. In the majority of cases this influence is not essential for bunch core measurements but is of extreme importance for measurements of a longitudinal halo. Information on halo intensity is vital for the new generation of high intensity linear accelerators. That is why a special measure for diminishing the influence of the detached electrons has been foreseen in BSMs developed for the SNS linac. Due to the difference in energy of the low energy secondary electrons used for bunch shape measurements and the detached electrons, an effective way of diminishing the influence of the latter ones is energy separation of the two electron fractions [3]. The standard configuration of the BSM (fig. 1) was modernised by adding bending magnet 5 along with slit 6 between output collimator 4 and electron collector 7. Bending magnetic field is selected to provide separation of electrons with the energy corresponding to target potential U_{targ} (typically 10 kV) Separated energy range must be sufficient to provide loss-less propagation of the low energy secondary electrons. With the radius of 47 mm, the slit size of 3 mm and the image size of 1 mm the energy range equals about 20%.

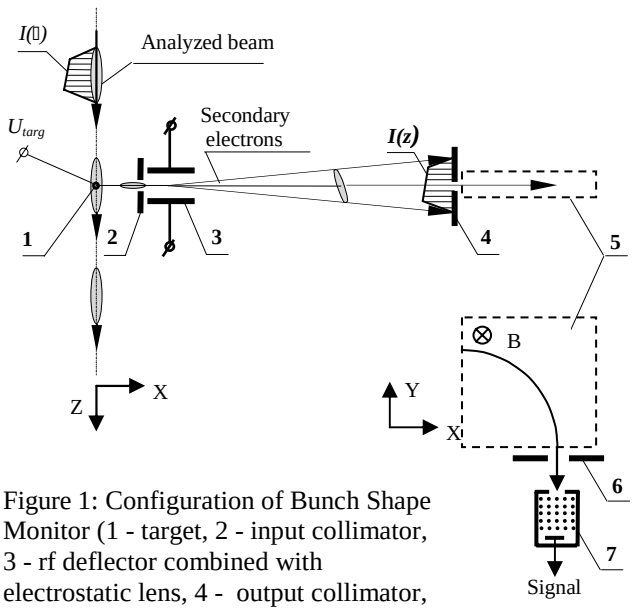

Figure 1: Configuration of Bunch Shape Monitor (1 - target, 2 - input collimator, 3 - rf deflector combined with electrostatic lens, 4 - output collimator, 5 – bending magnet, 6 – collimator, 7 – Secondary Electron Multiplier).

Energy separation also improves halo measurements due to decreasing the influence of electrons inelastically scattered on the plates of input collimator 2.

Three Bunch Shape Monitors have been built for the SNS linac. Now they are installed in intersegments 7, 9 and 11 of CCL Module #1. The first one, shown in fig. 2, was used during the commissioning of the DTL Tank 1 in autumn 2003.

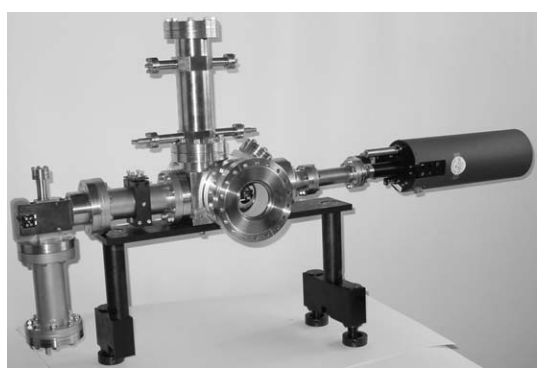

Figure 2: General view of BSM.

*feschenk@inr.troitsk.ru

BUNCH LENGTH MEASUREMENTS AT LEBRA

K.Yokoyama [#,*,A)], I.Sato [A)], K.Hayakawa [A)] , T.Tanaka [A)] , Y.Hayakawa [A)], K.Nakao[B)]
A) Laboratory for Electron Beam Research and Application, Institute of Quantum Science,
Nihon University 7-24-1 Narashinodai, Funabashi, 274-8501
B) College of Science and Technology, Nihon University
7-24-1 Narashinodai, Funabashi, 274 -8501 Japan

Abstract

The high-gain FEL amplification in near IR and SASE have been observed at LEBRA (Laboratory for Electron Beam Research and Application). A very short bunch of the electron beams have been achieved by the achromatic bending system, as the bunch compression system due to apt on the accelerating phase in the last accelerating section. The bunch length was estimated from the phase ellipse parameters which is deduced from the dependence of the beam spread on the accelerating phase. The bunch length of FWHM was estimated approximately 0.33 mm from the results of the experiments. Besides, the pulse length of the FEL lights around the wavelength of 1.5 micrometer was measured by means of the autocorrelation. The pulse length was less than 0.06 mm according to the number of interference waves. The pulse length of the FEL lights corresponds to around 20% of the electron bunch length.

INTRODUCTION

The high-gain FEL amplification has been obtained and the result of the simulation extracted from the FEL gain indicates that the bunch length could be around 1 ps or less [1]. SASE has also been observed using the electron beam with a low macropulse beam current and a very short bunch with considerable bunch compression in the achromatic bending system [2]. In order to investigate the bunch length which yields the high gain FEL amplification, the electron bunch length was measured by means of the simple theory about the phase ellipse instead of using a streak camera, which provides a direct and convenient way to measure bunch lengths but a high-accuracy one is very expensive. The pulse length of the FEL lights around the wavelength of 1.5 μm was also measured by means of the autocorrelation to compare the results of the bunch length.

The part of the main accelerating at LEBRA consists of three 4-m accelerating sections [3, 4]. The accelerating RF is provided by two 20-MW klystrons, which are operated at 2856 MHz with a pulse length 20 μs. The Phase flatness of the pulse error within 0.3° was achieved [5]. Klystron #1 is used for the injector and the first accelerating section and klystron #2 is used for the two accelerating sections. The electron beam accelerated in the linac is transported to the FEL system through the 90° achromatic bending and analyzer magnet system. The energy spread of the beam is restricted to about 1% by a slit of the momentum analyzer. The FEL system consists of an undulator of 50 periods of a Halbach-type permanent magnet array and an optical cavity and the cavity length is about 7 m.

#kazue.yokoyama@kek.jp
* Present affiliation: High Energy Accelerator Research Organization, KEK, 1-1 Oho, Tsukuba, 305-0801 Japan

EXPERIMENTAL METHOD [6]

The input RF phase of klystron #2 and the accelerating phase in accelerating section #3 can be changed by two phase shifters independently as shown in Fig. 1. The energy spectrum can be obtained by utilizing the first 45° bending magnet of the momentum analyzer as a spectrometer. The bunch length was estimated from the energy spread by using the method as below.

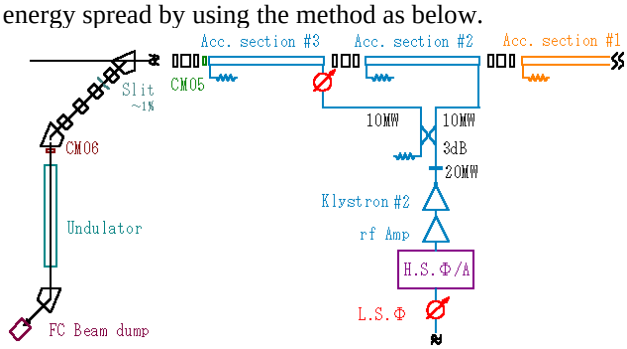

Figure 1: Layout of the FEL LINAC at LEBRA.

Maximum Energy Gain

The maximum electric field of the accelerating RF, E_P, is obtained from the maximum energy of the energy spectrum depending on the accelerating RF phase. E_0 is the total accelerating energy which beams obtain until acc-section #2 and the beam loading in acc-section #3, E_i is the beam energy after acc-section #3 and ϕ_i is the accelerating phase in acc-section #3. This correlation can be written

$$E_i = E_0 + E_P \cos\phi_i \qquad (1),$$

where the original point of ϕ_i is based on the phase with the maximum energy. E_0 and E_P can be obtained by the least-square method from the experimental data of E_i and ϕ_i.

Ellipse Parameters

To describe a beam in phase space, assuming that the distribution of the beam at any other place along the transport line is to be an ellipse space, it can be expressed

$$\gamma_0 \Delta l^2 - 2\alpha_0 \Delta l \Delta E + \beta_0 \Delta E^2 = \varepsilon \qquad (2)\ [7],$$

RF TUNING SCHEMES FOR J-PARC DTL AND SDTL

Masanori Ikegami, KEK, Tsukuba, Ibaraki 305-0031, Japan
Yasuhiro Kondo, Akira Ueno, JAERI, Tokai, Ibaraki 319-1195, Japan

Abstract

In the beam commissioning of J-PARC linac, RF phase and amplitude of RF cavities will be tuned based on the beam-phase or beam-energy measurement. In this paper, planned beam-based tuning schemes for the DTL and SDTL are presented together with the beam diagnostic layout for the tuning.

INTRODUCTION

In high-current proton linacs, precise tuning of RF amplitude and phase is indispensable to reduce uncontrolled beam loss and beam-quality deterioration. Especially, accurate RF tuning is essential for J-PARC linac [1, 2], because requirement for the momentum spread is severe ($\pm 0.1\%$ at the ring injection including jitter) to realize effective injection to the succeeding RCS (Rapid Cycling Synchrotron). To meet the requirement, tuning goals for the RF phase and amplitude are, respectively, set to ± 1 degree and $\pm 1\%$. In the beam commissioning of the linac, RF phase and amplitude are tuned based on the beam-phase or beam-energy measurement.

In this paper, planned tuning schemes for the DTL and SDTL (Separate-type DTL) are presented together with the beam diagnostic layout for the tuning. We have three DTL tanks and 32 SDTL tanks, which constitute middle energy portion of J-PARC linac. Each DTL tank is driven by a 3-MW klystron, and two neighboring SDTL tanks are driven by a 3-MW klystron. Only the klystron phase and amplitude is tuned based on the beam measurement. The relative phase and amplitude between the SDTL pair are tuned with low- and high-level RF measurements, and its procedure is out of scope of this paper.

TUNING SCHEMES

In the tuning of RF phase and amplitude of an RF cavity, a phase-scan method has widely been adopted [3]. There are a variety of phase-scan methods with different monitor setup and different approach. In the tuning of J-PARC DTL and SDTL, we are considering the following three schemes;

- Scheme I: Tank phase and amplitude are scanned with measuring the beam phase just after the tank under tuning. The output beam phase is measured with an FCT (Fast Current Transformer). Only the relative variation of output beam phase is used to find adequate RF phase and amplitude.
- Scheme II: Tank phase and amplitude are scanned with measuring the beam energy after the tank under tuning. The output beam energy is measured with two FCT's based on the TOF (Time Of Flight) method. While the beam energy is measured, only the relative variation of the beam energy is used to find adequate RF phase and amplitude.
- Scheme III: The setting is essentially the same with Scheme II, but the knowledge of the absolute output energy is used to find adequate RF phase and amplitude.

The setups for these tuning schemes are schematically shown in Fig. 1. It should be noted that the two FCT's in Scheme II and III have more than one DTL or SDTL tank in-between in our linac layout, and these tanks are detuned to avoid interference to the TOF measurement. In Scheme I and II, the required scanning ranges are modest, namely, the phase and amplitude are scanned about ± 10 deg and $\pm 5\%$, respectively. Contrary, we need a wider phase-scan (360 deg is desirable) for Scheme III. It is obvious that Scheme I is the most preferable considering its simplicity and the absence of the possible influence of idle detuned cavities, and that Scheme III is the least preferable where absolute beam energy measurements are involved. However, the applicability of these schemes is deeply dependent on the cavity characteristics. Then, we have determined the tuning schemes for each tank evaluating the applicability with PARMILA[4] simulations.

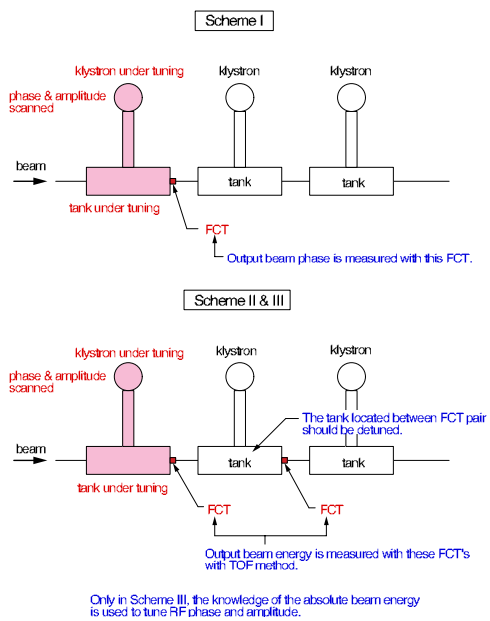

Figure 1: A schematic for RF tuning schemes.

AN ALTERNATIVE SCHEME FOR J-PARC SDTL TUNING

Masanori Ikegami , KEK, Tsukuba, Ibaraki 305-0801, Japan
Yasuhiro Kondo, Akira Ueno, JAERI, Tokai, Ibaraki 319-1195, Japan

Abstract

In the beam commissioning of J-PARC linac, we plan to perform phase-scan with precise TOF (Time Of Flight) beam-energy measurement to tune RF phase and amplitude of SDTL tanks. As a back-up method, we are considering to prepare a simpler RF tuning scheme with rough TOF measurement for SDTL which does not involve TOF measurements with idle SDTL tanks in-between. In this paper, the principle of this scheme is presented, and its advantages and disadvantages are discussed based on a systematic particle simulation.

INTRODUCTION

In the beam commissioning of J-PARC linac [1, 2], RF phase and amplitude are tuned based on the beam phase or beam energy measurement. As presented in a separate paper [3], we plan to perform phase-scan with precise TOF (Time Of Flight) beam-energy measurements in RF tuning of SDTL (Separate-type DTL) tanks. However, that scheme is presupposing an accurate TOF measurement of absolute beam energy having idle detuned cavities between beam phase monitors, which may involve technical difficulty. Then, we are considering to prepare an RF tuning scheme with rough TOF measurement as a back-up method for SDTL tuning. In this paper, the principle of this scheme is presented, and its advantages and disadvantages are discussed based on a systematic particle simulation.

ALTERNATIVE TUNING SCHEME

We have 30 SDTL tanks in SDTL section in 181-MeV operation [1], and the neighboring two SDTL tanks are driven by a 3-MW klystron. The beam energy measurement in SDTL section is performed based on the TOF (Time Of Flight) method utilizing two FCT's (Fast Current Transformers). Figure 1 schematically shows the FCT layout in SDTL section. Precise beam energy measurement is performed with a FCT pair which has three idle detuned SDTL tanks in-between. Although the accuracy of precise measurement is expected to reach 0.05 %, the measurement cannot be performed while nominal beam operation. For the beam energy measurement while nominal beam operation, additional FCT pairs with shorter drift length are prepared, to which we refer as "rough TOF pairs".

With these FCT pairs, we are able to perform rough TOF measurement of the beam energy without interfering with beam operation. The drift length in a rough TOF pair is around $2\beta\lambda$ with β and λ being the beam velocity scaled by the speed of light and the RF wave length, respectively. The accuracy of the beam energy measurement is limited to be around 0.5 % because of its short drift length. While the measurement accuracy is limited, it is advantageous that the measurement can be performed while nominal beam operation without possible influence of idle detuned cavities. We are considering two roles for the rough TOF pairs. One is the continuous watching of RF tuning to detect long-term drift or sway of RF properties. The other is the utilization for initial RF tuning of SDTL modules. The sensitivity of the former utilization is closely related to the achieved tuning accuracy of the latter. In this paper, we seek the possibility of using these pairs for initial RF tuning of SDTL tanks. It will also provide us information on the sensitivity for the watching of the long-term RF stability.

The accuracy of beam energy measurement is insufficient for precisely determining the RF phase and amplitude of an individual RF module. Our strategy for the RF tuning is to avoid undesirable build-up of the effect of errors, tolerating large phase and amplitude errors for individual RF modules. The rough TOF pairs are located after every SDTL module, and, hence, the output energy of every SDTL module can be monitored. In this tuning scheme, we first perform rough preset of the RF phase and amplitude of SDTL modules with, for example, low- and high-power RF

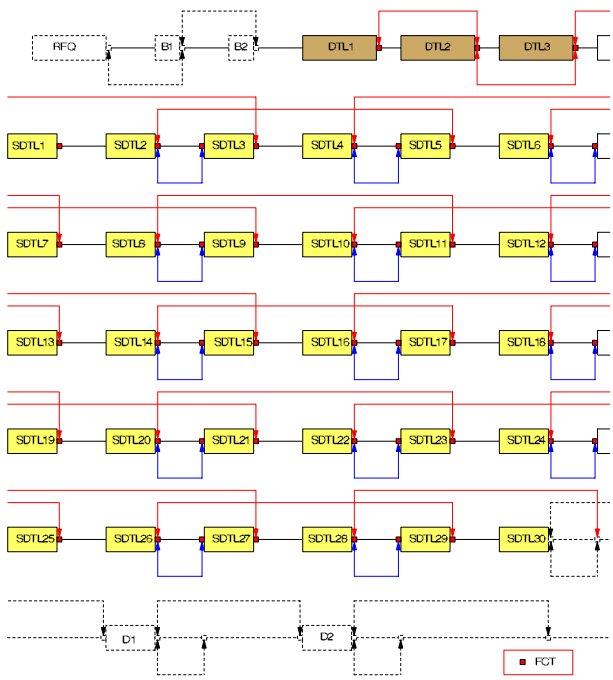

Figure 1: Schematic layout of FCT's in SDTL section (181-MeV operation). A red arrow indicates a FCT pair for presice TOF measurement, and a blue arrow rough TOF measurement.

BEAM-BASED ALIGNMENT MEASUREMENTS OF THE LANSCE LINAC*

R. C. McCrady#, L. J. Rybarcyk, LANL, Los Alamos, NM 87545, USA

Abstract

We have made measurements of the alignment of the Los Alamos Neutron Science Center (LANSCE) Drift Tube linac (DTL) and Side Coupled linac (SCL) using beam position measurements and analyzing them with linear models. In the DTL, we varied the injection steering and focusing lattice strengths, measured the beam position after each DTL tank, and analyzed the data with a linear model using R-matrices that were either computed by the Trace-3D computer program or extracted from analysis of the data. The analysis model allowed for tank-to-tank misalignments. The measurements were made similarly in the SCL, where the analysis model allowed for misalignments of each quadrupole doublet lens. We present here the analysis techniques and the resulting beam-based alignment measurements.

INTRODUCTION

The LANSCE linac accelerates protons and H^- ions from 750keV to 100MeV in a DTL and to 800MeV in an SCL. During beam operations, the presence of misalignments became apparent. During short (<1 day) accelerator development periods we used the particle beams to make measurements of the relative misalignment of the focusing elements in both the DTL and the SCL. These data were intended to supplement data from optical instruments that require more time, preparation and access to the beam tunnels.

Measurements of beam positions were made with profile monitors, as no beam position monitors are available in the areas of interest. To facilitate these measurements, a smaller emittance, 1mA peak beam was used.

DTL ALIGNMENT MEASUREMENTS

The DTL consists of four tanks. The drift tubes contain quadrupole magnets for transverse focusing of the beam. We can measure the beam position and angle at the entrance and exit of the DTL and the beam position between each pair of tanks. Two types of measurements were made: 1) We varied the position and angle of the injected beam and measured the effect on the beam position and angle downstream; 2) We varied the strength of the quadrupole magnets in the drift tubes and measured the effect on the beam position and angle downstream. The assumptions of the analysis models are: 1) The focusing lattice within each of the tanks is straight, 2) No x-y coupling is present, 3) A linear beam optics model is valid.

*Work conducted at Los Alamos National Laboratory, which is operated by the University of California for the United States Department of Energy under contract W-7405-ENG-36.

#mccrady@lanl.gov

Suppose the beam is injected into the DTL with measured injection position and angle (x_0,θ_0) and that there is a misalignment $(\delta_{0,1},\phi_{0,1})$ between the injection measurement system and tank 1. The position of the beam as it exits tank 1 of the DTL will be:

$$x_1 = R_{11}\left(x_0 + \delta_{0,1}\right) + R_{12}\left(\theta_0 + \phi_{0,1}\right) + \delta_1 \qquad (1)$$

where δ_1 is an offset in the measurement and R_{mn} is the $(m,n)^{th}$ element of the transport matrix[1] from the injection point through DTL tank 1 to the beam position measurement device. This equation can be applied to both the vertical and horizontal planes. A set of such equations can be formed by making N measurements of x_1 with different injection parameters or with different focusing lattice strengths (which varies the R-matrix elements.) To determine the misalignment parameters and measurement offset, the set of equations can be written in the form $A \cdot x = b$ where A is an $N \times 3$ matrix, b is a vector of the N measurements and x is the vector of the three quantities to be estimated. This over-determined matrix equation can be solved by a variety of techniques; we employed the method of singular value decomposition. (See, for example, reference [2].)

When the injection parameters are varied, the matrix equation is:

$$\begin{bmatrix} R_{11} & R_{12} & 1 \\ R_{11} & R_{12} & 1 \\ \vdots & \vdots & \vdots \end{bmatrix} \begin{bmatrix} \delta_{0,1} \\ \phi_{0,1} \\ \delta_1 \end{bmatrix} = \begin{bmatrix} x_1(1) - R_{11}x_0(1) - R_{12}\theta_0(1) \\ \vdots \\ x_1(N) - R_{11}x_0(N) - R_{12}\theta_0(N) \end{bmatrix}$$

When the focusing lattice strength is varied, the matrix is equation is:

$$\begin{bmatrix} R_{11}(1) & R_{12}(1) & 1 \\ \vdots & \vdots & \vdots \\ R_{11}(N) & R_{12}(N) & 1 \end{bmatrix} \begin{bmatrix} \delta_{0,1} \\ \phi_{0,1} \\ \delta_1 \end{bmatrix} = \begin{bmatrix} x_1(1) - R_{11}(1)x_0 - R_{12}(1)\theta_0 \\ \vdots \\ x_1(N) - R_{11}(N)x_0 - R_{12}(N)\theta_0 \end{bmatrix}$$

(The indices in parentheses indicate the measurement number.) The R-matrix elements can computed using a model of the DTL and the Trace-3D computer program[3], however for tank 1 we were able to extract the values of the R-matrix elements from the data.

One cannot distinguish the three fit parameters by varying the injection alone since each produces a constant offset in the measurements. These measurements can be useful when combined with those taken when the focusing lattice strength is varied.

For measurements of the beam position made downstream of DTL tanks 2, 3 and 4 additional terms for tank-to-tank misalignments must be included in Equation 1. The beam position measured downstream of tank j will be:

THE LANSCE LOW MOMENTUM BEAM MONITOR*

Rob Merl#, Floyd Gallegos, Chandra Pillai, Stuart Schaller, Fred Shelley, Andy Steck, Los Alamos National Laboratory, Los Alamos, NM 87545, USA
Benjamin J. Sanchez, ORNL, Oak Ridge, TN 37831, USA

Abstract

A diagnostic has been developed at the Los Alamos Neutron Science Center (LANSCE) for the purpose of identifying low momentum beam tails in the linear accelerator. These tails must be eliminated in order to maintain the transverse and longitudinal beam size. Instead of the currently used phosphor camera system, this instrument consists of a Multi Wire Proportional Chamber (MWPC) detector coupled to an EPICS compliant VME-based electronics package. Low momentum tails are detected with a resolution of 5 mm in the MWPC at a high dispersion point near a bending magnet. While phosphor is typically not sensitive in the nano amp range, the MWPC is sensitive down to about a pico amp. The electronics package processes the signals from each of the MWPC wires to generate an array of beam currents at each of the lower energies. The electronics has an analog front end with a high-speed analog to digital converter for each wire. Data from multiple wires are processed with an embedded digital signal processor and results placed in a set of VME registers. An EPICS application assembles the data from these VME registers into a display of beam current vs. beam energy (momentum) in the LANSCE control room.

ARCHITECTURE

The diagnostic is composed of a MWPC detector wired to a VME crate containing eight custom data acquisition and processing boards as shown in figure 1.

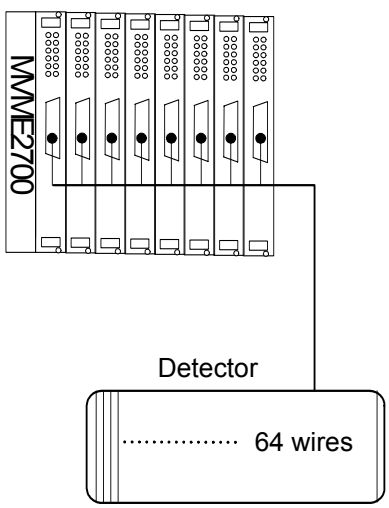

Figure 1: The 64 detector wires are supported by a remote VME crate with eight custom processing boards and a Motorola MVME2700 processor.

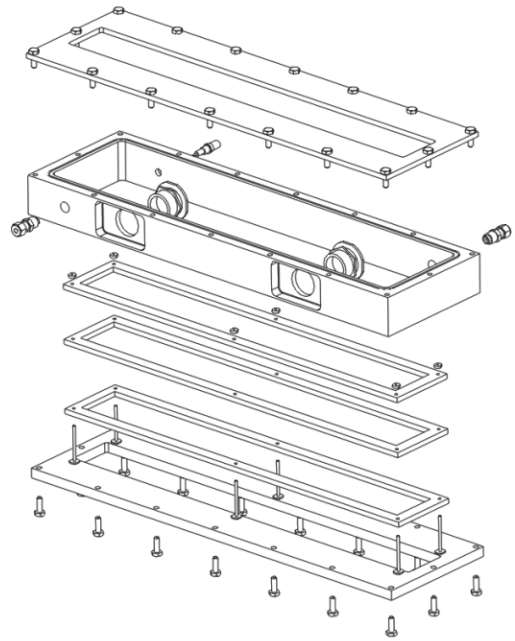

Figure 2: Solid Model drawing of detector assembly.

The detector is gas filled and contains 64 wires. The electronics supports them with 64 individual parallel processing channels in the VME crate.

There are cables containing 64 individual twisted pairs running from the detector to the VME crate. Each custom VME board handles eight of the 64 detector wires. The detector is located in the LANSCE beam tunnel just down stream and inboard from the XDBM04 bending magnet.

800 MeV beam entering this magnet is bent toward the experimental areas. Beam components at lower energies, however, are bent in a tighter radius and hit an inboard beam stop. These are the low energy components that should be eliminated. The detector is placed between this bending magnet and the beam stop so it can measure the magnitude spectrum of beam currents over a range of unwanted low energies [1].

MULTIWIRE CHAMBER

The chamber contains 64 gold plated tungsten wires that are stretched across a fiberglass frame. The wires are 5 mm apart and sit between two high voltage plates. The high voltage plates are made of 25 μm aluminum foil also supported by fiberglass frames. The area inside the frames is 50 cm x 6 cm or 300 square cm. The wires and high

*Work supported by the U.S. Department of Energy.
#merl@lanl.gov

PRECISION ALIGNMENTS OF STRIPLINE BPM'S WITH QUADRUPOLE MAGNETS FOR TTF2

D. Noelle, G. Priebe, M.Wendt and M. Werner,
Deutsches Elektronen Synchrotron DESY, Notkestr. 85, D-22603 Hamburg

Abstract

Due to the absence of synchrotron radiation in a linac like the TESLA Test Facility (TTF2), it is possible to install the beam position monitors (BPMs) inside the quadrupoles, defining the optical axis of the accelerator. This paper reports on an alignment setup and the procedure, using the stretched wire technique to calibrate the BPMs with respect to the magnetic axis of the quadrupole magnet.

INTRODUCTION

The control of the beam orbit is essential for the operation of linear accelerators for future linear colliders (LC), as well as for free electron laser (FEL) drive linacs. The transport of the beam, by preserving its low emittance, requires a precise measurement of the beam orbit with respect to the magnetic axis of the quadrupoles. As a beam based alignment procedure is not always applicable (common quadrupole power supplies), or sometimes may not give satisfactory results (shot-to shot beam jitter), a stretched wire alignment measurement for quadrupole and BPM pickup can be used as an alternative or add-on.

MEASUREMENT PRINCIPLE

The optical axis of an accelerator is defined by the magnetic axis of the focussing elements, i.e. the quadupoles. Only if the beam is following this axis as close as possible, the machine will achieve optimum performance. Therefore, it is essential to have the BPMs as close and as well aligned to the quadrupoles as possible. Since there is almost no synchrotron radiation in a linac, it is possible to install the BPM inside the quadrupoles without the danger that movements of the vacuum chamber due to heat load will move the quadrupole or the BPM with respect to the quadrupole.

Due to the rigid connection between the two units, it is also possible to determine the offset of the BPM and quadrupole, caused by manufacturing tolerances, before installation on a test bench.

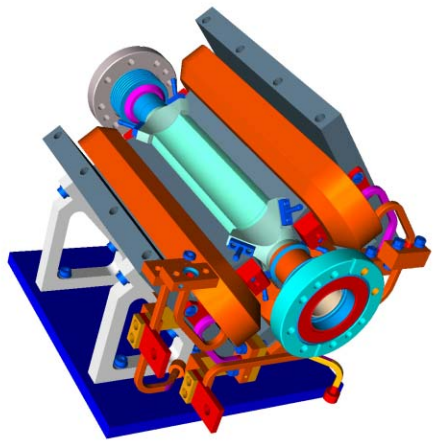

Figure 1: Drawing of a TTF2 stripline installed inside a quadrupole magnet.

The test bench uses a stretched wire, to determine

a) the magnetic axis of the magnets, by measuring an minimizing movements of the wire introduced by current pulses: If a current pulse is passing the wire, while the magnetic field of the quadrupole is present, Lorence force will induce movements of the wire, except if the wire is passing on the magnetic axis.
b) To determine the electrical axis of the BPM within the same reference frame, by using the wire as an antenna for incoupling of an RF signal. This signal is read by two opposite pickups of the BPM. If the wire is exactly on the electrical axis, the difference of the two signals will cancel.

Since we are dealing with no perfect mechanical systems, one has to find the minimum signal for wire movement and antenna signal. The difference of the transverse positions, where the minimum signals are found, is then the BPM offset, to be used as calibration data for the orbit measurement system.

THE STRECHED WIRE TEST BENCH

This idea [1] was already adapted for a few stripline BPM-quadrupole units, used at the S-Band Test Facility linac [2], and is now applied under cleanroom conditions for larger quantities for TTF2.

SYSTEMATIC CALIBRATION OF BEAM POSITION MONITOR IN THE HIGH INTENSITY PROTON ACCELERATOR (J-PARC) LINAC

S. Sato*#, Z. Igarashi†, S. Lee†, T. Tomisawa*, F. Hiroki*, J. Kishiro*,
M. Ikegami†, Y. Kondo*, K. Hasegawa*, A. Ueno*, T. Toyama†,
N. Kamikubota†, K. Nigorikawa†, M. Tanaka‡, H. Yoshikawa*
* JAERI: Japan Atomic Energy Research Institute, Tokai, Ibaraki, 319-1195 JAPAN
† KEK: High Energy Accelerator Research Organization, Tsukuba, Ibaraki, 305-0801 JAPAN
‡ Mitsubishi Electric System & Service, Tsukuba, Ibaraki, 305-0045 JAPAN

Abstract

As a joint project of KEK and JAERI, a MW class of high intensity proton accelerator (J-PARC), consisting of Linac, 3 GeV-RCS, 50 GeV-MR, is under construction. For this accelerator, it is required to minimize the beam loss (typically, lower than 0.1~1 W/m at the linac). To achieve the requirement, beam trajectory needs to be controlled with accuracy of some 100 μm. The first stage of the acceleration (up to 181 MeV during the first stage of construction) is done by linac. The beam position monitor (BPM) in the linac utilizes 4 stripline pickups (50 Ω) on the beam transportation chamber. In this paper, systematic calibration of the BPM is described.

DESIGN OF PICKUP LINE IN BPM

First stage of acceleration (181 MeV in the 1st phase of construction) in J-PARC is done by linac. For the beam position monitoring in the linac, stripline type of pickup electrodes (50 Ω) are placed inside beam transporting chambers. In order to minimize the space and to get the accuracy of the positioning of BPM, each BPM module is supported by pole faces of a quadrupole magnet. For the pickup electrodes it is important to maintain impedance matching, in order to avoid the reflection and to keep the signal balances between the electrodes. In the linac, there are 5 sizes of the beam transporting chamber, namely (from up stream) 37.7, 40, 70, 85, 120 mm in diameters. For BPMs in the 2 smaller types of diameter, flat-shape (in cross section) pickup plates are chosen because the mechanical structure is relatively simpler [1].

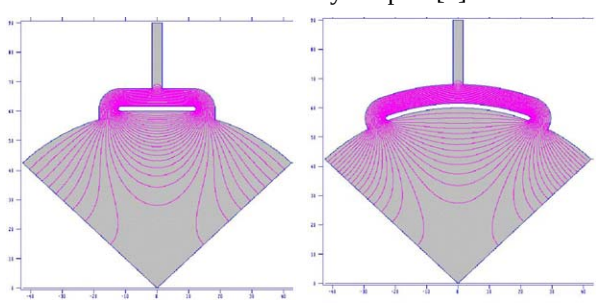

Figure 1: Cross section of the pickup electrode plates in BPM. Left; flat type. Right; round-shape type. (Due to the symmetry in the shape of BPM, only a quarter of BPM is shown.

#susumu.sato@j-parc.jp

For the BPMs in the 3 larger types of diameter, it is designed to use round-shape pickup plate along with the chamber circumference, in order to tale larger width of the electrode to achieve better sensitivity (S/N ratio). Figure 1 shows the two types of cross section of the pickup electrode plate with electric field shape in the BPM. The field shapes are calculated by POISSON [2] code which is used for the impedance optimization. As there are symmetries of the shape in each of 4 (up, down, right, left) electrodes, only a quarter of cross section is shown in the figure. The flat type and the round-shape type of pickups are shown in the left side and the right side, respectively.

CALIBRATION OF BPM

Calibrations of the BPM take two steps. The first step is taken before installation, and with the dedicated calibration bench which has a stainless wire (100μm) carrying 324 MHz (acceleration frequency) as dummy signal simulating the beam. In this step, an electrical zero point of pickup electrode is calibrated with respect to the mechanical center. The second step is taken after the installation with beam in low intensity, and is called beam based calibration (BBC). Displacement between the electrical center of BPM and the practical field center of the quadrupole magnet is calibrated.

Calibration before Installation (Calibration Bench Based)

Before installation, electrical zero point of pickup electrode for each BPM is calibrated by a calibration bench with a wire which carries 324 MHz simulating beam. Figure 2 shows a schematic (upper) and a photograph (lower) of the calibration bench, looking from the side. The BPM is sustained in the center of the calibration bench. The wire is placed inside the BPM and is straightened from both sides by hinges soldered on core pins of N-type connectors. The wire can be moved inside the BPM in order to simulate possible beam positions. On both edges of the BPM, dummy pipes are attached to simulate beam pipes, and are connected to the outer-line of the N-type connector. One side of the N-type connector is conducted to the 324 MHz generator and the other side is conducted to a terminator. Mechanical test of wire scanning has been already done.

HIGHLY SENSITIVE MEASUREMENTS OF THE DARK CURRENT OF SUPERCONDUCTING CAVITIES FOR TESLA USING A SQUID BASED CRYOGENIC CURRENT COMPARATOR

W. Vodel, S. Nietzsche, R. Neubert, Friedrich Schiller University Jena, Germany
A. Peters, GSI Darmstadt, Germany
K. Knaack, M. Wendt, K. Wittenburg, DESY Hamburg, Germany

Abstract

A newly high performance SQUID based measurement system for detecting dark currents, generated by superconducting cavities for the upcoming TESLA project (X-FEL) at DESY Hamburg, is proposed. It makes use of the Cryogenic Current Comparator principle and senses dark currents in the pA range with a measurement bandwidth of up to 70 kHz.

INTRODUCTION

The 2×250 GeV/c TESLA linear collider project, currently under study at DESY [1], is based on the technology of superconducting L-band (1.3 GHz) cavities. The two 10 km long main LINACs (linear accelerator) are equipped with a total of nearly 20,000 cavities. A gradient of 23.4 MV/m is required for a so-called superstructure arrangement of couples of 9-cell cavities. To meet the 2×400 GeV/c energy upgrade specifications, higher gradients of 35 MV/m are mandatory.

The dark current, due to emission of electrons in these high gradient fields, is an unwanted particle source. Two issues are of main concern:

- Thermal load: An emitted electron from the cavity surface follows a path along the electric field lines and will most probable hit somewhere else onto the cavity wall. This leads to an additional thermal load in the cryostat, which has to be covered by the liquid helium refrigerator.
- Propagating dark current: If the energy gain is sufficient, the electrons will generate secondary particles when hitting the cavity wall which then also may generate secondaries. In the following avalanche process some electrons may pass through the iris of the cavity cell and will be further accelerated. In this case the dark current along the LINAC would grow exponentially if on average more than one electron passes the complete FODO (focus/defocus lattice) cell.

Recent studies [2] show that the second case seems to be the more critical one. It limits the acceptable dark current on the beam pipe "exit" of a TESLA 9-cell cavity to approximately 50 nA. Therefore the mass-production of high-gradient cavities with minimum field emission requires a precise, reliable measurement of the dark current in absolute values. The presented apparatus senses dark currents in the nA range. It is based on the cryogenic current comparator (CCC) principle, which includes a highly sensitive LTS SQUID as magnetic field sensor. Further on the setup contains a faraday cup and will be housed in the cryostat of the CHECHIA cavity test stand.

REQUIREMENTS FOR DARK CURRENT MEASUREMENT APPARATUS

Electrons can leave the niobium cavity material if the force of an applied external electric field is higher than the bounding forces inside the crystal structure. The highest field gradients occur at corners, spikes or other discontinuities, due to imperfections of the cavity shape. Another potential field emitter is due to any kind of imperfection on the crystal matter, like grain boundaries, inclusion of "foreign" contaminants (microparticles of e.g. In, Fe, Cr, Si, Cu) and material inhomogeneity. At these imperfections the bounding forces are reduced and electrons are emitted under the applied high electromagnetic fields [3]. With a series of special treatments the inner surface of the TESLA cavities are processed to minimize these effects. A reliable, absolute measurement of the dark current allows the comparison of different processing methods and a quality control in the future mass-production.

TESLA will be operated in a pulse mode with 5 Hz repetition rate. The 1.3 GHz r.f. pulse duration is 950 µs. During this time the dark current is present and has to be measured. Therefore a bandwidth of 10 kHz of the dark current instrument is sufficient. As field emission is a statistical process, the electrons leave the cavity on both ends of the beam pipe. Thus, half of the dark current exits at each side, and has to be measured on one side only. With the 1.3 GHz r.f. applied, we expect that the dark current has a strong amplitude modulation at this frequency. This frequency has to be carefully rejected from the instrument electronics to insure its proper operation and to avoid a malfunction of the SQUID. This were done by the help of careful r.f. shielding, appropriate filtering of all leads feeding to the SQUID input coil, and the low pass characteristic of the transformer used.

The use of a cryogenic current comparator as dark current sensor has some important advantages:

- measurement of the absolute value of the dark current,
- independence of the electron trajectories,
- accurate absolute calibration with an additional wire loop, and
- extremely high resolution.

The required working temperature of 4.2 K (boiling temperature of LHe) for the apparatus is unproblematic to provide because the CHECHIA test stand includes the

TTF2 BEAM MONITORS FOR BEAM POSITION, BUNCH CHARGE AND PHASE MEASUREMENTS

D. Nölle, M. Wendt
Deutsches Elektronen Synchrotron (DESY),
Notkestr. 85, D-22607 Hamburg, Germany

Abstract

An overview of the basic beam instrumentation with regard to electromagnetic beam monitors for the TESLA Test Facility phase 2 (TTF2) is given. Emphasis is put on beam position monitor (BPM) and toriod transformer systems for beam orbit and bunch charge observations. Furthermore broadband monitors, i.e. wall current and bunch phase monitors, are briefly presented.

INTRODUCTION

During the past 10 years, the TESLA Collaboration has established the TESLA Test Facility (TTF) on the DESY site in order to develop the technology for a superconducting linear electron-positron collider and a X-ray free electron laser facility. The first phase of this project, TTF1, was successfully completed in 2002 with an extended operation period for first scientific applications of the saturated FEL beam below 100 nm wavelength [1].

Convinced of the unique possibilities provided by this new kind of radiation source, DESY is now upgrading the TTF accelerator and implementing the VUV-FEL user facility [2]. As in case of TTF1 the task in operating TTF2 will be twofold:

- Test accelerator for further development of superconducting L-Band (1.3 GHz) acceleration structures in the frame of a HEP linear collider, as well as for DESY's upcoming XFEL project.
- Drive linac for the 4th generation synchrotron radiation user facility based on a SASE FEL-undulator with a wavelength regime down to 6 nm.

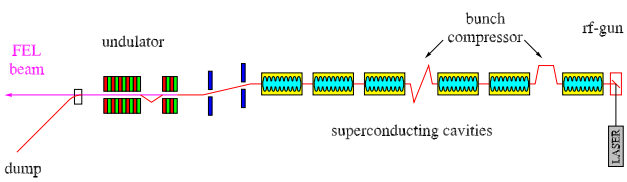

Figure 1: Schematic overview of TTF2.

Fig. 1 sketches the major components of TTF2, a new photoinjector (already tested with beam), five superconducting accelerator modules (a sixth module, for a 1 GeV upgrade, is under construction) of the TESLA type each containing eight L-band 9-cell cavities, two bunch-compressors, a collimation section and finally a 30 m long SASE FEL-undulator (divided in six 5 m long sections).

Based on the experience with TTF1 and other accelerators on the DESY side, a set of monitors for the basic beam instrumentation have been developed for TTF2. Emphasis was put on homogenous systems with high reliability, good maintenance and operational properties, rather than on "high-end instrumentation".

Table 1: Parameters of the TTF2 electron beam

max. beam energy	=	800 MeV (1 GeV)
max. rep. rate f_{rep}	=	10 Hz
macro pulse length t_{pulse}	=	800 μs
bunch spacing $\Delta\, t_b$	=	*110 ns or 1 μs*
N_e per bunch	=	*0.1...4 nC*
bunch length σ_z	$<$	50 μm
norm. emmittance ϵ_{norm}	=	2 mm mrad

Table 1 presents the beam parameters of TTF2, relevant for beam instrumentation. All monitors have to resolve single bunch information, thus the measurement (integration) time has to be $<$ 110 ns. Due to the use of high gradient superconducting cavities, special care has to be taken to avoid dust or other particles in the vacuum system, even though most of the diagnostics is installed outside of the cryostats.

BEAM POSITION MONITORS

About 60 *beam position monitors* (BPM) are installed in the warm sections of TTF2, half of them are stripline and half of them button BPMs, mainly installed in sections with limited space, e.g. in the undulator. Resonant cavity and re-entrant cavity type BPM's, with special read-out electronics, as they are used in the cold accelerating modules are not covered here.

Stripline BPM's

Based on a design for the S-Band LC test facility, the TTF2 *stripline-BPM's* are manufactured in two slightly different versions for the two standard vacuum chambers diameters of of 34 mm resp. 44 mm diameter. Since the outer shape of the BPMs maps to the contour of the poles inside the quadrupoles, it was possible to install the BPMs *inside* the quads, i.e. where the optical axis of the machine is defined. A stretched-wire calibration procedure was applied to these BPM-quadrupole units to measure the difference between electrical axis of the monitor and magnetic axis of the quad.

BEAM INSTRUMENTATION USING BPM SYSTEM OF THE SPring-8 LINAC

K. Yanagida*, T. Asaka, H. Dewa, H. Hanaki, T. Kobayashi,
A. Mizuno, S. Suzuki, T. Taniuchi, and H. Tomizawa
Japan Synchrotron Radiation Research Institute, Mikazuki, Hyogo, 679-5198, Japan

Abstract

Beam position monitors were installed in a SPring-8 linac's dispersive sections, and the entire beam trajectory could be measured along the linac. A fast and synchronized accumulating database system started, that accumulated beam position data from all forty-seven BPMs simultaneously at 10-pps operation of the linac. Feedback control of steering magnets and an energy compression system for beam position stabilization were also successfully examined.

INTRODUCTION

In a SPring-8 linac a beam position monitor (BPM) system has been developed and installed for several years. BPMs for the non-dispersive section were installed in August 2000. The non-dispersive section BPM is an electrostatic stripline monitor whose aperture is a circule of ϕ32 mm [1]. Its stripline length is 27 mm, and the detection frequency is 2856 MHz. Signal processors were installed in March 2001 whose basic processes are filtering by a band pass filter, detection by a logarithmic detector (AD8313), and analog-to-digital conversion [2]. At this time a simple data acquisition system from signal processors to an operator console was started to measure the trajectory of the non-dispersive section.

In August 2003 BPMs were installed in the dispersive section, and an entire beam trajectory could be measured along the linac. Finally, in November 2003 a fast and synchronized accumulating database system was started. After completion of the BPM system, the next task is to prepare beam instrumentation using the BPM system. The final goal is automatic tuning or operation of the linac. First beam position and energy feedback programs were developed, examined, and designed for long term stabilization in a top-up operation of the SPring-8 and the NewSUBARU storage rings [3] [4]. An examination of the programs was successfully carried out in July 2004, and they will be implemented from September 2004.

INSTALLATION OF DISPERSIVE SECTION BPM

The structure of the dispersive section BPM is the same as the non-dispersive section BPM, except that the cross-sectional aperture is larger. Its aperture is 62 $\times$ 30 mm ellipse as shown in Fig. 1 that was carefully designed to block RF noises around the detection frequency (2856 MHz), generated outside of BPM. Almost all BPMs were installed into quadrupole magnets. Figure 2 shows the location where the dispersive section BPMs were installed.

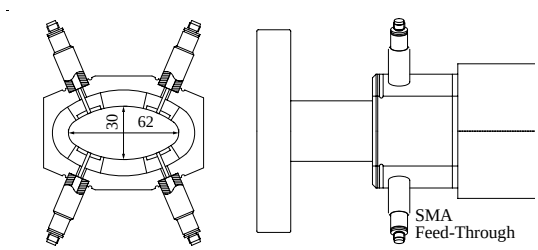

Figure 1: Schematic drawing of dispersive section BPM.

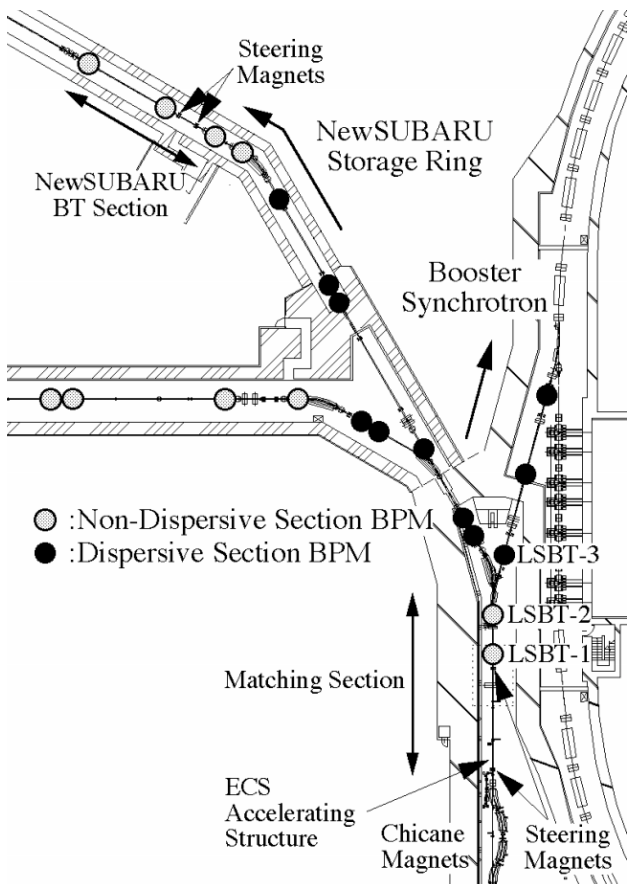

Figure 2: Location of installed dispersive section BPMs.

* ken@spring8.or.jp

THE BEAM DIAGNOSTICS SYSTEM IN THE J-PARC LINAC

S.Lee[A)], Z. Igarashi[A)], M.Tanaka[B)], S. Sato[B)], H. Akikawa[B)], F. Hiroki[B)], T.Tomisawa[B)], H.Yoshikawa[B)], J. Kishiro[B)] and T. Toyama[A)]
[A)] KEK, Tsukuba, Ibaraki, 305-0801, Japan
[B)] JAERI, Tokai, Naka, Ibaraki, 319-1195, Japan

Abstract

The beam diagnostics system has been developed to tune and investigate the high intensity proton beam in the J-PARC linac. Beam monitors are required to measure wide dynamic range of beam intensities and energies in linac. In this paper, construction and application of beam monitor system are described. Preliminary results of demonstration of beam position monitor (BPM), fast/slow current transformer (FCT/SCT), wire scanner (WS) and beam loss monitor (BLM) in the KEK-DTL1 (20MeV) are also discussed.

INTRODUCTION

The J-PARC (Japan Proton Accelerator Research Complex) linac aims to provide high intensity beams of peak current 50mA, kinetic energy 181/400MeV, pulse width 0.5mA and repetition rate 25Hz [1]. The goal of 133 kW beam power and hand-on maintenance will place significant demands on the performance and operational reliability of accelerator diagnostics systems. Beam diagnostics system is required to verify proper transverse focusing and matching of the magnetic focusing lattice of the linac. Large number of beam monitors will be installed in MEBT, DTL, SDTL, ACS and L3BT (Fig. 1). Progress and R&D results of beam monitors are evaluated in detail.

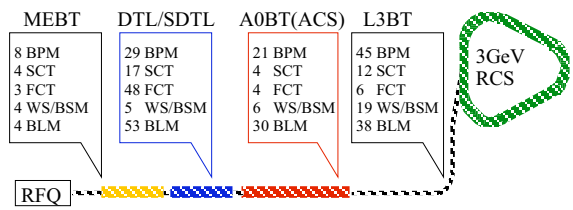

Figure 1: Designed beam monitor system in the J-PARC linac.

BEAM MONITORS IN THE J-PARC LINAC

Beam Position Monitor

Beam position monitors (BPM) have about 40mm-130mm bore and 4-stripline electrodes with one end shorted by 50 Ω terminations (Fig. 2) [2]. Electrostatic computations are used to adjust the BPM cross-section parameters to obtaine 50 Ω transmission lines. BPMs are sustained by pole edge of quadrupole magnet, and designed to reduce the offset between quadrupole magnet and BPM electrical centers of less than 0.1mm. A procedure of beam based calibration/alignment (BBC/BBA) method to evaluate the displacement of linac BPMs are examined [3]. The BPM electronics uses both amplitude-modulation-to-phase-modulation (AM-PM) method and conventional log-ratio method [4]. Prototype of BPM system with log-ration electronics have been constructed and examined in KEK MEBT1 and DTL1.

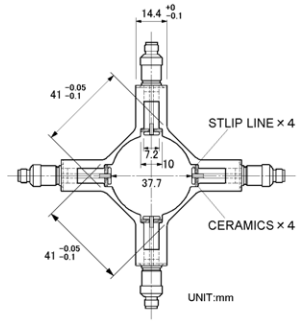

Figure 2: Schematic of beam position monitor in MEBT1.

Slow/Fast Current Transformer

Two types of current transformers have been developed to measure beam intensity and bunch phase (Fig. 3). The slow current transformer (SCT) have dynamic renge of 0.1-80 mA, a droop of 3% for a pulse width of 500 μs and time response of <50ns. The SCT has been chosen with 50 turns and additional winding to provide a calibration/test input capability. The fast current transformer (FCT) have response of relative bunch phase <1%. To measure the beam energy at every accelerator tank and injection point of 3GeV RCS, phase differences of two FCTs are used (time-of-flight: TOF), and 10^{-4} order energy resolutions can be expected. The SCT will also contribute to personal-protection-system (PPS). Integrated current signal will be evaluated to guarantee the normal operation of beam dumps.

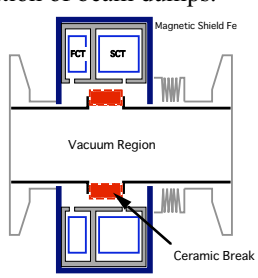

Figure 3: Cross sectional view of slow/fast combined type current transformer. FINEMET core is placed at outside the vaccum chamber to avoide the out gas. Outer wall is composed of iron to reduce the noise level.

Beam Loss Monitor

To prevent the activation and heat load by intense beam loss, fast time response of loss signals is required. The beam loss monitor (BLM) system is composed of scintillator (S-BLM) and Ar+CO_2 gas filled proportional

THE HIGH ACCURACY RF PHASE DETECTOR RESEARCH FOR 200 MEV LINAC

Dong Sai, Zhou Yingui, Li Ge, Huang Guirong, Jia Dachun,
National Synchrotron Radiation Laboratory,
University of Science and Technology of China,
Hefei, Anhui 230029, P.R.China

Abstract

The basic configuration of one experimental RF Phase detector and its application in Hefei 200MeV RF Linear accelerator are introduced. The 200MeV linac, which is the injector of Hefei Light Source (HLS), is cascaded by 5 accelerator tubes. The beam energy could be stabilized and controlled accurately by implementing RF Phase detectors of the 5 cascaded accelerator tubes into a phase locked system. The tabletop experiments are given and the RF Phase detector is tuned in the off-line status. The microwave in 2856MHZ under CW mode is differentiated accurately by the developed RF phase detector. The measured results are better than prediction. The accuracy of the basic configuration of the RF Phase detector is verified, which establishes foundations for further experiments.

INTRODUCTION

200 MeV electron linac is an injector of HLS (Hefei Synchrotron Radiation Light Source), as shown in Figure 1. The Linac has been running for 17 years. Its typical operation parameters are energy of 200 MeV, Current of 50 mA and energy spread of 0.8%[1]. Its energy shift during the injection period suggest its cure by implementing RF Phase detectors of the 5 cascaded accelerator tubes into a phase locked system.

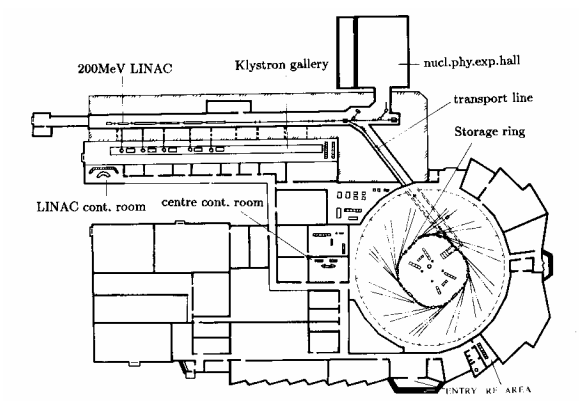

Figure 1: Layout of Hefei SLS.

In Phase-II Project of the National Synchrotron Radiation Laboratory, the old RF drive system of 200MeV Linac[2] is transformed into a high peak power RF solid-state amplifier as illustrated in Fig. 2. The main parameters of the RF power solid-state amplifier are operating frequency of 2856 MHz, peak power of 300W, pulse width (flat top) of 2.0μs, RF repetition rate of 300 pps. The new RF drive system consists of a medial power klystron amplifier and a medial power modulator. The RF solid-state amplifier drives the first high peak power klystron to amplify the 300Watt of the solid-state amplifier to a level of 8.5 MW. This power will be fed to the first accelerating tube, buncher and prebuncher. Simultaneously, a level of 15 kW from the first klystron is divided into 5 branches to drive other 5 high power klystrons along the new main drive line.

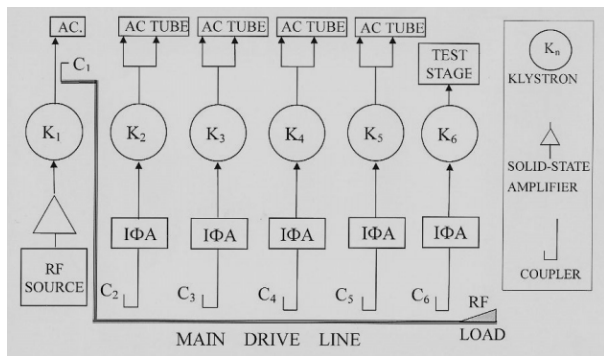

Figure 2: The New RF drive system of 200 MeV LINAC.

Free Electron Laser (FEL) is the only light source with over 20 eV photo energy and GW peak power [3-7], which covers the spectrum from mm wave to x-ray. Linac based FEL requires state-of-the-art performance from the all linear subsystems, especially RF power (within 0.1% shot-to-shot) and phase (less than 1^o rms jitter shot-to-shot and 5^o rms long-term drift). To satisfy such tight criteria, both low-level and high-power RF systems are under evaluation together with development of a precision on-line phase detector system for FEL [8-12].

The high accuracy RF Phase detector is not only necessary for reliable and stable operation of Linac as injector for storage ring [10-13], but also plays one important role in developing future Free Electron Laser system driven by the 200MeV Linac.

In 2003, National Synchrotron Radiation Laboratory, Univ. of Science and Technology of China was awarded

ADAPTIVE FEEDFORWARD CANCELLATION OF SINUSOIDAL DISTURBANCES IN SUPERCONDUCTING RF CAVITIES *

T. Kandil, T.L. Grimm, W. Hartung, H.K. Khalil, J. Popielarski, J. Vincent, R.C. York†
Michigan State University, East Lansing, MI 48824, USA

Abstract: A control method, known as adaptive feedforward cancellation (AFC) is applied to damp sinusoidal disturbances due to microphonics in superconducting RF (SRF) cavities. AFC provides a method for damping internal, and external sinusoidal disturbances with known frequencies. It is preferred over other schemes because it uses rudimentary information about the frequency response at the disturbance frequencies, without the necessity of knowing an analytic model (transfer function) of the system. It estimates the magnitude and phase of the sinusoidal disturbance inputs and generates a control signal to cancel their effect. AFC, along with a frequency estimation process, is shown to be very successful in the cancellation of sinusoidal signals from different sources. The results of this research may significantly reduce the power requirements and increase the stability for lightly loaded continuous-wave SRF systems.

INTRODUCTION

The control of the resonance frequency of SRF cavities is highly desirable in view of the narrow bandwidth of operation. Detuning of SRF cavities is caused mainly by the Lorentz force (radiation pressure induced by high RF field) and microphonics (mechanical vibrations). In continuous-wave (cw) accelerators, microphonics is the major concern. It is natural to think of using fast mechanical actuators to compensate for, i.e., attenuate, the effect of mechanical vibrations on detuning. This concept was applied successfully by Simrock et al [1] to a simple quarter wave resonator (QWR) with a fast piezoelectric tuner. However, the high-gain feedback approach used in [1] is too complex to apply to multi-cell elliptical cavities, which is the subject of this work. In fact, in a previous work by Simrock [2] for elliptical cavities it is stated that "the large phase shift over this frequency range makes it clear that feedback for microphonics control using the RF signal will not be possible with the piezo actuator." To date, there has been no demonstration of microphonics control on multi-cell SRF cavities, and the current paper presents the first such demonstration.

We start by formulating the microphonics control problem from a control theory viewpoint and exploring various standard control approaches. We conclude that AFC is the most appropriate for the task because it handles sinusoidal disturbances, which are the main source of microphonics, it is developed for stable systems, as in the current case, and it does not require an analytic model of the system to design a feedback controller. Then, we review the main elements of the theory of AFC, and present our experimental demonstration of its successful use in microphonics control of elliptical cavities.

PROBLEM FORMULATION AND PRELIMINARY WORK

The starting point is to develop a mathematical model that describes how the mechanical vibrations and the control actuator determine the cavity detuning. It is shown in [3, Section 3.2] that the relationship between the cavity detuning $\Delta\omega = \omega_0 - \omega$ and the phase angle ψ (between the driving current and cavity voltage) can be approximated by a parallel RLC circuit; consequently,

$$\tan\psi = 2Q_L\left(\frac{\Delta\omega}{\omega}\right) \tag{1}$$

where ω is the RF generator frequency, ω_0 is the cavity eigenfrequency, and Q_L is the loaded Q factor, defined by

$$Q_L = 2\pi\cdot\frac{\text{Stored energy}}{\text{Total power dissipation/cycle}}$$

From (1), we see that detuning can be reduced by reducing the phase angle ψ. Towards that end, we develop a model for ψ. Two basic assumptions in developing this model are:

- Mechanical vibrations, which affect the cavity in a distributed way, can be modelled by an equivalent lumped disturbance that affects the system at the same point where the control actuator is applied. In other words, the input to the system can be represented as the sum $u-d$, where d is the disturbance input and u is the control input.
- The system with input $u-d$ and output ψ is linear and time-invariant. Hence, it can be represented by a transfer function $G(s)$ from $u-d$ to ψ.

From a control theory viewpoint, the problem reduces to designing the control u to reject or attenuate the effect of the disturbance d on the output ψ. We started our investigation by examining six different control techniques for disturbance rejection: (1) Proportional (P), (2) Proportional-Integral (PI), (3) Proportional-Integral-Derivative (PID), (4) High-gain band-limited, (5) Servocompensator design, and (6) Adaptive Feedforward Cancellation (AFC). The six techniques were investigated in the internal report [4] using simulation of an experimentally-determined model of a

*This work was supported in part by the Michigan State University Foundation IRGP grant # 3699 and US Department of Energy under grant number DOE DE-FG02-00ER41144.

†T. Kandil and H.K. Khalil are with the Department of Electrical and Computer Engineering, and T.L. Grimm, W. Hartung, J. Popielarski, J. Vincent, and R.C. York are with the National Superconducting Cyclotron Laboratory.

STATUS OF RF CONTROL SYSTEM FOR ISAC II SUPERCONDUCTING CAVITIES

K. Fong, M. Laverty, S. Fang, TRIUMF, Vancouver

Abstract

The rf control system for the ISAC II superconducting cavities is a hybrid analogue/digital system using a self-excited feedback loop. It has undergone more than a year of testing. Improvements have been made to every aspect of the system including phase detection, loop regulation, data acquisition, as well as communication with EPICS. With a loaded Q of 100,000, amplitude regulation bandwidth of 400 Hz and phase regulation bandwidth of 100 Hz have been achieved. Simultaneous operation of 3 cavities under typical ISAC 2 operating conditions has also been demonstrated.

INTRODUCTION

The design of the RF system has been described in several previous papers[1][2]. Based on the experience gained in tests under superconducting conditions, the present system has eliminated some shortcomings in the original design and has incorporated several important improvements. Crosstalk between different feedback paths has been eliminated. This resulted in much improved regulation bandwidth in the phase/frequency loop. A higher dynamic range phase detector is used which enables self-excited operation at both high and low power levels. However, the most important improvements are in the supervisory software, particularly in the area of EPICS communication and multi-thread synchronization.

RF CONTROL SYSTEM

System Model

The transfer function representation of the self-excited system with quadrature control with perfect alignment in static loop phase is given by[3]:

$$\begin{bmatrix}\delta V\\ \delta\Omega\end{bmatrix}=\begin{bmatrix}G_{aa} & G_{ta}\\ G_{a\omega} & G_{t\omega}\end{bmatrix}\begin{bmatrix}\delta v_i\\ \delta v_q\end{bmatrix} \qquad (1)$$

where

$$G_{aa}=\frac{\gamma}{1+\tau s},\qquad G_{ta}=0,$$

$$G_{a\omega}=-\frac{1}{v_i}\frac{\Omega}{(1+\tau s)},\qquad G_{t\omega}=\frac{1}{v_i\tau}\equiv\eta, \qquad (2)$$

$\tau=\dfrac{2Q}{\omega_c}$ is the time constant of the cavity,

$\Omega=\omega-\omega_c$ is the detuning of the cavity, with γ is

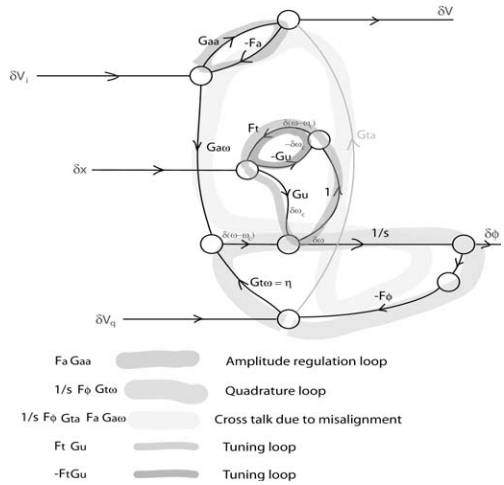

Figure 1: Signal Flow Graph of the Amplitude, Phase and Tuning Loops.

the voltage transformation ratio, ω_c the natural resonance frequency of the cavity and Q the loaded cavity quality factor. Eq. 1 is used to form the signal flow graph of the complete RF control system in Fig. 1, where F_a, F_ϕ and F_t/s are the amplitude, quadrature and tuner feedback coefficients, respectively. The $1/s$ factor from the tuner feedback coefficient arises due to that fact we have implemented velocity feedback in the tuner control. The sensitivity of frequency to tuner movement is given by

$$G_u=\frac{\partial\omega_c}{\partial x} \qquad (3)$$

and depends only on the geometries of the cavity and the tuning mechanism. From the signal flow graph we get the various open loop gains of the feedback system: Amplitude loop gain is given by:

$$G_a=F_aG_{aa}=\frac{\gamma F_a}{1+s\tau} \qquad (4)$$

and phase loop gain is given by:

DIAGNOSTICS FOR THE LOW LEVEL RF CONTROL FOR THE EUROPEAN XFEL

T.Jezynski*, P.Pucyk*, S.Simrock#
*Warsaw University of Technology, Inst. Electronic Systems, Poland, # DESY, Germany

Abstract

One of the most important goal of the diagnostic system is to provide the high reliability. This article describes the concept and the proposal for a diagnostics for the Low Level Radio Frequency system for EU-XFEL. It enables immediate location of faults and understanding of their causes, tests the functionality of LLRF system, tests each of the electronic boards and connections. The diagnostic system checks different LLRF subsystem components. Hardware, software and database aspect of diagnostic system is presented. The main part of this paper is devoted to the hardware and software specification of the diagnostic.

INTRODUCTION

The X -ray free-electron laser EU-XFEL, that is begin planed at the DESY research center will produce high-intensity ultra short X-ray flashes with the properties of laser light. The commissioning of the facility could start in 2012. The total length of the tunnel will be about 2.1 km. The access to the whole electronics placed inside the tunnel will be possible only during the maintenance day (once a month or even more seldom). One of the requirements for the electronic subsystems is the long lifetime and continues work. The LLRF devices will be installed inside the tunnel and exposed on some small level of the radiation. This radiation can cause Single Event Upset (SEU) an active electronic components. Therefore an additional systems redundancy is needed as well as the radiation hardness hardware to ensure the continues work. It is impossible to predict all ways it can fail. Therefore a diagnostic system is needed in order to monitor the hardware and in case of failure switch the system off or run the redundant one. It should also be able to perform offline tests of the device and diagnose the reason of the failure. Because of the scale of the accelerator it is also important to give the information about the placement of the broken part. Due to the complexity of the LLRF system and dependencies between its parts the diagnostic system should monitor as much devices as it is possible. All devices should also provide some hardware and software interfaces through which tests can be preformed. Diagnostic system itself should provide an user interface for experts and operators.

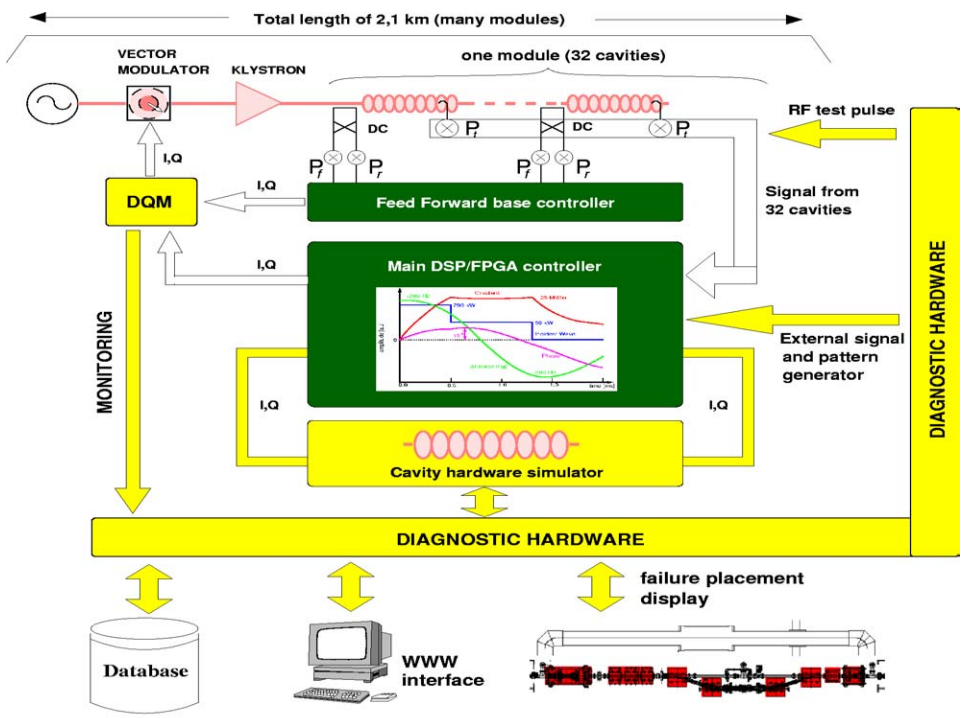

Figure 1: The structure of LLRF and the diagnostic system.

A NEW RF SYSTEM FOR THE CEBAF NORMAL CONDUCTING CAVITIES*

C. Hovater#, H. Dong, A. Hofler, G. Lahti, J. Musson and T. Plawski,
Jefferson Lab, Newport News, VA, USA

Abstract

The CEBAF Accelerator at Jefferson Lab is a 6 GeV five pass electron accelerator consisting of two superconducting linacs joined by independent magnetic transport arcs. CEBAF also has numerous normal conducting cavities for beam conditioning in the injector and for RF extraction to the experimental halls. The RF systems that presently control these cavities are becoming expensive to maintain, therefore a replacement RF control system is now being developed. For the new RF system, cavity field control is maintained digitally using an FPGA which contains the feedback algorithm. The system incorporates digital down conversion, using quadrature under-sampling at an IF frequency of 70 MHz. The VXI bus-crate was chosen as the operating platform because of its excellent RFI/EMI properties and its compatibility with the EPICS control system. The normal conducting cavities operate at both the 1497 MHz accelerating frequency and the sub-harmonic frequency of 499 MHz. To accommodate this, the new design will use different receiver-transmitter daughter cards for each frequency. This paper discuses the development of the new RF system and reports on initial results.

RF SYSTEM

The chopper and separator cavities are both beam deflecting cavities. In the case of the chopping cavities two orthogonal modes (Q_L 11,000) are excited in a single copper structure, with mode isolation being greater than 40 dB. The electron beam is chopped and then "de-chopped" after the beam has been modified. The separator cavities use a TEM dipole mode (Q_L 2500) that can deflect multiple beams [1]. The field control requirement for these cavities is relatively undemanding at 1% and 1 ps rms amplitude and phase control. In the case of the chopping cavities, the amplitude is rarely changed, but in the case of the separator, amplitude is adjusted to reflect the deflection needed for different beam energies. In both cases phase is adjusted upon initial start up of the accelerator and then tweaked as needed. Therefore the RF system can be rather simple.

Figure 1 shows a block diagram of the low level RF control system (LLRF). This architecture has become the common model for single cavity control LLRF systems, with 4 RF inputs and 2 RF outputs utilizing a modern large field programmable gate array (FPGA). We have chosen the VXI platform for both convenience and its RFI/EMI properties. The system utilizes a mother - daughter board with the FPGA on the motherboard and the daughterboard hosting the RF hardware and analog to digital converters (ADC) and digital to analog converters (DAC) for both the receiver and transmitter. The motherboard will also be used in other applications at CEBAF such as a cavity BPM [2].

The RF system down converts the cavity frequencies (499 MHz and 1497 MHz) to an IF of 70 MHz. This allows us to use the local oscillator (LO) and IF signals that are already distributed around CEBAF. The receiver IF signals are then quadrature demodulated using harmonic under sampling (56 MHz clock). The transmitter output is a single IF output at 70 MHz where the quadrature components are digitally recombined inside the FPGA [3]. The signal is then filtered and up converted to the cavity frequency. Both forward and reflected powers are also monitored. The control system is a digital generator driven resonator (GDR), using a basic proportional and integral (PI) algorithm for field control [4]. All adjustable parameters such as gain, phase and gradient are embedded in the FPGA.

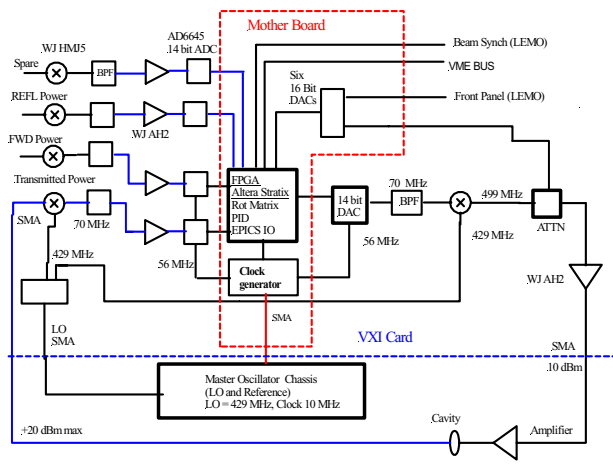

Figure 1: RF system block diagram.

Receiver/Transmitter

The receiver/transmitter mates as a daughterboard to a VXI motherboard. FET mixers (WJ HMJ5) were chosen because of their linearity (IP3 ~ 40 dBm) and high dynamic range. To minimize amplitude drifts a product called Thermopads is being considered (an attenuator product with selectable tempcos). This will allow us to offset any temperature induced amplitude drifts in the RF signal path. A commercial IF filter was chosen for its low group delay ~ 80 ns. In addition, a gentle lumped-element band pass filter designed to remove most of the out-of-band noise precedes the ADC. By including this we reclaim 1-2 bits of dynamic range in the ADC. The fast ADCs (AD6645) and a dual DAC (AD 9767) are included on this card. Because isolation between channels is also a

*This work was supported by DOE contract No. DE-AC05-84ER40150.
#hovater@jlab.org

A LONG-PULSE MODULATOR FOR THE TESLA TEST FACILITY (TTF)

W. Kaesler, Puls-Plasmatechnik GmbH, Feldstr.56, D-44141 Dortmund, Germany

Abstract

TESLA will be a TeV-Energy Superconducting Linear Accelerator where superconducting (sc) 9-cell Niob-cavities with field gradients of more than 25MV/m will be the key elements. For the TESLA Test Facility (TTF) "long-pulse"-klystron modulators must generate 1.6 ms output pulses with an output power up to 20 MW which is flat to within 1% during 1.5 ms. The main goal of the development at PPT is to optimize the existing modulator design towards a reliable and cost-effective design to allow for a industrial series production of pulse modulators for sc-accelerator operation.

Based on the first design of Fermilab [1] the main features of the redesigned new pulse modulator sub-assemblies are: 1) a compact 300-kW/12-kV switched mode power supply; 2) a volume optimized 1.4-mF storage capacitor bank using high energy capacitors with self-healing segmented PP-foil technology; 3) a rugged , compact solid-state switch stack with seven 4.5-kV IGCT`s, integrated gate units and a current turn-off capability up to 4 kA; 4) a solid-state crowbar switch assembly based on light-triggered high current thyristors replacing the ignitron tubes.

INTRODUCTION

The TESLA cavities will be used in the linac cryo-modules of the TTF2-Free Electron Laser (FEL) project, further for the 35-GeV-linac, driving the European X-ray FEL at DESY and the planned electron-positron linear collider TESLA. One important characteristic number of sc-cavities is the 'quality factor' Q. Q_{sc}-values > 10^{10} exceed the Q-values of conventional normal conducting cavities by more than 10^5. This high Q_{sc}-values increase the filling time of cavities; the TESLA-cavities with an operating frequency of 1.3 GHz need a filling time of more than 0.5 ms. With a required rf-flattop of up to 1.0ms the TESLA rf-source must generate ms-pulse lengths.

In the TTF-project different accelerator subsystems are under test. For the rf-generation different types of 1.3-GHz-klystron tubes are in operation: A 5-MW conventional single beam klystron TH2104, a special developed 10-MW multibeam klystron TH1801 from THALES and at the end of 2004 alternative multibeam klystrons from CPI and Toshiba.

Tab. 1 shows some features of the THALES-klystron.

Table 1: Technical data of "Long-pulse" klystrons

Klystron		TH2104	TH1801
		max	max
Klystronperveance	$AV^{-1.5}$	2,0E-06	3,4E-06
Number of beams		1	**7**
Cathode Voltage	kV	130	120
Anode Current	A	92	140
Impedance	kOhm	1,41	0,86
Input Power	MW	11,96	16,80
Efficiency (min)	**%**	42	60
Output Power	MW	5,0	10,1

TTF MODULATOR

HV-Power Supply

To operate the TTF-klystron modulators the HVPS´s must be able to deliver an electrical peak power up to17 MW with a dc-output voltage up to 12 kV. The load is a 1.4-mF capacitor bank with a storage energy up to 100 kJ - which must deliver periodically current pulses up to 1700 A and pulse lengths up to 1.6 ms. The maximum droop of the the capacitor voltage is about 16 % which must be recharged by the HVPS. The pulse repetition rate may vary in steps from 0.1 to 10 Hz. This operation modus requires a rms-power of about 300 kW. To run large numbers of modulators this units mustbe operated in "constant-power-mode" in order to minimize the generation of low-frequency disturbances on the mains. An essential HVPS-part to achieve this constant power mode is a fast intelligent regulating system which has been developed at DESY.

Pulse Generator

The pulse generator is a solid-state-switched capacitor discharge which will be droop-compensated by an appropriate L-C-ringing circuit (bouncer) [1]. The main components of the pulse generator are: The storage capacitor bank, the crowbar switch, the solid-state high power switch, the droop-compensating bouncer circuit, the undershoot circuit and the backup switch.

PPT tries to reduce the construction efforts and to minimize costs focussing on components widely used in industrial applications.

The main redesigned sub-assemblies of the new, improved pulse generator are:

A volume optimized storage capacitor bank using self-healing Polypropylen capacitors; a rugged, compact12-kV IGCT-switch stack with a 4-kA current turn-off capability and a 100-kA solid-state crowbar switch with light-triggered thyristors.

SUPERSTRONG ADJUSTABLE PERMANENT MAGNET FOR A LINEAR COLLIDER FINAL FOCUS

T. Mihara, Y. Iwashita, Kyoto University, Kyoto, Japan
M. Kumada, NIRS, Chiba, Japan
C. M. Spencer, SLAC, CA, USA
E. Sugiyama, NEOMAX, Osaka, Japan

Abstract

A superstrong permanent magnet quadrupole (PMQ) is one of the candidates for the final focus lens for the linear collider because of its compactness and low power consumption. The first fabricated prototype of our PMQ achieved a 300T/m superstrong field gradient with ϕ100mm overall magnet radius and ϕ7mm bore radius, but a drawback is its fixed strength. Therefore, a second prototype of PMQ, whose strength is adjustable, was fabricated. Its strength adjustability is based on the "double ring structure", rotating subdivided magnet slices separately.

This second prototype is being tested. Some of the early results are presented.

INTRODUCTION

A 4.45T high magnetic field has been demonstrated with just permanent magnets. It is based on the modified Halbach's configuration, which introduces some saturated iron to enhance the field strength [1,2]. This technique has been applied to a quadrupole to generate a high gradient (see Fig. 1). The first prototype was fabricated and tested [3]. This PMQ, which is compact and strong, is good to use as the final focus lens in a linear collider because the outgoing beam from the interaction point passes very close to the final focus lens (separated by only 7cm).

The remanent field strength of a permanent magnet changes with temperature. NdFeB, which is used for the PMQ has a relatively large temperature coefficient. A special temperature compensation alloy, MS-1, was added to the core to cure this problem. Then the temperature coefficient decreased from -7×10^{-4} to -3×10^{-5} [4,5].

DOUBLE RING STRUCTURE

The final focus lens for the linear collider needs a strength-adjustable quadrupole with 1% adjustment steps. A method for varying the strength is to divide the magnet into sections along the beam axis and rotate the sections separately [3, 4, 5]. Any section is rotated only by 90° so as not to introduce any skew multipoles.

Because mechanical errors in rotation may introduce unwanted skew components and a shift in the magnetic field axis (i.e. the magnetic center where the field is zero), we extended this technique into a "double ring structure" (Fig. 2). The inner region of a PMQ has a larger influence on its field quality in the bore than its outer region. If we split a PMQ into two nested concentric rings and rotate only the outer ring or parts of it, to change the total strength, while the inner ring is fixed, then, we supposed, the skew component would be reduced, and also any shift of the quad's magnetic axis. We confirmed this by calculations and computer modeling [4].

We fabricated a second prototype of a PMQ with a double ring structure. This prototype also has the temperature compensation material. We will make long term measurements to confirm these features.

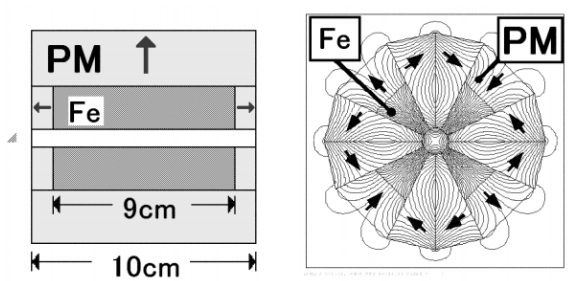

Figure 1: The first prototype of the PMQ.

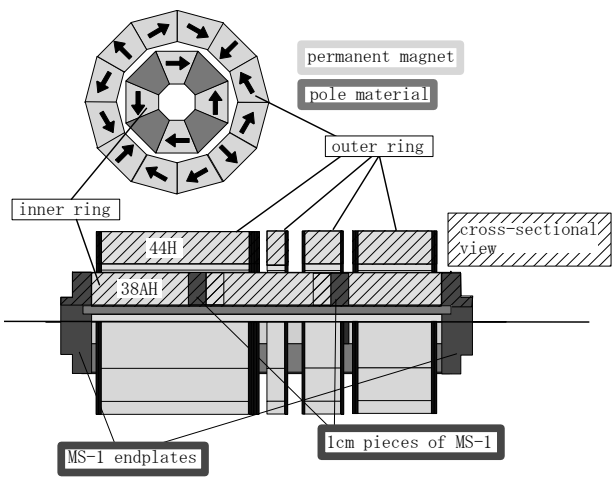

Figure 2: The double ring structure.

SECOND PROTOTYPE OF THE PMQ

Figure 3 shows the second prototype of a PMQ, with the "double ring structure" and hence adjustable. The outer rings are rotated by worm gears powered by DC motors [6]. The design parameters are shown in Table 1. The pole material is Permendur. Four poles are welded onto two endplates made of MS-1, which compensates for the NEOMAX strength variation with temperature [4]. Considering that the maximum length of a permanent magnet piece that can be fabricated is about 5cm, three

LOW ENERGY BEAM TRANSPORT USING SPACE CHARGE LENSES

O. Meusel, A. Bechtold, J. Pozimski, U. Ratzinger, A. Schempp, H. Klein,
Institut für Angewandte Physik der Johann Wolfgang Goethe Universität,
Robert-Mayer-Str. 2-4, D-60054 Frankfurt am Main, Germany

Abstract

At the frontend of an accelerator the transversal focusing suffers from high space charge forces. Space charge lenses (SCL) provide strong cylinder symmetric electrostatic focusing by a confined nonneutral plasma. The density distribution of the enclosed space charge is defined by the enclosure conditions in transverse and longitudinal direction. For a homogeneous charge density distribution the resulting electrostatic field and therefrom the focusing forces inside the space charge cloud are linear. Additionally, in case of a positive ion beam, the space charge of the confined electrons causes compensation of the ion beam space charge forces.
To study the capabilities of a Gabor double lens system to match an ion beam into an RFQ a testinjector was installed at the IAP and put into operation successfully. Beam profiles and emittance measurements as well as measurements of the beam energy and energy spread have already been performed and show satisfactory results and no significant deviation from the theoretical predictions. To investigate the beam focusing of bunched beams using this lens type at beam energies up to 500 keV a new high field Gabor lens was built and installed behind of the RFQ.

THEORY

The focal strength of a SCL is determined by the spatial space charge density distribution. The space charge density distribution is a function of the transversal and longitudinal enclosure conditions [1,2]. Gabor showed [3] for a radial confinement by a magnetic field, that in absence of external electric fields, the transversal enclosure condition is given by the Brillouin flow [4] and therefrom the maximum electron density can be calculated by:

$$n_{e,rad} = \frac{\varepsilon_0}{2m_e} B_z^2 \qquad (1)$$

The upper limit for the longitudinal enclosure can be calculated by the space charge potential of a homogeneous cloud of radius r_A, which has to be smaller then the anode potential V_A, resulting in:

$$n_{e,l} = \frac{4\varepsilon_0 V_A}{e r_A} \qquad (2)$$

Both of these relations solely overestimate the space charge density significantly. Additionally the longitudinal enclosure condition is drastically influenced by thermalization of the enclosed particles and therefrom due to losses of fast particles in the Maxwellian tail. By measurement of the focal length the average electron density can be determined. Applying the thin lens approximation for a homogeneously space charge filled cylinder the average electron density is given by:

$$\frac{1}{f} = \frac{r'}{r_0} = k^2 \cdot l = \frac{\bar{n}_e \cdot e}{4\varepsilon_0 \cdot W_B} \cdot l \qquad (3)$$

(refraction power k, divergence angel r´, beam radius r_0 and energy W_B, the length of the space charge cloud l, focal length f). The length of the cloud can be estimated by the distance between the two grounded electrodes (see fig. 5). Introducing the radial and longitudinal filling factors [5] $\kappa_{r,l}$ [$0 \leq \kappa_{r,l} \leq 1$] and using Eq. (1),(2) and (3) the trapping efficiency can be expressed by:

$$\kappa_r = \frac{\bar{n}_e}{n_{e,r}} \quad ; \quad \kappa_l = \frac{\bar{n}_e}{n_{e,l}} \qquad (4)$$

THE HE^+ - TEST INJECTOR

A test injector to study the matching of a space charge dominated ion beam into an RFQ has been constructed and installed at IAP. The schematic layout of the experiment is shown in figure 1.

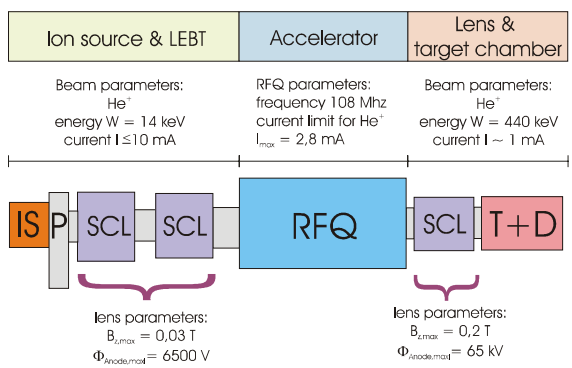

Figure 1: Schematic drawing of the experimental set up.

RESULTS OF THE MAGNETIC FIELD MEASUREMENTS OF THE DTL QUADRUPOLE MAGNETS FOR THE J-PARC

E. Takasaki#, F. Naito, H. Tanaka, K. Yoshino, KEK, Tsukuba, Japan
T. Ito, JAERI, Tokai, Japan
H. Ino, Z. Kabeya, S. Kakizaki, T. Kawasumi, MHI, Nagoya, Japan

Abstract

A quadrupole electromagnet is installed in the drift tube, which has an outer diameter of 140 mm and its minimum length of 53 mm. Hence, a coil of this magnet was made by the advanced periodic reverse copper electroforming method (PR-method) instead of the conventional hollow conductor. 149 quadrupole electromagnets were completed and then installed in the drift tube within a high accuracy. The magnetic field measurements have been carried out by a rotating coil at each stage of the manufacturing process of the drift tube. The discrepancies between the magnetic field center and the mechanical center are within about ± 25 μm after installation of the quadrupole magnet inside the drift tube. Recently, drift tubes have been aligned into 9 unit-tanks. This paper describes results of the magnetic field measurements and summarizes results of the drift tube alignments in the unit tanks.

INTRODUCTION

The Alvarez-type drift tube linac (DTL) accelerates the H^- ion beams from 3 MeV to 50 MeV. It consists of the three tanks (DTL-1, DTL-2 and DTL-3), of which the length is about 9 m. Each tank is composed of three short unit tanks. The inner diameter of the tank is 560 mm.

The 149 drift tubes, in which an electromagnetic quadrupole magnet (Q-magnet) is installed, are aligned into DTL precisely within the required accuracy. The specifications of all the Q-magnets in the DTL are given in Table 1 with the size of the drift tube.

Now all the magnets have been completed and installed into the drift tubes (DT). All the drift tubes have been aligned into the 9 unit tanks within the high accuracy of ± 50 μm, which was determined from requirement of the beam dynamics. The first tank (DTL-1) accelerates the H^- ion beam from 3 MeV to 19.7 MeV, successfully.

CONSTRUCTION OF QUADRUPOLE

Since the resonance frequency of the DTL is 324 MHz, the size of the DT becomes smaller. The pulsed Q-magnet is selected to suppress deformation of the DT by the released heat of the coil. Hence, as a coil, the electroformed hollow coil [1-3] has been developed at KEK. Furthermore, beam dynamics requires that the deviation of the quadrupole center from the mechanical center should be within ± 50 μm. Hence, we decided on ± 25 μm as a tolerable deviation of the magnetic field center from the mechanical center of the Q-magnet and the DT. Figure 1 shows some components for the Q-magnet.

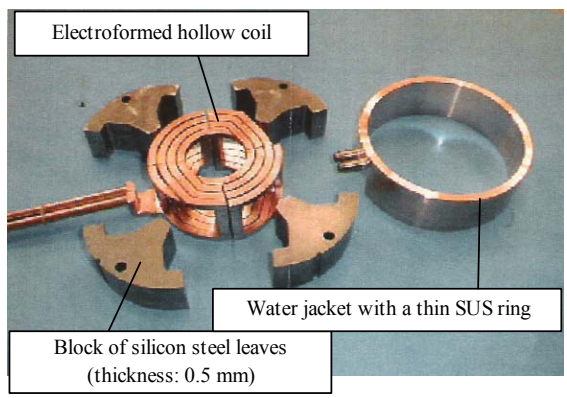

Figure 1: Components for the Q-magnet

Especially, the water jacket with a thin SUS ring has been used to fasten four long blocks together with thermal shrinkage of a water jacket.

The magnetic field of the Q-magnet has been measured by a rotating coil to investigate if the deviation of the magnetic field center from the bore center would be within the required accuracy. The measured results are shown in Figure 2. As seen in the Fig. 2, the discrepancies of all the magnets are within ± 25 μm.

Table 1: Specifications of all quadrupoles in the DTL

DTL tank	DTL-1					DTL-2		DTL-3
DT Nos.	1 to 6	7 to 23	24 to 56	57	58 to 77	78	79 to 121	122 to 149
Type of Q-mag.	A type	B type	C type		D type		E type	F type
Outside diameter of Q-mag./ DT (mm)	115/140	115/140	115/140	115/140	115/140	115/140	115/140	115/140
Core length (mm)	33	35	50	76	80	80	90	125
Bore diameter (mm)	15.6	16	16	21	21	25	25	29
Number of magnets	6	17	33	1	20	1	44	28
Inside diameter of beam pipe (mm)	13	13	13	13|18	18	22	22	26

#eiichi.takasaki@kek.jp

SPECTROGRAPHIC APPROACH TO STUDY OF RF CONDITIONING PROCESS IN ACCELERATING RF STRUCTURES

H. Tomizawa[1], T. Taniuchi[1], H. Hanaki[1], Y. Igarashi[2], S. Yamaguchi[2], A. Enomoto[2]
Accelerator Division, Japan Synchrotron Radiation Research Institute (SPring-8)
1-1-1 Kouto, Mikazuki-cho, Sayo-gun, Hyogo 679-5198, Japan[1]
High-Energy Accelerator Research Organization (KEK)
1-1 Oho, Tsukuba, Ibaraki 305-0801, Japan[2]

Abstract

The acceleration gradient of a linac (linear accelerator) is limited by rf breakdown in its accelerating structure. We applied an imaging spectrograph system to study the mechanism of rf breakdown phenomena in accelerating rf structures. Excited outgases emit light during rf breakdown, and the type of outgases depend on surface treatments and rinsing methods for their materials. To study rf breakdown, we used 2-m-long accelerating structures and investigated the effects when high-pressure ultrapure water rinsing (HPR) treatment was applied.

We performed experiments to study the outgases under rf conditioning with quadruple mass spectroscopy and imaging spectrography. As a result, we were able to observe instantly increasing signals at mass numbers of 2 (H_2), 28 (CO), and 44 (CO_2) but not 18 (H_2O) just after the rf breakdown. We also conducted spectral imaging for the light emissions from atoms in a vacuum that are excited by rf breakdown. Without HPR, we observed atomic lines at 515 nm (Cu I), 622 nm (Cu II), and 711 nm (C I). With HPR, 395 nm (O I), 459 nm (O II), 511 nm (Cu I), 538 nm (C I), 570 nm (Cu I), 578 nm (Cu I), 656 nm (H I), and 740 nm (Cu II) were observed.

INTRODUCTION

Recently, rf structures have become necessary for higher-gradient acceleration. A range of contaminants and micron-sized particles may remain on the surface following different treatments. Those contaminants are field emitters, and outgassed due to the rf breakdown in rf structures. The lower the outgassing rates and the fewer the contaminating particles, the lower the breakdown rate.

It has been reported that the high-pressure ultrapure water rinsing (HPR) technique is very effective in improving the field gradients for normal conducting and superconducting rf structures [1]. This is because HPR treatment eliminates particle contamination on the surface, which is thought to be one of the causes of field emission.

To study rf breakdown, we applied this technique to the S-band 2-m-long disk-loaded accelerating structure. Microsecond-pulsed rf power (average accelerating field of 45 MV/m at maximum) was fed into these rf structures.

We performed experiments using quadrupole mass spectroscopy and imaging spectrography of atomic lines to study outgassing from the surface of rf structures. This imaging spectrograph system is useful for observing irreproducible phenomena such as rf breakdown, even for non-ultra-high vacuum conditions. Condensed gas and electrons play important roles in triggering the formation of aggressive plasma that acts against the copper surface. In our work, excited neutral and ionized gases in this plasma were observed as atomic lines in the real accelerating structures. Additionally, to reduce outgas rate, we applied chemical etching for rf pill-box-type single cavity (rf gun). With this treatment, we could achieve 206 MV/m of the maximal surface field.

EXPERIMENTAL SETUP

Tested accelerating structure

We performed experiments using the high-power test stand at KEK. We chose two S-band 2-m-accelerating structures which were prepared with the following fabrication processes:

A. A high-precision turning lathe with a diamond byte machined the disks and cylinders.
B. The electroplating fabrication method was applied to fix the disks and cylinders together.
C. HPR was applied to the assembled accelerating structure.

Note that these accelerating structures have a crescent-shaped cut opposite the waveguide iris (see Figure 1) to correct the asymmetry of the electromagnetic field.

For comparison, we prepared two different treated accelerating structures with and without HPR treatment (process C). One of the accelerating structures, while moving vertically (60 mm/min) and rotating (6.5 rpm), was rinsed by a nozzle-equipped pipe that jets high-pressure ultrapure water under optimal conditions.

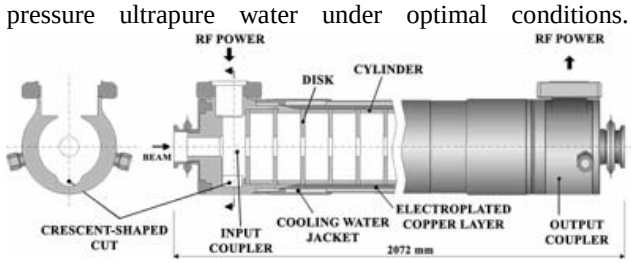

Figure 1: Schematic drawing of the accelerating structure

J-PARC LINAC ALIGNMENT

Masanori Ikegami, Fujio Naito, Hirokazu Tanaka, Kazuo Yoshino, Chikashi Kubota, Eiichi Takasaki
KEK, Tsukuba, Ibaraki 305-0801, Japan
Takatoshi Morishita, Hiroyuki Ao, Takashi Ito, Naoki Nakamura, Akira Ueno, Kazuo Hasegawa
JAERI, Tokai, Ibaraki 319-1195, Japan

Abstract

J-PARC lianc has the total length of more than 400 m including the beam transport line to the succeeding synchrotron. In this paper, planned schemes for the linac alignment is presented together with instrumentation for the long-term ground-motion watching.

INTRODUCTION

J-PARC linac has the total length of more than 400 m including the beam transport line to the succeeding RCS (Rapid Cycling Synchrotron) [1, 2]. In high-current proton accelerators, precise alignment of accelerator components is indispensable to reduce uncontrolled beam loss and beam-quality deterioration. It is of essential importance to achieve precise alignment and to maintain its long-term accuracy for realization of the high-power proton beams.

Although we originally planned to develop a laser-based alignment system for J-PARC linac [3], we totally revised the alignment scheme to reduce construction cost and R&D burden. Main difficulty in the original system was the avoidance of the effect of air-turbulence on the measurement. It was also anticipated to be difficult to use the system for continuous observation of the alignment, because its silicon-photo-diode sensors are supposed to be vulnerable to radiation damage. In the revised system, the emphasis is put on the continuous watching of the ground motion as well as the accuracy of the initial alignment. In this paper, the revised alignment scheme for J-PARC linac is described.

ALIGNMENT GOALS

Tolerances for the transverse displacement from the design axis, Δx and Δy, the longitudinal displacement from the adjacent elements Δz, and the roll error, θz, are listed in Table 1. These tolerances are not margins for the alignment procedure, but include various errors in the machining and assembling procedures of a component. The requirement for the transverse displacement of quadrupole magnets, including DTQ (Drift Tube Quadrupole), is especially severe to avoid orbit distortion and resulting emittance growth. However, it has been confirmed that a gradual deflection of the alignment axis is tolerable, and the tolerance for the monotonous deflection is around 0.05 mm/10 m.

INITIAL ALIGNMENT

Link to the Global Survey

Before the commencement of the accelerator alignment, we need to know the relative position of the linac building with the other J-PARC buildings. To this end, we set up a metrological network on the ground which covers the whole J-PARC facility. It also has a few GPS (Global Positioning System) measurement points to link with a global coordinate system. Because the metrological network is set up on the ground level, we need to have access holes to the linac accelerator tunnel (that is located at 13.5 m underground) to introduce the coordinate. We have three access-holes to the linac accelerator tunnel from the ground level (klystron gallery). Just below the access-holes, we have three "primary reference points" for the linac tunnel, which will be the starting points of the linac tunnel survey. Through the access-holes, the height reference of the whole J-PARC facilities is also introduced into the linac tunnel.

Alignment Reference on the Components

The horizontal and longitudinal alignment are planned to be performed with a laser-tracker. Although a laser-tracker can be used for the vertical measurement, we plan to use a digital level (Leica DNA03) for the vertical alignment to improve the accuracy [4, 5]. As a back-up scheme for the horizontal alignment of straight sections, we are preparing a stretched-wire method with capacitive wire-position sensors (Fogale nanotech WPS2D). In addition, we will use an alignment-telescope (Taylor-Hobson 112/2582) in prealignment of the accelerator elements. The rotation about the beam axis will be avoided with a digital inclinometer (Wyler Minilevel NT). To enable these alignments, each accelerator element has "alignment reference bases" which are standardized for J-PARC accelerators. The alignment base is a stainless steel plate which has a standardized reference hole at the center of its top surface. The position of the reference hole is adjusted to a certain position with respect to the beam axis before the installation of the component. Various targets, including a CCR (Corner Cube Reflector) for a laser-tracker, an optical target for an alignment telescope, a leveling staff for a digital level, and a capacitive wire-position sensor, can be mounted on the reference base via dedicated attachments with precise position reproducibility. Figure 1 shows an example of these attachments, in which a drawing of a wire-position-sensor holder for DTL and SDTL tanks is shown. To attain the precise position reproducibility, we use a preside attach/detach sys-

COUPLER DEVELOPMENT AND GAP FIELD ANALYSIS FOR THE 352 MHz SUPERCONDUCTING CH-CAVITY*

H. Liebermann, H. Podlech, U. Ratzinger, A. Sauer,
Institut für Angewandte Physik, Frankfurt, Germany

Abstract

The cross-bar H-type (CH) cavity is a multi-gap drift tube structure based on the H-210 mode currently under development at IAP Frankfurt and in collaboration with GSI. Numerical simulations and rf model measurements showed that the CH-type cavity is an excellent candidate to realize s.c. multi-cell structures ranging from the RFQ exit energy up to the injection energy into elliptical multi-cell cavities. A 19-cell, beta=0.1, 352 MHz, bulk niobium prototype cavity is under fabrication at the ACCEL-Company, Bergisch-Gladbach. This paper will present detailed MicroWave Studio [1] simulations and rf model measurements for the coupler development of the 352 MHz superconducting CH-cavity. It describes possibilities for coupling into the superconducting CH-cavity. First results of the measurements of different coupler concepts, e.g. capacitive and inductive coupling at different positions of the CH-cavity are reported.
Additionally the rf quadrupole content in CH-type gaps was investigated quantitatively.

INTRODUCTION

Present H-mode structures are all operated at room temperature. Many future accelerator projects require cw operation. But the achievable gradients of room temperature cw operated H-mode cavities are limited due to power losses and cooling problems. The superconducting CH-cavity can be realized in the frequency range from 150 to 800 MHz, the beam energy can be chosen between 5 AMeV and 150 AMeV which corresponds to a β-range from 0.1 to 0.5. The CH-structure can be used for proton as well as for heavy ion beams. The superconducting version seems to be quite attractive for high current proton linacs like XADS [2] or deuteron linacs like IFMIF [3].

SUPERCONDUCTING (SC) STRUCTURES

In sc cavities there is no cooling problem as in cw operated rt (room temperatur) linacs. In general, sc linacs can be operated at higher gradients above a certain duty factor. On the other hand, at low duty factors and high beam currents rt structures are very favourable because they are less expensive and can tolerate dark current contributions. To demonstrate the capabilites of the CH-DTL, it is foreseen to test a sc CH cavity prototype. A design and engineering study has been performed in close cooperation with industry[1]. This study shows the feasibility of the production of superconducting CH cavities. The cavity production started in 2003 and the delivery is expected in October 2004 [4]. The CH protoype with 19 gaps will be made of

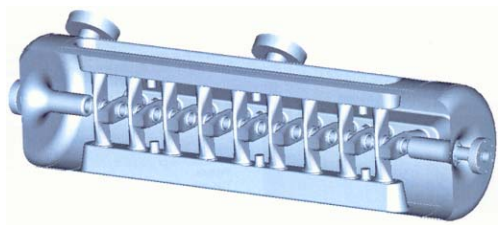

Figure 1: The sc 352 MHZ CH prototype with matched end cell geometry.

bulk niobium, the diameter is 28 cm, the length is 105 cm. At an operation frequency of 352 MHz, this corresponds to a particle β of 0.1. One important issue during the design phase was the minimization of the electric and magnetic peak fields to reduce the risk of field emission and of thermal break down. An accelerating gradient of 4 MV/m results in an electric peak field of 26.4 MV/m and in a magnetic peak field of 30 mT which is a moderate value.

Table 1: Main design parameter of the s.c. prototype CH-cavity

β	0.1
Frequency [MHz]	352
Diameter [m]	0.28
Tank length [m]	1.05
$R_a/Q[\Omega]$	3220
E_p/E_a	6.59
B_p/E_a [mT/(MV/m)]	7.29
$Q_0(R_s = 150n\Omega)$	$3.7 \cdot 10^8$

METHODE FOR THE EXTERNAL Q VALUE

For calculation of the external Q value, we use the method described by Balleyguier [5]. If a lossless cavity is weakly coupled to an infinite line, this line drives out a certain RF power P and the energy stored in the cavity gradually decreases. The external Q then is:

$$Q_{ext} = \omega W/P.$$

If we assume, that the line mode is a TEM and the dielectric is vacuum: $\eta^2 = \mu/\epsilon$. Then, the external Q can be

* Supported by GSI Darmstadt, EU and by BMBF, contr. no. 06F134I
[1]ACCEL Company, Bergisch Gladbach, Germany

TECHNOLOGIES OF THE PERIPHERAL EQUIPMENTS OF THE J-PARC DTL1 FOR THE BEAM TEST

K. Yoshino#, C. Kubota, E. Takasaki, E. Kadokura, F. Naito, H. Tanaka, T. Kato, Y. Fukui, KEK, Tsukuba, Japan
T. Ito, JAERI, Tokai, Japan

Abstract

First beam test of the DTL1 was performed in November of 2003 at KEK site. A 30-mA H^- beam was successfully accelerated from 3 to 19.7 MeV. In order to accomplish the successful beam test, various peripheral equipments were developed: the electrode plates for connecting the hollow-conductor coil and the power cable were developed since quadrupole electromagnets are built in all DTs (77 sets) of the DTL1 [1], the water-cooled multiconductor copper tubes (Control Copper Tube) were used as the power cable from the electrode plates to power supplies, and the interlock system assembled by PLCs (Programmable Logic Controller) was also prepared for the surveillance of many cooling channel.

INTRODUCTION

High Energy Accelerator Research Organization (KEK) and Japan Atomic Energy Research Institute (JAERI) are together constructing the high intensity proton accelerator at Tokai site, which is called Japan Proton Accelerator Research Complex (J-PARC) Project. We are conducting the beam test of the first tank of DTL (DTL1) at the Proton linac test facility at KEK site. A negative hydrogen beam was accelerated to its design value of 19.7 MeV. A peak current of 30 mA was achieved with almost 100 % transmission at a 12.5 Hz repetition rate in a 20-microsecond pulse width [2].

It is required for the beam test that the wiring from the power supply to the quadrupole magnet (Q-magnet) copes with the following technical subjects:

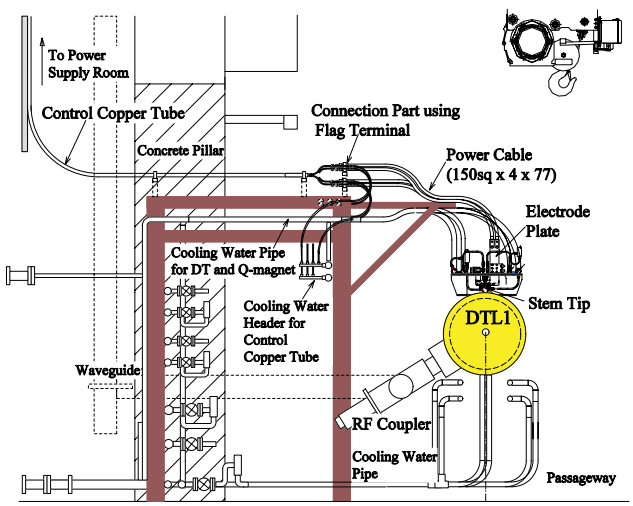

Figure 1: Schematic drawing of the wiring in the tunnel.

1) Suppressing cable vibration with the pulse excitation of the Q-magnet.
2) Design of the electrode which connects the power cable and the Q-magnet in small installation space.
3) Assembling procedure of the electrode in order to minimize the effects on the position of the stem. (Because the electrode can push the stem, it may shift the position of the drift tube.)
4) The performance test of the busduct which is intended to use mainly as the power cable in Tokai site.
5) Construction of a local interlock system for errors in the magnet power supplies, the cooling water system and the vacuum pump controllers.

Investigated results for these subjects are described in the following sections.

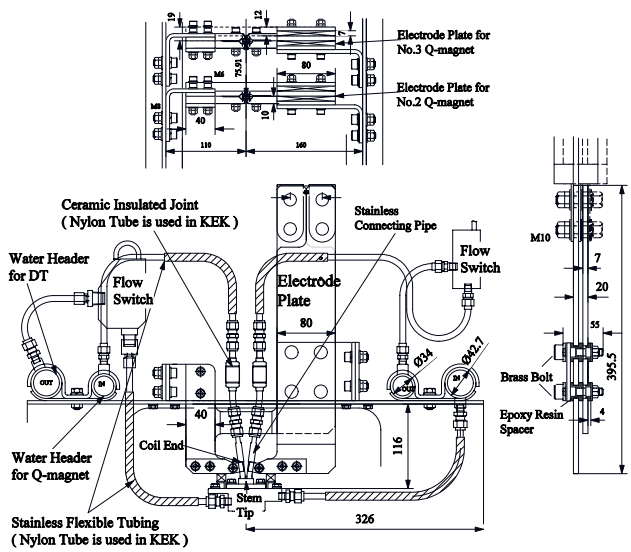

Figure 2: Schematic drawing of the connection part between the power cable and the electrode at the top of the stem.

WIRING COMPONENTS

Schematic drawing of the wiring in the tunnel at kek is shown in Fig. 1. All magnets were wired by the cables which satisfy the pulse excitation specification (Max. 1000 A, 50 Hz). Therefore wiring was done after the confirmation test that the effects of the pulse vibration of those cables were negligible for the DT alignment.

#kazuo.yoshino@kek.jp

CLIC MAGNET STABILIZATION STUDIES

S. Redaelli*, R. Aßmann, W. Coosemans, G. Guignard,
D. Schulte, I. Wilson, F. Zimmermann. CERN, Geneva, Switzerland.

Abstract

One of the main challenges for future linear colliders is producing and colliding high energy e^+e^- beams with a transverse spot size at the collision point in the nanometre range ("nanobeams"). The Compact LInear Collider (CLIC), presently under investigation at CERN, aims at colliding e^+e^- beams with a vertical spot size of 0.7 nm, at a centre-of-mass energy of 3 TeV. This requires a vertical stability to the 1.3 nm level for the 2600 linac quadrupoles and to the 0.2 nm level for the two final doublets at either side of the interaction point. In the framework of the CLIC Stability Study, it has been demonstrated for the first time that CLIC prototype quadrupoles can be stabilized to the 0.5 nm level in a normal working area on the CERN site.

INTRODUCTION

The Compact LInear Collider (CLIC) study [1] at CERN is investigating the feasibility of building an e^+e^- linear collider with centre-of-mass energies up to 5 TeV, at a luminosity of 10^{35} cm^{-2}s^{-1}. High luminosities will be achieved by colliding opposing e^+e^- beams with transverse spot sizes of $\approx 60 \times 0.7$ nm^2 (horizontal$\times$vertical), which imposes tight tolerances on the stability of the focusing quadrupoles. The CLIC tolerances for a 2 % luminosity reduction for uncorrelated RMS displacements above 4 Hz are summarized in Table 1 for the 2×1300 linac quadrupoles and for the 2×2 final focus quadrupoles [2]. The SLC experience has shown that beam-based feedback systems can efficiently compensate *slow* motions up to $\approx 1/25$ of the pulse repetition frequency [3] (100 Hz for CLIC). *Fast* vibration above ≈ 4 Hz must then be mechanically stabilized to ensure the required luminosity performance. To achieve the ambitious CLIC stability goal, it is not possible to rely only on the stability of a given site because the natural ground stability is strongly increased by the accelerator environment (pumps, ventilation, cooling water, ...). This was demonstrated by vibration measurements at LEP [4], where the motion was increased from 0.2 nm to more than 20 nm. Dedicated stabilization technologies must therefore be developed to meet the requirements of future linear colliders.

In the last years, the magnet stabilization problem has attracted the interest of various high-energy physics laboratories and universities worldwide. At CERN, a CLIC stability study was started in 2001 [5] to investigate the feasibility of colliding nanometre-size beams in CLIC in a realistic accelerator environment. Following the encouraging results obtained in stabilizing low-energy nanobeams for electron transmission microscopy [6] and in various other domains, the CLIC study pursued the approach of using state-of-the-art stabilization devices to find out what level of magnet stability could be achieved by using the presently available technology from industry (see Fig. 1). This report summarizes the experimental achievements obtained from January 2001 to December 2003.

Table 1: Tolerance on the uncorrelated RMS motion above $f_{\min}$ of the CLIC quadrupoles for a 2 % luminosity loss

Magnet type	N_{magnet}	$f_{\min}$	I_x	I_y
Linac	2600	4 Hz	14.0 nm	1.3 nm
Final focus	2	4 Hz	7.8 nm	0.2 nm

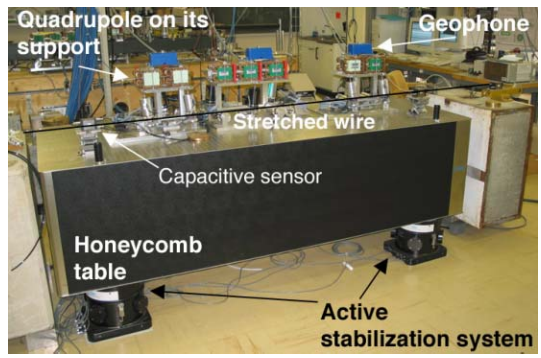

Figure 1: Photograph of the CLIC stability study test stand, with the detail of a geophone installed on a quadrupole.

THE CLIC TEST STAND

Basic notation

Vibration measurements are performed with high-resolution *geophones*, which measure vibration velocities versus time. The employed sensors have a sub-nanometre resolution in the 4 Hz to 315 Hz range (e.g., 0.28 nm resolution on the RMS motion above 4 Hz). Detailed comparisons with several other vibration devices [7], indicate an error of 10 % on the geophone calibration provided by the manufacturer. Here, the basic notation for data analysis is briefly reviewed. The vibration velocity, $v(t_n)$, is measured at the discrete times $t_n = n\Delta t$, with $n = 1, 2, ...N$ ($\Delta t = 0.001$ s). The power spectral density of the displacement, $P(f_k)$, is defined for the discrete frequencies $f_k = \frac{k}{N\Delta t}$ as:

$$P(f_k) = \frac{N\Delta t^3}{2\pi^2 k^2} \left| \sum_{n=1}^{N} v(n) e^{-2\pi i \frac{kn}{N}} \right|^2 . \qquad (1)$$

The integrated RMS displacement induced by vibrations

* Work done in the framework of a PhD program at the University of Lausanne, CH, High Energy Physics Institute (UNIL-IPHE).

STATIC ABSOLUTE FORCE MEASUREMENT FOR PRELOADED PIEZOELEMENTS USED FOR ACTIVE LORENTZ FORCE DETUNING SYSTEM

P. Sekalski, A. Napieralski, DMCS, Technical University of Lodz, Poland
S. Simrock, L.Lilje, DESY, Hamburg, Germany
A. Bosotti, R. Paparella, F. Puricelli, INFN, Milan, Italy
M. Fouaidy, IN2P3, Orsay, France

Abstract

To reach high gradients in pulsed operation of superconducting (SC) cavities an active Lorentz force detuning compensation system is needed. For this system a piezoelement can be used as an actuator (other option is a magnetostrictive device). To guarantee the demanded lifetime of the active element, the proper preload force adjustment is necessary. To determine this parameter an absolute force sensor is needed which will be able to operate at cryogenic temperatures. Currently, there is no calibrated commercial available sensor, which will be able to measure the static force in such an environment. The authors propose to use a discovered phenomenon to estimate the preload force applied to the piezoelement. The principle of the proposed solution based on a shape of impedance curve, which changes with the value of applied force. Especially, the position of resonances are monitored. No need of specialized force sensor and measurement in-situ are additional advantages of proposed method.

INTRODUCTION

For the X-Ray Free Electron Laser (XFEL) and for the TeV Superconducting Linear Collider (TESLA) a tuning system is developed. Its main goal is to keep the internal resonance frequency of the cavity constant. Perturbations in cavity shape have two main sources. One of them is a microphonics and another is a Lorentz force [1÷3].

One tuning system was designed to compensate both effects. Moreover, it is integrated with the existing step motor system, used for cavity pretuning [1]. The tuning system consists of the frame in which two piezo elements (PEs) are assembled. One of them works as a dynamic force sensor, while the second one as an actuator. PE devices are identical, hence there is possible to use them as a sensor or an actuator or use both as actuators.

The PEs must work during each pulse, thus the proper lifetime must be guaranteed. For ten years working period without any breakdown with repetition rate up to 20Hz more than 10^{10} cycles is foreseen. The PEs might reach such a lifetime, only if they are properly preloaded. From literature and manufacturers datasheets of piezostacks, one might conclude that the best preload is around a half of the blocking force. For our case the blocking force is 3kN, hence the preload should be set between 1,0kN and 1,5kN. Unfortunately, an access to PE is only possible during module assembly but mentioned preload ought to be reached at the cryogenic temperature (CT) - below 2K and low pressure (several mBars). The precise preload force adjustment becomes difficult task due to the complexity of system and the different thermal coefficient of expansion (TCE) of used materials. Also during changing the pressure additional forces appears. As a consequence it is very hard to calculate or estimate the preload force change during cooling down and pumping. Even if a proper approximation will be done, there is need to verify the result. Therefore an absolute force measurement is needed. Currently, a commercial-use absolute force sensor for temperature below 10K does not exist.

The authors propose to use one of two observed effect caused by applied force: either a capacitance change of PE or a impedance resonances shift of the PE. The detailed information about performed experiment is presented in following chapters.

Currently, five types of PEs are investigated in three institutes (DESY, INFN, IN2P3). The devices come from five different manufacturers: EPCOS (PZT/Nd34), PI Ceramics (PICMA), PiezoMechanik (PSt150/10/60), NOLIAC (Pz27 and Pz29) and Piezo JENA (#9222). The EPCOS PE has been tested for 2 years; the others are quite new ones. As a consequence this publication will focus mainly on the EPCOS PE.

Four types of experiment were done. Firstly, the resonances were measured at room temperature (RT); secondly the characteristic of the PEs was investigated at CT. Then, the calibration was used to determine the preload force in real system in CHECHIA cryostat. At the end, the capacitance change due to the applied force at RT is presented.

ROOM TEMPERATURE EXPERIMENTS

The electrical impedance was first measured at RT, during PE classification. The impedance resonances were the parameters, which were investigated.

Each PE was characterized individually. It was assembled in series with a piezoresistive force sensor - model 8415-6002 from BURSTER Company. At the top of the fixture there was a screw to adjust the force applied to devices. The stiffness of the frame was more than 10 times higher than stiffness of PE.

The impedance was measured using a dynamic Signal Analyzer (SR785) for frequency range from 50Hz up to 100kHz.

IMPROVEMENTS OF RF CHARACTERISTICS IN THE SDTL OF THE J-PARC PROTON LINAC

S. Wang*, IHEP, P.O.Box 918, 100039, Beijing, China
T. Kato, KEK, Oho, Tsukuba-shi, Ibaraki-ken, 305-0801, Japan
V.V.Paramonov, RAS/INR, Moscow, Russian Academy of Sciences Institute for Nuclear Research

Abstract

A separated drift tube linac (SDTL) was adopted as an accelerating structure of Japan Proton Accelerator Complex (J-PARC), which follows the DTL. The SDTL of J-PARC consists of 32 five-cell short tanks, ranging from 1.5 to 2.5 m in length. A design of frequency tuners of the SDTL was performed by taking account of 3-D field distribution calculated with MAFIA. The effects of stems on the resonant frequency and field distribution were also analyzed. An easy and effective compensation method for perturbation by stems of both end cells was proposed and applied to the SDTL tanks.

INTRODUCTION

An Alvarez drift-tube linac (DTL) is widely used for accelerating low-energy proton beams. It is a complicated and sophisticated structure since drift-tubes contain focusing magnets. A separated-type drift-tube linac (SDTL) was proposed [1] as an accelerating structure for the medium-energy region because of both high shunt impedance and ease of construction. Higher shunt impedance can be realized by eliminating focusing devices from drift tubes. Instead, the focusing elements are placed between two adjacent SDTL tanks. Since one of the merits of the SDTL structure is simplicity of both rf properties and mechanical issues in construction, any kinds of stabilizing devices (post couplers or multi-stems) are not usually installed. Thus, the number of cells in a tank is also important from the viewpoint of rf stabilization.

The SDTL was adopted as the accelerating structure of J-PARC linac [2], which connects the DTL and the ACS. The SDTL of J-PARC consists of 32 short five-cell tanks. A normal unit cell in the tank consists of an accelerating gap, two tubes of half-size and two half stems. Table 1 shows the parameters of the SDTL tank.

Table 1. Parameters of SDTL tank for J-PARC

Frequency	324 MHz
Tank diameter	520 mm
Drift tube diameter	92 mm
Stem diameter	36 mm
Cell length	0.29– 0.51m
Tank length	1.47 – 2.56m
Energy	50 – 190 MeV

As the first constructed SDTL linac in the world, the tuner of the SDTL was designed based on the detailed calculation by using MAFIA. The special attention should be taken for both end cells, where there is no half stem on the end plate usually. An easy and effective compensation method for the perturbation of the stem to the accelerating field was studied by the simulations.

*Email: wangs@ihep.ac.cn

THE DESIGN OF THE TUNER

The Positions for Installing Tuners

As shown in Table 1 for J-PARC, the maximum length of SDTL tanks is 2.56 m, and the number of the tuner is expected within three. Fig.1 shows the sketch of a five-cell SDTL tank and the candidate positions for tuners in the longitudinal direction.

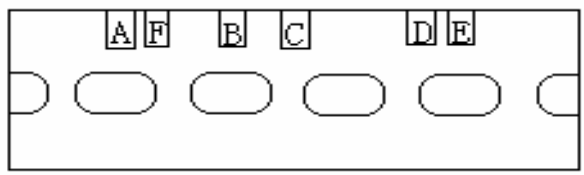

Figure 1: The sketch of a five-cell SDTL tank and the candidate positions (A~F) for tuner in the longitudinal direction.

In case of adopting 3 tuners, there are two choices for the distribution of tuners in the longitudinal direction. One choice is installing in the positions of F, C and D, in which C is in the center of the tank, and F and D are at L/4 from the both end plates respectively, with L the length of the tank. In this case, the distribution of the tuner is uniform in longitudinal direction, but all the tuners are not located in the center of the tube, where is the most effective tuning position. The other choice is installing in the positions of A, B and E, with A, B and E the center of the drift tube, but in this case three tuners are not regularly distributed in the longitudinal directions. To decide the distribution of the tuner, the simulations were made by MAFIA, for investigating the difference of the tuning efficiency among different positions. For all SDTL tanks, the diameter of the tuner was chosen as 90 mm.

Fig. 2 shows the simulated frequency shift of one tuner with different insertion length for different positions in the 97-MeV tank. For the insertion length more than 5 cm, the tuner positioned at A is much more effective than tuners positioned at the other two places. The power losses on the tuner surface at different positions were almost equal.

According to the simulation results, the tuners should be positioned at the position of the center of the drift tube in longitudinal direction. In case of installing three tuners,

COMPACT ELECTRON-LINAC DESIGN CONCEPT FOR A GAMMA RAY SOURCE

K. C. Dominic Chan, Bruce E. Carlsten, Gregory E. Dale, Robert W. Garnett, Hugh C. Kirbie, Frank L. Krawczyk, Steven J. Russell, Thomas P. Wangler, LANL, Los Alamos, NM87545, USA
Edward Wright, CPI, Palo Alto, CA 94303, USA

Abstract

Gamma-ray sources, particularly sources that are easily transportable, are in high demand for different applications. We have carried out a review of commercially available electron-linac-based sources, and have investigated alternative compact electron-linac systems that use updated technologies compared with sources that are available commercially. As a result, we propose to develop a new source using an electron linac operating at 17-GHz. It uses a klystron, instead of a magnetron, and an IGBT-switched HV power supply. The source design takes advantages of the advances in X-band linac technology and solid-state HV technology. The higher frequency and upgraded technologies offer smaller size, lighter weight, better efficiency, easier operation, and higher reliability, compared with commercially available linacs. In this paper, we will describe the source design and our choice of technologies.

REQUIREMENTS OF AN ELECTRON-LINAC-BASED GAMMA-RAY SOURCE

For most applications, an electron-linac-based gamma-ray source is required to produce a dose rate up to 1500 cGy/min on axis one meter away from the source. The electron beam energy is typically between 6-10 MeV. The exact dose rate and energy will depend on the specific application and material to be penetrated. A pulsed linac is usually needed to allow for beam-off time for data acquisition. The typical pulse format is a repetition rate of 50 Hz, a 10-μs pulse length, and a nominal peak current of 70 mA. For some applications, a compact system is also required. A compact system provides transportability, ease of radiation shielding, and low cost. Ease of use and reliability will also be important.

STATUS OF TECHNOLOGY

We have carried out a study of electron-linac-based sources and associated technologies. The results are summarized in a report [1] and this paper is a summary of that report.

Presently, commercially available electron-linac-based gamma-ray sources are derived from medical linac technology. Such sources usually consist of a Linac Subsystem, a RF Subsystem, an HV Subsystem, and a Support Subsystem for cooling, vacuum, and control. The general features of presently available gamma-ray sources include:

- A S-band (3 GHz) linac
- Powered by magnetrons
- High-voltage modulated by a pulse-forming network (PFN) and a HV transformer
- Limited flexibility in energy and pulse format
- Dimensions of each component about a few feet on each side
- Weight of each component about 500-1000 pounds; with total weight about 1800 pounds.

AN GAMMA-RAY SOURCE WITH IMPROVED TECHNOLOGY

In our study, we concluded that using an electron linac at 17 GHz, a klystron as the RF source, and a solid-state Marx generator as modulator can make an improved electron-linac-based gamma-ray source. By updating the technology in these three aspects, the system will improve in efficiency, reliability, flexibility, size, weight, and cost. In this section, we will describe the subsystems using these updated technologies.

Linac Subsystem

The nominal parameters of the Linac Subsystem are given in Table 1. The linac will operate at an optimum frequency of 17 GHz. A higher-frequency linac operating at 17 GHz offers many advantages over the currently available S-band linacs because linac performance improves with linac frequency. The copper loss is reduced by a factor of 2.3. The linac is less prone to RF field breakdown with the breakdown limit higher by the same factor. The structure radius decreases linearly with frequency, resulting in a structure weight reduction by a factor of 25.

Table 1: Nominal Parameters of a Linac Subsystem

Linac frequency (GHz)	17
Beam energy (MeV)	8
Beam current (mA)	68.2
Beam Power (kW)	545
Structure power (kW)	1170
Total power required (kW)	1715
Length of structure (cm)	25
Acceleration gradient (MeV/m)	32
Diameter of structure (cm)	2.7
Number of cells	55
Ratio of mode spacing to mode width	3.2
Shunt impedance (MΩ/m)	219
Unloaded quality factor	5725
Cell to cell coupling coefficient	0.048

Our investigation shows that 17 GHz is nearly the optimum linac frequency for this application. Frequencies higher than 17 GHz, even better in linac efficiency, may lead us to linac operation with multiple RF-structure modes [2], and consequently unstable

RESULTS OF A 3D-EM-CODE COMPARISON ON THE TRISPAL-CAVITY BENCHMARK

P.Balleyguier CEA/DPTA Bruyères-le-Châtel, France

Abstract

Several 3D electromagnetic codes (MAFIA, CST MicroWave-Studio, Vector-Fields Soprano, Ansoft HFSS, SLAC Omega3P) have been tested on a 2-cell cavity benchmark. Computed frequencies and Q-factors were compared to experimental values measured on a mock-up, putting the emphasis on the effect of coupling slots. It comes out that MAFIA limitations due to the staircase approximation is overcome by all other codes, but some differences still remain for losses calculations in re-entrant corners.

INTRODUCTION

Up to recent times, we mainly used the MAFIA code to design cavities for particle accelerators applications in Bruyeres-le-Chatel. Despite of its proper quality, the meshing method used by this software introduces a "staircase" approximation causing some artifacts on calculated results. In many cases, a proper choice of the mesh grid and a proper post-processing permit to get rid of these artifacts (see for example [1]).

To correct the artifacts, the first step is to start from an accurate 2D simulation, and in a second step, to take into account every 3D aspect of the structure: coupling holes, tuning plungers, RFQ vane ends, pumping grids... Their effect can be estimated individually with a fair accuracy by the comparison of two simulations using an identical mesh, with and without each considered 3D aspect. This method gives good results for global structure parameters (frequency resonance, Q-value, R/Q, external Q), but can be difficult to apply for local parameters such as local losses or peak fields. And, of course, it can only be applied on "2D-like" structures.

Because of these limitations, and to take advantage of computer and software evolutions, we considered to change our tool, and compared on the same benchmark MAFIA and four other 3D EM codes (fig. 1):

- Microwave Studio 4.3 (CST)
- Soprano (Vector Fields)
- High Frequency Structure Simulator 9.0 (Ansoft)
- Ω3p (eigen mode solver developed at SLAC)

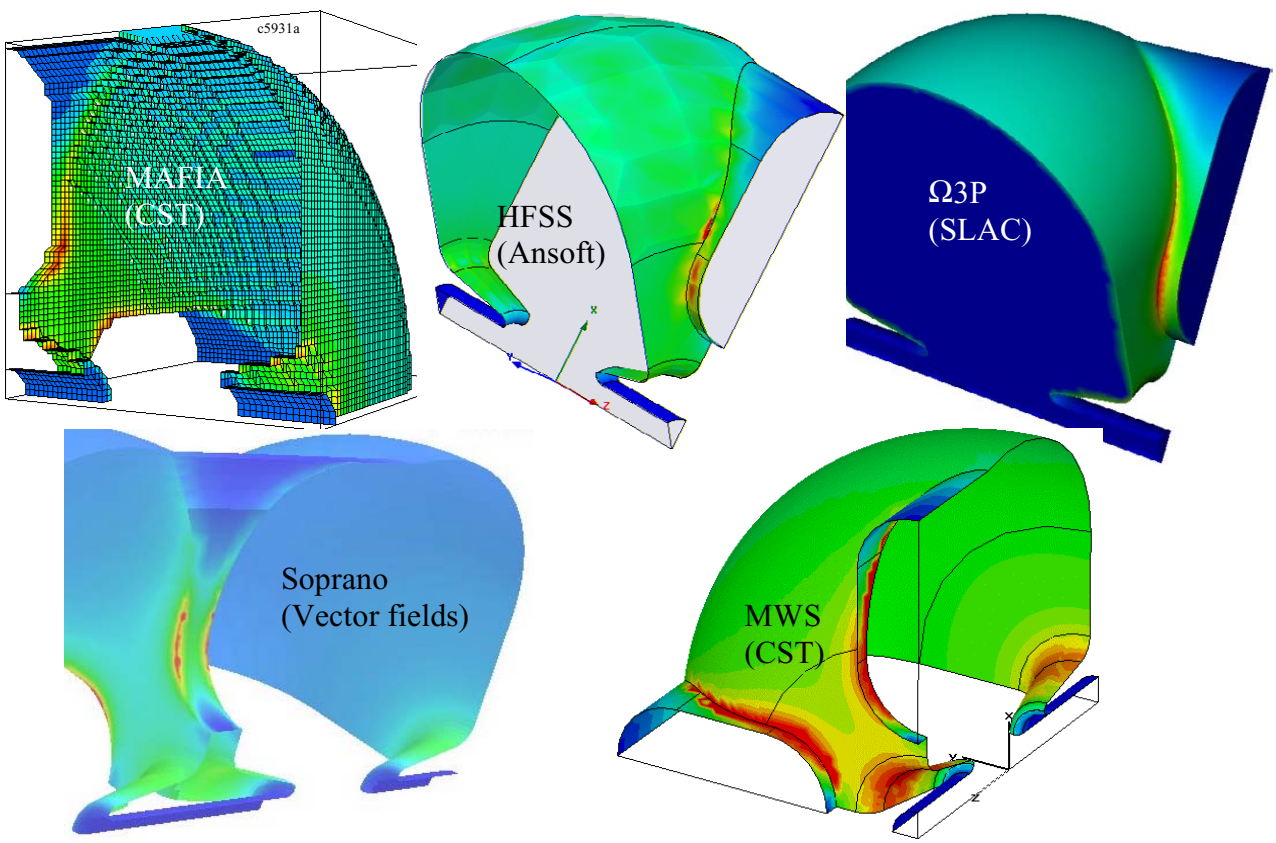

Figure 1: Losses in Trispal benchmark for tested 3D-codes (pi-mode).

PARALLEL PARTICLE IN CELL COMPUTATION OF AN ELECTRON GUN WITH GdfidL

W. Bruns, WBFB, Berlin, Germany *

Abstract

The paper describes an efficient algorithm to integrate the equations of a fast moving charge cloud of small size in a large electron gun. Particle in cell computation of a realistic electron gun is challenging due to the large discrepancy between the size of the cavity and the size of the cloud. A fine grid must be used to resolve the small volume of the charge, with a grid spacing in the order of 0.1 mm. The cavity has extensions of about 100 mm. Therefore one has to deal with about 1000 million gridcells. Such a large grid is handled best with parallel systems. Each node of the parallel system computes the electromagnetic field in its subvolume. As the extension of the charge keeps being small during the flight, at each timestep the charged particles will be located in only a few subvolumes of the nodes of the parallel system. This would lead to a strong load imbalance, if the particle related computations for each particle would be performed by the node where the particle is in. GdfidL instead spreads the data of most particles over all processors, which then perform the particle related computations, and send back the results to the processors where the particles are in.

THE PHOTO GUN

The resonator has a diameter of 10cm, and the height of the most interesting part of the gun is about 10cm. At the bottom of the gun, a charge with a diameter of 3mm is emitted via a laser-pulse. The duration of the pulse is so short, that the emitted charged cloud has a length of 5 mm. Because the gradient in the gun is about 100 MV/m, the emitted charge is accelerated very rapidly to relativistic velocities. The size of the charge cloud therefore stays small.

The geometry itself is rotational symmetric, and the charge ideally would be rotational symmetric. To investigate what effect an offset of the laser pulse from the axis would have, one needs to perform a three dimensional computation, without any planes of symmetry.

Because the charge has an extension in the order of 3 mm, one needs a gridspacing of 0.1 mm or less. Because we want to resolve small effects due to a small deviation from a rotational symmetric case, we want to compute with a homogeneous grid, minimising dispersion errors and reflections due to an inhomogeneous grid. This leads to a total number of gridcells in the order of 1000 millions. A naive implementation of the FDTD-algorithm would then require about 50 GBytes of RAM. Such large grids are best handled by clusters of PCs.

* bruns@gdfidl.de

DOMAIN SUBDIVISION

The computational volume is partitioned in many more subvolumes than the number of available processors. Each subvolume is inspected, whether it is filled only with electric conducting material. The fully electric conducting subvolumes are discarded and the remaining ones are spread evenly over the processors. This way, each processor has about the same number of interesting gridcells to compute the fields in, leading to a good load balancing for the field computation.

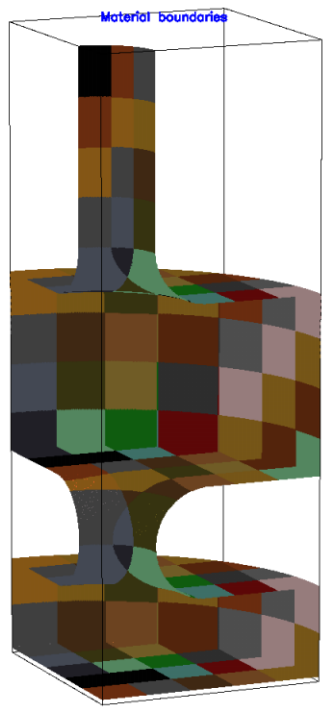

Figure 1: A model of the gun. The grid spacing is 0.1 mm. The total number of gridcells in this quarter of the total volume is 212 millions. Less than 40% of the computational volume is filled with vacuum cells. The different colours indicate the used subvolumes. The shown volume is partitioned in 325 subvolumes, of which 167 are discarded, since they do not have a single vacuum cell. A naive implementation of FDTD in this quarter of the volume would require 10 GBytes of RAM. GdfidL uses 4.3 GBytes, spread evenly over the available processors.

Local Field Computation

Each processor computes the electromagnetic fields in its local subvolumes. The tangential electric and magnetic fields of the neighbour volumes are boundary conditions

EVALUATION OF MAGNETIC FIELD ENHANCEMENT ALONG A BOUNDARY

Y. Iwashita, ICR, Kyoto Univ., Kyoto, JAPAN
T. Higo, KEK, Tsukuba, JAPAN

Abstract

Only the high electric field gradient on boundaries has been thought to cause sparking in a cavity, and designers have been taking much attention on avoiding sharp edges in such an area to reduce peak electric field gradient. Recently, not only the electric field but also magnetic field on an edge can cause the spark problem through heating up of the very local surface material by concentration of the magnetic field density. The effects were numerically evaluated through a simplified model.

INTRODUCTION

There are three requirements for the accelerator structure of the main linac of the linear collider GLC/NLC[1]:

1) high gradient (50MV/m),
2) suppression of wake field and
3) low cost in mass production.

The first two items are of concern in the present paper. The second requirement was proved to be met by the DDS (Damped Detuned Structure) that can suppress the long wake field [2]. In order to meet the first requirement, the design parameters have been evolved for a few years to date to adopt low group velocity and high phase advance features [3]. The resultant recent shape of the relevant constituent disk is shown in Fig. 1.

It was known that the magnetic field that crosses a ridge-like geometry was enhanced at the ridge. The enhanced field results in a huge temperature rise within a pulse (see Fig. 2). Typical example was described in [4] where copper surface with low electric field but high magnetic field was cracked and/or eroded identified after numerous number of breakdowns near the ridge. Considering these, we designed and fabricated the HDDS disks, which does not have any area where severe magnetic field enhancement did not appear. In the present paper are described the enhancement characteristics relevant to this HDDS disks. Understanding the sensitivities on relevant parameters and proper tolerance setting is very important to pursue the structure mass production stably in an inexpensive manner.

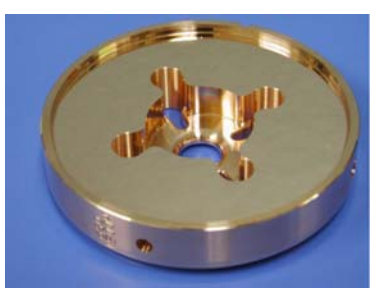

Figure 1: The HDDS cell.

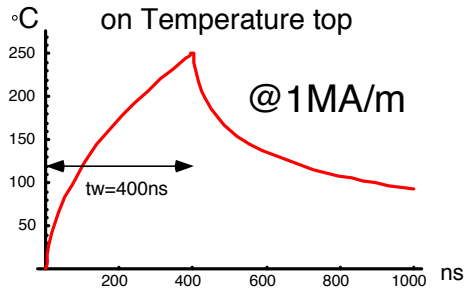

Figure 2: Pulse temperature rise on a flat copper surface where the pulse surface current is 1MA/m and the duration is 400ns. The temperature value should be scaled with the square of the surface current. A reference value of a surface current for a 2D cell without a local enhancement is 0.2MA/m, which reaches 1MA/m when the enhancement factor at a convex corner is 5. This temperature rise becomes more at a convex corner, where a heat capacity is less.

SURFACE CONFIGURATION

As seen in Fig. 3, there are two areas, shown in red, where magnetic field is naturally large. The first is the opening from accelerator cell to HOM manifold. The second is located at each slot, which is needed to extract HOM dipole filed to manifold. From these features, the enhancement at these two areas is inevitable. We evaluated on these geometries.

The assumed geometry is a parallel cut into the outer diameter of a pillbox. The width of the opening and the edge angle are the important parameters. The very edge of the opening is assumed to be rounded by 5 microns reflecting to the fact that these disks are chemically etched by about 3 microns in the fabrication stage so that the similar amount of rounding, 5-micron radius, is assumed at the very edge.

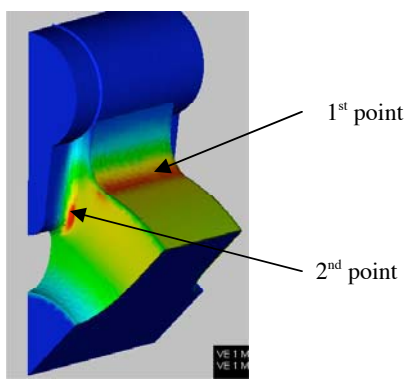

Figure 3: Magnetic field distribution on the surface.

MECHANICAL STABILITY SIMULATIONS ON A QUARTER WAVE RESONATOR FOR THE SPIRAL II PROJECT

H. Saugnac, G. Olry, S. Blivet, J.L. Biarrotte, S. Bousson, T. Junquera, M. Fouaidy, IPN Orsay, CNRS/IN2P3, France

Abstract

In the framework of the SPIRAL II project, IPN Orsay is studying a 88 MHz beta 0.12 super conducting quarter wave resonator prototype. Due to its low RF bandwidth (around 60 Hz) the resonator must have a very high mechanical stability and have small sensitivity to dynamic mechanical loads. To simulate the effects of geometrical deformations on the fundamental RF frequency a three dimensional analysis is required. The simulations were made by coupling mechanical FEM analysis performed in COSMOS/GEOSTAR© with the RF electromagnetic FEM code MICAV© integrated in the COSMOS/GEOSTAR© interface.

Static mechanical loads were first studied to reduce the effects of external pressure on the RF frequency shift and evaluate the tuning sensitivity of the cavity. Then, simulations of the dynamic response of the resonator, using the modal superposition analysis method, with random external pressure variations and harmonic excitation of the cavity were performed.

This paper presents the results of the simulations and mechanical solutions chosen to increase the cavity RF frequency stability.

NUMERICAL CODES AND METHODS

Numerical simulations where performed with the finite element codes COSMOS/GEOSTAR© for the mechanical study and MICAV/EMW© for the RF frequency simulations. MICAV© being integrated in COSMOS© it is possible, after some data treatments on the input and output files, to create a shell mechanical model and a solid RF model with corresponding meshing patterns. RF frequency perturbations are then computed without numerical interpolation [2].

Dynamic simulations are performed using the modal superposition analysis method [3] where the overall response of the structure is the sum of a set of modal responses for specific loading and boundary conditions.

Each mode *i*, considered as a single freedom degree element, has the harmonic stationary relative response :

$$u_i(t) = \frac{1}{2\xi_i\sqrt{1-\xi_i^2}} \cdot X \cdot \sin(\omega_i t + \pi/2)$$

Assuming, for small displacements, proportionality between RF frequency shift, and cavity wall deformation:

$$\Delta f_i \approx \left(\frac{\Delta f}{u}\right)_i \cdot u_i = K_i \cdot u_i$$

K_i is computed with COSMOS/GEOSTAR© and MICAV©.

For a combination of harmonic excitations having the same phase, and amplitude X_j and pulsation Ω_j once have the overall response :

$$\Delta f\ (t) \approx \frac{1}{N}\sum_j\sum_i H(h_{i,j}) \cdot X_{i,j} \cdot K_i \cdot \sin(\Omega_j t + \varphi_{i,j})$$

$$H(h_{i,j}) = \sqrt{\frac{1}{(1-h_{i,j}{}^2)^2 + 4\cdot\xi_i{}^2\cdot h_{i,j}^2}} \quad \& \quad \varphi_{i,j} = \arctan\left(2\xi_i \cdot \frac{h_{i,j}}{1-h_{i,j}^2}\right)$$

$$\xi_i = \frac{1}{2Q_i} \qquad \& \qquad h_{i,j} = \frac{\Omega_j}{\omega_{0i}}$$

Q_i being the modal mechanical quality factor.

$X_{i,j}$ is the harmonic excitation amplitude.

For harmonic acceleration of amplitude γ_j or harmonic displacement of amplitude Z_{mj} once have:

$$X_{i,j} = \frac{\gamma_j}{\omega_i^2} \qquad \text{or} \qquad X_{i,j} = h_{i,j}^2 \cdot Z_{mj}$$

STATIC ANALYSIS

Simulations on static changes of cavity geometry were performed to stand cavity and cold tuning system design parameters. The tuning sensitivity was calculated at various positions on the external cavity body in order to optimise the ratio between the tuning sensitivity and the mechanical stiffness.

Static pressure variation effects as well as cool down and chemical etching induced frequency shift are presented in table 1 for two studied models (figure 1).

Table 1: Static frequency shifts numbers

	Model I	Model II
Tuning. Sens.	~ 15 kHz/mm	~ 15 kHz/mm
Tuning stiffness	~ 15 kN/mm	~ 15 kN/mm
Pressure. Sens.	-5.5 kHz/bar	-4.5 kHz/bar
Chemical etching sens.	~ -5kHz/0.1mm	~ -5kHz/0.1 mm
Therm. sens. @4K	~150 kHz	~150 kHz

These data will give a first evaluation of the design frequency target and the overall tuning range taking into account the manufacturing incertainities that will be measured on a first prototype planed for October 2004.

SOME ESTIMATIONS FOR CORRELATION BETWEEN THE RF CAVITY SURFACE TEMPERATURE AND ELECTRICAL BREAKDOWN POSSIBILITY

V.V. Paramonov, INR, 117312 Moscow, Russia

Abstract

The electrical breakdown in accelerating cavities is the complicated phenomenon and depends on many parameters. Some reasons for breakdown can be avoided by appropriate vacuum system design and the cavity surface cleaning. This case for normal conducting accelerating cavities free electrons - the dark currents due to Fowler-Nordheim emission can be considered as the main reason of possible electrical breakdowns. It is known from the practice the combination of the high electric field at the cavity surface with high surface temperature is the subject for risk in the cavity operation. In this paper the dependence of the dark current density on the surface temperature is considered and effective electric field enhancement is discussed.

INTRODUCTION

As it is well understood now, the electron current, emitted from the rf cavity surface, is one reason for electrical breakdown. When the electron current reach some threshold value, the sparking and further breakdown take place.
The investigation of electron emission is a special branch of technical physics and a lot of researchers worked in this field. Extensive special bibliography exists related to the investigation of emitting surface parameters on the emitting current. The systematic review one can find in [2] with related references.
The purpose of this report is not to find new relationships - just, referring to the well known in the emission study effects, estimate the influence of the surface temperature in normal conducting cavities on the dark current emission.

ELECTRON EMISSION

The electron emission from metals is quantum tunneling effect through potential barrier. The probability of the electron tunneling depends on both the barrier parameters - width, height - and the electrons energy state. Several physical processes can change the electron energy state - the external electric field, the temperature of material, the external photons. The quantitative description of electron emission, taking unto account all processes, is very complicated and just under simplifications we can obtain some analytical conclusions.
The electron field emission has been explained in [1] for the limiting case $T_c = 0^o K$,

$$j_0(E_s) = \frac{A(\beta E_s)^2}{\phi} exp(-\frac{B\phi^{3/2}}{\beta E_s}), \qquad (1)$$

where E_s is the surface electric field, in $\frac{MV}{m}$, ϕ is the work function of the material, in eV ($\phi = 4.47eV$ for copper), $A = 1.54 \cdot 10^6 \frac{eVA}{(MV)^2}$, $B = 6830 \frac{MV}{m(eV)^{3/2}}$, β is the ratio of local field at the emitter to the average surface field E_s. For the case of very high electric fields it can be corrected [3] as:

$$j_0(E_s) = \frac{A(\beta E_s)^2}{\phi} exp(-\frac{B\phi^{3/2}}{\beta E_s})(1 - \frac{5\beta E_s}{18B\phi^{(3/2)}}). \quad (2)$$

Anyhow, both (1) and (2) are obtained in the assumption of absolute zero material temperature. The estimations of the material temperature influence were done in [4] and extended in [5]. The parameter with temperature dimension is the inversion temperature T_i, K^o, related with the external field strength E_s as:

$$T_i = \frac{0.567 E_s}{\sqrt{\phi}}. \qquad (3)$$

Emitting electrons can either absorb the heat from thee emitter ($T_i > T_c$), or generate it, if ($T_i < T_c$) - Nottingham effect. The inversion temperature T_i is the linear function of the external electric field E_s and, to estimate values, $T_i = 134K^o$ for $E_s = 500 \frac{MV}{m}$.
Analytical results in [4], [5] are obtained for the case of 'low temperature' and 'high electric field', when temperature addition can be considered as small. According [4], the current density j_{T_c}, emitted from the surface with the temperature T_c is:

$$j_{T_c} = j_0 \frac{\frac{\pi T_c}{2T_i}}{sin(\frac{\pi T_c}{2T_i})}, \qquad (4)$$

for the temperature range $0 < T_c < 1.2T_i$. Extended temperature region $1.2T_i < T_c < 2.2T_i$ is considered in [5] and

$$j_{T_c} = j_0 \cdot 1.16 \cdot exp(0.31 \frac{T_c^3}{T_i^3}). \qquad (5)$$

The plot of the current ratio densities $\frac{j_{T_c}}{j_0}$ for temperature range $0 < T_c < 2.2T_i$ is shown in Fig. 1. The plot in Fig. 1 exhibits fast rise of the current density for $T_c > 1.5T_i$. Unfortunately, we can not extend the plot for higher ratio values $T_c > 2.2T_i$ - it is out of physical assumptions, done in the obtaining these analytical estimations.
The extension to higher temperatures requires numerical simulations. Such results are known, see, for example [6], and shows significant current density rise with the surface temperature increasing (up to order) for relatively low electric fields. For higher temperatures T_c the current density

THE FINITE STATE MACHINE FOR KLYSTRON OPERATION FOR VUV-FEL AND EUROPEAN X-FEL LINEAR ACCELERATOR

W. Cichalewski, B. Kosęda, A. Napieralski, Technical University of Lodz, POLAND
F.R. Kaiser, S.N. Simrock, Deutsches Elektronen-Synchrotron Hamburg, GERMANY

Abstract

In order to provide a pulsed RF power signal that fulfills all designers and users demands the development on power supplies, pulse transformers, wave-guides, and klystrons has to be well coordinated. Because operators and not experts engineers will operate the user facility therefore software has to be implemented in order to automate the enormous quantity of hardware operation accompanying regular operation of *linear accelerator*. A finite state machine provides an adequate formal description of reactive systems that has become starting point for designing our control software. To present the complexity of the task that establishing a FSM for klystron and modulator system would be, one has to become acquainted with the complexity of the system itself. Therefore this article describes the construction and principles of the klystron and modulator as well as ideas concerning the implementation of a FSM for such a system.

INTRODUCTION

In present time all this equipment, which work for VUV-FEL and X-FEL together with hardware control systems, has to be monitored and operated through a computer system. At DESY DOOCS has been developed (Distributed Object Oriented Control System DOOCS [3]) that is a computer system of multi layer servers working together for optimal operation of the whole system. Beside the typical hardware servers like ADC or DAC servers, there are also servers designed especially for Finite State Machine purposes. Such FSM allows minimizing user intervention during system operation to “one button” action. One of the part of the whole system that requires such a structure is a system responsible for supplying cavities with energy necessary for particle acceleration.

Superconducting cavities are supplied with RF power needed for electron acceleration from multibeam 10MW klystrons working in pulse mode.

KLYSTRON SYSTEM DESCRIPTION

In order to provide a pulsed power signal that fulfils all designers and users demands the work on power supplies, pulse transformers waveguides and klystrons has to be well coordinated. As in the phase of commissioning the device (like VUV-FEL) such a system can be operated manually that in a final solution operator has to be replaced by robust FSM software working in the DOOCS environment

In the whole klystron and modulator system one can distinguish several subsystems that form main sections. Each of this section has to be carefully managed to achieve best system performance.

Modulator - High Voltage Power Supply (HV-PS)

HV-PS is a section responsible for high voltage (HV) pulse for klystron. There is possibility to regulate HV pulse parameters as duration or voltage level and repetition rate in order to achieve requested portion of the energy for the klystron.

Electrical power is delivered to the system as AC 440V 50Hz signal in 3 phases. After conversion (in a transformer) the signal is filtered and the energy is stored in 1,4mF capacitor (*Cap Bank*). Next to the capacitor *the crowbar* system is installed. If there is an arcing effect in the klystron tube this system makes a short circuit for the Capbank and sends the energy from the capacitor to the ground. This system is not used during normal operation.

The switch is present for releasing the energy from capacitor bank. This *main switch* is based on seven Integrated Gate-Commutated Thyristors devices.

This power is send to *the pulse transformer*.

Because of the slope that occurs on a high voltage envelope there is compensation needed. In order to achieve a flattop the bouncer system is used. A bouncer is a resonance circuit that stores energy and when triggering signal appears this energy is released in order to compensate the slope on the main circuit signal. Bouncers counterbalance signal minimizes the fluctuations of the high voltage signal to the level of +-0,5 %.

Pulse Transformer

The *pulse transformer* (PT) is a subsystem that converts signal achieved from HVPS to the HV signal that supplies the klystron tube [4]. For the efficient use of magnetic core, there is also biasing introduced through one of the section of the secondary windings.

In order to decrease thermal power losses, the whole pulse transformer body is cooled by mineral oil. The level, temperature and also humidity of the oil are monitored at all times.

Klystron Section

The HV pulse is delivered to the klystron, where *collector* is grounded and high voltage is applied to the *cathode*.

To achieve sufficient electron emission from the cathode, this part of the klystron must be heated to the particular temperature. *The filament* subsystem is responsible for this process. A heater subsystem contains special controller hardware for slow increasing the temperature that is necessary for efficient and longtime filament and cathode use.

According to the data achieved from cathode examination the pearvance of the klystron is measured. Afterwards some correction of the filament preparation

GRADIENT LIMITATIONS FOR HIGH-FREQUENCY ACCELERATORS*

S. Döbert, SLAC, Menlo Park, CA 94025, USA

Abstract

The main gradient limitation for high frequency accelerators is rf breakdown. While the physics of this gradient limitation still lacks a full theoretical understanding, a fairly complete empirical picture has emerged from the experimental work done in the past few years to characterize this phenomenon. Experimental results obtained mostly in the framework of the NLC/GLC project at 11 GHz and from the CLIC study at 30 GHz will be used to illustrate the important trends. The dependence of achievable gradient on pulse length, operating frequency and fabrication materials will be described. Also, the performance results most relevant to linear colliders will be presented in some detail. Specifically, these related to the requirements that the structures sustain a certain gradient without incurring damage, and that more importantly, they run reliably at this gradient, with breakdown rates less than one in a million pulses. In this context, long term operation results will be discussed as well as the result of controlled venting experiments. Finally, a very brief idea of the theories related to rf breakdown will be presented.

INTRODUCTION

Choosing a high rf operating frequency offers the advantage of a more compact accelerator design and less rf energy per pulse for efficient acceleration. Drawbacks include the difficulty of generating high peak powers at higher frequency and the tighter alignment tolerances required to cope with the higher transverse wakefields. However, these impediments can be overcome, and high rf frequencies were chosen by normal-conducting linear collider projects, specifically, NLC and GLC [1] and by CLIC [2], which aims for multi-TeV energies. The NLC/GLC collaboration has developed accelerating structures at 11.4 GHz with an unloaded design gradient of 65 MV/m with 400 ns long pulses. The CLIC group studies structures at 30 GHz aiming for an unloaded gradient of 170 MV/m at a pulse length of 130 ns (recent optimization studies suggest a much shorter pulse length of about 60 ns). These gradient choices were motivated in part by early measurements that showed achievable gradient increases monotonically with frequency. Recent results suggest that this assumption is probably not valid anymore at frequencies above X-band [3]. Beyond just achieving these gradients, the structures must operate reliability for decades in a linear collider, which makes it imperative that rf breakdown limitations be well understood. Although a dynamical model of rf breakdown has yet to be fully developed, the phenomenon can be sketched from an empirical view as follows: rf breakdown is a fast and local dissipation of stored energy. Several Joules of rf energy can be absorbed in a single cell, and in the process, surface melting and evaporation occurs in an area of a few 100 μm^2. Strong electron emission, acoustic waves, gas desorption, X-rays and visible light is observed during a breakdown event. The majority of breakdowns are concentrated in areas of high surface electric fields. However a strong exponential correlation between surface field distribution and breakdown location is not always observed, as would be expected from a purely field emission driven process. In areas with high surface currents but not necessarily high electric fields, surface defects like particles, voids and contaminants have been found to be sources of breakdown. The stress imposed on the copper surface by pulsed heating resulting from high surface currents alone is also believed to lead to breakdown. Structure designs with a pulsed temperature rises < 50 K appear to be safe in this respect.

HIGH GRADIENT PROCESSING

High frequency accelerators have to be conditioned to their high operational gradients. The process of rf conditioning is not well understood but it is believed to be a combination of physically smoothening, degassing and cleanup of the surface as a result of the energy dissipated during breakdown. Clean fabrication and assembly procedure seem to speed up rf conditioning but never eliminate it. Typically, the conditioning starts with a pulse width much shorter than the design value. The structure is processed to a field 10-25% above the design gradient and then this process is repeated with progressively longer pulses. As an example, Figure 1 shows the processing

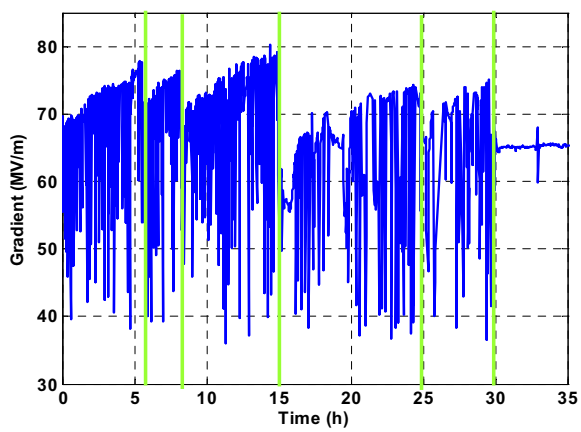

Figure 1: Processing history of a pair of 60 cm structures. The green vertical lines indicate changes in the rf pulse length (50, 100, 170, 240,400 ns).

* Work supported by the US Department of Energy, under contract DE-AC03-76SFF00515

STATE OF THE ART SRF CAVITY PERFORMANCE

Lutz Lilje#, DESY, Hamburg. Germany

Abstract

The paper will review superconducting RF cavity performance for β=1 cavities used in both linear and circular accelerators. These superconducting cavities are used in two kinds of applications: High current storage rings and efficient high duty cycle linacs. In recent years the performance of those cavities has been improving steadily. High accelerating gradients have been achieved using advanced surface preparation techniques like electropolishing and surface cleaning methods like high pressure water rinsing. High intensity beams can be handled with advanced higher-order-mode damping schemes.

INTRODUCTION

Superconducting radiofrequency (SRF) cavities are used for several applications. All species of particles are accelerated using SRF for several reasons:

- Surface resistance at microwave frequencies is a few nOhm (10^6 times smaller than for normal conductors)
- High efficiency for transforming wall-plug to beam power
- Continuous-wave operation
- Low frequencies
  - Large aperture
  - Large acceptance
  - Smaller wakefields
- Potential for energy recovery operation
- High accelerating gradients

This paper will describe the state-of-the-art for cavities used for electron acceleration (β=v/c=1). Electron accelerators are used for elementary particle physics (storage rings, linear collider) or light sources (storage rings, linacs).

SUPERCONDUCTING CAVITY TECHNOLOGY

For superconducting cavities at very high electrical and magnetical surface field great care has to be taken during manufacturing and preparation for beam acceleration. Normalconducting inclusions in the material and contaminations on the surface need to be avoided. For example, the preparation and assembly in in clean rooms and ultrapure water supplies for rinsing the surfaces are a must. In this paper the focus will be on the surface preparation with electrochemical methods before the final high pressure rinsing.

Material Quality

The niobium bulk material used for cavity fabrication needs to have good thermal conductivity as the heat produced on the inner side of the cavity needs to be conducted to the coolant (liquid helium) on the outside. The thermal conductivity is usually not quoted as the figure of merit but the RRR (residual-resistivity ratio) value. Typical RRR values in the cavities described in this paper is around 200-300 and 500-600 for cavities subjected to a postpurification using a furnace treatment at 1300°C with a titanium getter layer.

As an example of quality control for the niobium sheet material an eddy-current scanning system which currently is used for SNS (build by company based on a design by Bundesanstalt für Materialforschung and DESY) is shown in figure 1. A similar system is in use for the TESLA cavities [1,2]. The eddy-current system also allows to certain degree to determine the type of inclusion. Any niobium sheet showing defects is rejected from the cavity manufacturing process. The rejection rate is about 5 %. Most of the rejected sheets will be recoverable by applying some chemical etching. The iron inclusions were caused by mechanical wear of the rolls used for sheet rolling. In the meantime new rolls have been installed. The eddy-current check has turned out to be an important quality control not only for the cavity manufacturer but also for the supplier of the niobium sheets.

Figure 1: Setup for quality control of niobium sheet material for SNS.

Surface Treatment

The niobium sheets are deep drawn and electron beam welded to fabricate a cavity. A damage layer of about 100 μm thickness is removed from the inner surface to obtain optimum performance in the superconducting state. Often cavities have been chemically etched [2,3]. Niobium metal has a natural Nb_2O_5 layer with a thickness of about 5 nm which is chemically rather inert and can be dissolved only with hydrofluoric acid (HF). Chemical etching of niobium consists of two alternating processes: dissolution of the Nb_2O_5 layer by HF and re-oxidation of the niobium by a strongly oxidizing acid such as nitric acid (HNO_3) [4,5]. To reduce the etching speed a buffer substance is added, for example phosphoric acid H_3PO_4 (concentration of 85%) [6], and the mixture is cooled

#lutz.lilje@desy.de

STATE OF THE ART IN RF CONTROL

S.N. Simrock, DESY

Abstract

Nowadays the designer of a new rf control system has access to a wealth of powerful digital, analog, and rf circuitry. The requirements for the rf control system have changed from only controlling the amplitude and phase of the accelerating field to the required degree to stability. Additional tasks include exception handling and extensive build-in diagnostics while pursuing issues related to reliability, operability, and maintainability. Also operation close to the performance limit must be supported while maximizing the availability of the accelerator. With many accelerator projects in planning or under construction several state-of-the art rf control designs have evolved. This paper will present an overview of this new technology and discuss its performance.

INTRODUCTION

The architecture of a typical RF control system is shown in Figure 2. A power amplifier provides the rf power necessary for establishing the accelerating fields in the cavities. The cavity field is measured and the compared to a setpoint. The resulting error signal is amplified and filtered and drives a controller for the incident wave to the cavity. A frequency and phase reference system provides the necessary rf signals. The requirements for the stability of the accelerating fields range from 1% in amplitude and 1 degree in phase for high power H^- accelerators to 0.01% in amplitude and 0.01 degree in phase for the critical sections such as compressors in XFELs. Since many of the present and near future accelerator based facilities are employing superconducting cavity technology this review will focus on rf control systems for sc-cavities. Accelerator projects making use of the present state of the art technology include SNS, J-PARC, CEBAF upgrade, RIA, the European X-FEL, the BESSY soft X-Ray Laser, the Cornell ERL, and many others. Descriptions of the design of the llrf system that have been developed recently for the various accelerator projects can be found in [1-21].

RF CONTROL SUBSYSTEMS

The subsystems shown in the architecture of the rf system in Figure 2 are shown in more detail in Figure 5. Most recent advances in technology have been achieved in the area of the digital controllers including high speed analog I/O and powerful signal processing, the area of field detection, frequency conversion and actuators for field control, fast piezoelectric and magnetostrictive cavity frequency tuners, low noise reference frequency oscillators and highly stable frequency distribution systems.

CAVITY FIELD DETECTION

The cavity field detection can be accomplished with traditional amplitude and phase detectors or with IQ detectors which operated directly at the rf operation frequency or at an intermediate IF frequency which contains the amplitude and phase information. Another possibility if the a scheme employing digital IQ detection where the IF (or the RF signal) is sampled directly by an ADC which usually samples alternating the real and imaginary components of the cavity. This of course requires correct timing of the data acquisition.

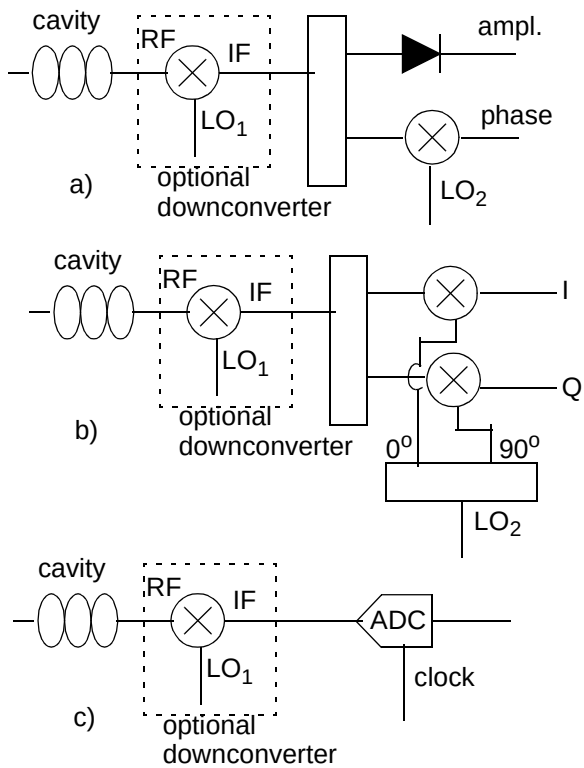

Figure 1: Field detection schemes. a) amplitude and phase detection, b) IQ detection, c) digital IQ detection.

With the rapid development of the telecommunication market industry had developed a variety of single chip solutions for amplitude detection, phase detection, and IQ detection based on analog multipliers. Examples are:

- AD8343 analog multiplier
- RF2411 analog multiplier
- AD8361 linear video detector (temperature stabilized)
- AD8302 logarithmic video detector and phase detector
- HMC 439 digital phase detector

STATE-OF-THE-ART ELECTRON BUNCH COMPRESSION

P. Piot *
Fermi National Accelerator Laboratory, Batavia, IL 60510, USA

Abstract

Many accelerator applications such as advanced accelerator R&D, free-electron laser drivers and linear colliders, require high peak current electron bunches. The bunch is generally shortened via magnetic compression. In the present paper we review various bunch compression schemes and discuss their limitations.

INTRODUCTION

There is a growing demand for generating and transporting very bright electron bunches. Applications range from linac-based light sources (both free-electron laser (FEL) and spontaneous emission-based), future linear colliders, to novel electron beam-driven acceleration schemes (e.g. plasma wake-field acceleration). The generation of bright electron bunches directly out of an electron sources is generally not an easy task. Instead it is preferred to create relatively low peak current bunches at the source. Beam manipulations are subsequently implemented in the downstream transport in order to obtain short electron bunches. Several proposed projects [1, 2] call for peak current in the multi-kiloamps regime resulting in bunch length of as low as $\sim 20\mu$m (corresponding to a duration of $\sim$ 70 fs). The process of manipulating an electron beam so to enhance its peak current is called bunch compression. Many other schemes aimed to produce short bunches have been proposed, either with special design of electron source [4] or by selecting only one part of the bunch, e.g. via dispersive collimation or spoiling. These latter "selective" techniques are not addressed in the present paper and a review in the context of light source short radiation pulse production is given in Reference [3]).

MAGNETIC COMPRESSION SCHEMES

Principle

A magnetic bunch compressor, in its simplest form, consists of two elements: an energy "modulator" and a non-isochronous achromatic sections. The energy modulator provides a time-energy correlation (or chirp) along the bunch length, the non-isochronous section introduces an energy-dependent path length. Thus a proper tuning of the modulator parameters to impart the needed chirp along the bunch results in compression as the bunch propagates in the non- isochronous section.

* piot@fnal.gov

Let's first discuss the magnetic compression scheme by considering a single particle linear model. Consider an electron with longitudinal phase space coordinate (z_0, δ_0) w.r.t. the bunch center upstream of the energy modulator (δ denotes the fractional energy offset of the electron with respect to the bunch center). Downstream of the modulator, the longitudinal phase space coordinate, (z_m, δ_m), are

$$\begin{aligned} z_m &= z_0, \text{ (assuming } \gamma \gg 1) \qquad (1)\\ \delta_m &= \frac{eV_{rf}}{\mathcal{E}_m}\left(\cos(kz_0+\varphi)-\cos\varphi\right) \doteq \kappa z_0 + \mathcal{O}(z^2) \end{aligned}$$

wherein e is the electron charge, V_{rf} and φ are the accelerating voltage and operating phase of the energy modulator section, k is the rf wavenumber ($k = 2\pi/\lambda_{rf}$, λ_{rf} being the rf-wavelength), and $\mathcal{E}_m \doteq \mathcal{E}_0 + eV_{rf}\cos(\varphi)$ ($\mathcal{E}_0$ being the initial electron energy). After passing through a non-isochronous section characterized by its first order momentum compaction, R_{56}, the electron coordinates are mapped, to first order, to the following:

$$z_c = z_0 + R_{56}\delta_m, \text{ and } \delta_c = \delta_m. \qquad (2)$$

Thus the final electron position with the bunch, z_c, is related to the initial position, z_0, via $z_c = (1+\kappa R_{56})z_0$ which gives the longitudinal matching condition $\kappa = -1/R_{56}$ for minimizing the bunch length in a single stage magnetic compressor. The constant κ is the bunch chirp and can be tuned via V_{rf} and/or φ variable. If one consider rms quantities, the final rms bunch length downstream of the compressor is:

$$\sigma_{z,c} = \left((1+\kappa R_{56})^2\sigma_{z,0}^2 + (R_{56}\sigma_{\delta,0}\mathcal{E}_0/\mathcal{E}_m)^2\right)^{1/2}. \qquad (3)$$

When the longitudinal matching condition is satisfied, we have $\sigma_{z,c} = R_{56}\sigma_{\delta,0}\mathcal{E}_0/\mathcal{E}_m$. Therefore compression at higher energy ($\mathcal{E}_m \to \infty$) would results in shorter minimum bunch length. The above linear theory holds under the condition (i.e. $k\sigma_z \ll 1$). In a real accelerator such a condition is not a fortiori satisfied: e.g. in a photo-injector it is common [5] to generate a long bunch length so to properly compensate transverse emittance growth. The bunch compression is then performed once this bunch has been accelerated to high enough energy to sufficiently damp space charge forces. As the bunch is accelerated in the structure, the longitudinal phase space accumulates some curvature due to the cos-like time dependence of the rf-field and the fractional energy spread downstream of the accelerating structure is expanded as $\delta_m = \kappa z_0 + \mu z_0^2 + \mathcal{O}(z_0^3)$ instead of Eq. 1. In turn the bunch compressor needs to be

RESULTS FROM THE INITIAL OPERATIONS OF THE SNS FRONT END AND DRIFT TUBE LINAC*

A. Aleksandrov for SNS collaboration, ORNL, Oak Ridge, TN 37830 USA

Abstract

The Spallation Neutron Source accelerator systems will deliver a 1 GeV, 1.44 MW proton beam to a liquid mercury target for neutron scattering research. The accelerator complex consists of an H^- injector, capable of producing one-ms-long pulses at 60 Hz repetition rate with 38 mA peak current, a 1 GeV linear accelerator, an accumulator ring, and associated transport lines. The 2.5 MeV beam from the Front End is accelerated to 86 MeV in a Drift Tube Linac, then to 185 MeV in a Coupled-Cavity Linac and then to 1 GeV in a Superconducting Linac. The staged beam commissioning of the accelerator complex is proceeding as component installation progresses. The Front End and Drift Tube Linac tanks 1-3 have been commissioned at ORNL. The primary design goals of peak current, transverse emittance and beam energy have been achieved. Beam with 38 mA peak beam current, 1 msec beam pulse length and 1 mA average beam current have been accelerated through the DTL tank 1. Results and status of the beam commissioning program will be presented.

INTRODUCTION

The Spallation Neutron Source accelerator complex will provide a 1 GeV, 1.44 MW proton beam to a liquid mercury target for neutron production. The accelerator complex consists of an H^- injector, capable of producing one-ms-long pulses at 60 Hz repetition rate with 38 mA peak current, a 1 GeV linear accelerator, an accumulator ring, and associated transport lines. The SNS accelerator systems are comprehensively discussed elsewhere [1]. The baseline linac beam has a 1 msec pulse length, 38 mA peak current, is chopped with a 68% beam-on duty factor and repetition rate of 60 Hz to produce 1.6 mA average current. The staged beam commissioning of the accelerator complex is proceeding as component installation progresses. At this point, the H^- injector (Front End) and Drift Tube Linac tanks 1, 2 and 3 (of 6) have been commissioned at ORNL. A summary of baseline design parameters and beam commissioning results is shown in Table 1.

FRONT-END PERFORMANCE AND COMMISSIONING RESULTS

The front-end for the SNS accelerator systems is a 2.5 MeV injector consisting of the following major subsystems: the rf-driven H^- source, the electrostatic low energy beam transport line (LEBT), a 402.5 MHz RFQ, the medium energy beam transport line (MEBT), a beam chopper system and a suite of diagnostic devices. The front-end is required to produce a 38 mA beam of 2.5 MeV energy at 6% duty factor. The 1 ms long H^- macro-pulses are chopped at the revolution frequency of the accumulator ring (~1 MHz) into mini-pulses of 645 ns duration with 300 ns gaps. After construction and initial commissioning at LBNL the Front End was shipped to Oak Ridge in the summer of 2002, installed at the SNS site and re-commissioned using a dedicated beam stop. The Front End has been providing beam for commissioning the rest of the linac since then and more than 2000 hours of operation time have been accumulated so far.

Table 1. SNS design vs. achieved beam parameters

	Baseline Design or Goal	Achieved
MEBT peak current [mA]	38	52
DTL1 peak current [mA]	38	40
DTL1-3 peak current [mA]	38	38
DTL1 beam pulse length [msec]	1.0	1.0
DTL1 average current [mA]	1.6	1.05
MEBT horiz. emittance [π mm mrad (rms,norm)]	.27	< .3
MEBT vertical emittance [π mm mrad (rms,norm)]	.27	< .3
DTL1 horiz emittance [π mm mrad (rms,norm)]	0.3	0.30 (fit), 0.40
DTL1 vertical emittance [π mm mrad (rms,norm)]	0.3 (RMS)	0.21 (fit), 0.31 (RMS)
DTL1 beam duty factor	6.0%	3.9%
MEBT Beam Energy [MeV]	2.5	2.45 ± 0.010
DTL2 output energy [MeV]	22.89	22.94 ± 0.11

Ion Source and LEBT Performance

Details of the ion source and LEBT design can be found in [2]. General performance of the ion source during commissioning is summarized in Fig.1, where operational current is shown for each day of the last commissioning run. Since there are no beam diagnostics in the ion source or LEBT, the beam current is measured in the MEBT after the RFQ. A maximum current of 51 mA was achieved, significantly exceeding the base line requirement of 38 mA. An R&D program on the ion-source hot spare stand [3] yielded a significant increase of the ion source

* SNS is managed by UT-Battelle, LLC, under contract DE-AC05-00OR22725 for the U.S. Department of Energy. SNS is a partnership of six national laboratories: Argonne, Brookhaven, Jefferson, Lawrence Berkeley, Los Alamos and Oak Ridge.

RECENT RESULTS IN THE FIELD OF HIGH INTENSITY CW LINAC DEVELOPMENT FOR RIB PRODUCTION

A. Pisent, INFN/LNL, Legnaro, Padova, Italy

Abstract

High Intensity CW Linacs have been proposed as driver accelerators for RIB production in various projects, since they can drive in steady conditions a MW power range target for the production of spallation neutrons that induce fission in a natural uranium target. The necessity to develop a superconducting intermediate energy part with good power conversion efficiency is particularly important for this application, with a relatively low beam current. The second specific requirement of RIB facility drivers, which is also fulfilled by a superconducting intermediate energy linac, is the necessity to keep some flexibility in the species that can be accelerated (deuterons or light ions). In EURISOL RTD project, a 1 GeV 5 mA proton linac has been proposed for this application. In the SPES project, recently approved for its initial phase at LNL, a lower energy proton beam will be used on a solid target. The results of the specific R&D programs in the field of CW RFQ and superconducting low energy linacs will be illustrated. In particular for LNL the status of the RFQ construction and the superconducting cavities prototype tests will be given.

HIGH INTENSITY FOR RIB PRODUCTION

In the last years the availability of new intense radioactive ion beams (RIB) has been recognized as a fundamental tool for future research in Nuclear Physics, and new major facilities have been proposed worldwide (Table 1). By means of RIBs it is possible to study the properties of nuclei that, due to their short life-time, cannot be used as a target. Therefore RIBs allow to extend the knowledge of nuclear structure to exotic compounds and to study conditions that are relevant for the understanding of the early stage of the Universe and for the nucleo-synthesis.

Of the two complementary methods for RIB production, the In Flight (IF) and the ISOL (Isotope Separation On Line), the second one takes directly advantage of the development of cw high intensity linacs.

The basic scheme of an ISOL facility [1] is the following: the primary accelerator beam induces a nuclear reaction in a thick target, producing unstable nuclei. During their short life-time the isotopes evaporate from the target (kept at high temperature), are pumped into an ion source, ionized, extracted, selected by a magnetic spectrometer, accelerated and sent into the experimental apparatus. The RIB intensity actually delivered to the experiments is mainly the product of the primary beam intensity, the cross section of the specific production and the various efficiencies. These efficiencies take into account the particle losses occurred during the effusion from the hot target and the diffusion in the ion source, the nuclei that decay before reaching the experiment and the transmission of the spectrometer and of the reaccelearator. Even if the improvement of the efficiencies and of the ion selectivity of the spectrometer are under many aspect the key points for the success of an ISOL facility, a large flux of primary particles is the initial point.

In Europe the future for the IF method is assured by the GSI project FAIR[2], while for the ISOL method a large group of research institutions, including the major Nuclear Physics laboratories, have joined the EURISOL project, funded by EU, for the determination of the most competitive new generation ISOL facility for Europe. The resulting EURISOL report[3] has been published last year, and more recently the EU has positively evaluated a second stage design work (EURISOL-DS), now in negotiation stage, that includes the funding of prototypes of some critical issues.

Thanks to the complementarity with FAIR, EURISOL is mainly concentrated on the use of a 1 GeV high power proton linac, while the American project RIA, including IF method, considers a lower intensity linac able to accelerate ions up to uranium. For this reason this paper will be centred on European development, even if at present the most performing cw proton beam for RIB production is produced by a cyclotron in America (ISAC at TRIUMF[4]).

In particular in EURISOL design the direct use of a p beam of "moderate" intensity (tenths of mA) on a solid target will allow in most cases to operate at the limit of the target possibility (in terms of power dissipation density) with RIBs intensity much larger than the one available today.

Neutron reach isotopes are instead most efficiently produced by fission reaction with the two targets method: a very high fission rate (exceeding $10^{15}s^{-1}$) can be induced in a depleted uranium carbide target by fast neutrons; the fast neutrons are produced by spallation in a MW class (liquid metal) target.

Therefore, the EURISOL reference facility foresees three 100 kW target stations and one 5 MW target. Correspondently, the linac will have two modes of operation, at 100 μA and at 5 mA. Moreover, the possibility to accelerate light ions with the same driver has been explored; in particular the upgrading of the injectors needed to accelerate ions with A/q=2 up to 500 A MeV and A/q=3 up to 100 A MeV have been considered.

To assure the continuity in RIB research development some new ISOL facilities are proposed in Europe for the next decade (Tab. 2). In EURISOL-DS proposal and in NuPECC Long Range Plan a "EURISOL road map"

Challenges of Linac Driven Light Sources

C. Bocchetta, ELETTRA, Basovizza, Trieste

Abstract

The use of linacs allows novel light sources to be conceived by not being limited by equilibrium dynamics or IBS effects. These new sources can be single pass or recirculated (with or without energy recovery) or linac augmented storage rings. They allow tuneable polarised radiation of unprecedented brilliance, short pulse lengths that may reach the atto-second scale and full coherence. Both SC and NC machines are being proposed, designed and constructed. Photon output characteristics range from incoherent synchrotron radiation to SASE to seeded HGHG. The proposed beams can be low to high average current and pulse time structures range from CW to highly variable with mutual exclusion amongst different forms of operation. The multiple challenges of these machines reside not only in the requirement of beams of extremely high quality (energy, emittance, energy-spread and temporal stability) for the brightest, shortest wavelength sources but also in the demanding technologies and control of beam-machine interactions for the high current energy recovery ones. The paper gives an overview of these broad challenges and of the directions taken to reach the objectives of a user facility.

NO SUBMISSION RECEIVED

PAL LINAC UPGRADE FOR A 1-3 Å XFEL

J. S. Oh, W. Namkung, Pohang Accelerator Laboratory, POSTECH, Pohang 790-784, Korea
Y. Kim, Deutsches Elektronen-Synchrotron DESY, D-22603 Hamburg, Germany

Abstract

With the successful SASE FEL saturation at 80-nm wavelength at TTF1, TTF2 will begin re-commissioning in the fall of 2004 as an FEL user facility to 6 nm with 1-GeV beams. The high gain harmonic generation is also confirmed by the DUV-FEL experiments at 266 nm with seeding wavelength at 800 nm. In order to realize a hard X-ray SASE FEL (SASE XFEL) with a lower energy beams, we need a long in-vacuum mini-gap undulator and a GeV-scale FEL driving linac that can supply an extremely low slice emittance, a high peak current, and an extremely low slice energy spread. PAL is operating a 2.5-GeV electron linac as a full-energy injector to the PLS storage ring. By adding an RF photo-cathode gun, two bunch compressors, and a 0.5-GeV S-band injector linac to the existing PLS linac, and by installing a 60-m long in-vacuum undulator, the PLS linac can be converted to a SASE XFEL facility (PAL XFEL) which supplies coherent X-ray down to 0.3-nm wavelength. The third harmonic enhancement technique can supply coherent hard X-ray beams to 0.1 nm. The technical parameters related to these goals are examined, and preliminary design details are reviewed for the PAL linac upgrade idea for a 1-3 Å PAL XFEL.

INTRODUCTION

The requirements of X-ray from scientific users are radiation wavelength of 0.1nm, pulse length of 20 fs (FWHM). PAL operates a 2.5-GeV electron linac, the 3rd largest in the world, as a full-energy injector to the PLS storage ring [1]. The PAL 2.5-GeV linac can be converted to an X-ray free electron laser (XFEL) facility driven by a self-amplified spontaneous emission (SASE) mode, which supplies coherent X-rays down to 0.3-nm wavelength. The third harmonic enhancement technique on the electron beam or advanced X-ray laser optics will be applied to obtain radiation wavelengths of 0.1 nm. The design goal is for the undulator to be less than 60 m in total length. The linac should supply highly bright 3-GeV beams to a 60-m long in-vacuum undulator with a 3-mm gap and a 12.5-mm period, of which emittance of 1.5 mm-mrad, a peak current of 4 kA, and a low energy spread of 0.02% [2].

Table 1 shows the comparison of single bunch specifications between the PLS linac and PAL XFEL. Normalized emittance should be 100 times improved, which requires a low emittance gun and high gradient acceleration at low energy region to preserve the emittance. The suitable bunch compression is one of key technique to realize the high peak current, also.

Questions are how to utilize the existing 2.5-GeV linac and how to keep the operation mode as a full energy injector for PLS 2.5-GeV storage ring.

Therefore we have to minimize the modification of existing linac layout. We have to find matching conditions to provide flexible beam operation for both applications. Also the site is already fixed and limits the maximum size of a new machine scale. The performance and stability of the 2.5-GeV linac is also challenging to meet the strict SASE requirements.

Table 1: Bunch specifications of PLS linac and XFEL

Parameter	PLS Linac	XFEL
Beam energy	2.5 GeV	3.0 GeV
Normalized emittance	150 μm-rad	1.5 μm-rad
FWHM bunch length	13 ps	0.23 ps
RMS energy spread	0.26%	0.02%
Bunch charge	0.43 nC*	1.0 nC
Peak current	33 A*	4 kA
Repetition rate	10 Hz	60 Hz

* 2-A gun current and 62% transmission

PAL XFEL PROGRAM

The fundamental radiation wavelength λ_x of an undulator is given by

$$\lambda_x = \frac{\lambda_u}{2\gamma^2}(1 + K^2/2), \quad \gamma = E_o / 0.511, \quad K = 0.934 B_u \lambda_u ,$$

where E_o is the beam energy in MeV, B_u is the peak magnetic field of the undulator in Tesla, and λ_u is the undulator period in cm. The peak magnetic field B_u of a 45°-magnetized undulator with $H = \lambda_u/2$ is given by

$$B_u = \frac{4\sqrt{2}B_r}{\pi} \sum_{n=1,5,9}^{\infty} \frac{1}{n}(1 - e^{-2n\pi H/\lambda_u}) e^{-n\pi g/\lambda_u} ,$$

where B_r is assumed 1.19 Tesla with $Nd_2Fe_{14}B$ magnets, H is the block height, and g is full-gap length [3]. Fig. 1 shows the undulator geometry with 45°-magnetization.

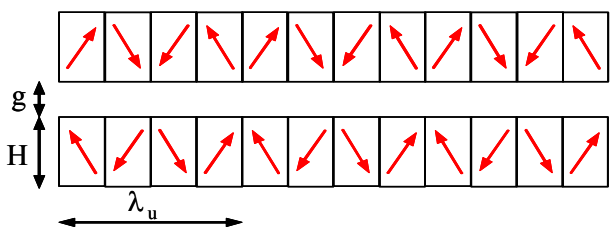

Figure 1: Undulator geometry with 45°-magnetization.

KEKB INJECTOR LINAC AND UPGRADE FOR SUPERKEKB

S. Michizono#, for the KEK electron/positron Injector Linac and the Linac Commissioning Group, KEK, Tsukuba, Japan

Abstract

The KEB injector linac delivers electrons and positrons to four rings (KEKB LER, KEK HER, PF and PF-AR). The operational status of the KEKB injector linac is summarized. The R&D work concerning diagnostics of the klystrons and the beam-quality are also described. An upgrade plan of the injector linac using a C-band rf system is under consideration for SuperKEKB. A C-band acceleration structure was installed in the KEKB linac after rf conditioning at more than 40 MW. An energy gain of more than 40 MV/m was confirmed by the beam acceleration. The C-band acceleration unit has been operated continuously for a stability test.

INTRODUCTION

The KEKB Injector linac has provided 8 GeV electrons to KEKB HER and 3.5 GeV positrons to KEKB LER [1]. KEKB has recorded the highest luminosity to which the linac contributes with an advanced operational stability for about 7,000 hours per year. Double bunch injection and continuous injection (CI) schemes have been adopted.

The SuperKEKB project [2], aiming for a ten-times higher luminosity, is under consideration as an upgrade of KEKB. In this upgrade, the injector linac has to increase the positron acceleration energy from 3.5 GeV to 8 GeV [3]. One of the plans for this upgrade is to double the acceleration field (from 20 to 40 MV/m) with a C-band (5712 MHz) rf system. The newly developed components are summarized.

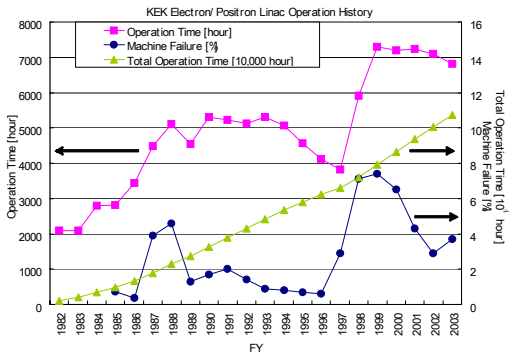

Figure 1: Operation history of the KEKB linac.

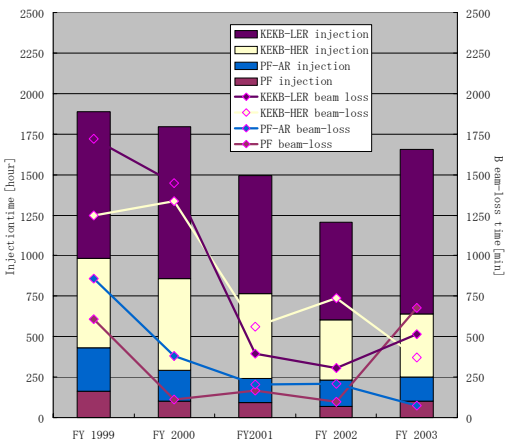

Figure 2: Injection time and beam-loss time to PF, PF-AR, KEKB LER and KEKB HER.

#shinichiro.michizono@kek.jp

OPERATION STAUS OF KEKB LINAC

Operation History and Statistics

Construction of the linac started in 1978, and operation started in 1982. Electron/positron beams were injected to Tristan from 1986 to 1994. The KEKB rings started their operations from 1998. The operation time is presently about 7,000 hours per year. The history of the operation time is shown in Figure 1. The accumulating operation time reached 100,000 hours on Mar. 3, 2003. The failure ratio has been about 5%. Figure 2 shows the injection time delivered to 4 kinds of rings. The KEKB injection time is more than 80% of the total injection time. The beam-loss time is shorter than the value obtained from the machine failure in Figure 1 because many of failed modules can be replaced by one of the stand-by modules before beam operation. The larger beam-loss time at PF in FY 2003 was caused by a problem of old modules in the trigger system. It was replaced last spring.

Continuous Injection (CI) Scheme

From January, 2004, the CI scheme to KEKB started for higher luminosity operation. CI operation enables us to increase the accumulation luminosity by about 20-

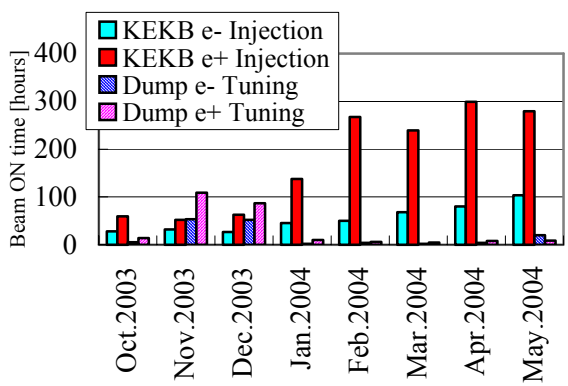

Figure 3: Status of the beam on time. The CI scheme started from Jan, 2004, the beam on time for LER (e+) increased and the tuning time (Dump) decreased.

STATUS OF THE J-PARC LINAC, INITIAL RESULTS AND UPGRADE PLAN

Y. Yamazaki for the J-PARC Accelerator Group,
JAERI, Shirakata-Shirane 2-4, Tokai-mura, Naka-gun, Ibaraki-ken, Japan, and KEK, Oho 1-1, Tsukuba-shi, Ibaraki-ken, Japan

Abstract

The J-PARC linac comprises the voulume-production type negative hydrogen ion source, the 50-keV low-energy beam transport, the 3-MeV RFQ linac with π-mode stabilizing loop, the 50-MeV, 324-MHz Dift-Tube Linac (DTL) with electro quadrupole magnets therein, and 180-MeV separate-type DTL. The construction is on schedule for starting the beam commissioning in September, 2006. The first cavity of DTL already accelerated the beams up to 20 MeV in November, 2003. The beam study results are reported with the measured values of the emittances. The chopper installed to the medium-energy beam transport was already beam-tested with designed rise and falling times. Since the expected beam power of the 3-GeV rapid-cycling synchrotron is only 0.6 MW with an injection energy of 180 MeV, the construction budget for the linac energy recovery to 400 MeV will be immediately submitted to the funding agency after the completion of the present phase of the project. The further upgrade plans to several-MW neutron source and neutrino factory are also presented.

INTRODUCTION

The High-Intensity Proton Accelerator Facility in Japan [1-9], which is a joint project between JAERI (Japan Atomic Energy Research Institute) and KEK (High Energy Accelerator Research Orgainzation), has been referred to as J-PARC, which is the acronym of Japan Proton Accelerator Research Complex. The J-PARC project as agreed by JAERI and KEK comprises the 600-MeV linac, the 3-GeV rapid-cycling synchrotron (RCS), and the 50-GeV proton synchrotron (Main Ring, MR). The 400-MeV beams from the linac are injected to the RCS with a repetition rate of 25 Hz, while the beams are further accelerated up to 600 MeV by the superconducting (SC) linac to be used for the basic study of the Accelerator-Driven Nuclear Waste Transmutation System (ADS). The maximum average current is 333 μA for each of RCS and ADS. The 1-MW beams from the RCS are mostly extracted to the Materials and Life Science Experimental Facility (MLF), where the muon-production and neutron-production targets are located in a series. The 10 % of the beams are used for the muon production. Every 3.3 second, the beams are transported and injected to the MR four times. The ramping time is 1.9 s, while the deceleration takes 0.9 s. The accelerated beams are slowly extracted to the Nuclear and Fundamental Particle Physics Experimental Facility (NPF), and are fast extracted to produce the neutrino beams, which are sent to the SUPERKAMIOKANDE detector located 300-km west. The MR beam power is 0.75 MW at 50 GeV (15 μA). This is a full scope of the J-PARC project as agreed between JAERI and KEK.

When the project was funded to start in Japanese Fiscal Year (JFY) 2001 as a six-year project, the following facilities were shifted to the Phase II (the funded project is referred to as Phase I).

1) The Neutrino Facility
2) The ADS Facility
3) The SC linac from 400 MeV to 600 MeV
4) Half of the NPF Experimental Hall
5) The fly-wheel electric power generator for the MR, which means that the MR can be operated only up to 40 GeV with the above ramping time (if the ramping time is longer, the acceleration up to 50 GeV will be possible).

In the next section the project status and the overall schedule will be reported. Then, the linac scheme is summarized together with its reasoning. After the construction status is reported, the initial results of the beam commissioning up to the 20-MeV Drift-Tube Linac (DTL) are presented in detail. Finally, the upgrade plans proposed so far are described.

PROJECT STATUS

The following three major changes came into the project. First, the Neutrino Facility was approved for the construction starting from April 2004 to complete in March 2009, implying that the Neutrino Facility was moved up from Phase II to Phase I.

Second, the linac energy was decreased from 400 MeV to 180 MeV in order to compensate the budget overflow in the linac and RCS. Here, we will construct all the accelerating structures up to 190 MeV, but the two cavities, to accelerate the beams from 180 MeV to 190 Mev in future, will be used as debunchers rather than accelerators for the time being. Although the RCS beam power is reduced from 1 MW to 0.6 MW by this, the MR the same beam power may be kept as original by increasing the time duration of the injection from the RCS to the MR. The present building can accommodate the 400-MeV linac, and the energy recovery to 400 MeV will be submitted to the funding agency immediately after the completion of Phase I. Since it needs several-year beam operational experience to achieve the full performance of 0.6 MW, the 1-MW full power operation will not be delayed by recovering the linac energy to 400 MeV within a few years.

OVERVIEW OF HIGH INTENSITY LINAC PROGRAMS IN EUROPE

M. Vretenar, R. Garoby, CERN, Geneva, Switzerland

Abstract

Recent years have seen a boost in the support by the European Union (EU) of accelerator research in Europe. Provided they coordinate their efforts and define common goals and strategies, laboratories and institutions from the member states can receive a financial support reaching 50% of the total project cost. In the field of High Intensity Linacs, the EU has already supported the EURISOL initiative for nuclear physics, which this year is applying for funding of a Design Study, and the development of linacs for Waste Transmutation. More recently, an initiative for high-energy physics has been approved, which includes a programme for the development of pulsed linac technologies. The coordination and synergy imposed by the EU rules increase the benefit of the allocated resources. Combined with the ongoing internal projects in the partner laboratories, these European initiatives represent a strong effort focussed towards the development of linac technologies.

This paper summarises the requests from the various European communities and gives an overview of linac R&D activities sponsored by the EU, together with some information on parallel national/local projects. The parameter choices as well as the main technical features of the different projects are presented and compared.

INTRODUCTION

Recent years have seen an increasing worldwide interest in high-intensity linear accelerators for protons and H^- primarily aimed at the production of intense beams of secondary particles. Secondary beams of scientific interest include:

- Intense neutrino beams for particle physics, produced by the decay of pions, muons or radioactive beta emitters.
- Radioactive ions for nuclear physics, astrophysics and natural science.
- Spallation neutrons as a probe for condensed matter studies or feeding sub-critical reactors for energy production and waste transmutation.

In these applications as "proton drivers", linacs are attractive with respect to circular accelerators for their capability to operate at high repetition rates, up to CW, with limited current per bunch. For pulsed applications at low duty cycle and high energy (1 GeV and above), they are in competition with Rapid Cycling Synchrotrons, while for CW applications at low energy, they compete with cyclotrons. In the past, linacs have always been considered expensive in comparison to circular accelerators. However, thanks to the recent advances in superconducting RF technology and to the increasing optimisation of linac designs, their energy reach, size and cost are improving, so that more projects rely on high-energy high-intensity linear accelerators. Moreover, the strict limits on acceptable beam loss required to minimise radiation and allow hands-on maintenance are more easily met in linear machines, less disturbed by harmful beam resonances than circular machines.

EUROPE AND ACCELERATOR R&D

Any one of these future high energy and high power linacs has such important needs in terms of space and overall infrastructure that it can only be hosted in a large laboratory. With the exception of CERN, the landscape of European accelerator research is rather made-up of a large number of small national laboratories and Universities, with very competent teams, but none having the critical mass required either for a large scale project or for its associated R&D. The basic mission of CERN is for large projects in high energy physics, however its present resources are focused on the construction of the LHC with a very limited support for future options beyond its start-up. Therefore R&D for new European accelerator projects can only be pursued through the collaboration of many different laboratories.

This situation in accelerator research is common to many branches of European science, a fact that is pushing the European Union (EU) commission towards taking a more active role in creating a real European Research Area. In the frame of the 6th EU Framework Programme (FP), covering the period 2004-2009, European research institutions are invited to propose Integrated Projects (IP), i.e. a coordinated research programme for a particular topic involving a certain number of EU scientific centres, which establish a common schedule and share their resources and the results of their work. The approved projects can be financially funded up to a maximum of 50% of the total cost (material and personnel). The evaluation is made not only on the scientific case, but also on the level of integration involved in the proposal.

For high intensity proton linacs, the EU has expanded the support already given to pioneering projects in the FP5, by approving the CARE (Coordinated Accelerator Research in Europe) Initiative. The EURISOL and EUROTRANS Design Studies have also been positively evaluated and are expecting approval. In parallel, support for the ADS (Accelerator Driven Systems) activities is continuing through the EURATOM agency of the EU.

It must be stressed that, due to the fierce competition, projects are never funded at the maximum allowed level, the priorities being defined by the EU committees. For example, inside the CARE initiative, the Joint Research Activity (JRA) dedicated to R&D for high-intensity low-energy linacs, has been very positively evaluated but has obtained EU funding for only about 25% of the total

SUMMARY OF THE ARGONNE WORKSHOP ON HIGH GRADIENT RF

J. Norem*, Argonne National Laboratory, Argonne, IL 60439, USA

Abstract

The Workshop on High Gradient rf was held at Argonne, Oct. 7-9, 2003. This workshop reviewed the progress in a number of accelerator technologies approaching high gradient limits. In addition to progress reports, one aim of the workshop was to involve materials scientists and look at trigger mechanisms and surface interactions. Talks were presented on superconducting rf, progress with high and low frequency copper cavities, and dielectrics. The focus was on both experimental and theoretical aspects of the problem. The overall picture presented at the workshop will be summarized.

INTRODUCTION

This paper will attempt to review the highlights presented at the workshop, summarize in a little more detail ongoing work not otherwise mentioned at this conference, and discuss some of the open questions in the field of high gradient rf. Since many of the participants in this workshop are also presenting more recent results at LINAC 2004, and it is desirable to avoid repetition and discussion of older data, the emphasis will be on topics not covered in this conference, and on general conclusions that could be extracted from the workshop.

Effort on the Workshop was begun as an attempt by members of the Muon Collaboration to explore how much overlap there was between the problems of building muon cooling linacs, with very low frequencies (200 MHz) but comparatively high gradients, and the better understood problems of high frequency electron linacs. There was also a strong feeling that the material dependence of rf breakdown was an important and not well understood aspect of this problem, and it might be possible to productively involve materials scientists in a study of this problem. There was an organizational meeting at PAC03, in Portland Oregon and the workshop was held at Argonne, Oct. 7-9, 2003. A short summary of the workshop was published in the CERN Courier [1].

The website, with copies of all talks given at the workshop, is located at http://www.hep.anl.gov/rf/ [2]. In order to simplify this paper, contributions will be identified by name and not referenced individually.

LINAC DEVELOPMENTS

The majority of the effort on high gradient rf has been done as part of the NLC, CLIC and TESLA effort to produce TeV scale electron linacs for the next generation of particle accelerators. This work has been done by an international group centered at SLAC, FNAL, KEK, DESY and CERN, with important contributions from many other laboratories and individuals.

* norem@anl.gov

Linear Collider Work

Although the emphasis of the workshop was on normal conducting rf, two talks were given on superconducting rf technology. A. Matheisen described SRF surface preparation techniques, and K. Saito discussed recent results with high field SC cavities. The techniques used in this technology involve enormous effort to insure that the metals and surfaces are as free of defects and contamination as possible, the manufacturing process are clean, and assembly and testing do not further contaminate the structures. In many cases this has been done to the point where there is no field emission even at the highest fields. While these methods are widely respected, there is some doubt if they are applicable to high frequency cavities, which are somewhat harder to clean and seem prone to produce damage sites when first exposed to high powers.

The majority of the effort devoted to the linear collider has been adequately summarized elsewhere in this conference. At the workshop C. Adolphsen gave an overview the NLC structure tests done by KEK, SLAC and others, showing that the specifications of the NLC design were being met by prototypes. This was followed by S. Tantawi, who talked about breakdown experiments in waveguides of different dimensions (local B/E ratios) and single cell traveling wave structures. V. Dolgashev described the effects of magnetic fields and input power levels on test cells in the NLCTA and simulations of breakdown. S Doebert looked at gradient limitations on high frequency accelerators showing how breakdown depended on a number of variables (pulse length, power, electric field etc.), but ultimately seemed to occur when the product $\beta E_s \sim 7$ GV/m. S. Harvey presented results of autopsies on structures following high power processing, which showed cracks, craters, and a variety of inclusions and sparking sites, extending the description of surface defects from that published recently by Pritzkau and Siemann [3]. T Higo, showed some preliminary data on the effects of high pressure rinsing of cavities and other treatments. Some of these resulets are shown in Figs. 1-4.

The CLIC effort was summarized by W. Wuensch, who described the work done at the CLIC test facility, which produces high power rf from structures exposed to high energy bunched beams, and uses this power to drive accelerating structures. Results were presented which showed that the breakdown rates seemed to be essentially independent of frequency and initial temperature.

Other Structures

High gradient structures are under construction at other facilities. S. Yamaguchi described a very thorough construction, cleaning and conditioning program for a high gradient test of a new S band structure at KEK.

INDUSTRIAL RF LINAC EXPERIENCES AND LABORATORY INTERACTIONS *

M. Peiniger, ACCEL Instruments GmbH, Bergisch Gladbach

Abstract

For more than two decades ACCEL Instruments GmbH at Bergisch Gladbach (formerly Siemens/ Interatom) has supplied accelerator labs worldwide with key components like rf cavities and power couplers, s.c. magnets, insertion devices, vacuum chambers and x-ray beamline equipment. Starting with the design and production of turn key SRF accelerating modules in the late 80th, meanwhile ACCEL is now engineering, manufacturing, on site commissioning and servicing complete accelerators with guaranteed beam performance. Today, with a staff of more than 100 physicists and engineers and about the same number of manufacturing specialists in our dedicated production facilities, ACCEL's know how and sales volume in this field has accumulated to more than 2000 man years and several hundred Mio €, respectively. Basis of our steady development is a cooperative partnership with the world's leading research labs in the respective fields. To give an example, we established a very fruitful partnership with DESY for the supply of a turn key 100 MeV injector linac for the Swiss Light Source, and meanwhile also for the Diamond Light Source as well as for the Australian Synchrotron Project.

INTRODUCTION

In the last years there have been different talks by people from industry [1], [2] or labs [3] on international accelerator conferences concerning the relation between the labs and the supplying industry for this worldwide research market. The scope of industrial supplies and services ranges from job shop and build to print work over standard and special equipment to turn-key systems. The lab's choice of type of relation is generally depending on their individual capabilities and strategies. While there exist a broad range of companies for performing work on a job shop/build to print level or supplying standard and special equipment there exist only very few companies worldwide with the know-how and capabilities for supplying complete accelerator systems or subsystems with guaranteed beam performance.

ACCEL Instruments GmbH is supplying advanced technology special equipment as well as turn-key linear and circular accelerators for research, industry and medical purposes worldwide. In the following I will try to give a picture on ACCEL's experiences and interactions with the international accelerator labs in the field of rf linac components and complete systems within the last years.

SRF CAVITIES AND MODULES

Within the last two decades ACCEL has manufactured more than 600 superconducting rf cavities out of bulk niobium, by Nb sputter coating of copper cavities or by Nb/Cu explosion bonding techniques. As examples we built all the 360 niobium cavities for CEBAF, the 109 medium and high ß cavities for SNS/ORNL (fig. 1) [4] and in the meantime more than 50 TESLA type cavities (fig. 1) for DESY, Stanford University, FZ Rossendorf and BESSY [5]. Our production know-how for these key components is based on a very intense, long term co-operation especially with DESY, CERN, JLAB, Cornell and Wuppertal University.

Figure 1: SNS (upper) und TESLA (lower) Cavity.

While in the past the cavity production was performed more or less on best effort basis, today customers are asking more and more on a performance guarantee especially for the accelerating field (E) and the cavity Q of the naked cavity, sometimes including the LHe vessel.

For BESSY we have been contracted for manufacturing, chemically treating (BCP) and high pressure rinsing (HPR, fig. 2) two TESLA type cavities [5]. The 800 °C heat treatment (fig. 2) and the vertical cold test have been performed at DESY with the help of DESY personnel. In fig. 3, the resulting Q versus E curves are shown in comparison with results of TESLA cavities manufactured by us but finally treated by and at DESY. We think these first results of accelerating fields above 20 MV/m at a Q of 1 E10 are very promising.

For future projects upon customer's request we plan to perform all preparation steps on TESLA type cavities under full responsibility of ACCEL, using DESY Nb material inspection, furnace and test infrastructure under service contract.

IOT RF POWER SOURCES FOR PULSED AND CW LINACS

H. Bohlen, Y. Li, R. Tornoe,
CPI Eimac Division, San Carlos, CA, USA

Abstract

For many years, klystrons have been the preferred RF power amplifiers for both pulsed and CW linacs at UHF and higher frequencies. Their properties have earned them that position. But in recent years, in UHF terrestrial television transmitters, the earlier predominant klystron has been replaced by the Inductive Output Tube (IOT) because the IOT provides higher efficiency and , due to its excellent linearity, can handle the simultaneous amplification of both the vision and the sound signal. Its robustness and life expectancy equals that of a klystron, and it more than compensates its lower gain by a lower price and a smaller size. Pulsed operation of an IOT can be achieved without the help a high-voltage modulator. Since the beam current is grid-controlled it is sufficient to pulse the drive power. For linac operation, derivates of UHF TV IOTs, capable of up to 80 kW CW output power, are already available and operating. In L-Band, they are presently joined by recently developed 15 to 30 kW CW IOTs. HOM-IOTs are expected to extend the CW range in UHF to 1 MW and beyond.

LINAC RF SOURCE REQUIREMENTS AND BASIC IOT PROPERTIES

Every linac has certain requirements regarding its RF power source. The most common ones are (not necessarily in this order): high efficiency, reliability and ruggedness, long-term stability, low pushing factors (AM/AM and AM/PM), long life, and all that at a price that does not jeopardize the project. For many years, klystrons have provided most of these properties, and they still do so. So, why and when use IOTs instead?

In now almost two decades of TV operation the IOT has developed into a device that equals the klystron in terms of reliability and ruggedness, long-term stability and life. That by itself is remarkable, but it would not serve as a prudent reason for a change. However, there are areas where the IOT shows significant superiority compared to the klystron.

Efficiency and Linearity

The IOT, also known as a klystrode*, is by its nature a special tetrode. The bunches in its electron beam are generated by means of a control grid and not by velocity modulation, as in a klystron. This results in several advantages. The first one is basic efficiency. Like a tetrode the IOT can be operated in class C mode, providing efficiency figures in the order of 73 % and higher. The second advantage is that the IOT's high basic efficiency can actually be fully exploited.

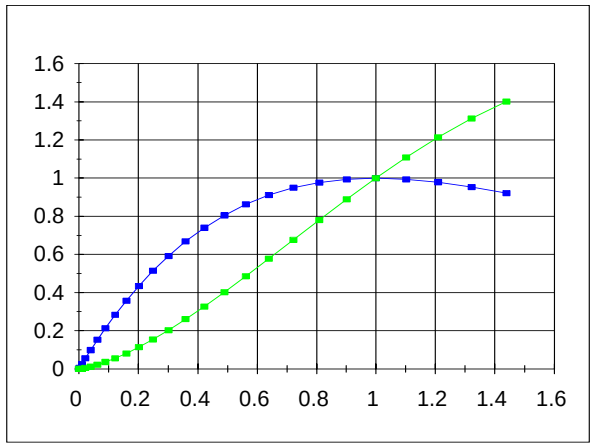

Figure 1: Normalized characteristics of output power (vertical axis) vs. drive power (horizontal axis) for klystrons (blue, saturating) and IOTs (green, not saturating).

Figure 1 highlights this very important feature for accelerator operation. In order to apply fast feedback control when using a klystron, a back-off in the order of 10 % of output power from the point of maximum efficiency (1/1 in the figure) is necessary, due to the change of slope in the characteristic at that point. An IOT, on the other hand, does not require a back-off; full use of its already higher basic efficiency can be made since its characteristic does not saturate at its nominal output power level.

A third advantage is superior linearity, resulting in low pushing factors. The characteristic in Figure 1 already reveals the lower AM/AM conversion in the vicinity of the operation point, compared to that of a klystron. AM/PM conversion is likewise much more benign in an IOT.

Costs

IOTs are simple devices. Basically, they contain only one RF circuit (the so-called input circuit is merely an impedance-matching device between the input line and the low-impedance cathode-grid structure). The whole tube is considerably shorter than a comparable klystron, resulting in a significantly lower price for both the IOT proper and the assembly hardware, including the focusing magnet.

A drawback is the lower gain of the IOT (in the order of 23 dB) which requires a more powerful driver, but this is usually more than compensated by reduced costs for power supplies and cooling devices, due to the higher efficiency. And, naturally, there are considerable savings in the power bill, especially in CW operation.

In pulsed operation, the power bill savings may not be that attractive. But in this case, another IOT feature that is

* Klystrode® is a trademark of CPI

REVIEW OF FAST BEAM CHOPPING

F. Caspers, CERN, Geneva, Switzerland

Abstract

Several types of fast beam chopping systems in use or under construction are presented. Emphasis is given to their specific technologies and in particular their various fields of application. Important parameters are duty cycle, rise- and fall-time, ringing and overall bandwidth. Certain systems have very specific driver concepts, since the generation of multi-kW peak power with nanosecond transients, high repetition rate and very good pulse shape fidelity is not a trivial issue. The design of driver amplifier and actual chopper structure are not always mutually independent and thus some of the limiting aspects will be discussed.

INTRODUCTION

Over the recent years different chopper structures and chopper systems (e. g. RAL-ESS, LANL-SNS, JAERI CERN-SPL) have been designed and tested. Some of them are already in operation, others still under construction and / or in development. Many of these chopper structures contain slow wave deflectors, since the beam to be chopped has a fairly low momentum, usually with $\beta = v/c$ values between 5 and 10 %. The specifications for the chopper systems differ largely in terms of duty cycle, rise-and fall-time as well as required deflection angle. Thus there is no unique solution for all existing machines and the structures and hardware presently available has been optimised for each individual application.

DISCUSSION OF CHOPPER CONCEPTS

In the following sections the properties and design concepts of the four chopper systems mentioned above will be shown and subsequently discussed. Obviously this selection cannot be complete and priority is deliberately given to the most recent projects.

THE RAL-ESS CHOPPING SCHEME#

This is an example of a chopping scheme for a next generation spallation neutron source [1]. Chopping is restricted to the 2.5 MeV medium energy beam transfer (MEBT) line, where a low level of emittance growth is predicted [2,5]. The proposed 'fast-slow' chopping technique addresses the requirements for a ~ 2 ns transition time, a 200 ns to 0.1 ms chopping duration, and a programmable duty cycle [2]. Components of the European Spallation Source (ESS) front-end are shown in schematic form in Fig. 1. ESS front-end specifications call for significant technical development and the design may be considered to be very relevant for next generation spallation sources and neutrino factories [3].

#Supported by EC Research Infrastructure Activity FP6 "Structuring the European Research Area" program, CARE –RII3-CT-3003-506395

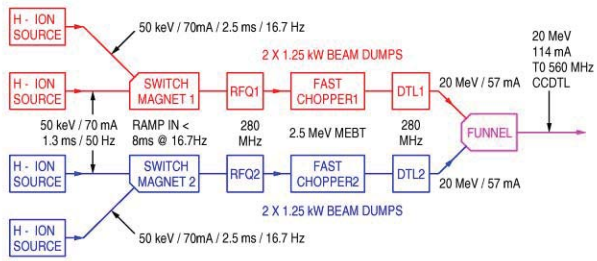

Figure 1: ESS front-end schematic [2].

A schematic drawing of the 2.5 MeV ESS MEBT line is shown in Fig. 2. and a corresponding table of key parameters can be found in [2].

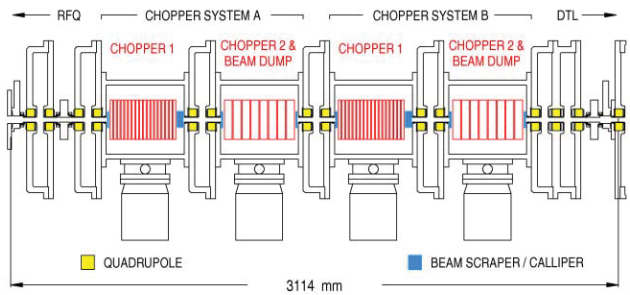

Figure 2: ESS MEBT line with 'Tandem' chopper [2].

The configuration has evolved from a previously reported design [4], and utilises two slow-wave E-field chopper systems operating in 'Tandem'. The design reduces beam dump power dissipation, and high voltage pulse generator repetition frequency by a factor of two, without incurring excessive emittance growth.

Simulated r.m.s beam radii and emittances from a revised optical design [5] return beam radii around 2 mm in both planes [2]. Input matching from the RFQ, use of regular lattice functions with the same beam aspect ratios in the channel cells, and a final six parameter output matching section, result in an acceptably low level of emittance growth and halo development. Optical amplification of beam deflection has not been attempted, and chopping fields are therefore higher than in other designs [6]. Key parameters and a timing schematic for one sub-system of the 'Tandem' chopper configuration are shown in Table 1, and Fig. 3, respectively.

'Tandem' sub-systems are identical in operation and operate alternately at a repetition frequency of 25 Hz. Each sub-system consists of an upstream fast chopper with a meander type slow-wave electrode structure [7]

High Power Targets

H. Kirk, BNL, Upton, Long Island, New York

Abstract

The accelerator physics community is responding to developing theoretical arguments for the search of new physics beyond the Standard Model by conceiving and proposing new high-intensity proton machines in the multi-megawatt class. These new machines will allow for the production of a variety of useful secondary beams but only if the proper target configurations are first developed and then implemented. In this paper, important target issues will be discussed and world-wide approaches and prospects for new targets will be reviewed.

NO SUBMISSION RECEIVED

END-TO-END BEAM DYNAMICS SIMULATIONS FOR THE ANL RIA DRIVER LINAC*

P.N. Ostroumov#, Physics Division, ANL, 9700 S. Cass Avenue, Argonne, IL, 60439

Abstract

The proposed Rare Isotope Accelerator (RIA) Facility consists of a superconducting (SC) 1.4 GV driver linac capable of producing 400 kW beams of any ion from hydrogen to uranium. The driver is configured as an array of ~390 SC cavities, each with independently controllable rf phase. For the end-to-end beam dynamics design and simulation we use a dedicated code, TRACK [1]. The code integrates ion motion through the three-dimensional fields of all elements of the driver linac beginning from the exit of the electron cyclotron resonance (ECR) ion source to the production targets. TRACK has been parallelized and is able to track large numbers of particles in randomly seeded accelerators with misalignments and a comprehensive set of errors.

INTRODUCTION

A detailed configuration of the 1.4-GV RIA driver linac was described in ref. [2]. The linac consists of a front-end and three sections of SC linac: low-, medium- and high-β sections. The front-end includes an ECR ion source, a Low Energy Beam Transport (LEBT) system, a Multi-Harmonic Buncher (MHB), a Radio Frequency Quadrupole (RFQ) and a Medium Energy Beam Transport (MEBT) system. The three sections of the linac are each separated by two stripper areas with a stripper foil or film and a post-stripper Magnetic Transport System (MTS). Beam dynamics in the driver linac are the most challenging for the multiple-charge-state uranium beam [2]. The baseline design of the driver linac has been optimized for simultaneous acceleration of two charge states (28^+ and 29^+) in the front-end and the first section of the linac up to the first stripper and optimized for five charge states between the two strippers (average charge state is 74^+) and five charge states in the high-β section (average charge state is 88^+). The acceleration of multi-q beams not only increases the total intensity but also reduces significantly the power to dump at the strippers. For example, the five charge states after the second stripper represent 98% of the total intensity. The linac lattice is optimized for multiple-charge-state uranium beams and includes 220 SC drift tube based resonators between the front end and the second stripper. The stripping energies for uranium beam, 12 MeV/u and 89.86 MeV/u, are optimized to minimize the longitudinal effective emittance of multi-q beams at the location of the strippers. The baseline design includes 172 SC cavities of elliptical type beyond the second stripper. The most recent parameters of the RIA driver baseline design were reported in the RIA R&D workshop [3].

With cw operation of the driver linac, the space charge effects are negligible in all accelerator sections except the ECR source, the ECR extraction optics and the LEBT. The required beam intensity in the LEBT is 500 μA for protons and 250 μA for uranium to produce 400 kW accelerated cw beams. After separation and selection of ion species the beam optics become emittance dominated and the space charge effects produce small perturbations with respect to the "zero-current" beam optics. Downstream of the LEBT the space charge effects are negligible.

FRONT END

ECR-LEBT

Detailed design, optimization and simulation of the front-end is extremely important to produce a realistic beam distribution in the six-dimensional phase space at the entrance of the SC linac. Several publications have been devoted to this problem [4-6].

Beam parameters at the entrance of the LEBT have been obtained from simulations of multi-component ion beams through extraction and acceleration system of the ECR, including the extraction electrodes, solenoid lens and accelerating tube (Fig. 1). The total accelerating voltage is 100 kV. The calculations performed by the code TRACK, including static electric and magnetic field distributions and beam space charge, are consistent with the recent experimental data [7]. The achromatic section of the LEBT has been optimized to select two charge state heavy-ion beams and obtain a ~6 mm diameter beam at the location of the MHB. Figure 2 shows transverse phase space plots of dual charge state ion beam at the location of mass-analyzing slits and at the entrance of the MHB. The total extracted beam current is 3.9 mA with each charge state of U^{28+} and U^{29+} carrying 125 eμA. The simulations show that the system separates charge states reliably over full range of total input beam currents and provides at the MHB similar Twiss parameters for transverse emittances for both charge states.

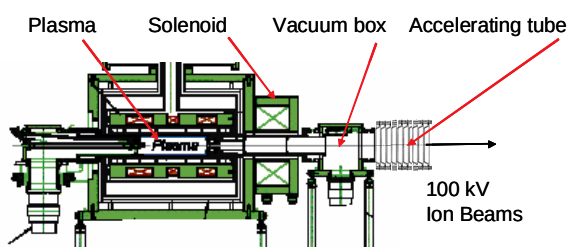

Figure 1: Beam extraction from the ECR.

Work supported by the U.S. Department of Energy, Office of Nuclear Physics, under Contract No. W-31-109-ENG-38.
#ostroumov@phy.anl.gov

INTERMEDIATE-VELOCITY SUPERCONDUCTING ACCELERATING STRUCTURES*

J. R. Delayen#, Thomas Jefferson National Accelerator Facility, Newport News, VA 23606, USA

Abstract

In the last decade, one of the most active areas in the applications of the superconducting rf (SRF) technology has been for the acceleration of ions to medium energy (~1 GeV/amu). One such accelerator is under construction in the US while others are being proposed in the US, Japan, and Europe. These new facilities require SRF accelerating structures operating in a velocity region that has until recently been unexplored, and new types of structures optimized for the velocity range from ~0.2 to ~0.8 c have been developed. We will review the properties of these intermediate-velocity structures, the status of their development, as well as present an over view of the medium-energy superconducting ion accelerator designs being developed world-wide.

OVERVIEW OF MEDIUM-ENERGY ION ACCELERATORS

Medium-energy superconducting ion accelerators can be grouped into three broad categories: high-current cw, high-current pulsed, and low-to medium current cw.

High-current cw accelerators

The main application of cw high-current ion accelerators is for accelerator driven systems, either for energy production, waste transmutation or (some time ago) tritium production [1-3].

The main technical issues and challenges are:

- Beam losses (< 1 W/m in order to allow hands-on maintenance)
- Activation
- High cw rf power
- Higher order modes
- Cryogenics losses

The implications for SRF technology are:

- Cavities with high acceptance
- Development of high cw power couplers
- Extraction of HOM power
- Cavities with high shunt impedance

High-current pulsed accelerators

Accelerators in this category are mostly H^- or proton accelerators for neutron production; the best example of these machines is the Spallation Neutron Source (SNS) under construction at ORNL as collaboration between several laboratories [4], or the proposed European Spallation Source. A different application, although with similar beam parameters, is the 8 GeV injector linac at Fermilab [5].

The main technical issues and challenges are:

- Beam losses (~ 1 W/m)
- Activation
- Higher order modes
- High peak rf power
- Dynamic Lorentz detuning

The implications for SRF technology are:

- Cavities with high acceptance
- Development of high peak power couplers
- Extraction of HOM power
- Development of active compensation of dynamic Lorentz detuning

Low-to-medium current cw accelerators

The best example of low-to-medium current cw accelerator is the Rare Isotope Accelerator (RIA) under consideration in the US [6]. The RIA driver would be capable of initially producing a 100 kW, 400 MeV/u uranium beam and also a ~ 1 GeV proton beam.

The main technical issues and challenges are:

- Microphonics, frequency control
- Cryogenic losses
- Wide charge to mass ratio
- Multicharged-state acceleration
- Activation

The implications for SRF technology are:

- Cavities with low sensitivity to vibration
- Development of microphonics compensation
- Cavities with high shunt impedance
- Cavities with large velocity acceptance (few cells)
- Cavities with large beam acceptance (low frequency, small frequency transitions)

ACCELERATING STRUCTURES

The majority of the superconducting structures that are being developed for medium-energy accelerators fall into two categories: those based on $\lambda/2$ resonant transmission line modes (TEM-like) and those based on a transverse magnetic (TM) mode [7-9]. The former can be of either the coaxial half-wave or spoke geometry, the latter are compressed versions of the familiar "elliptical" geometry used in high-energy accelerators.

* Work supported by the U.S. Department of Energy under contracts DE-AC05-84-ER40150 and DE-AC05-00-OR22725.
#delayen@jlab.org

END-TO-END BEAM SIMULATIONS FOR THE MSU RIA DRIVER LINAC*

X. Wu†, M. Doleans, D. Gorelov, Q. Zhao, T. L. Grimm, F. Marti and R. C. York,
National Superconducting Cyclotron Laboratory, Michigan State University, E. Lansing,
MI 48824, USA

Abstract

The Rare Isotope Accelerator (RIA) [1] driver linac proposed by Michigan State University (MSU) will use a 10th sub-harmonic based, superconducting, cw linac to accelerate light and heavy ions to final energies of ≥ 400 MeV/u with beam powers of 100 to 400 kW. The driver linac uses for acceleration superconducting quarter-wave, half-wave, and six-cell elliptical cavities with frequencies ranging from 80.5 MHz to 805 MHz, and for transverse focusing superconducting solenoids and room temperature quadrupoles. For the heavier ions, two stages of charge-stripping and multiple-charge-state acceleration will be used to meet the beam power requirements and to minimize the requisite accelerating voltage. End-to-end, three-dimensional (3D), beam dynamics simulations from the Front End to the output of the driver linac have been performed. These studies include a 3D analysis of multi-charge-state beam acceleration, evaluation of transverse misalignment and rf errors on the machine performance, and modeling of the charge-stripping foils and stripping-chicane performance. The results of these beam dynamics studies will be presented, and further planned beam dynamics studies will be discussed.

INTRODUCTION

RIA beam dynamics studies [2,3] have been performed at Michigan State University since 1999 as part of an overall effort to establish a comprehensive design for RIA and in support of the on-going Superconducting Radio Frequency (SRF) R&D program. To meet the beam power (≤400 kW) specification, multi-charge state beam acceleration for heavy ions is required. To meet beam loss criteria ($\leq 10^{-4}$) for hand-on maintenance, adequate acceptances and limited emittance growths must be achieved. The MSU RIA driver lattice design [4] was predominantly motivated by the minimization of technical risk and maximization of simplicity, leading to higher probability of achieving performance and increased operational efficiencies. The 10th sub-harmonic or 80.5 MHz was chosen, compared to 14th sub-harmonic or 57.5 MHz proposed by ANL [5], as the lowest linac frequency to significantly reduce microphonics in the first segment of the Superconducting Linac (SCL), allowing a simple solution utilizing a mechanical damper and modest rf while avoiding the VCX tuner reliability concerns. The design requires only three rf frequencies and six SRF cavity types for the driver linac.

*Work supported by MSU and DOE.

†xwu@nscl.msu.edu

Figure 1 shows the Rare Isotope Accelerator (RIA) driver linac layout that is being evaluated at MSU. A folded MSU RIA driver linac option also exists by bending the beam 180° in the 2nd charge-stripping chicane. It consists of a room temperature Front End, and three segments of superconducting rf linac, separated by two charge-stripping sections that provide a cost-effective method of achieving the final beam energy for a wide range of ions from proton to uranium. A beam switchyard will deliver up to 400 MeV/u ion beams to the Isotope Separation On Line (ISOL) and Particle Fragmentation (PF) target area. The RIA driver linac will be operated in a continuous-wave (cw) mode, effectively providing a 100% duty factor.

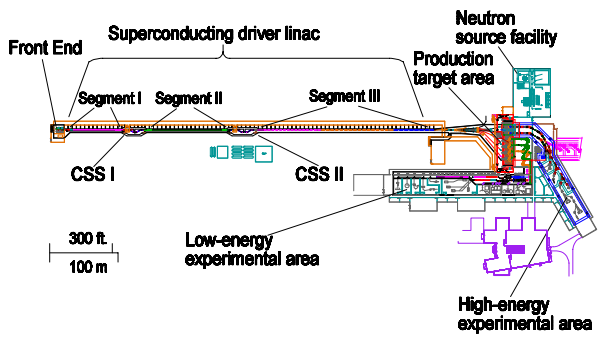

Figure 1: Layout of the MSU RIA driver linac.

End-to-end beam simulations were performed to quantify the driver linac performance and evaluate the full effects of alignment and rf errors through all three segments of the driver linac, given a realistic initial input beam from the ECR ion source. A model of the charge stripping foil including the effects of multiple scattering, energy loss and straggling, and variation in foil thickness was also included in the simulations. Since the multi-charge state beam acceleration for heavy ions [6] is the most challenging, our end-to-end simulations assumed an initial beam consisting of a two-charge state ^{238}U beam from the ECR going through two charge-stripping targets during acceleration in RIA driver linac. Charge states of 28+ and 29+, 71+ to 75+, and 87+ to 89+ will be accelerated in Segments I, II and III, respectively.

Various computer codes were used for beam dynamics studies. The simulations for the Front End were done primarily using PARMELA and PARMTEQ to include space-charge effects. LANA [7] was used for the longitudinal beam dynamics studies, 6-D phase space particle tracking, and rf error analysis in the SCL segments. DIMAD [8] and COSY INFINITY were used to study the transverse focusing structure, beam matching,

DESIGN IMPROVEMENT OF THE RIA 80.5 MHZ RFQ

Q. Zhao*, V. Andreev, M. Doleans, D. Gorelov, T. Grimm, W. Hartung, F. Marti, S.O. Schriber, X. Wu, R.C. York, NSCL, Michigan State University, East Lansing, MI 48824, USA

Abstract

An 80.5 MHz, continuous-wave, normal-conducting, radio-frequency quadrupole (RFQ) was designed for the front end of the Rare Isotope Accelerator (RIA) driver linac. It will accelerate various ion beams (hydrogen up to uranium) from 12 keV/u to about 300 keV/u. The 4-meter-long RFQ accepts the pre-bunched beams from the low energy beam transport (LEBT) and captures more than 80% of the beams with a current of ~0.3 mA. Beam dynamics simulations show that the longitudinal output emittance is small for both single- and two-charge-state ion beams with an external multi-harmonic buncher. A 4-vane resonator with magnetic coupling windows was employed in the cavity design to provide large mode separation, high shunt impedance, and a small transverse dimension. The results of beam dynamics as well as the electromagnetic simulations are presented.

INTRODUCTION

To minimize beam losses in the RIA driver linac, the superconducting (SC) linac requires the front end to provide a longitudinal beam emittance of about 1.2 π·keV/u·ns (99.5% particles) with minimum transverse emittance growth. Since the beam current is not very high in the RIA driver linac, the dc beam selected from the ion source can be efficiently pre-bunched by an external multi-harmonic buncher before injection into the RFQ. This scheme can produce a smaller longitudinal output emittance [1], and enhance the RFQ's acceleration efficiency. In previous designs of the front end RFQ [2,3], the longitudinal output emittance was larger than the requirement when using a more realistic input beam from LEBT that includes unbunched particles. Therefore, we optimized the initial longitudinal acceptance and its evolution to remove the tails while still maintaining the transverse emittance. Beam dynamics simulations showed about 83% of the injected beam was accelerated with required output emittances. In addition, an improved 4-vane RFQ structure with coupling windows was adopted to achieve improved mode separation and smaller power dissipation.

The driver linac will provide ion beams from protons up to uranium. To meet the final beam power requirement for heavier ions, two charge-state beams will be injected and accelerated in alternate longitudinal buckets of the RFQ [4]. Since the heaviest ion beams are the most challenging, the baseline design has been primarily focused on the uranium beam with charge states of 28+ and 29+. Therefore, the RFQ must be able to operate with a wide range of power levels to accommodate the different ion species. To minimize the range of voltages, we proposed to use triatomic hydrogen molecule ions (e.g. H_3^+ instead of H^+ for proton) from the ion source through the RFQ and first segment of SC linac until stripped into monatomic ions at first stripper, which also reduces the beam current by a factor of 3 at the low energy side.

* zhao@nscl.msu.edu

DESIGN PHILOSOPHY

The 100% duty factor, normal conducting RFQ will accelerate ion beams from 12 keV/u to about 300 keV/u. The input energy is determined by the high voltage platform of ion source, while the output energy is set to obtain a transit time factor of 0.5 for the first SC cavity in the driver linac and is a tradeoff between the acceptance of the SC linac and the size of RFQ. The 80.5 MHz frequency is chosen to be the same as the successive quarter-wave superconducting structures.

The design goals are the minimization of the longitudinal and transverse emittance, RF power requirements and structure size. For the RIA beam currents, an external harmonic buncher with a quasi-linear bunching field can generate a small longitudinal emittance beam for RFQ. To obtain a low output emittance, the RFQ should only accept the well-bunched core particles for further acceleration avoiding capture of the small fraction particles in the tails of the distribution. Since the beam is already bunched at the entrance of RFQ, an initial synchronous phase of –30° and a modulation factor of 1.03 are chosen so that the longitudinal acceptance is truncated, as shown in Fig. 1. These values represent an optimization between the removal of tail particles and providing a linear field for the bunched particles. The modulation factor as well as the synchronous phase is then smoothly increased to accelerate just the core particles.

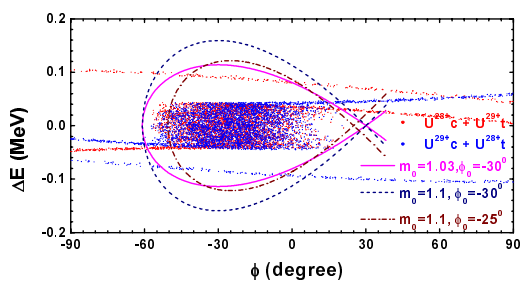

Figure 1: Initially reduced separatrices with bunched beams.

Even though the beam is pre-bunched, a four-cell radial matcher was found to be of benefit especially for a two-charge-state beam. A reduced adiabatic bunching design before the acceleration section is necessary to achieve stable bunches and control the blowup of emittances. Particles with large transverse amplitudes may result in

FABRICATION OF SUPERCONDUCTING CAVITIES FOR SNS

M. Pekeler, S. Bauer, J. Schwellenbach, M. Tradt, H. Vogel, P. vom Stein,
ACCEL Instruments GmbH, Friedrich-Ebert-Str. 1, 51429 Bergisch Gladbach, Germany

Abstract

During the last three years ACCEL fabricated almost all 109 superconducting cavities for the Spallation Neutron Source (SNS) in Oak Ridge, Tennessee. Two series of 35 medium beta (beta=0.61) and 74 high beta (beta=0.81) cavities will be delivered until October 2004. Besides cavity manufacturing ACCEL also performed RF tuning and chemical surface preparation. We give an outline on the current manufacturing experience and comment on future developments for industrial cavity production.

INTRODUCTION

In August 2001 the contract for the production of in total 109 elliptical 6-cell 805 MHz superconducting niobium cavities was awarded to ACCEL by JLAB. Two families of cavities had to be produced, 35 cavities of the medium beta type optimised for β=0.61 particle velocity and 74 cavities of the high beta type optimised for β=0.81 particle velocity needed to be produced within a 3 years period.

In addition to the manufacturing, the contract also included the surface removal of 30 µm from the outside and 100 µm from the inside by buffered chemical polishing.

The last step before delivery is field flatness tuning of the π-mode to accuracy better than 5% in amplitude and adjustment of the external Q of the fundamental mode of the HOM couplers to values above 10^{12}.

CAVITY MANUFACTURING

At the time of the contract award prototype cavities of both families were already produced at Jefferson Laboratory. After contract award major milestones for the successful run of the project were:

- Engineering review of manufacturing procedures of the prototype cavities.
- Develop production drawings to reflect different manufacturing methods used at ACCEL compared to the JLAB used procedures for the prototype cavities.
- Establish QA plan for the cavity production and detailed workshop travellers.
- Design and manufacturing of all tooling for metal forming, turning, milling, electron beam welding, leak check, tuning, inner and outer BCP needed for the series production.
- Determine optimum electron beam welding parameters for all weld geometries.

The engineering review of the cavity manufacturing methods lead to the decision to change production details compared to the prototype cavities. The main changes were:

- Deepdrawing of half cells using a stamp and a cushion instead of inner and outer die. This technique requires fewer production steps and results in better accuracy of cell geometry.
- Production of raw end groups (see figure 1) out of one sheet of reactor grade niobium by deep drawing and nipple pulling.
- Production of the HOM coupler bodies out of reactor grade niobium cans (ordered from Heraeus GmbH).

The finished cavities can be seen in Figure 2 (medium beta cavity) and Figure 3 (high beta cavity) ready for shipment to JLAB.

Figure 1: Raw end groups produced for SNS cavities by deep drawing and nipple pulling from one reactor grade niobium sheet.

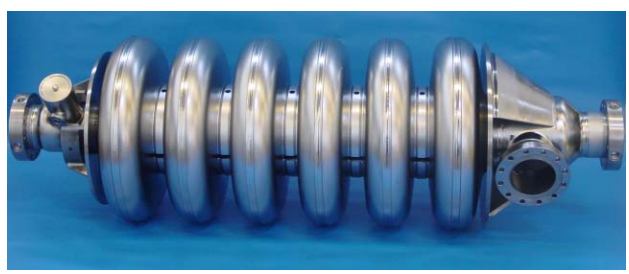

Figure 2: Medium beta 6 cell 805 MHz cavity produced for the Spallation Neutron Source Linac. The production of the medium beta cavities is finished.

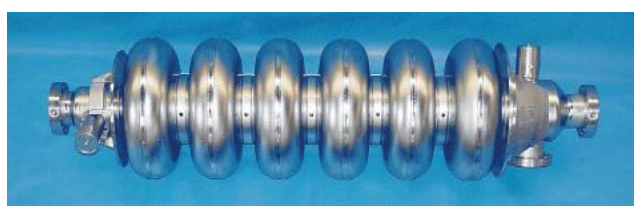

Figure 3: High beta 6 cell 805 MHz cavity for SNS. The series production of the 74 high beta cavities is scheduled to be completed in October 2004.

SUPERCONDUCTING β=0.15 QUARTER-WAVE CAVITY FOR RIA

M.P. Kelly, Z.A. Conway, J.D. Fuerst, M. Kedzie, K.W. Shepard
Argonne Physics Division, Argonne National Laboratory, Argonne, IL 60439, USA

Abstract

A 109 MHz niobium quarter-wave cavity, fully configured with an integral stainless steel helium jacket, has been built and tested as part of the R&D for the Rare Isotope Accelerator (RIA) driver linac. The two-gap cavity is designed to accelerate ions over the velocity range 0.14<β<0.24. Final processing of the cavity RF surfaces, including high-pressure rinsing and assembly of the cavity with a high-power, variable rf coupler, were all performed under clean-room conditions. Cold test results including high-field cw operation, microphonics, and helium pressure sensitivity are discussed..

INTRODUCTION

A superconducting (SC) linac for the Rare Isotope Accelerator (RIA) ion driver requires several hundred SC cavities of several different types spanning the velocity range 0.02<β<0.8 [1]. We report here on the first cold tests of a prototype for one of these types, a β=0.15 niobium quarter-wave resonator (QWR). Although the QWR cavity discussed here will initially be used in an energy upgrade of the existing ATLAS accelerator, it has been developed specifically for the RIA driver linac as one of a set of three SC cavities spanning the intermediate velocity range 0.12<β<0.5. The other two cavities are a half-wave cavity, reported elsewhere at this conference [2], and a two-cell spoke-loaded cavity which has been reported previously [3]. The cold-test results for the QWR cavity discussed below represent the completion of development of the entire set of three cavities, in all of which the performance substantially exceeds the requirements of RIA.

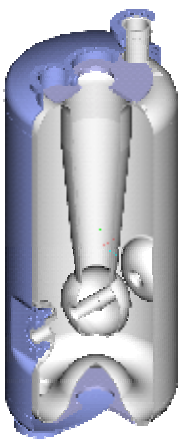

Figure 1: A partially cut away view of the RIA quarter-wave cavity generated in Pro/Engineer. The active length along the beam axis is 25 cm.

DESIGN AND CONSTRUCTION

The design of the β=0.15 QWR is shown in Figure 1. The inner niobium shell is shown in gray while the stainless-steel helium vessel is shown in blue. Electromagnetic parameters are listed in Table I. The cavity design was developed using numerical finite-element models in full 3D, using Pro/Engineer for the mechanical properties and CST Microwave Studio for the electromagnetic properties..

The useful accelerating range spans the velocity region 0.10<β<0.30, a velocity somewhat higher than for most existing quarter-wave structures. A correction for beam steering, inherent in quarter-wave structures due to the rf magnetic field in the beam region, has been incorporated by tilting the drift-tube faces by approximately 9° [4] The top and bottom of the QWR cavity are terminated in a large-radius toroid to avoid sharp corners and facilitate both chemical processing and rinsing, and also high-pressure water rinsing.

Frequency	109.13	MHz
Geometric Beta	0.144	v/c
Active Length	25	cm
QRs	40	ohm
R/Q	548	
below for Eacc = 1 MV/m		
Epeak	3.2	MV/m
Bpeak	58.3	Gauss
RF Energy	0.17	Joule

Table I: Electromagnetic properties of the QWR cavity

The cavity was formed of high-purity, RRR > 250, 3mm niobium sheet. The center conductor, toroids, and drift-tube faces were hydroformed, while the outer housing was rolled from flat niobium sheet. The niobium cavity-shell is enclosed in an integral stainless-steel helium vessel, as is the case for all of the ANL-developed RIA cavities. The stainless jacket is joined to the niobium at the cavity ports by a vacuum braze with pure copper. All nb-nb joints are electron-beam welded..

SURFACE PROCESSING

Chemical processing

It is well established that electropolishing of a niobium surface gives a substantially smoother and brighter rf surface than a heavy buffered chemical polish (BCP) and experimental data indicate that rf losses are reduced

COLD TESTS OF A SUPERCONDUCTING CO-AXIAL HALF-WAVE CAVITY FOR RIA

M.P. Kelly, J.D. Fuerst, M. Kedzie, K.W. Shepard
Argonne Physics Division, Argonne National Laboratory, Argonne, IL 60439, USA

Abstract

This paper reports cold tests of a superconducting niobium half-wave cavity with integral helium vessel, the design of which is suitable for production for the Rare Isotope Accelerator (RIA) driver linac. The cavity operates at 172 MHz and can provide more than 2 MV of accelerating voltage per cavity for ions with $0.24<\beta<0.37$. Cavity rf surfaces were prepared using electropolishing, high-pressure rinsing and clean assembly. Measurements of Q_0 show a residual rf surface resistance R_S = 5 nΩs in both 2 K and 4 K operations. The cavity can be operated at 4.5 K with E_{Acc} >10 MV/m (E_{Peak} >30 MV/m). Performance exceeds RIA specifications of an input power of 12 Watts at 4.5 K and E_{Acc} = 6.9 MV/m. RMS frequency jitter is only 1.6 Hz at E_{Acc} = 8 MV/m and T = 4.5 K as determined from microphonics measurements in a realistic accelerator environment connected to the ATLAS refrigerator.

INTRODUCTION

The Rare Isotope Accelerator (RIA) superconducting (SC) multi-ion driver requires ~390 SC cavities of several different types spanning the velocity range $0.02<\beta<0.8$ [1]. We report here on the cold tests of a prototype for one of these types, a β=0.26 niobium half-wave resonator (HWR). The HWR cavity discussed here will initially be used in an energy upgrade of the existing ATLAS accelerator, however, it has been developed specifically for the RIA driver linac as one of a set of three SC cavities spanning the intermediate velocity range $0.12<\beta<0.5$. The other two cavities are a quarter-wave cavity, reported elsewhere at this conference [2], and a two-cell spoke-loaded cavity which has been reported previously [3]. The complete set of three cavities all substantially exceed the performance requirements of RIA.

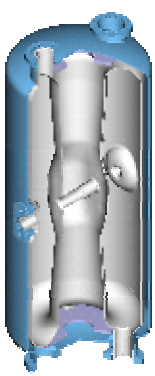

Figure 1: A partially cut away view of the RIA half-wave cavity generated in Pro/Engineer. The active length along the beam axis is 30 cm.

FABRICATION

The design of the β=0.25 half-wave resonator (HWR) is shown in Figure 1. with electromagnetic parameters in Table I. The inner niobium shell is shown in gray while the stainless-steel helium vessel is shown in blue. The cavity design was developed using numerical finite-element models in full 3D, using Pro/Engineer for the mechanical properties and CST Microwave Studio for the electromagnetic properties.

Table 1: Electromagnetic properties of the HWR cavity

Frequency	170	MHz
Geometric Beta	0.26	v/c
Active Length	30	cm
QRs	57	ohm
R/Q	241	
below for Eacc = 1 MV/m		
Epeak	2.9	MV/m
Bpeak	78	Gauss
RF Energy	0.338	Joule

The useful accelerating range spans the velocity region $0.24<\beta<0.40$. The top and bottom of the HWR cavity are terminated in a large-radius toroid to avoid sharp corners and facilitate both chemical processing and rinsing, and also high-pressure water rinsing.

The cavity was formed of high-purity, RRR > 250, 3 mm niobium sheet. The center conductor, toroids, and drift-tube faces were hydroformed, while the outer housing was rolled from flat niobium sheet. The niobium cavity-shell is enclosed in an integral stainless-steel helium vessel, as is the case for all of the ANL-developed RIA cavities. The stainless jacket is joined to the niobium at the cavity ports by a vacuum braze with pure copper. All nb-nb joints are electron-beam welded.

PROCESSING AND ASSEMBLY

Electropolishing

Electropolished surfaces like those shown in Figure 4. are known to be substantially smoother than those achieved using standard buffered chemical polish (BCP). Electropolishing has been used here to remove between 100 and 150 microns of niobium from all of the critical rf surfaces. Results shown here together with other recent results for ANL cavities indicate that electropolishing

PERFORMANCE IMPROVEMENT OF THE MULTICELL CAVITY PROTOTYPE FOR PROTON LINAC PROJECTS

B. Visentin#, J.P.Charrier, G. Devanz, Y. Gasser, J.P. Poupeau, D. Braud, P. Sahuquet, B. Coadou,
CEA-Saclay, DSM/DAPNIA/SACM - 91191 Gif / Yvette Cedex - France
H. Saugnac, H. Gassot, S. Bousson, Ph. Szott
IPN-Orsay, Accelerator Division - 91406 Orsay Cedex - France

Abstract

The CEA-Saclay / IPN-Orsay collaboration allowed to manufacture a multicell superconducting RF cavity prototype for proton linac. Since the first experimental results [1], obtained in a vertical cryostat and the horizontal cryostat CryHoLab, the accelerating field E_{acc} has been recently increased up to 19 MV/m with a quality factor $Q_0 = 9.10^9$ and a limitation by quench.

However some improvements are still needed, in particular to suppress the field emission above 16 MV/m.

INTRODUCTION

The French R&D program on superconducting RF cavities dedicated to fit the high energy section (>100 MeV) of high intensity proton linear accelerators (see Fig.1) is mainly supported by two European projects:

- XADS, Preliminary Design Study of an eXperimental Accelerator Driven System. In this concept, neutrons are produced from spallation processes induced by the proton beam interaction with a heavy material target (Pb). These neutrons make up the external neutron source for a subcritical nuclear reactor to sustain transmutation of nuclear wastes,
- EURISOL, Research and Technical Development for the EURopean Isotope Separator On-Line, a radioactive beam facility in Europe. Rare isotopes are produced after the proton beam interaction with the target.

In this context, the CEA-Saclay and IPN-Orsay Laboratories started few years ago a collaboration to design, build and test a multicell cavity prototype for medium beta (β=0.65). At the same time an international collaboration was also established with INFN-Milan for the low beta superconducting cavities (β=0.47) for the Italian TRASCO program [2]. This R&D on multicell superconducting cavities should be continuing within the 6th European framework program with the Integrated Project EUROTRANS (XADS continuation), the EURISOL Design Study and the CARE-HIPPI (High Intensity Pulsed Proton Injector) program linked to the SPL (Superconducting Proton Linac) project at CERN.

CAVITY FEATURES

The five-cell A5-01 cavity (700 MHz, β=0.65), manufactured by CERCA from Wah Chang Niobium sheets (thickness 4 mm - RRR>250), is characterized by ratios of E_{peak}/E_{acc} and B_{peak}/E_{acc} surface peak to accelerating fields, respectively about 2.32 and 4.48 mT/(MV/m). Conflat® flanges, and liquid helium vessel, made from 316 L stainless steel, are copper-brazed on niobium. The mechanical stiffness of the cavity is ensured by the stainless steel frame (20 mm thick) and bracing rods, without stiffening rings between cells. Moreover, the cavity has been annealed under vacuum in furnace (650°C, ~ 1.10^{-7} mbar) to prevent the Q-disease during the RF test in the horizontal cryostat.

EXPERIMENTAL RESULTS

Preliminary Results

The first RF results achieved on this cavity have been discussed in previous papers [1,3]. During these tests, some problems occurred:

- a vacuum leak due to the acid attack of the brazing metal. This leak was temporarily sealed with a Stycast® epoxy compound,

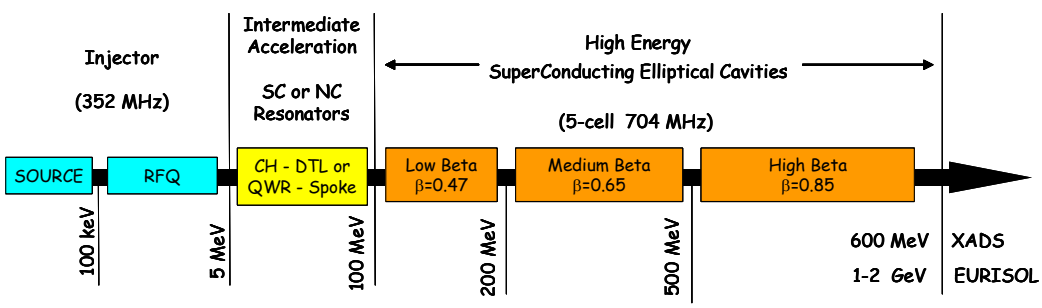

Figure 1: Schematic layout of a high intensity proton linear accelerator.

bvisentin@cea.fr

THE FRANKFURT FUNNELING EXPERIMENT*

J. Thibus†, U. Bartz, N. Müller, A. Schempp, H. Zimmermann, IAP,
J.W. Goethe-University, Frankfurt a.M., Germany

Abstract

Funneling is a procedure to multiply beam currents of rf-accelerators at low energies. In the ideal case the beam current can be multiplied in several stages without emittance growth. The Frankfurt Funneling Experiment consists of two ion sources, a Two-Beam RFQ accelerator, two different funneling deflectors and a beam diagnostic equipment system. The whole set-up is scaled for He^+ instead of Bi^+ for the first funneling stage of a HIIF driver. The progress of our experiment and the results of the simulations will be presented.

INTRODUCTION

The maximum beam current of a linac is limited by the beam transport capability at the low energy end of the accelerator. For a given ion source current and emittance the linac current limit is proportional to $\beta = v/c$ for electric and to β^3 for magnetic focusing channels and ideal emittance conservation. The funneling scheme is making use of the higher current limits at higher beam energies by doubling the beam current combining two bunched beams preaccelerated at a frequency f_0 with an rf-deflector to a common axis and injecting into another rf-accelerator at frequency $2 \cdot f_0$ as shown in figure 1. Ideally the beam emittance could be staying as low as for one single beam. Extracting twice the beam from a single ion source would result in at least twice the emittance for the following accelerators.

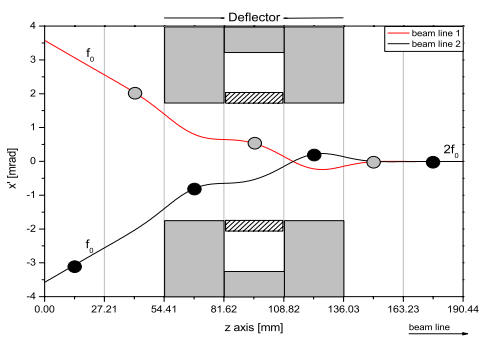

Figure 1: Principle of funneling demonstrated at a 3 cell deflector. To reduce the bending voltage drift tubes can be placed in the wider electrode apertures (shaded rectangle).

* Work supported by BMBF
† thibus@iap.uni-frankfurt.de

A tree of ion linacs is planned to increase the heavy ion beam current from 25 mA Bi^+ at the first linac to 400 mA at 10 MeV/u for the main linac.

The first linac is an RFQ with two beam channels in one resonator. By the use of the Two-Beam RFQ the distance of the two beams are very small while they are still radially and longitudinally focused. Additional discrete elements like quadrupole-doublets and -triplets, debunchers and bending magnets, as they have been proposed in first funneling studies, might not be necessary [1, 2, 3]. A short rf-funneling deflector is placed at the beam crossing position behind the RFQ [4].

EXPERIMENTAL SETUP

The Two-Beam RFQ accelerator is designed for He^+-ions instead of Bi^+ to reduce experimental expenses, facilitate operation and beam diagnostics (fig. 2,3). Two small multicusp ion sources [5, 6] and electrostatic LEBT lenses are used. The LEBTs are directly mounted at the front of the RFQ. The angle of both beam axes is 75 mrad.

Figure 2: Picture of the experiment.

The Two-Beam RFQ consists of two sets of quadrupole electrodes, where the beams are bunched and accelerated driven by one resonant structure. The RFQ electrodes are divided in two sections. The first section, which is about two thirds of the total length of 2 meters, bunches and accelerates the beam to a final energy of 160 keV. At first the second part has been used as a transport section with unmodulated RFQ electrodes. For first beam tests only one RFQ-channel has been replaced by a section that matches the beam to the funneling deflector to optimize beam radius and phase width. This allowed us to compare both RFQ channels directly.

TUNER DESIGN FOR HIGH POWER 4-ROD-RFQs*

A. Schempp#, L. Brendel, B. Hofmann, H. Liebermann
Institut für Angewandte Physik
Johann Wolfgang Goethe-Universität, 60054 Frankfurt am.Main, Germany

Abstract

The performance of high power RFQ linacs, as used in spallations sources and proposed for projects like ADxy, IFMIF or high duty factor drivers for RIB application are limited by beam dynamic properties as well as technical limits like sparking, power density, cooling and thermal stresses. A "one piece structure" even possible in theory has to have means for tuning the real fields like exchangable or moving tuners. Tuner design features will be discussed and results will be presented.

INTRODUCTION

The low energy section of a modern ion linac consist of an RFQ-DTL combination in which the beam from the ion source is shaped to match the experiment or the following accelerator, an high energy linear or circular accelerator.

The beam dynamics and rf-structure designs for moderate beam currents and pulsed structures are proven and there is a lot of experience and tools to match and shape for different special requirements.

For high average beam power and e.g. cw-operation of linacs the freedom of parameter is limited and the interference of beam dynamics with rf-design and mechanical engineering is much stronger.

There are high duty factor heavy ion machines and some experience with cw high current RFQ prototypes but new projects like the IFMIF / XADS [1] type of projects require new parameter ranges which cannot be achieved by just extrapolating low power structures.

The succesful tests of the LEDA RFQ with 100mA cw proton beam illustrates the magnitude of problems to be solved [2].

One important point is the tuning of a long structure. Starting from designs for an ideal cavity the frequency of the resulting structure can be determined in the order of some percents precision. The more homogenous the structure the more precise the simulation can be. But, e.g. with the modulation of the RFQ electrodes structure and by this varying capacity along the RFQ the simulation are less precise and in addition some design ask for a tilted field distribution, while in the normal designs the field amplitude is just a constant factor.

Tilted field designs are even more difficult to simulate and mechanical tolerances bring unavoidable field and frequency errors.

One point which brought some reduction in length sensitivity was the development of resonantly coupled sections and distributed rf-feeds and vacuum pumping ports. Still the LEDA-RFQ has 132 tuners to compensate for discontinuities and field balance.

The 4-rod-RFQ-structure is less sensitive to mechanical asymmetries, a typical number is 10 tuners for a 4 m long RFQ at 200 MHz. There are two kind of tuners: static ones to tune the frequency and dynamic ones to compensate for temperature changes. For lower average rf-powers this is no real problem. 30A/cm scale down to average currents of less than 1A/cm and rather low power losses on the contacts between tuner blocks and the tank base, which can be simple spring fingers, special developed finger stock like for tunable cyclotrons or metal vacuum seals.

We have made an attempt to investigate these problems, because for possible application of the 4-Rod as cw structure the straightforward finger stock material used so far is at its limits.

RFQ TUNER

The 4-Rod-RFQ consists of a chain of interlaced $\lambda/2$ resonators operating in π0-mode, generating the homogenous quarupole voltage distribution along the RFQ electrodes. Basicly the capacitively loaded stem structure is a loaded chain of strongly coupled resonators. The frequency of theses resonators should be identical, then the fields will be constant along the RFQ. Mechanical inhomogeneities, ports etc. and the varying electrode shape detune the chain.

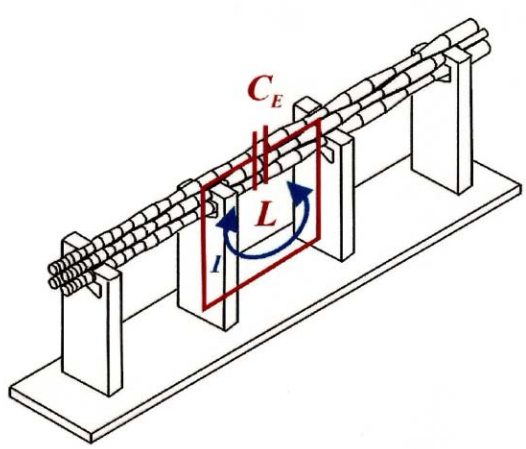

Figure 1: Basic 4-Rod-RFQ cell.

*supported by the BMBF
#a.schempp@em.uni-frankfurt.de

DESIGN OF A 352 MHZ-PROTON-RFQ FOR GSI *

B. Hofmann, L. Brendel, A. Schempp#,
Institut für Angewandte Physik,
Johann Wolfgang Goethe-Universität, 60054 Frankfurt am.Main, Germany

Abstract

Part of the future project of GSI is a new p-linac for the production of Antiprotons. The 4-Rod-RFQ operating at 352 MHz has to accelerate up to 100mA protons from an ECR source. Design studies have been made using the RFQsim- and Microwave Studio codes to optimize beam dynamics properties and the field distribution of the RFQ. Results of the design studies will be presented.

INTRODUCTION

The plan for the future GSI accelerator system is based on the existing UNILAC and SIS18 as injectors to a complex Synchrotron storage ring system, which should be able to deliver unique beams for the study of the structure of matter [1]. A key feature of the facility is the generation of intense, high-quality secondary beams of rare isotopes as well as antiprotons. To serve as an injector, the UNILAC intensity has to be upgraded by a factor of appr. 100. Refering to the experience of CERN the primary proton beam pulse intensity for the production of antiprotons has to be in the order of 50mA, while the maximum proton beam currents from the UNILAC, which is optimized for Uranium beams, are only I_p < 1mA. Therefore plans to built a new dedicated P-linac have a high priority.

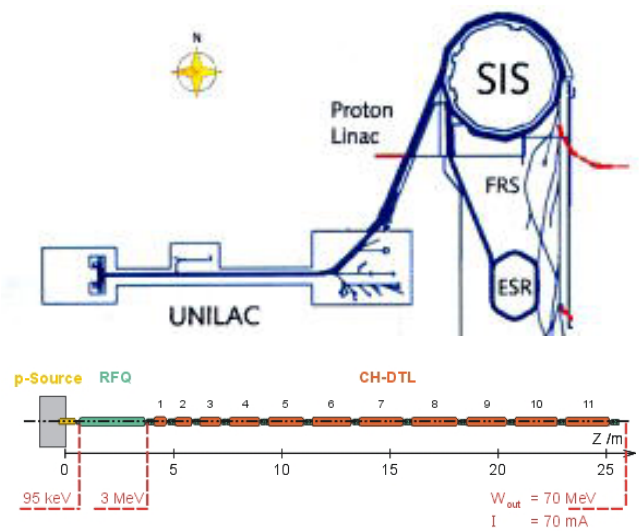

Figure 1: Scheme of the future GSI-p-linac with ECR-source, RFQ and CH-DTL linac.

*supported by the BMBF
#a.schempp@em.uni-frankfurt.de

Table 1: Basic P-Linac Parameters

Frequency	352 MHz
pulse rate,length	5 Hz, 0.1msec
Output energy	70 MeV
Beam current	70 mA
transv, emittance rms norm.	1.5 π mm mrad
energy spread	± 1%

This new 70 MeV proton linac will directly inject into the SIS18 and should deliver high quality 70 mA beams. It is planned to built a very compact linac, making use of the recent progress in accelerator technology by building an ECR-RFQ-CH linac with a total length of ca. 26 m. The choice of the operating frequency of 352 MHz is set by the availability of LEP-type Klystrons which shall drive the linac [2,3].

RFQ-BEAM DYNAMICS

Preliminary design studies fixed the injection energy of the RFQ to 95 keV and the final energy to 3 MeV. The beam current should be 70 mA, but a current upgrade up to 90mA should be possible without big changes.

Table 2: Basic RFQ Parameters

Frequency	352 MHz
Input energy	95 keV
Output energy	3.0 MeV
Beam current	70/90 mA
output emittance rms norm.	0.4 π mm mrad
energy spread rms	150 deg.keV
Electrode voltage	90 kV
RFQ length	3.22 m
cell number	272
min - max aperture	2.35-3.6 mm

The beam dynamics design is based on the results for the proton RFQs for DESY, RAL and Debtec with adiabatic variation of electrode parameters, it aims at a short structure at low electrode voltage to save rf-power and facilitate rf-tolerances and peak power problems preserve emittance and high transmission.

The beam dynamics design,based on the parameters of Table 1, led to a RFQ with electrode voltage of 90 kV and a length of 3.2 m as summarized in table 2.

The design procedure allows for a transmission of more than 95% even at the high input current of 100 mA, with a very small emittance growth.

SUPERCONDUCTING RFQS IN THE PIAVE INJECTOR*

G. Bisoffi, G. Bassato, G. Bezzon, A. Calore, S. Canella, F. Chiurlotto, A. Lombardi, P. Modanese, A.M. Porcellato, S. Stark, INFN LaboratoriNazionali di Legnaro, I 35020 Legnaro (Italy)

Abstract

Two superconducting (sc) RFQ's (SRFQ1 and SRFQ2, resonating at 80 MHz, 0.8 m in diameter and 1.34 m and 0.74 m long), were mounted in their common cryostat and connected to the TCF50 refrigerator in the linac building. The SRFQs follow an ECR source on a 350 kV platform and external bunching, and precede 8 sc quarter wave resonators. They are the very low velocity accelerating structures of the new heavy ion injector PIAVE [1], which will soon expand the mass range of accelerated projectiles at INFN-Legnaro up to the heaviest ones. After thorough "off-line" resonator testing was completed and dealt with on previous publications ($E_{sp,n}$> 25.5 MV/m – the design value, Q-values between 5 and 8 x10^8, stability issues in He-to-recovery mode), this paper describes the very first on-line results.

THE BUMBY ROAD TOWARDS BEAM COMMISSIONING

After assemblying both RFQs in their common final cryostat more than a year ago, a number of inconveniences had to be overcome and tests to be made, before the resonators could undergo on-line tests in June this year, prior to their use for beam acceleration.

First of all, their delicate alignment with respect to the beam line (~0.2 mm precision) was complicated by manufacturing errors of the cryostat, which were brought up both at room T and at 77 K (April-September 2003). Then a few months were intensely invested in searching for a cold leak, which was eventually found on one innermost indium sealing (September 2003 – January 2004). At that stage, we had already realized that both mechanical tuners of SRFQ1 were not working at cold temperatures. Aware that an additional disassembly was hence unavoidable later, after fixing the problem, we opted for proceeding anyway with the overall assembly of the cryostat in the linac vault, with a view of addressing then all possibly arising problems in once. Automatic refrigeration with Linde Kr. TCF50 was hence successfully performed on the SRFQ cryostat between February and March 2004. Immediately afterwards, the first on-line testing started, till the beginning of April. Two months were then spent to perfect a significant refurbishing of the slow tuners mechanics (new articulated joints, ball and roller bearings wherever appropriate), to perform their warm and cold off-line tests and to assemble the cryostat once more (see fig.1). June 2004 was then dedicated to prepare the resonators, check the linear response of the slow tuners and eventually investigate the best possible locking conditions, while stepwise approaching with the cryogenic system the conditions of best pressure stability in operation.

Figure 1: Assembly of SRFQ1 and SRFQ2 on the final cryostat.

PREPARATION FOR THE LOCKING TESTS

Following cryostat evacuation, both SRFQs underwent bakeout at 340÷350 K for about 30 h. With the intermediate shields at 77 K, resonant field emission (RFE) was processed at room temperature. After cool-down to 4 K, residual RFE low level processing (up to peak surface fields $E_{s,p}$ = 3.2 MV/m for SRFQ1 and up to $E_{s,p}$ = 6.2 MV/m for SRFQ2) took 8 h and 2.5 h respectively. Both cavities have always shown a very last RFE level at ~ 9 MV/m: to overcome this and to He-process non resonant field emission (FE) took further 2 h and 9 h respectively.

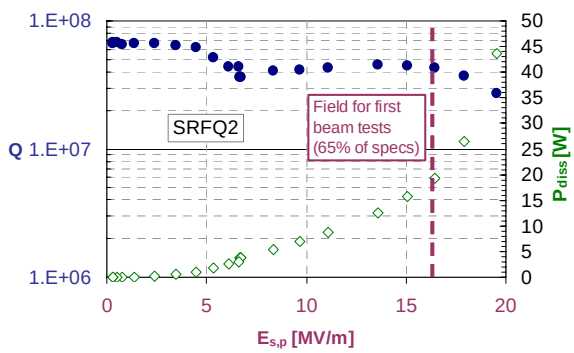

Figure 2: On-line Q-curve of SRFQ2 (Q and P_{diss} are loaded by the VCX, cooled at 77 K)

Construction of a 161 MHz, β=0.16 Superconducting Quarter Wave Resonator with Steering Correction for RIA

A. Facco, INFN/LNL, Legnaro, Padova
C. Compton, T.L. Grimm, W. Hartung, F. Marti, R.C. York, NSCL, East Lansing, Michigan
V. Zvyagintsev, TRIUMF, Vancouver

Abstract

We have built a 161 MHz, β=0.16 superconducting Quarter Wave Resonator with steering correction for the low beta section of RIA. This bulk niobium, double wall cavity, compatible with both separate vacuum between beam line and cryostats or unified one, was designed in collaboration between MSU-NSCL and LNL. The design is suitable for extension to other frequencies, e.g. to obtain the 80 MHz, β=0.085 cavity required in RIA. The shaped drift tube allows correction of the residual QWR steering that can cause emittance growth especially in light ions; this could make this resonator a good alternative to Half-Wave resonators in high intensity proton-deuteron linacs, like the SPES injector project at LNL. First test results will be presented.

NO SUBMISSION RECEIVED

HIGH BETA CAVITY OPTIMIZATION FOR ISAC-II

R.E. Laxdal and V. Zvyagintsev, TRIUMF, Vancouver, Canada
Z.H. Peng, CIAE, China Institute of Atomic Energy, Beijing, China

Abstract

The linac for ISAC-II comprises twenty cavities of medium β quarter wave cavities now in the production phase. A second stage will see the installation of ~ 20 MV of high β quarter wave cavities. The cavity structure choice depends on the efficiency of operation, cost, stability, beam dynamics and schedule. Two main cavity types are considered; a low frequency 106 MHz option and a high frequency 141 MHz cavity. We compare and contrast the cavity choices.

INTRODUCTION

TRIUMF is now constructing an extension to the ISAC facility, ISAC-II, [1], to permit acceleration of radioactive ion beams up to energies of at least 6.5 MeV/u for masses up to 150. Central to the upgrade is the installation of a heavy ion superconducting linac designed to accelerate ions of $A/q \leq 7$ to the final energy. The superconducting linac is composed of two-gap, bulk niobium, quarter wave rf cavities, for acceleration, and superconducting solenoids, for periodic transverse focussing, housed in several cryomodules. The cryomodules are grouped into low, medium and high beta sections corresponding to cavities with optimum velocities of $\beta_o = 4.2\%$, $\beta_o = 5.8, 7.1\%$ and $\beta_o = 10.4\%$ respectively.

Due to experimental pressure and budget limitations the installation of the linac has been grouped into three stages highlighted in Fig. 1. The initial Stage 0 to be completed in 2005 includes the installation of a transfer line from the ISAC DTL ($E = 1.5$ MeV/u) and the medium beta section to produce 18 MV of accelerating voltage for initial experiments. Stage 1 to be completed two years later includes the installation of the three high beta modules for a further 18 MV. The ISAC-II accelerator final Stage 2 is foreseen for 2010. The twenty medium beta cavities are installed four per cryomodule in a total of five modules now in production. The design effort on the high beta section is now intensifying.

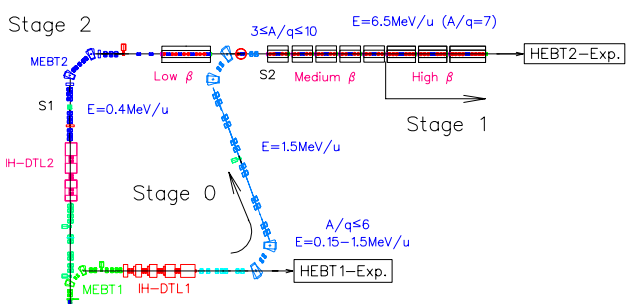

Figure 1: Stages 0, 1 and 2 for the ISAC-II upgrade.

CAVITY VARIANTS

Three cavity variants are considered and shown in Fig. 2. The benchmark cavity, (a) *round141*, has identical transverse dimensions to the medium beta cavity[2] but is designed as a 141 MHz cavity by shortening the overall length and adjusting the gap. In a second variant, (c) *round106*, the cavity frequency is kept at 106 MHz but the cavity transverse dimensions are scaled to increase the beta from 7.1% to 10.4%. The quadrupole asymmetry in the accelerating fields [3] is somewhat larger in the high frequency case by virtue of the smaller inner conductor. A third variant, (b)*flat141*, is also considered where the 141 MHz cavity inner conductor is flattened near the beam ports to produce a smaller quadrupole asymmetry. This variant has a lower optimum beta, 9%, suitable for use in the beginning of the high beta section.

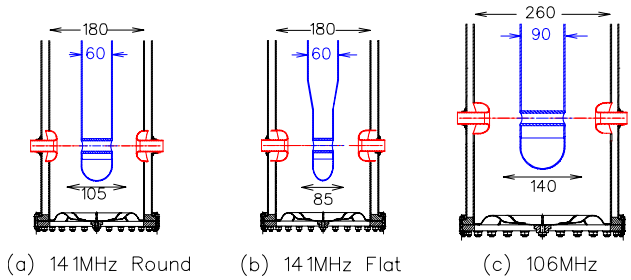

Figure 2: Three cavity variants considered in the study.

BEAM DYNAMICS

The field asymmetries from the three models are summarized in Fig. 3 over the operating velocity range required of the cavity for an accelerating gradient of 6 MV/m, an ion of $A/q = 3$, and a phase of $\phi_s = -30°$. Shown are the corrected vertical steering components and the vertical and horizontal defocussing perturbations for a 1 mm displacement from the electrical axis. The dipole steering components can be reduced to less than 0.1 mrad over the whole velocity range, for even the lightest beams, by shifting the cavities down by 1.3,1.0 and 2 mm respectively for the *round141*, *flat141* and *round106* cases with respect to the beam and solenoid axis. In particular the beam port position with respect to the inner conductor tip is varied to reduce the required shift and minimize the steering effect.

Linac Variants

The beam dynamics of the three cavity types are studied in three linac variants. The benchmark variant consists of twenty 141 MHz high beta cavities divided into two modules of six cavities and one module of eight cavities with one solenoid in each module. In a second vari-

ENGINEERING AND CRYOGENIC TESTING OF THE ISAC-II MEDIUM BETA CRYOMODULE

G. Stanford, Y. Bylinsky, R.E. Laxdal, W. Rawnsley, T. Ries and I. Sekachev,
TRIUMF, 4004 Wesbrook Mall, Vancouver, BC, Canada, V6T 2A3

Abstract

The medium beta section of the ISAC-II Heavy Ion Accelerator consists of five cryomodules each containing four quarter wave bulk niobium resonators and one superconducting solenoid. A prototype cryomodule has been designed and assembled at TRIUMF. This paper describes the system engineering, alignment procedures and test results.

INTRODUCTION

The ISAC-II[1], superconducting linac is composed of two-gap, bulk niobium, quarter wave RF cavities, for acceleration, and superconducting solenoids (9 T), for periodic transverse focusing, housed in several cryomodules and grouped into low, medium and high-beta sections. Each cryomodule has a single vacuum system for thermo-isolation and beam. This demands extreme cleanliness of internal components and precludes the use of volatile lubricants or flux as well as particulate generators to avoid superconducting surface contamination. An initial stage to be completed in 2005 includes the installation of the medium-beta section consisting of five cryomodules. An initial cryomodule[2] has been designed and assembled at TRIUMF.

CRYOMODULE ENGINEERING

The stainless steel vacuum tank has dimensions $\sim 2 \times 2 \times 1$m. The superconducting elements are supported on a beam that is suspended from the lid by struts (Fig. 1). The struts are slung from three support points, two upstream and one downstream, that are laterally and vertically adjustable. There is an independently mounted liquid helium reservoir (120ℓ inventory) suspended from the lid attached to the superconducting elements by soft bellows. Except for the niobium cavities the cold mass is predominantly made from 316L stainless steel. The efficiency of cooldown is improved by a manifold and distribution system 'spider', connected to the LHe transfer line, that delivers cold gas and liquid to the bottom of each element through 5 mm Cu tubing. Once the liquid begins to collect in the reservoir a pre-cool valve on the distribution manifold is opened and LHe flows directly into the reservoir.

The entire cold mass is surrounded by a forced flow, liquid nitrogen cooled, thermal shield. The shield consists of several Cu panels riveted together to form a box with 10 mm ID Cu tubing soldered to the panels to form a serial LN2 circuit. After soldering the panels are nickel plated to improve emissivity. A μ-metal magnetic shield, consisting of 1 mm Conetic panels is attached to the inside of the vacuum tank outside the LN2 shield. A single LN2 panel

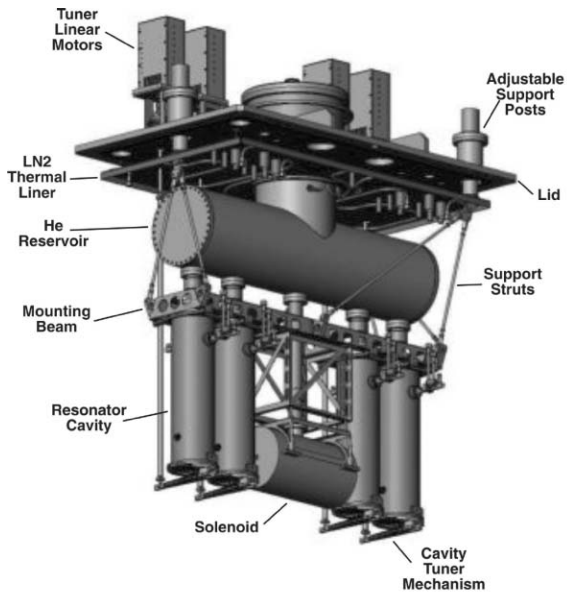

Figure 1: Cryomodule top plate assembly.

and μ-metal shield suspended from the lid make up the top thermal and magnetic enclosure respectively.

Alignment During Assembly and Installation

An assembly stand (Fig.2) is used to assemble the tank internals to the lid. The stand mimics the vacuum tank and uses the same lid location dowel arrangement. The line of sight (LOS) location of the beam and wire position monitor (WPM) ports on the tank are transferred to the adjustable end plates on the assembly stand via a transfer fixture and optical telescope. The tank internals are aligned with respect to the LOS using optical targets in the beam ports. The WPM alignment monitors are aligned with respect to the line of wire (LOW) also with optical targets.

The WPM system[3] provides an off-axis measure of the cavity and solenoid positions during cooldown. The monitors, each consisting of four striplines, are attached to the cavities and solenoid by brackets that position them 0.31 m horizontally from the beam axis. A wire running parallel to the beam axis and through the monitors carries an rf signal that is measured by the striplines and is converted to an x-y position. The cryomodule tank is also outfitted with a pair of optical windows and alignment targets to set up and monitor an external optical reference line with a telescope. Optical targets are installed in each cavity and in the upstream and downstream ends of the solenoid. Optical measurements, taken periodically, serve to check for

PROGRESS IN THE DEVELOPMENT OF THE TOP LINAC

L. Picardi, C. Ronsivalle, ENEA, Frascati (Rome), Italy, S. Frullani, ISS, Rome, Italy

Abstract

The TOP Linac (Oncological Therapy with Protons), under development by ENEA and ISS is a sequence of three pulsed (5 μsec, 300 Hz) linear accelerators: a 7 MeV, 425 MHz RFQ+DTL (AccSys Model PL-7), a 7-65 MeV, 2998 MHz Side Coupled Drift Tube Linac (SCDTL) and a 65-200 MeV, variable energy 2998 MHz Side Coupled Linac (SCL). The first SCDTL module is composed by 11 DTL tanks coupled by 10 side cavities. The tanks has modified to overcome vacuum leakage that occurred during brazing, and now the module has been completed, and is about to be ready to be tested with protons. The 7 MeV injector will be installed in September at the ENEA Frascati laboratories for preliminary test, before being transferred to a large oncologycal hospital in Rome (Istituto Regina Elena or Ospedale S. Andrea).

INTRODUCTION

Protontherapy is nowadays a reality in the oncologycal radiotherapy and several accelerators are being developed worldwide for this application, but they are mainly cyclotrons and synchrotrons while the accelerator described in this paper is the only linac. The reasons why walking this unusual road are: the modularity of the construction, as the linac can be expanded in at least 3 steps, each of them able to be operated for a specific task, the compactness, as the linac extends in the area used by beam transport lines in other types of machine, and the flexibility, as a fully 3D scanning irradiation with energy, current and position variable on a pulse-to pulse basis is possible.

Moreover, the use of 3 GHz accelerating structures in a large part of the machine makes the use of the facility closer to the electron conventional radiotherapy accelerators as to time structure, maintenance and dosimetry.

The TOP (Terapia Oncologica con Protoni) Linac [1] is a proton medical linac designed to produce at least the following beams (fig. 1):

- a 7 MeV, 700 W beam for F-18 radioisotope production;
- a 65 MeV, 10nA (average) beam for proton eye therapy;
- a 100-200 MeV, 10 nA (average) beam for deep seated tumours proton therapy.

The linac is composed of a 7 MeV 425 MHz injector, a 7-65 MeV 3 GHz linac booster, named SCDTL (Side Copled Drift Tube Linac) from the accelerating structure name, a second 65-200 MeV 3 GHz linac booster named SCL, and the various beam lines to the application rooms. The time structure is pulsed with typical hundreds of Hz rep rate and a few μs pulses. The fully 3-D scanning irradiation of deep seated tumours requires a beam whose position, energy and pulse charge can be varied on a pulse-to pulse basis, that is energy between 130 and 200 MeV, pulse current between 0.1 and 10 μA (a factor 100) and pulse duration between 1 and 5 μs pulses at 100-250 Hz repetition frequency.

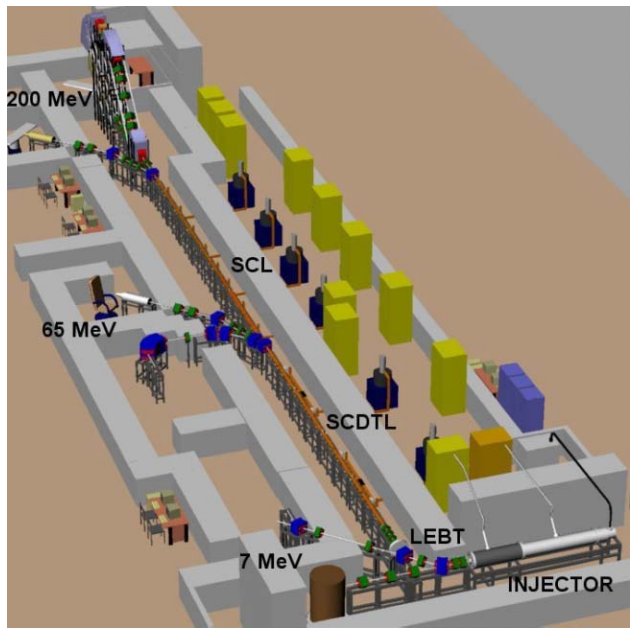

Figure 1: TOP Linac design layout.

The design [2] was developed by ENEA in collaboration with CERN, INFN and TERA and it was approved by ISS (National Institute of Health) and funded in 1997 but only with about 4.5 M€ against the 22 M€ estimated for the high technology devices of the facility. Despite this, construction started within a cooperation agreement between ENEA and ISS and installation was agreed to be done in Rome at a large Oncologycal Hospital. Up to now unfortunately no additional funding has been available so that work is carried on at ENEA Frascati laboratories, where a proper temporary site was set up for the first machine tests, up to 20 MeV. Interest for the installation has been evidenced by S. Andrea Hospital in Rome.

THE 7 MEV LINAC INJECTOR

The injector linac was bought from AccSys Inc., USA. It is a PL-7 model modified to meet the TOP requirements [3]. It is actually installed in a test bunker at Frascati and scheduled to be put in operation in September. It will be used for three main purposes: Fluorine-18 production (F-Mode, high current), Protontherapy beam injection and radiobiology experiments (P-mode, low current). In the high-current mode the pulse current will be 8 mA for 60 μs and 60-100 Hz rep. rate. In the low-current mode the pulse current

THE ACCELERATION TEST OF THE APF-IH LINAC

K.Yamamoto[a) b)], M. Okamura[a)], T. Hattori[b)],S. Yamada[c)]
[a)] The Institute of Physical and Chemical Research (RIKEN), Japan
[b)] Tokyo Institute of Technology (TITech), Japan
[c)] National Institute of Radiological Sciences (NIRS), Japan

Abstract

An IH linac with Alternating Phase Focusing scheme has been fabricated to study a high efficiency cavity for a medical accelerator injector. This linac was designed to accelerate C4+ ions from 39 keV/u up to 1.9MeV/u. In order to test this linac, a test stand was just assembled which consists of a P.I.G. ion source, bending magnets and focus lenses. The total length of the test stand is less than 5 m including 1.5 m of linac tank length. The operation frequency of the cavity is 97.6MHz. We will report linac design, fabrication and the test bench.

INTRODUCTION

Now tumor therapy is being one of major applications of hadron accelerators. Typically a chain of linacs occupies large area in tumor therapy facilities. For instance, an injector of HIMAC (Heavy Ion Medical Accelerator in Chiba; Japan), consists of RFQ linac and Alvarez linac, accelerates C4+ ions up to 6MeV/u and the length is over 30 m[1)]. In particularly such a medical accelerator complex, not only machine performance but also construction cost and operation cost are very important. Therefore compact and reliable linac design is needed. For this purpose, we designed an Interdigital-H mode linac with alternating phase focusing (APF) as a new high efficiency cavity for the injector. The IH structure has an advantage of high shunt impedance in low energy region. The technique of APF has been proposed for the design of short low beta structures, because its inherent focusing capability could eliminate the need of external transverse focusing by drift tube quadrupoles[2)-5)].

DESIGN

Initial parameters were determined for C4+ acceleration. An injection energy, output energy and operation frequency are 2 MeV/u, 40 keV/u, and 100 MHz respectively. Electric field strength in gaps is limited by twice of Kirpatric's limit and an acceleration ratio is 5MeV/m. Based on this condition, a length of the linac is 1.5m long. A number of cell was determined as 22 which was given by the linac length divided by an average cell length (about 70mm).

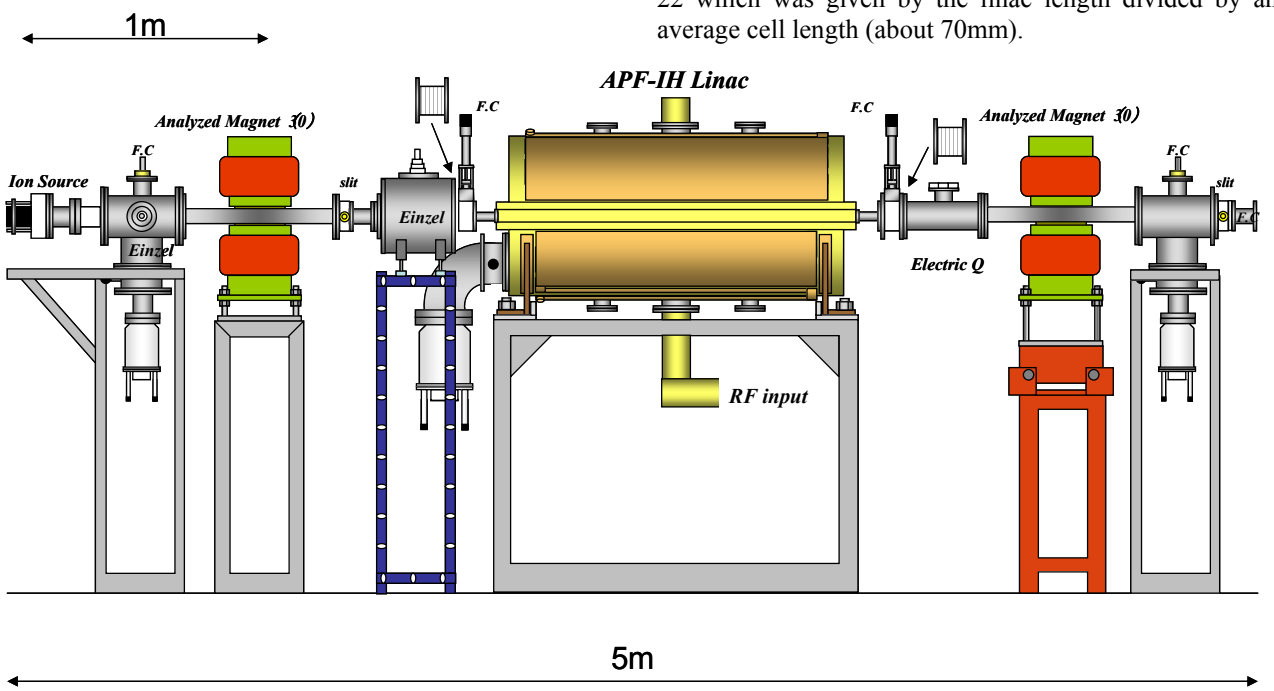

Figure 1: Acceleration test bench.

CALCULATION OF ELECTRON BEAM DYNAMICS OF THE LUE−200 ACCELERATOR

A.P. Sumbaev#, V.S. Aleksandrov, N.Yu. Kazarinov, V.F. Shevtsov,
JINR, Moscow region, 141980, Dubna, Russia

Abstract

The results of calculations of the focusing and transportation systems of the electron beam of LUE-200 accelerator – the driver of a pulse source of resonant neutrons IREN [1], JINR (Dubna), are presented. Simulations of the beam dynamics in the traweling wave accelerator were carried out by means of PARMELA code [2]. The calculations have been fulfilled for various parameters of the focusing magnetic field in the accelerator and the channel, various currents of the beam and various initial distributions of electrons.

INTRODUCTION

The intense resonant neutron pulse source IREN is a traditional JINR combination of a driver (an electron LINAC) and a converter - target with a booster multiplier. The LINAC is designed at the Budker INP of the Siberian Branch of the Russian Academy of Sciences. The design prototype is the preinjector of the VEPP-5 accelerator complex [3]. For ensuring the design parameters of the IREN, the average power of the electron beam must be about 10 kW that defines the electron energy to be 200 MeV if the pulse duration is 250 ns, the electron current is 1.5 A, and the repetition frequency is 150 Hz. The mean rate of the energy gain in the accelerating structures should not be less than 35 MeV/m because the restrictions related to the placement of the accelerator in the available building.

LUE-200 ACCELERATOR

The accelerator (Figure 1) consists of an electron gun (C−A), an accelerating system, and an electron beam transport channel up to the target (T).

The accelerating system consists of a buncher (B) and two accelerating sections (AS1, AS2).

The *buncher* [4] is four coupled resonators (3 cells and a converter of wave type) with an operational frequency 2855.6 MHz and 4π/3 operating mode. Figure 2 shows the distribution of the longitudinal electric field along the axis of the buncher.

The accelerating sections are round disk-loaded waveguides of constant impedance. The major parameters of the section are given in [3]. Each section is fed by RF power from independent klystron amplifiers based on the 5045 SLAC klystron operating at the frequency 2856 MHz.

The *focusing system* consists of a solenoid focusing channel and a quadrupole focusing channel.

The *solenoid focusing channel* is used at the bunching step and at initial acceleration from the energy 200 keV to 100 MeV. It consists of magnetic lenses AS, ML1 and ML2 of the electron source, and of a solenoids system of the buncher (BC) and the first accelerating section (S1). During the design, the configuration of the solenoid focusing channel was evolved. In the first version of the design [3], focusing of the beam in the first accelerating section was performed by two solenoids S1 (length ~0.75 m, field strength ~1.5 kG) and S2 (length ~2.1 m, field strength ~4.0 kG) with opposite directions of the field. After optimization of the fields, the system of two solenoids was replaced by a single sectioned solenoid S1 (16 coils).

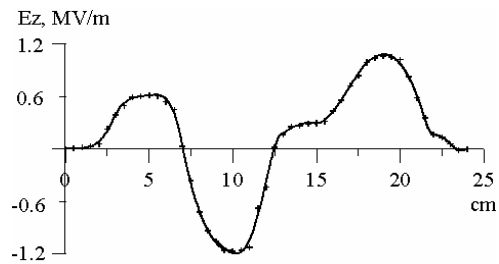

Figure 2: Distribution of the longitudinal electric field strength along the axis of the buncher.

The *quadrupole focusing channel* is used after the exit of the first accelerating section. The channel consists of nine quadrupole lenses Q1–Q9. The correcting lens Q1 is combined with the beam displacement corrector. Two doublets Q2–Q3 and Q4–Q5 are mounted on the second accelerating section and aimed at guiding the beam through the small-aperture channel inside the section.

Two more doublets Q6–Q7 and Q8–Q9 aimed at guiding and focusing the beam to the target (T).

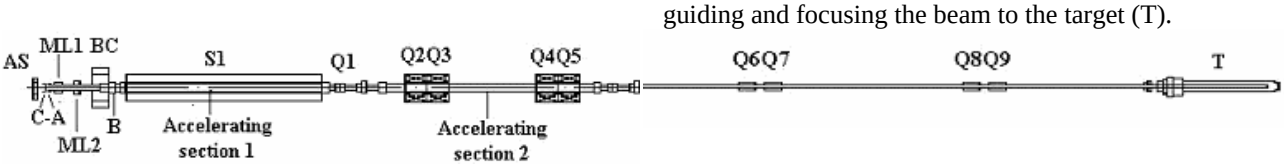

Figure 1: Layout of LUE-200 accelerator.

#sumbaev@nf.jinr.ru

3D BEAM DYNAMICS SIMULATION IN UNDULATOR LINAC*

E.S. Masunov, S.M. Polozov, MEPhI, Moscow, 115409, Russia

Abstract

The ion beam can be bunched and accelerated in linear undulator accelerator (UNDULAC). The acceleration and focusing of beam can be realised without using a synchronous wave. In this paper the computer simulation of high intensity ion beam dynamics in UNDULAC-RF was carried out by means of the "particle-in-cell" method.

INTRODUCTION

The beam focusing and acceleration can be realized without using a synchronous wave of RF field, as it discussed in Ref. [1-2]. In this case accelerating force is to be driven by a combination of two non-synchronous waves (two undulators). Such linac was called linear undulator accelerator (UNDULAC). The ribbon ion beams can be accelerated in two types of undulator linac UNDULAC-E [1] and UNDULAC-RF [2]. In first case beam bunching, acceleration and transverse focusing are realised in combined wave field which is produced by one spatial RF field harmonic in a periodical resonator and field of electrostatic undulator. In second case the accelerator force is driven by two fundamental RF field harmonics. It should be noted that the ion beams can be accelerated in UNDULAC in low energy range using transverse or longitudinal fields [1].

The beam dynamics in UNDULAC can not be investigated by means of traditional analytical methods because it is no synchronous wave in this linac. The computer simulation and optimization of ion dynamics consist of two steps. At the first the equations of particles motion in polyharmonic fields is devised by means of smooth approximation. Hamiltonian analysis of this equation allows to find a velocity of reference particle in polyharmonic field and to formulate the conditions of effective longitudinal bunching and transverse beam focusing [3]. These conditions define the structure period and the field amplitudes distribution. At the second, using above founded characteristics, the 3D ion beam dynamics numerical simulation in an UNDULAC is provided. The space charge influence on the beam dynamics is investigated also by this simulation

The results of beam dynamics analytical study and numerical simulation for UNDULAC-E are discussed in Ref. [4-5]. The analytical investigation for UNDULAC-RF is provided in [3]. Let us consider briefly the results of this investigation. It helps to realize the numerical simulation.

*The work was supported by RFBR. Grant 04-02-16667

THE RESULTS OF BEAM DYNAMICS ANALYTICAL STUDY

The analytical investigation was provided for UNDULAC-RF using RF field with $\mu = 0$ and $\mu = \pi$ modes in Ref. [3]. The main results of ribbon ion beam dynamics analytical study in UNDULAC-RF:

1. The two sub-sections are necessary for providing of beam bunching in UNDULAC-RF. The reference particle phase must be chosen linearly decreased and fields amplitudes increased as sine function in first bunching sub-section. The synchronous phase and amplitudes are constant in second accelerating sub-section. These dependencies are providing the minimal particle loses.
2. It was shown that the optimal bunching conditions and maximal current transmission coefficient could to be driven with the optimal RF field harmonics ratio $\chi = E_1 / E_0$. The optimal value is equal χ=0.3-0.4 in UNDULAC-RF using $\mu = \pi$ mode of RF field and χ>1 for $\mu = 0$ mode.
3. In the smooth approximation the current transmission coefficient K_T is equal 90-95 % for UNDULAC-RF using $\mu = \pi$ mode of RF field (for both transverse and longitudinal fields) and 85-90 % for $\mu = 0$ mode.
4. The two bunches per one period of RF field will be configured.

BEAMDULAC CODE

The beam dynamics can not be studied completely using analytical methods only. The time-averaged motion equation and effective potential function are obtained using smooth approximation. The influence of particle phase and velocities oscillations on beam dynamics does not take into account in this approximation. The numerical simulation in polyharmonic field is also necessary. The new code BEAMDULAC has been developed specially for beam dynamics simulations in undulator linear accelerator. This code is carried out by means of Cloud-in-Cell (CIC) method for accurate treat of space charge effects that is especially important in the case of high intensity beam. The motion equation for each particle is being solved including forces due to external fields and inter-particle Coulomb field. field The Poisson equation is solving on the grid with periodic boundary conditions in order to find the potential of Coulomb. The Dirichlet boundary conditions are applied at transverse boundaries of the simulation domain. The interaction of the bunch space charge with the accelerating channel is taken into account. The Fast Fourier Transform algorithm is used to solve the Poisson equation on 3D grid with given charge density distribution. The external potential is

AN ELECTRODE WITH MOLYBDENUM-CATHODE AND TITANIUM-ANODE TO MINIMIZE FIELD EMISSION DARK CURRENTS

T. Nakanishi[a], F. Furuta[a], S. Okumi[a], T. Gotou[a], M. Yamamoto[a], M. Kuwahara[a], N. Yamamoto[a], K. Naniwa[a], K. Yasui[a], H. Matsumoto[b], M. Yoshioka[b] and K. Togawa[c]

[a]Department of Physics, Nagoya University, Nagoya 464-8602, Japan
[b]KEK High Energy Accelerator Research Organization, 1-1 Oho, Tsukuba 305-0801, Japan
[c]SPring-8 /RIKEN, 1-1-1 Koto, Mikazuki-cho, Sayo-gun 679-5148, Japan

Abstract

A series of dark current measurements are performed for Molybdenum (Mo) and Titanium (Ti) electrodes, and the results are analyzed to separate the primary field emission current from the total observed dark current. The analysis shows that Mo exhibits very low primary field emission current as a cathode, and Ti also exhibits a lower enhancement effect of dark current due to electron and ion bombardments of cathode and anode. An electrode configuration with Mo cathode and Ti anode is thus examined, and it is confirmed that a field gradient of as high as 130 MV/m for 1 nA total dark current is possible for an electrode gap of 0.5 mm and an effective cathode area of 7 mm^2.

INTRODUCTION

The initial phase of dark current or pre-breakdown phenomenon, dominated by primary field emission is usually weak, and does not cause fatal damage in high-voltage devices. More serious breakdown phenomena that degrade device performance are triggered by the same field emissions but are enhanced by an additional positive feedback mechanism. However, for photoemission source using GaAs-type photo-cathodes with a negative electron affinity (NEA) surface to extract electrons into vacuum, even a weak pre-breakdown current significantly reduces the cathode lifetime [1]. The NEA surface realized by a surface dipole layer of Ga(−)–Cs(+) is delicate and easily destroyed by small disturbances induced by dark current. Thus, technology for reducing pre-breakdown dark current is essential for the photoemission devices using an NEA-GaAs surface. Polarized electron source (for linear collider) and low-emittance electron source (for ERL) are representatives of such devices.

The dark current properties of SUS and Cu surfaces have already been investigated using a compact test stand constructed at KEK. Based on these experiments, it has been suggested that the magnitude of dark current is dependent on both the electrode fabrication process and the purity of the crystal structure of the material [2]. Thus, using the same apparatus, our group undertook a systematic study of the dark current from Ti and Mo electrodes. This paper presents the results of these experiments, and introduces a new analysis method for separating primary field emission current from total dark current based on experimental data for the gap-separation dependence.

APPARATUS AND ELECTRODE

The test stand was built for basic study of field emission dark current under the high DC-field gradient condition (~200 MV/m) with ultra-high vacuum of $<10^{-11}$ Torr. In order to obtain a high-quality UHV, the main vacuum chamber was fabricated using re-melted stainless steel (NK-Clean-Z), which contains much less non-metallic impurities than SUS316L. The applied field gradient could be changed by controlling the gap separation of the electrodes (0–20 mm) and the bias voltage (0–100 kV), allowing the dark current under a given field gradient to be measured with respect to different gap separations. The Ti electrode was machined from JIS grade-2 pure Ti, and a mirror-like surface was obtained by buff-polishing. The Mo electrode was machined from a single-crystal Mo block (purity: 99.999%), and a mirror-like surface was prepared by diamond paste polishing. The specimens were finally treated by high-pressure rinsing (80 kg/cm^2, 5 min) with ultra-pure water in the class-100 clean room.

DARK CURRENT MEASUREMENT

To avoid trivial electrical breakdown, the dark current measurements were done very carefully using the long time current conditioning for a few days to 2 weeks. The results of dark current measurements are shown in Fig. 1, where the dark current is plotted as a function of applied field gradient at the cathode surface. The Ti and Mo electrodes exhibited no dark current up to 80 and 83 MV/m, reaching 1 nA at 103 and 115 MV/m at a gap separation of 0.5 mm, respectively. This represents much higher performance than either SUS or Cu.

The dependence of dark current on gap separation is also shown in Fig. 1. For Ti, it exhibits a dark current of ~1 pA with a 0.5 mm gap and > 100 pA with a 1.0 mm gap under the same field gradient of 80 MV/m. A stronger dependence is observed for Mo. It has a dark current of less than 1 pA for 0.5 mm gap separation, but a dark current of over 1 nA for 1.0 mm gap separation under a field gradient of 83 MV/m.

Fowler-Nordheim theory provides a fundamental viewpoint for field emission phenomena, but it is unable

HIGHLY POLARIZED ELECTRONS FROM GaAs-GaAsP AND InGaAs-AlGaAs STRAINED LAYER SUPERLATTICE PHOTOCATHODES

T. Nakanishi[a], T. Nishitani[a], M. Yamamoto[a], S. Okumi[a], F. Furuta[a], M.Kuwahara[a], N. Yamamoto[a], K. Naniwa[a], K. Yasui[a], O. Watanabe[b], Y. Takeda[b], H. Kobayakawa[b], Y. Takashima[b]
H. Horinaka[c], T. Matsuyama[c]
[a]Department of Physics, Nagoya University, Nagoya 464-8602, Japan
[b]Faculty of Engineering, Nagoya University, Nagoya 464-8602, Japan
[c]Faculty of Engineering, Osaka Prefecture University, 599-8531, Japan

Abstract

GaAs-GaAsP and InGaAs-AlGaAs strained-layer superlattice photocathodes are presented as emission sources for highly polarized electron beams. The GaAs-GaAsP cathode achieved a maximum polarization of 92(±6)% with a quantum efficiency of 0.5%, while the InGaAs-AlGaAs cathode provides a higher quantum efficiency (0.7%) but a lower polarization (77(±5)%). Criteria for achieving high polarization using superlattice (SL) photocathodes are discussed based on experimental spin-resolved quantum efficiency spectra.

INTRODUCTION

Polarized electron beams are conventionally produced by photoemission from GaAs-type semiconductors. The degeneracy between heavy hole (hh) and light hole (lh) bands at the valence band maximum can be resolved through the use of a strained GaAs layer, a GaAs-AlGaAs superlattice SL layer, or a strained InGaAs-GaAs SL layer, and our group has achieved experimental ESPs of 86% [1], 70% [2] and 83% [3], respectively.

In these studies it became clear that by using a modulation-doping method, the SL cathode is capable of achieving much higher quantum efficiency (QE) than the strained-layer GaAs. Thus, while heavy doping is used for surface layers to achieve large band-bending, medium doping is better for SL layers in order to avoid spin-flip depolarization.

More importantly, however, SL cathodes were found to provide a solution for the surface charge limit (SCL) problem, whereby the maximum current density that can be extracted from the NEA surface is much lower than that determined by the space charge limit. This effect is caused by a decrease in band bending at the NEA surface due to the surface photo-voltage (SPV) effect. However, a GaAs-$Al_{0.31}Ga_{0.69}As$ cathode has been demonstrated to produce a space charge-limited current of 14 A (2.3×10^{11} electrons in a 2.5 ns bunch) using a 120 keV gun with a QE of 2.0% at a laser wavelength of 752 nm [4]. This means that the use of a modulation-doped SL photocathode solves the SCL problem for this beam condition.

Encouraged by these successful results, the present authors have continued research on the development of new types of InGaAs-AlGaAs and GaAs-GaAsP strained SL structures [5]. We have also investigated the SCL problem in more detail using the SL photocathodes irradiated by a nanosecond double-bunch laser with 2.8 ns separation time [6]. In this paper, we describe experimental results demonstrating the improvements in ESP, QE and SCL effect achieved using a GaAs-GaAsP cathode. Criteria for obtaining the highest ESP are also proposed based on the spin-resolved QE spectra.

PHOTOCATHODE PREPARATION

The InGaAs-AlGaAs SL samples were fabricated by molecular beam epitaxy (MBE) at NEC, and the GaAs-GaAsP SL samples were made by metal-oxide chemical vapor deposition (MOCVD) at Nagoya University. The InGaAs-AlGaAs sample was prepared with a protective surface film of amorphous As, which was removed by heat-cleaning at 400 ºC in a vacuum. The GaAs-GaAsP sample had no protective film and was heat cleaned at 550 ºC for 2 h in a vacuum.

A number of different SL samples with various materials and crystal parameters were fabricated and tested, but in this paper, the SLSA#2 and SLSP#9 samples are selected from InGaAs-AlGaAs and GaAs-GaAsP SL families, for detailed analysis. The crystal structure and doping densities for SLSP#9 are shown in Fig. 1.

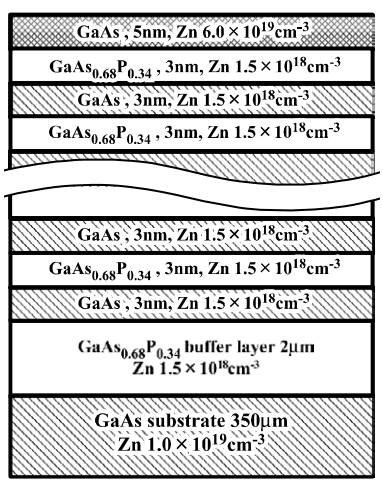

Figure 1: Crystal structure and doping density of the SLSP#9 sample.

A commercially available GaAs wafer with high Zn dopant content was used as a substrate, and a strain-

DEVELOPMENT OF FIELD-EMISSION ELECTRON GUN FROM CARBON NANOTUBES

Y. Hozumi[1,A)], S.Ohsawa[B)], T. Sugimura[B)], M. Ikeda[B)]
[A)]*The graduate university for advanced studies,* [B)]*KEK, 1-1 Oho, Tsukuba, JAPAN*

Abstract

Aiming to develop a high intensity electron beam with narrow energy-spread for injector guns, we have been tested field emission cathodes of carbon nanotubes (CNTs), which have some features of easy handling and low cost. Experiments for these three years brought us important suggestions and a few rules of thumb. Now at last, anode current of 3.0 A/cm^2 was achieved with 8 kV acceleration voltage by applying short grid pulses between cathode and grid electrodes[1]. In order to proof utility, 100-kV gun system had been designed and constructed since last year. Then the value of 100 mA was obtained based on 10^{-5}~10^{-6} Pa back ground pressures. With some improvements it would be expected that anode currents of Ampere order will be obtained from the CNTs cathode gun.

INTRODUCTION

The heater-less electron guns (e-guns) are desired because of its excellent emission properties, i.e., low emittance, high brightness and low cost driving. Field emission (FE) e-guns are under investigation for injector linacs. This time, we have been fabricated and tested a new type of FE-gun using the promising material emitter called “carbon nanotubes (CNTs)”. The CNTs have strong potentials as a field emitter; actually, 1×10^9 A/cm^2 of current density has recently obtained in Japan. In the last year, it was reported that anode current of 3.0 A/cm^2 was achieved from CNT-FE e-gun by applying short grid pulses between cathode and grid electrodes [1]. The CNTs cathode which had enough current density and long life-time could be developed by some companies’ cooperation[2]. The report results were obtained with as low acceleration voltage as 8 kV, and this time, we have constructed a 100 kV practical test stand and started test of performance of the e-gun which were also designed to suited EIMAC-Y796 standard. This paper describes the basic design and the characteristics of the CNTs FE-gun.

COMPOSISIONS OF THE E-GUN SYSTEM

Measurement System and Electrical Circuits

At the gap distance between the grid and cathode (G-C) electrodes, short pulses of 50 ~ 100 ns width and 0.1 ~ -3.4 kV are applied through a BNC connector with a repetition rate of 7～10 Hz. 50 ns is the lower limit of the pulse generator PVX-4140 produced by DIRECTED ENERGY, INC. Figure 1 shows this system outline. The 50 Ω resistance connected to the pulser in series has a role of mitigating damage of the cathode from discharge, and reflected pulses due to impedance miss match. The emitted electrons are accelerated by DC high voltage of 100 kV between the anode and grid electrodes, and then emerge from the e-gun through an anode hole. Then, electron beams are adjusted by a magnetic lens to focus on the beam catcher (BC) in solenoidal fields. The values of beam currents are measured by monitors such as a wall current monitor (WCM), a core monitor (CM) and BC, which are set along the beam line. Furthermore, a fluorescence screen is available, if necessary, by inserting in the beam line instead of BC at the same place.

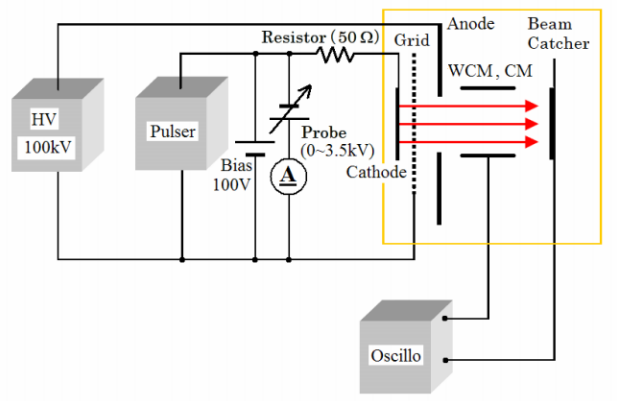

Figure 1: The main components of the e-gun system

Structures of the E-Gun

Figure 2: The e-gun view

Figure 2 shows e-gun structure viewed from the grid side. A standard vacuum flange ICF88 is adopted for the e-gun in order that it is compatible with the often used cathode EIMAC-Y796. The distance between the G-C is very important, because it determines the field gradient between the G-C with grid pulses, namely beam currents. Therefore we designed the structure of the G-C assembly

[1)] hozumiy@post.kek.jp

COMPARISON OF 2 CATHODE GEOMETRIES FOR HIGH CURRENT (2 KA) DIODES

M. Caron, F. Bombardier, E. Merle, Ch. Noël, O. Pierret, R. Rosol, C. Vermare

CEA/DIF Polygone d'Experimentation de Moronvilliers – 51 Pontfaverger-Moronvilliers, France

N. Pichoff, DPTA/SP2A, A. Piquemal, DPTA/SPPE, CEA/DIF 91 Bruyères-le-Chatel, France

D.C. Moir, LANL-DX6 – NM Los Alamos – USA

Abstract

AIRIX (FRANCE) and DARHT axis-1 (USA) facilities are two high current accelerators especially designed for X-ray flash radiography. The produced electron beam (2 kA, 60 ns, 3.5 to 3.8 MeV at the diode output) is extracted from a velvet cold cathode. Specific calculations have demonstrated the influence of the cathode geometry on the emitted beam profiles [1]. In order to check this assumption two different experiments (DARHT march 2003 – AIRIX march 2004) have been performed. The beam characteristics with two different geometries have been compared both theoretically and experimentally. The beam simulations have been done with 3 codes: a home-made one (M2V) and 2 commercial ones (PBGUNS and MAGIC). The extracted beam current and transverse profiles, for the first experiment, have been measured and compared to simulations results. In the second one, we have mainly compared the primary current intensity that can be drawn with the two different K-designs for a given energy.

INTRODUCTION

Since the first reports on the X-ray sources like DARHT Axis 1 or AIRIX [1] [2] [3], some efforts have been devoted to improving the overall electron beam quality in order to reduce for instance the beam focal spot. One of the most relevant parameters to assess the ability for a beam to be more focused is the so-called emittance ε. ε can be seen as an intrinsic beam characteristic that can only increase all along the acceleration line. At first glance, the smaller ε onto the X-ray converter, the smaller the spot size is. Therefore, the main challenges we have to face are on the one hand to reduce the emittance as much as possible at the e-beam production stage and on the other hand to limit its growth during regular transport. This paper rather deals with the first point since reducing ε remains a key issue in the successful development of new cathode designs. We present in the first section the two different cathode geometries taken into consideration in this report as well as the numerical simulations exhibiting the expected gain in terms of beam quality. Then section 2 is dedicated to the description of the two experiments performed so far at DARHT Axis 1 and AIRIX facilities. A comparison between theoretical predictions and experimental results is done in section 3.

THEORETICAL BACKGROUND

The driving forces responsible for the major cathode developments have been quite extensively described elsewhere [1] [4] and have lead to an evolution from our regular standard K-geometry to a modified one: the so-called Pierce geometry. The main differences between them become clear from figure 1.

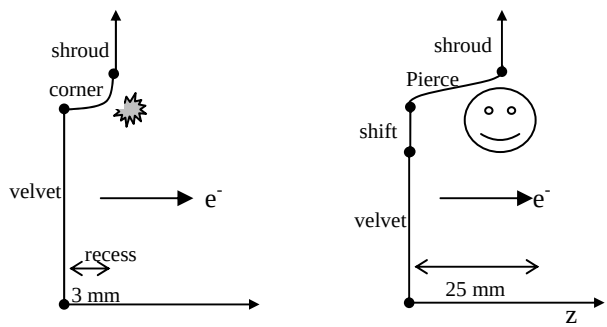

Figure 1: Cathode geometries: a: Standard; b: Pierce.

These geometrical modifications have been implemented into numerical simulation tools independently developed. The entire diode theoretical description has not only been performed by means of a home made code called M2V [5], but also with two commercial codes PBGUNS [6] and MAGIC [7] which are based on very different models. In any cases, the beam is always extracted from the cathode under space-charge limited flow. Electrons are focused out of the diode by means of a solenoid whereas another coil brings the residual magnetic field on top of the cathode down to zero. Up to now, it has been shown that the beam distribution into the (x,x') phase space simulated nearest to the anode level with M2V, PBGUNS or even MAGIC look very similar provided that stationary conditions are considered (front edges excluded) [8] [9].

According to the theoretical calculations, the main improvement expected from the use of the newest type of cathode is to get an emittance reduction of about 10 to 30 % for the same values of primary currents and energies.

ULTRA-LOW EMITTANCE ELECTRON GUN PROJECT FOR FEL APPLICATION

R. Ganter, M. Dehler, J. Gobrecht, C. Gough, G. Ingold, S.C. Leemann, M. Paraliev,
M. Pedrozzi, J.-Y. Raguin, L. Rivkin, V. Schlott, A. Streun, A. Wrulich,
Paul Scherrer Institut, Villigen, Switzerland
A. Candel, K. Li, Swiss, Federal Institute of Technology, Zürich, Switzerland

Abstract

Most of the current 1 Å Free-Electron Laser (FEL) projects are based on thermionic or photocathode guns aiming at an electron beam emittance of 0.5 to 1 mm·mrad. The design of a gun capable of producing a beam with an emittance one order of magnitude lower than the state of the art would reduce considerably the cost and size of such a FEL. Due to the recent advances in nanotechnologies and vacuum microelectronics, a field-emitter based gun is a promising alternative scheme. We present first measurements on commercial field-emitter arrays as well as 3-D numerical simulations of the electron beam dynamics for typical bunch distributions generated from field emitters in realistic gun geometries.

MOTIVATIONS

In a LINAC-driven FEL, the normalized electron beam emittance ε_n has to satisfy the condition [1]:

$$\varepsilon_n < \beta\lambda\gamma / 2\pi L_g ,$$

where λ is the radiated wavelength, β the beta function, γ the relativistic factor and L_g the gain length. For a given wavelength, a small normalized beam emittance would considerably reduce the required beam energy and thus the cost and size of the accelerator facility [2]. The required peak current to drive efficiently a FEL is also reduced when the emittance is smaller. Moreover, the emittance is limited by its initial value at the cathode which can be expressed as follows:

$$\varepsilon_n = \frac{\gamma r_c}{2}\sqrt{\frac{E_{r,kin}}{m_o c^2}} ,$$

where r_c is the cathode radius and $E_{r,kin}$ the mean transverse kinetic energy just after emission. Reducing the the size of the cathode and the mean transverse energy of the emitted electrons leads then to a lower emittance.

FIELD-EMISSION CATHODES

The standard emission mechanisms of the cathodes used in the accelerator electron guns are photoemission and thermionic emission. In both cases, the mean transverse energy of the extracted electrons is several hundreds meV due either to the difference between photon energy and cathode work function or to the cathode temperature. This already limits the minimum achievable initial transverse kinetic energy of the produced electron beam. One alternative technology is field-emitter arrays (FEA) where electrons are emitted with energies close to the Fermi level. In such cathodes, the mean transverse energy is mainly determined by the geometry of the electric field lines [3].

These FEAs consist of thousands of conductive tips in the micrometer size range separated from a conductive gate layer by a one micrometer thick dielectric layer (see Fig. 1 and 2). By applying a voltage V_{ge} between the tips and the gate layer electrons are emitted from the tip's apexes. Additional control of the electron trajectories can be achieved by integrating a focusing second grid layer.

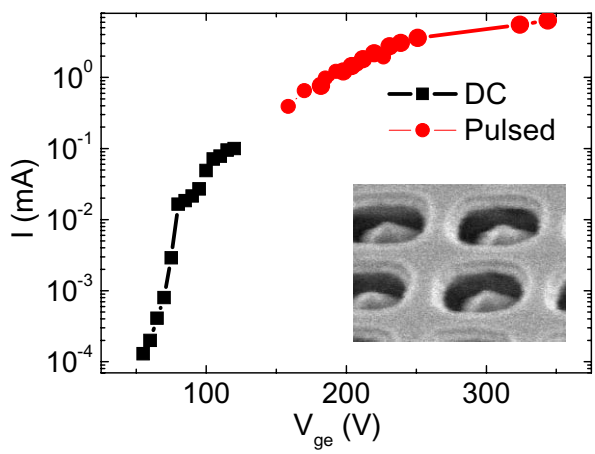

Figure 1: Current-voltage characteristic in DC and pulsed regime for a XDI Inc. FEA (170 µm diameter, 3,000 diamond tips). Insert: SEM picture of some pyramidal diamond tips.

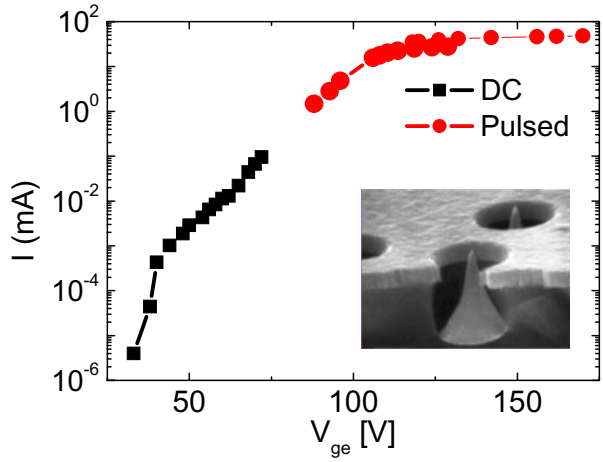

Figure 2: Current-voltage characteristic in DC and pulsed regime for a SRI Inc. FEA (1 µm diameter, 50,000 Mo tips) Insert: SEM picture of some conical Mo tips (SRI website [3]).

MULTI-MODE SLED-II PULSE COMPRESSORS

S.V. Kuzikov, Yu.Yu. Danilov, G.G. Denisov, D.Yu. Shegol'kov, A.A. Vikharev,
Institute of Applied Physics, Russian Academy of Sciences, Nizhny Novgorod, Russia
I. Syratchev, CERN, Geneva, Switzerland
V.G. Paveliev, Nizhny Novgorod State University, Russia

Abstract

Compact SLED-II pulse compressors are considered. The primary idea to use a set of the cylindrical multi-mode cavities, to be free of high-Q resonances around the 11.4 GHz, is analyzed [2]. This idea is developed, in order to provide more delaying time per miter of the line. Another idea to provide compactness is to avoid two-channel scheme with 3dB coupler usually used for SLED-II pulse compressors. A reflectionless delay line is built in this case, using coupling in a form of the non-symmetrical mode converter. SLED-II pulse compressors of higher frequency bands also are considered. It is suggested to shape these compressors on a base of the multi-mirror transmission lines. The operating mode in this case is a Gaussian wavebeam traveling between mirrors.

PULSE COMPRESSORS BASED ON A SET OF CYLINDRICAL MULTI-MODE CAVITIES

The SLED-II pulse compressor consists of two delaying lines, operated with TE_{01} modes, which are coupled by means of 3 dB coupler [1].

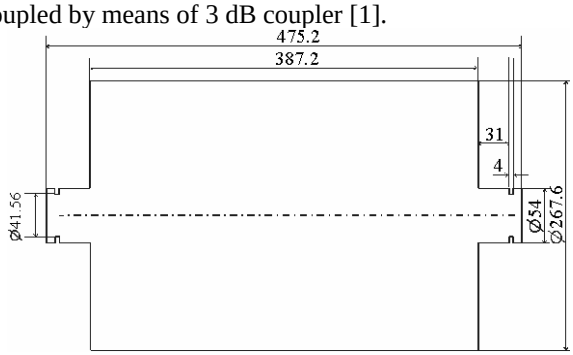

Figure 1: The 11.4 GHz elementary delaying cell.

In order to reduce the total length of delay waveguides, the idea to use a set of cavities, which are to be an equivalent of delaying line, was suggested [2]. One of cells of the mentioned type, which was calculated for 11.424 GHz, is shown in Fig. 1. Near the operating frequency the cavity does not have any high-Q resonances. The incident power in a form of TE_{01} mode passes many times inside the cavity. This provides several times larger delay time comparing to the straight waveguide of the same length as the cavity's length. Several cavities, connected in a chain, can provide delaying time up to hundreds of nanoseconds.

The necessary condition for the mentioned solution is to avoid spurious high-Q resonances in the frequency band which at least wider than spectrum width of the output compressor's pulse:

$$|f - f_0| >> \Lambda f, \qquad (1)$$

where f – is a real part of the eigen frequency of the nearest eigen mode, f_0 – is an operating frequency, and Δf – is a width of spectrum of the output pulse. The low-Q resonances are not dangerous if Q-factors are much less than:

$$Q^* = f_0 / \Lambda f. \qquad (2)$$

The conditions (1-2) are satisfied, in particular, if the cavity has spectrum of eigen modes consisted of the quasi-degenerated modes. This situation takes place in the solution presented in [2].

In order to test at low power level the idea of compact pulse compressor, the cavity with the shape, shown in Fig. 1, was chosen. The transmission and reflection characteristics of the delay line consisted of this chain are plotted in Fig. 2. Near the operating frequency the reflection is less than 1% on power. The dependence of the phase on frequency is practically linear one (Fig. 3). This means that the incident pulse has delaying only (23 ns/m) without distortions on amplitude and phase.

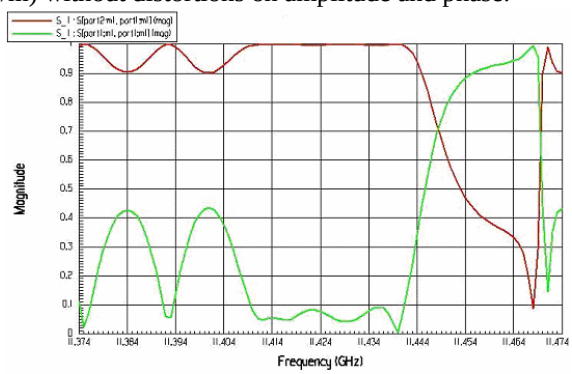

Figure 2: Reflection and transmission for the 4-cell chain (the cell shape is shown in Fig. 1).

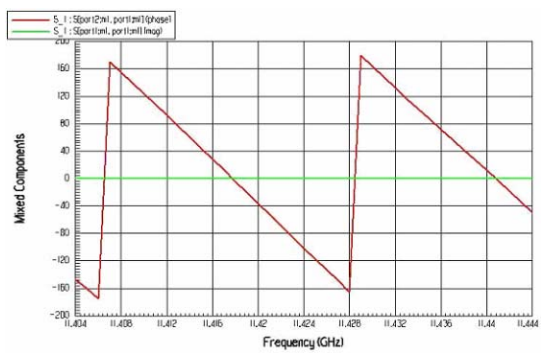

Figure 3: Phase of the reflected (red curve) wave for the 4-cell chain.

The low power tests were carried out at 34.27 GHz with the one-channel prototype (Fig. 4), where the last cell was closed by means of movable cut off reflector. This reflector was used for precise frequency tuning. The design of each cavity with scaling to 34.27 GHz

DEVELOPMENT OF C-BAND ACCELERATING SECTION FOR SUPERKEKB

T. Kamitani*, N. Delerue, M. Ikeda, K. Kakihara, S. Ohsawa, T. Oogoe, T. Sugimura,
T. Takatomi, S. Yamaguchi, K. Yokoyama, KEK, Tsukuba, Japan
Y. Hozumi, Graduate University for Advanced Studies Department
of Accelerator Science, Tsukuba, Japan

Abstract

In a future luminosity upgrade from the present KEK-B factory to the SuperKEKB, the injector linac is required to increase the positron acceleration energy from 3.5 GeV to 8.0 GeV. It could be realized by replacing some of the present S-band accelerator modules to the C-band module and doubling the acceleration field gradient (21 → 42 MV/m). Research and development of the components for the C-band module has been performed since 2002. This paper reports on the development of the first prototype of the C-band accelerating section whose design is based on a half-scale dimension of the present S-band 2-m long section. Details in the design and the fabrication are described. Results of the high-power test, beam acceleration test and ten months' operation in the KEKB injector linac are given.

INTRODUCTION

The KEK-B factory has achieved the world highest luminosity of 1.39×10^{34} cm^{-2}s^{-1} [1] but further upgrade aiming 2.5×10^{35} cm^{-2}s^{-1} has been considered [2]. In this upgrade, the stored beam energies of the electrons (8.0 GeV) and of the positrons (3.5 GeV) will be exchanged against positron beam-instability due to the electron-cloud effect. Consequently, the injector linac has to increase positron acceleration energy from 3.5 GeV to 8.0 GeV. In the present injector, the positron generation target is placed in the midway of the linac. Only the accelerator modules after the target contributes to the positron acceleration and it is sufficient for 3.5-GeV injection but not for 8.0 GeV. The 8.0-GeV positron beam is obtained if we could double the acceleration field gradient (21 → 42 MV/m). It is a general strategy to use higher rf frequency for higher field gradient as seen in the active R and D works for the linear colliders [3]. We have adopted the C-band (5712 MHz) accelerator module to replace some of the present S-band (2856 MHz) modules. The rf frequency is exactly twice of the present S-band frequency to accomodate the remaining S-band modules. Design studies of the C-band components have been performed to fit them to the specification for the KEKB injector upgrade [4]. The C-band accelerating section which cope with the rf breakdowns in the structure is one of the key components in the C-band accelerator module development.

* takuya.kamitani@kek.jp

DESIGN AND FABRICATION

The design of the first prototype of the C-band accelerating section is based on a half-scale dimension of the present 2 m long S-band section used in the KEKB linac [5]. We could take advandages of determining many design parameters just by scaling. Thus, the length of the first prototype C-band section is 1 m. It has a disk-loaded waveguide structure whose disk-iris diameter decrease linearly along the section to achieve quasi-constant field gradient. Specifications and a figure of the C-band section are shown in Table 1 and in Fig. 1.

Table 1: Specifications of the first prototype 1-m long C-band accelerating section.

operation frequency	5712.000 (MHz)
operation temperature	30.0 (degC)
no. of cells	54 regular cells + 2 couplers
section length	926.225 (mm) (55 cells)
phase advance per cell	$\frac{2\pi}{3}$-mode
cell length	17.495 (mm)
disk thickness (t)	2.500 (mm)
iris diameter (2a)	12.475 ∼ 10.450 (mm)
cavity diameter (2b)	41.494 ∼ 41.010 (mm)
shunt impedance (r_0)	74.6 ∼ 85.1 (MΩ/m)
Q factor	9703 ∼ 9676 (mm)
group velocity (v_g/c)	1.9 ∼ 1.0 (%)
filling time	234 (ns)
attenuation parameter (τ)	0.434

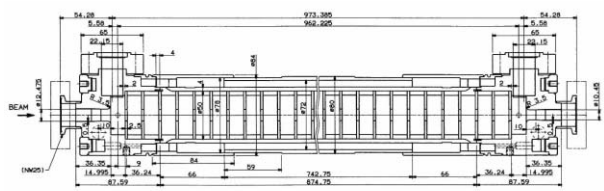

Figure 1: First prototype of C-band accelerating section.

The disks and cylindrical spacers forming regular cells of the accelerating section were made of oxygen-free copper and individually machined. The inner diameters of the spacers were adjusted by the Nodal shift measurements to achieve $2\pi/3$ phase advance per cell. After this resonant frequency adjustment of each cell, the central 50 cells out of total 54 cells were joined together by electroplating with copper. Typical radial thickness of the spacers was 4 mm

PRODUCTION OF S-BAND ACCELERATING STRUCTURES

Kai Dunkel, Christian Piel, Hanspeter Vogel, Peter vom Stein,
ACCEL Instruments GmbH, Bergisch Gladbach, Germany

Abstract

ACCEL currently produces accelerating structures for several scientific laboratories. Multi-cell cavities at S-band frequencies are required for the projects CLIC-driver-linac, DLS and ASP pre-injector linac and the MAMI-C microtron. Based on those projects differences and similarities in design, production technologies and requirements will be addressed.

CLIC DRIVER LINAC

The production of 18 CLIC Driver Linac structures [1] is under way at ACCEL Instrument GmbH [2]. Meanwhile more than 12 structures are delivered and successfully tested at CERN. The structure consists of 35 accelerating cells including the coupling cells with symmetric rf ports. Each cell contains four Silicon Carbide absorbers, which are coupled to the accelerating cells by the slotted cavity iris for HOM suppression. The operating frequency is 2998.55 MHz in 2π/3 mode. The structure is designed for extreme high beam loading of nearly 98 %. The nominal input power is 30 MW at a pulse length of 1.5 µs resulting to an unloaded accelerating voltage of 13.5 MV.

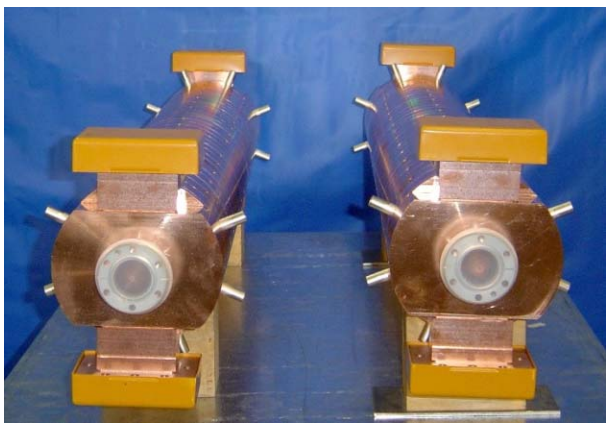

Figure 1: Two 1.22 m long CLIC Drive Linac structures ready for delivery.

The slotted iris geometry of the accelerating cells requires extreme care during the manufacturing process. After the turning and milling operations on the accelerating cells, which is similar to other standard S-Band structures, the cell is cut from the iris up to 10 mm away from the cell equator by wire spark erosion. This makes the cells fragile and sensitive to any mechanical deformations.

To assure the correct phase and amplitude tuning of the finished structure the frequency of each cell is measured before final brazing (Figure 2). A special test setup was built up at ACCEL for the measurement of the 0-mode and π- mode frequencies of each cell. This allows to calculate the 2π/3 mode frequency of the individual cells. After the final brazing the phase advance and field distribution of each structure is checked by a bead pull measurement (Figure 3).

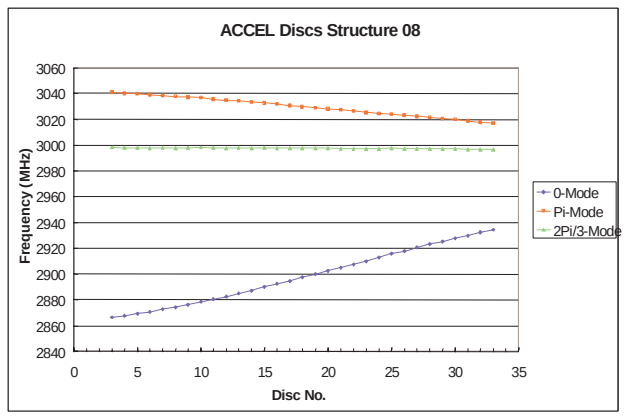

Figure 2: RF measurement of CLIC structure half cells.

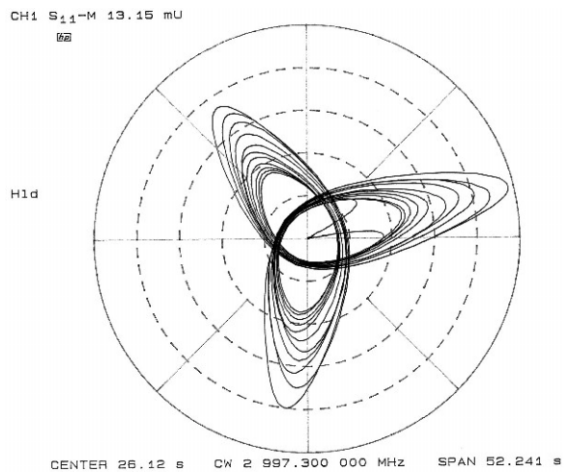

Figure 3: Bead pull measurement of a CLIC structure.

DLS AND ASP INJECTOR LINAC

ACCEL currently manufactures the 100 MeV injector linacs for the Diamond Light Source DLS [3],[4] and for the Australian Synchrotron Project ASP [5] based on 2π/3 mode travelling wave S-Band structures, operating at 2.997912 GHz.

Already four structures of this type had been delivered in the past. Two structures serve the SLS [6] injector linac at moderate accelerating fields of 11 MeV/m very reliable since April 2000. Another two structures are used at MaxLab at much higher gradients of 25 MeV/m. The manufacturing technology and design allow as well the production of 6m long structures. The design of the 5.2m long structures has been transferred from DESY to ACCEL under a technology transfer contract.

A FOUR-CELL PERIODICALLY HOM-DAMPED RF CAVITY FOR HIGH CURRENT ACCELERATORS *

G. Wu†, R. Rimmer, H. Wang, Jefferson Lab, Newport News, VA 23606, USA
J. Sekutowicz, DESY, Notkestrasse 85, 22607 Hamburg, Germany
Sun An, Oak Ridge National Lab, Oak Ridge, TN 37830, USA

Abstract

A periodically Higher Order Mode (HOM) damped RF cavity is a weakly coupled multi-cell RF cavity with HOM couplers periodically mounted between the cells. It was studied as an alternative RF structure between single-cell and superstructure cavities in high current application requiring strong damping of HOMs. The acceleration mode in this design is the lowest frequency mode (zero mode) in the pass band, in contrast to the traditional "π" acceleration mode in multicell superconducting cavities. The acceleration mode of the four-cell cavity has been studied, along with the monopole and dipole HOMs. The frequency response through HOM ports has been simulated in HFSS™ with waveguide couplers, which shows almost constant Q_{ext} for several important HOMs, even with different number of cells. A 4x1 zero-mode cavity was studied with MAFIA time domain analysis. To understand the tuning challenge for this weakly-coupled cavity, ANSYS® and SUPERFISH codes were used to simulate the cavity frequency sensitivity and field flatness change, which will influence the design of the tuner structure. This paper presents the computer simulation of this novel accelerating structure that may be used for variety of accelerator applications.

INTRODUCTION

High current linacs require heavily HOM-damped RF cavities. In other words, the high-current accelerating structure should only confine the accelerating mode or at most the only modes within the first pass band. One such RF structure is a HOM well-damped single cell cavity, which is used in storage rings [1, 2]. To get higher voltage gain within the same machine length, one would use multi-cell cavities [3], or a superstructure cavity [4]. The multi-cell structure inevitably traps some HOMs. One would naturally think that something in between should provide a trade off between effective accelerating voltage per unit length and the good HOM damping.

One solution could be packing individually HOM damped single cell cavities in a chain to form a periodical structure, which we call the Zero Mode cavity. The other would be packing single cell cavity back to back, which is essentially a superstructure of two-cell cavities. The latter has been proposed and studied earlier [5]. This note investigates the former case, the Zero Mode cavity.

*Work performed under DOE Contract #DEAC0584ER40150
†Electronic mail: genfa@jlab.org

ZERO MODE CAVITY

An enlarged beam pipe connects individual cells. Cell-to-cell coupling is expected to be quite weak. Since the high current RF cavity would mostly run in energy recovering mode, the weak coupling is thought to be less detrimental in terms of energy re-filling. The beam test of a 2x7 superstructure indicated that the energy flow between weakly coupled subunits was not a problem at least for TESLA's beam current [6].

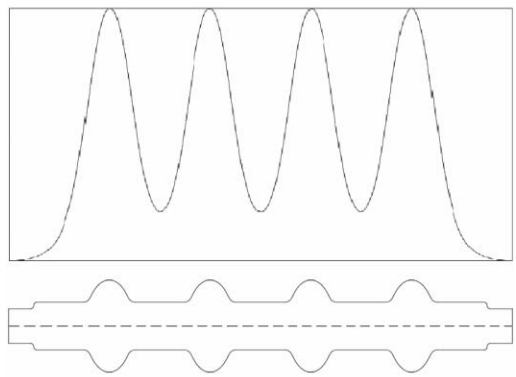

Figure 1: The four cell Zero Mode cavity and its on-axis electric field for acceleration mode.

A four-cell Zero Mode cavity is shown in Figure 1. Due to the non-zero field in the interconnecting beam pipe, lower R/Q is expected for the accelerating mode. The RF parameters are also listed in Table 1. From the E_p/E_{acc} ratio, a peak surface field 50 MV/m would be needed for a 10 MV/m accelerating gradient. The frequencies of the first pass band modes are plotted in Figure 2.

Table 1: RF parameters of Zero Mode cavity

Accelerating mode [MHz]	0	1498.703
Mode 2 [MHz]	π/4	1499.048
Mode 3 [MHz]	2π/4	1500.110
Mode 4 [MHz]	3π/4	1501.167
Cell number		1x4
Cell to cell coupling		7.91E-04
R/Q [Ohm] of accelerating mode		239
Geometric factor		277
Epk/Eacc		5.07
Bpk/Eacc [mT/(MV/m)]		8.42

NEW ACCELERATING MODULES RF TEST AT TTF

D. Kostin for the TESLA collaboration, DESY, D-22607 Hamburg, Germany

Abstract

Five new accelerating modules were installed into the TTF tunnel as a part of the VUV FEL Linac. They are tested prior to the linac operation. The RF test includes processing of the superconducting cavities, as well as maximum module performance tests. The test procedure and the achieved modules cavities performance are presented.

TTF ACCELERATING MODULES

The TESLA Test Facility (TTF) VUV FEL LINAC [1], [2], [3], [4] has now 5 accelerating modules (see Fig. 1), each module (see Fig. 2) consists of 8 9-cell niobium cavities with input RF power couplers (see Table 1) and a quadrupole in the cryomodule [5].

Figure 1: Accelerating modules ACC1 – ACC5 at TTF.

Figure 2: Accelerating module in the VUV-FEL tunnel.

Table 1: Accelerating Modules.

pos.	mod.	ready	coupler type	cold win.	warm win.
ACC 1	2*	Jan. 2004	FNAL/ TTF III	Conical /Cyl.	Planar /Cyl
ACC 2	1*	Mar. 2000	FNAL/ TTF II	Conical /Cyl.	Planar (WG)
ACC 3	3*	Feb. 2003	TTF II	Cyl.	Planar (WG)
ACC 4	4	Jul. 2001	TTF II	Cyl.	Planar, (WG)
ACC 5	5	Mar. 2002	TTF III	Cyl.	Cyl.

The cavities are operated at 2 K and have an accelerating gradient between 12 and 35 MV/m. The RF power sources for the accelerating modules are the 5 and 10 MW 1.3 GHz klystrons connected to the modules through the waveguide power distribution system (see Fig. 3). The RF power measurements are done using the waveguide directional coupler (DC) (1 coupler, forw. and refl., 1 DC pro module installed). The probe power measurement is done for the one cavity (where DC is also installed) pro accelerating module using the power meter. Power meters connected through GPIB-Ethernet network to the computers, controlling the test procedure using LabVIEW program.

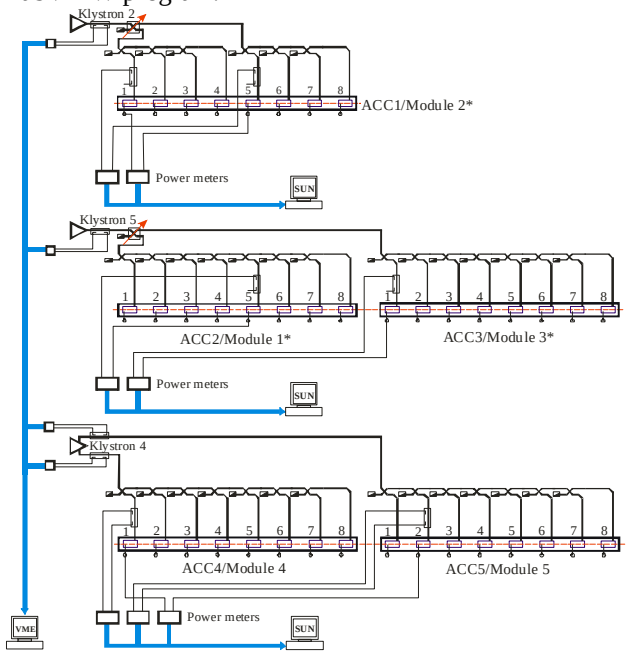

Figure 3: RF power distribution / measurement diagram.

Downconvertor/ADC channel for P_{for}, P_{ref} (from circulators) and P_{trans} (cavity probes) for each cavity is used to monitor the forward, reflected and transmitted power pulse shape. To measure power precisely enough proper power line calibration measurement must be ensured in order to get attenuation values between the power meter (PM) and measurement point. All measurement cables were calibrated before the test. To measure the accelerating gradient (E_{acc}) cavity pickup (transmitted) power value was used, calibration coefficient k_t is to be measured at lower power rectangular pulse, when pulse shape is precisely defined and E_{acc} is calculated (see Eq. 1).

$$E_{ACC} = \frac{\sqrt{4\frac{R_{sh}}{Q}Q_{load}P_{for}}}{L_{cavity}} \times \left[1 - e^{-\frac{\pi f_0 t_{fill}}{Q_{load}}}\right] = k_t \times \sqrt{P_{trans}}, [V/m] \quad (1)$$

PROGRESS TOWARD NLC/GLC PROTOTYPE ACCELERATOR STRUCTURES*

J.W. Wang#, C. Adolphsen, G. Bowden, D.L. Burke, J. Chan, J. Cornuelle, S. Doebert, V. Dolgashev, R.M. Jones, J. Lewandowski, Z. Li, R.H. Miller, C. Nantista, N. Baboi, C. Pearson, R.D. Ruth, S. Tantawi, P.B. Wilson, L. Xiao SLAC, USA
T. Higo, Y. Higashi, T. Kumi, Y. Morozumi, N. Toge, K. Ueno, KEK, Japan.
T. Arkan, C. Boffo, H. Carter, D. Finley, I. Gonin, T. Khabiboulline, S. Mishra, G. Romanov, N. Solyak, FNAL, USA

Abstract

The accelerator structure groups for NLC (Next Linear Collider) and GLC (Global Linear Colliders) have successfully collaborated on the research and development of a major series of advanced accelerator structures based on room-temperature technology at X-band frequency. The progress in design, simulation, microwave measurement and high gradient tests are summarized in this paper. The recent effort in design and fabrication of the accelerator structure prototype for the main linac is presented in detail including HOM (High Order Mode) suppression and design of HOM couplers and fundamental mode couplers, optimized accelerator cavities as well as plans for future structures.

HIGH GRADIENT TEST STRUCTURES

Since 2000, more then thirty structures with different length, aperture, phase advance and coupler design have been built and tested at the NLCTA.[1] Through the thorough comparison and analysis we have selected the following main accelerator parameters: 60 cm of length, 5π/6 phase advance /cell, low group velocity with optimal attenuation factor of 0.5-0.6 for optimal RF efficiency.

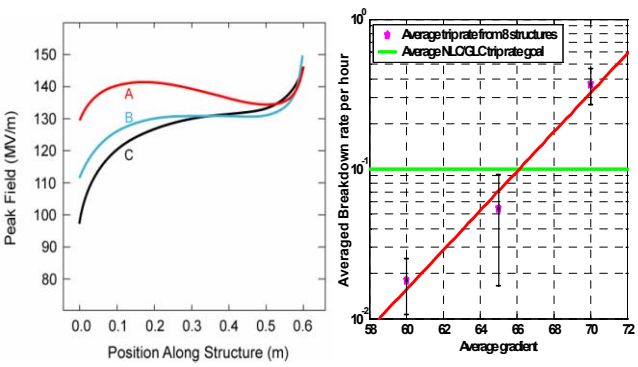

Figure 1: Maximum surface field for three types structures at unloaded gradient of 65 MV/m (left) and high power test results for eight structures (right).

The parameters of A (H60VG3S18), B (H60VG3S17) and C (H60VG4S17) are shown on Table 1. With reduced aperture a/λ=0.17, B and C have 10% higher RF efficiency than A. With asymmetric dipole mode detuning distribution, C has lowest surface field at the input end.

Table 1: Basic parameters for three typical structures

Structure Type	H60VG3S18	H60VG3S17	H60VG4S17
Other Names	FXBs (2D), KX01 (2D)	FXCs	FXDs, KX02, H60VG4SL17
Length	62 cm	62 cm	62 cm
Number of Cells	53 cells + 2 Matching Cells	53 cells + 2 Matching Cells	53 cells + 2 Matching Cells
Iris Radius	$<a/\lambda>$ =0.18	$<a/\lambda>$ = 0.17	$<a/\lambda>$ = 0.17
Phase Advance	5π/6 Per Cell	5π/6 Per Cell	5π/6 Per Cell
Group Velocity	3.27–1.24 % Speed of Light	3.56–0.78 % Speed of Light	4.50-0.82 % Speed of Light
Attenuation τ	0.533 0.508 (2D)	0.630	0.636
Filling Time	105 ns	116.5 ns	117.6 ns
Q_0 Value	~ 6640 ~ 6990 (2D)	~ 6670	~ 6660
Shunt Impedance	46.5-73.5 49.1-77.2 (2D) MΩ/m	54.7 – 68.8 MΩ/m	50.9 – 69.0 MΩ/m
Coupler Type	Mode Converter or Wave Guide Type	Waveguide Type	Wave Guide type
1st Band Dipole Mode Detuning	kdn/df Symmetric Gaussian Δf/f~10% (4.0σ)	kdn/df Symmetric Gaussian Δf/f~9.37% (3.94σ)	kdn/df Asymmetric $Sech^{1.5}$ with Δf/f~12.5% (5.1σ)
Es /Ea	2.06 - 1.90	2.04 -1.99	2.10 -1.97
Required Input Power	69 MW 63.2 MW (2D)	59 MW	58.2 MW
Unloaded Gradient	65 MV/m	65 MV/m	65 MV/m

The right plot of Fig. 1 show a summary of performance for the recent eight accelerator structures. The horizontal line is the goal line for GLC/NLC stable high power operation – less than 1 breakdown per 10 hours per 60 cm section at unloaded 65 MV/m gradient for 60 Hz RF pulses. The tilted line is a fit for average trip rates for

*Work supported by U.S. Department of Energy, contract DE-AC02-76SF00515 and part of JapanUS Collaboration Program In High Energy Physics Research.
jywap@slac.stanford.edu

A HIGH-POWER TEST OF AN X-BAND MOLYBDENUM-IRIS STRUCTURE

W. Wuensch, A. Grudiev, S. Heikkinen, I. Syratchev, M. Taborelli, I. Wilson, CERN, Geneva, Switzerland
S. Döbert, C. Adolphsen, SLAC, Palo Alto, California, USA

Abstract

In order to achieve accelerating gradients above 150 MV/m, alternative materials to copper are being investigated by the CLIC study. The potential of refractory metals has already been demonstrated in tests in which a tungsten-iris and a molybdenum-iris structure reached 150 and 193 MV/m respectively (30 GHz and a pulse length of 15 ns). In order to extend the investigation to the pulse lengths required for a linear collider, a molybdenum-iris structure scaled to X-band was tested at the Next Linear Collider Test Accelerator (NLCTA). The structure conditioned to only 65 MV/m (100 ns pulse length) in the available testing time and much more slowly than is typical of a copper structure. However the structure showed no sign of saturation and a microscopic inspection of the rf surfaces corroborated that the structure was still at an early stage of conditioning. The X-band and 30 GHz results are compared and what has been learned about material quality, surface preparation and conditioning strategy is discussed.

INTRODUCTION

The CLIC accelerating gradient specification is 150 MV/m, indisputably high, and a substantial development program is underway to achieve it [1]. One aspect of the program is an rf design study with the objective to design and optimize structures within experimentally determined high-power rf and simulated beam-dynamics constraints [2]. Another aspect is an experimental study which seeks to find alternative materials to copper which are able both to sustain a higher surface electric field and to resist damage during breakdown. A significant success of this experimental study has been the demonstration in CTF2 of a 193 MV/m, 15 ns peak accelerating gradient in a molybdenum iris structure [3].

The logical next step is to repeat the test at a longer pulse length since the CLIC design pulse length is 150 ns. However 30 GHz power will only become available for testing (in CTF3) at the end of 2004. In order make the test as soon as possible and to utilize the highly-developed NLCTA test area, an agreement was made to test a CERN-built molybdenum iris structure scaled to 11 GHz at the NLCTA at SLAC.

THE STRUCTURE AND INSTALLATION

The 11 GHz structure geometry was exactly scaled from the 30 GHz test in order to be able to make as direct a comparison to the previous test and also to provide frequency scaling of gradient data. The structure characteristics are summarized in table 1. The same mode-launcher coupler was used as in the 30 GHz test with only slight dimensional changes to match to WR-90 rather than WR-28 waveguide.

In addition, the irises were manufactured from the same 99.95% purity sintered and forged molybdenum bar produced by the same supplier as those of the 30 GHz test. Finally the method of assembly by clamping, a cell and iris are shown in fig.1, was maintained to keep to a minimum the number of differences between the structures.

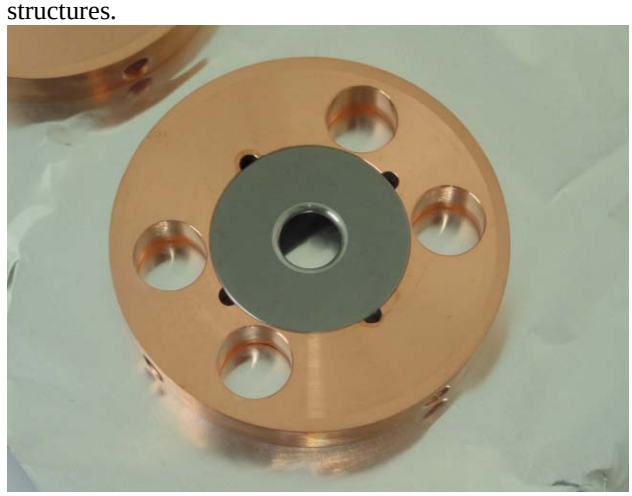

Figure 1: A molybdenum iris mounted in the copper disk which forms the cell.

Table 1: Structure Specifications

Frequency	11.424 GHz
Number of cells	30+2 matching cells
Phase advance	$2\pi/3$
Beam aperture	9.19 mm (constant)
Group velocity, v_g/c	4.6 %
Fill time	20 ns
$E_{surface}/E_{accelerating}$	2.2
Power for $E_{accelerating}$=100 MV/m	175 MW

The structure was assembled and installed in a dedicated vacuum tank at CERN and shipped to SLAC under vacuum. However the structure arrived vented and was therefore purged with hot (100°C) nitrogen for 72 hours in an attempt to reduce the water content in the rest gas. The structure vacuum level was measured by a gauge mounted directly on the tank and operated with a static pressure of the order of 10^{-8} mbar.

DEVELOPMENT OF A NON-MAGNETIC INERTIAL SENSOR FOR VIBRATION STABILIZATION IN A LINEAR COLLIDER*

Josef Frisch, Valentin Decker, Eric Doyle, Linda Hendrickson, Thomas Himel, Thomas Markiewicz, Andrei Seryi, SLAC, Stanford CA, USA
Allison Chang, Richard Partridge, Brown University, RI, USA

Abstract

One of the options for controlling vibration of the final focus magnets in a linear collider is to use active feedback based on accelerometers. While commercial geophysics sensors have noise performance that substantially exceeds the requirements for a linear collider, they are physically large, and cannot operate in the strong magnetic field of the detector. Conventional nonmagnetic sensors have excessive noise for this application. We report on the development of a non-magnetic inertial sensor, and on a novel commercial sensor both of which have demonstrated the required noise levels for this application.

SENSOR REQUIREMENTS

Room temperature linear colliders require relative position stability of the electron and positron beams at the Interaction point at the nanometer lever. The most sensitive beam line elements for vibration effects on the beam are the final focus doublets, which produce approximately one-to-one motion of the beam spots at the IP. With a beam rate of 120Hz, a feedback based on the beam interaction typically has unity gain around 10Hz. Gain at 1Hz is 10-1000 [1].

An accelerometer-based feedback system to mechanically stabilize the final doublets, with gain at frequencies above ~1 Hz can reduce the beam / beam motion at the IP [2]. While there is not a simple relationship between the accelerometer noise and ultimate feedback performance, it is clear that an integrated sensor noise of < 1nm for frequencies above ~1Hz is desirable, corresponding to a sensor acceleration noise of $<3x10^{-8}M/s^2/Hz^{1/2}$ at frequencies above 1Hz.

The acceleration sensors are attached to the final doublet magnets, and must operate in a detector magnetic field of the order of one Tesla. They must also be physically compact (approximately 20x20x10cm) due to volume constraints in the final focus design.

COMMERCIAL SENSORS

Good commercial piezoelectric seismometers have specified noise of $\sim 6x10^{-7}M/s^2/Hz^{1/2}$ at 1Hz [3]. Tests at SLAC measured a noise level of these sensors of $2x10^{-6}M/s^2/Hz^{1/2}$ at 1Hz with an integrated noise of 50nm above 1Hz. [4], too large for this application.

A commercial magnetic geophone of the type used in vibration stabilization experiments at SLAC [5], the GS-1 from Geospace [6] has a moving mass of 700 grams and a mechanical Q of ~0.5. The theoretical thermal noise of the sensor is $5x10^{-10}M/s^2/Hz^{1/2}$ (see below), however the actual sensor noise is not specified and may be higher.

Previous measurements of a similar sensor, a Mark Products L-4C at SLAC gave a noise of $<4x10^{-8}M/s^2/Hz^{1/2}$ (measurement limit), with an integrated noise of 0.3nm above 1Hz. This meets the noise requirements for final focus stabilization, but this type of sensor can not be used in the strong magnetic field of the detector.

Geophysics feedback seismometers such as the Streckeisen STS-2 have noise levels of $\sim 10^{-9}M/s^2/Hz^{1/2}$ with a corresponding integrated noise above 1Hz of ~.07nm [7], much better than our requirements. All commercial sensors of this type use magnetic internal components for temperature compensation and for force feedback, and cannot be used for our application. The prototype NLC vibration uses the same basic design concept, adapted for non-magnetic operation.

Micromachined accelerometers such as the "Si-flex" [8] accelerometer from Applied Mems have a specified noise of at $3x10^{-7}M/s^2/Hz^{1/2}$ at 1Hz. This does not meet our requirements, but future devices may improve on this performance.

Electrochemical Sensor

A novel commercial sensor SP-400 based on electrochemical detection of motion has recently been developed by PMD/Eentec [9]. This sensor is specified at $10^{-8}M/s^2/Hz^{1/2}$ at 1Hz, sufficient for our application. However this sensor uses magnetic coils for force feedback and cannot be used in this application without modification. The company estimates that replacing the magnetic components (which would remove the force feedback) would increase the noise by a factor of ~3, still within our requirements.

NLC SENSOR DESIGN

The lack of suitable sensors for NLC final focus stabilization led to the design of a low noise, nonmagnetic sensor. The sensor operates on the same principal as geophysics feedback seismometers, however the non-magnetic and compact size requirements lead to some design changes. The prototype sensor was designed for vertical sensing as this was considered to be the more technically challenging problem.

Sensor Noise Sources

All acceleration sensors can be modeled as a suspended mass, with a position measurement between the mass and the body of the sensor. The ultimate thermal noise of the

* Work Supported by DOE Contract DE-AC03-76SF0515

VIBRATION STABILIZATION OF A MECHANICAL MODEL OF A X-BAND LINEAR COLLIDER FINAL FOCUS MAGNET*

Josef Frisch, Allison Chang, Valentin Decker, Eric Doyle, Leif Eriksson, Linda Hendrickson, Thomas Himel, Thomas Markiewicz, Richard Partridge, Andrei Seryi, SLAC, Stanford CA, USA

Abstract

The small beam sizes at the interaction point of a X-band linear collider require mechanical stabilization of the final focus magnets at the nanometer level. While passive systems provide adequate performance at many potential sites, active mechanical stabilization is useful if the natural or cultural ground vibration is higher than expected. A mechanical model of a room temperature linear collider final focus magnet has been constructed and actively stabilized with an accelerometer based system.

PROTOTYPE SYSTEM

One option for the warm linear collider is to use a permanent magnet final focus. The small beam sizes at the IP of the linear collider require nanometer scale stabilization of the final doublets. Passive stabilization, interferometer based stabilization, and inertial stabilization have been considered. This paper describes a prototype of the inertial stabilization system.

The prototype system is designed to have mechanical properties similar to an actual permanent magnet final doublet and support raft, but is constructed somewhat differently, figure 1. It is referred to as the "extended object" to distinguish it from an earlier prototype consisting of a simple suspended block. [1]

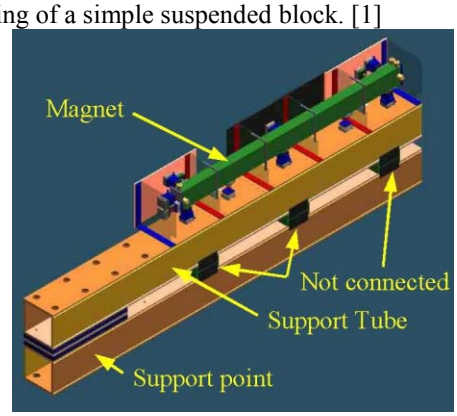

Figure 1: Vibration stabilization demonstration system.

Extended Object Mechanical Design

The extended object contains a simulated magnet support raft constructed of 4 thick-wall welded steel plates. It has the same dimensions, weight, and first two internal design mode frequencies as one of the designs for the NLC final doublet support raft.

Table 1: Simulated magnet properties

Length	3 Meters
Height	21 cm
Width	11.4 cm
Wall thickness	2.54 cm
Weight	240 Kg

The simulated magnet is supported on 6 spring mounts, designed to give the 6 rigid body degrees of freedom resonant frequencies of 2.5 to 6 Hz. This low support resonant frequency provides good attenuation of high frequency motions, which limits excitation of internal modes of the extended object and simplifies feedback.

The springs are mounted on a steel beam which has the same mass and resonant frequencies as the support tube which in an actual final focus would be cantilevered into the detector. Note that mounting the support tube rigidly to the detector risks coupling vibrations from the detector.

Table 2: Support tube properties

Length	3.35M (unsupported length)
Height / Width	40.6 cm
Wall thickness	1.6cm
Weight	1090 Kg

Figure 2: Photo of stabilization demonstration system.

Vibration Sensors

The position of the magnet mass is measured using 8 Geospace GS-1 1Hz magnetic coil seismometers [2]. These seismometer are not suitable for use in the magnetic field of a physics detector, however they have noise similar to the non-magnetic prototype seismometer being developed for the NLC [3]. These sensors are

* Work Supported by DOE Contract DE-AC03-76SF0515

APPROACHES TO BEAM STABILIZATION IN X-BAND LINEAR COLLIDERS*

Josef Frisch, Linda Hendrickson, Thomas Himel, Thomas Markiewicz, Tor Raubenheimer, Andrei Seryi, SLAC Stanford CA USA
Philip Burrows, Stephen Molloy, Glen White, Queen Mary University, London UK,
Colin Perry, Oxford University, Oxford UK

Abstract

In order to stabilize the beams at the interaction point, the X-band linear collider proposes to use a combination of techniques: inter-train and intra-train beam-beam feedback, passive vibration isolation, and active vibration stabilization based on either accelerometers or laser interferometers. These systems operate in a technologically redundant fashion: simulations indicate that if one technique proves unusable in the final machine, the others will still support adequate luminosity. Experiments underway for all of these technologies have already demonstrated adequate performance.

STABILIZATION OVERVIEW*

The NLC X-band linear collider is designed to operate at a 120Hz train rate with 192 bunches spaced at 1.4 nanoseconds per train. The linacs each contain approximately 600 quadrapoles containing beam position monitors, and 40 feedback corrector magnets. Beam position monitors and correctors are distributed throughout the beam delivery system. Beam stabilization simulations are described elsewhere [1], here we only quote results. Beam stabilization can be characterized with respect to its timescale, in this paper we primarily discuss feedback on relatively short timescales:

Beam Based Alignment

On approximately one month timescales, the effective centers of the Linac beam position monitors relative to the quadrapole magnetic centers are found through either quad shunting, or dispersion free steering [2].

On several hour timescales, the Linac quadrapoles are moved based on a global optimization algorithm to minimize the orbit errors in the BPMs, to minimize the corrector strengths, and to overall center the beam.

The accelerator structures contain beam position monitors (using signals from the higher order mode ports). Mechanical movers on the structures are used to minimize the transverse wakes when the quadrapoles are aligned.

Beam Based Feedback

Feedbacks distributed throughout the accelerators operate on a pulse to pulse basis at the 120Hz repetition rate of the accelerator[1]. These feedbacks are cascaded, allowing each to have information about the operation of the upstream feedbacks[3].

* Work Supported by DOE contract DE-AC03-76SF0515

The beam / beam deflection at the Interaction Point provides information on the beam separation. This deflection signal is used in a 120Hz feedback in the final focus to maintain beam collisions.

Vibration feedback

The final doublet magnets have the tightest vibration tolerances of any of the machine components [4] with an approximately 1:1 response of beam motion to magnet motion. As the 120Hz beam rate limits the effective frequency of feedbacks to frequencies below a few Hz, several options for mechanical stabilization of the final doublets have been considered, including passive, inertial based, and interferometer based feedback. To date most of the work has been directed to using accelerometers mounted on the doublets, with force feedback to control the magnet positions. The loop speed is typically 1-2 kilohertz, providing gain at frequencies from approximately 1-100 Hz. Current status of this work is described in [5], and the results are used here.

Fast Intratrain Feedback

A fast beam position monitor and kicker located near the interaction point can provide closed feedback on a timescale of tens of nanoseconds[6]. This feedback operates essentially independently from the other beam feedbacks (due to the different timescale), and can significantly improve luminosity under noisy beam conditions.

STABILIZATION STUDIES

The beam stabilization studies use a combination of real and simulated data to provide an estimated luminosity. The simulations are described in [7]. The basic procedure is:

- A series of initial machines with random errors (BPM offsets, magnet positions, etc) based on design tolerance are constructed.
- A simulated ground motion model, in this case the model "B", power spectrum shown in figure 1 is applied to the beamline components EXCEPT for the final doublet. [8].
- An additional 15nm of random jitter is applied to the linac quadrapoles to simulate, for example, water flow induced vibration . An addition 5nm of random jitter is added to the beam delivery quadrapoles.
- 120Hz linac beam feedbacks are simulated
- Final doublet positions are taken from measured data from the vibration stabilization test system [5] – a

HIGH PRECISION SURVEY AND ALIGNMENT OF LARGE LINEAR ACCELERATORS

J. Prenting, M. Schlösser, A. Herty[⊗], DESY, Hamburg, Germany
J. Green, G. Grzelak, A. Mitra, A. Reichold, University of Oxford, United Kingdom

Abstract

Future linear accelerators require new survey techniques to achieve the necessary alignment precision. For TESLA, the demanded accuracy for the alignment of the components is 0.5mm horizontal and 0.2mm vertical, both on each 600m section. Other proposed linear colliders require similar accuracies. These demands can not be fulfilled with common, open-air geodetic methods, mainly because of refraction in the tunnel. Therefore the RTRS (Rapid Tunnel Reference Surveyor), a 25m long measurement train performing overlapping multipoint alignment on a regular tunnel reference network is being developed. Two refraction-free realizations of this concept are being developed at the moment:

GeLiS measures the horizontal co-ordinates using multipoint alignment with stretched wires as strightness reference. In areas of the tunnel where the accelerator is following the earth curvature GeLiS measures the vertical co-ordinate using a new hydrostatic levelling system (HLS).

LiCAS is based on laser straightness monitors (LSM) combined with frequency scanning interferometry (FSI) in an evacuated system. LiCAS measures both co-ordinates with respect to its LSM-beam and thus is suitable for geometrically straight tunnel sections. Both measurement systems will be placed on a train, which could do the reference survey autonomous or semi-autonomous.

GEODETIC TASKS

A very high accuracy is demanded for the alignment of all accelerator components to run the linear collider successfully. The standard deviation of every component is postulated to be $\sigma_{l,h}$ = 0.2mm in lateral and height over the maximum betatron wavelength (e.g. 600m). Because of the influence of refraction, this requirement can not be achieved with any open-air optical survey.

CONCEPT

A basic network of reference points fixed to the wall in an equidistance of approximately 5m is installed in the tunnel. The alignment of the accelerator is split up in two major steps:

1) The reference points will be determined by an automated system (Rapid Tunnel Reference Surveyor, RTRS) in 3D space. The RTRS is described here.
2) The coordinates are transferred to the machine components with a tacheometer. This step is geodetic standard work and is not described in this paper. It is planned to integrate this second step into the RTRS.

Multipoint Alignment

With the technique of multipoint alignment the effects of refraction can be eliminated or reduced if a mechanical structure or a laser beam in vacuum is used as straightness reference. Multipoint alignment in a simplified 2D context means that the lateral distances s_{i-1}, s_i and s_{i+1} (see Fig. 1) between the straightness reference and several reference points are measured. Together with the distances $s_{i-1,i}$ and $s_{i,i+1}$ the angle β and the distances d can be calculated. This is done sequentially for every reference point in the tunnel (see Fig. 1). A traverse then is used to estimate the coordinates of the reference points. LiCAS extends this concept to a 3D-measurement

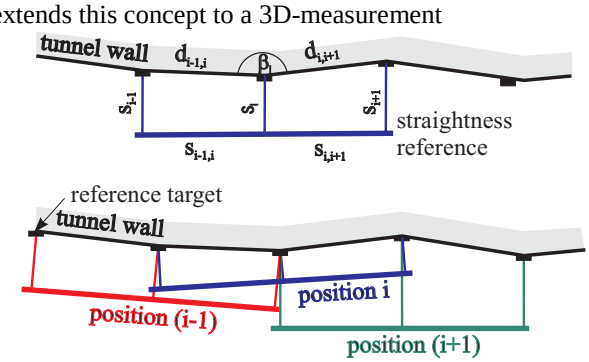

Figure 1: concept of geodetic reference survey, simplified 2D.

Rapid Tunnel Reference Surveyor, RTRS

A train with six measurement cars (blue, see Fig. 2) will overdetermine the multipoint alignment problem and provide enough redundancy to obtain the desired accuracy and reliability. For electronics and drives additional service cars (grey) are needed. This train can act autonomous and moves through the tunnel without user interaction.

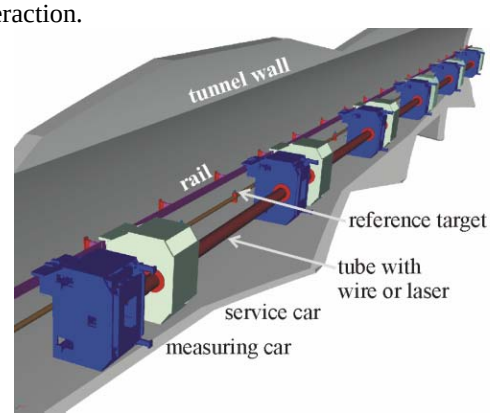

Figure 2: Measuring train on the tunnel wall.

[⊗]now CERN, Geneva, Switzerland

Operation of a 1.3 GHz, 10 MW Multiple Beam Klystron

H.P. Bohlen, A. Balkcum, M. Cattelino, L. Cox, M. Cusick,
S. Forrest, F. Friedlander, A. Staprans, E. Wright, L. Zitelli,
CPI, Palo Alto, California
K. Eppley, SAIC, Boston

Abstract

Results will be reported for a 1.3 GHz, 10 MW multiple beam klystron that is being developed for the TESLA linear accelerator facility. The design parameters for the device are 10 MW peak RF output power with 150 kW average power, 1.5 ms pulse length, 65% efficiency, 50 dB gain, and 2.0 A/cm^2 maximum cathode loading. Initial testing of the device has validated the basic design approach. Six 120 kV electron beams of measurably identical currents of 22.9 A each have been successfully propagated through the klystron circuit with 99.5% DC beam transmission at full operating video duty and with 98.5% saturated RF transmission. A peak power of 10 MW at 1.3 GHz with 60% efficiency and 49 dB of gain has been measured.

NO SUBMISSION RECEIVED

DEVELOPMENT OF HIGH RF POWER DELIVERY SYSTEM FOR 1300 MHZ SUPERCONDUCTING CAVITIES OF CORNELL ERL INJECTOR*

S. Belomestnykh#, M. Liepe, V. Medjidzade, H. Padamsee, V. Veshcherevich,
Laboratory for Elementary-Particle Physics, Cornell University, Ithaca, NY 14853, USA
N. Sobenin, Moscow Engineering Physics Institute (State University), Moscow, Russia

Abstract

Development of a 150 kW CW RF power delivery system for 1300 MHz superconducting cavities is under way at Cornell University in collaboration with MEPhI. The system is based on a twin-coupler consisting of two identical coaxial antenna-type couplers derived from the TTF III input coupler design. Because the average power is much higher than in the TTF III coupler, the required coupling is stronger and to avoid multipacting phenomena, major changes were made to the prototype design. Presented coupler has completely redesigned cold part and significantly improved cooling of warm bellows. The results of thermal and mechanical stress calculations are reported. The magnitudes and phases of RF fields applied to each side of the twin-coupler must be very close to each other. This imposes very strict requirements upon a power dividing system. These requirements and proposed layout of a system satisfying them are discussed.

INTRODUCTION

In the Cornell Energy Recovery Linac project (ERL) [1], each of the two-cell 1300 MHz injector cavities will deliver 100 kW of CW RF power to the 100 mA beam. Individual 150 kW klystrons will drive the cavities via high-power delivery systems. Each system consists of a twin input coupler [2] and a waveguide distribution network with an adjustable hybrid and a two-stub phase tuner for precise setting of RF power split. The twin coupler consists of two identical antenna type couplers, and the magnitudes and phases of RF fields applied to each of these couplers must be very close to each other. A difference of field magnitudes on individual coupler antennae should not exceed 1-2%, and a phase difference should not exceed 1° [2]. A scheme of the power dividing system for ERL injector cavities is shown in Figure 1. This paper describes latest results in developing components of the high power delivery system that would satisfy such strict requirements.

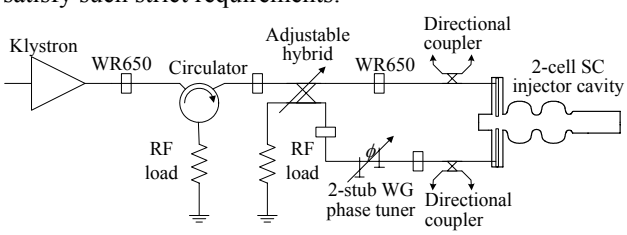

Figure 1: RF power splitting scheme for ERL injector.

*Supported by Cornell University
#sab@lepp.cornell.edu

POWER SPLIT

We proposed to use a short slot hybrid as a power divider for this precise RF power dividing system [3]. This type of hybrids seems to have better electrical properties compared with other four-port hybrid designs: low sensitivity to mismatch, a wide frequency band, and the best high power handling. For power balance, an adjustable stub in the middle point of the short slot hybrid can be used. By varying its penetration into the waveguide, one can adjust the power ratio between hybrid output arms with a very small phase error. Two versions of an adjustable short slot hybrid design were studied recently [4]. The first one uses uniform standard waveguide arms of the WR650 type and has a narrower frequency band. The second one uses narrower waveguide arms and needs additional transition pieces for connection to standard waveguides. On the other hand, it has a wider frequency band. Both types are adequate to the Cornell ERL RF system.

A two-stub device can be used as a phase tuner. Insertion of a stub into a waveguide produces capacitive admittance and an additional phase shift, these two values depending on the depth of the stub insertion. Using optimal stub separation one can reach the phase range of 20° keeping reflection below –40 dB [3].

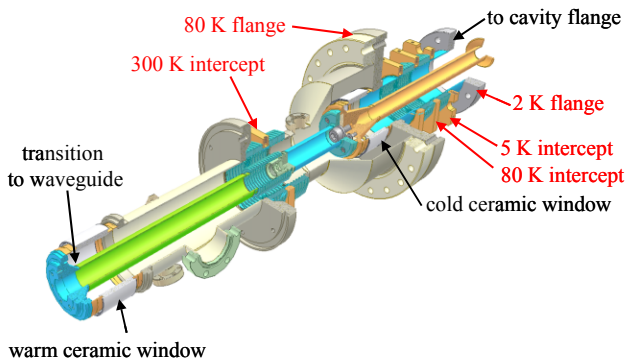

Figure 2: 3D view of the injector cavity coupler.

INPUT COUPLER

A design of the coaxial antenna type couplers is derived from the TTF III input coupler [5]. The following major modifications were made to meet our requirements. The cold part of the original coupler was completely redesigned. Instead of a 40 mm 70 Ω coaxial line, a 62 mm 60 Ω line was chosen for stronger coupling, better handling the high power and avoiding multipacting [2]. The coupler has large profiled antenna tip and the 16 mm travel range for getting the required coupling variation.

NLC HYBRID SOLID STATE INDUCTION MODULATOR*

R.L. Cassel, J.E. deLamare, M.N. Nguyen, G.C. Pappas @SLAC,
E. Cook, J. Sullivan @ LLNL, C. Brooksby @ Bechtell Nevada

Abstract

The Next Linear Collider accelerator proposal at SLAC requires a high efficiency, highly reliable, and low cost pulsed power modulator to drive the X band klystrons. The original NLC envisions a solid-state induction modulator design to drive up to 8 klystrons to 500kV for 3µS at 120 PPS with one modulator delivering greater than 1,000-megawatt pulse, at 500kW average. A change in RF compression techniques resulted in only two klystrons needed pulsing per modulator at a reduced pulse width of 1.6µS or approximately 250 megawatts of the pulsed power and 80kW of average powers. A prototype Design for Manufacturability (DFM) 8-pack modulator was under construction at the time of the change, so a redirection of modulator design was in order. To utilities the equipment, which had already be fabricated, a hybrid modulator was designed and constructed using the DFM induction modulator parts and a conventional pulse transformer. The construction and performance of this hybrid two-klystron Induction modulator will be discussed. In addition the next generation DFM induction modulator utilizing a ten-turn secondary and fractional turn primary transformer well be presented.

PROTOTYPE MODULATOR

The prototype Solid State induction modulator for the NLC Klystron was original designed to drive eight X-band klystron in parallel requiring 500kV 2000A pulses for 3.2µS flat top at 120 PPS. [1] [2] The prototype was fabricated and tested in a water load to 500kV and into two 5045 klystron up to 420kV. The NLC program for the RF testing was modified requiring a change in the modulator to operate only four XL4 klystron at 400kV, 1300 Amps, 1.6µS flattop at 60Hz. (See figure 1)

Figure 1: "8-pack" Solid State modulator installation.

To better match the operating condition of the klystron the two parallel drivers were reduced to one driver operating at 2kV at 3600A.

The stray capacitance to ground of the XL4 klystrons, was twice that of the X-band klystron resulting in a voltage overshoot of greater than 20%. This overshoot was eliminated by delaying the turning on of 18 of the 76 driver cells. (See figure 2)

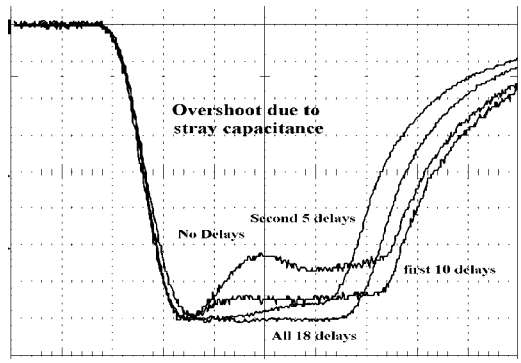

Figure 2: Overshoot correction by delaying triggers.

Delaying eliminated the overshoot without compromising the rise time and adjusted the flattop to a flatness of < 0.5%. (See figure 3)

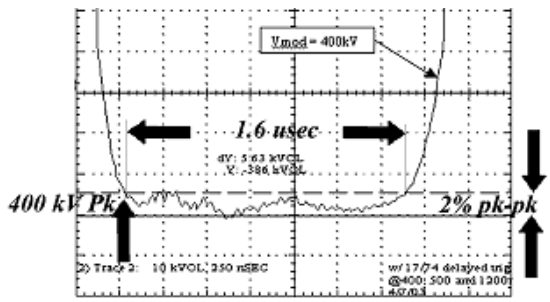

Figure 3: Pulse flattop regulation.

The prototype solid-state modulator has been operating at 60 Hz 24 hours a day for months >600hr with a minimum of intervention. Even with more than a thousand interruptions of operation for RF vacuum faults the modulator continues to operate.

Klystron Arcs

There were numerous (>15) klystrons arc at different points along the flattop pulse with no discernable effect on either klystron of modulator. (See Figure 4) The klystron and modulator resumed operation after the klystron arcs with no klystron damage. From the measurements of the klystron arcs, it is clear that the joules and coulombs under which a klystron can recover from are considerably higher than previously predicted.

* Work supported by DOE, contract DE-AC03-76SF0051

REDUCTION OF RF POWER LOSS CAUSED BY SKIN EFFECT

Y. Iwashita, ICR, Kyoto Univ., Kyoto, JAPAN

Abstract

Skin effect on a metal foil that is thinner than a skin depth is investigated starting from general derivation of skin depth on a bulk conductor. The reduction of the power loss due to the skin effect with multi-layered conductors is reported and discussed. A simple application on a dielectric cavity is presented.

INTRODUCTION

RF current flows on a metal surface with only very thin skin depth, which decreases with RF frequency. Thus the surface resistance increases with the frequency. Because the skin depth also decreases when the metal conductivity increases, the improvement of the conductivity does not contribute much; it is only an inverse proportion to the square root of the conductivity. Recently, it is shown that such a power loss can be reduced on a dielectric cavity with thin conductor layers on the surface, where the layers are thinner than the skin depth [1]. The thin foil case is analyzed after a review of the well-known theory of the skin effect. Then an application to a dielectric cavity with TM0 mode is discussed [2].

SKIN DEPTH OF BULK MATERIAL

In materials with conductance σ ($>>i\omega\varepsilon$), Ampere's law becomes:

$$\nabla\times\mathbf{H}=(\sigma+i\omega\varepsilon)\mathbf{E}. \tag{1}$$

Suppose a system as shown in Fig. 1, Eq.1 finally becomes:

$$\partial_x^2 j = i\omega\mu\sigma j, \quad j=\sigma E_y. \tag{2}$$

Under the condition of $\sigma>>i\omega\varepsilon$, the solution of Eq.2 is:

$$j(x)=j_0 e^{-(1+i)x/\delta}, \quad \delta=\sqrt{2/\omega\mu\sigma}, \tag{3}$$

where δ is the skin depth. Considering that $\nabla\times\mathbf{E}$ has only one nonzero component of $\partial_x E_y=\partial_x j/\sigma$, the magnetic field in the conductor is derived from Faraday's law $\partial_x E_y=-i\omega\mu H_z$ as

$$H_z(x)=\frac{\partial_x E_y}{-i\omega\mu}=\frac{\partial_x j}{-i\sigma\omega\mu}=\frac{\delta^2\partial_x j}{-2i}=\frac{\delta}{2}(1-i)j(x). \tag{4}$$

Thus $j(x)$ is expressed by the magnetic field on the conductor surface $H_z(0)$:

$$j(x)=\frac{1+i}{\delta}H_z(0)e^{-(1+i)x/\delta}. \tag{5}$$

A typical value of δ in copper at the frequency of 3GHz is 1μm. Figure 2 shows the current j as a function of x/δ. By integrating j, we obtain total current in the conductor:

$$J=\int_0^\infty j\,dx=H_z(0). \tag{6}$$

The power loss in the conductor can be calculated as

$$P_{bulk}=\int_0^\infty |j|^2/\sigma\,dx=\frac{H_z(0)^2}{\sigma\delta}=\sqrt{\frac{\omega\mu}{2\sigma}}H_z(0)^2, \tag{7}$$

where $1/\sigma\delta$ is often written as surface resistance Rs.

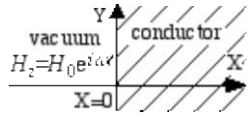

Figure 1: Half of the space is filled by conductor.

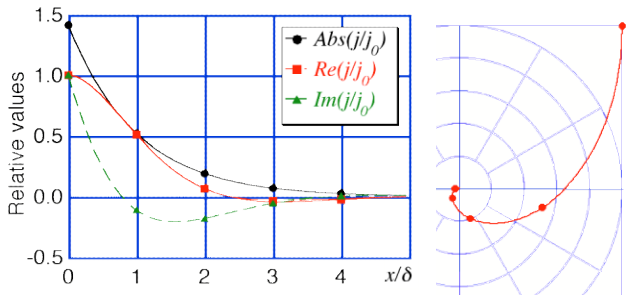

Figure 2: Left: j as a function of x/δ. Right: polar plot. Markers are put in every unit.

Although it is necessary to increase the conductance for lower RF power loss, the higher conductance leads to higher current density and thus the thinner skin depth reduces the improvement by the good conductance. It may be possible to cure this situation if we can control the current density independent of the conductance.

Typical value of σ is 5.8×10^7 [S] for copper metal and that of $\omega\varepsilon$ is 1 in vacuum at 18 GHz. Reminding the Eq.1, if low loss dielectric material with relative permittivity of more than 10^7 at such a high frequency were available, the RF power loss could be determined by the dielectric loss other than the conductor loss. Composite material such as seen in multilayered capacitors may have such characteristics. This will be investigated in future.

SKIN EFFECT ON THIN FOIL

Let us consider a case that the thickness of the conductor is thinner than the skin depth δ (see Fig. 3) and the both sides have electromagnetic fields with different amplitudes. The solution of Eq.2 becomes:

$$j(x)=H_z(0)\left(j_f e^{-(1+i)x/\delta}+j_b e^{-(1+i)(\alpha\delta-x)/\delta}\right), \tag{8}$$

$$j_f=\frac{(1+i)e^{(1+i)\alpha}\left(e^{(1+i)\alpha}-\xi\right)}{\delta\left(e^{2(1+i)\alpha}-1\right)}, j_b=\frac{(1+i)e^{(1+i)\alpha}\left(\xi e^{(1+i)\alpha}-1\right)}{\delta\left(e^{2(1+i)\alpha}-1\right)}.$$

Figure 4 shows polar plots for $j(x)$ for the case when the magnetic fields of both sides have the same amplitude(ξ=1). They are symmetrical with respect to the origin because the currents from both sides cancel each other. The linear behaviour can be seen when the

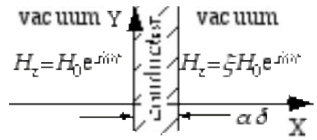

Figure 3: The thickness is thinner than the skin depth.

THE DESIGN AND PERFORMANCE OF THE SPALLATION NEUTRON SOURCE LOW-LEVEL RF CONTROL SYSTEM *,**

M. Champion, M. Crofford, K. Kasemir, H. Ma, C. Piller, Spallation Neutron Source, Oak Ridge National Laboratory, Oak Ridge, TN, USA
L. Doolittle, C. Lionberger, M. Monroy, A. Ratti, Lawrence Berkeley National Laboratory, Berkeley, CA, USA
J. Power, H. Shoee, Los Alamos National Laboratory, Los Alamos, NM, USA

Abstract

The Spallation Neutron Source (SNS) linear accelerator low-level RF control system has been developed within a collaboration of Lawrence Berkeley, Los Alamos, and Oak Ridge national laboratories. Three distinct generations of the system, previously described, have been used to support beam commissioning at Oak Ridge. The third generation system went into production in early 2004, with installation in the coupled-cavity and superconducting linacs to span the remainder of the year. The final design of this system will be presented along with results of performance measurements.

INTRODUCTION

The LLRF controller for the SNS linac has been designed with a collaborative effort among three US national laboratories, Oak Ridge, Lawrence Berkeley and Los Alamos.

The three main components of the SNS LLRF Control System are the RF field control module (FCM), the High Power Protection Module (HPM), and the reference system. The HPM and the reference systems have been described elsewhere.

The FCM is a digital feedback controller that uses a Field Programmable Gate Array (FPGA) for fast data processing. The work presented here covers the test performance and production of the field control module.

The FCM is the result of the evolution of the FPGA-based data acquisition and processing systems developed for the SNS project by Los Alamos and Berkeley[1].

The SNS project is currently under construction. The equipment described here has been used during beam commissioning of the front end and DTL systems, and is ready to support CCL commissioning. The beam commissioning for the entire linac is planned for 2005.

* This work is supported by the Director, Office of Science, Office of Basic Energy Sciences, of the U.S. Department of Energy under Contract No. DE-AC03-76SF-00098.

** The SNS project is being carried out as a collaboration of six US Laboratories: Argonne National Laboratory (ANL), Brookhaven National Laboratory (BNL), Thomas Jefferson National Accelerator Facility (TJNAF), Los Alamos National Laboratory (LANL), E. O. Lawrence Berkeley National Laboratory (LBNL), and Oak Ridge National Laboratory (ORNL). SNS is managed by UT-Battelle, LLC, under contract DE-AC05-00OR22725 for the U.S. Department of Energy.

PROTOTYPING AND TESTING

Throughout the project, we took a gradual and incremental approach towards accomplishing our goals. As a consequence of this decision, we leveraged from the experience of the first and second-generation LLRF systems, as well as that of similar components in the BPM system[2].

Shortly after deciding on the basic approach, we designed and built a prototype system, which we used for debugging and performance testing purposes[3,4]. This system was used to power up both a superconducting RF system, using the JLAB SRF cavity test stand, and a warm system at SNS.

The prototype system was an expansion over the interim system built at Berkeley and used as a benchmark and a development platform for the final system[5]. This allowed us to compare most of the performance measurements and make the necessary adjustments to enhance performance as described below before going into final production.

PRODUCTION EXPERIENCE

Once the system was successfully prototyped, we went to commercial production. In this process we combined the fabrication of the FCMs with that of the HPMs and requested that the vendor be responsible for both the manufacturing of the PC boards and the loading of its components.

In order to meet our aggressive schedule, we procured all electrical components in advance; the vendor was responsible for board procurement, nuts & bolts, loading, and flying-probe testing.

Since we need to deploy 98 systems, we planned for a full production of 100 boards, plus 25 spares. This process had no big surprises; the only problem was caused by damage to the filters in the output circuit, which were not sealed and were damaged in the cleaning process. This was discovered in a pre-production run, so for the final run we attached the filters to the board after the rest of the board was soldered and cleaned.

TEST STRATEGY

We approached testing in two phases. The first was in support of the development of the hardware and was aimed at maximizing performance and optimizing the design. The second is the ongoing acceptance testing of

THE TOSHIBA E3736 MULTI-BEAM KLYSTRON

A.Yano#, S.Miyake,
TOSHIBA ELECTRON TUBES & DEVISES Co., Ltd, Otawara, Tochigi 324-8550, Japan
S. Kazakov, A. Larionov, V. Teriaev, BINP, Branch of Institute of Nuclear Physics, Russia
Y. H. Chin, KEK, High Energy Accelerator Research Organization, Tuskuba, 305-8550, Japan

Abstract

A 10-MW, L-band multi beam klystron (MBK) for TESLA linear collider and TESLA XFEL has been under development at Toshiba Electron Tubes & Devices Co., Ltd. (TETD) in collaboration with KEK. The TESLA requires pulsed klystrons capable of 10 MW output power at 1300 MHz with 1.5 ms pulse length and a repetition rate of 10 pps. The MBK with 6 low-perveance beams in parallel in the klystron enables us to operate at lower cathode voltage with higher efficiency. By choosing the coaxial cavities operated in TM_{010} mode, the cathode loading can be reduced for long life operation. This klystron is a six-cavity klystron. The 2nd harmonic cavity was employed as the 3rd cavity to satisfy the phase sensitivity requirement due to the change in the beam voltage. Tow pillbox windows with WR650 waveguide were chosen for power transmission. From the space limitation, a low-height waveguide was coupled to an output cavity. The design work and the fabrication have been accomplished and the testing is under way. We started conditioning and testing of prototype #0 from the beginning of August 2004. The preliminary testing up to a beam voltage of 100kV (specification=115kV) demonstrated the output power more than 6.2MW with an efficiency of 59%. The testing at higher voltage will start soon. The design overview and the initial test result at the factory are presented.

INTRODUCTION

Each author The TESLA project is a 33km long 500 to 800GeV electron/positron linear collider.[1] The TESLA X-FEL laboratory is a 1.5km long 20Gev electron linear accelerator for free electron laser application. [2] The superconducting cavity technology is adapted to the accelerators. The 500GeV TESLA project requires 572 klystrons operating at 10MW output power with 1.5ms pulse length. [3]

KEK has investigated a basic design X-band multi-beam klystron as power sources of Global linear collider (GLC) main linac. [4] Our design work started based on our experience of this X-band MBK design. TOSHIBA/KEK team improved the preliminary design to meet the DESY's requirements. The design parameters for the TOSHIBA E3736 klystron are shown in Table 1.

#atsunori.yano@toshiba.co.jp

Table 1: Design parameters of the E3736 MBK

Parameter	Value	Units
Frequency	1300	MHz
Output Power	10	MW
Average Output Power	150	kV
Beam Voltage	115	kV
Beam Current	132	A
Efficiency	>65	%
RF Pulse Width	1.5	ms
Repetition Rate	10	pps
Saturation Gain	47	dB
Number of Beams	6	
Cathode Loading	<2.1	A/cm^2
Structure	6	cavities
RF Window	Pill Box WR-650	
Tube Length	2270	mm
Solenoid Power	<4	KW

MULTI-BEAM KLYSTRON [5]

Fig. 1 shows the cut-away view of the multi-beam klystron E3736.

Symons reported the relationship of an RF efficiency η and the beam perveance P ($I/V^{3/2}$) can be expressed as below: [6]

$$\eta(\%) = 90 - 20 \times P(\mu perv.)$$

If a microperveance $P(\mu perv.)$ is to be chosen to be 2.0 that are typically selected for the conventional (shingle beam) klystrons operated at 10MW output power, expected RF efficiency is 50% at the maximum. A low microperveance klystron must operate at higher beam voltage. In case of long pulse klystrons, it might be cause of breakdown problem at electron gun and hence reduce the klystron reliability.

By using several low perveance electron beams in parallel in a klystron, a higher RF efficiency is expected due to the lower space charge forces that enable a tighter beam bunching.

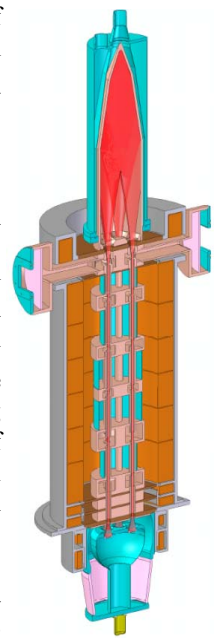

Figure 1: Cut-away view of the TOSHIBA E3736 multi-beam klystron.

CABLE INSULATION BREAKDOWNS IN THE MODULATOR WITH A SWITCH-MODE HIGH-VOLTAGE POWER SUPPLY*

A. Cours#, Argonne National Laboratory, 9700 S. Cass Ave.,
Argonne, Illinois, 60439, USA

Abstract

The Advanced Photon Source modulators are PFN-type pulsers with 40-kV switch-mode charging power supplies (PSs). The PS and the PFN are connected to each other by 18 feet of high-voltage (HV) cable. Another HV cable connects two separate parts of the PFN. The cables are standard 75-kV x-ray cables. All four cable connectors were designed by the PS manufacturer. Both cables were operating at the same voltage level (about 35 kV). The PS's output connector has never failed during five years of operation. One of the other three connectors failed approximately five times more often than the others. In order to resolve the failure problem, a transient analysis was performed for all connectors. It was found that transient voltage in the connector that failed most often was subjected to more high-frequency, high-amplitude AC components than the other three connectors. It was thought that these components caused partial discharge in the connector insulation and led to the insulation breakdown. Modification of the PFN eliminated one HV cable and significantly reduced the AC components during the pulse. A connector with higher partial discharge inception voltage was chosen as a replacement.

THE MODULATOR CIRCUITRY

The modulator power circuitry is shown in Fig. 1.

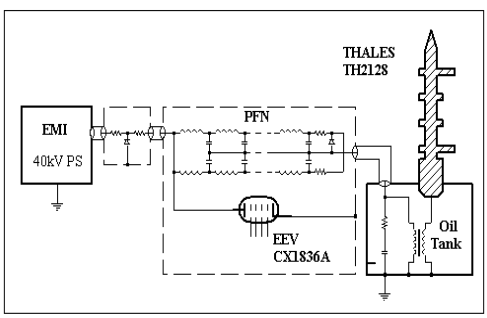

Figure 1: Modulator power circuitry.

The main elements are a 40-kV, 30-kJ/s Lambda-EMI power supply, a 2×8-cell PFN, an EEV thyratron switch, and a 15.3:1 step-up pulse transformer (PT). The charging supply charges the PFN capacitors to up to 40 kV (normal operational voltage is 34 to 36 kV), and then the thyratron switch discharges the PFN into the matched 4-Ω reflected load of the klystron cathode. The process then repeats at a 30 p.p.s. rate. The modulator has a fairly standard design and has been presented at various particle accelerator and power modulator conferences [1- 3].

HIGH-VOLTAGE CABLES

Cable Configuration

The Lambda-EMI PSs have been installed in five operational linac modulators between March 1999 and April 2000. Old PFNs have been utilized in the new modulator design. In addition to the PSs, a copper box with a PS protection circuit (PSPC) consisting of two resistors and a diode stack was placed between the PFN box and the PS (see Fig. 1).

The PS and the PSPC were connected to each other by 18 feet of high-voltage cable (Dielectric Science, model 2060). The PSPC and the PFN were connected by 10 feet of the same cable. Both cables were terminated at the ends with connectors designed by the manufacturer of the PSs (Fig. 2).

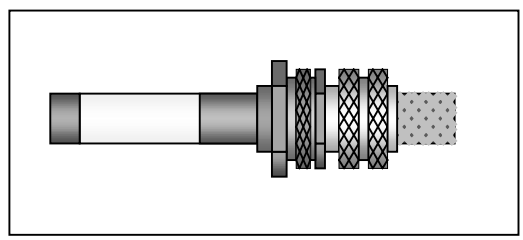

Figure 2: High-voltage cable termination.

Cable Failures

Since the first PS with the PSPC and the cables were installed in 1999, we have experienced 24 connector failures. Failure distribution over the years is presented in Fig. 3.

* Work supported by U.S. Department of Energy, Office of Basic Energy Sciences, under Contract No. W-31-109-ENG-38.
# cours@aps.anl.gov

THE RF-SYSTEM FOR A HIGH CURRENT RFQ AT IHEP

Zhang Zonghua, Qiao Jimin, Li Jian, Xu Xinan,
IHEP, Institute of High Energy Physics, Beijing100039, China

Abstract

The R&D of a high current proton RFQ is one of the most important research tasks of the Accelerator Driven Sub-critical system (ADS) basic research project. In preliminary research phase, the 352.2MHz RF system will be operated in pulse mode. CERN kindly provided IHEP with some RF equipment. Because the given RF system was used for CW operation at CERN before, to apply them to our pulse mode operation, some modifications and improvements are necessary. We have made some indispensable assemblies, and also did some tests and commissioning of every sub-system. At present, the initial high power conditioning of the klystron is carried out. A description of RF power system is given, in particularly, the performance of HV power supply, thyratron crowbar and capacitors, hard tube modulator and its control electronics, and klystron power conditioning are presented.

INTRODUCTION

The programme of building our RF power system, in brief, includes two phases--the 1st phase is to modify CERN LEP / RF equipment and to install a RF power test stand of our own for pulse mode operation. That is, klystron amplifier is directly connected to dummy load and meanwhile, R&D of long pulse hard tube modulator for klystron TH2089 is carried out. The 2nd Phase is fabrication of RF power transmission and distribution system from the klystron amplifier to the RFQ cavity; at last, we will perform RFQ power delivering and conditioning. Design features and parameters of RF system are shown in Table 1. The picture of RF power test stand can be seen in Fig. 1.

Table 1: Design features and parameters

Frequency	352.209MHz
Pulsed output RF power	1 MW max.
Waveguide system	WR2300
Klystron cathode voltage	95 kV max.
Klystron modulation anode voltage	62 kV to 0

Figure 1: Panorama picture of our RF power test stand.

HV POWER SUPPLY

General Layout

The power supply of a klystron is a 100kV, 20A power converter. It consists of four basic units: step-down transformers TR1 and TR2 (10 / 1 kV), a thyristor AC line controller and its electronics, high voltage transformers TR3 and TR4 (1 / 52 kV), diode rectifier and the filter chokes unit.

Step-down Transformers

Original HV power supply at CERN was fed from the 18 kV, 50 Hz, three-phase mains, but in China the mains feeding voltage is 10kV, therefore we specially redesigned and manufactured the step-down transformer unit in China to match CERN LEP power supply equipment. The primaries of the two step-down transformers TR1 and TR2 are fed from the 10kV, 50Hz, three-phase mains. The secondary output voltage of each transformer is 1kV line-to-line. The two transformer units are housed in one tank and are immersed in mineral oil. They are air natural / oil natural cooled. The winding configuration of the two step-down transformers is extended delta / star, so their secondaries can form phase-shift of 30 degrees between TR1 and TR2. A twelve-phase system at the HV DC output terminals is obtained. This can help to reduce the DC output ripple. The ripple of the whole power supply is no more than 1%.

Vector group of TR1 is dyn 11.5, and TR2's is dyn 0.5. That means, the phase-shift of the TR1 secondary voltage with respect to the feeding mains is +15 degrees, and the TR2's is –15 degrees. Thus, the required phase-shift of 30 degrees between TR1 and TR2 is obtained. The two transformers are designed symmetrically. It can limit the difference between the two halves of the converter and minimize sub-harmonic generation. Under the acceptance test, the phase-shift between TR1 and TR2 is 30.03 degrees. The design allowable tolerance of phase shift is 30 ± 0.1 degrees. So the result of the acceptance test is satisfying.

Thyristor AC Line Controller

The power converter can provide 0 to 100kV continuously variable output voltage. This is realized by controlling firing angle of the thyristors of the thyristor AC line controller. The different firing angle corresponds to the different current in each branch of the thyristors. The input voltage of the thyristor AC line controller is fixed at 1kV, and the output voltage can be adjusted from

A HIGH-RESOLUTION S-BAND DOWN-CONVERTING DIGITAL PHASE DETECTOR FOR SASE FEL USE

A.E. Grelick, N.D. Arnold, J. Carwardine, N.P. DiMonte, A. Nassiri, T.L. Smith,
Argonne National Laboratory, Argonne, IL 60439, USA

Abstract

Each of the rf phase detectors in the Advanced Photon Source linac [1] consists of a module that down converts from S-band to 20 MHz followed by an analog I/Q detector. Phase is calculated from one digitized sample per pulse each of I and Q. The resulting data have excellent long-term stability but are noisy enough so that a number of samples must be averaged to get a usable reading. The more recent requirement to support a self-amplified spontaneous emission (SASE) free-electron laser (FEL) has presented the need to accurately resolve the relative phase of a single pulse. We replaced analog detection with digital sampling and replaced internal intermediate frequency (IF) reference oscillators with a lower-noise external oscillator in order to control the two largest components of noise. The implementation of a central, ultra-low-noise reference oscillator and a distribution system capable of maintaining the low phase noise is described, together with the results obtained to date. The principal remaining technical issue is determining the processing power required as a function of measurement channels per processor, measured pulse repetition rate, intrapulse data bandwidth, and digital filter characteristics. The options and tradeoffs involved and the present status are discussed.

DEFINITION OF PROBLEM

Existing System and Limitations

The existing LANL-designed linac phase detectors utilize down conversion from 2856 MHz to 20 MHz (Downconverter VXI Module), followed by ovenized analog I and Q detectors that produce one 12-bit digitized sample per pulse for each of the I and Q waveforms (Vector Detector 2 slot VXI module). Software in the input/output controller (IOC) performs a rectangular-to-polar conversion on the data samples, extracting phase and suppressing amplitude. Excellent long-term stability has been achieved. However, these detectors have exhibited over one degree of noise on the measurement.

Requirements for Improved Performance

The more recent requirement to support a SASE FEL [2] has presented the need to accurately resolve the relative phase of a single pulse. The following requirements have been determined as goals for upgrade efforts.

- Compatibility with existing, VXI-based, down-converting (to 20 MHz) hardware
- Resolution of ≤ 0.1 degree rms based on single-pulse data (without averaging multiple pulses)
- Capability of supporting up to four measurements/subsystem in the operational environment
- Operational Environment:

Pulse rep. freq.	30 Hz max
Sampled pulse width	1.3 μs max
Intrapulse data bandwidth	10 MHz

DIGITAL CONCEPT AND EXPERIMENTS

An internal APS presentation [3] identified phase detection as one of a number of applications that could potentially benefit from cost-effective performance improvements associated with the use of digital signal processing (DSP).

In order to maximize the pulse envelope bandwidth, the existing design employs minimal filtering of the IF carrier. DSP easily incorporates high performance filters that could reduce carrier noise. Newly announced sampling modules using state-of-the-art flash analog-to-digital converters that could support the desired 80-MHz sampling rate were identified. DSP would allow acquisition of the phase waveform of the portion of interest of a complete pulse, which could then be averaged in different ways for different purposes. For instance, one point in a pulse could be averaged over a number of pulses to get an extremely steady phase value for screen display and long-term auto phase correction. At the same time, the entire portion of interest of a pulse could be averaged into a composite phase value, which would have low enough effective noise to be effectively compared with the equivalent value for an adjacent pulse.

A frequency quadrupler was constructed and experiments were performed comparing digital sampling to the existing analog system. A key finding from the initial experiments was that the phase noise of the 20-MHz IF reference oscillator, used by the Downconverter Module, constitutes the most critical limitation that constrains the phase measurement performance. This implementation is especially sensitive since the approximately 143X down conversion adds phase noise that is 43 dB greater than the reference oscillator phase noise to both the down-converted signal and the down-converted 2856-MHz reference. Furthermore, the digitally sampled data is degraded even more than the analog data when the noise level is as great as that of the existing system.

ULTRA-LOW-NOISE OSCILLATOR

An ultra-low-noise oscillator, from the Wenzel Associates ULN series, has been procured. This oscillator

THE RF-STATION INTERLOCK FOR THE EUROPEAN X-RAY LASER

T. Grevsmühl, S. Choroba, P. Duval, O. Hensler, J. Kahl, F.-R. Kaiser, A. Kretzschmann, H. Leich, K. Rehlich, U.Schwendicke, S. Simrock, S. Weisse, R. Wenndorff, DESY, Germany

Abstract

The RF-station interlock for the European X-ray laser will be based on a 19"- 3U crate incorporating a controller with the 32-bit RISC NIOS-processor (ALTERA). The main task of the interlock system is to guarantee safety of personnel and prevent any damage from the components of the RF station and connected cavities. The interlock system must also guarantee a maximum time of operation of the RF stations which implies the implementation of self diagnostics and repair strategies on a module basis. Additional tasks are: collection and temporary storage of status information of the individual channels of the interlock system, transfer of this information to the control system, slow control functions (e.g. HV setting and monitoring) and control of inputs and outputs from and to other subsystems. In this paper we present the implementation using an ALTERA-FPGA running a 32-bit RISC NIOS-processor. Connection to the accelerator main control is provided by Ethernet using BSD-style socket routines based on ALTERA's plugs-library. The layout of the system is presented and first hardware components are shown.

INTRODUCTION

The RF system for the European XFEL consists of 35 RF stations supplying RF power at 1.3GHz for the superconducting cavities of the linear accelerator of the XFEL [1]. Each RF station generates RF pulses up to 10MW at a pulse duration up to 1.5ms and a repetition rate up to 10Hz. A station consists of a klystron, pulse transformer, pulsed high voltage power supply, a low level RF system, auxiliary power supplies and an interlock system [2]. A simplified view is shown Figure 1. The pulsed high voltage power supplies will be installed in a separate hall above ground whereas all other components will be installed in the accelerator tunnel under ground near to the cavities. Connection between the components in the hall and in the tunnel is accomplished by high voltage pulse cables and control and interlock connections. The main task of the interlock system is the protection of the different subsystems of the RF stations and of the components connected to the station. In addition it provides slow control functions for the subsystems. Since the interlock system is installed in the accelerator tunnel, where no access is allowed during beam operation, the interlock system has to provide monitoring functions, allowing the localization of failures of the RF station remotely which sets the service personnel in a position to exchange broken subunits quickly during a scheduled maintenance time. In addition all monitored signals will be transferred to the accelerator main control system, where correlations between accelerator and RF station operation can be determined. The interlock system is a modular system so that malfunctioning interlock boards can be exchanged without renewing a complete system.

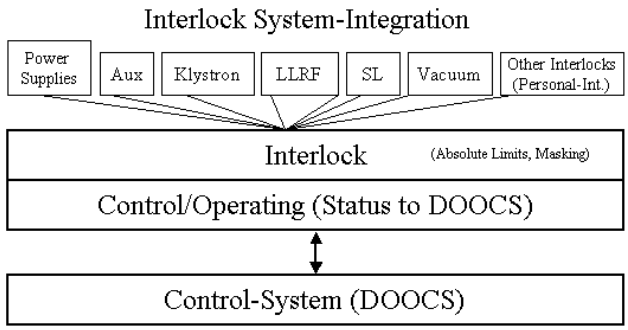

Figure 1 : RF-Station components (simplified).

REQUIREMENTS

To serve its main task the interlock system has to deal with 3 types of errors:

-hard component failures (non-reversible hardware mal-function like broken cables, damaged contacts, dead sensors, ...)
-soft errors (e.g. sparks in the klystron or wave guide system, temperature above a threshold, water-flow...)
-error conditions caused by transient noise from the RF station itself (caused by the pulsed power operation)

Errors should be treated with two types of thresholds and channel masking.

Absolute max./min. thresholds: any violation of these thresholds will force the shutdown of one ore more subsystems or of all components of the RF station.

Programmable (soft) thresholds: a violation of these boundaries will generate an alarm message to the control system. Soft thresholds are only available for analog input channels.

For any individual input channel a mask function should be implemented which allows to exclude this channel from all of the interlock functions. Masking operations via the control system are secured by password mechanism and must cause an entry into a log file [3,4].

Besides additional tasks like setting operational parameters, collecting status and diagnostic information and providing it to the main control system, a system self test at power-up has to ensure the proper operation of all interlock components. This is also true for a test during normal operation. In case of power-down status-information should be saved for diagnostics. The RF-

THE CEBAF RF SEPARATOR SYSTEM UPGRADE*

C. Hovater#, M. Augustine, A. Guerra, Rick Nelson, R. Terrel, and M. Wissmann,
Jefferson Lab, Newport News, VA, USA

Abstract

The CEBAF accelerator uses RF deflecting cavities operating at the third sub-harmonic (499 MHz) of the accelerating frequency (1497 MHz) to "kick" the electron beam to the experimental halls. The cavities operate in a TEM dipole mode incorporating mode enhancing rods to increase the cavity's transverse shunt impedance [1]. As the accelerators energy has increased from 4 GeV to 6 GeV the RF system, specifically the 1 kW solid-state amplifiers, have become problematic, operating in saturation because of the increased beam energy demands. Two years ago we began a study to look into replacement for the RF amplifiers and decided to use a commercial broadcast Inductive Output Tube (IOT) capable of 30 kW. The new RF system uses one IOT amplifier on multiple cavities as opposed to one amplifier per cavity as was originally used. In addition, the new RF system supports a proposed 12 GeV energy upgrade to CEBAF. We are currently halfway through the upgrade with three IOTs in operation and the remaining one nearly installed. This paper reports on the new RF system and the IOT performance.

INTRODUCTION

The CEBAF accelerator has been operating for 10 years steadily increasing the beam energy from 4 GeV up to 5.75 GeV. In that time the original RF amplifiers used to separate the electron beam have been pushed to their operational limit. This has resulted in increased system down time. Three years ago the RF group began an investigation to find a replacement power amplifier for the RF system. An additional requirement was to make the new amplifier compatible with the CEBAF energy upgrade. We settled on what is known as an Inductive Output Tube (IOT). The concept of the IOT was first proposed in the late 1930's – early 1940's but it was only in the last 20 years that they have become commercialized, primarily used in the broadcast industry [2, 3]. The system will ultimately incorporate four IOTs operating from a single high voltage power supply. The IOT and power supply is completely autonomous from the RF controls and self protected. The RF control system for the separator RF cavities has also changed. Where as before we had one cavity/amplifier, we now have multiple cavities/amplifier and control the field on the vector sum. To support this RF system we have incorporated inline high power coaxial phase shifters for system alignment. The existing LLRF controls have been modified to support these changes. Three of the IOTs are now operational and the system has been very reliable.

*This work was supported by DOE contract No. DE-AC05-84ER40150.
#hovater@jlab.org

RF SYSTEM

The CEBAF accelerator has the capability of extracting any one of the 5 passes and sending it to an experimental hall [4]. Each pass has a bank of RF separator cavities that can kick the beam out. The three highest energy passes all are powered by an individual IOT. While the IOT is capable of 30 kW we have limited them to 10 kW. The lowest energy passes (1 and 2) share an IOT in a slave configuration. Figure 1 shows the RF system for pass 5, the highest energy pass. A single IOT output is split 3 ways and then drives the three cavities. In two of the legs, electronically controlled high power coaxial phase shifters have been installed for phase adjustments. In addition, the RF cables from the splitter to the cavity coupler were meticulously measured and trimmed to within ~ two degrees of one another. In a similar fashion the cables for the cavities' transmitted powers have been measured and cut to a similar accuracy. Field control is maintained by summing the transmitted signals and controlling on the average. Cavity control is presently provided by the original analog CEBAF LLRF system, though this will change in the near future with the addition of a new digital controller [5].

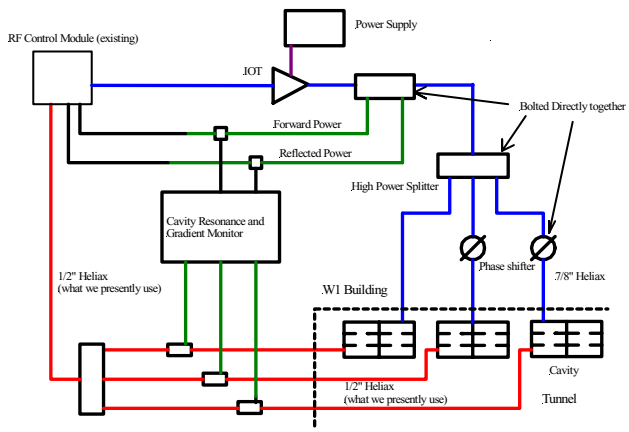

Figure 1: 5th Pass Separator RF System.

First and Second Pass

The first and second passes share a single IOT. Since required RF power goes as the square of the beam energy this can be implemented fairly easily. The energy essentially doubles between pass one and two thereby a 6 dB coupler is needed to divide the output of the IOT. For 6 Gev operations pass one needs approximately 400 watts so pass two would need 1600 watts. Figure 2 shows the First and second passes with one IOT. A coaxial jumper will allow one to choose to operate both passes or just one pass. The RF from the pass not in operation is then fed to

TUNING OF EXTERNAL Q AND PHASE FOR THE CAVITIES OF A SUPERCONDUCTING LINEAR ACCELERATOR

V.Katalev, S.Choroba, DESY, Germany

Abstract

The RF power required for a certain gradient of a superconducting cavity depends on the beam current and coupling between the cavity and waveguide. The coupling with the cavity may be changed by variation of Q_{ext}. Different devices can be used to adjust Q_{ext} or phase. In this paper three stub and E-H tuners are compared and their usability for the RF power distribution system for the superconducting accelerator of the European X-Ray Laser and the TESLA linear collider is considered. The tuners were analyzed by using the scattering matrix. Advantages and limitations of the devices are presented.

INTRODUCTION

The linear accelerators of the European XFEL and TESLA linear collider make use of the same type of superconducting cavities [1],[2]. The cavities are operated at a frequency of 1.3 GHz and an unloaded quality factor of Q_0>10^9.The accelerating gradient is 23.4 MV/m with a beam current of 9.5 mA for the TESLA linear colder and 22.9 MV/m with 5 mA of a beam current for the XFEL.

The power required by the cavity is 122 kW for the XFEL and 231 kW for TESLA with a pulse duration of 1.5 ms at a repetition rate of 10 Hz and 5 Hz respectively. To accelerate the beam with optimum consumption of RF power it is necessary to change the loaded quality factor of the cavity within several units of 10^6. With constant coupling between the cavity and the waveguide this can be achieved by changing the external losses namely by changing of Q_{ext}.

The cavities are connected to the RF power source, a klystron, by a waveguide distributing system with a circulator and a fixed dummy load in front of each cavity. In order to change the external losses of the cavity it is necessary to use an additional impedance transformer between the cavity and the circulator like a three stub tuner or an E-H tuner.

RF POWER FOR BEAM ACCELERATION

Let us consider the case of cavity operation at resonance and beam acceleration on-crest. It is possible to neglect power dissipation in the walls of the cavity in comparison with losses in the external load because Q_0>> Q_{ext}. The required RF power [3] for filling of the superconducting cavity with energy up to the required accelerating voltage V_{c0} is

$$P_{g0} = \frac{V_{c0}^2}{4\frac{R}{Q_0}Q_{ext}} \frac{1}{(1-e^{-\frac{t_{inj}}{\tau}})^2}$$

With R/Q_0 – normalized shunt impedance for a linac
τ = $Q_{ext}/\pi f$ time constant of the cavity
t_{inj} – time of beam injection

In order to accelerate the DC beam current I_b the RF power

$$P_{gb} = \frac{V_{c0}^2}{4\frac{R}{Q_0}Q_{ext}}\left(1+\frac{I_b\frac{R}{Q_0}Q_{ext}}{V_{c0}}\right)^2$$

for flattop operation is required. It is the well-known formula for the power of a generator connected to a cavity with heavy beam loading [4].

Fig. 1 shows the RF power for the XFEL and TESLA cavity P_g as a function of the external quality factor Q_{ext}. The minimum RF power for cavity filling or for beam acceleration has a minimum for different conditions. For cavity filling the condition is

$$\frac{t_{inj}\pi f}{Q_{ext}^0} = 1.256,$$

whereas for beam accelerating it is

$$Q_{ext}^b = \frac{V_{c0}}{I_b\frac{R}{Q_0}}$$

Typically Qext is chosen between these two minima.

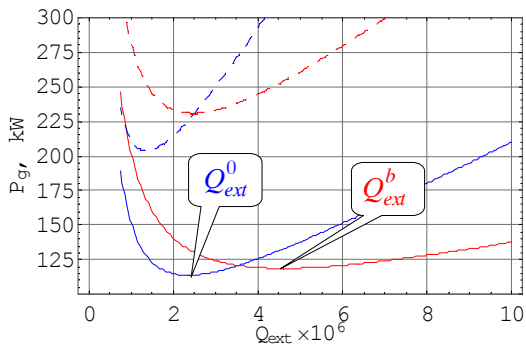

Figure 1: Cavity forward power P_{g0} (blue) and P_{gb} (red) for a XFEL cavity with gradient E=22.9 MV/m, I_b=5 mA and t_{inj}=720 μs. TESLA cavity – E=23.4 MV/m, I_b=9.5 mA t_{inj}=420 μs (dashed).

The conditions of minimum RF power for cavity filling and beam acceleration are fulfilled with $Q_{ext}^0 = 2.36\times10^6$ and $Q_{ext}^b = 4.59\times10^6$ in the XFEL case and with $Q_{ext}^0 = 1.36\times10^6$ and $Q_{ext}^b = 2.47\times10^6$ in the TESLA case, respectively. For the case of operation at a reduced cavity gradient one has to reduce the external quality factor in order to operate at minimum of RF power consumption . In the other case of a reduced beam current one might consider increasing Q_{ext} to meet the minimum condition for Q_{ext}^b. But one has to observe that by increasing Q_{ext} the RF power for cavity filling would increase dramatically (see Fig. 1). Therefore the recommended Q_{ext} value are in the range from 2.3 up to

RF REFERENCE DISTRIBUTION SYSTEM FOR THE J-PARC LINAC

T. Kobayashi†, E. Chishiro, JAERI, Tokai, Naka, Ibaraki, Japan
S. Anami, S. Yamaguchi, S. Michizono, KEK, Tsukuba, Ibaraki, Japan

Abstract

The J-PARC (Japan Proton Accelerator Research Complex) linac, which is 300 m long, consists of a 324-MHz accelerating section of the upstream part and a 972-MHz section of the downstream part. In the klystron gallery, a total of about 60 RF source control stations will drive the klystrons and solid-state amplifiers.

The error of the accelerating field must be within ±1° in phase and ±1% in amplitude. Thus, high phase stability is required as an RF reference for all of the low-level RF control systems and the beam-monitor systems. The RF reference (12 MHz) is distributed to all stations optically. Low-jitter E/O and O/E with temperature stabilizers were developed. The reference is optically amplified, divided into 17 transfer lines, and delivered through PSOF (phase-stabilized optical fiber), the temperature of which is stabilized by cooling water. Each of the transmitted signals is divided more into 4 signals by an optical coupler.

Our objective concerning the phase stability of the reference aims at less than ±0.3° at a frequency of 972 MHz.

INTRODUCTION

J-PARC accelerators [1] are now under construction at the JAERI Tokai site. The linac of the J-PARC, which is about 300 m long, provides 181-MeV (400-MeV in the future) proton beam to the 3-GeV, 1-MW rapid-cycling synchrotron (RCS). For this linac, the RF source will power 20 accelerating cavity modules (an RFQ, 3 DTLs and 16 SDTL modules) operated at a frequency of 324 MHz, and 21 ACS cavities operated at a frequency of 972 MHz (Refer Fig. 1). Furthermore, solid-state amplifiers will drive the buncher, chopper and debuncher cavities. In addition to the RF systems, the beam-monitor systems, the magnet power supply, and so on, are installed in the klystron gallery. Totally, 60 arrays of 12 EIA-standard 19-inch racks will be installed as the control stations for these systems over the whole area of the klystron gallery. An RF reference signal must be distributed to all of these control stations.

Because the momentum spread (Δp/p) of the RCS injection beam is required to be within 0.1%, the RF sources must maintain the correct accelerating field within an amplitude error of ±1% and a phase error of ±1°. Therefore, the RF reference signal should be more highly stable. Our objective for the RF reference aims at within ±0.3° at a 972-MHz frequency for phase stability.

On account of pulse operation of 500-μs beam duration and 50-Hz repetition, the timing control signals must be distributed in analogy with the RF reference.

This paper presents the final design of the RF reference distribution system in detail, including the timing reference distribution.

RF REFERENCE DISTRIBUTION LINE

A block diagram of the RF reference distribution system is shown in Fig. 1. The 12-MHz RF reference is distributed to about 60 low-level RF (LLRF) control systems of klystron and solid-state amplifier stations (RFQ,

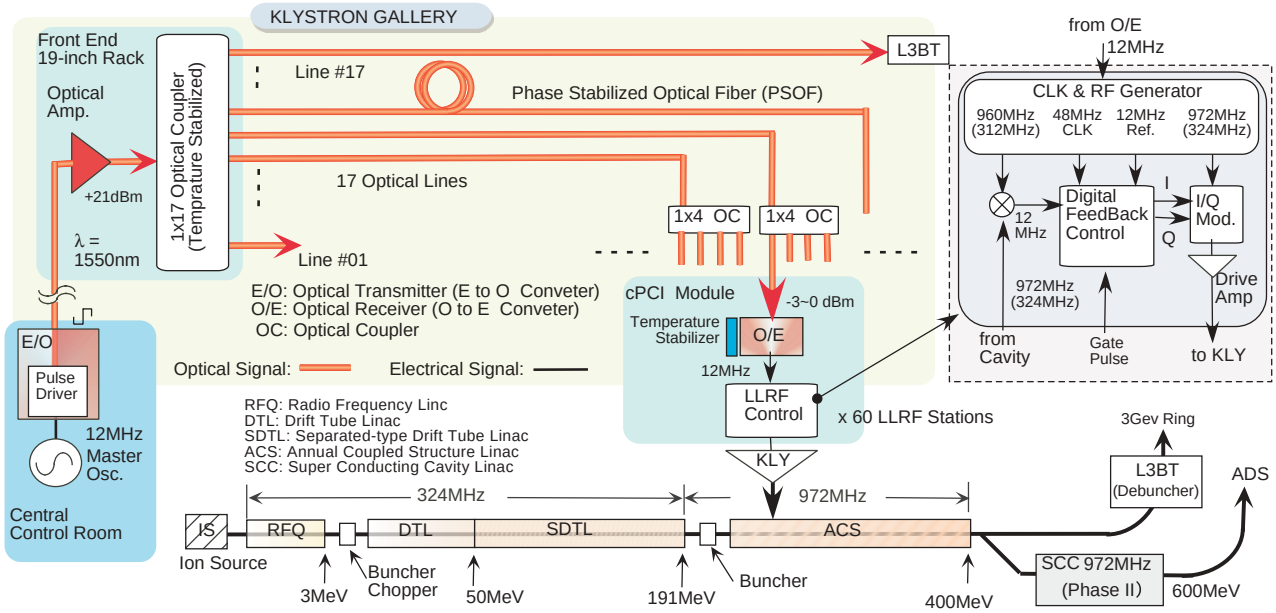

Figure 1: Block diagram of the RF reference distribution system.

†tetsuya.kobayashi@j-parc.jp

QUASI-OPTICAL COMPONENTS FOR FUTURE LINEAR COLLIDERS

S. Kuzikov, G. G. Denisov, M.Yu. Smelyov, Institute of Applied Physics, Russian Academy of Sciences, Nizhniy Novgorod, Russia
J.L. Hirshfield, Omega-P, Inc., New Haven, Connecticut, USA

Abstract

This paper presents a concept of the quasi-optical RF system for future Ka-band electron-positron linear collider. According to this concept a quasi-optical Delay Line Distribution System (DLDS) is considered. The DLDS is based on oversized waveguides. In such waveguides the so-called image multiplication phenomena are used for power launching, extracting, combining, and splitting of waves. Recent low power tests of mode launchers and other DLDS components are discussed.

INTRODUCTION

The DLDS concept is considered as one of prospect solutions for feeding of high-gradient accelerators at 11.424 GHz [1-2]. According to the projected schemes the DLDS is based on relatively oversized delay lines operated with one or several modes and mode launchers completely or partially constructed on the base of single-mode waveguides. Scaling of the mentioned projects to Ka-band seems to be not acceptable because of higher Ohmic attenuation as well as bigger RF power density, which causes a threat of breakdown. More natural way is to use pure quasi-optical solutions in the design of each DLDS component.

MODE LAUNCHERS

A key component of any DLDS project is a mode launcher, which allows feeding consequently different acceleration sections by means of proper setting the phases of RF pulses from different amplifiers. In the scheme, shown in Fig. 1, the mode launcher has four input channels and the same number of output channels providing four times power gaining. The delay lines behind the mode launcher are assumed to be oversized circular cross-section waveguides operated with axis-symmetrical TE_{01} mode.

We considered two possible versions of the mode launcher both based on image multiplication phenomena in an oversized waveguide [3-6].

Mode Launcher Based on Rectangular Cross-Section Waveguide

In this version (Fig. 2) the mode launcher is shaped of a smooth oversized (waveguide size is a) rectangular waveguide, where image multiplication occurs at one coordinate only. Four TE_{01} modes at the input of rectangular waveguide are combined into one of four output channels. The position of the resulted channel depends on the mutual phases at the input. The required length of the waveguide equals to a^2/λ.

The mode launcher was calculated using Kirhgof's approach, and results were published in paper [3]. According to these results the wider waveguide the higher efficiency of the launcher. For example, at 34 GHz, width a=120 mm, and length L=1600 mm provide 99% efficiency of the power summarizing.

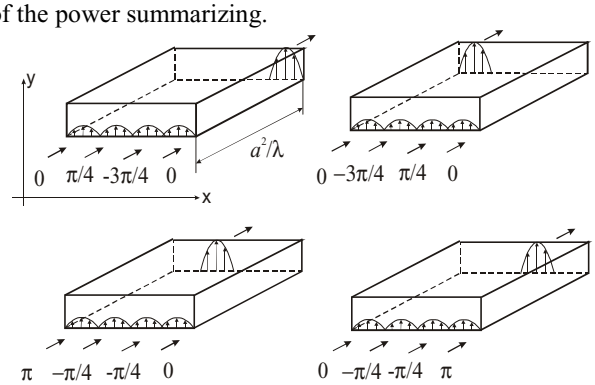

Figure 1: Mode launcher based on rectangular cross-section waveguide (principal scheme).

Figure 2: Mode launcher based on rectangular cross-section waveguide (photograph of the prototype).

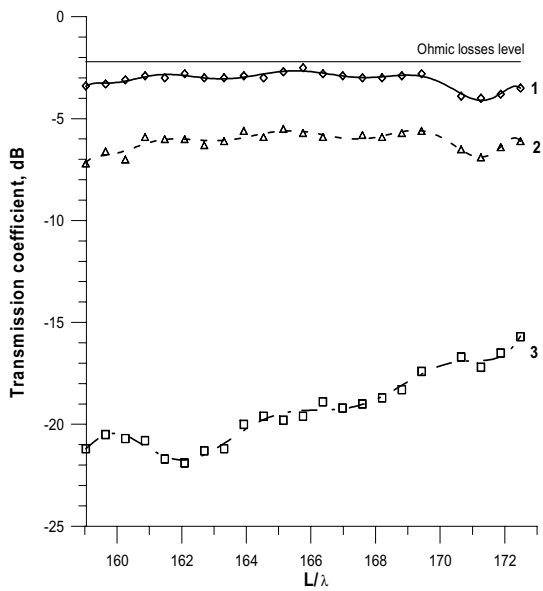

Figure 3: Measurements of mode launcher efficienc when incident wave is launched into a channel near the wall.

MOSCOW MESON FACTORY DTL RF SYSTEM UPGRADE

A.I.Kvasha•, Institute for nuclear research RAS, Moscow

Abstract

The last paper, devoted to description of the first part (DTL) RF system of Moscow Meson Factory upgrade, was published in Proceedings of PAC95 Conference in Dallas [1]. Since then some new works, directed at improvement of reliability and efficiency of the RF system, were carried out. Among them there are a new powerful pulse triode "Katran" installed in the output RF power amplifiers (PA) of three channels, modifications of the anode modulator control circuit and crow-bar system, new additional RF channel for RF supply of RFQ and some alterations in placing of the anode modulator equipment, decreasing a level of interference's at crow-bar circuits. Some new, checked at MMF RF channels, ideas concerning of PA tuning are of interest for people working in this sphere of activity.

INTRODUCTION

Developed more than 30 years ago the DTL RF system equipment of the MMF (frequency 198,2 МГц, RF pulse length - 400 μs, repetition rate - 50 Гц, pulse RF power - up to 2,5 MW, amount of RF channels - 6, including RFQ), has successfully operated for 16 years. Since the last information [1] the RF system has been in operation about 18 thousand hours. During all this time the continuous work, directed at increasing of reliability and efficiency of the RF system has been fulfilled. Some results of this activity have found the reflection in papers [2,3]. Moreover, due to improvement of the water quality in the powerful vacuum tubes cooling system, realization of preventive works and more strict maintenance of the exploitation conditions it got possible to appreciably increase powerful vacuum tubes service life. So at service life of 1000 hours, guaranteed by the manufacturer of powerful modulator (GMI-44A) and RF amplifiers (GI-51A and GI-54A) vacuum tubes, it achieves now about 5000 hours for triode GI-54A, installed in the RF output power amplifier (PA), about 6000 for tetrode GI-51A, installed in the PA driver, and about 7000 for modulator tube GMI-44A. A few vacuum tubes were in operation more than 16 thousand hours. It is necessary to have in view, that these data concern to the vacuum tubes that were manufactured 20-25 years ago.

Each RF channel consists of two main parts - the four-stage RF amplifier and two pulse modulators.

PULSE MODULATORS

There are two pulse modulators in each RF channel. The first modulator provides anode supply for the first two RF amplifiers vacuum tubes; the second one provides anode supply of the last two powerful RF amplifier vacuum tubes GI-51A and GI-54A. The first modulator also serves as a driver for the more powerful second modulator. In both anode modulators were recently used a few vacuum tubes for driving and control of output pulse voltage, because stabilization of RF amplitude voltage in the DTL tank is realized by means of the modulator pulse amplitude control (see fig.1).

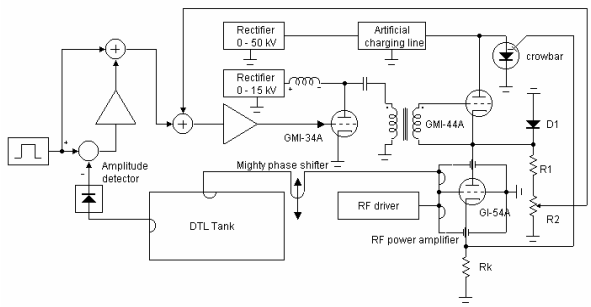

Figure 1: Common view of the DTL RF channel

During the last modernization of the pulse power supply systems were developed and established transistor pulse drivers (TPD) in all modulators. Inputting of TPD has allowed removing six vacuum tubes in each RF channel and appreciably increasing reliability of modulators operation. Besides, installation of the TPD has allowed realizing rather simply the negative feedback path around of the anode modulator (see Fig.1). The feedback increased output pulse stability and essentially improved frequency response of the modulator, which, in turn, has resulted in improvement static and dynamic characteristics of RF amplitude stabilization system in the tank. So now there are only seven vacuum tubes in every RF channel - four in RF amplifiers and three in two modulators.

Structure of the artificial charging line (ACL), as a storage device for the powerful anode modulator vacuum tube GMI-44A, was also changed so that during breakdowns in load of ACL, accompanied by crowbar operation, overcharge of ACL took place. In that way, fast (about 400μs) and reliable lock-out of crowbar thyristors is achieved. This is particularly important in a case of using the induction regulators, demanding of constant load for their operation, in alternating-current high voltage circuit. Obviously, the faster the thyristors are closed, the less load perturbations an induction regulator "fills" during crowbar operation. Besides, some useful rearrangements of high voltage equipment were performed. In particular, diode network D1 (see fig.1) was carried out from ACL chamber into the GMI-44A case. That resulted in the strong shortening of the HV

• kvasha@inr.ru

ELECTROMAGNETIC DESIGN OF NEW RF POWER COUPLERS FOR THE S-DALINAC

M. Kunze#, W.F.O. Müller, T. Weiland, TEMF, TU Darmstadt, Darmstadt, Germany
M. Brunken, H.-D. Gräf, A. Richter, IKP, TU Darmstadt, Darmstadt, Germany

Abstract

The electromagnetic design and design results of new rf waveguide-coax input power couplers for the S-DALINAC are presented. Special consideration is spent on the minimization of the transverse electromagnetic field on the beam axis which would cause an emittance growth of the electron beam.

INTRODUCTION

The superconducting Darmstadt electron linear accelerator (S-DALINAC) is a recirculating machine operating at 3 GHz [1]. Since its first operation in 1987 the S-DALINAC has continuously be improved. Presently, the third generation of components for this accelerator is under development. To allow future nuclear physics experiments with cw beam currents from 150 to 250 µA at electron energies of 14 MeV behind the injector linac rf power of up to 2 kW has to be transferred to the electron beam. The present coax-coax input power couplers at the S-DALINAC with variable coupling are limited to a maximum power of 500 W. To reach power operation up to 2 kW while keeping the emittance growth of the electron beam small waveguide power couplers [2, 3] with minimized transverse kick should be used in the accelerator upgrade.

Recently, the electromagnetic design of a single-waveguide-coax and a twin-waveguide-coax coupler, respectively, for the S-DALINAC has been published [4]. It was mentioned that the single-waveguide-coax coupler allows for a more compact design whereas the rf behavior in terms of S-parameters is similar to that of the twin-waveguide-coax coupler.

In this paper a modified design of the twin-waveguide-coax coupler and its electromagnetic design procedure is presented. It is shown that a compact design similar to that of the single-waveguide-coax coupler is possible.

COUPLER DESIGN

Fig. 1 shows the geometry of the twin-waveguide coupler and the electric field patterns of the two lowest coaxial (TEM, H_{11}) and circular waveguide modes (TM_{01}, TE_{11}), respectively. At the 3 GHz operating frequency of the S-DALINAC the TEM mode and the H_{11} mode can propagate on the coaxial line while the TM_{01} and the TE_{11} mode of the circular waveguide (beam tube in Fig.1) are still evanescent modes. At transition 2 the TE_{11} mode with its asymmetric field distribution is mainly excited by the H_{11} mode. Since the asymmetric electromagnetic field of the TE_{11} mode generates an emittance growth, the excitation of the H_{11} mode must be minimized at transition 1.

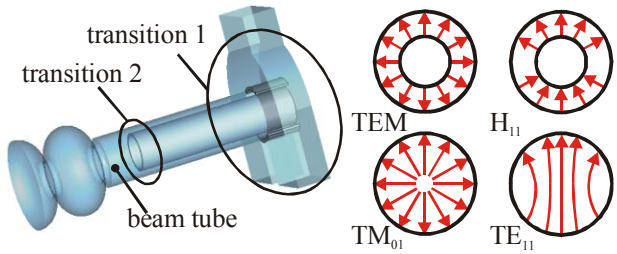

Figure 1: The twin-waveguide coupler and the electric field patterns of the two lowest coaxial modes (TEM, H_{11}) and of the circular waveguide modes (TM_{01}, TE_{11}).

In Fig. 2a the geometry of the twin-waveguide-to-coax transition (transition 1 in Fig. 1) and its parameters are given. The single-waveguide-to-coax transition presented before in [4] is again given in Fig. 2b. In both designs diaphragms are used to minimize the transverse coupler kick. The suppression of the H_{11} mode can be adjusted choosing the opening angle $\varphi_1+\varphi_2$. Once the angle $\varphi_1+\varphi_2$ is chosen the power transfer from the fundamental rectangular waveguide mode H_{10} to the TEM mode of the coaxial waveguide can be maximized by adjusting the height *h* and the stub length *s* for the single-waveguide-to-coax transition and additionally the gap width *g* and the waveguide width *w* for the twin-waveguide-to-coax transition, respectively.

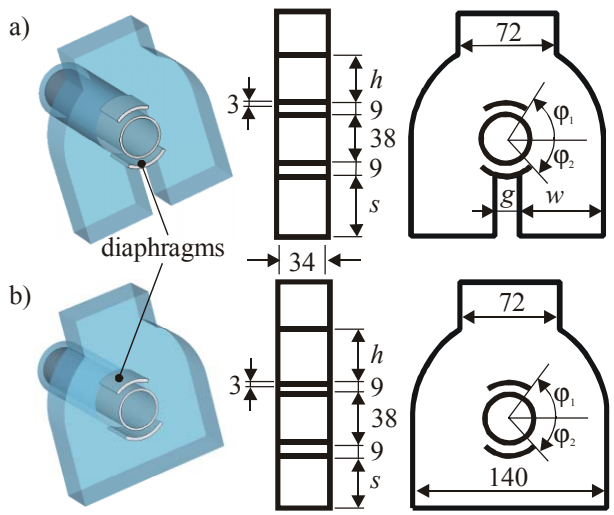

Figure 2: The twin-waveguide-to-coax (a) and the single-waveguide-to-coax (b) transition of the waveguide-to-coaxial couplers under investigation (unit of length is mm).

#kunze@temf.tu-darmstadt.de - This work is supported by the Deutsche Forschungsgemeinschaft (DFG) under contract SFB 634.

CONTROL OF THE LOW LEVEL RF SYSTEM FOR THE J-PARC LINAC

S. Anami#, E. Kadokura, S. Michizono, S. Yamaguchi, KEK, 1-1 Oho, Tsukuba, Ibaraki, 305-0801,Japan; E. Chishiro, T. Kobayashi, H. Suzuki, JAERI, 2-4 Shirakata-Shirane, Tokai, Naka, Ibaraki, 319-1195, Japan

Abstract

The J-PARC 181-Mev proton linac requires twenty-four RF systems, which operate at a 620-μs pulse width, 50-Hz repetition rate, and 324-MHz frequency. The required basic functions of the low level RF (LLRF) control system for the klystron RF source are: field control, high-power protection, analog and status monitor and klystron drive. To perform these functions a programmable logic controller (PLC) is used as the main system controller. The PLC will be locally operated by a touch panel on PLC LAN and remotely by an EPICS Operator Interface (OPI) on EPICS LAN. This paper describes the LLRF hardware configurations and the system control using the PLC.

INTRODUCTION

The RF source of the J-PARC 181-MeV proton Linac is composed of four solid-state amplifiers and twenty klystron amplifiers. In each RF source, the cavity field will be stabilized within an accuracy of ± 1% in amplitude and ± 1° in phase. This field control, which is implemented by a combination of feedback (FB) and feed-forward (FF) algorithms, is the most important key function in the low level RF (LLRF) system, and requires much of our efforts [1][2]. However, seeing from the viewpoint to control the whole LLRF system, the field control is one embedded system, all of the LLRF components, such as a high power protection unit, status and analog monitors and a klystron driver, are controlled by a system controller with interfaces for local and remote operation. We adopt a programmable logic controller (PLC) as the main system controller.

OVERVIEW OF THE LLRF SYSTEM

There are twenty-four LLRF systems corresponding to each of the solid-state and klystron amplifier stations. A block diagram of the LLRF system for the klystron station, including an interface with the EPICS control system (VME/IOC and NIM/Timing), is shown in Figure 1. The required fundamental functions for the LLRF system are: 1) generation of the accelerating RF (324 MHz) and clock (12 MHz, 48 MHz and 312 MHz) signals phase-locked with a 12-MHz optical signal provided with the rf reference distribution system [3], 2) cavity field and tuning control (cPCI/Digital FB), 3) high-power protection and RF monitor (Fast Interlock, Arc Detector and VSWR Meter), and 4) klystron drive (Analog FB, 20-dB and 40-W amplifiers).

The signal generation and the cavity field and tuning control are performed by a cPCI crate system, which is composed of a host CPU module, a control input/output module (CTRL I/O), a mixer and I/Q modulator module (MIX&I/Q-M), a DSP module attached with a FPGA mezzanine card, and an RF and clock generator module (RF&CLK). All of the LLRF hardware components which are listed in Table 1 are installed in two 19”

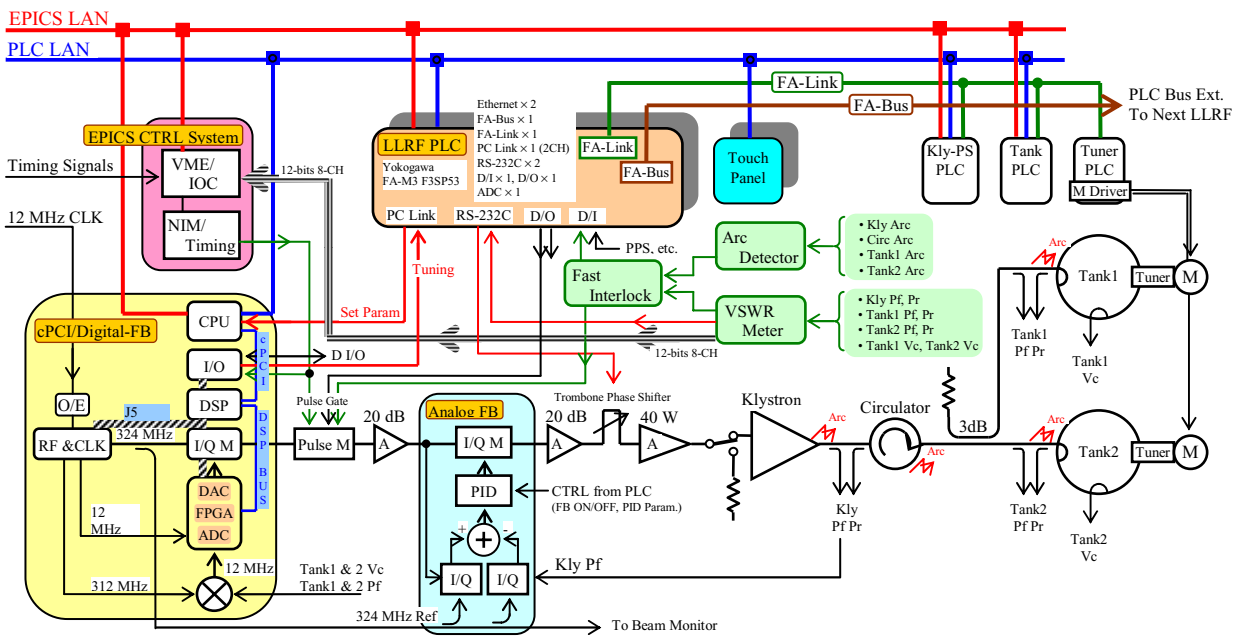

Figure 1: Block diagram of LLRF System.

#anami@post.kek.jp

DIGITAL FEEDBACK SYSTEM FOR J-PARC LINAC RF SOURCE

S. Michizono#, S. Anami, S. Yamaguchi, KEK, Tsukuba, Japan
T. Kobayashi, JAERI, Tokai, Japan

Abstract

At the proton linac of J-PARC (Japan Proton Accelerator Research Complex), an accelerating electric field stability of ±1% in amplitude and ±1° in phase is required for the RF system. In order to accomplish these requirements, a digital feedback system is adopted for flexibility of the feedback (FB) and feedforward (FF) algorism implementation. FPGAs are used for the real-time FB system. A DSP board is also utilized for data processing and communication between FPGAs and a crate control CPU (Host). The system was examined with the SDTL cavity, and satisfied the stability specification.

INTRODUCTION

Twenty klystrons (324 MHz, 3 MW) will be installed in the J-PARC linac. An RFQ, 3 DTLs and 16 SDTL modules are driven by klystrons [1]. The maximum pulse width and repetition rate are 620 μs, including the cavity build-up time, and 50 pps, respectively. Because the rf source should maintain the accelerating field within an amplitude stability of ±1% and phase stability of ±1°, a highly intelligent feedback system should be constructed. A digital feedback system using the FPGAs combined with DSPs has been developed for these requirements. The FPGAs are in charge of fast feedback for the cavities and the DSPs will be operated for data/program exchange and a slow feedback system, such as tuning the cavities. In this report, the hardware developments and performance of the feedback system are described.

FEEDBACK EQUIPMENT

The digital feedback system is installed in a compact PCI (cPCI crate). The backplane of the cPCI crate is specially designed so as to separate the ground line between digital and analog boards. The digital equipment, such as the CPU, DSP (Spectrum Signal Processing Inc. 'Barcelona', 4xTMS320C6701) and I/O boards, are located on left side of the cPCI crate, and analog boards, such as the RF&CLK (rf and clock generator) and Mixer&I/Q (mixers and I/Q modulators) boards, are installed on the right side. The RF&CLK board creates timing clock (f_{Tim}:12 MHz, f_{Trig}: 48MHz, f_{LO}: 312 MHz) and RF (f_{RF}: 324 MHz) signals synchronized with a distributed reference signal [2]. Since the accuracy of around 2 ps is required especially to the LO signal (312 MHz), the reference signal is planned to change from 12

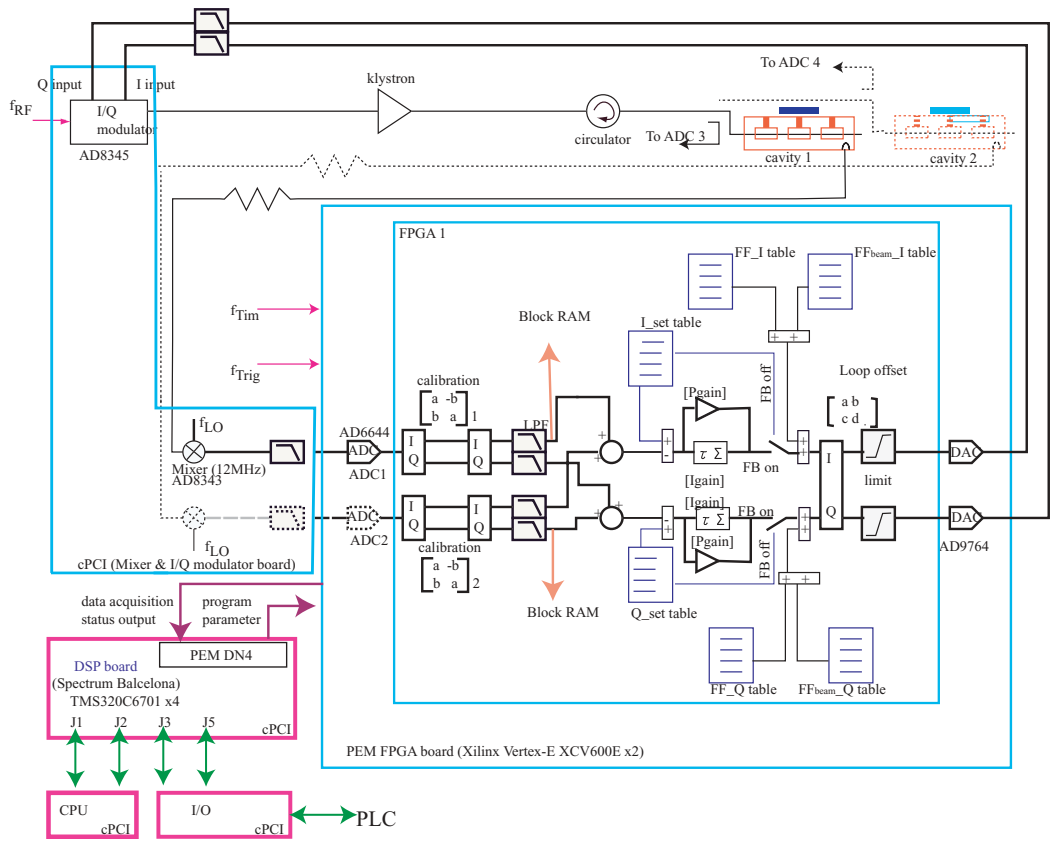

Figure 1: Schematic diagram of the digital feedback system.

#shinichiro.michizono@kek.jp

DEVELOPMENT OF C-BAND HIGH-POWER MIX-MODE RF WINDOW

S. Michizono#, T. Matsumoto, K. Nakao, T. Takenaka, S. Fukuda, KEK, Tsukuba, Japan
K. Yoshida, Mitsubishi Electric Corporation, Amagasaki, Japan

Abstract

A high-power C-band (5712 MHz) rf system (40 MW, 2 μs, 50 Hz) is under consideration for an electron-linac upgrade aimed for the super KEKB project. An rf window, which isolates the vacuum and passes rf power, is one of the most important components for the rf system. The window consists of a ceramic disk and a pill-box housing. The mix-mode rf window is designed so as to decrease the electric field on the periphery of the ceramic disk. A resonant ring has been assembled in order to examine a high-power transmission test. The window was tested up to a transmission power of 300 MW. The rf losses were also measured during rf operation.

INTRODUCTION

An upgrade of the KEKB injector linac is under consideration for the SuperKEKB project [1]. C-band rf sources (5712 MHz, 2 μs, maximum 50 MW) will be installed in the upgrade for a higher acceleration gradient of more than 40 MV/m [2]. The rf power (~40 MW) will be transmitted through an rf window and a pulse compressor, and delivered to acceleration structures. The rf window consists of an alumina ceramic disk and pill-box housing, which enables us to transmit the rf and separate the vacuum, which is one of the important components for this upgrade. A surface discharge due to electron emission at the edge of the ceramic under high rf fields results in excess surface heating, leading to punctures.

In this paper, the design of a mix-mode window [3], where the electric fields at the edge of the ceramic decrease, is described. The results of high-power tests using a resonant ring are also summarized.

DESIGN OF THE RF WINDOW

The new rf window is required to transmit rf power of 50 MW (2 μs, 50 pps). The criteria of the new C-band rf window are determined based on the electric fields of the S-band rf window. The S-band window has a long life with an MTBF of more than 100,000 hours [4] under an rf transmission of 50 MW (2856 MHz, 4 μs, 50 pps), and is reliable for long-time rf operation, even though leakage of the klystrons is one of the reasons for klystron failures. The electric field at the edge and center of the ceramic disk should be less than that of the S-band disk (84 mm in diameter and 3.2 mm in thickness). The bandwidth of the rf window should be more than 100 MHz, which is sufficiently wider than the performance of the klystron and/or the acceleration structure. The calculated values are given in Table 1. The electric fields at the edge and at the center of the ceramic are about 1.7 MV/m and 3.7 MV/m, respectively. In order to satisfy these requirements, it is necessary to enlarge the diameter of the alumina ceramic disk compared with the wavelength of the C-band, which indicates the transmission of the higher modes, such as a TM_{11} mode. By mixing the TE_{11} mode and the TM_{11} mode, lower electric fields can be accomplished, thus making a 'mix-mode window'. A high-purity alumina ceramic of HA-997 (99.7% purity, NTK Co.) having a high durability for the transmission of high power [5] has been adopted. A diameter of 78 mm and a thickness of 4 mm were chosen in order to avoid any resonant frequencies around the operation frequency (5712 MHz).

Table 1: Electric properties of the S-band rf window

Center of the ceramic	3.7 [MV/m@50MW]
Edge of the ceramic	1.7 [MV/m@50MW]
Maximum electric field on the surface of the ceramic	5.5 [MV/m@50MW]
Bandwidth (VSWR<1.2)	600 [MHz]

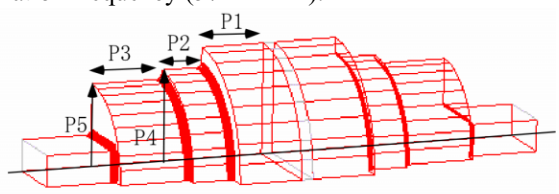

Figure 1: Schematic of the C-band window. The length of the first ring (P1), second ring (P2), third ring (P3) and inner radius of second (P4) and third ring (P5) are the parameters to be optimized.

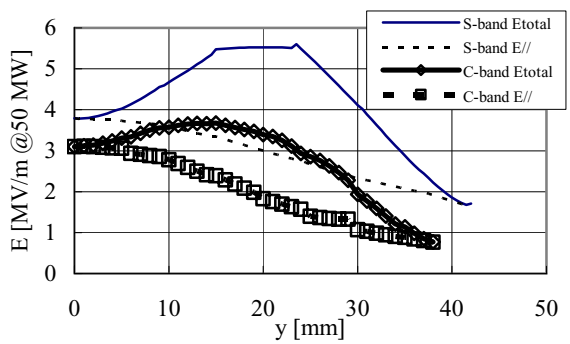

Figure 2: Electric fields on the ceramic disk calculated for C-band and present S-band rf window.

The window is constructed with a combination of three rings. Five parameters (Figure 1), which are necessary to match the two different modes in a same length, are optimized using HFSS. In order to avoid any volume resonance of TE_{012}-like and TM_{014}-like modes, the rf waves do not propagate as complete travelling waves in the ceramic disk (quasi-travelling wave). However, the

#shinichiro.michizono@kek.jp

LOW LEVEL RF INCLUDING A SOPHISTICATED PHASE CONTROL SYSTEM FOR CTF3

J. Mourier, R. Bossart, J.-M. Nonglaton, I. Syratchev and L.Tanner
CERN, Geneva, Switzerland

Abstract

CTF3 (CLIC Test Facility 3), currently under construction at CERN, is a test facility designed to demonstrate the key feasibility issues of the CLIC (Compact LInear Collider) two-beam scheme. When completed, this facility will consist of a 150 MeV linac followed by two rings for bunch-interleaving, and a test stand where 30 GHz power will be generated. In this paper, the work that has been carried out on the linac's low power RF system is described. This includes, in particular, a sophisticated phase control system for the RF pulse compressor to produce a flat-top rectangular pulse over 1.4 μs.

INTRODUCTION

An international collaboration is currently building CTF3 (CLIC Test Facility 3) at CERN. When completed, this facility will consist of a 150 MeV 3 GHz linac followed by two rings for bunch-interleaving and a test stand where 30 GHz power will be generated [1]. Its aim is to demonstrate the key feasibility issues of the CLIC (Compact LInear Collider) two-beam scheme [2]. At present, the linac is being constructed and commissioned in stages and well over half is completed. Six 35 MW to 45 MW 3 GHz klystrons are operational. One powers two standing-wave pre-buncher cavities and a travelling-wave buncher. The others each power two damped travelling-wave accelerating structures with a loaded gradient of 6.5 MV/m. Commissioning results in 2003 demonstrated full beam loading operation of these structures with the nominal beam current of 3.5 A [3].

CTF3 uses a large part of the infrastructure of LPI, the now decommissioned LEP pre-injector linac. This includes re-use of modulators, klystrons and LIPS pulse compressor cavities at the klystron output [4]. RF pulse compression is mandatory in order to reach the required power level of over 30 MW for the 1.5 μs pulses at each structure's input. In LPI, the phase function for compression consisted of a straightforward 180^{O} phase inversion at the klystron driver's output. However in CTF3, with much longer bunch trains of 1.4 μs, a much more sophisticated phase function was required and this was one of the principal reasons why the low level RF system needed a complete re-design. In this paper, an overview of the current status of the CTF3 low level RF system is presented, concentrating on the pulse compression phase control scheme.

AMPLITUDE AND PHASE CONTROL

The layout of the low power system for one klystron is shown in Figure 1. The 3 GHz is distributed from a master synthesizer to the low level equipment of each klystron over low-loss phase-stable 7/8-inch coaxial cable. To minimize differential phase variations with temperature, equal lengths of cable are used (100 m ±1 cm). The 360^{O} "digital" phase shifter (analogue with integrated DAC) is slow and is used for adjusting the

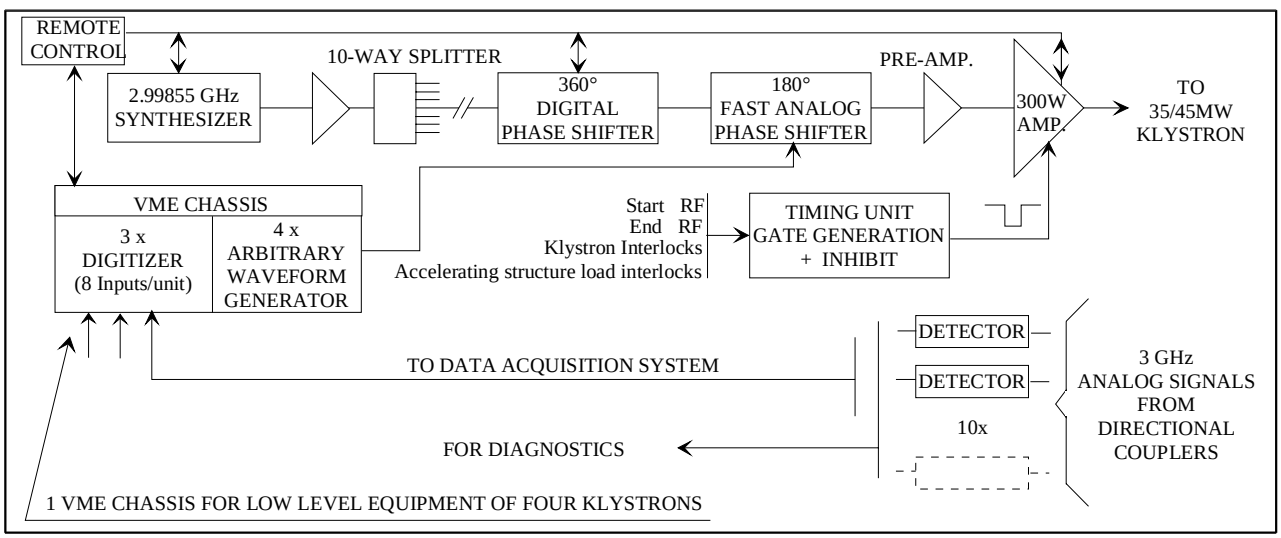

Figure 1: Simplified block diagram of low level system.

HIGH-POWER RF DISTRIBUTION SYSTEM FOR THE 8-PACK PROJECT*

Christopher Nantista, Sami Tantawi, Jose Chan, David Schultz, SLAC, Menlo Park, CA 94025, USA, Dennis Atkinson, LLNL, Livermore, CA 94550, USA, Sergey Kazakov, KEK, Tsukuba, Japan

Abstract

The 8-Pack Project at SLAC is a prototype rf system whose goal is to demonstrate the high-power X-band technology developed in the NLC/GLC (Next/Global Linear Collider) program. In its first phase, it has reliably produced a 400 ns rf pulse of over 500 MW using a solid-state modulator, four 11.424 GHz klystrons and a dual-moded SLED-II pulse compressor [1]. In Phase 2, the output power of our system has been delivered into the bunker of the NLCTA (Next Linear Collider Test Accelerator) and divided between several accelerator structures for beam acceleration. We describe here the design, cold-test measurements, and processing of this power distribution system. Due to the high power levels and the need for efficiency, overmoded waveguide and components are used. For power transport, the TE_{01} mode is used in 7.44 cm and 4.064 cm diameter circular waveguide. Only near the structures is standard WR90 rectangular waveguide employed. Components used to manipulate the rf power include transitional tapers, mode converters, overmoded bends, fractional directional couplers, and hybrids.

INTRODUCTION

As part of the research and development for the future linear collider, SLAC has undertaken the 8-Pack Project, its goal being the realization of a working prototype rf system of the type envisioned for a machine powered by warm X-band technology, as in the NLC/GLC (Next/Global Linear Collider) designs. Employing a state-of-the-art solid-state modulator, four 50 MW klystrons, dual-moded transmission waveguides, and a novel dual-moded SLED-II pulse compression system, this project has had remarkable success in reliably generating 400 ns flat compressed pulses of 500 MW and above. This phase of the project is reported on elsewhere [1,2].

In this paper, we describe Phase 2 of the 8 Pack Project, in which the power produced in Phase 1 is used to conduct gradient tests and accelerate beam in accelerator structures. To this end, we have designed and constructed an rf distribution system to transport the high power pulses into the NLCTA (Next Linear Collider Test Accelerator) bunker and distribute them between several structures. As the use of overmoded waveguide and components is dictated by the need for high power-handling capacity and reasonable efficiency, such a system is non-trivial. Indeed, the interface between power sources and the accelerator represents an important part of an rf module, increasingly so as the design has moved toward higher peak-power pulses and shorter structures, requiring more division.

* Work supported by the U.S. Department of Energy under contract DE-AC02-76SF00515.

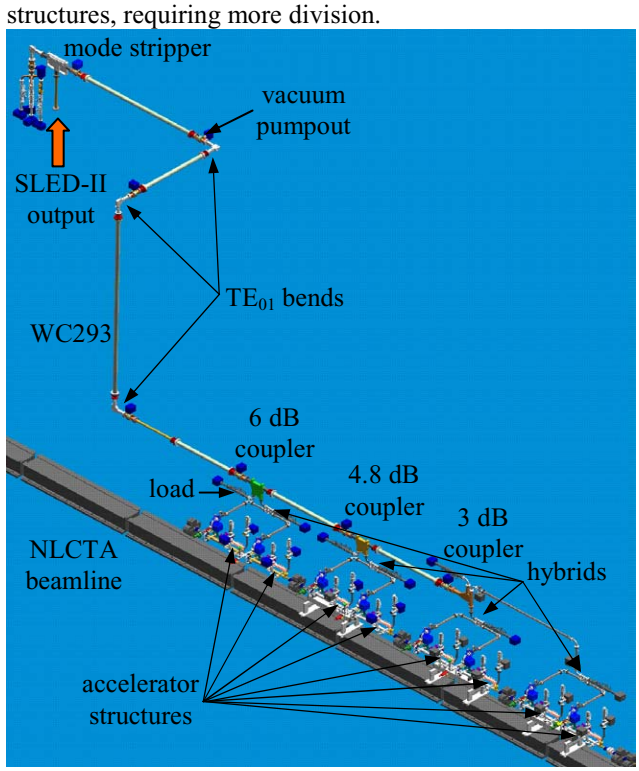

Figure 1: Physical layout of the distribution system from the 8-Pack pulse compressor to the accelerator structures.

SYSTEM LAYOUT

A scaled graphical representation of the distribution waveguide system, picking up from the output of the SLED-II system, is shown in Figure 1. The dual-moded nature of the Phase 1 system [3], along with the project title, is a vestige of the originally conceived configuration (retained for power source versatility and to test components capable of accommodating either option). The distribution system uses only the TE_{01} mode in circular waveguide. A "mode stripper" thus replaces the splitter that previously divided the output power into a series of eight loads. It directs any TE_{11} power due to source mismatch/misphasing into a smaller four-load tree while bending the desired power horizontally.

Due to the position and orientation of our pulse compression system, three more overmoded 90° bends are required to bring the power parallel and in close proximity to the NLCTA beamline. The vertical run penetrates the roof of the concrete bunker housing the

SKIP - A PULSE COMPRESSOR FOR SUPERKEKB

T. Sugimura, T. Kamitani, K. Yokoyama, K. Kakihara, M. Ikeda and S. Ohsawa
KEK, 1-1, Oho, Tsukuba, Ibaraki, Japan

Abstract

A C-band RF pulse compressor "SKIP", which stand for SuperKEKB Injector Pulse compressor, has been developed for the SuperKEKB project aiming luminosity upgrade of the present KEK-B factory. The design of the compressor using $TE_{0,3,8}$ mode cylindrical cavity is based on the "LIPS" used in the LEP injector S-band linac. Detailed dimensions of the cavity have been optimized for C-band (5712 MHz) with low power models. In the high power test of the pulse compressor, a peak output power of 200 MW is achieved with the input RF power of 43MW in 2 μsec duration.

INTRODUCTION

KEKB attained the highest luminosity ($1.3\times10^{34}cm^{-2}s^{-1}$) in the world. SuperKEKB, an upgrade of KEKB whose target luminosity is 1-5 $\times10^{35}$ $cm^{-2}s^{-1}$ is under consideration [1]. In the SuperKEKB project, energy exchange of beams has an important role. In order to escape the influence of electron clouds, the energy of an electron beam is lowered to 3.5 GeV from 8 GeV, and the energy of a positron beam is raised from 3.5 GeV to 8 GeV. Although it is easy to lower the energy of an electronic beam, it is not easy to raise the energy of a positron beam. A positron is a secondary particle, and after generating it, the space in which a positron beam is accelerated is restricted. One of solutions is to double an acceleration field. Thus the C-band accelerator module which has double acceleration field has been developed [2]. In the summer of 2003, an accelerating structure was installed into the beam line and beam acceleration has been performed since. The acceleration gain with the accelerating structure is 40 MeV/m, feeding power from a klystron into one 1m-long structure. In the complete composition of accelerator module, one klystron feeds two 2m-long structures. Since peak power runs short with the present 50 MW class klystron in such a case, an RF pulse compressor is essential.

Modified RF pulse compressors of SLED are used in the sections of S-band [3]. The half-scale model of S-band structure was adopted in the design of an accelerating structure [4]. In the design of a pulse compressor, when the scale down model of S-band is considered, sufficient Q factor is not acquired. Then, another design plan is needed. We considered using the cavity in the $TE_{0,3,8}$ mode adopted in the LIPS cavities [5]. The Q factor of about 150,000 is expected in $TE_{0,3,8}$-mode cavity. Thereby, an energy multiplication factor of the same as SLED for S-band can be obtained.

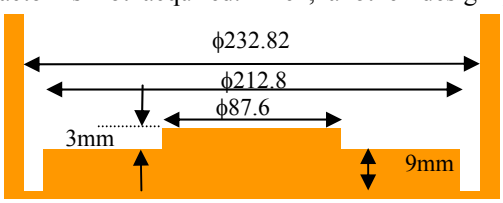

Figure 1: Sectional view of the groove

DESIGN

As already stated, the cavity in the $TE_{0,3,8}$ mode was adopted. Considering a simple cylindrical cavity, there are two adjustable parameters such as diameter and height. For the first step, a scale down model of LIPS cavity is considered. The diameter of 232.82 mm is as almost same as the present S-Band SLED type pulse compressor in KEKB injector linac. It is necessary to investigate the resonance modes of a cylindrical cavity with such form. The mode which should be most careful of is the $TM_{1,3,8}$ mode which is degenerating with the $TE_{0,3,8}$ mode. It is also necessary to take care about the $TE_{12,1,1}$ mode. In order to detune these modes, there is a groove on the base plate as shown in a Fig1. In the numerical computation by MAFIA, these modes are detuned, as shown in the Table1.

Table 1: Frequency shift by groove

Mode	F_0(MHz)	ΔF from $TE_{0,3,8}$ (MHz)
$TM_{1,3,8}$	5684.525	-12.723
$TE_{12,1,1}$	5708.321	11.073
$TE_{0,3,8}$	5697.248	0

An energy multiplication factor M is given by [6]

$$M = \gamma e^{-T_a/T_c}\left[1-(1-g)^{1+\nu}\right]\left[g(1+\nu)\right]^{-1} - (\alpha - 1),$$

where T_a is the filling time of the accelerating structure, T_c is the filling time of the cavity, $\alpha=2\beta/(1+\beta)$ and $\nu=T_a/T_c[ln(1-g)]$. The group velocity vg varies linearly with the position z according to $v_g(z)= v_{g0}(1-gz/L)$, where v_{g0} is a group velocity at position $z=0$, L is the length of the accelerating structure and g is the quantity about the gradient of a group velocity v_g variation along the structure. For the case of C-band accelerator, characteristic parameters of RF are given in Table 2. Using these values, relation between coupling factor β and energy multiplication factor is represented in Fig. 2.

Table 2: Main RF parameter

Frequency	5712 MHz
Q_0	130000
T_a	350 nsec
g	0.6
L	1.924
Full RF pulse width	2.00 μsec
Pulse width before phase inversion	1.65 μsec

WAVEGUIDE STUB TUNER ANALYSIS FOR CEBAF APPLICATION*

H. Wang#, M. Tiefenback, Jefferson Lab, Newport News, VA 23606, USA

Abstract

Three-stub WR650 waveguide tuners have been used on the CEBAF superconducting cavities for two changes of the external quality factors (Q_{ext}): increasing the Q_{ext} from 3.4~7.6×10^6 to 8×10^6 on 5-cell cavities to reduce klystron power at operating gradients and decreasing the Q_{ext} from 1.7~2.4×10^7 to 8×10^6 on 7-cell cavities to simplify control of Lorenz Force detuning. To understand the reactive tuning effects in the machine operations with beam current and mechanical tuning, a network analysis model was developed. The S parameters of the stub tuner were simulated by MAFIA and measured on the bench. We used this stub tuner model to study tuning range, sensitivity, and frequency pulling, as well as cold waveguide (WG) and window heating problems. Detailed experimental results are compared against this model. Pros and cons of this stub tuner application are summarized.

INTRODUCTION

Most applications of a three-stub tuner modifying a superconducting cavity input coupling are on storage rings, to match RF power to heavy beam loading and off-crest conditions. An early implementation was at DESY [1]. The analysis method used an equivalent circuit including the three-stub tuner. Recently, a similar application has been employed at CESR, Cornell. The analysis method has been improved from lumped elements to a network distributed system [2]. Reactive tuning by H or E stubs and other fast response tuning devices could also compensate Lorenz Force detuning and microphonic problems in the SRF control system [3]. In a WG iris/stub tuning design [4], reactive tuning was dominated by the fixed inductance of an iris. The stubs only change the frequency pulling. So the Q_{ext} can only be increased. Three stubs can act as both frequency tuner and reactive device to increase or decrease the Q_{ext}.

The WR650 waveguide three-stub tuners have been used at JLab on 5-cell (mean value of Q_{ext}=5.5±0.8×10^6) cavities to reduce required klystrons' power [5]. They were also installed on the SL21 cryomodule, with new 7-cell cavities and Q_{ext}=1.7~2.4×10^7. The heating effect on the SL21's cold WG fundamental power coupler (FPC) and warm ceramic windows have been observed [6] with little understanding. Under existing RF low level control (amplitude modulation) and high level power (5kW klystron) systems, the system Q at 8×10^6 is more tolerable. Then there is motivation to decrease the Q_{ext} to overcome the problem of Lorenz-force bump during cavity gradient ramp-up [7]. Otherwise a manual tuning of up to 3 bandwidths (225Hz) and slow increase of gradient are necessary. A network model has been developed to analyze stub tuner tuning properties, such as range, sensitivity and reactive heating effect.

NETWORK ANALYSIS MODEL

A two-port microwave network can be described by a 2×2 transmission matrix **T**:

$$\begin{pmatrix} a_1 \\ b_1 \end{pmatrix} = \begin{pmatrix} T_{11} & T_{12} \\ T_{21} & T_{22} \end{pmatrix} \begin{pmatrix} b_2 \\ a_2 \end{pmatrix} \quad (1)$$

Here a_1 and b_1 are incident and reflected waves (or voltages) on input port 1 respectively. The a_2 and b_2 are for output port 2 and reversed in raw position. So a total **T** matrix represents a cascaded wave transmission from three-stub tuner to the Field Probe (FP) of the cavity.

$$T_{tot} = T_{3st} \bullet T_{wg2} \bullet T_{tp} \bullet T_{hb} \bullet T_{wg1} \bullet T_{FPC} \bullet T_{ca} \bullet T_b \bullet T_{FP} \quad (2)$$

Here T_{wg1} and T_{wg2} are WR650 WG matrices in two section lengths l_1 and l_2 with attenuation α and propagation β constants for TE01 mode.

$$T_{wg} = \begin{pmatrix} e^{(\alpha+j\beta)l} & 0 \\ 0 & e^{(\alpha-j\beta)l} \end{pmatrix} \quad (3)$$

The T_{FPC} and T_{FP} are ideal transformer matrices for FPC (subscript 1) and FP (subscript 2), with $n_1 = \sqrt{Q_0 / Q_{1ext}}$, and $n_2 = \sqrt{Q_0 / Q_{2ext}}$ respectively:

$$T_{FPC} = \begin{pmatrix} \frac{1+n_1^2}{2n_1} & \frac{n_1^2-1}{2n_1} \\ \frac{n_1^2-1}{2n_1} & \frac{1+n_1^2}{2n_1} \end{pmatrix} \quad T_{FP} = \begin{pmatrix} \frac{1+n_2^2}{2n_2} & \frac{1-n_2^2}{2n_2} \\ \frac{1-n_2^2}{2n_2} & \frac{1+n_2^2}{2n_2} \end{pmatrix} \quad (4)$$

The T_{ca} and T_b corresponds normalized cavity and beam load shunt susceptances:

$$T_{ca} = \begin{pmatrix} 1+\frac{Y_{ca}}{2} & Y_{ca} \\ -\frac{Y_{ca}}{2} & 1-\frac{Y_{ca}}{2} \end{pmatrix} \quad T_b = \begin{pmatrix} 1+\frac{Y_b}{2} & Y_b \\ -\frac{Y_b}{2} & 1-\frac{Y_b}{2} \end{pmatrix} \quad (5)$$

The Y_{ca} is a function of cavity's intrinsic quality factor Q_0, drive frequency f (1497MHz for CEBAF) and cavity tuned resonance frequency deviation *df*.

$$Y_{ca} = 1 + iQ_0\left(\frac{f+df}{f} - \frac{f}{f+df}\right) \quad (6)$$

The Y_b is a function of beam current I_0, cavity's shunt impedance per unit length $(r/Q)Q_0$, acceleration gradient E_{acc} and the beam current to RF voltage's phase Φ_b.

$$Y_b = \frac{I_0 (r/Q) Q_0}{E_{acc}} e^{i\phi_b} \quad (7)$$

The T_{3st} is the transmission matrix for the three-stub tuner. The T_{tp}, a WG taper, transforms from WR650 to a reduced height WG (5.292″×0.986″). The T_{hb} is for a reduced height 90^o H-bend. Their transmission matrices can be converted from their S-parameters.

* Work supported by the US DOE Contract No. DE-AC0584ER401050
# haipeng@jlab.org

LOW-POWER RF TUNING OF THE SPALLATION NEUTRON SOURCE WARM LINAC STRUCTURES

C. Deibele, ORNL, Oak Ridge, TN, 38830 USA
J. Billen, LANL, Los Alamos, NM, 87545, USA
L. Young, TechSource, Santa Fe, NM, USA
A. Vasyuchenko, RAS/INR, Moscow, Russia
J. Error, P. Gibson, G. Johnson, ORNL, Oak Ridge, TN, 38830 USA
N. Bultman, J. Stovall, LANL, Los Alamos, NM, 87545, USA
J. Manolitsas, D. Trompetter, Accel Instruments, Bergisch Gladbach, Germany

Abstract

The Spallation Neutron Source (SNS) is an accelerator-based neutron source being built at Oak Ridge National Laboratory. A conventional 402.5-MHz drift-tube linac (DTL) accelerates the H^- beam from 2.5 to 86 MeV, followed by a 805-MHz coupled-cavity linac (CCL) to 186 MeV. Tuning the six DTL tanks involves adjusting post-coupler lengths and slug tuners to achieve the design resonant frequency and stabilized field distribution. A 2.5-MW klystron feeds RF power into a DTL through a ridge-loaded waveguide. The CCL consists of 4 RF modules operating in the π/2 mode. Each module contains 96 accelerating cavities in 12 segments of 8 cavities each, 11 active bridge coupler cavities, and 106 nominally unexcited coupling cavities. For each RF module, power from a 5-MW klystron splits and drives bridge couplers 3 and 9. We will discuss the procedures and special tools developed for the structure tuning.

INTRODUCTION

We describe the low-power RF tuning of the SNS warm linac designed by LANL. For each of 10 RF structures (6 DTL tanks and 4 CCL modules), the tuning goals are:

- Resonant frequency within ±20 kHz of design under normal operating conditions.
- Field distribution within ±2% of design.
- Fields stable against frequency perturbations.
- Cavity-to-waveguide coupling matched for full beam current.

We convert all frequency measurements made under ambient conditions to 20 C structure temperature under vacuum. Flowing dry nitrogen through the cavities avoids any uncertainty from inaccurate or varying humidity measurements.

DRIFT-TUBE LINAC

The six 402.5-MHz DTL cavities have between 22 and 60 1-βλ-long cells with half drift tubes on the end walls. A tank contains three (two for tank 1) ~2-m-long, copper-plated steel sections bolted together. Tank 1 with 60 cells and tank 2 with 48 cells have a ramped field distribution. Tanks 3-6 with 34, 28, 24, and 22 cells all have a flat field distribution. Slug tuners evenly spaced along the tank bottom (4 per section) provide each tank with 2.1 MHz of static tuning to correct for expected manufacturing dimensional tolerances. In operation, water coolant temperature controls the frequency. Water-cooled copper drift tubes (DTs) mounted on copper-plated steel stems contain focusing, steering, or diagnostic elements. The FFODDO focusing lattice uses permanent-magnet quadrupole lenses in 2/3 of the DTs. In each tank, 4 downstream DTs contain dipole steering magnets and 2 upstream DTs contain beam-position monitors. Some DTs are empty.

Post couplers (PCs) are quarter-wave resonators that provide field stabilization. Rotating the bent the PC adjusts the longitudinal field distribution. A DT-to-tank-wall spacing of ~0.95λ/4 ensures adequate coupling between the PC tip and DT. Tank 1 has 19 PCs, one at every third DT and alternating side to side. Tanks 2 and 3 have 23 and 17 PCs (one at every other DT), and tanks 4,5,and 6 have a PC at every DT location.

RF power enters the cavity through a tapered ridge-loaded waveguide that terminates in a barbell shaped iris (see Fig. 1). Because the iris is small (~2 mm wide), it has a negligible effect on the cavity frequency and field distribution.

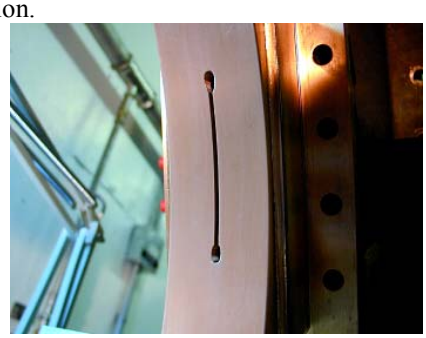

Figure 1: Iris viewed from the DTL side.

DTL Tuning

For low-power DTL tuning we adjust temporary aluminum slug tuners (STs) and PCs (see Figs. 2 and 3). Upon completed, fixed copper parts are finish machined to the measured final dimensions. For low PC excitation during operation, we adjust the STs to achieve the design field distribution before installing PCs. The PCs raise tank frequency 100 to 200 kHz when installed. From this point forward, we move all STs together to maintain the tank target frequency.

MEASUREMENT AND CONTROL OF MICROPHONICS IN HIGH LOADED-Q SUPERCONDUCTING RF CAVITIES*

T.L. Grimm, W. Hartung, T. Kandil, H. Khalil,
J. Popielarski, C. Radcliffe, J. Vincent, R.C. York,
Michigan State University, East Lansing, MI 48824

INTRODUCTION

Superconducting radio frequency (SRF) linacs with light beam loading, such as the Rare Isotope Accelerator (RIA), S-DALINAC, CEBAF upgrade, and energy recovery linacs, operate more efficiently with loaded-Q, Q_L, values greater than 10^7. The resulting narrow bandwidth puts stringent limits on acceptable levels of vibration, also called microphonics, which detune the SRF cavities and require additional rf power to maintain amplitude and phase.

RIA will use six-cell 805 MHz elliptical cavities for acceleration of uranium from 88 MeV/u to 400 MeV/u (β=v/c=0.41 to 0.72) with a final beam power of 400 kW [1]. To cover this velocity range, three geometric β, β_g, values of 0.47, 0.61 and 0.81 are used [2,3]. A multi-charge state uranium beam with three charge states centered on $^{238}U^{89+}$ and a total beam current, I_{beam}, of 0.37 mA are accelerated in the elliptical cavity section of RIA.

A prototype RIA 805 MHz β_g=0.47 cryomodule has been tested in realistic operating conditions [4]. For Q_L~10^7 operation of RIA, rf power requirements are determined, and measurement and control of microphonics have been demonstrated.

BEAM LOADING & RF REQUIREMENTS

Superconducting cavities require very little rf power to generate the accelerating gradient, and therefore, have intrinsic quality factors, Q_o, greater than 10^8. Additional rf power is required for beam acceleration and control of microphonics. If the beam current is high, beam loading is large enough so that the system bandwidth is much larger than any microphonics detuning. Under these circumstances, the rf generator power (P_g) equals the beam power (P_{beam}). But, if the cavity resonant frequency is shifted, then additional rf power is required to maintain amplitude and phase. The required P_g for a given beam loading, coupler strength ($Q_{ext} \cong Q_L$), and maximum detuning ($\pm\delta f$) is given by [5]

$$\frac{P_g}{P_{beam}} = \frac{1}{4}\frac{Q_{beam}}{Q_L}\left[\left(1+\frac{Q_L}{Q_{beam}}\right)^2+\left(\frac{\delta f}{\Delta_{beam}}\frac{Q_L}{Q_{beam}}\right)^2\right]$$

$$Q_{beam} = \frac{2\pi f U}{I_{beam} V_a \cos\phi_s} = Q_o \frac{P_o}{P_{beam}}$$

$$\Delta_{beam} = half\ \ beam\ bandwidth = \frac{f}{2Q_{beam}}$$

*Work supported by Michigan State University and DOE DE-FG02-00ER41144

Table 1: Beam loading requirements for 400 kW, 400 MeV/u uranium in RIA elliptical cavities

Type	6-cell	6-cell	6-cell
β_g	0.47	0.61	0.81
V_a(MV)	5.12	8.17	13.46
P_{beam}(W)	1660	2640	2600*
Q_{beam}	9.1×10^7	9.1×10^7	1.4×10^8
P_g(W)	3320	5280	5200
Q_L	3.0×10^7	3.0×10^7	4.7×10^7
$\Delta_{allowed}$(Hz)	25	25	16

*β_g=0.81 decreased from the maximum value due to transit time factor

For RIA, the rf generator requirements are chosen to be twice the maximum beam power. From the previous equation it can be shown that the maximum allowable detuning occurs when Q_L/Q_{beam}=0.33 for these conditions. The maximum allowable detuning for which amplitude and phase can be maintained is then $\delta f=2.8\Delta_{beam}$. Therefore, the microphonics can detune the cavity over a full bandwidth, $\Delta_{allowed}=2\delta f=5.6\Delta_{beam}$, and the amplitude and phase can still be maintained. The control bandwidth is slightly smaller than the Q_L bandwidth (f/Q_L) due to the generator requirements.

The design beam for the driver linac is 400 MeV/u uranium with a total power of 400 kW. For this case, the beam loading values are shown in Table 1 for a synchronous phase, ϕ_s, of -30°. The accelerating voltages, V_a, correspond to peak surface electric fields of 32.5 MV/m and accelerating gradients of 10-15 MV/m. Because the β_g=0.81 cavity does not accelerate uranium at the peak of its transit time curve, the maximum beam power is nearly the same as the maximum value for the β_g=0.61 cavity. The allowable detuning for RIA, assuming a generator power that is twice the beam power, is also shown in Table 1. Due to transit time effects, most of the cavities do not supply the maximum power to the beam. Therefore, most of the cavities will be able to handle significantly higher detuning than shown here. The measured microphonics with and without passive and active damping on the prototype RIA cryomodule show that the values in Table 1 are adequate for RIA.

Operation of SRF cavities with $Q_L=3\times10^7$ is done at the S-DALINAC in Darmstadt [6], and a Q_L in the low 10^7 range is proposed for the CEBAF upgrade [7]. Energy recovery linacs would benefit from Q_L in the 10^8 range. Therefore, the design bandwidth values proposed here for RIA are consistent with the goals of other projects and will be able to capitalize on the advances made for other accelerators.

TRAVELLING WAVE AND STANDING WAVE SINGLE CELL HIGH GRADIENT TESTS *

V.A. Dolgashev, S.G. Tantawi, C.D. Nantista, SLAC, Menlo Park, CA, 94025, USA
Y. Higashi, T. Higo, KEK, Tsukuba, Ibaraki 305, Japan

INTRODUCTION

Accelerating gradient is one of the crucial parameters affecting the design, construction and cost of next-generation linear accelerators. The present Next Linear Collider (NLC) / Global Linear Collider (GLC) designs specifies unloaded accelerating gradient of 65 MV/m at 11.4 GHz [1]. This is almost three times the present operating gradient of the S-band SLAC linac. The major obstacle to higher gradient is rf breakdown.

RF breakdown limits working power and produces irreversible surface damage in high power rf components and rf sources. For a given rf frequency, the maximum working gradient depends on the rf circuit, structure geometry and material. It is also a function of the input power, pulse width, and surface electric and magnetic fields. Here we define working gradient as a gradient with very low breakdown rate — less then one breakdown in 2×10^6 rf pulses.

The complexity of rf breakdown phenomena and the absence of a proven theory for it make it difficult to apply experimental results on breakdown limit from one rf structure to another. For example, working gradients in specialized small cavities are usually much higher than in high power waveguides and practical accelerating structures. To date, dozens of full-scale travelling wave (TW) structures [1, 2] and standing wave (SW) structures [3] have been tested at SLAC in an effort to produce accelerating structures that satisfy NLC/GLC requirements on gradient and breakdown rate. The requirements were met mainly by reducing length of a structure. To reach the same gradient while keeping average iris size, the power fed into a structure had to be reduced. Many questions about the physics of rf breakdown remain unanswered. The experiments described in this paper are designed to study the breakdown phenomena. They allow economical testing of structures with different cell geometries, materials and preparation techniques with short turn around time. The requirements were met mainly by reducing the power fed into a structure. To reach the same gradient while keeping average iris size, structure length had to be reduced. Many questions about the physics of rf breakdown remain unanswered.

MOTIVATION

The shape of the cell is one of the parameters that determines the high power performance of an accelerating structure. To study the effect of cell shape on the rf breakdown behavior of a TW structure is difficult because the geometry of the cells varies along its length and rf power decays toward the end of the structure. Here we refer to 11.424 GHz, near-constant-gradient TW structures developed for the NLC [2].

In order to study the effect of cell shape alone, we will perform an experiment with *single cell TW* structures. The idea is to build a structure that in only one cell mimics the fields near the input of a full-scale TW structure and has high electric and magnetic fields only in that cell, not in matching elements or *couplers* that transform the TE_{10} mode of rectangular waveguide into the "accelerating" circular TM_{01} mode. Another feature of the setup is the couplers, or mode launchers, which can be connected to the single cell structure with rf-compatible circular waveguide vacuum flanges. The flanges allow re-use of the same mode launchers for different structures, significantly reducing the cost of the experiments and allowing fast turn-around between tests of different structures.

We emphasize the difference between our proposed tests and earlier experiments with single cell structures [4]: the power available for breakdown and the field configuration in the single TW cell are similar to the power and fields at the beginning of the full TW accelerating structure. This was not the case in earlier experiments, which were done mostly with standing wave structures. We note that available rf power was shown in experiments [2] to have an effect on the breakdown limit in full TW structures.

Since breakdown behavior in TW structures and SW structures is different [3, 5], to study this difference and effect of SW cell shape on breakdown, we will perform *single cell SW* experiments. These will employ one of the mode launchers to feed rf power into a SW structure. Fields in the middle cell of the SW structure are similar to fields of a large-aperture SW structure already tested at high power (structure SW20a565 [3]). Fields in the other two cells are designed to be at most one half of the middle cell fields, so breakdowns will likely occur in the middle cell.

We note that shapes and field distributions in both single cell TW and single cell SW structures are identical to shapes and fields of full-length structures. We speculate that this similarity will allow us to predict the behavior of practical structures from the tests. We note another advantage of the single cell structures: small geometry allows better diagnostics of breakdown events and makes possible detailed 3D simulation of breakdown processes observed in the experiments.

SETUP

The TW single cell setup consists of two mode launchers with a TW structure in between. The SW single cell setup consists of one mode launcher and a SW structure. Mode

* This work was supported by the U.S. Department of Energy contract DE-AC03-76SF00515.

The Simulation Calculations And Dielectric Characteristics Investigation of a Hybrid Dielectric-Iris-Loaded Traveling Accelerating Structure

C.-F. Wu, USTC/NSRL, Hefei, Anhui

Abstract

Mafia code has been used to calculate the RF properties versus the geometric parameters and dielectric permittivity of the X-band (f=9.37 GHz) hybrid dielectric-iris-loaded travelling accelerating structure. The simulation results show that when the range of the permittivity is about 59 and the geometric parameters are optimized, the new structure may have lower ratio (about 1) of peak surface electric field at the iris to axial accelerating electric field , while r, Q, r/Q of the new structure being comparable to iris-loaded accelerating structure. The experimental investigation of the permittivity of the dielectric (ceramic)has been made by using the cavity perturbation technique. The results show that the permittivity of the ceramic is about 5.8 at the X-band and its stability is good.The above results will be applied to the design of the new accelerating structure, which may be a potential candidate of high gradient Linear accelerator.

NO SUBMISSION RECEIVED

THE TUNING STUDY OF THE COUPLED CAVITIES FOR THE RF CHOPPER SYSTEM OF J-PARC

S. Wang*, S. Fu, IHEP, P.O. Box 918, Beijing 100039, People's Republic of China
T. Kato, KEK, 1-1 Oho, Tsukuba-shi, Ibaraki-ken 305-0801, Japan

Abstract

A 3-MeV medium-energy beam transport line (MEBT) is located between the RFQ and the DTL in the linac of the Japan Proton Accelerator Research Complex (J-PARC). The MEBT accomplishes beam matching and chopping. An rf deflector (RFD) was adopted as a chopper in the J-PARC linac. A coupled RFD system was proposed in the design of chopper system for saving the cost of rf power source. The tuning of the coupled RFD system was successfully performed. The longer rise time of the second RFD and the delay of the second RFD excitation were found during the tuning of the coupled RFD system, and these phenomena were further analyzed and investigated. Both in the high power and beam tests, the chopper worked well without any discharge under 36 kW peak driving power.

INTRODUCTION

A Medium-Energy Beam-Transport line (MEBT) of Japan Proton Accelerator Research Complex (J-PARC) was installed in KEK for the beam test [1]. As a key component of MEBT, an rf deflector was proposed[2] and designed[3] as a chopper, because of its merits of high deflecting field, compact structure and easy to manufacture. An rf chopper, composed of two RFD (RFD-A and RFD-B), has been successfully developed. Because of the very low loaded-Q of the RFD, a coupled RFD system was adopted in operation for decreasing the demanded rf power by half.

Some frequency deviation was found after the construction of the RFDs. Although the bandwidth of the RFD is very large (~30 MHz), the frequency deviation of about 2 MHz still induces some negative effects: additional reflection and mismatch between two RFDs. The modifications of the RFDs were made for tuning the resonant frequency to the operation frequency of 324 MHz. In a low-level rf test, the fundamental rf properties showed good agreement with those in a design simulation. In a high-power test, the chopper worked well without any discharge under 36 kW peak driving power, and the longer rise time of the second RFD and the delay of the second RFD excitation were investigated in the coupled RFD system.

THE IMPROVEMENT OF THE RFD CAVITY DISIGN

The RFD cavity consists of two parts: the cavity body and the two end plates with large coupling loops. Fig. 1 shows the deformed waveform of the first RFD (RFD-A) when a mismatch of the resonant frequencies (~2 MHz) between RFD-A and B exists in the coupled RFD system.

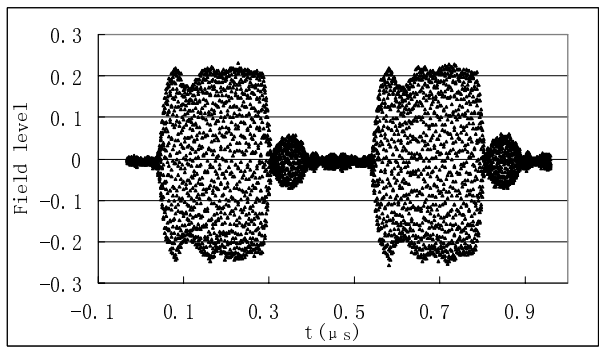

Figure1: The deformed waveform of the RFD-A of the coupled system due to mismatch (36 kW driving power).

To tune the resonant frequency back to 324 MHz, one idea is to move the large coupling loops about 3 mm towards the electrode. In practice, just about a 3mm gasket is needed between the loop and the end plate, then the resonant frequency is tuned to 324 MHz. But in this case the bandwidth of the RFD cavity is increased to 36 MHz, this means much more input power is needed than design.

To tune the resonant frequency to 324 MHz and keep the bandwidth and the other parameters unchanged, a new coupling loop was proposed, and designed by the RF simulation code HFSS.

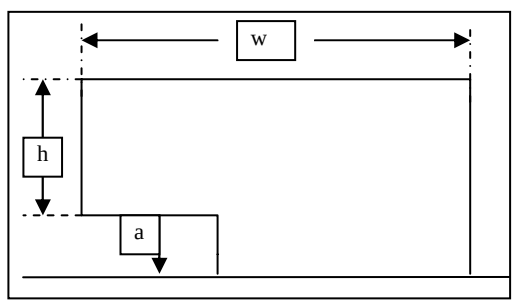

Figure 2: The shape and parameters of coupling loop.

Figure 2 shows the shape and parameters of the coupling loop. The thickness of the loop was 3mm. In design calculations by HFSS, the resonant frequencies were firstly tuned to the measured values by changing the gap distance, for RFD-A and RFD-B, respectively. In order to compensate the manufacture error of the cavities, the width *w* and height *h* of the loop of the two RFDs are

*Email: wangs@ihep.ac.cn

EXPERIMENTAL STUDY OF AN 805 MHz CRYOMODULE FOR THE RARE ISOTOPE ACCELERATOR*

T. L. Grimm, S. Bricker, C. Compton, W. Hartung, M. Johnson, F. Marti, J. Popielarski, R. C. York
National Superconducting Cyclotron Lab, Michigan State University, East Lansing, Michigan, USA
G. Ciovati, P. Kneisel, L. Turlington
Thomas Jefferson National Accelerator Facility, Newport News, Virginia, USA

INTRODUCTION

The driver linac for the Rare Isotope Accelerator (RIA) is designed to accelerate heavy ions to 400 MeV/u ($\beta = v/c = 0.72$) with a beam power up to 400 kW [1]. To obtain these intensities, partially stripped ions are accelerated in a 1400 MV superconducting linac. The high energy section of the linac uses 805 MHz six-cell elliptical cavities with geometric $\beta \equiv \beta_g = 0.47$, 0.61, and 0.81. The first cavity was developed specifically for RIA [2]; the last two were developed for the Spallation Neutron Source (SNS) [3].

A rectangular cryomodule design that can accommodate all of the superconducting cavity and magnet types is proposed for RIA [4]. The proposed cryomodule is more compact than the SNS cryomodule, allowing for a smaller tunnel cross-section and a higher real estate gradient. The cold mass alignment is accomplished with titanium rails supported by adjustable nitronic links, similar to that used for superconducting magnet cryostats at MSU.

A prototype cryomodule for the RIA $\beta_g = 0.47$ elliptical cavities was completed in February 2004. The prototype contains 2 multi-cell cavities instead of the 4 cavities planned for production cryomodules, since the critical issues of cavity gradient, quality factor, and microphonics (which drive the linac cost via module count, cryo-plant capacity, and RF amplifier power) can still be addressed. The first cryogenic and RF tests on the prototype cryomodule were completed in May 2004. Experimental results will be presented in this paper, including alignment, cryogenic performance, RF performance, and frequency tuning. Measurements on microphonics and microphonics control for the cryomodule cavities are presented elsewhere [5, 6].

PROTOTYPE DESIGN AND CONSTRUCTION

Figure 1 shows the prototype cryomodule. The cavities were chemically treated and tested in a vertical cryostat at Jefferson Laboratory (JLab) to verify their performance before installation into the module [2]. The field unflatness between cells was less than 10%, and the π mode frequency was tuned for 805 MHz at 2 K.

The titanium helium vessel was TIG welded to Nb-Ti adapter flanges that were electron beam welded to the cavity beam tubes. Nb-Ti flanges with Al alloy gaskets were used for vacuum sealing. The cold mass was assembled in Jlab's class 10 clean room and shipped by truck to MSU. The cavities were shipped under partial vacuum due to a leaky valve, which was subsequently replaced.

Two μ-metal shields that also serve as passive thermal shields reduce stray fields to 0.5–1 μT. Liquid N_2 was used in the thermal shield, but in the RIA linac 50 K He gas will further decrease the static load to the liquid He.

The required RF power for beam loading and microphonics control is less than 10 kW [5]. The same ceramic window as SNS was used with a smaller diameter coaxial coupler [7, 8].

A room temperature external tuner with piezo-electric actuator was designed for ease of maintenance. Since RIA operates continuous wave (CW), Lorentz detuning will not require fast compensation.

A simple fixture was used to verify cavity alignment to the beam axis within ± 0.25 mm. Fiducials on the Ti rails were monitored through viewports during the cool-down.

COOL-DOWN

The cool-down to 20 K was done rapidly to avoid Q disease. Below 20 K, we proceeded slowly to economise liquid He while the cryomodule approached steady state. The cavities reached 24 K in about 2.5 hours and became superconducting after another 2.5 hours. He gas was introduced into the insulation vacuum space for about 3 hours during the cool-down to increase the heat transfer to the liquid N_2 shield. The cryomodule temperatures were nearly at their steady state values with a full He reservoir 16 hours after the cool-down started. The cavities were cooled from 4.3 K to 2 K by pumping on the He reservoir.

In the initial attempt to cool down to 4 K, the insulation vacuum was not spoiled and the He reservoir was filled rapidly—this caused problems due to the inner μ-metal shield and Ti rails still being warm. In the production cryomodules, it may be worthwhile to improve the heat sinking for these elements to simplify the cool-down.

In initial attempts to cool down to 2 K, there were 2 trapped gas volumes in the liquid He space, one in the supply bayonet and the other associated with a viewport on top of the module. These trapped gas volumes produced thermo-acoustic oscillations near the λ-point, resulting in a pressure instability. Once the liquid level was low enough so that the gas was no longer trapped, we were able to reach 2 K. This problem was eliminated by removing the supply bayonet and the viewport and plugging the holes with teflon-tipped G10 spears. (A supply bayonet was installed in the He reservoir to replace the original bayonet feeding liquid directly to the cavities.) Trapped gas volumes will

*Work supported by Michigan State and the U.S. Department of Energy under Grant DE-FG02-03ER41247.

FIRST EXPERIENCE WITH DRY-ICE CLEANING ON SRF CAVITIES

D. Reschke#, A. Brinkmann, DESY, D-22603 Hamburg, Germany
D. Werner, Fraunhofer IPA, D-70569 Stuttgart, Germany
G. Müller, FB C, University of Wuppertal, D-42097 Wuppertal, Germany

Abstract

The surface of superconducting (s.c.) accelerator cavities must be cleaned from any kind of contamination, like particles or chemical residues. Contaminations might act as centers for field emission, thus limiting the maximum gradient. Today's final cleaning is based on high pressure rinsing with ultra pure water. Application of dry-ice cleaning might result in additional cleaning potential. Dry-ice cleaning relies on the sublimation-impulse method and removes particulate and film contaminations without residues. As first qualifying step intentionally contaminated niobium samples were treated by dry-ice cleaning. It resulted in a drastic reduction of the particle numbers and of DC field emission up to fields of 100 MV/m. The dry-ice jet caused no observable surface damage. First cleaning tests on single-cell cavities showed Q-values at low fields up to $4x10^{10}$ at 1.8K. Gradients up to 33 MV/m were achieved, but field emission still is the limiting effect. Further tests are planned to optimise the dry-ice cleaning technique.

INTRODUCTION

Despite the substantial improvement of the preparation procedures, enhanced field emission still imposes the major high gradient limitation of superconducting accelerator structures, e.g. for the 1.3 GHz nine-cell structures used in TTF at DESY [1]. In order to achieve a gradient of 23 MV/m required for the XFEL [2] or to push the performance to 35 MV/m required for TESLA [3], electric surface fields of at least 46 MV/m and 70MV/m, respectively, should be achieved reliably without field emission loading of the Q-value. Therefore, advanced final cleaning and handling procedures must be applied to avoid surface contaminations like particles, hydrocarbons, etc. and mechanical damages like scratches. The above mentioned have been shown to cause enhanced field emission (EFE) at the envisaged field levels. Though high pressure rinsing with ultrapure water has been proven to be a powerful technique to reduce the enhanced field emission of cavities [1, 4, 5], dry–ice cleaning might have additional cleaning potential. Moreover it avoids a wet cavity surface with its enhanced sensitivity against recontamination. It should be applicable to ceramics (coupler windows) without loosing the gain of an earlier conditioning. Due to these properties dry-ice cleaning is considered as very attractive for the final treatment of horizontally assembled cavities with its power coupler. According to the stimulating first results on flat Nb samples [6], the adoption of this technique to srf cavities will be reported in this paper.

#detlef.reschke@desy.de

DRY-ICE CLEANING

A jet of pure carbon dioxide snow loosens and removes different types of surface contaminations by its unique combination of mechanical, thermal and chemical effects. The cleaning process acts locally, mildly, dryly, without residues and requires no additional cleaning agent. The spontaneous relaxation of liquid carbon dioxide leaving the nozzle results in a snow/gas mixture with app. 45 % snow and a temperature of 194.3 K (-78.9°C). This jet is surrounded by supersonic nitrogen, which firstly gives an acceleration and focussing of the jet and secondly prevents partially the condensation of humidity at the cleaned object. The cleaning effect is based on thermo mechanical and chemo mechanical forces. The former are created by three effects: brittling the contamination as a result of rapid cooling (shock-freezing), the tough pressure and shearing forces due to the high momentum of the snow crystals hitting the surface and the powerful rinsing due to the 500 times increased volume after sublimation. Particles down to 100 nm can be removed. Chemo mechanical forces occur, when high momentum snow particles hitting the surface partially are melting at the point of impact. In its liquid phase carbon dioxide is a good solvent for non-polar chemicals, especially for hydrocarbons and silicones. The thermal effect of shock-freezing is thereby directly correlated with the snow intensity. The mechanical effect however depends on the velocity and angle of the jet and the chemical effect depends on the momentum of the crystals. An optimal cleaning impact is achieved, if the thermal gradient between contamination and substrate is high. To avoid recontamination an effective and well-defined exhaust system is necessary. In summary the advantages of the carbon dioxide dry-ice cleaning are:

- dry cleaning process,
- no cleaning agents,
- removal of particulate and film contaminations,
- no polluting residues.

NB SAMPLE EXPERIMENTS

Flat samples with a diameter of 28 mm were machined from high purity niobium (RRR = 300) and etched 80 µm with standard BCP ($HF:HNO_3:H_3PO_4$ volume ratio 1:1:2). In order to get typical EFE, each test sequence started with a new surface treatment, i.e. etching and rinsing inside a cavity [7] or intentional contamination with particles [6]. The chosen particle materials are typically ambient during the assembly of accelerating structures like latex (gloves), metal oxides, copper, iron and stainless steel. At first, these samples were inspected with

A NEWLY DESIGNED AND OPTIMIZED CLIC MAIN LINAC ACCELERATING STRUCTURE

A. Grudiev, W. Wuensch, CERN, Geneva, Switzerland

Abstract

A new CLIC main-linac accelerating-structure design, HDS (Hybrid Damped Structure), with improved high-gradient performance, efficiency and simplicity of fabrication is presented. The gains are achieved in part through a new cell design which includes fully-profiled rf surfaces optimized to minimize surface fields and hybrid damping using both iris slots and radial waveguides. The slotted irises allow a simple structure fabrication in quadrants with no rf currents across joints. Further gains are achieved through a new structure optimization procedure, which simultaneously balances surface fields, power flow, short and long-range transverse wakefields, rf-to-beam efficiency and the ratio of luminosity to input power. The optimization of a 30 GHz structure with a loaded accelerating gradient of 150 MV/m results in a bunch spacing of seven rf cycles and 32 % rf-to-beam efficiency.

INTRODUCTION

In order to reach the CLIC design luminosity and energy (~10^{35} $cm^{-2}sec^{-1}$ and 3 TeV, respectively) in power-efficient way, multiple-bunch trains of about 0.5 nC each are accelerated on each machine cycle with an average gradient of 150 MV/m [1]. The design of an accelerating structure capable of this is constrained by a number of very demanding beam dynamics requirements and rf effects: a short-range transverse wakefields limit, long-range transverse wakefield suppression, rf breakdown and rf pulsed surface heating.

As more experimental data about rf breakdown has become available and when these constraints have been considered simultaneously, it has become clear that the existing designs of the CLIC main linac accelerating structure, the TDS (Tapered Damped Structure) [2] and later the XDS (conveX Tapered Structure) [3], are not satisfactory. In this paper, a new geometry and design approach is described giving a structure which not only finally satisfies both beam dynamics and rf constraints (at least to our present level of knowledge of them) but also brings a distinct improvement in rf-to-beam efficiency of 32% and a novel assembly technique.

The first key improvement has been to increase higher order mode damping by combining iris slots and radial waveguides – hybrid damping and hence the name HDS (Hybrid Damped Structure) - allowing the bunch spacing to be reduced from 20 to 7 rf cycles. The second key improvement is a new optimization procedure which is based on the interpolation of the structure parameters and allows millions of structures to be analysed taking into account the full and extremely complex interplay between rf and beam dynamics parameters.

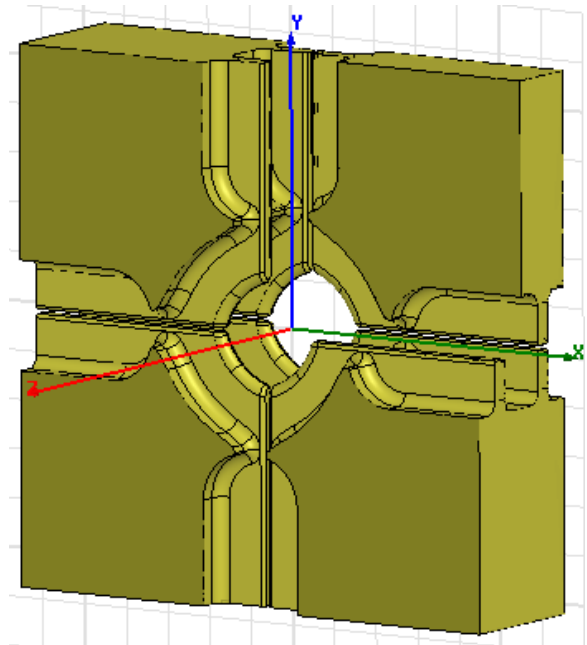

Figure 1: Geometry of the HDS cell. Two cells are shown to better demonstrate shape of the cell cavity, slotted iris and damping waveguides. For the same reason one quarter of one of the cells is removed from the picture.

HDS DESIGN

The HDS design was illuminated by the idea that iris slots could be introduced in addition to the damping waveguides in order to improve suppression of long-range transverse wakefields with little increase of the pulsed surface heating. The geometry of the HDS cell is shown in Fig. 1. In fact, the coupling in the HDS of the (dominant) lowest dipole mode to the slots becomes significantly stronger than the coupling to the damping waveguides. The waveguides are retained because there are higher-order transverse modes with the rf phase advance per cell close to 0 and longitudinal higher-order modes (TM_{0n}), which are weakly or not at all coupled to the slots. These modes are generally well damped by the waveguides.

Because the lowest dipole mode is coupled mainly to the slots rather than to the waveguides, and the weak dependence of this coupling on the damping waveguide aperture size, the surface of the cell outer wall can be increased compared to the XDS. This *reduces* pulsed surface heating, due to a lower current density, while simultaneously improving damping.

The slots however introduce a number of difficulties which have had to be addressed. One of them is that the surface electric field is enhanced in the area where the slots end in the center of the iris. This field enhancement is eliminated by composing the beam aperture out of four

LASER PRODUCED IONS AS AN INJECTION BEAM FOR CANCER THERAPY FACILITY*

A. Noda, M. Hashida, Y. Iwashita, S. Nakamura, S. Sakabe, S. Shimizu, T. Shirai,
T. Takeuchi, H. Tongu, ICR, Kyoto University, Uji-city, Kyoto, 611-0011, Japan
A. Fukumi, Z. Li K. Matsukado, NIRS, Inage-ku, Chiba, 263-8555, Japan
H. Daido, Kansai Research Establishment, JAERI, Umemi-dai, Kizu, Kyoto, 619-0215, Japan
T. Hosokai, H. Iijima, K. Kinoshita, K. Yoshii, T. Watanabe, M. Uesaka
Graduate School of Engineering, Univ. of Tokyo, Naka, Tokai, Ibaraki, 319-1188, Japan

Abstract

Ion production from a solid target by a high-power short-pulse laser has been proposed to replace the injector linac for the synchrotron dedicated for cancer therapy in order to reduce the size of the facility. For the reduction of the energy spread of the laser-produced ions up to ±5 %, a scheme of phase rotation is to be utilized. A quarter wave length resonator with the resonant frequency of 79.3~82.7 MHz and its power amplifier of the maximum power of 30 kW are designed and fabricated. Ion production from the solid target has also been studied and experimental results suggest the ion production from under dense plasma for the case with the presence of pre-pulse.

INTRODUCTION

High energy ion production from the solid target by a high-power laser has recently been reported [1, 2]. In such a process, target normal sheet acceleration is expected [3]. The lasers utilized for such purpose had been high power lasers mainly oriented for laser fusion and their repetition rates are, in general, very low and less than once per twenty minutes, which does not match the real application for medical use and so on. For the purpose of demonstrating the feasibility of utilization of the laser-produced ion-beam as the injection beam for cancer dedicated synchrotron, possibility of inducing target normal sheet acceleration of ion beam from the solid target with the pulse laser of much shorter pulse width and higher repetition rate as 10 Hz has been investigated. By focusing the laser to the size ~10μm in diameter, ion production up to 1 MeV has been observed even for the rather limited laser power density of ~10^{18} W/cm^2. The intensity of the laser-produced ions, however, decreases exponentially according to the increase of the ion energy. In order to remedy this situation, a scheme of phase rotation with use of the laser-synchronized RF electric field has been proposed [4], which has been developed assuming the experiments utilizing 100 TW, 20 fs, 10 Hz laser at JAERI, Kansai Research Establishment.

In the present paper, the preliminary results of experimental research on laser ion production is presented together with the design and fabrication of the quarter wave length RF cavity for phase rotation.

PRELIMINARY TEST OF LASER ION PRODUCTION

Ion production by the laser with the power ~10 TW and short pulse width (50 fs) has been performed as the preparatory work for ion production and its phase rotation with use of 100 TW, 20 fs laser, because the available time of the latter laser is rather limited.

Wth use of a 30TW, 50 fs laser at Nuclear Engineering Research Laboratory, Graduate School of Engineering, University of Tokyo, ion production from various solids targets such as polyethylene, Ti, Ta and so on, has been performed. Among these targets, Ta target, 5 μm in thickness was most preferable. In Fig. 2, comparison of energy distribution among the metal targets is shown together with the data taken using the 10 TW, 50 fs laser

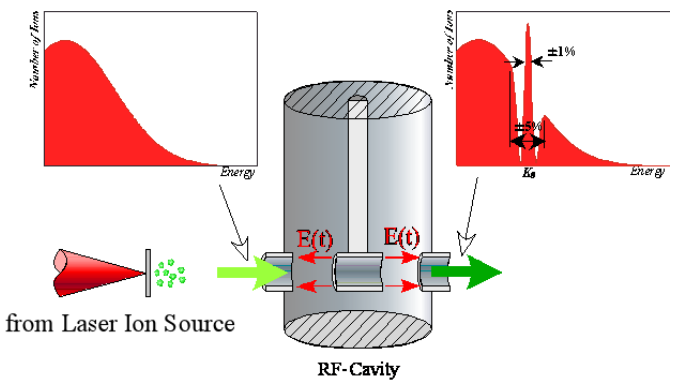

Figure 1: Schematic illustration of phase rotation of laser produced ions by a laser-synchronized laser.

*noda@kyticr.kuicr.kyoto-u.ac.jp

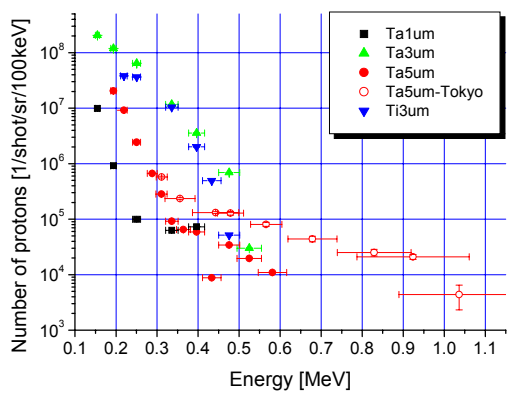

Figure 2: Comparison of energy distributions of laserproduced proton from various metal targets.

SUPERCONDUCTING ACCELERATING STRUCTURE WITH GRADIENT AS 2 TIMES HIGHER AS TESLA STRUCTURE

P. Avrakhov, V. Balakin, Physical Technical Center of P.N.Lebedev Physical Institute, Protvino, Russia

Abstract

A proposed new accelerating structure for TESLA is assumed to have an effective gradient 2 times more than existing 9-cell cavity [1]. This structure is an interlaced combination of two side-cavity-coupled standing wave substructures with $\lambda/4$ cells length. Intercell coupling provides side-coupled cavities, which are made from a special shape waveguide section. The high accelerating gradient is accomplish by 4 factors:

1) The shortened accelerating cells have transit time factor 0.9 instead of 0.64 for conventional standing wave cells with $\lambda/2$ length.

2) The side magnetic coupling has made it possible to reduce the cells beam aperture that reduce relation between the maximum surface field and the acceleration gradient.

3) Stronger intercell coupling allows extending the accelerating cavity and improving a duty factor of linac.

4) Availability of the side coupling elements enables to use them for power input and HOM-couplers. It reduces intercavity distance and enhances duty factor too.

INTRODUCTION

Under development of a superconducting linear accelerator the greatest efforts are applying to increase its effective accelerating gradient. The next significant parameter is shunt impedance. But shunt impedance of a superconducting linac is higher than 5-6 orders of magnitude for "warm" accelerators and is not so important to choice of a geometry superconducting linac. A few methods for improvement of acc. gradient are known. They are including an application of shortened cells for accelerating structure, reducing linac aperture and increasing of active length of accelerators by shortening of inter-cavity spacing. The first two methods increase acc. gradient due to reducing surface electric and magnetic fields into an accelerating cell. And third method extends effective length of accelerator. In this report a novel type of standing wave accelerating structure, which combines all these methods, is suggested.

DOUBLE-CHAIN BIPERIODIC STANDING WAVE STRUCTURE

Experience of employment of biperiodic accelerating structures with side coupled resonators (see Fig.1) showed their high efficiency in comparison with ordinary iris-loaded cavities. Due to side magnetic coupling large intercell coupling coefficient is easily obtained for any

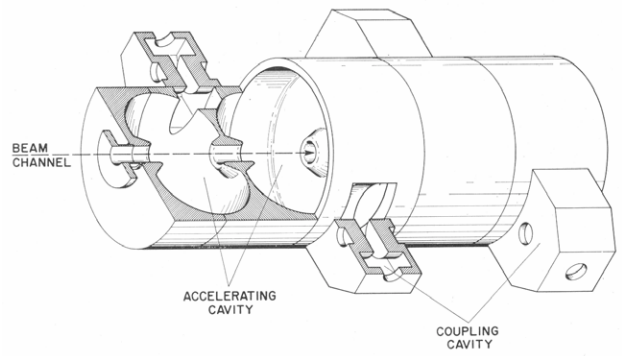

Figure 1: The side-coupled cavity chain [1].

size of beam holes. Low aperture accelerating cells have low field ratios E_{surf}/E_{acc} and H_{surf}/E_{acc}, where E_{surf}, H_{surf} means the maximal electric and magnetic fields into the cell and E_{acc} is the accelerating gradient.

In addition the high coupling allows to use long accelerating cavity because the main limitation factor of cell number for superconducting structure is field nonuniformity [4], which is proportional to $\Delta f/f \cdot N^{3/2} \cdot K_{coup}^{-1}$, where $\Delta f/f$ means average relative error of cells frequency, N is number of cells in the cavity and K_{coup} is the intercell coupling coefficient. Existence of the side resonators allows to carry out main power and HOM couplers into these resonators. Filling factor for such biperiodic structure can achieve 1.

If an accelerating cavity consists of $\lambda/4$ instead of $\lambda/2$ length cells it gives considerable gain in accelerating gradient due to rising of transit time factor. Transit time factor for single pillbox resonator can be expressed from length of pillbox as:

$$T = \frac{\sin(\theta/2)}{\theta/2} = \frac{\sin(\pi \cdot D/\lambda)}{\pi \cdot D/\lambda}$$

Where θ is transit angle and D is the resonator length. In case of $D=\lambda/2$ $T=2/\pi=0.637$ and for $D=\lambda/4$ $T=2\cdot\sqrt{2}/\pi=0.9$. Since transit time factor means ratio of effective accelerating voltage to maximum cell voltage, accelerating rate of $\lambda/4$ pillbox obtains as $\sqrt{2}=1.41$ times higher than in $\lambda/2$ length pillbox.

However the well-known biperiodic structure [2, 3] with side coupling cavity is not quite suitable for superconducting accelerator because of prohibitive gain of magnetic field in coupling slot area. It is caused by

EXPERIENCES IN FABRICATION AND TESTING THE PROTOTYPE OF THE 4.90 GHZ ACCELERATING SECTIONS FOR MAMI C[#]

A. Jankowiak, H. Euteneuer, S. Schumann, O. Tchoubarov,
Institut für Kernphysik, Johannes Gutenberg-Universität, D-55099 Mainz, Germany

Abstract

The fourth stage of the Mainz Microtron (MAMI C) is under construction as a Harmonic Double Sided Microtron [1]: by 43 recirculations through two anti-parallel linacs, one working at the MAMI-frequency of 2.45GHz, the other at 4.90GHz, the beam energy is raised from 855 to 1500MeV. The biperiodic accelerating structures used are of the on axis coupled type [2], well proven in high power cw-operation at MAMI since 1978. For 4.90GHz a further optimisation of the cavity profile was done [3]. In addition, to ensure an efficient industrial production of the ten 35AC-sections needed, a prototype section was designed, built and power tested fully in house.

We report the final cavity profile and the configuration of this 4.90GHz-section with its cooling arrangement, tuning plungers and diagnostic probes. Details of machining, fine tuning and brazing the resonator discs are given. Finally the results of the high power test up to 22kW (1.29MV/m) are presented: the conditioning behaviour and the irreversible permanent as well as the reversible dynamic changes of passband gap and resonance frequency as a function of rf input power.

RESONATOR PROFILE

A detailed discussion of our modifications of the cavity profile compared with the just 2:1 scaled 2.45GHz dimensions was given in [3]. These changes were: a larger beam hole ($\varnothing_B$=7 → 10mm) for a relaxed loss free beam transmission along the 12m long linac; a further outward positioning of the coupling slots for higher coupling (k=-4.1% → -8.7%), i.e. less stringent tuning demands, and a less sharp nose cone for easier precision machining. The total sacrifice in shunt impedance by these measures was calculated to be 18%.

With MAFIA and URMEL the sensitivities of the AC- and CC-frequencies to small changes of cavity dimensions were calculated (Table 1). Because of the high sensitivity of ν_{CC} to the CC-length l_{CC} (+163MHz/mm), bearing in mind the layer of brazing alloy with not precisely known final thickness between the endfaces, as a final modification l_{CC} was enlarged from 1.94 → 2.94mm, sacrificing 0.5mm in web thickness. The sensitivity decreased to +99MHz/mm, the coupling increased by 0.5% and the final CC- and AC-diameter is 40.23 resp. 45.39mm. In addition in Table 1 the calculated sensitivities of ν_{AC} and ν_{CC} to special cuts applied by us for fine tuning (cf. 3) are given, as well as the range of empirical values (e) gained during this tuning. For the full end cells (EC) with only one pair of coupling slots a by 50MHz higher frequency was compensated by a 0.52mm larger diameter, and the magnetic coupling slot (22.1×5.5mm through a min. 3.1mm wall) in the input coupler (IC) demanded for compensation of -47MHz by a 0.49mm smaller diameter.

SETUP OF THE 35AC-SECTION

The design of the section is shown in Fig. 1. The number of 35AC (electr./mech. length = 1.071/1.121m) was chosen for two sections being fed by one 55kW cw-klystron (THALES / TH2166): dissipated power 2×15kW, max. beam load 2×4kW, and a margin for waveguide losses and controlling the rf-amplitude to $<10^{-3}$ via the klystron input power. The coupling slot pairs in the AC were chosen to be oriented parallel: for compensation of their rf-quadrupole effect [4], a larger splitting of the TM_{110}-BBU-mode [5] and a clear fulfilling of the mirror boundary conditions when tuning finite resonator stacks. The IC is located at the symmetry point AC18, so the next excitable modes are ±19MHz away from the π/2-mode. Detailed calculations with LOOP [6] were done for this section design, concerning its tuning tolerances and the optimum position of tuning plungers and probes. It e.g.

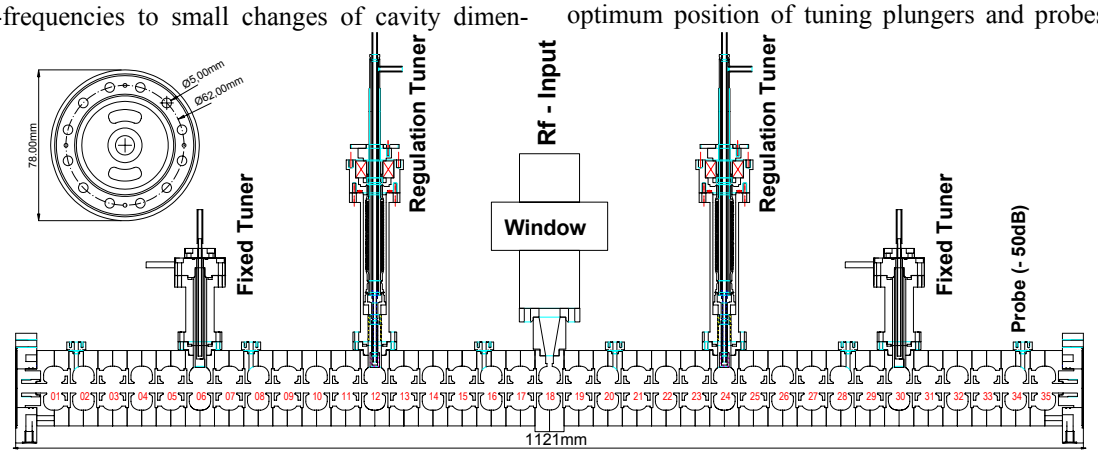

Figure 1: Scheme of the 4.90GHz section (already adapted for series production).

[#] Work supported by HBFG and DFG (SFB443)

MEASUREMENTS OF HIGH ORDER MODES IN HIGH PHASE ADVANCE DAMPED DETUNED ACCELERATING STRUCTURE FOR NLC

Gennady Romanov, Tug Arkan, Harry Carter, Timergali Khabiboulline,
FNAL, Batavia, IL 60510, USA
Gregory Linder, University of Illinois, Champaign, IL, USA

Abstract

The RF Technology Development group at Fermilab is working together with the NLC and JLC groups at SLAC and KEK on developing technology for room temperature X-band accelerating structures for a future linear collider. We have built several series of structures for high gradient tests. We have also built 150 degrees phase advance per cell, 60cm long, damped and detuned structures (HDDS or FXC series). Five of these structures have been successfully used for the 8-pack test at SLAC this summer, as part of the JLC/NLC effort to demonstrate the readiness of room temperature RF technology for a linear collider. HDSS structures are very close to the final design for the linear collider, and it was very interesting to study the properties of high order modes in the structures produced by semi-industrial methods. In this study advanced RF techniques and methods developed at Fermilab for structure low power testing and tuning have been used. The results of these measurements are presented in this paper.

INTRODUCTION

There are three basic requirements on the NLC structure design [1]: it must transfer the rf energy to the beam efficiently and demonstrate stable, long-term operation at 65-70 MV/m accelerating gradient to keep the machine cost low; it must be optimized to reduce the short-range wakefields which depend on average iris radius; and it must suppress the long-range transverse wakefield to prevent multibunch beam breakup and achieve high luminosity. During the past four years, an aggressive program has been underway by groups at SLAC, KEK and FNAL to build structures that meet the gradient requirements. Though the major emphasis has been on proving high gradient operation, an optimization of the structure for the NLC has been continuing as well, resulting in the development and adoption of a structure design (H-type Damped Detuned Structure) that basically meets performance requirements [2]. Now that significant progress in structure high gradient performance has been achieved [3], the high order modes issue must be revisited.

The NLC will require 10,000 to 20,000 accelerator structures. Each structure is comprised of about 50 accelerating cells, thus the total number of cells required is roughly one million [1]. Due to the tight tolerance requirements for these cells, quality control (QC) of RF parts is one of critical steps for this program. The full scope of QC includes many topics such as single cell and full structure QC, and RF and mechanical QC. At Fermilab, we have developed QC set-ups utilizing different microwave techniques to ensure that the machined cells are within the design tolerances, and to confirm overall RF performance of the completed structure [4]. Thus far, our routine QC procedures have not included direct control of high order modes.

The long-range dipole wakefield is suppressed in the structure design by detuning the dipole mode frequencies and damping the fields with dipole coupling channels (HOM manifolds) [2]. The dipole wakefields are the main cause of emittance increase and beam break-up in high-energy accelerators, thus understanding them is essential. Recently, we have developed methods for direct measurements of high order modes in completed structures in order to study their properties and to gain a better understanding of their relationship to single disk and full structure production.

MEASUREMENT SETUP

General

HOM measurements in a completed brazed structure requires the implementation of powerful automated bead-pull techniques. The high order modes of interest do not propagate along the axes of a tapered, detuned structure. Instead, they exist as a set of standing wave modes of different frequencies trapped in corresponding groups of cells, and it is difficult to excite and detect them in a completed brazed structure. Since the modes of interest should be coupled to the HOM manifolds and the manifolds are designed to provide good propagation for such modes, we were able to utilize the HOM manifolds for high order mode excitation and indication. For our experiments we used the FXC-001 structure (a Fermilab designation for an intermediate version of a 52 cell HDDS structure).

Simulation of Measurements

The experiments were simulated before measurements to predict what we should observe. Fig.1 shows a model of an FXC structure consisting of disks ##1,10,20,30,40,50 and 60 (there is no disk #60 in a real FXC structure, this one has extrapolated parameters). As shown in [5], a model developed with

DESIGN OF A 300 GHZ BROADBAND TWT COUPLER AND RF-STRUCTURE*

Frank L. Krawczyk#, Bruce E. Carlsten, Lawrence M. Earley, Floyd E. Sigler, LANL, Los Alamos, NM 87545, USA, James M. Potter, JP Accelerator Works, Inc., Los Alamos, NM 87544, USA, Martin E. Schulze, General Atomics, Los Alamos, NM 87544, USA, Evgenya Smirnova, MIT, Cambridge, MA 02139, USA

Abstract

Recent LANL activities in millimeter wave structures focus on 95 and 300 GHz structures [1]. They aim at power generation from low power (100W-2kW) with a round electron beam (120kV, 0.1-1.0 A) to high power (2-100 kW) with a sheet beam structure (120 kV, 20 A). Applications cover basic research, radar and secure communications and remote sensing of biological and chemical agents. In this presentation the design of a 300-GHz RF structure with a broadband (> 6% bandwidth) power coupler is presented. The choice of two input/output waveguides, a special coupling region, and the structure parameters are presented. As a benchmark also a scaled up version at 10-GHz was designed and measured. These results will also be presented.

INTRODUCTION

We are investigating planar micro-fabricated traveling-wave tube amplifiers as sources for the generation of millimeter waves from 95 to 300 GHz. While for low energy applications narrow structures with pencil beams are proposed, for high-energy operation flat, thin sheet beams are required. For the latter, vane-loaded rectangular waveguides that operate in a slow-wave mode matched to the velocity of the electron beam are especially well suited. The 300-GHz effort initially is limited to narrow structures for pencil beams. The main emphases for this work are the study of fabrication issues and the understanding of features that allow a broadband operation (5-10% bandwidth.)

THE GEOMETRY

The design work is focused on the RF-structure. This structure is made up of the resonator, the power couplers to couple power to the structure, and the coupling regions between the RF-structure and the couplers.

The Base Geometry

The base geometry is a vane-loaded rectangular waveguide (see Fig. 1). We opted for a double-sided waveguide with vanes on the top and the bottom. The vane thickness, height and spacing are given by the desired phase velocity that has to match the energy of the electron beam. A second consideration is maximizing the achievable gain in the structure. The vane parameters that match these criteria, have been determined by simulations with the DETER code [2].

*Work supported by DOE/DOD

#fkrawczyk@lanl.gov

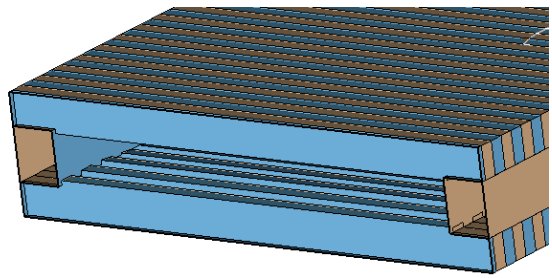

Figure 1: 3D model of the vane loaded waveguide. The top and bottom vanes can be seen inside the waveguide. The bars on the sides define the width and the proper spacing of the top and bottom halves of the resonator.

The Power Coupler

The power has to be fed to the structure off the central plane, away from the entrance path of the electron beam. We opted for two rectangular waveguides operated in a TE mode. These waves that are 180 degrees out of phase at the entrance into the structure combine into the operating TM mode. Figure 2 shows the arrangement of the couplers and the combination of the properly phased electric fields. In the central plane also the waveguide opening for the beam to enter the structure is included.

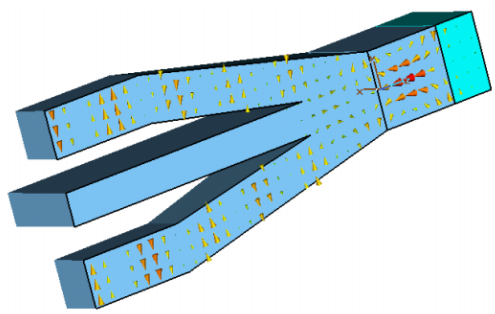

Figure 2: A cross-section through the input waveguides and their combination at the entrance of the RF-resonator are shown. For RF-considerations the inside volume, not the outside material is modeled. The cones indicate the amplitude and direction of the electric field.

The parameters for matching the coupler are the distance of the top and bottom waveguides, the length of the tapered section and a side taper that opens up the waveguide cross-sections towards the entry into the structure. An identical coupler is attached to the outlet of the structure as a load to remove the generated power.

TEST RESULTS OF THE 3.9 GHz CAVITY AT FERMILAB*

N. Solyak, L. Bellantoni, T. Berenc, M. Foley, H. Edwards, I. Gonin, T. Khabiboulline, D.Mitchell, A.Rowe, FNAL, Batavia, IL 60510, USA

Abstract

Two types of 3.9GHz superconducting RF cavities are under development at FNAL for using in the upgraded A0 photo-injector facility. A TM_{010} mode cavity (3rd harmonic of 1.3GHz, frequency of accelerating capture cavity) will be used to linearize energy distribution in the bunch before compression for better emittance. A TM_{110} mode cavity (deflecting or "CKM" cavity) will provide streak capability for bunch slice diagnostics. In paper we present current status of both cavities and results of testing niobium and copper prototypes.

INTRODUCTION

Both cavities have strong motivation for development [1,2]. The design of cavities, infrastructure development and material study can be found in [3,4], R&D work on both cavities were presented at PAC'03 and SRF'03 conferences [2,5]. Here we discuss status and latest results of high gradient test and studies of the high order modes.

STATUS

Before building final design of each type of the cavity a few prototypes were produced and tested to finalize cavity design. Below we discuss current status of design work and production activity at Fermilab.

3rd Harmonic Cavity

Cavity is made of 9 cells with elliptical shape in iris and equator areas. End-cells have bigger iris (r=20mm) from the tube side, than the regular cells (r=15mm). It allows increased coupling with main coupler and facilitates HOM damping [3]. Two HOM couplers mounted in both ends of the cavity provide good damping. To study HOM performances of the cavity and RF properties for accelerating mode we have built two full-scale copper models, each equipped with main and HOM couplers. We also built short 3-cell niobium cavity for the low temperature high gradient tests. Briefly the current status of 3rd harmonic cavity is the following:

- Cavity design is finished, including helium vessel, magnetic shielding and frequency blade-tuner.
- 9-cell cavity in production, all components are ready and partly welded.
- Helium vessels and blade tuners for two cavities are placed an order, stepper motors with controllers are in hand.
- Main coupler and cryomodule for installation on photo-injector A0 are under design.

* Supported by the U.S. Department of Energy.
#solyak@fnal.gov

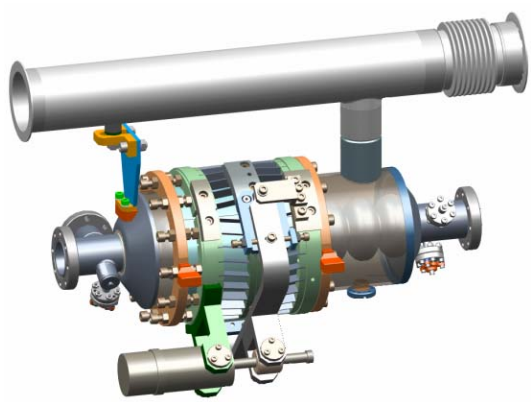

Figure 1: 3rd cavity, equipped with helium vessel and frequency tuner (design).

CKM Cavity

Eight TM_{110} mode cavities have been made, mostly shorter (3, 5 and 9 cells) structures, but there is one full 13-cell prototype. One more short structure is in production, and one more 13-cell is planned. First prototypes were made of 1.6mm niobium sheet, but cavity shape wasn't rigid enough. Last prototypes were built out of 2.2 mm niobium to improve mechanical properties. Helium vessel and frequency tuner are built, assembled and are under testing (see Fig.2). CKM cryomodule for two cavities are ready and will be tested soon. Small cryomodule (for single cavity) for A0 installation will be the same design as for 3rd harmonic cavity.

Figure 2: 13-cell CKM cavity, assembled with the helium vessel.

TEST RESULTS

Short niobium prototypes of both cavities were tested at helium temperature down to 1.6°K in a vertical dewar to investigate cavity performances and field limitations (fig.3). The results of cold tests are presented below.

LOW POWER MEASUREMENTS ON A FINGER DRIFT TUBE LINAC*

K. Kühnel[1], A. Schempp, IAP Frankfurt, Germany
C. Welsch, MPI-K Heidelberg, Germany

Abstract

The efficiency of RFQs decreases at particle energies higher than a few MeV/u and thus typically DTL structures are used in this energy region. However, the rf field in the gap always has a defocusing influence on the beam. In order compensate this effect, fingers with quadrupole symmetry were added to the drift tubes. Driven by the same power supply as the spiral drift tubes, the focusing fingers do not need an additional power source or feedthrough.

Beam dynamics have been studied with the code RFQSIM . Detailed analysis of the field distribution was done and the geometry of the finger array has been optimized with respect to beam dynamics. A prototype cavity with finger drift tubes was built, and low power measurements were done. In this contribution, the results of the rf simulation with Microwave Studio are compared to bead perturbation measurements and the focusing effect on the beam is discussed.

INTRODUCTION

At low energies, RFQs are widely used to accelerate ions up to energies of a few MeV/u. Since they can capture relatively high current dc beams and convert them with a high efficiency into a bunched beam, they have found numerous applications [1-3]. However, at velocities above 0.1c, the efficiency of RFQ accelerators decreases.

Spiral loaded cavities have been developed over many years at IAP and are the ideal tool to further accelerate and bunch the beam [4, 5]. Their characteristic parameters can be calculated with high precision, and their compact design and large energy acceptance allows a usage in most beam lines.

A 4-gap spiral loaded cavity was planned as a booster after the 4 m RFQ of the COSY SCL upgrade, which consists of a room temperatur RFQ with a booster cavity to inject into a superconducting linac [6]. In order to accelerate deuterons from 2 MeV/u to 2.5 MeV/u an overall voltage of 1 MV is needed in the booster. A four gap structure was chosen in order to keep the required peak voltages in each section low. Table 1 gives an overview of the design parameters.

Table 1: Parameters of the booster cavity

Input Energy	2 MeV/u
Length	300 mm
Diameter	280 mm
Beam aperture radius	10 mm
Gap / total voltage	250 kV / 1 MV
Power consumption	150 KW
$\beta\lambda/2$	62 mm

While the desired energy gain can be realized with this structure, the rf-defocusing from the fields in the acceleration gaps would lead to a growth of the transverse dimensions of the beam. Therefore, fingers in quadrupole symmetry were added to the drift tubes in order to focus the ions. A prototype cavity, designed and built at IAP, is shown in fig. 1.

Figure 1: View of the spiral loaded cavity with finger drift tubes.

* Work supported by BMBF
[1] k.kuehnel@iap.uni-frankfurt.de

ACCELERATOR STRUCTURE BEAD PULL MEASUREMENT AT SLAC*

J. R. Lewandowski, G. Bowden, R. H. Miller, J. W. Wang, SLAC, Menlo Park, Ca 94025, USA

Abstract

Microwave measurement and tuning of accelerator structures are important issues for the current and next generation of high energy physics machines. Application of these measurements both before and after high power processing can reveal information about the structure but may be misinterpreted if measurement conditions are not carefully controlled. For this reason extensive studies to characterize the microwave measurements have been made at SLAC. For the bead pull a reproducible measurement of less than 1 degree of phase accuracy in total phase drift is needed in order to resolve issues such as phase changes due to structure damage during high power testing. Factors contributing to measurement errors include temperature drift, mechanical vibration, and limitations of measurement equipment such as the network analyzer. Results of this continuing effort will be presented

INTRODUCTION

The measurement of an accelerator's internal electric field by the bead pull method is an established and trusted measurement. The bead pull measurement consists of pulling a small metallic bead attached to a string through the accelerator structure while a small amount of rf power is fed into the structure at the frequency of the mode you wish to investigate. Real and imaginary S_{11} data is acquired by a network analyzer as the bead moves through the accelerator structure. The electric field amplitude and phase is then calculated for each bead position in the structure.

At SLAC the measurement serves several roles: it is used to quantitatively judge engineering and fabrication issues, to tune newly fabricated accelerator structures and also to characterize any differences that might arise from high power processing by comparing pre and post processing bead pull measurements.

For the purpose of tuning the measurement is well established and its accuracy is trusted. When the measurement is used to investigate changes due to high power processing, which can be on the order of 1° degree of phase integrated across the structure, understanding errors with the measurement becomes essential. At this level there are many things that may contribute to the accuracy of the measurement including: temperature of the room and structure, stability of RF source in the network analyzer, data analysis techniques,[1] atmospheric pressure, and water vapor content of the air. This paper will address issues of temperature, mechanical vibration and network analyzer stability by using statistical analysis of multiple bead pull's with the goal of quantifying a phase measurement error that can be generalized for future measurements. Atmospheric pressure and humidity will not be addressed since a dry nitrogen purge is used during the measurements.

*Work supported by U.S. Department of Energy, contract DE-AC03-76F00515

TEMPERATURE CONSIDERATIONS

At SLAC we have introduced a commercial water temperature control system to stabilize the structure temperature during the measurement. The system consists of a Thermo Haake DC-30 circulator and temperature control unit along with the Themo Haake K-20 Chiller. The DC-30 is specified to control the water temperature to 0.1° Celcius.

The bead pull measurement is performed with the controller temperature set near the ambient room temperature typically around 20°C. Though the controller is specified to regulate the water temperature to $.1^{\circ}$C, temperature excursions during the measurement on this scale can occur due to the control algorithm of the DC-30. The consequence of the temperature control is a sawtooth variation in temperature data during the bead pull scan. S_{11} data for a non moving bead centered in the last cell of the structure is presented. Phase data is sampled at 5 Hz while temperature data is sampled at 1 Hz.

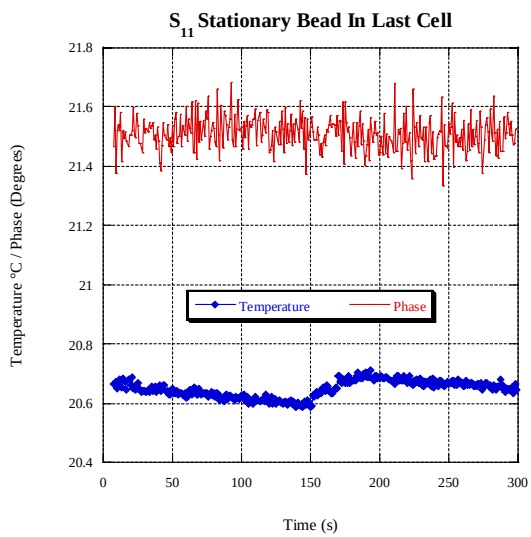

Figure 1:S_{11} phase measurement of a stationary bead in last cell for 5 minute scan.

The Figure 1 data address the phase stability of the bead measurement with the bead in the position where it is most sensitive to temperature and frequency variations. A

LONGITUDINAL BUNCH SHAPE MONITOR USING THE BEAM CHOPPER OF THE J-PARC

F. Naito*, KEK, Tsukuba, Japan

Abstract

We propose the longitudinal bunch shape monitor for the beam from the RFQ of the J-PARC linac. The monitor uses the beam chopper cavity installed in the MEBT line between the RFQ and the DTL of the J-PARC as a kind of the bunch rotator. Consequently the longitudinal bunch shape can be measured along the horizontal direction. If we can measure the energy distribution of the bunch also, the longitudinal emittance of the beam is derived. In the paper, the basic idea of the monitor is being discussed.

INTRODUCTION

The construction of Japan Proton Accelerator Research Complex (J-PARC) has been started in the Tokai campus of the JAERI. The injector linac consists of the radio-frequency quadrupole (RFQ) linac, the drift-tube linac (DTL), the separated DTL (SDTL) and several beam transport lines[1]. The beam from the linac is injected into the rapid cycle synchrotron (RCS) ring. For the beam injection into RCS without beam losses, the beam from the linac has to be chopped before the DTL by a chopper.

The measurement of the beam properties is quite important for the stable beam operation. In particular, the emittance of the beam is one of the most important parameters since the behavior of the beam in the phase space must be compared to the results of the beam dynamics calculation in order to improve the linac system of the J-PARC.

The shape of the 3-MeV beam, emitted from the RFQ, is tuned to be matched to the DTL by the Q-magnets and bunchers in the medium energy beam transport (MEBT) line between the RFQ and the DTL [2].

STRUCTURE OF THE CHOPPER

The chopper cavity is installed in the MEBT. As the chopper deflects the micro bunch in order to chop the beam by rf power, it is an rf deflector (RFD) [3]. The resonant frequency of the chopper cavity is 324 MHz which is the same frequency as that of RFQ and DTL. The chopper consists of two RFD both of which are coupled resonantly[4]. The each micro bunch of the beam is kicked horizontally by the crest of the rf electric field applied to the cavity. The performance of the chopper has been confirmed by using the beam from RFQ [5].

The photograph of the inside of the chopper cavity is shown in figure 1. The principle of the chopper is shown in figure 2. The deflected beam by the chopper is removed by the scraper. Figure 3 shows the layout of the MEBT components which include the chopper and the scraper.

* fujio.naito@kek.jp

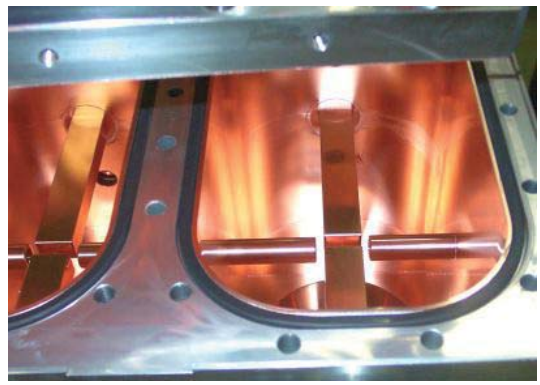

Figure 1: Inside of the chopper.

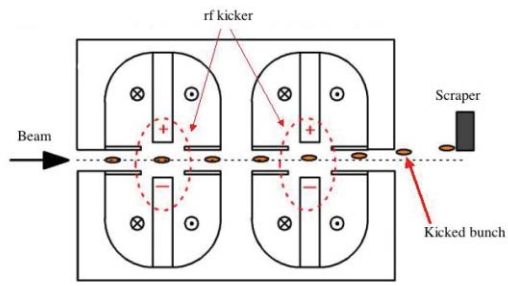

Figure 2: Principle of the chopper.

PRINCIPLE OF THE MONITOR

Measurement of the Longitudinal Bunch Shape

The chopper cavity is a main component of a longitudinal bunch shape monitor we proposed. Because the rf-system of the chopper is very flexible, we can easily use the cavity for another purpose by changing the rf phase. The principle of the bunch shape monitor is following:

1. Shift the rf-phase by $\pm\pi/2$ for the chopper cavity from the normal chopping mode as shown in figure 4. In this case the chopper cavity spreads the longitudinal distribution horizontally. Namely it woks as a kind of the bunch rotator. The middle part of the figure 5 shows the behavior of the bunch;

2. Measure the horizontal shape bunch at the down stream of the chopper by a wire scanner for instance. The measured width has the information about the longitudinal distribution of the micro bunch.

3. Set the slit which limits the bunch horizontal width before the chopper. It increases the spatial resolution for the longitudinal bunch distribution;

MEASURED RF PROPERTIES OF THE DTL FOR THE J-PARC

H. Tanaka#, T. Kato, F. Naito, E. Takasaki, KEK, Tsukuba, Japan
H. Asano, T. Itou, T. Morishita, JAERI, Tokai, Japan

Abstract

RF properties of the second DTL tank for the J-PARC have been measured at KEK. The required flatness and stability of the accelerating field of the second tank have been obtained by the tuning of the post-couplers, whose shapes were modified to tune the resonant frequency to 324MHz. Consequently we have confirmed the following: (1) the achieved flatness of the field is 0.5% in maximum deviation, (2) the stabilized field can bear the perturbation of a 25% tilt of the field distribution.

INTRODUCTION

The J-PARC consists of a 181-MeV linac, a 3-GeV rapid cycle synchrotron and a 50-GeV synchrotron. The 181-MeV injection linac is comprised of an H^- ion source, a radio-frequency quadrupole (RFQ) linac, a drift-tube linac (DTL), a separated DTL (SDTL) and several beam transport lines. The linac will be extended to obtain a 400-MeV beam by adding the annular coupled structure (ACS) linac at the downstream of the SDTL in the next phase of the project.

The Alvarez-type DTL accelerates the H^- ion beam from 3 to 50 MeV. It consists of three independent tanks of which the length is about 9 m. Furthermore each tank is comprised of three short unit tanks (about 3 m in length). The inside diameter of the tank is 560 mm. The resonant frequency is 324 MHz. Each drift tube (DT) accommodates a tunable electromagnetic quadrupole magnet.

At this stage the assembling of all DTs for the DTL-2 and the DTL-3 has been completed. Moreover the first tank (DTL-1) already accelerates a 3 MeV beam from the RFQ up to an energy of 20 MeV at KEK [1]. Some RF properties were already described in the reference [2].

For the second DTL tank (DTL-2), which is designed to accelerate the beam from 20 to 37 MeV, some RF properties have been measured. A uniform accelerating field has been achieved by the fine adjustment of the post couplers and the fixed tuners. The field stabilization by the post-couplers against perturbations has been confirmed also. In order to achieve the stabilized-uniform distribution of the average field at the final target frequency of 324MHz, the following techniques have been applied for the post-coupler tuning: (1) non-uniform insertion length of the post-couplers from the tank wall; (2) increment of diameter of all post-couplers of the wall side.

Furthermore measurements of RF properties of the third tank (DTL-3) which will be used for beam acceleration from 37 MeV to 50 MeV, has been started.

#hirokazu.tanaka@kek.jp

STRUCTURE OF THE DTL-2 AND THE DTL-3

The second DTL tank consists of 42 full-size drift tubes, 42 post-couplers and 10 fixed tuners. Bore diameter of the DT is 22 mm. The third DTL tank consists of 26 full size drift tubes, 26 post-couplers and 8 fixed tuners. Bore diameter of the DT is 26 mm. Both tanks have two movable tuners and two half drift tubes. The layout of the tuners and the input couplers are shown in figure 1. The first and the third unit tanks for the DTL-2 and these for DTL-3 have four and three fixed tuners, respectively. The second unit tank has two fixed tuners and two movable ones. Diameter of the tuner is 90 mm. There are two ports for the input couplers in the tank in order to reduce the RF power per coupler. Each coupler is located at one fourth of the total length from the end plate in order to suppress the excitation of the TM_{011} mode.

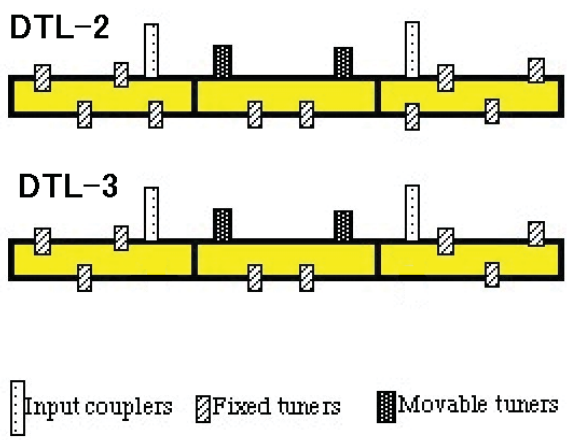

Figure 1: Layout of tuners.

TUNING OF THE DTL-2

Adjustment of the Tuners

The accelerating-field measurement for the DTL-2 has been done by using a bead-pull perturbation technique [3]. Initial field distribution of the TM010 mode without the tuners and the post-couplers is shown by the square marks in figure 2. The ordinate of figure 2 shows the normalized electric field of each gap. The DTL-2 tank has two movable tuners and 10 fixed ones as described above. The length of each fixed tuner was adjusted in order to tune the resonant frequency and to obtain the uniform accelerating field along the beam axis. (During the tuning, the ”fixed” tuners are replaced by the ”movable” model.)

THE TECHNIQUE FOR THE NUMERICAL TOLERANCES ESTIMATIONS IN THE CONSTRUCTION OF COMPENSATED ACCELERATING STRUCTURES

V. V. Paramonov, A.K. Skassyrskaya, INR, 117312 Moscow, Russia

Abstract

The requirements to the cells manufacturing precision and tuning during multi-cells accelerating structures construction came from the required accelerating field uniformity, based on the beam dynamics demands. The standard deviation of the field distribution can be expressed in terms of accelerating and coupling cells frequencies deviations, stop-band width and coupling coefficient deviations. The deviations of the cells frequencies and coupling coefficient can be expressed from 3D fields distributions for accelerating and coupling modes and the cells surface displacements. With the modern software possibilities it can be done separately for every specified part of the cell surface. Finally, the surface displacements are expressed through characteristic cells dimensions deviations. This technique allows both qualitatively to define the critical regions and quantitative to optimize the tolerances definition.

INTRODUCTION

In the multi-cell accelerating structures all time exists the problem of cells identity - to realize the structure design parameters, the cells should be identical within the defined tolerances. The tolerances for cells parameters are directly related to tolerances for geometrical parameters. And the tolerances for cell geometry are directly related to the price (and possibility) of the cavity construction. The cavity mast realize design parameters, so, tolerances can not be too soft. But extremely rigid tolerances lead, at least, to the extra costs in the construction. The tolerances definition is all time the important part in the cavity development.

COUPLED CIRCUIT ANALYSIS

The original demands originate from the beam dynamics, which provides the requirements to the accelerating field distribution - the standard (rms) field deviations in accelerating gaps σ_E or field tilt along the cavity. The relation between σ_E value and deviations in cells rf parameters can be obtained by using well known coupled circuit model [1]. The rms value of the accelerating electric field deviation σ_E is [2]:

$$\sigma_E^2 = \sigma_{E_f}^2 + \sigma_{E_k}^2, \quad \sigma_{E_k}^2 = \sigma_{k_c}^2 \frac{N_p + 2}{3}, \qquad (1)$$

and

$$\sigma_{E_f}^2 \approx \frac{16\sigma_{f_a}^2}{k_c^4}(\sigma_{f_c}^2 \frac{N_p^2 + 3N_p}{12} + (\frac{\delta f}{f_a})^2 \frac{N_p^3 + 4N_p^2 + 6N_p}{3}), \qquad (2)$$

where σ_{f_a} and σ_{f_c} are the rms frequency deviations for the accelerating (f_a) and coupling (f_c) cells, $\delta_f = f_c - f_a$ is the stop-band width, N_p - number of structure periods in the cavity, σ_{k_c} is the rms deviation of coupling coefficient k_c. As it usually is supposed in coupled circuit approach, the influences of δk_c and $\delta f_{a,c}$ on the operating field distribution are independent.

Suppose the cell geometry (the shape and dimensions) are defined with the set of geometrical parameters x_i. Assuming the deviations of different parameters as independent, for relative rms deviations $\sigma_{f_{a,c}}, \sigma_{k_c}$ it is valid:

$$\sigma_{f_{a,c}} = \frac{\sqrt{\sum_i (\frac{\partial f_{a,c}}{\partial x_i})^2 \sigma_{x_i}^2}}{f_{a,c}}, \sigma_{k_c} = \frac{\sqrt{\sum_i (\frac{\partial k_c}{\partial x_i})^2 \sigma_{x_i}^2}}{k_c}, \qquad (3)$$

where $\frac{\partial f_a}{\partial x_i}, \frac{\partial f_c}{\partial x_i}, \frac{\partial k_c}{\partial x_i}$ are the sensitivities of the cell parameters f_a, f_c, k_c with respect the small deviation in the geometrical cell parameter x_i, σ_{x_i} is the rms x_i deviation. The value σ_{x_i} corresponds to the tolerance $\pm 3\sigma_{x_i}$ for the parameter x_i.

To estimate values in numbers, we need in the sensitivities values.

Coupling Coefficient Deviations

Considering k_c deviations, we have to distinguish symmetrical and nonsymmetrical k_c distortions with respect coupling cells. Suppose k_c value of the j-th coupling cell with adjacent $j-1$-th and $j+1$-th accelerating cells has the same deviation δk_c^s. The total coupling between the coupling cell and adjacent accelerating cells remains equal. As it is easy to see from coupled equations, [1], the fields in $j-1$-th and $j+1$-th accelerating cells will be equal.

Estimating k_c deviations, we have to exclude from consideration the symmetrical (with respect coupling cells) parts.

3D NUMERICAL MODELS

The sensitivity values $\frac{\partial f_a}{\partial x_i}, \frac{\partial f_c}{\partial x_i}, \frac{\partial k_c}{\partial x_i}$ depend on the field distributions of both accelerating and coupling cells (modes).

Suppose the structure period has a length $d = 2l, -l \leq z \leq l$, z is the structure axis, and at least the accelerating cells has a plate of mirror symmetry. It means, at $z = \pm l$, in the middles of accelerating cells, one can apply boundary conditions of electric walls (to simulate accelerating mode) or magnetic ones (to simulate coupling mode).

3D fields distributions and frequencies can be calculates for accelerating ($\vec{E}_a, \vec{H}_a, f_a$) and coupling ($\vec{E}_c, \vec{H}_c, f_c$) modes

EFFECT OF THE TUNER ON THE FIELD FLATNESS OF SNS SUPERCONDUCTING RF CAVITIES

An Sun, Oak Ridge National Laboratory, Oak Ridge, TN 37830*
Haipeng Wang, Genfa Wu, Jefferson Lab, Newport News, VA 23606#

Abstract

The field flatness (FF) in a multi-cell superconducting cavity affects not only net accelerating voltage, but also peak surface field [1] and Lorentz detuning coefficient [2]. Our measurements indicate that the tuner's motion changes not only the cavity frequency but also its FF. This field amplitude change is a linear tilt and proportional to the distance between each cell center and the cavity's geometric center. This tilt also changes the coupling of the Fundamental Power Coupler (FPC) and Field Probe (FP) on either side of the cavity. The tilt has been measured and simulated, and is ~20%/MHz on the Spallation Neutron Source (SNS) medium β cavities. The FF change is not only due to the uneven volume change within the cell, but also due to the cell-to-cell coupling.

INTRODUCTION

The FF in a multi-cell cavity can be derived from its original definition [2].

$$\eta_{ff} = \frac{E_{c\max} - E_{c\min}}{\frac{1}{N}\sum_{i=1}^{N} E_{ci}} \times 100\% \qquad (1)$$

Here E_{ci} is the peak axial electric field in the ith cell.

The FF specification for SNS production cavities is less than 8%. The FF was tuned after manufacture at ACCEL and qualified at JLab by the bead-pulling measurement during the cavity tuning. After final cavity etching and rinsing, there is no way to check or correct the FF.

The SNS cavity tuner uses a stepper motor to drive a tuner frame. The frame is seated on the one end of the helium tank to compress the cavity end dish [3]. The resulting frequency tuning range is ~±245kHz for an axial spring distance of 1.8mm.

From our cold (2K) cryomodule measurement, we found that when the tuner changes the cavity's frequency, it also changes the external Q of both fundamental power coupler (FPC) and field probe (FP). After excluding other causes, we concluded that it relates to the relative RF field change at each end cell or the FF has been altered. A later warm bead-pulling measurement and numerical simulations confirmed this speculation.

MEASUREMENT IN CRYOMODULE

The measurements were done on a medium β cryomodule in the Cryomodule Test Facility at JLab. The power transfer function from FPC to FP can be measured by the S21 parameter on a network analyzer. With a stable cryogenic system and a well matched circuit, a -3dB bandwidth of the |S21| resonance peak can lead to a relatively accurate measurement of the external Q of the FPC, (Q_{eFPC}) which is the lowest Q for the coupled superconducting cavity.

Only a relative measurement on S21 is needed [2] to get the external Q of FP Q_{eFP} in order to get the relative FF information.

$$\frac{Q_{eFP}}{Q_{eFP0}} = \frac{Q_{eFPC}}{Q_{eFPC0}} \cdot 10^{\frac{S21-S21_0}{10}} \qquad (2)$$

Here subscript 0 corresponds to the values at the operation frequency of f_0=805MHz. Figure 1 shows this measurement data. It indicates that the field amplitude decreases at the FPC-end cell and increases at the FP-end cell, when the cavity frequency is increased by the tuner stretching the cavity. Supposing the cavity FF (η_{ff}) is perfect at f_0=805MHz (η_{ff}=0), and the electric field tilt is a linear function of frequency as the fits illustrate in Figure 1, then the FF can be expressed as:

$$\eta_{ff} = \frac{\left|\sqrt{Q_{eFPC0}/Q_{eFPC}} - \sqrt{Q_{eFP0}/Q_{eFP}}\right|}{\sqrt{Q_{eFPC0}/Q_{eFPC}} + \sqrt{Q_{eFP0}/Q_{eFP}}} \times 200\% \qquad (3)$$

Figure 2 shows this calculation from Figure 1's data. The FF change can be estimated as ~20%/MHz.

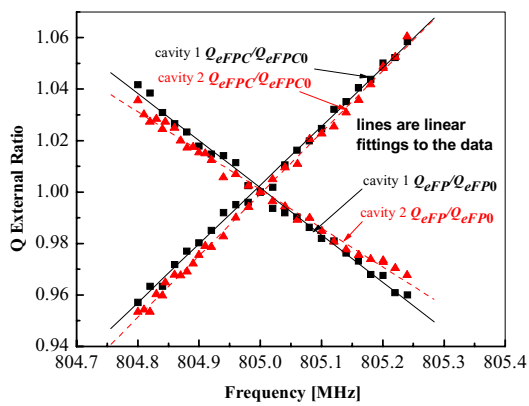

Figure 1: The relative external Q changes on FPC and FP measured on a medium beta cryomodule operated at 2K when tuner changes the cavity frequency.

BEAD-PULL MEASUREMENT

To verify the above result, we did a bead-pull experiment on cavity MB-19 with attached helium vessel to measure axial electric field profiles. To measure the helium vessel effect, we performed the bead-pull on

* Work supported in part by an appointment to the Oak Ridge National Laboratory Postdoctoral Research Associate Program.
# Work supported by the U.S. Department of Energy under contract DE-AC05-00OR22725

A 3D SELF-CONSISTENT, ANALYTICAL MODEL FOR LONGITUDINAL PLASMA OSCILLATION IN A RELATIVISTIC ELECTRON BEAM

Gianluca Geloni, Evgeni Saldin, Evgeni Schneidmiller and Mikhail Yurkov
Deutsches Elektronen-Synchrotron (DESY), Notkestrasse 85,
22607 Hamburg, Germany

Abstract

Longitudinal plasma oscillations are becoming a subject of great interest for XFEL physics in connection with LSC microbunching instability [1] and certain pump-probe synchronization schemes [2]. In the present paper we developed the first exact analytical treatment for longitudinal oscillations within an axis-symmetric, (relativistic) electron beam, which can be used as a primary standard for benchmarking space-charge simulation codes. Also, this result is per se of obvious theoretical relevance as it constitutes one of the few exact solutions for the evolution of charged particles under the action of self-interactions.

INTRODUCTION

Longitudinal space-charge oscillations have been treated only from an electrodynamical viewpoint, or using limited one-dimensional models: in this paper we report a fully self-consistent solution to the initial value problem for the evolution of a relativistic electron beam under the action of its own fields in the (longitudinal) direction of motion. The beam is accounted for any given radial dependence of the particle distribution function. For a more detailed description of our work and references see [1]. An initial condition is set so that the beam, which is assumed infinitely long, is modulated in energy and density at a given wavelength. When the amplitude of the modulation is small enough the evolution equation can be linearized. An exact solution can be found in terms of an expansion in (self-reproducing) propagating eigenmodes.

Our theoretical findings constitute one of the few exact solutions known up to date to the problem of particles evolving under the action of their own fields. Yet, particle accelerator and FEL physics make large use of simulation codes to deal with space-charge fields, and these codes are benchmarked against exact solutions of Poisson equation only; recently partial attempts based on one-dimensional theory (which can only give some incomplete result) have been made to benchmark them against some analytical model accounting for the system evolution. We claim that our findings can be used as a standard benchmark for any space-charge code from now on. Our results are of relevance to an entire class of practical problems arising in state-of-the-art FEL technology when (optically) modulated electron beams are feed into an FEL (optical seeding or certain two-color pump-probe schemes): given the parameters of the system, plasma oscillations turn out to be an effect to be accounted for. It is also important to mention the relevance of plasma oscillation theory in the understanding of practical issues like longitudinal space-charge instabilities in high-brightness linear accelerators which may lead to beam microbunching and break up.

[1] E. Saldin et al. Longitudinal Spacs Charge Driven Michrobunching instability in TTF linac, TESLA-FEL-2003-02, May 2003

[2] J. Feldhaus et al. Two-color FEL amplifier for femtosecond-resolution pump-probe experiments with GW-scale X-ray and optical pulses DESY 03-091, July 2003

THEORY

We describe longitudinal plasma waves in a relativistic electron beam assuming that transverse coordinates enter as parameters in the description of fields and particle distribution. Our beam is initially modulated at some wavelength λ_m, in density and energy. It is natural to define the phase $\psi = \omega_m\,(z/v_z(\mathcal{E}_0) - t)$, where $v_z(\mathcal{E}_0) \sim c$ is the longitudinal electron velocity at the nominal beam kinetic energy $\mathcal{E}_0 = (\gamma - 1)mc^2$, $\omega_m = 2\pi v_z/\lambda_m$, t is the time and z the longitudinal abscissa. We operate in energy-phase variables (P, ψ), P being the deviation from the nominal energy.

A small energy deviation P is assumed; then the equations of motion for our system can be interpreted as Hamilton canonical equations corresponding to the Hamiltonian $H(\psi, P, z) = e\int d\psi E_z + \omega_m P^2/(2c\gamma_z^2\mathcal{E}_0)$. The bunch density distribution is then represented by $f = f(\psi, P, z; \boldsymbol{r}_\perp)$. Linearization of the evolution equation for f is possible when $f(\psi, P, z; \boldsymbol{r}_\perp)_{|z=0} = f_0(P; \boldsymbol{r}_\perp) + f_1(\psi, P, z; \boldsymbol{r}_\perp)_{|z=0}$, f_0 being the unperturbed solution of the evolution equation with $f_1 \ll f_0$ for any value of dynamical variables or parameters. Moreover we assume $f_0(P; \boldsymbol{r}_\perp) = n_0(\boldsymbol{r}_\perp)F(P)$, where the local energy spread function $F(P)$ is normalized to unity. The initial modulation can be written as a sum of density and energy modulation terms: $f_1(\psi, P, z; \boldsymbol{r}_\perp)_{|z=0} = f_{1d}(\psi, P; \boldsymbol{r}_\perp) + f_{1e}(\psi, P; \boldsymbol{r}_\perp)$ where $f_{1d}(\psi, P, z; \boldsymbol{r}_\perp) = a_{1d}(\boldsymbol{r}_\perp)F(P)\cos(\psi)$ and $f_{1e}(\psi, P, z; \boldsymbol{r}_\perp) = a_{1e}(\boldsymbol{r}_\perp)dF/dP\cos(\psi + \psi_0)$. Here ψ_0 is an initial (relative) phase between density and energy modulation. Finally it is convenient to define complex quantities $\tilde{f}_{1d} = a_{1d}F$, and $\tilde{f}_{1e} = a_{1e}(dF/dP)e^{i\psi_0}$ so that $f_{1_{|z=0}} = (\tilde{f}_{1d} + \tilde{f}_{1e})e^{i\psi} + CC$. Further definition of $\tilde{E}_z = \tilde{E}_z(z; \boldsymbol{r}_\perp)$ in such a way that $E_z = \tilde{E}_z e^{i\psi} + \tilde{E}_z^* e^{-i\psi}$ allows one to write the Vlasov equation linearized in $\tilde{f}_1$:

$$\frac{\partial \tilde{f}_1}{\partial z} + i\frac{\omega_m P}{c\gamma_z^2\mathcal{E}_0}\tilde{f}_1 - e\tilde{E}_z\frac{\partial f_0}{\partial P} = 0\,. \qquad (1)$$

Let us now introduce the longitudinal current density $j_z(z; \boldsymbol{r}_\perp) = -j_0(\boldsymbol{r}_\perp) + \tilde{j}_1 e^{i\psi} + \tilde{j}_1^* e^{-i\psi}$, where $j_0(\boldsymbol{r}_\perp) \simeq$

COLD TESTS OF A 160 MHZ HALF-WAVE RESONATOR

R.Stassen#, R.Eichhorn, F.M.Esser, B.Laatsch, R.Maier, G.Schug, H.Singer, FZ Juelich, Germany

Abstract

A new linac was projected based on superconductive half-wave resonators to fill the COoler SYnchrotron COSY Juelich up to the space charge limit.

The first prototype of a 160 MHz HWR has been built and tested. RF measurements in CW as well as in a pulsed operation will be presented. A second prototype with a slightly different way of fabrication will be completed soon.

All measurements have been performed using the 4 kW loop-coupler that was here developed especially for the HWR linac. The use of a cold window allows to change the coupling from $1*10^6$ to $1*10^{10}$ without any risk of contamination. The mechanical tuner consisting of a stepper-motor-driven coarse tuner and a fast piezo system has successfully integrated into the vertical test-cryostat. The piezos also allow to compensate for the Lorentz-force detuning.

HALF-WAVE RESONATORS

The design of the HWRs was dominated by the parameters of a linac concept to fill the synchrotron COSY at FZ-Juelich with polarized protons and deuterons up to the space charge limit [1].

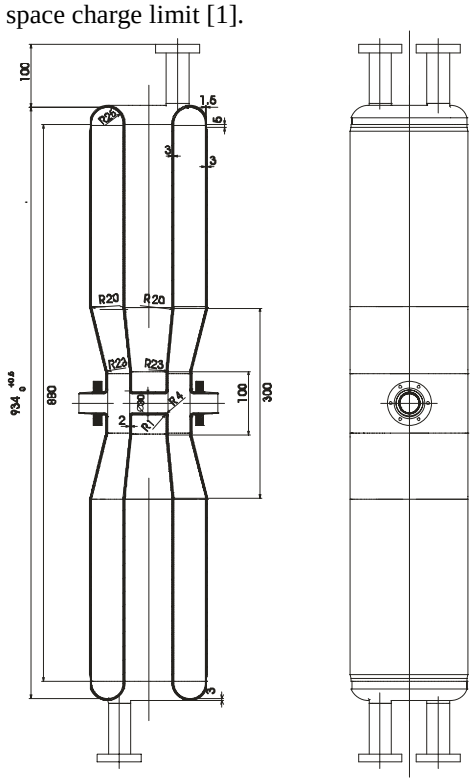

Figure 1: Layout of 160 MHz HWR.

Two prototypes had been ordered at different companies and show slight changes basically at the end-plates (fig. 2). These changes have no impact on the cavity parameters that are summarized in table 1.

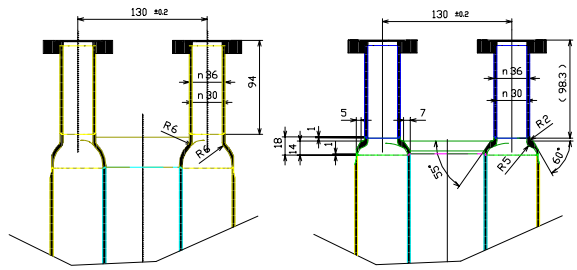

Figure 2: Different end-plate geometries of the HWRs.

Table 1: Main parameters of 160 MHz HWRs related to an accelerating length of $l = ß\lambda$

β	0.11
R/Q in Ohm	249
B_{peak}/E_{avg} in mT/MV/m	10.4
E_{peak}/E_{avg}	4.2
E_{avg} in MV/m peak	8

The first prototype of the 160 MHz HWRs was tested at room temperature prior to any chemical treatment. Figure 3 shows the good conformity of the field profiles measured and calculated by the simulation tool CST-MicroWaveStudio MWS [2].

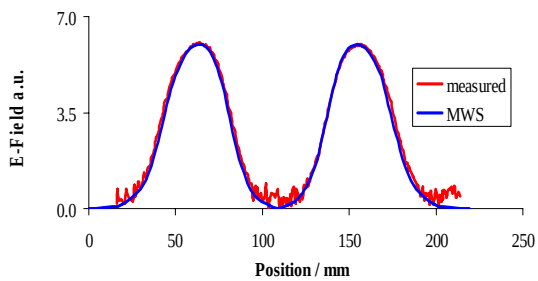

Figure 3: Field profiles, measured and calculated.

The measurements of the resonant frequency during the production process and each step towards operation (like pumping, cool-down and tuning-sensitivity) agree to the simulations [3].

Coupler

The coupler design differs from normally used concepts for superconducting cavities. One of the cavity access-ports, which are required for a good preparation of the cavity surface, has been chosen to hold the RF main coupler. The coupling is essentially magnetic via a current loop. It is variable and has been designed to match the beam-current as well as the unloaded cavity for an on-line

#r.stassen@fz-juelich.de

Electro Polishing of Niobium Cavities at DESY

A.Matheisen, L. Lilje, H.Morales, M.Schmökel, B. Petersen, N. Steinhau-Kuehl,
Deutsches Elektronen Synchrotron DESY, Hamburg, Notkestraße 85, 22602 Hamburg, Germany

Abstract

At DESY a facility for electro polishing (EP) of the super conducting (s.c.) TESLA/TTF cavities has been built and is operational since summer 2003. The EP infrastructure is capable to handle single - cell structures and the standard TESLA/ TTF nine - cell cavities.
Several electro polishing processes have been made since and acceleration voltage up to 40 MV/m have been reached in nine cell structures. We report on measurements and experiences gained since 2003 as well as on handling procedures developed for the preparation of electro polished resonators. Specific data like heat production, variation of current density and bath aging will be presented. Another important point for reproducible results is the quality control of the electro polishing process.

INTRODUCTION

At DESY an electro-polishing stand (EPS) was built in 2003 [1;2;3]. According to the good experiences gained with electro polishing (EP) at KEK and CERN, constant voltages and a mixture of 9 volume parts of sulphuric acid (96%) and 1 part fluoric acid (48%) are chosen for the baseline parameters set of the EP process [3].
A total of 14 cavities are electro polished since summer of 2003. Voltages of 14 to 18 V have been tested. The well-established handling procedures for cavities processes with buffered chemical polishing (BCP) had to be changed to meet the needs of EP resonators. On three single cell and one 9-cell resonator acceleration voltages up to 40 MV/m are reached using the DESY EP set up and adapted handling procedures. During the EP processes all relevant parameters are monitored and stored for documentation. From these data set's a first analysis is made to find system parameters, gain online analysis of the process and find parameter sets for reproducible high gradient resonator preparation.

ELECTRO POLISHING INFRASTRUCTURE

The DESY EP set-up (EPS) is designed as a closed loop acid circuit with one acid supply barrel of about 150 –180 l storage volume, the cavity rotating horizontally on the EPS bench and a heat exchanger in line [1]. The acid is pumped into the resonators via the pure aluminium cathode and is distributed homogenously into the 9 cells via holes with adopted diameters. Main parameters to determine the EP process are the acid volume sent into the resonator (Q), the temperature at the inlet of the electrode (T3), the temperature at the cavity outlet (T4), the current (I) and the current oscillation (dI).

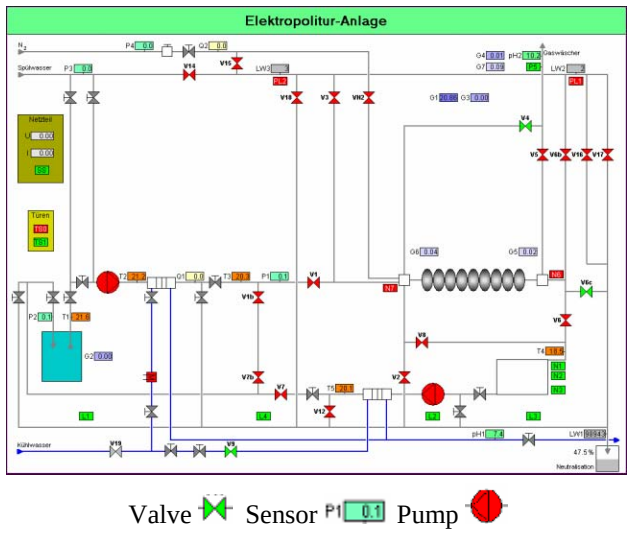

Figure 1: Flow chart of the DESY electro polishing infrastructure.

All other are Sensors are mainly installed to control the safety of the system and the automated process sequences [2] (Figure 1).

PROCEDURES

The procedures in use for processing the EP cavities are close to the once, which are well established for BCP cavities [6]. For safety reasons the EPS is located outside of the DESY TTF cleanroom. To enter the cleanroom after EP, the cavities have to under go an additional cleaning procedure by rough outside surface cleaning (solvent + DI water rinse at 80 bars pressure), ultrasonic cleaning and rinsing with ultra pure water (R=>18 Mohm cm, particle filtered to <= 0,2 µm). The number of high-pressure water (HP) rinses, following the assembly procedure, is increased from 2 to 6 rinses. Assembly and RF test at 2 K as well as heat treatment at 800 C resp. 1400 C (post purification) are identical to the standard BCP treatments. Up to now no technical solution for EP of cavities dressed with the helium vessel is available. The procedures for tank welding and tuning of cavities are modified and are still under investigation and optimization. The cavities, vented to normal pressure by argon gas are sealed inside the cleanroom and stay hermetically closed during electron beam welding (Nb cone to Ti connections) as well as during tuning of the field profile and tank welding by TIG weld. Major item developed for this process is a new flange system with

OVERVIEW OF LINEAR COLLIDER TEST FACILITIES AND RESULTS

H. Hayano, High Energy Accelerator research organization (KEK), Tsukuba, Japan

Abstract

In order to promote realization of Linear Collider (LC), the formation of international co-operation for unified LC design and efficient R&D share are thought to be necessary. As a first step of this co-operation, the International Technology Recommendation Panel (ITRP) will recommend a technology for the global LC design to the International Linear Collider Steering Committee (ILCSC). Towards this recommendation, many efforts of the developments and the output results of each technology have been made to satisfy the requirements of the technical review committee report (TRC)[1]. The test facilities of each LC design are the place of the key technology demonstration and realization. The summarized overview of the LC test facility activities and outputs of TTF, NLCTA, ATF&GLCTA and CTF will give information of LC technology direction.

INTRODUCTION

Major laboratories in the world began to start LC developments in late 1980s. LC workshop and many related workshop have been held from that time, having R&D information exchange and design review. After about 15 years R&D, LC designs of each laboratory became more realistic based on the demonstrations of technologies in their test facilities. The test facilities in this overview are the active facilities conducted by the leading laboratories. By the order of the main linac frequency, TTF (TESLA Test Facility) conducted by DESY, NLCTA (NLC Test Accelerator) conducted by SLAC, ATF (Accelerator Test Facility)&GLCTA (GLC Test Accelerator) conducted by KEK, and CTF (CLIC Test Facility) conducted by CERN, are briefly summarized in this text.

TESLA TEST FACILITY (TTF)

The TTF at DESY includes infrastructure labs and shops for superconducting cavity treatment, test stands and the accelerator module assembly and a test linac for an integrated system test of the TESLA[2] accelerator prototype with beam. The functions of this facility are development of accelerating module compatible to TESLA, integrated system test of the TESLA linac components with beam and application of SASE FEL in the VUV wavelength regime[3]. The performance of the TESLA superconducting cavities are well advanced by the electro-polishing (EP) processing as well as chemical etching of the inner surfaces, high temperature treatment at 1400degC, and high pressure rinsing with ultra-pure water. The design gradient 23.8 MV/m has been attained on average with cavities of the standard treatment. By application of new EP method to 9-cell cavities, another 6 cavities have reached gradients between 31 and 35 MV/m. Some of them are assembled into the TTF cryomodule. TTF linac is now in the phase 2 stage construction, which is planned for 2μm emittance, 1nC electron beam by upgraded laser-driven photocathode RF gun, 1 GeV acceleration by 6 cryomodules each containing 8 superconducting 9 cell cavities, and 50μm RMS bunch length by 2 stage bunch compressors. A 6.4nm wavelength FEL light will be generated by modified 27m undulator magnets, and will be transported to the downstream user experimental area. The photocathode RF gun injector is capable of delivering bunch trains with parameters very close to the TESLA linear collider specifications in terms of beam current and pulse length. It also delivers bunches with sufficiently low emittance for successful operation of the FEL. The TTF-I program is being concluded in autumn 2002. The last tests are devoted to one more accelerator module (named module 1*, because it is the original module 1 equipped with new cavities), which is expected to yield an average accelerating gradient of 25 MV/m, and to a beam test with a first version of the so-called superstructure concept. In a superstructure, two cavities are fed with RF power by a single coupler, which saves length (the fill factor is increased by 6% in comparison with the present TTF modules) and cost by reducing the number of couplers. First beam tests with two superstructures at a gradient of 15 MV/m have been performed successfully, proving the principle of this concept and confirming very satisfactory damping of higher order modes in the structures. After completion of that experimental program, the linac is lengthened by three more modules (two of which contain only cavities which have reached 25 MV/m or more on the test stand) in an already completed additional tunnel, and the FEL installations is modified to prepare for phase 2 (TTF-II) of the user facility, commissioning of which will begin in the second half of 2004[4].

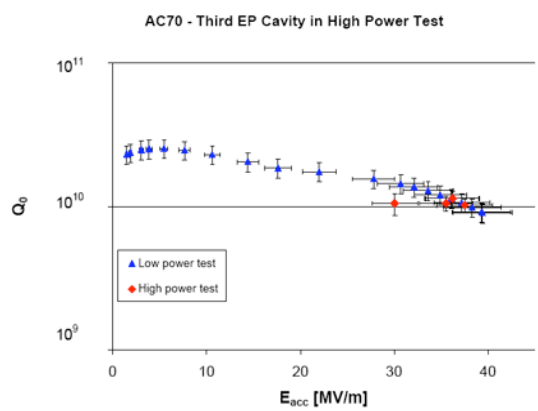

Figure 1: 35MV/m result of AC70 EP cavity.

MUON IONIZATION COOLING EXPERIMENT (MICE)*

M. S. Zisman†, LBNL, Berkeley, CA, 94720, USA, for the MICE Collaboration

Abstract

There is presently considerable activity worldwide on developing the technical capability for a "Neutrino Factory" based on a muon storage ring and, later, a muon collider. Muons are obtained from the decay of pions produced when an intense proton beam hits a high-Z target, so the initial muon beam has a large 6D phase space. To increase the muons' phase-space density (i.e., decrease the emittance), we use ionization cooling, which is based on energy loss in an absorber, followed by re-acceleration with high-gradient, normal-conducting RF cavities. A superimposed solenoidal focusing channel contains the muons. The international MICE collaboration will demonstrate ionization cooling in a short section of a realistic cooling channel, using a muon beam at Rutherford Appleton Laboratory (RAL). We will measure the cooling effects of various absorber materials at several initial emittance values using single-particle measurement techniques. The experiment layout and goals are discussed, as is the status of component R&D.

INTRODUCTION

It is now widely believed that a Neutrino Factory based on a muon storage ring will be the most effective tool to probe the physics of the neutrino sector. Depending on the values of presently unknown parameters, it may also offer the first means to observe charge-conjugation–parity (*CP*) violation in the lepton sector. Scientific results from a Neutrino Factory will test theories about neutrino masses and oscillation parameters, and thus provide important information for both particle physics and cosmology.

A high-performance Neutrino Factory—one capable of delivering roughly 4×10^{20} ν_e aimed at a remote detector in a 10^7 s "year"—depends on ionization cooling of the muon beam. As will be described below, this cooling process involves straightforward physics, but the technique has not been experimentally demonstrated. As a Neutrino Factory is expected to be an expensive facility, it is highly appropriate to carry out a demonstration of this key principle.

The cooling demonstration we propose aims to:

- design, engineer, and build a section of cooling channel capable of giving the desired performance for a Neutrino Factory
- place this apparatus in a muon beam and measure its performance in a variety of operating modes and beam conditions

*Work supported by U.S. Dept. of Energy, Office of High Energy Physics, under contract no. DE-AC03-76SF00098.

†mszisman@lbl.gov

The experiment will verify that our design tools (simulation codes) agree with observations. This will give confidence that we can optimize the design of an actual facility. No matter what configuration we test today, it is likely that there will be changes made before construction of a Neutrino Factory facility actually begins. Validating the design tools will permit their use in someday developing a full proposal for a Neutrino Factory. It is important to note, however, that this approach depends on both the equipment being tested and the simulation codes being as realistic as possible. Thus, full engineering details of all components must be included in the simulations—a nontrivial task.

The main challenge of MICE is that, for cost reasons, we use only a single cell of a cooling channel, which means that the expected cooling effect is small, about 10%. We therefore wish to measure the emittance reduction to a precision of about 10^{-3}. Other challenges include:

- operating high-gradient RF cavities in a solenoidal field and with field terminations (windows or grids)
- safely operating LH_2 absorbers with very thin windows
- integration of cooling channel components while maintaining functionality

Fortunately, these challenges are being worked on via R&D activities that fall outside of MICE, mainly carried out by the U.S. Neutrino Factory and Muon Collider Collaboration (MC).

NEUTRINO FACTORY INGREDIENTS

A Neutrino Factory is a relatively complex facility. It starts with a proton driver capable of providing a MW-level beam directed at a production target, such as a Hg-jet. Pions from the interaction are captured into a solenoidal decay channel, where they decay to muons. The muon beam is then bunched and "phase rotated" to reduce its energy spread (effectively exchanging energy spread for bunch length). Thereafter, an ionization cooling channel is used to reduce the transverse emittance of the beam. This is the aspect that is the focus of this paper. After cooling, the muon beam is rapidly accelerated to its final energy by means of Recirculating Linear Accelerators (RLAs) or Fixed-Field Alternating Gradient (FFAG) machines. Finally, the muon beam is injected into a storage ring where it circulates for about 500 turns. A long straight section of the ring is oriented toward a neutrino detector located several thousand kilometers from the accelerator site.

STATUS OF THE SNS* LINAC: AN OVERVIEW

N. Holtkamp, ORNL, Oak Ridge, TN 37831, USA

Abstract

The Spallation Neutron Source (SNS) is a second generation pulsed neutron source and under construction at Oak Ridge National Laboratory. The SNS is funded by the U.S. Department of Energyís Office of Basic Energy Sciences and is dedicated to the study of the structure and dynamics of materials by neutron scattering. A collaboration composed of six national laboratories (ANL, BNL, TJNAF, LANL, LBNL, ORNL) is responsible for the design and construction of the various subsystems. With the official start in October 1998, the operation of the facility will begin in 2006 and deliver a 1.0 GeV, 1.4 MW average power proton beam with a pulse length of approximately 700 nanoseconds on a liquid mercury target sixty times a second. The multi-lab collaboration allowed access to a large variety of expertise in order to enhance the beam power delivered by the accelerator by almost an order of magnitude compared to existing neutron facilities. The SNS linac consists of a combination of room temperature and superconducting structures and will be the first pulsed high power sc linac in the world. The challenges and the achievements will be described in the paper.

GENERAL PROJECT OVERVIEW

The Spallation Neutron Source (SNS) [1, 2], authorized for construction in fiscal year 1999, is 85% complete. The accelerator, Central Laboratory and Office Building (which includes the central control room) and the Center for Nanophase Material Sciences (CNMS), are shown in Figure 1. The Joint Institute for Neutron Sciences (JINS) will be operated in conjunction with the University of Tennessee in support of the users program. CNMS is one out of five nanophase science centers under construction in the United States.

Currently, all of the SNS accelerator-associated buildings and tunnels are completed with installation and staged commissioning of the accelerator components ongoing. The project goal for SNS is to deliver a proton beam of up to 1.4-MW beam power to a mercury target for neutron spallation. Longer term, higher beam power operation by increasing the beam energy and doubling the user access with a second target station is envisioned as summarized in DOEís 20 year outlook of science facilities for the future [3]. These upgrades are incorporated in the site layout with an identified area for the second target station. Also, empty spaces in the tunnel allow for installation of an additional nine cryomodules to increase the energy to more than 1.3 GeV. The accelerator systems, basically a full-energy injector linac and an accumulator ring, operate at a repetition rate of 60 Hz and an average current of 1.6 mA. The accelerator systems consist of a negative hydrogen (H-) RF volume source; a low-energy beam transport (LEBT) housing a first-stage beam chopper; a 4-vane RF quadrupole (RFQ) for acceleration up to 2.5 MeV; a medium-energy beam transport (MEBT) housing and a second-stage chopper; a 6-tank drift-tube linac (DTL) up to 87 MeV; a 4-module coupled-cavity linac (CCL) up to 186 MeV and a superconducting linac (SCL) with 11 medium-β cryomodules (up to 379 MeV) and 12 high-β cryomodules (up to 1000 MeV). The linac produces a 1 msec long, 38 mA peak, chopped beam pulse at 60 Hz for accumulation in the ring. A high-energy beam

Figure 1: The photograph shows the SNS site with the finished accelerator facilities in the upper left and the Target building, Central Laboratory Office and the Center for Nanophase Material sciences in the foreground, with civil construction still ongoing.

Table 1: Summary of SNS Facility Parameters

Proton beam energy on target	1.0	GeV
Proton beam current on target	1.4	mA
Proton beam power on target	1.4	MW
Pulse repetition rate	60	Hz
Beam macropulse duty factor	6	%
H- peak current from front end	>38	mA
Aver. current per macropulse	26	mA
Chopper beam-on duty factor	68	%
Linac length, incl. front end	335	m
Ring circumference	248	m
Ring fill time	1	ms
Ring extraction gap	250	ns
Protons per pulse on target	1.5×10^{14}	
Liquid mercury target	18 tons	1 m^3
Number of moderators	4	
Minimum initial instruments	8	

* SNS is managed by UT-Battelle, LLC, under contract DE-AC05-00OR22725 for the U.S. Department of Energy. SNS is a partnership of six national laboratories: Argonne, Brookhaven, Jefferson, Lawrence Berkeley, Los Alamos and Oak Ridge

OVERVIEW OF HIGH-BRIGHTNESS ELECTRON GUNS*

J.W. Lewellen, Argonne National Laboratory, Argonne, IL, USA†

Abstract

In most electron linear accelerators, the beam brightness is set by the beam source. It is very difficult to improve the overall beam brightness after it has been produced; on the other hand, providing a brighter beam source can provide an "instant upgrade" to the performance of a brightness-limited electron-linac-based facility. The development and routine operation of high-brightness guns, therefore, is critical to the success of next-generation linac-based light sources. This includes sources already under construction, as well as proposed and as-yet completely theoretical machines.

In recent years, other potential applications of high-brightness electron beams have been identified, including high-average-power IR and UV free-electron lasers, and (relatively) high-energy electron microscopes.

The source requirements are discussed for these application areas, along with a description of some sources currently under development to meet those requirements.

AREAS OF INTEREST

High-brightness electron gun development can be broadly categorized into four distinct categories. Injectors for national facility-scale linac-based light sources represent one broad category. This includes both x-ray free-electron lasers and energy-recovery linacs; the main differences lie in the required beam repetition rates, as the desirable single-bunch characteristics are quite similar.

Second, there is presently strong interest in the use of small energy-recovery linacs to provide beams for high-power IR and UV free-electron lasers. The injectors for this category of device generally have (relatively) relaxed transverse emittance requirements, strong longitudinal emittance requirements, and very high (~ 1 A) average beam current requirements.

Third, a tantalizing possibility is the use of high-brightness injectors for use as electron microscope beam sources. Typical electron microscope beams have excellent emittance but very low (tens of keV) beam energies; among other things, this limits the depth of the sample that can be studied in transmission electron microscopes (TEMs). A high-energy (500 kV–5 MeV) electron gun, if transverse emittance and energy spread requirements can be met, represents a very interesting possible path towards dramatically expanding existing capabilities.

Finally, electron beam sources for next-generation linear colliders represent a combination of several fascinating challenges. The ability to produce a "flat" beam with a high transverse emittance ratio could at worst reduce the requirements on the e^- linac damping ring, and at best eliminate the need for one altogether. There is also a strong interest in developing photoinjectors capable of producing beams of polarized electrons.

* This work supported by the U.S. Department of Energy, Office of Basic Energy Sciences, under Contract No. W-31-109-ENG-38.

† Lewellen@aps.anl.gov

LINAC-BASED LIGHT SOURCES

The next generation of x-ray user facilities are widely seen as being driven by electron linacs, rather than storage rings. Thus, the electron beam source will be of critical importance to the performance of the facility.

In general, one can consider improving an x-ray source by increasing the flux (photons/s), the average or peak brightness, the coherence, or the temporal structure of the radiation pulse.

Linac-based light sources will probably offer the greatest potential enhancements in peak (and, to an extent, average) brightness, coherence, and temporal structure. They can be roughly categorized depending on whether the source provides spontaneous undulator radiation at a large number of photon beamlines, or uses a gain mechanism to provide coherent radiation at a relatively few number of photon beamlines. The former will be referred to as storage-ring replacements (SRRs), while the latter are known as x-ray free-electron lasers (X-FELs).

Although most future facilities will probably encompass combinations of these two basic categories of machines, the injector requirements can be derived separately. This is done more thoroughly in [1]; a synopsis is presented here.

For X-FEL injectors, we require the LCLS wavelength performance at the minimum practical electron beam energy, given present undulator technology. For storage-ring replacement injectors, we require a factor of at least 100 times peak brightness increase over existing third-generation storage rings such as the APS or ESRF.

X-ray Free-Electron Lasers

The equation relating the operational wavelength of a free-electron laser (FEL) to the electron beam energy and undulator parameters is

$$\lambda = \lambda_u \frac{1+\tfrac{1}{2}K^2}{2\gamma^2}, \qquad (1)$$

where λ is the photon wavelength generated, λ_u is the undulator period, γ is the electron beam Lorentz factor, and K is the normalized undulator magnetic field strength. K scales with λ_u as well as the on-axis undulator field.

To minimize the overall length of the accelerator Eq. (1) implies that one should minimize λ_u and K; this results in the smallest possible electron Lorentz factor for a given wavelength. Given practical limits on undulator

ACCELERATOR CONTROL AND GLOBAL NETWORKS – STATE OF THE ART*

D. Gurd, SNS, ORNL/LANL, Oak Ridge, TN, USA

Abstract

As accelerators increase in size and complexity, demands upon their control systems increase correspondingly. Machine complexity is reflected in complexity of control system hardware and software and careful configuration management is essential. Model-based procedures and fast feedback based upon even faster beam instrumentation are often required. Managing machine protection systems with tens of thousands of inputs is another significant challenge. Increased use of commodity hardware and software introduces new issues of security and control. Large new facilities will increasingly be built by national (e.g. SNS) or international (e.g. a linear collider) collaborations. Building an integrated control system for an accelerator whose development is geographically widespread presents particular problems, not all of them technical. Recent discussions of a "Global Accelerator Network" include the possibility of multiple remote control rooms and no more night shifts. Based upon current experience, observable trends and rampant speculation, this paper looks at the issues and solutions - some real, some probable, and some pie-in-the-sky.

INTRODUCTION

The phrase "state-of-the-art" can mean either of two quite different things. Whereas literally it describes current practice, it is also often used to describe "cutting edge" concepts, perhaps not yet quite ready for prime time. This paper will discuss some trends in accelerator controls which may be expected to lead from current practice to practical systems of the future.

Three main factors drive developments in accelerator control: the ever increasing scale and complexity of accelerators themselves; their ever more demanding reliability requirements and the fast pace of technology change in our discipline. Trends can be discerned by following the proceedings of the biennial accelerator controls conferences – The International Conference on Accelerator and Large Experimental Physics Controls Systems (ICALEPCS). Last year's conference was held in Gyeongju, Korea, and next year's is scheduled for Geneva, Switzerland. Many of the observations in this discussion are derived from those conferences. Although this conference is focused on linacs, the techniques and technology of linac control systems do not differ significantly from those applied to circular machines, and the following discussion applies equally to both.

* Work supported by the US Department of Energy under contract DE-AC05-00OR22725

THE CONTROLS "STANDARD MODEL"

For many years, the controls community has referred to a "Controls Standard Model." Although this three-layer distributed model has evolved in the details of its various implementations, it has remained surprisingly constant for over a decade. A good example, drawn from the LHC Design Report, is the architectural representation of the LHC control system shown below in figure 1. The three layers are known respectively as the "presentation" tier, the "application" or "server" tier and the "resource" tier.

Although well-established institutions (DESY, CERN, SLAC, BNL, Fermilab, etc) have built new facilities based upon this standard model but using legacy control system tools and technologies, it is not an exaggeration to suggest that the last decade has been dominated by the use of EPICS – the Experimental Physics and Industrial Control System [1] – developed jointly by Los Alamos National Laboratory and Argonne National Laboratory and embracing the contributions of many collaborators. The EPICS collaboration includes well over 100 licensees, and most "green-field" facilities started in the past ten years – including KEKB, SNS, ISAC at TRIUMF, SLS and Diamond – have opted to use EPICS, benefiting from a reliable, high-performance base and well-defined user interfaces that allow easy interfacing and widespread sharing of locally-developed applications and embellishments. As many as 50% of papers presented at recent ICALEPCS meetings come from the EPICS community, and the semi-annual EPICS collaboration meetings sometimes draw over one hundred participants. More recently, EPICS, which had been available free only to not-for-profit institutions and two competitively licensed companies, has been released as open software and distributed to industries and individuals, expanding its use even further. Several companies advertise products and instruments with EPICS drivers, and industry has been successfully contracted by SNS, SLS and others to develop EPICS-based subsystems for integration into otherwise home-built systems.

EPICS represents one possible approach to implementation of the standard model. Although EPICS users select from a variety of available tools, all implementations have two things in common – a communication protocol known as "Channel Access" and a common distributed database design. Without these it isn't EPICS; but after these almost anything goes. EPICS continues to be selected for new machines because its open architecture allows the use of modern (state-of-the-art) technology at all levels. Channel Access is layered upon the Ethernet TCP/IP protocol, and so EPICS has benefited from the ever-improving performance and cost

STATUS OF HIGH-POWER TESTS OF DUAL MODE SLED-II SYSTEM FOR AN X-BAND LINEAR COLLIDER*

Sami G. Tantawi, Christopher D. Nantista, Valery A. Dolgashev, SLAC, Menlo Park, CA94025

Abstract

Future linear colliders and accelerators require rf systems and components that are capable of handling multi-hundred-megawatt peak power levels at X band frequencies and higher. We present a set of RF components capble of handling these levels of powers. We also present a system implementation that uses these components. We carry out all of the RF manipulations in more easily handled over-moded rectangular waveguide. We present a smooth transition from circuilar to rectangular waveguide. This transition is perfected for two modes simultaneously. We show a set of rectangular overmoded components that can handle the same two modes simultaneously. Using these sets of components we constructed a fully dual moded rf pulse compression system. The system has produced 400 ns flat-top rf pulses of greater than 500 MW at 11.424 GHz. The system ran for hundreds of hours. After 39 million pulses the system tripped only 14 times; indicating the high reliability of these sets of components.

INTRODUCTION

Recently, ultra-high-power rf systems at X-band and above have received a lot of attention in different laboratories around the world because of the desire to design and construct a future linear collier. For a review of these activities the reader is referred to [1-2]. These systems are required to generate and manipulate hundreds of megawatts. Standard rf components that have been in use for a long time such as waveguide bends, directional couplers and hybrids, cannot be used directly because of peak field considerations. Usually, these components are made with oxygen-free high-conductivity copper and the operation takes place under ultra-high vacuum conditions. Experimental work at X-band showed that peak electric fields should not exceed 500 kV/cm [3]. Peak magnetic field should be limited so that the pulsed surface heating does not exceed 30 C^o [4].

To reduce the losses and to enhance the power handling capabilities one must use overmoded waveguides. Manipulating rf signals in highly overmoded waveguide is not trivial. With even simple functions, such as bends, the designs are quite complicated in order to insure the propagation of a single mode without losses due to mode conversion to other modes.

Also, most proposed designs for future linear colliders contain long runs of waveguides. In X-band room temperature designs, these runs are on the order of 100 km or more. To reduce the length of these waveguides, we suggested multimoded systems [5]. In these systems the waveguide is utilized multiple times, carrying different modes simultaneously. At first glance, one might think that this would lead to extra complications in the design of most rf components. Indeed, one has to invent a whole new set of multimoded components. However, since simple manipulations such as bending an overmoded waveguide tend to couple the modes together anyway, it turns out that designs of multimoded components are not much more complex. This is also true from the mechanical design point of view; most of these components are compact.

Manipulation of multiple modes in a single component can be easier in rectangular waveguide than circular. The philosophy of our designs is to do all the manipulation in two dimensions, i.e. planar designs. We leave the height of the waveguide as a free parameter to reduce the fields. To transport the the rf signals we need to use the low-loss circular waveguides. To take advantage of this, we present an rf taper which maps modes in circular waveguide into modes in rectangular guide. The modes of choice are TE_{10} and TE_{20} in rectangular waveguides and TE_{11} and TE_{01} in circular waveguides.

We present the design methodologies for these components, which can handle these two modes simultaneously. These designs feature smooth transitions to minimize field enhancements and at the same time they are virtually losses. We also present a pulse compression system based on these components. This system produced a peak rf signal of about 580 MW. In a reliability test, it ran for hundreds of hours at a power level of about 500 MW with pulse energy of more than 200 joules. The repetition rate varied from 30 Hz to 60 Hz. This exceeds the previous state of the art [3] by increasing the pulse energy by more than a factor of 3 and the pulse power by more than 25%.

DUAL-MODED CIRCULAR-TO-RECTANGULAR TAPERS

We assumed that all these tapers will be built using wire electron discharge machining (EDM). When tapering from one shape, e.g. a circle, to another shape, e.g. a rectangle, the length of the taper, *l,* and the connecting points between the two shapes uniquely define the taper. In cylindrical coordinates a shape *i* placed with cylindrical symmetry around the z-axis can be described by a relation $r_i(\phi)$, which gives the radius as a function of the angle ϕ. The taper between two shapes $r_1(\phi)$, and $r_2(\phi)$ is then given by $r(\phi, z) = r_1(\phi) + (r_2(\phi) - r_1(\phi))/l\ z$.

*This work is supported by the US Department of Energy, Contract number DE-AC03-76SF00515

The Science of Radioactive Ion Beams

B. Sherrill, NSCL, East Lansing, Michigan

Abstract

The primary intellectual challenge of nuclear physics is to understand the nature of strongly interacting matter and how the features of nuclear many-body systems derive from the fundamental forces and properties of their constituent parts. In nuclear science, interestingly, atomic nuclei present one of the most difficult problems to address. However, a comprehensive understanding of nuclear properties is essential to our ability to model the chemical evolution of the Universe, use nuclei for tests of the fundamental symmetries of nature and assess any number of nuclear technologies. Until recently, the fact that experiments had to be carried out with the limited range of stable isotopes found in nature has severely constrained our understanding. However, the current and next generation of radioactive ion beam facilities will remove this constraint. This talk will endeavor to summarize the most important opportunities made available with the next generation of radioactive ion beam facilities.

NO SUBMISSION RECEIVED

THE PHYSICS PERSPECTIVES AT THE FUTURE ACCELERATOR FACILITY FAIR

J. Stroth, GSI, Darmstadt, Germany*

Abstract

The future international accelerator Facility for Antiproton and Ion Research FAIR at Darmstadt, Germany will serve as research facility for a large community of scientists in Europe and around the world. It will expand on experiences made at GSI in combining synchrotrons with storage rings, and will open access to a broad spectrum of experimental approaches. The physics of strongly interacting systems is the main research field, but also aspects of atomic and plasma physics as well as material science will be addressed. The key features of the facility are high intensities, multi-user parallel operation and brilliant beams of secondary reaction products, i.e. exotic instable nuclei and anti-protons. The opportunities have attracted by now three large communities interested in nuclear structure studies using rare isotopes, hadron spectroscopy exploiting collisions of anti-protons with various targets and physics of ultra-dense nuclear matter created in central collisions of very heavy ions. Moreover, many smaller groups of scientists have proposed exiting experiments to investigate e.g. anti-matter, QED in strong fields and strongly correlated plasmas.

INTRODUCTION

At the end of the past decade the Gesellschaft für Schwerionenforschung (GSI), together with Universities and various international user groups, triggered an initiative aimed at providing the European and international science community with a new, world-wide unique accelerator complex. The Conceptual Design Report [1] was presented to the German Ministry for Education and Research in 2002 and was finally approved in 2003 after evaluation by an International Expert Committee put in charge by the German Science Council. The projected facility has been optimized to guarantee excellent conditions for future challenging experiments on open questions concerning - in broadest terms - many-body system governed by the strong interaction and also in related fields. The concept of the future facility founds on the positive experiences made at GSI with combining a synchrotron and a storage ring. Its layout is depicted in Fig. 1.

About 100 years after Rutherford's discovery of the atomic nucleus compelling information about the structure and reaction of nuclei has been collected. As of this, nuclear physics nowadays is concerned with a much broader scope of questions ranging from the dynamics of the elementary quarks and gluons to the evolution of super-nova explosions and the formation of neutron stars. Objects, which differ in size by almost 20 orders of magnitude,

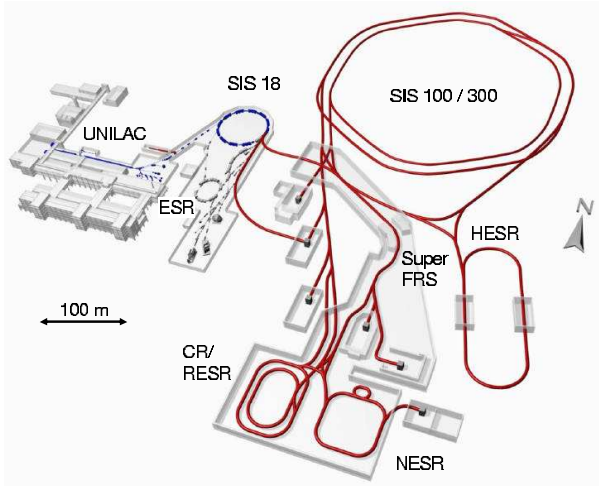

Figure 1: Projected layout of FAIR. The future facility (plotted in red) will be arranged around the old GSI accelerator complex (plotted in blue) comprising the Universal Linear Accelerator UNILAC, a 18 Tm synchrotron (SIS 18) and the Experimental Storage Ring (ESR). The new complex is composed of a rapid cycling 100 Tm synchrotron SIS 100 and a stretcher synchrotron SIS 300 for maximum beam energy and slow extraction. The new super fragment separator (Super FRS) will catch secondary reaction products after dissociation of stable beams of highest intensities. A set of three storage rings is used for collection and pre-cooling (CR), deceleration (RESR) and in-ring experiments with secondary beams in the New Experimental Storage Ring (NESR). The large high energy storage ring (HESR) will provide circulating brilliant beams of antiprotons.

but all essentially governed by the strong interaction. Recently, various national and international advisory committees have outlined the most important avenues for nuclear research in the next decade [2, 3, 4]. Among the top priority research direction are:

- Properties of hot and dense nuclear matter and new phases of matter.
- Non-perturbative effects of QCD and the formation of hadrons.
- Structure and reactions of short-lived, exotic isotopes.
- Symmetries and physics beyond the standard model.

Besides their importance in their own, these fields are intimately linked to the microscopic understanding of cosmological and astrophysical processes.

Although the larger part of the user community will work in nuclear and hadron physics, a still growing fraction of

* j.stroth@gsi.de